Mechanics of Fluid Flow

Scrivener Publishing
100 Cummings Center, Suite 541J
Beverly, MA 01915-6106

Publishers at Scrivener
Martin Scrivener (martin@scrivenerpublishing.com)
Phillip Carmical (pcarmical@scrivenerpublishing.com)

Mechanics of Fluid Flow

Kaplan S. Basniev
Gubkin State University of Oil and Gas, Russia

Nikolay M. Dmitriev
Gubkin State University of Oil and Gas, Russia

and

George V. Chilingar
University of Southern California, USA

Science/technical editors
Misha Gorfunkel
Amir G. Mohammad Nejad

Scrivener

WILEY

Co-published by John Wiley & Sons, Inc. Hoboken, New Jersey, and Scrivener Publishing LLC, Salem, Massachusetts.
Published simultaneously in Canada.

Cover design by Kris Hackerott.

Library of Congress Cataloging-in-Publication Data:

ISBN 978-1-118-38506-7

Printed in the United States of America

10 9 8 7 6 5 4 3 2 1

Contents

DEDICATED TO

***Dr. Henry Chuang**, Chairman*
and Director of "Willie International
Holdings Limited" (Hong Kong, China)
for his outstanding contributions
to the World Petroleum Industry

and

***Dr. John Mork**, President of*
"The Energy Corporation of America" (USA)
for his outstanding contributions
to the Petroleum Industry and education
of petroleum and engineering students

PREFACE

The mechanics of fluid (gas, oil, water) flow is a fundamental engineering discipline explaining various natural phenomena and human-induced processes. It is of utmost importance in aviation, shipbuilding, petroleum industries, thermodynamics, meteorology, and chemical engineering.

This basic applied scientific discipline enables one to understand and describe mathematically the movement of fluids (gas, oil, water) in various media: channels, subsurface formations, pipelines, etc. to describe various phenomena and applications associated with fluid dynamics, the writers used the unified systematic approach based on the continuity and conservation laws of continuum mechanics. Mathematical description of specific applied problems and their solutions are presented in the book.

The present book is an outgrowth of copious firsthand experience of the writers in the fields of hydrodynamics, thermodynamics, heat transfer, and reservoir engineering, and teaching various university courses in fluid mechanics and reservoir characterization. The continuity principle, the equations of fluid motion, momentum theorem (Newton's second law), and steady-flow energy equation (first law of thermodynamics) are emphasized and used for development of engineering solutions of applied problems in this book. The similarities and differences between the steady-flow energy equations and integrated forms of differential equations of motion for nonviscous fluids (Bernoulli Equation) are pointed out.

Differential equations describing the flow of gas and liquid in fractures and fractured-porous reservoir rocks are presented. The two-phase fluid flow is discussed in detail. By applying the unified approach of continuum mechanics, the writers achieved better understanding of fluid properties (density, viscosity, surface tension, vapor pressure, etc) and basic laws of mechanics and thermodynamics. Some chapters of the book are devoted exclusively to incompressible and others to compressible fluid flow, with comparison of the flow of gas and flow of water in the open channels.

This book can be used both as a textbook and a handbook by undergraduate and graduate students, practicing engineers and researchers working in the field of fluid dynamics and related fields.

Authors are very grateful to the Academician of Russian Academy of Sciences S. S. Grigoryan who attentively read through the manuscript and has made a number of valuable remarks.

K. S. Basniev, N. M. Dmitriev, G. V. Chilingar

Mechanics of Fluid Flow
by Kaplan S. Basniev, Nikolay M. Dmitriev and George V. Chilingar

PART I. FUNDAMENTALS OF THE MECHANICS OF CONTINUA

CHAPTER I

BASIC CONCEPTS OF THE MECHANICS OF CONTINUA

Introduction

The theoretical mechanics is a scientific discipline dealing with general laws of equilibrium, movement and interaction between the material bodies. Systems to be analyzed are not real physical bodies but the *models*: material points, material point systems, rigid (non-deformable) bodies. Using model makes the description of processes simpler with the preservation of major specifics of the phenomena.

Frequently, not only the movements of the bodies but their deformations are important. In such cases the models of theoretical mechanics are inapplicable.

An extensive scientific discipline dealing with the theoretical mechanics is the mechanics of continua. It views physical bodies as continuous deformable media. Thus, likewise the theoretical mechanics, it operates with *models*.

In many situations (for instance in gas movements) the processes in deformable media are closely interrelated with thermodynamic phenomena in these media. That is why both the laws of the *theoretical mechanics* and *thermodynamics* are in the base of the mechanics of continua.

The mechanics of continua is the theoretical basis for disciplines such as hydromechanics of Newtonian and non-Newtonian fluids, gas dynamics, subsurface hydromechanics, elasticity theory and plasticity theory.

1. Continuity hypothesis

The phenomena analyzed in the mechanics of continua (particularly in liquids and gas mechanics) are of macroscopic nature. This fact allows for abstracting from the molecular structure of the matter and considers physical bodies as continuous media.

Continuous medium is a material continuum. What it means is that it is a continuous multitude of material points over which the kinematic, dynamic, thermodynamic and other physicochemical parameters of the reviewed medium are continuously (in the general case, piecewise-continuously) distributed.

Physically, the acceptance of the continuous medium model signifies that when macroscopically described, any "infinitely small" volume contains sufficiently great number of molecules. For instance, a 10^{-9}-mm cube of air contains $27*10^6$ molecules suggesting that the idealization will not apply in the case of very high vacuum.

The concept of the "continuous medium" is a model of real medium. The application of such model in the fluid mechanics and other disciplines is based on the experimental results and comprehensive practical confirmation. The examples would be the flow computation in pipelines of diverse purposes, gas and liquid outflow through nozzles, filtration through porous media, etc.

2. Movement of continuous medium: description techniques

When movement is quantitatively studied, it is assumed that some coordinate system is locked relative to which this movement is analyzed. Let us assume that an $Ox_1x_2x_3$ coordinate system with the orthonormal basis[1] $\bar{e}_1$, $\bar{e}_2$, $\bar{e}_3$ is locked in space (Fig. 1.1).

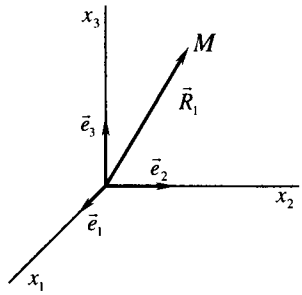

Fig. 1.1

The movement of an individual material point is determined by a time function of its coordinates:

$$x_i = x_i(t) \tag{1.1}$$

or in vector format:[2]

$$\bar{R} = \bar{e}_i x_i(t). \tag{1.2}$$

x_i values are in the *space coordinates*.

The description of continuous medium movement by definition means the assignment of movements of all material points, which form the continuum under consideration. The spatial coordinates of the point at a moment in time $t = t_0$ may be used as "flags" for distinguishing one material point from another one.

Let us assign the spatial coordinates of material points in a continuous medium at $t = t_0$ as X_i. Then the movement of the continuous medium movement may be described as:[3]

$$x_i = x_i(X_1, X_2, X_3, t) = x_i(X_j, t). \tag{1.3}$$

Or, in vector format:

$$\bar{R} = \bar{e}_i x_i(X_j, t). \tag{1.4}$$

---

[1] Orthonormal basis is an aggregate of three mutually perpendicular single vectors.

[2] Here and thereafter, unless specifically stated otherwise, letter subscript assume values of 1, 2, 3, and the summation is performed for the repeated subscripts, i. e., $\bar{e}_i x_i = \sum_{i=1}^{3} \bar{e}_i \cdot x_i$

[3] When specifying $a = a(b_j,t)$ we thereafter mean that $a = a(b_1,b_2,b_3,t)$

A conclusion from the "marker" assigning rule is that the Eqs. (1.3) and (1.4) must satisfy equalities as:

$$X_i = x_i(X_j,t_o),\ \bar{R}_o = \bar{e}_i x_i(X_j,t_o).$$

The X_i coordinates are called the *material coordinates.*

Note: any mutually univalent functions of material coordinates $q_i = q_i(X_j)$ may be used as "markers".

Function (1.3) is considered to be continuous, having continuous partial derivatives for all of its arguments. Physical considerations say that one and only one point in the space corresponds at any moment in time to each material point of a continuous matter. The inverse is also true: only one material point corresponds to each point in space. Therefore, at $t \geq t_o$ function (1.3) assigns a mutually univalent correspondence between material coordinates X_i and spatial coordinates x_i. The latter means that the Jacobian:

$$J = \frac{D(x_1,x_2,x_3)}{D(X_1,X_2,X_3)} = \begin{vmatrix} \frac{\partial x_1}{\partial X_1} & \frac{\partial x_1}{\partial X_2} & \frac{\partial x_1}{\partial X_3} \\ \frac{\partial x_2}{\partial X_1} & \frac{\partial x_2}{\partial X_2} & \frac{\partial x_{21}}{\partial X_3} \\ \frac{\partial x_3}{\partial X_1} & \frac{\partial x_3}{\partial X_2} & \frac{\partial x_3}{\partial X_3} \end{vmatrix} \neq 0,$$

And Eq. (1.3) may be solved relative to the material coordinates:

$$X_j = X_j(x_i,t). \tag{1.5}$$

Two different techniques can be used for describing movement of the continuous medium.

The first one is the Lagrange's technique. The Lagrange's variables X_i and time t are used as independent variables for the description of the movement. On assigning a physical value A (either a vector or scalar value) as a function of the Lagrange's variables and time:

$$A = A(X_j,t) \tag{1.6}$$

At fixed value of material coordinates X_j, the Eq. (1.6) describes the change in the value of A with time in a fixed material point of the continuous medium. At fixed value of material coordinates t, the Eq. (1.6) describes the distribution of value A within the material volume at a fixed moment in time. Therefore, the physical sense of the Lagrange's technique is in the description of a continuous medium by way of describing the movement of individualized material points.

The second way is the Euler's technique. The spatial coordinates x_i (Euler's variables) and time t are utilized for the description of the movement. In this case various parameters of the continuous medium (such as velocity, temperature, pres-

sure, etc.) must be assigned as functions of the Euler's variables. On assigning value A (either a vector or scalar value) as a function of the Euler's variables:

$$A = A(x_j,t) \tag{1.7}$$

At fixed spatial coordinates x_j, Eq. (1.7) describes change in the value A in a given point in space with time. Therefore, the physical sense of the Euler's technique is in the description of a continuous medium behavior at fixed points in space, and not at points in a moving continuous medium.

The application of either technique depends on the setting of the problem. When deriving the basic laws of motion, the Lagrange's technique should be used as it is formulated for the fixed material objects. Likewise, in solving specific hydromechanical problems, the Euler's technique is preferred as in this case, as a rule, it is important to know the medium parameters distribution in space.

The Lagrange's and Euler's techniques are equivalent in the sense that if a description of the movement is established under one of them, it is always possible to switch to the movement description under another one.

The transition from the Lagranges variables to the Euler's variables in a case where the value A is assigned as a function of the Lagranges coordinates (i. e., the Eq. (1.6) is established and the motion law (1.3) is known) boils down to the solution of Eq. (1.3) relative to X_j values, i. e., to find Eq. (1.5) and replace with X_j by $X_j(x,t)$. Then, from (1.5) and (1.6):

$$A(X_j,t) = A(X_j(x_i,t),t) = A(x_i,t). \tag{1.8}$$

If the law of motion (1.3) is assigned and the A value is assigned as a function of the Euler's coordinates, i. e., Eq. (1.7) is given, then by reversing the transformation in the Eq. (1.8), one obtains:

$$A(x_i,t) = A(x_i(X_j,t),t) = A(X_j,t). \tag{1.9}$$

If the law of motion is not assigned but the velocity vector distribution $\bar{v} = e_i v_i(x_j,t)$ is known[4] then it follows from (1.3) or (1.4) that:

$$v_i(x_j,t) = \frac{\partial x_i}{\partial t}. \tag{1.10}$$

By integrating Eq. (1.10) one obtains $x_i = x_i(C_1, C_2, C_3, t)$, where C_j are integration constants, which represent x_i values at some moment in time t_o and may be taken as the "markers" that individualize material points of the continuous medium. Therefore, by integrating Eq. (1.10) one can define the law of motion of the continuous matter (Eq. 1.3), and the transition from the Euler's technique to the Lagrange's technique using the Eq. (1.9).

Thus, only technical difficulties may occur in solving Eq. (1.1) or integrating the Eq. (1.8) when switching from the Lagrange's to the Euler's technique and vice versa, as theoretically such transition is always possible.

[4] If the Euler's description is known, then the velocity distribution is also known, i. e., the $v_i(x_j,t)$ functions are known.

3. Local and substantive derivative

The change of *any property A*, for instance velocity, density, temperature of a fixated material point in a moving continuous medium with respect to time is called a substantive (material, individual or total) time derivative and is denoted by $\frac{dA}{dt}$.

The A value may be a scalar or vector and may be assigned as a function of the Lagrange's or Euler's coordinates, i. e., $A = A(X_i,t)$ or $A = A(x_i,t)$. As the material point is moving along its own trajectory, the A value may also be assigned as $A = A(s,t)$ where s is the length of the arc along the trajectory. When a fixed point is moving, its material coordinates do not change:

$$\frac{d}{dt}A(X_i,t) = \frac{\partial A(x_i,t)}{\partial t}. \tag{1.11}$$

Conversely, its spatial coordinates are a function of time:

$$\frac{d}{dt}A(x_i,t) = \frac{\partial A(x_i,t)}{\partial t} + \frac{\partial A(x_i,t)}{\partial x_j}\frac{\partial x_j}{\partial t}, \tag{1.12}$$

or

$$\frac{d}{dt}A(s,t) = \frac{\partial A(s,t)}{\partial t} + \frac{\partial A}{\partial s}\frac{\partial s}{\partial t}. \tag{1.13}$$

Obviously, $\frac{\partial s}{\partial t} = v$ is the modulus of the velocity vector, and $\frac{\partial x_i}{\partial t}$ are components of the velocity vector of the point under consideration. Then, taking Eq. (1.10) into account, Eqs. (1.12) and (1.13) may be represented as:

$$\frac{d}{dt}A(x_i,t) = \frac{\partial A(x_i,t)}{\partial t} + v_j\frac{\partial A(x_i,t)}{\partial x_j}, \tag{1.14}$$

$$\frac{d}{dt}A(s,t) = \frac{\partial A(s,t)}{\partial t} + v\frac{\partial A(s,t)}{\partial s}. \tag{1.15}$$

If A is a scalar value:

$$v_j\frac{\partial A(x_i,t)}{\partial s} = \bar{v}\,\mathrm{grad}A = \bar{v}\nabla A, \tag{1.16}$$

the directional derivative s is equal to:

$$\frac{\partial A(s,t)}{\partial s} = \bar{s}^o\nabla A, \text{ and } v\frac{\partial A(s,t)}{\partial s} = v\bar{s}^o\nabla A = \bar{v}\nabla A, \tag{1.17}$$

where $\bar{s}^o$ is a singular vector, tangential to the trajectory; $\bar{v} = \bar{e}_i v_i$ is the velocity vector.

Considering Eqs. (1.16) and (1.17), Eqs. (1.14) and (1.15) may be rewritten as:

$$\frac{dA}{dt} = \frac{\partial A}{\partial t} + v\nabla A. \tag{1.18}$$

If A is a vector (i. e., $\bar{A} = \bar{e}_i A_i$), then according to Eq. (1.14)

$$\frac{dA_i}{dt} = \frac{\partial A_i}{\partial t} + v_j \frac{\partial A_i}{\partial x_j},$$

then:

$$e_i \frac{dA_i}{dt} = \frac{d\bar{e}_i A_i}{dt} = \frac{d\bar{A}}{dt}, \quad e_i \frac{\partial A_i}{\partial t} = \frac{\partial \bar{e}_i A_i}{\partial t} = \frac{\partial \bar{A}}{\partial t},$$

$$\bar{e}_i v_j \frac{\partial A_i}{\partial x_j} = v_j \frac{\partial \bar{e}_i A_i}{\partial x_j} = v_j \frac{\partial A_i}{\partial x_j} = (\bar{v} * \nabla)\bar{A}$$

and

$$\frac{d\bar{A}}{dt} = \frac{\partial \bar{A}}{\partial t} + (\bar{v} * \nabla)\bar{A}, \tag{1.19}$$

where $(\bar{v} * \nabla)$ is a symbolic operator which is equal to:

$$(\bar{v} * \nabla) = v_j \frac{\partial}{\partial x_j}.$$

The first term in Eqs. (1.12)–(1.15) and (1.18), (1.19) describes the change in velocity of the property A at the fixed point of space and is called a local derivative. The second term in these equations is called a convective derivative and describes the change in A due to displacement of the material point in space. The convective derivative value is determined by the motion of the material point $(\bar{v} \neq 0)$ as well as by non-uniformity of A value distribution in space $(\frac{\partial A}{\partial x_i} \neq 0)$.

4. Scalar and vector fields

If a scalar (vector) value corresponds to each point of the spatial volume D and to each temporal moment t, it means that *a scalar (vector) field is defined in the volume D*. Thus, the *field* of a certain value is defined as the aggregation of its numerical values established at each point of the volume D and within the assigned time interval. For instance, if the functions of scalar values are established

$$\rho = \rho(x_i,t), \; T = T(x_i,t), \tag{1.20}$$

where ρ is density and T is temperature, then the functions (1.20) define the scalar fields of density and temperature. If a vector function is established, for instance,

$$v_k = v_k(x_i,t) \text{ or } \bar{v} = \bar{v}(x_i,t), \tag{1.21}$$

then the function (1.21) defines the vector field of velocities.

Thus the concept of the field with a physical value is applicable for the motion description only through the Euler's technique.

A scalar (vector) field is called *continuous* if any representing function is continuous over x_i and t. If a function representing the field does not depend on time t, the field is called *stationary*.

If all fields describing the motion of the continuous medium are stationary, such a motion is called *transient-free* or *stationary*. However, if these fields (or either of them) depend on time, the motion is called *transient* or *non-stationary*. In the case of the transient-free motion all local derivatives (partial derivatives over time) are equal to zero, i. e.,

$$\frac{\partial \rho}{\partial t} = 0, \quad \frac{\partial T}{\partial t} = 0, \quad \frac{\partial v_i}{\partial t} = 0, \ldots$$

The notion of transient-free or transient motion is applicable only if the motion is described using the Euler's technique relative to a reference coordinates. One motion may be transient-free relative to one coordinate system and transient relative to the other one. For instance, when a solid is moving at a constant velocity in a liquid, the liquid's motion is transient-free in the coordinate system associated with the solid, and transient in an immovable coordinate system.

For any vector field, a notion of *a vector line* may be introduced. The vector line is a tangent line at each point at a given moment in time coinciding with the direction of the field of vectors . It follows from this definition that if a vector field $\bar{A}(x_i,t)$ is established, then at a given moment in time the condition $\bar{A} \| d\bar{s}$ is accomplished in the vector line points. Here, $d\bar{s}$ is infinitely small vector of the tangent, or $d\bar{s} = \bar{A} d\lambda$ where $d\lambda$ is a scalar parameter (Fig. 1.2).

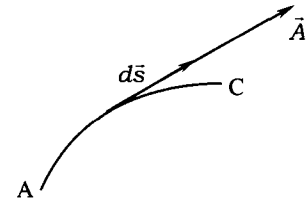

Fig. 1.2

The velocity field vector lines are called *the flow lines*. As by definition for the $d\bar{s} = \bar{e}_i dx_i = \bar{v} d\lambda = \bar{e}_i v_i d\lambda$, the equation flow lines can be presented as:

$$\frac{dx_i}{d\lambda} = v_i(x_j,t). \tag{1.22}$$

Please note that the following equality is true along the motion trajectory of the material point:

$$\frac{dx_i}{dt} = v_i(x_j,t). \tag{1.23}$$

In Eq. (1.22), the time is the parameter and in Eq. (1.23), it is an independent variable.

The solution of the system of equations (1.22) has a form of $x_i = x_i(c_j, \lambda, t)$, where c_j are integrating constants, and the flow lines (vector lines) may have different shapes at different moments in time.

At the transient-free motion, Eqs. (1.22) and (1.23), respectively, have the following form:

$$\frac{dx_i}{d\lambda} = v_i(x_j), \quad \frac{dx_i}{dt} = v_i(x_j),$$

And the distinction boils down to the parameter over which the differentiation is conducted. Therefore, at the transient-free motion the flow-lines and material point trajectories coincide.

If the equation system (1.22) has a solution, and the solution is singular, then the only one flow line runs through each point in space. However, there are some points of the velocity field where the conditions of the existence and singularity may be broken. In particular, the solution singularity conditions may be broken at the points where velocity vector components approach zero or infinity.

The points where velocity approaches zero or infinity are called *singularities*. Fig. 1.3 shows an example of the velocity field that occurs when the liquid flows around a solid. The velocity at point A equals zero, and the flowline bifurcates.

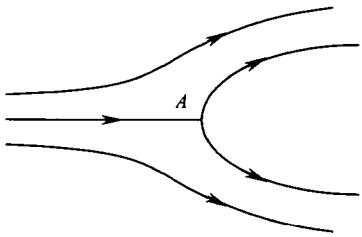

Fig. 1.3

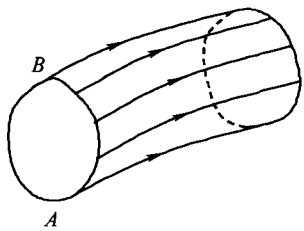

Fig. 1.4

Next, the writers examine some aspects of the velocity field with no singularities. Drawing flowlines within the area of the curve AB, one flowline may be carried through each point of the curve AB. The aggregation of these flowlines forms a surface at each point in which the velocity vector lies in the plane tangent to this surface. Such a surface is called *a flow-surface*. As the only flowline runs through each point of the flow-surface, this surface is impermeable for the particles of the liquid. If the AB line is closed (Fig. 1.4), the surface is called *the flow-tube*.

Next, one can assume that $f(x_1,x_2,x_3) = 0$ is the equation of flow-surface. Inasmuch as

$$\nabla f = \bar{e}_i \frac{\partial f}{\partial x_i}$$

is the vector normal to this surface, and the velocity vector $\bar{v} = \bar{e}_i v_i$ lies on the plane tangent to the flow-surface, then:

$$\bar{v}\nabla f = v_i \frac{\partial f}{\partial x_i} = 0 \tag{1.24}$$

is the condition necessarily fulfilled on the flow-surface.

On cutting the flow-tube with some surface, if the vector at each point of this surface is directed normally to this surface, it is called effective cross-section. On assuming $\varphi(x_1, x_2, x_3) = 0$ is the equation of the effective cross-section, the velocity vector $\bar{v}$ is parallel to the normal to this cross-section, $\nabla\varphi \| \bar{v}$, or $\bar{v} * \nabla\varphi = 0$.

If the *AB* line length is infinitely small, the flow-tube is called elementary. The flow parameters (velocity, density, etc.) within the elementary flow-tube are uniformly distributed on the effective cross-section.

5. Forces and stresses in the continuous medium. Stress tensor

A continuous medium and a rigid body move upon acting forces. Theoretical mechanics deals mostly with concentrated forces, but mechanics of continua deals mainly with distributed forces.

Depending on the nature of acting forces, regardless of the specific physical nature, mechanics of continua distinguishes two types of forces, the mass forces and the surface forces. The mass forces are those whose value is proportional to the mass of the medium they act on. Gravity, electromagnetic forces, and inertia are examples of these types of forces. The surface forces are those whose value is proportional to the surface of the medium they act on such as pressure and friction.

Mechanics of continua deals not with the mass and surface forces but rather with the *stress* (*distribution density*).

The stress of mass forces is defined as the limit of a ratio:

$$\lim_{\Delta m \to 0} \frac{\Delta \bar{R}}{\Delta M} = \bar{F}(M),$$

Where $\Delta \bar{R}$ is the main vector of mass forces acting on the mass Δm contained in an elementary volume ΔV, which includes the point M (Fig. 1.5). The dimension for mass force's stress is that of acceleration. For the gravity force, the stress $\bar{F} = \bar{g}$ where $\bar{g}$ is the vector of the gravity acceleration.

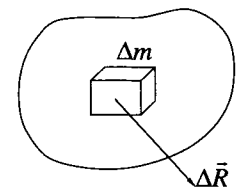

Fig. 1.5

To determine the surface forces, consider an elementary area ΔS on the surface S placed within the continuous medium. The ΔS area includes point M

(Fig. 1.6). The stress of the surface force at point M is determined by the limit of a ratio

$$\lim_{\Delta S \to 0} \frac{\Delta \bar{P}}{\Delta S} = \bar{p}(M).$$

It is obvious that an infinite number of surfaces S may be carried through point M. In a general case, the stress at point M may be different for different surfaces (Fig. 1.7). Therefore, the stress of a surface force is not only a spatial function but a function of the orientation of the elementary area ΔS.

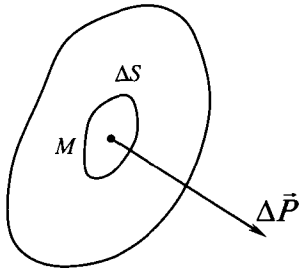

Fig. 1.6

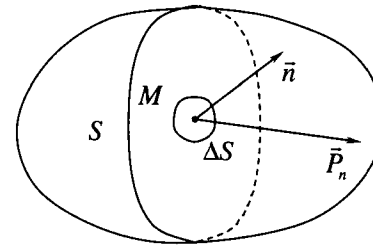

Fig. 1.7

Thus, contrary to stress of the mass forces (they are spatial functions, therefore, they form a vector field), the surface force stress does not form a vector field.

The orientation of the ΔS area in space may be established by a singular vector of the normal $\bar{n}$ to the surface S at point M. Considering $\bar{p} = \bar{p}(\bar{n}, M)$, $\bar{p}$ as function of $\bar{n}$ is denoted by a subscript: $\bar{p} = \bar{p}_n(M)$.

However, the surface S is bilateral. Two normals may be carried through point M, $\bar{n}$ and $-\bar{n}$ (Fig. 1.8). That is why a convention of the normals positive direction is necessary. *Assume the positive direction points toward the part of the continuous medium, from which the surface forces are acting on the area* ΔS. It follows that when the $\bar{n}$ and $\bar{p}_n$ directions coincide, surface forces are extension forces, and if these directions are opposite, they are contractive forces.

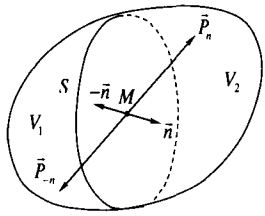

Fig. 1.8

It is desired to divide the continuous medium volume V into parts V_1 and V_2 by surface S (Fig. 1.8). Considering the surface S and the boundary of the volume V_1 the force acting on the ΔS area from the side of volume V_2, is equal to $\bar{p}_n(M)\Delta S$, and the force acting on the entire surface S is given by:

$$\int_S \bar{p}_n(M)dS.$$

However if, the surface S to the boundary of the volume V_2 is considered, the force acting on the ΔS area is equal to $\bar{p}_{-n}(M)\Delta S$, and the force acting on the entire surface S is given by:

$$\int_S \bar{p}_{-n}(M)dS.$$

Under the Newton's third law of motion:

$$\int_S [\bar{p}_n(M) + \bar{p}_{-n}(M)]dS = 0.$$

the surface S is chosen arbitrary such that:

$$\bar{p}_n(M) = -\bar{p}_{-n}(M). \tag{1.25}$$

the stress $\bar{p}_n$ may be expanded into the normal p_{nn} and tangential p_r components:

$$\bar{p}_n = \bar{n}p_n + \bar{\tau}p_r, \tag{1.26}$$

where $\bar{\tau}$ is a singular vector and $\bar{n} * \bar{\tau} = 0$.

Carrying coordinate axes x_1, x_2, x_3 through any point of the continuous medium yields an infinitely small tetrahedron $ABCM$ (Fig. 1.9). The verges of the tetrahedron will be dx_1, dx_2, dx_3. By default, the tetrahedron faces BCM, AM, CAM are perpendicular to the corresponding basis vectors. Therefore, $\bar{n}_1 = -\bar{e}_1$, $\bar{n}_2 = -\bar{e}_2$ and $\bar{n}_3 = -\bar{e}_3$. The ABC face orientation is arbitrary and is established by the vector of the normal $\bar{n} = -\bar{e}_i\alpha_{ni}$, where $\alpha_{ni} = \overline{ne}$ are directing cosines of the normal. Then the stresses on the corresponding faces is given by $\bar{p}_{-i}$, and $\bar{p}_n$.

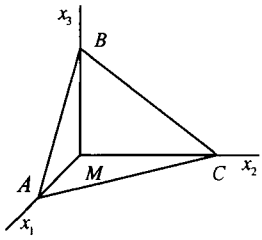

Fig. 1.9

Denoting the area of the ABC face as dS, the areas of the other faces may be computed as projections of the areas of the face on the corresponding coordinate planes: $dS_1 = \alpha_{n1}dS$ for the face BCM, $dS_2 = \alpha_{n2}dS$ for the face ABM, and $dS_3 = \alpha_{n3}dS$ for the face ACM, or

$$dS_1 = (\bar{n} * \bar{e}_i)dS = \alpha_{ni}dS. \tag{1.27}$$

Surface forces $\bar{p}_{-i}dS_i$, $\bar{p}_n dS$ and the mass force $d\bar{R} = \bar{F}dm = \rho\bar{F}dV = \rho\bar{F}\,{}^1/_3 hdS$ are acting on the tetrahedron $ABCM$ (dm is the mass within the tetrahedron dV, and h is the tetrahedron height). Under the Newton's second law of motion, the sum of forces acting on the tetrahedron $ABCM$ is equal to the product of its mass and the acceleration, i. e., demonstrated in Eq. (1.27),

$$\frac{1}{3}\rho h\bar{F}dS + \bar{p}_{-i}\alpha_{ni}dS = \frac{d\bar{v}}{dt}dm = \frac{1}{3}\rho h\frac{d\bar{v}}{dt}dS. \tag{1.28}$$

Canceling all dS's in Eq. (1.28), and constricting the tetrahedron to a point (i. e., assuming $h \to 0$):

$$\bar{p}_{-i}\alpha_{ni} + \bar{p}_n = 0,$$

or, like Eq. (1.25):

$$\bar{p}_n = \bar{p}_i \alpha_{ni}. \tag{1.29}$$

The $\bar{p}_i$ vectors can be presented in the following format:

$$\bar{p}_i = e_j p_{ji}. \tag{1.30}$$

Here, p_{ji} is the j^{th} component of vector p_i.

The Eq. (1.30) vector equality is equivalent to the following equations expressed in the component format:

$$\begin{aligned} p_{n1} &= p_{11}\alpha_{n1} + p_{21}\alpha_{n2} + p_{31}\alpha_{n3}, \\ p_{n2} &= p_{12}\alpha_{n1} + p_{22}\alpha_{n2} + p_{32}\alpha_{n3} \\ p_{n3} &= p_{13}\alpha_{n1} + p_{23}\alpha_{n2} + p_{33}\alpha_{n3}. \end{aligned} \tag{1.31}$$

Thus, the state of stress at any given point is determined by the aggregation of three stress vectors p_i or by the nine-component-p_{ij} defined over three mutually perpendicular areas. The Eq. (1.29) is the definition of tensor.

The p_{ij} components form a second rank tensor like:

$$p_{ij} = \begin{pmatrix} p_{11} & p_{12} & p_{13} \\ p_{21} & p_{22} & p_{23} \\ p_{31} & p_{32} & p_{33} \end{pmatrix}. \tag{1.32}$$

The first subscript of the p_{ij} stress tensor component indicates the direction of the coordinate axis to which the normal vector $\bar{n}$ is parallel. The second subscript of the p_{ij} stress tensor component indicates the direction of the coordinate axis onto which the stress vector is projected (Fig. 1.10). For instance, p_{21} represents the projection of $\bar{p}_2$ vector, attached to the area perpendicular to the x_2 axis, onto the x_1 axis.

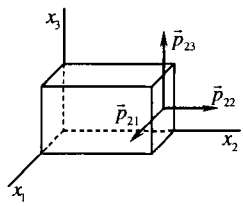

Fig. 1.10

The components with the same subscripts p_{ii} are called *normal stresses*, and the components p_{ik} $(i \neq k)$ are called *tangential stresses* or *shear stresses*.

The p_{ij} stress tensor depends on coordinates x_i and time t forming a tensor field.

It is necessary to note here that the concept described above is the classical theory of the state of stress. It is important to note that the moments of the surface and mass forces at point M are equal to zero. However, there are more detailed theories considering continuous series with distributed moments of surface and mass forces. These theories are dealing with special branches of the mechanics of continua, for instance in studies of liquid and elastic media with a micro-structure.

Mechanics of Fluid Flow
by Kaplan S. Basniev, Nikolay M. Dmitriev and George V. Chilingar

CHAPTER II

CONSERVATION LAWS. INTEGRAL AND DIFFERENTIAL EQUATIONS OF CONTINUOUS MEDIUM

1. Integral parameters of a continuous medium and the conservation laws

Basic equations for the continuous medium are derived from the conservation laws which are the fundamental laws of nature. The major conservation laws in the mechanics of continua are the conservation laws of mass, variation in momentum, moment of momentum, energy and entropy balance. For a mathematical formulation of the conservation laws, a *material* (*movable*) or *control volume* is reviewed.

The *material* (*movable*) volume is such a volume composed at all time from the same material points.

A volume of space whose boundaries are open to material, energy, and momentum transfer is called the control volume, and the limiting boundary is called the control surface. The control surface may change its position in space but usually it is considered static.

When considering the material volume, it is assumed that it represents a singular physical body with mass:

$$M = \int_{V(t)} \rho dV, \tag{2.1}$$

with its corresponding momentum:

$$\bar{J} = \int_{V(t)} \rho \bar{v} dV, \tag{2.2}$$

moment of momentum:

$$\bar{M} = \int_{V(t)} \rho \left(\bar{r} \times \rho \bar{v}\right) dV, \tag{2.3}$$

energy:

$$E = \int_{V(t)} \rho \left(u + \frac{v^2}{2}\right) dV, \tag{2.4}$$

which is a sum of the kinetic energy:

$$K = \int_{V(t)} \rho \frac{v^2}{2} dV \tag{2.5}$$

internal energy:

$$U = \int_{V(t)} \rho u dV, \tag{2.6}$$

and entropy:

$$S = \int_{V(t)} \rho s dV, \tag{2.7}$$

where $\rho = \rho(x_j,t)$ is density, $\bar{v} = \bar{v}(x_j,t)$ is velocity, $u = u(x_j,t)$ is per-unit-mass internal energy, $s = s(x_j,t)$ is per-unit-mass entropy, $\bar{r}$ is radius-vector of a material particle with the origin at a point relative to which the kinetic momentum is determined, $V(t)$ is the material (movable) volume.

Under the law of mass conservation, the mass of a material volume (2.1) remains constant. Therefore, the total derivative of Eq. (2.1) is equal to zero, i. e.,

$$\frac{dM}{dt} = \frac{d}{dt} \int_{V(t)} \rho dV = 0. \tag{2.8}$$

Under the Newton's second law of motion, the rate of variation in momentum of a liquid volume equals to the sum of all external forces acting on this volume. Thus, the material derivative of the Eq. (2.2) is equal:

$$\frac{d\bar{J}}{dt} = \frac{d}{dt} \int_{V(t)} \rho \bar{v} dV = \bar{F}^{(e)}, \tag{2.9}$$

where $\bar{F}^{(e)}$ is the total sum of all mass and surface forces attached to the volume $V(t)$.

The sum of all mass forces may be presented in the following format (Fig. 2.1):

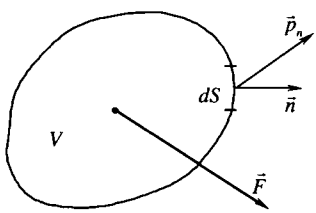

Fig. 2.1

$$\int_{V(t)} \rho \bar{F} dV.$$

The sum of all surface forces (Fig. 2.1) obviously is equal to:

$$\int_{S(t)} \bar{p}_n dV,$$

where $S(t)$ is a closed surface delimiting the material volume $V(t)$.

Taking all these remarks into account, the law of kinetic momentum Eq. (2.9) may be presented in the following format:

$$\frac{d\bar{J}}{dt} = \frac{d}{dt}\int_{V(t)} \rho \bar{v} dV = \int_{V(t)} \rho \bar{F} dV + S. \tag{2.10}$$

Considering the law of kinetic momentum, the rate of change in the kinetic momentum of a material volume in relation to any point is equal to the main momentum of all external mass and surface forces in relation to the same point. Equation for the momentums is given by:

$$\int_{V(t)} (\bar{r} * \rho \bar{F}) dV, \quad \int_{S(t)} \bar{r} * \bar{p}_n dS,$$

then the relationship for the variation of kinetic momentum of a given material volume is given by:

$$\frac{d\bar{M}}{dt} = \frac{d}{dt}\int_{V(t)} (\bar{r}\rho\bar{v}) dV = \int_{V(t)} (\bar{r} * \rho \bar{F}) dV + \int_{S(t)} \bar{r} * \bar{p}_n dS. \tag{2.11}$$

As it can be seen from the kinetic momentum relationship, the rate of change of a material volume $V(t)$ is equal to the sum of mechanical work W of the external mass and surface forces per unit time (external force power) and of the other energy inflow Q per unit time. Therefore, the material derivative of Eq. (2.4) is associated with the W and Q values as follows:

$$\frac{dE}{dt} = \frac{d}{dt}\int_{V(t)} \rho(u + \frac{v^2}{2}) dV = W + Q. \tag{2.12}$$

From now on, in this book it is assumed that Q is only the rate of heat in-flow The law of the energy conservation is also called the first law of thermodynamics.

Power of the external volume forces W_1 is equal to:

$$W_1 = \int_{V(t)} \rho \bar{F} * \bar{v} dV,$$

and that of the surface forces W_2:

$$W_2 = \int_{S(t)} \bar{p}_n * \bar{v} dS.$$

Heat inflow Q per unit time may be presented as:

$$Q = \int_{V(t)} \rho q_e dV,$$

where q_e is heat delivered per unit volume of fluid $V(t)$ per unit time.

The energy conservation law following from Eq. (2.12) is given by:

$$\frac{dE}{dt}=\frac{d}{dt}\int_{V(t)}\rho(u+\frac{v^2}{2})dV=\int_{V(t)}\rho\bar{F}\bar{v}dV+\int_{S(t)}\bar{p}_n\bar{v}dS+\int_{V(t)}\rho q_e dV. \qquad (2.13)$$

Along with the laws of conservation of mass, variation in momentum, moment of momentum and energy, a theorem (law) may be formulated for the relationship between the variations of kinetic energy (theorem of live force). As opposed to the other mentioned laws, the kinetic energy theorem is not an independent law. Considering the theoretical mechanics law, kinetic energy theorem is derived from the momentum theorem (law).According to this theorem; the changes in kinetic energy in time for a given fluid volume is equal to the sum of works (powers) done by the external and internal forces acting on this volume. The material derivative of Eq. (2.5) is given by:

$$\frac{dK}{dt}=\frac{d}{dt}\int_{V(t)}\rho\frac{v^2}{2}dV=\int_{V(t)}\rho\bar{F}\bar{v}dV+\int_{S(t)}\bar{p}_n\bar{v}dS+\int_{V(t)}\rho N^i dV, \qquad (2.14)$$

where N^i is the magnitude of internal forces per-unit mass of the medium.

Please notice that Eq. (2.14), as opposed to the energy conservation law Eq. (2.13), includes the magnitude of external and of internal forces.

The change in the entropy of a given fluid volume $V(t)$ can never be less than the sum of entropy inflow through its boundary $S(t)$ and entropy generated within it by the external sources. This is the definition of the second law of thermodynamics or so called the law of the entropy balance. The mathematical expression of this law is formulated through an inequality as follows:

$$\frac{d}{dt}\int_{V(t)}\rho s dV\geq\int_{V(t)}\rho e dV-\int_{S(t)}\frac{\bar{q}*\bar{n}}{T}dS, \qquad (2.15)$$

This inequality is called the Klausius-Dughem inequality, where, s is *entropy per unit mass*, e is power of local external sources of entropy per unit mass, $\bar{q}$ is the heat flow vector through a unit area per unit time. The Eq. (2.15) equality is valid for the reversible processes, and the Eq. (2.15) inequality is valid for the irreversible processes.

The left portions of the Eqs. (2.8), (2.10), (2.11), (2.13) and (2.14) can be written in a general form as:

$$\frac{d}{dt}\int_{V(t)}\varphi(x_j,t)dV=\Phi,$$

where $\varphi(x_j,t)$ can be one of the values of ρ, $\rho\bar{v}$, $\bar{r}*\rho\bar{v}$, $\rho(u+v^2/2)$, $\rho v^2/2$, and Φ representing the right portions of the above formulas. In order to attribute the corresponding mathematical formulation to Eqs. (2.8), (2.10), (2.11), (2.13) and (2.14), it is necessary to compute the total (material) derivative over the material (movable) volume.

2. Time differentiation of the integral taken over a movable volume

To derive the formula for time derivative, it is necessary to review the position of the control volume $V(t)$ at time moments t and Δt (Fig. 2.2). From the definition of the total derivative:

$$\frac{d}{dt}\int_{V(t)}\varphi(x_j,t)dV = \lim_{\Delta t\to 0}\frac{1}{\Delta t}\left[\int_{V(t+\Delta t)}\varphi(x_j,t+\Delta t)dV - \int_{V(t)}\varphi(x_j,t)dV\right], \quad (2.16)$$

where $V(t+\Delta t)$ is the position occupied by the fluid volume $V(t)$ at the time $t+\Delta t$.

As

$$\int_{V(t+\Delta t)}\varphi(x_j,t+\Delta t)dV = \int_{V(t)}\varphi(x_j,t+\Delta t)dV + \int_{V(t+\Delta t)-V(t)}\varphi(x_j,t+\Delta t)dV,$$

the Eq. (2.16) may be rewritten as:

$$\frac{d}{dt}\int_{V(t)}\varphi(x_j,t)dV = \lim_{\Delta t\to 0}\int_{V(t)}\frac{\varphi(x_j,t+\Delta t)-\varphi(x_j,t)}{\Delta t}dV + \lim_{\Delta t\to 0}\frac{1}{\Delta t}\int_{V(t+\Delta t)-V(t)}\varphi(x_j,t+\Delta t)dV. \quad (2.17)$$

According to Eq. (2.17), the first component is equal to:

$$\lim_{\Delta t\to 0}\int_{V(t)}\frac{\varphi(x_j,t+\Delta t)-\varphi(x_j,t)}{\Delta t}dV = \int_{V(t)}\frac{\partial\varphi(x_j,t)}{\partial t}dV. \quad (2.18)$$

Considering (Fig. 2.2), the change in the volume can be formulated by $V(t+\Delta t) - V(t) = V_2 + V_3 - V_3 - V_1 = V_2 - V_1$. Here, V_2 and V_1 are volumes of space, respectively, freed and occupied again over the period of time Δt, and V_3 is the shared portion of volumes $V(t+\Delta t)$ and $V(t)$.

For the volume V_2, the volume element dV may be computed as the volume of a cylinder (Fig. 2.2) with the base dS and height $V_n\Delta t - \bar{v}*\bar{n}\Delta t$, where v_n is the projection of velocity on the external normal $\bar{n}$ to the surface S_2 separating volumes V_2 and V_3.

Then:

$$\int_{V_2}\varphi(x_j,t+\Delta t)dV = \int_{S_2}\varphi(x_j,t+\Delta t)v_n\Delta t dS.$$

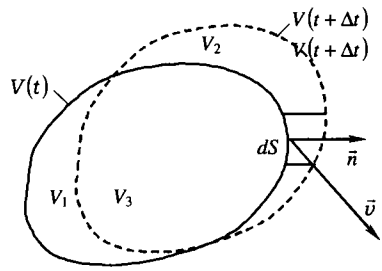

Fig. 2.2

Similarly for the volume V, the height of the elementary cylinder is: $\bar{v} * \bar{n}\Delta t = -v_n\Delta t$ and

$$\int_{V_1} \varphi(x_j, t+\Delta t)dV = -\int_{S_1} \varphi(x_j, t+\Delta t)v_n \Delta t dS,$$

where S_1 is the surface separating volumes V_1 and V_2.

This lead to a conclusion that the second component in the right hand side of Eq. (2.17) can be formulated as follows:

$$\lim_{\Delta t \to 0} \frac{1}{\Delta t} \int_{V(t+\Delta t)-V(t)} \varphi(x_j, t+\Delta t)dV = \lim_{\Delta t \to 0} \frac{1}{\Delta t} [\int_{V_2} \varphi(x_j, t+\Delta t)dV -$$

$$-\int_{V_1} \varphi(x_j, t+\Delta t)dV] = \lim_{\Delta t \to 0} [\int_{S_2} \varphi(x_j, t+\Delta t)v_n dS - \tag{2.19}$$

$$-\int_{S_1} \varphi(x_j, t+\Delta t)v_n dS] = \int_{S(t)} \varphi(x_j, t)v_n dS,$$

where $S(t)$ is a closed surface limiting volume $V(t)$.

Replacing Eqs. (2.18) and (2.19) into Eq. (2.18) yields:

$$\frac{d}{dt} \int_{V(t)} \varphi(x_j, t)dV = \int_{V(t)} \frac{\partial \varphi(x_j, t)}{\partial t} dV + \int_{S(t)} \varphi(x_j, t)v_n dS. \tag{2.20}$$

In Eq. (2.20), the normal $\bar{n}$ is considered external relative to the closed surface $S(t)$.

For further transformations of Eq. (2.20), the Gauss–Ostrogradsky theorem is used in the following format:

$$\int_S a_n dS = \int_S \bar{a} * \bar{n} dS = \int_S a_i \alpha_{ni} dS = \int_V \frac{\partial a_i}{\partial x_i} dV = \int_V div\bar{a}\, dV, \tag{2.21}$$

where $\bar{a} = \bar{e}_j a_j$, α_{ni} are directing cosines of the normal $\bar{n}$, and divergence of the vector $\bar{a}$ is:

$$div\bar{a} = \frac{\partial a_i}{\partial x_i}.$$

According to Eq. (2.21), $\bar{a} = \varphi\bar{v}$, deriving from Eq. (2.20):

$$\frac{d}{dt} \int_{V(t)} \varphi(x_j, t)dV = \int_{V(t)} \left(\frac{\partial \varphi}{\partial t} + div\varphi\bar{v} \right) dV, \tag{2.22}$$

where, arguments of the $\varphi(x_j,t)$ are not shown.

As $div\varphi\bar{v} = \varphi div\bar{v} + v_i \frac{\partial \varphi}{\partial x_i}$,

and:

$$\frac{\partial \varphi}{\partial t} + v_i \frac{\partial \varphi}{\partial x_i} = \frac{d\varphi}{dt},$$

Eq. (2.22) can be rewritten as follows:

$$\frac{d}{dt}\int_{V(t)}\varphi dV = \int_{V(t)}\left(\frac{d\varphi}{dt}+\varphi div\bar{v}\right)dV\,. \tag{2.23}$$

The Eqs. (2.20) and (2.23) preserve their appearance even when $\varphi(x_j,t)$ is a vector function of its arguments.

3. Continuity equation (law of mass conservation)

The continuity equation is a differential form of the mass conservation law for the continuous medium. Assuming $\varphi = \rho$ in Eq. (2.23) and using the condition of a fluid volume mass constancy Eq. (2.8):

$$\int_{V(t)}\left(\frac{d\rho}{dt}+\rho div\bar{v}\right)dV = 0\,. \tag{2.24}$$

As this equation is true for any fluid volume, the expression under integral in Eq. (2.24) is equal to zero:

$$\frac{d\rho}{dt}+\rho div\bar{v} = 0\,. \tag{2.25}$$

Eq. (2.25) is called the continuity equation. If Eq. (2.22) is substituted rather than Eq. (2.23), the continuity equation changed to the following format:

$$\frac{\partial\rho}{\partial t}+div\rho\bar{v} = 0\,. \tag{2.26}$$

To derive the continuity equation for a flow-tube, Eqs. (2.8) and (2.20) are used. Replace $\varphi = \rho$ in Eq. (2.20):

$$v(t)\int\frac{\partial\rho}{\partial t}dV + \int_{S(t)}\rho v_n dS = 0\,. \tag{2.27}$$

Eq. (2.27) is called the integral form of the continuity equation.

Next, Eq. (2.27) is applied to the fluid flow through a flow-tube. Carrying the effective cross-sections S_1 and S_2 (Fig. 2.3), the control surface S is composed of three parts: the effective sections S_1 and S_2 (through which the fluid flows in and out of the flow-tube segment under consideration), and its side surface S_3.

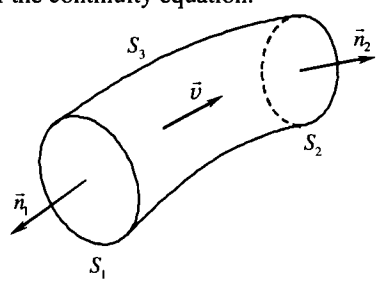

Fig. 2.3

By definition of a flow-tube, at the points of the side surface S_3, $v_n = 0$. Thus, Eq. (2.27) forms the following format:

$$\int_V \frac{\partial \rho}{\partial t} dV + \int_{S_1} \rho v_n dS + \int_{S_2} \rho v_n dS = 0. \tag{2.28}$$

Substituting the definitions of effective cross section for S_2 as $v_n = v$, and for S_1 as $v_n = -v$ into Eq. (2.28) yields:

$$\int_V \frac{\partial \rho}{\partial t} dV = \int_{S_1} \rho v dS - \int_{S_2} \rho v dS. \tag{2.29}$$

In the case of a transient-free motion, $\frac{\partial \rho}{\partial t} = 0$, and from Eq. (2.29):

$$\int_{S_1} \rho v dS = \int_{S_2} \rho v dS = Q_m = \text{const}. \tag{2.30}$$

The $Q_m = \int_S \rho v dS$ is the fluid mass per unit time, running through the effective cross-section or so-called the mass throughflow. It can be concluded from Eq. (2.30) that under the transient-free flow environment, the mass throughflow along the tube is constant.

For the elementary flow-tube, Eq. (2.30) takes the following format:

$$\rho_1 v_1 S_1 = \rho_2 v_2 S_2 = \text{const}. \tag{2.31}$$

A fluid is called incompressible if the density of any particle within that fluid is a constant value, i. e., if $\frac{d\rho}{dt} = 0$. Eq. (2.25) for incompressible fluid is: $div\bar{v} = 0$. If $div\bar{v} = 0$, and as $div\bar{v} = \frac{\partial v_i}{\partial x_i}$, this condition is valid for $\bar{v} = \bar{v}(x_j)$ as well as for $\bar{v} = \bar{v}(x_j, t)$.

Then, under the Gauss–Ostrogradsky theorem:

$$\int_V div\bar{v} dV = \int_S v_n dS = 0. \tag{2.32}$$

Repeating the procedure similar to the previous one, from Eq. (2.32) the equation for the flow-tube of an incompressible fluid is:

$$\int_{S_1} v dS = \int_{S_2} v dS = Q(t). \tag{2.33}$$

The $Q = \int_S vdS$ value is the fluid volume running through the effective cross-section per unit time or so-called *throughflow*. Therefore, Eq. (2.33) demonstrates that when an incompressible fluid is flowing through the tube, the throughflow in all of its effective cross-sections at any time is constant whether the flow is transient-free or not.

In the case of an elementary flow-tube, Eq. (2.33) follows:

$$V_1 S_1 = v_2 S_2, \tag{2.34}$$

which shows that the smaller the effective cross-section area, the greater the flow velocity, and *vice versa*.

4. Motion equation under stress

The formulation of the momentum law Eq. (2.10) includes the $\rho\bar{v}$ value, which is the momentum of a unit volume, and the surface force stress $\bar{p}_n$. Thus, to derive the motion equations expressed in stresses, by taking $\varphi = \rho\bar{v}$ in Eq. (2.23):

$$\begin{aligned} \frac{d}{dt}\int_V \rho\bar{v}dV &= \int_V \left(\frac{d(\rho\bar{v})}{dt} + \rho\bar{v}div\bar{v} \right) dV = \\ &= \int_V \left(\frac{d\bar{v}}{dt} + \bar{v}\left(\frac{dt}{dt} + \rho div\bar{v} \right) \right) dV = \int_V \rho \frac{dv}{dt} V \end{aligned} \tag{2.35}$$

According to the continuity Eq. (2.25), the expression in parentheses is equal to zero. Substituting Eq. (2.35) into the momentum law Eq. (2.10):

$$\int_V \rho \frac{d\bar{v}}{dt} dV = \int_V \rho \bar{F} dV + \int_S \bar{p}_n dS, \tag{2.36}$$

where from Eq. (1.29)

$$\bar{\rho}_n = \bar{p}_i \alpha_{ni}. \tag{2.37}$$

Assuming $a_2 = a_3 = 0$ in the Gauss–Ostrogradsky theorem Eq. (2.21):

$$\int_S a_1 \alpha_{n1} dS = \int_V \frac{\partial a_1}{\partial x_1} dV. \tag{2.38}$$

Similarly, for the components a_2 and a_3:

$$\int_S \bar{a}\ \alpha_{n1} dS = \int_V \frac{\partial \bar{a}}{\partial x_1} dV. \tag{2.39}$$

It follows from Eqs. (2.37) and (2.39) that

$$\int_S \bar{p}_n dS = \int_S \bar{p}_i \alpha_{n1} dS = \int_V \frac{\partial \bar{p}_i}{\partial x_1} dV. \tag{2.40}$$

Substituting Eqs. (2.40) into (2.36):

$$\int_V \left(\rho \frac{d\bar{v}}{dt} - \rho F - \frac{\partial \bar{p}_i}{\partial x_i} \right) dV = 0, \tag{2.41}$$

Eq. (2.41) is applicable for all kinds of material volumes. The expression under integral is equal to zero, i. e.:

$$\rho \frac{d\bar{v}}{dt} = \rho \bar{F} + \frac{\partial \bar{p}_i}{\partial x_i}, \tag{2.42}$$

or in coordinate format:

$$\rho \frac{dv_j}{dt} = \rho F_j + \frac{\partial p_{ij}}{\partial x_i}. \tag{2.43}$$

Eqs. (2.42) and (2.43) are called equations of motion of a continuous medium and expresses the law of kinetic momentum (or the law of variation of momentum).

The law of kinetic momentum for a flow-tube can be derived from Eqs. (2.10) and (2.20) and by taking $\varphi = \bar{\rho}\bar{v}$. as follows:

$$\int_V \frac{\partial(\bar{\rho}\bar{v})}{\partial t} dV + \int_S \bar{\rho}\bar{v}\bar{v}_n dS = \int_V \rho \bar{F} dV + \int_S \bar{p}_n dS. \tag{2.44}$$

Eq. (2.44) is the integral form of the kinetic momentum law.

Consider a closed surface S composed of effective cross-sections of the flow-tube S_1 and S_2 and its side surface S_3 (Fig. 2.4). Repeating the procedure followed to the derivation of Eqs. (2.28) and (2.29), one can obtain from Eq. (2.44):

$$\int_V \frac{\partial(\bar{\rho}\bar{v})}{\partial t} dV - \int_{S_1} \bar{\rho}\bar{v}\bar{v} dS + \int_{S_2} \bar{\rho}\bar{v}\bar{v} dS = \int_V \rho \bar{F} dV + \int_S \bar{p}_n dS. \tag{2.45}$$

Calling G the mass force acting on the identified volume V of the flow-tube:

$$\int_V \rho \bar{F} dV = \bar{G}, \tag{2.46}$$

and $\bar{P}$, results of the surface forces acting from the fluid in the S_1 and S_2 sections:

$$\int_{S_1+S_2} \bar{p}_n dS = \bar{P}. \tag{2.47}$$

By using factorization presented in Eq. (1.26) forces acting on surface S_3 can be determined (the S_3 surface may, in particular, be a solid wall). Assigning

$$\bar{N} = \int_{S_3} n \bar{p}_{nn} dS, \; \bar{T} = \int_{S_3} \bar{\tau} p_{n\tau} dS, \tag{2.48}$$

where $\overline{N}$ is resultant of the normal forces, and $\overline{T}$ is resultant of the tangential forces applied to surface S_3.

Substituting Eqs. (2.46), (2.47) and (2.48) into Eq. (2.45) results in the mathematical expression for the momentum law for a flow-tube:

$$\int_V \frac{\partial(\rho\bar{v})}{\partial t} dV + \int_{S_2} \rho\bar{v}\bar{v}dS - \int_{S_1} \rho\bar{v}\bar{v}dS = \overline{G} + \overline{P} + \overline{N} + \overline{T}. \tag{2.49}$$

For the transient-free motion, $\frac{\partial(\rho\bar{v})}{\partial t} = 0$, and Eq. (2.49) reduces to:

$$\int_{S_2} \rho\bar{v}\bar{v}dS - \int_{S_1} \rho\bar{v}\bar{v}dS = \overline{G} + \overline{P} + \overline{N} + \overline{T}. \tag{2.50}$$

Using the mean value theorem in the integral calculus:

$$\int_S \rho\bar{v}\bar{v}dS = \bar{v}^{(mean)} \int_S \rho v dS = \bar{v}^{(mean)} Q_m,$$

where $\bar{v}^{(mean)}$ is mean integral value of the velocity vector in cross-section S. Because in the transient-free motion $Q_m = \text{const}$, Eq. (2.50) may be rewritten as follows:

$$Q_m(\bar{v}_2^{(mean)} - \bar{v}_1^{(mean)}) = \overline{G} + \overline{P} + \overline{N} + \overline{T}, \tag{2.51}$$

where $\bar{v}_1^{(mean)}$ and $\bar{v}_2^{(mean)}$ are flow velocity mean values, respectively, in cross-sections S_1 and S_2. Keep in mind that expressions (2.44), (2.45), (2.49), (2.50) and (2.51) are vector equations, so the variation of momentum may occur at a change in the velocity value as well as its direction.

Eq. (2.51) is convenient for the solution of a number of practical problems (examples will be provided in Chapter VII).

5. Law of variation of kinetic momentum. Law of pairing of tangential stresses

Eq. (2.11), the law of kinetic momentum, includes the term $\bar{r} * \rho\bar{v}$. Substituting the expression $\varphi = \bar{r} * \rho\bar{v}$ into the Eq. (2.23):

$$\begin{aligned}
\frac{d}{dt}\int(\bar{r} * \rho\bar{v})dV &= \int_{V(t)} \left[\frac{d}{dt}(\bar{r} * \rho\bar{v}) + (\bar{r} * \rho\bar{v})div\bar{v}\right] dV = \\
&= \int_V \left[\frac{d\bar{r}}{dt} * \rho\bar{v} + \bar{r} * \bar{v}\frac{d\rho}{dt} + \bar{r} * \rho\frac{d\bar{v}}{dt} + (\bar{r} * \rho\bar{v})div\bar{v}\right] dV = \\
&= \int_V \left[\frac{d\bar{r}}{dt} * \rho\bar{v} + (\bar{r} * \bar{v})\left(\frac{d\rho}{dt} + \rho div\bar{v}\right) + \bar{r} * \rho\frac{d\bar{v}}{dt}\right] dV.
\end{aligned} \tag{2.52}$$

Using the continuity Eq. (2.25) and taking into account that $\frac{d\bar{r}}{dt} = \bar{v}$ and consequently $\frac{d\bar{r}}{dt} * \rho\bar{v} = 0$, Eq. (2.52) may be transformed into:

$$\frac{d}{dt}\int_V (\bar{r} \times \rho\bar{v}) dV = \int_V \bar{r} * \rho \frac{d\bar{v}}{dt} dV . \tag{2.53}$$

It follows from Eqs. (2.37) and (2.39) that:

$$\int_S \bar{r} * \bar{p}_n dS = \int_S \bar{r} \times \bar{p}_i \alpha_{ni}) dS = \int_V \frac{\partial(\bar{r} * \bar{p}_i)}{\partial x_i} dV . \tag{2.54}$$

Substituting Eqs. (2.53) and (2.54) into Eq. (2.11):

$$\int_V \left[\bar{r} * \rho \frac{d\bar{v}}{dt} - \bar{r} * \rho\bar{F} - \frac{\partial(\bar{r} * \bar{p}_i)}{\partial x_i} dV \right] = 0 , \tag{2.55}$$

Because Eq. (2.53) is true for any arbitrary volume, the under-integral expression must be equal to zero, i. e.:

$$\bar{r} * \rho \frac{d\bar{v}}{dt} = \bar{r} * \rho\bar{F} + \frac{\partial(\bar{r} * \bar{p}_i)}{\partial x_i} . \tag{2.56}$$

Eq. (2.56) represents the law of the kinetic momentum. This law has one important implication discussed below.

First, multiply the motion vector Eq. (2.42) by the radius-vector $\bar{r}$:

$$\bar{r} * \rho \frac{d\bar{v}}{dt} = \bar{r} * \rho\bar{F} + \bar{r} * \frac{\partial \bar{p}_i}{\partial x_i} . \tag{2.57}$$

Then subtract Eq. (2.57) from Eq. (2.56):

$$\frac{\partial(\bar{r} * \bar{p}_i)}{\partial x_i} - \bar{r} * \frac{\partial \bar{p}_i}{\partial x_i} = \frac{\partial \bar{r}}{\partial x_i} * \bar{p}_i = 0 . \tag{2.58}$$

As $\bar{r} = \bar{e}_i x_i$, and $\frac{\partial \bar{r}}{\partial x_i} = \bar{e}$, then Eq. (2.58) may be rewritten as follows:

$$\bar{e}_i * \bar{p}_i = 0 . \tag{2.59}$$

Using a known vector equation:

$$\bar{a} * \bar{b} = \begin{vmatrix} \bar{e}_1 & \bar{e}_2 & \bar{e}_3 \\ a_1 & a_2 & a_3 \\ b_1 & b_2 & b_3 \end{vmatrix} ,$$

where a_1 and b_1 are projections of vectors $\bar{a}$ and $\bar{b}$ onto coordinate axes. From Eq. (2.59):

$$\bar{e}_i * \bar{p}_i = \begin{vmatrix} \bar{e}_1 & \bar{e}_2 & \bar{e}_3 \\ 1 & 0 & 0 \\ p_{11} & p_{12} & p_{13} \end{vmatrix} + \begin{vmatrix} \bar{e}_1 & \bar{e}_2 & \bar{e}_3 \\ 0 & 1 & 0 \\ p_{21} & p_{22} & p_{23} \end{vmatrix} + \begin{vmatrix} \bar{e}_1 & \bar{e}_2 & \bar{e}_3 \\ 0 & 0 & 1 \\ p_{31} & p_{32} & p_{33} \end{vmatrix} =$$

$$= e_1(p_{23} - p_{32}) + e_2(p_{31} - p_{13}) + e_3(p_{12} - p_{21}) = 0,$$

and from this:

$$p_{12} = p_{21},\ p_{31} = p_{13}, p_{23} = p_{32} \text{ or } p_{ik} = p_{ki}. \tag{2.60}$$

The Eq. (2.60) represents the law of pairing or reciprocity of tangential stresses. It follows from this law that the stress tensor Eq. (1.33) is symmetric meaning the stress tensor contains only six different components. Thus, the number of variables in the Eq. (2.43) decreases.

6. The law of conservation of energy

The law of conservation of energy was shown previously in Eq. (2.13). To transform this equation, it is assumed $\varphi = \rho\left(u + \frac{v^2}{2}\right)$ in Eq. (2.23). Then:

$$\frac{d}{dt}\int_V \rho(u+\frac{v^2}{2})dV = \int_V \left[\frac{d}{dt}\rho(u+\frac{v^2}{2})dV + \rho(u+\frac{v^2}{2})div\bar{v}\right]dV =$$
$$= \int_V \left[\rho\frac{d}{dt}(u+\frac{v^2}{2}) + (u+\frac{v^2}{2})(\frac{d\rho}{dt} + \rho div\bar{v})\right]dV. \tag{2.61}$$

Taking the continuity equation Eq. (2.25) into account, Eq. (2.61) changes into the following format:

$$\frac{d}{dt}\int_V \rho(u+\frac{v^2}{2})dV = \int_V \rho\frac{d}{dt}(u+\frac{v^2}{2})dV. \tag{2.62}$$

It follows from Eq. (2.37) and the Gauss–Ostrogradsky theorem Eq. (2.39) that:

$$\int_S \bar{p}_n \bar{v} dS = \int_S \bar{p}_i \bar{v}\alpha_{ni} dS = \int_V \frac{\partial(\bar{p}_i \bar{v})}{\partial x_i} dV. \tag{2.63}$$

By substituting Eqs. (2.62) and (2.63) into Eq. (2.13):

$$\int_V \left[\rho\frac{d}{dt}(u+\frac{v^2}{2}) - \rho\bar{F}\bar{v} - \frac{\partial(\bar{p}_i \bar{v})}{\partial x_i} - \rho q_e\right]dV = 0. \tag{2.64}$$

Because this equation is valid for an arbitrary volume, the under-integral expression must be equal to zero:

$$\rho\frac{d}{dt}(u+\frac{v^2}{2})=\rho\bar{F}\bar{v}+\frac{\partial(\bar{p}_i\bar{v})}{\partial x_i}+\rho q_e. \tag{2.65}$$

Eq. (2.65) is a mathematical expression of the law of energy conservation for the thermo-mechanical continuum. It shows that the change of total energy is equal to the sum of all external forces and the amount of heat supplied per unit time. Remember that Eq. (2.65) includes *per unit volume* values.

Now it is desired to derive the law of energy conservation for the flow-tube. Assuming $\varphi=\rho(u+\frac{v^2}{2})$ in Eq. (2.20) and substituting into Eq. (2.13):

$$\int_V\frac{\partial}{\partial t}\rho(u+\frac{v^2}{2})dV+\int_S\rho(u+\frac{v^2}{2})v_n dS=\int_V\rho\bar{F}\bar{v}dV+\int_S\bar{p}_n\bar{v}dS+\int_V\rho q_e dV. \tag{2.66}$$

It is assumed that the stress of the internal force has potential, i. e., $\bar{F}=\nabla\Pi$. Then, by taking the continuity equation Eq. (2.26) into account:

$$\rho\bar{F}\bar{v}=\rho\bar{v}\nabla\Pi=div\rho\Pi\bar{v}-\Pi div\rho\bar{v}=div\rho\Pi\bar{v}+\Pi\frac{\partial\rho}{\partial t},$$

And, based on the Gauss–Ostrogradsky theorem Eq. (2.21):

$$\int_V\rho\bar{F}\bar{v}dV=\int_V\left(div\rho\Pi\bar{v}+\Pi\frac{\partial\rho}{\partial t}\right)dV=\int_V\Pi\frac{\partial\rho}{\partial t}dV+\int_S\rho\Pi v_n dS. \tag{2.67}$$

Consider a closed surface, the surface composed of the flow-tube effective cross-sections S_1 and S_2 and its side surface S_3 (Fig. 2.4). In the effective cross-section S_1, $\bar{v}=-\bar{n}v$, in S_2, $\bar{v}=-\bar{n}v$, and on the side surface S_3, $\bar{v}=\bar{\tau}_1 v$ where $\bar{\tau}_1$ is a singular vector positioned on the plane tangential to the flow-tube. Then, taking Eq. (1.26) into account:

$$\int_S\bar{p}_n\bar{v}dS=-\int_{S_1}p_{nn}vdS+\int_{S_2}p_{nn}vdS+\int_{S_3}\bar{p}_n vdS. \tag{2.68}$$

Now by substituting Eqs. (2.67) and (2.68) into Eq. (2.66) and repeating the same procedure used for the derivation of Eqs. (2.26) and (2.27), one obtains:

$$\begin{aligned}\int_V\left[\frac{\partial}{\partial t}\rho(u+\frac{v^2}{2})-\Pi\frac{\partial\rho}{\partial t}\right]dV+\int_{S_2}\rho(u+\frac{v^2}{2})v\,dS-\int_{S_1}\rho(u+\frac{v^2}{2})v\,dS=\\ =\int_{S_2}(\Pi\rho+p_{nn})vdS-\int_{S_1}(\Pi\rho+p_{nn})vdS+\int_{S_3}\bar{p}_n\bar{\tau}_1 vdS+\int_V pq_e dV.\end{aligned} \tag{2.69}$$

Eq. (2.69) is an expression of the energy conservation law for the flow-tube in the presence of the mass force stress potential. In the case of a transient-free motion:

$$\int_{S_2}\rho(u+\frac{v^2}{2})\rho v\, dS-\int_{S_1}\rho(u+\frac{v^2}{2})\rho v\, dS= \\ =\int_{S_2}(\Pi+\frac{p_{nn}}{\rho})\rho v dS-\int_{S_1}(\Pi+\frac{p_{nn}}{\rho})\rho v dS+\int_{S_3}p_n\,\beta\tau_1 v dS+\int_V\rho q_e dV. \tag{2.70}$$

Using the mean value theorem:

$$\int_S(u+\frac{v^2}{2})\rho v\, dS=(u+\frac{v^2}{2})^{mean}\int_S\rho v\, dS=(u+\frac{v^2}{2})^{mean}Q_m,$$

$$\int_S(\Pi+\frac{p_{nn}}{\rho})\rho v dS=(\Pi+\frac{p_{nn}}{\rho})^{mean}\int_S\rho v dS=(\Pi+\frac{p_{nn}}{\rho})^{mean}Q_m,$$

and because in the transient-free motion in the flow-tube $Q_m=\text{const}$, Eq. (2.70) may be rewritten as follows:

$$(u+\frac{v^2}{2})^{mean}_{\ 2}-(u+\frac{v^2}{2})^{mean}_{\ 1}=(\Pi+\frac{p_{nn}}{\rho})^{mean}_{\ 2}- \\ -(\Pi+\frac{p_{nn}}{\rho})^{mean}_{\ 1}+\frac{1}{Q_m}\int_{S_3}\bar{p}_n\bar{\tau}_1 v dS+\frac{1}{Q_m}\int_V\rho q_e dV, \tag{2.71}$$

where subscripts "1" and "2" denote the corresponding cross-sections.

7. Teorem of variation of kinetic energy

In order to develop mathematical expression of the kinetic energy theorem, it should be denoted $\varphi=\rho\frac{v^2}{2}$ in Eq. (2.23). Then, by considering the continuity equation Eq. (2.25):

$$\frac{d}{dt}\int_V\rho\frac{v^2}{2}dV=\int_V\left[\frac{d}{dt}(\rho\frac{v^2}{2})+\rho\frac{v^2}{2}div\bar{v}\right]dV= \\ =\int_V\left[\rho\frac{d}{dt}\frac{v^2}{2}+\frac{v^2}{2}(\frac{d\rho}{dt}+\rho div\bar{v})\right]dV=\int_V\rho\frac{d}{dt}(\frac{v^2}{2})dV \tag{2.72}$$

Substituting Eqs. (2.63) and (2.72) into Eq. (2.14):

$$\int_V\left[\rho\frac{d}{dt}\frac{v^2}{2}-\rho\bar{F}\bar{v})-\frac{\partial(\bar{p}_i\bar{v})}{\partial x_i}-\rho N^{(i)}\right]dV, \tag{2.73}$$

And because this equation is valid for an arbitrary volume, then:

$$\rho\frac{d}{dt}\frac{v^2}{2}=\rho\overline{F}\overline{v}+\frac{\partial(\overline{p}_i\overline{v})}{\partial x_i}+\rho N^{(i)}. \tag{2.74}$$

It follows from Eq. (2.74), i. e., from the theorem of forces for the continuous medium, that the rate of kinetic energy variation is equal to the sum of all external and *internal* forces. Both Eqs. (2.74) and (2.75) deal with per-unit volume values.

In order to obtain the force theorem for the flow-tube, it is assumed $\varphi=\rho\frac{v^2}{2}$ in Eq. (2.20). Then by using Eq. (2.14):

$$\int_V\frac{\partial}{\partial t}\left(\frac{\rho v^2}{2}\right)dV+\int_S\frac{\rho v^2}{2}v_n dS=\int_V\rho\overline{F}\overline{v}dV+\int_S\overline{p}_n\overline{v}dS+\int_V\rho N^{(i)}dV, \tag{2.75}$$

which represents the integral format of the theorem of kinetic energy variation.

Consider a closed surface S, the surface limited by the effective cross-sections S_1 and S_2 of a flow-tube and its side surface S_3 (Fig. 2.3). It is also assumed that the mass force stress has potential, i. e., $\overline{F}=\nabla\Pi$. Following the procedure similar the one used to derive Eq. (2.69) and using Eqs. (2.67) and (2.68), one can obtain from Eq. (2.75):

$$\begin{aligned}&\int_{S_2}\left[\frac{\partial}{\partial t}\left(\frac{\rho v^2}{2}\right)-\Pi\frac{\partial\rho}{\rho t}\right]dV+\int_{S_2}\frac{v^2}{2}\rho vdS-\int_{S_1}\frac{v^2}{2}\rho vdS=\\&=\int_{S_2}\left(\Pi+\frac{p_{nn}}{\rho}\right)\rho vdS-\int_{S_1}\left(\Pi+\frac{p_{nn}}{\rho}\right)\rho vdS+\int_{S_3}\overline{p}_n\overline{\tau}_1 vdS+\int_V\rho N^{(i)}dV,\end{aligned} \tag{2.76}$$

which represents an expression of the kinetic energy theorem for the flow-tube with the presence of potential of the mass forces.

At transient-free motion, Eq. (2.76) takes the following format:

$$\begin{aligned}&\int_{S_2}\left(-\Pi-\frac{p_{nn}}{\rho}+\frac{v^2}{2}\right)\rho vdS-\int_{S_1}\left(-\Pi-\frac{p_{nn}}{\rho}+\frac{v^2}{2}\right)\rho vdS=\\&=\frac{1}{Q_m}\int_{S_3}\overline{p}_n\overline{\tau}_1 vdS+\frac{1}{Q_m}\int_V\rho N^{(i)}dV\end{aligned} \tag{2.77}$$

or

$$\begin{aligned}&\left(-\Pi-\frac{p_{nn}}{\rho}+\frac{v^2}{2}\right)_2^{mean}-\left(-\Pi-\frac{p_{nn}}{\rho}+\frac{v^2}{2}\right)_1^{mean}=\\&=\frac{1}{Q_m}\int_{S_3}\overline{p}_n\overline{\tau}_1 vdS+\frac{1}{Q_m}\int_V\rho N^{(i)}dV,\end{aligned} \tag{2.78}$$

where the averaging over cross-sections S_1 and S_2 has the same implication as in Eq. (2.71).

In order to compute the internal force magnitude per-unit, $N^{(i)}$, consider Eq. (2.68). After a scalar (non-vectorial) multiplication of the motion equation in stresses Eq. (2.42) by the velocity vector $\bar{v}$:

$$\rho\bar{v}\frac{d\bar{v}}{dt} = \rho\frac{d}{dt}(\frac{v^2}{2}) = \rho\bar{F}\bar{v} + v\frac{\partial\bar{p}_i}{\partial x_i}. \tag{2.79}$$

Subtracting Eq. (2.79) from Eq. (2.78) term-by-term:

$$\frac{\partial\bar{p}_i\bar{v}}{\partial x_i} + \rho N^{(i)} - v\frac{\partial\bar{p}_i}{\partial x_i} = p_i\frac{\partial\bar{v}}{\partial x_i} + \rho N^{(i)} = 0.$$

But, as $\bar{p}_i = \bar{e}_j p_{ij}$, and $v = \bar{e}_k v_k$:

$$\rho N^{(i)} = -p_i\frac{\partial\bar{v}}{\partial x_i} = -e_j p_{ij}\frac{\partial\bar{e}_k v_k}{\partial x_i} = -p_{ik}\frac{\partial v_k}{\partial x_i}. \tag{2.80}$$

It follows from Eq. (2.80) that, if all points of the continuous volume under consideration move at the same velocity, i. e., if $v_k = v_k(x_j,t)$, the $N^{(i)} = 0$. Therefore, the work of the internal forces may be different from zero only in a spatially non-uniform velocity field where $\frac{\partial v_k}{\partial x_i} \neq 0$.

8. Heat flow equation

In order to obtain an equation describing variation in the internal energy, subtract, Eq. (2.74) from the equation of the total energy conservation law (Eq. 2.65) term-by-term results in:

$$\frac{du}{dt} = q_e - N^{(i)}. \tag{2.81}$$

Eq. (2.81) includes internal energy u per-unit mass, heat input q_e, internal forces $N^{(i)}$ and is called *heat flow equation*. It shows that under the adiabatic process, i. e., if $q_e = 0$, changes of the internal energy can occur only at the expense of work of the internal forces.

Using Eq. (2.80), this equation may be rewritten as follows:

$$\frac{du}{dt} = q_e + \frac{p_{ik}}{\rho}\frac{\partial v_i}{\partial x_k}. \tag{2.82}$$

Eq. (2.82) implies that in the uniform velocity field (i. e., at $v_i = v_i(t)$) changes in the internal energy are determined only by the external heat supply.

Note that the heat flow equation like the kinetic energy variation theorem is not an independent equation but is a consequence of the main conservation laws.

Examples of the heat flow equation applications are reviewed in Chapter IV.

9. Continuous medium motion equations

The continuous medium motions as defined by the fundamental physical laws of mass conservation, kinetic momentum conservation, energy conservation are described by a system of equations comprised of Eqs. (2.25), (2.42) and (2.65):

$$\frac{\partial \rho}{\partial t} + \rho div \bar{v} = 0$$

$$\rho \frac{d\bar{v}}{dt} = \rho \bar{F} + \frac{\partial \bar{p}_i}{\partial x_i} \tag{2.83}$$

$$\rho \frac{d}{dt}(u + \frac{v^2}{2}) = \rho \bar{F}\bar{v} + \frac{\partial(\bar{p}_i \bar{v})}{\partial x_i} + \rho q_e .$$

Therefore, the system of equations describing the motion of any continuous medium consists of one vector and two scalar equations, or of five scalar equations. In a general case, the system Eq. (2.83) includes 11 scalar variables[1]: v_i, p_{ij}, ρ, u. Therefore, it is not closed. This circumstance implicates the fact that the conservation laws do not include any parameters describing the properties of specific continuous media. As a result, the derived equations need to be supplemented by the corresponding interrelations (connections), assigning physical properties of a specific continuous medium. It should be noticed that for different continuous media (such as fluids, elastic bodies, plastic bodies, etc.) these connections are different, and the resulting, now closed, systems of equations for different continuous media are also different.

The establishment of connections necessary for specific media requires a preliminary study of the continuous medium deformations or deformation rates.

The relation between stresses and deformations or between stresses and deformation rates are called *rheologic equations*. Thus, different rheologic equations correspond to different continuous media.

It is important to note that in this Chapter it is assumed that there is a postulate in the classical mechanics of continua under which the main conservation laws are considered valid not only for the entire body under consideration (in our case, a material volume) but for any section of a body. This postulate is called the principle of locality, and the differential equations – results of the integral laws of conservation, are called local formulations of the conservation laws.

It is also important that, if the coordinate system, in which the continuous medium motion is considered, is moving then all equations in this coordinate system preserve their format; however, the mass forces also include the inertia forces appearing in the relative motion.

[1] The stress of mass forces $\bar{F}$ and heat input q_e are exeternal actions and are considered given.

CHAPTER III

CONTINUOUS MEDIUM DEFORMATION RATE

1. Small particle deformation rate. Helmholtz theorem

Let's review a small particle in the continuous medium as shown in Fig. 3.1. Here, point O is the particle's center with the spatial coordinates x_j, point O' is any point within the particle, vector $\bar{R}(\xi_j) = \overline{OO'}$ is totally enclosed within the particle.

The rate distribution within the particle at a given moment in time t_1 is determined by the rate (velocity) field, i. e., velocity values of points O and O', correspondingly, $\bar{v}_o = \bar{v}(x_i, t_1)$ and $\bar{v}' = \bar{v}(x_j + \xi_j, t_1)$, or $\bar{v}_{oi} = \bar{v}_i(x_j, t_1)$, $\bar{v}'_i = \bar{v}(x_j + \xi_j, t_1)$. The motion within the particle is assumed to be continuous and differentiable.

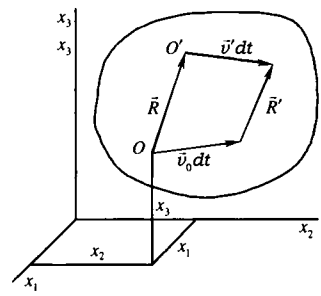

Fig. 3.1

Expanding v'_i by Taylor's series polynomials:

$$v'_i = v_{oi} + \xi_j \frac{\partial v_i}{\partial x_j} + ... = v_i + \bar{R}\nabla v_i + ..., \tag{3.1}$$

where all derivative are taken at point 0. The particle is assumed to be small, i. e., ξ are assumed to be small compared with the linear module in the problem under review. Hence, truncating Eq. (3.1) only to the terms of first-order gives:

$$v'_i = v_{oi} + \xi_j \frac{\partial v_i}{\partial x_j} = v_{oi} + \bar{R}\nabla v_i \tag{3.2}$$

or

$$\bar{v}' = \bar{v}_o + (\bar{R}\nabla)\bar{v} = \bar{v}_o + \Phi\bar{R}. \tag{3.3}$$

Eqs. (3.2) and (3.3) show that the velocity difference $\bar{v}' - \bar{v}_o$ is defined by the matrix:

$$\Phi = \begin{pmatrix} \frac{\partial v_1}{\partial x_1} & \frac{\partial v_1}{\partial x_2} & \frac{\partial v_1}{\partial x_3} \\ \frac{\partial v_2}{\partial x_1} & \frac{\partial v_2}{\partial x_2} & \frac{\partial v_2}{\partial x_3} \\ \frac{\partial v_3}{\partial x_1} & \frac{\partial v_3}{\partial x_2} & \frac{\partial v_3}{\partial x_3} \end{pmatrix}, \tag{3.4}$$

whose elements are multipliers for the terms of first order in the expanding v'_i with the Taylor's series.

Matrix Φ can be represented as the sum of two matrices, one symmetric and another one, asymmetric:

$$\begin{aligned} \varepsilon_{ik} &= \left(\frac{\partial v_1}{\partial x_k} + \frac{\partial v_k}{\partial x_1} \right), \omega_1 = \left(\frac{\partial v_3}{\partial x_2} - \frac{\partial v_2}{\partial x_3} \right) \\ \omega_2 &= \left(\frac{\partial v_1}{\partial x_3} - \frac{\partial v_3}{\partial x_2} \right), \omega_3 = \left(\frac{\partial v_2}{\partial x_1} - \frac{\partial v_1}{\partial x_2} \right) \end{aligned} \tag{3.5}$$

Rearranging the matrix Eq. (3.4) similar to Eq. (3.5):

$$\Phi = \begin{pmatrix} \varepsilon_{11} & \varepsilon_{12} & \varepsilon_{13} \\ \varepsilon_{21} & \varepsilon_{22} & \varepsilon_{23} \\ \varepsilon_{31} & \varepsilon_{32} & \varepsilon_{33} \end{pmatrix} + \begin{pmatrix} 0 & -\omega_3 & \omega_2 \\ \omega_3 & 0 & -\omega_1 \\ -\omega_2 & \omega_1 & 0 \end{pmatrix} = D + \Omega . \tag{3.6}$$

It can be seen from Eq. (3.5) that $\varepsilon_{ik} = \varepsilon_{ki}$.

Substituting Eq. (3.6) into Eq. (3.3):

$$\bar{v}' = \bar{v}_o + D\bar{R} + \Omega\bar{R}_o . \tag{3.7}$$

Rewriting Eq. (3.7) in the coordinate form:

$$\begin{aligned} v'_1 &= v_{o1} + \varepsilon_{11}\xi_1 + \varepsilon_{12}\xi_2 + \varepsilon_{13}\xi_3 - \omega_3\xi_2 + \omega_2\xi_3 , \\ v'_2 &= v_{o2} + \varepsilon_{21}\xi_1 + \varepsilon_{22}\xi_2 + \varepsilon_{23}\xi_3 - \omega_3\xi_1 + \omega_1\xi_3 , \\ v'_3 &= v_{o3} + \varepsilon_{31}\xi_1 + \varepsilon_{32}\xi_2 + \varepsilon_{33}\xi_3 - \omega_2\xi_1 + \omega_1\xi_2 . \end{aligned} \tag{3.8}$$

It follows from Eq. (3.5) that ω_k values are components of vector $\bar{\omega} = \bar{e}_k\omega_k$ which may be written symbolically as:

$$\bar{\omega} = \frac{1}{2} \begin{vmatrix} \bar{e}_1 & \bar{e}_2 & \bar{e}_3 \\ \frac{\partial}{\partial x_1} & \frac{\partial}{\partial x_2} & \frac{\partial}{\partial x_3} \\ v_1 & v_2 & v_3 \end{vmatrix} = \frac{1}{2} rot\bar{v} . \tag{3.9}$$

Vector $\bar{\omega}$ is called velocity rotor.[1]

Introducing a quadratic function:

$$F = \frac{1}{2}\varepsilon_{ik}\xi_i\xi_k, \tag{3.10}$$

Because $\varepsilon_{ik} = \varepsilon_{ki}$, it follows from Eq. (3.10):

$$\frac{\partial F}{\partial \xi_i} = \frac{1}{2}\varepsilon_{ik}\xi_k. \tag{3.11}$$

Using Eqs. (3.9) and (3.11), Eq. (3.8) may be rewritten as:

$$v'_i = v_{oi} + \frac{\partial F}{\partial \xi_i} + (\bar{\omega} * \bar{R})_i$$

or

$$\bar{v}' = \bar{v}_o + (\bar{\omega} * \bar{R})_i + \nabla F. \tag{3.12}$$

If the small particle under consideration was perfectly rigid, then, from the theoretical mechanics postulate, the velocity distribution within it would have been:

$$\bar{v} = \bar{v}_o + \bar{\omega}\bar{R}, \tag{3.13}$$

where $\bar{v}_o$ is velocity of progressive advance, and $\bar{\omega}$ is vector of instantaneous angular velocity. Therefore, it follows from Eqs. (3.12) and (3.13) that $\nabla F = v' - v$, i. e., the ∇F is the deformation velocity.

Comment: the population of points O_1 surrounding the point O forms a fluid particle. Over the time dt, the point O experiences a displacement of $\bar{v}_o dt$, and the point O_1, a displacement of $\bar{v}'_o dt$. Fig. 3.1 shows that $\bar{R} + \bar{v}'dt = \bar{R}' + \bar{v}_o dt$ or, taking Eq. (3.12) into account:

$$d\bar{R} = \bar{R}' - \bar{R} = (\bar{v}' - \bar{v}_o)dt = (\bar{\omega} \times \bar{R} + \nabla F)dt. \tag{3.14}$$

Assuming $\bar{R}' = \bar{e}_k \xi'_k$, combining Eqs. (3.3) and (3.14):

$$\bar{R}' = \bar{e}_k \xi'_k = \bar{R} = (\bar{v}' - \bar{v}_o)dt = \bar{R} + (\bar{R}\nabla F)\bar{v}dt.$$

Or, in the coordinate format:

$$\xi'_i = \xi_i + \xi_k \frac{\partial v_i}{\partial x_k} dt. \tag{3.15}$$

Eqs. (3.15) can be considered as the fluid particle coordinate transformation during the dt time interval. Because the $\frac{\partial v_i}{\partial x_k}$ values, as indicated earlier, are com-

[1] Some authors recognize $\overline{rot\bar{v}} = 2\bar{\omega}$ as velocity rotor.

puted at point 0 they are independent of ξ_k, and the transformation (3.15) is linear. Thus, during the *dt* time interval this transformation transforms the second order surfaces into second order surfaces, planes into planes, and straight lines into straight lines. For instance, a sphere is transformed into an ellipsoid.

Let's recall:

$$dR = R' - R(dR \neq d\bar{R}), \quad \varepsilon_R = \frac{dR}{Rdt}, \tag{3.16}$$

where ε_R is *relative extension* of vector $\bar{R}$ per unit time. It follows from Eqs. (3.10), (3.11), (3.14) and (3.16) that:

$$\varepsilon_R = \frac{dR}{Rdt} = \frac{\bar{R}d\bar{R}}{R^2 dt} = \frac{\vec{R}(\omega * R * \nabla F)}{R^2} = \frac{\vec{R}\nabla F}{R^2} = \frac{\varepsilon_{ik}\xi_i\xi_k}{R^2} = \frac{2F}{R^2}. \tag{3.17}$$

Because $\frac{\xi_i}{R} = \alpha_i$ are the directing cosine of vector $\bar{R}$:

$$\varepsilon_R = \frac{\varepsilon_{ik}\,{}_i\xi_k}{R^2} = \varepsilon_{ik}\alpha_i\alpha_k = 2F(\alpha_j), \tag{3.18}$$

and the relative extension ε_R does not depend on the length of vector $\bar{R}$ but only on its direction.

Assuming that $\varepsilon_R = 0$, then it follows from Eq. (3.17) that :

$$\varepsilon_R = \frac{\bar{R}}{R^2}\nabla F = \frac{\bar{R}^o}{R}\nabla F = 0, \tag{3.19}$$

where $\bar{R}^o = \frac{\bar{R}}{R} = \frac{1}{R}e_k\xi_k$ is the singular direction vector $\bar{R}$. As Eq. (3.19) is valid for any $\bar{R}^o$ (taking Eq. (3.11) in consideration):

$$\nabla F = \bar{e}_i\frac{\partial F}{\partial \xi_i} = \bar{e}_i\varepsilon_{ik}\xi_k = 0,$$

Therefore, $\varepsilon_{ik}\xi_k = 0$ and, as ξ_k are arbitrary, $\varepsilon_{ik} = 0$. The inverse statement is: if all $\varepsilon_{ik} = 0$ then $\varepsilon_\rho = 0$, and the particle behaves as it is perfectly rigid.

It follows from the same argument that $\bar{v}^* = \nabla F$ is indeed the deformation velocity.

Now Eq. (3.12) can be rewritten into the following format: $\bar{v}' = \bar{v}_m + \bar{v}^* = \bar{v}_o + \bar{\omega}^*\bar{R} + \nabla F$. This equation is the form of the First Helmholtz theorem: the motion of an elementary fluid volume may be presented at any given point in time

as expanded into the quasi-rigid motion with the velocity $\bar{v}_m$ (which is equal to the sum of the translation velocity $\bar{v}_o$ and rotation velocity $\bar{\omega} * \bar{R}$) and the deformation motion with velocity $\bar{v}^* = \nabla F$.

2. Tensor of the deformation velocity

Let's review the scalar product $\bar{R}\nabla F$ first. It follows from Eq. (3.11) and from the vector $\bar{R}$ definition that $\bar{R}\nabla F = \bar{e}_i \xi_i \bar{e}_k \dfrac{\partial F}{\partial \xi_k} = \varepsilon_{ik} \xi_i \xi_k$.

The scalar product in its concept is invariant relative to coordinate conversion, thus:

$$\varepsilon \ \xi_i \xi_k = \bar{\varepsilon}_{mn} \tilde{\xi}_m \tilde{\xi}_n , \tag{3.20}$$

where ξ_i are coordinates of the old coordinate system, and $\tilde{\xi}_i$ coordinates of the new one.

The vector $\bar{R}$ in both old and new coordinate systems is expressed as $\bar{R} = \bar{e}_k \xi_k = \tilde{\bar{e}}_j \tilde{\xi}_j$ where $\tilde{\bar{e}}_j$ are unit vectors of the new coordinate system. By multiplying this relationship by $\bar{e}_k$, the equations for the coordinate transformation can be obtained:

$$\xi_k = \tilde{\bar{e}}_j \bar{e}_k \tilde{\xi}_j = \tilde{\xi}_j \alpha_{jk} = \tilde{\xi}_m \alpha_{mk} = \tilde{\xi}_n \alpha_{nk} , \tag{3.21}$$

where α_{jk} are cosines of the angles between the axes of the new and old coordinate systems.

Substituting Eq. (3.21) into Eq. (3.20) results: $\varepsilon_{ik} \xi_i \xi_k = \varepsilon_{ik} \tilde{\xi}_m \alpha_{mi} \tilde{\xi}_n \alpha_{nk} = \tilde{\varepsilon}_{mn} \tilde{\xi}_m \tilde{\xi}_n$. This equation is valid for any $\tilde{\xi}_m$ and $\tilde{\xi}_n$, so:

$$\tilde{\varepsilon}_{mn} = \varepsilon_{ik} \alpha_{mi} \alpha_{nk} . \tag{3.22}$$

Eq. (3.22) is the definition of an affine ortagonal vector of second rank. Thus, the deformation velocities are symmetric ($\varepsilon_{ik} = \varepsilon_{ki}$) tensors of second rank, components of which are established by the following matrix:

$$D = \begin{pmatrix} \varepsilon_{11} & \varepsilon_{12} & \varepsilon_{13} \\ \varepsilon_{21} & \varepsilon_{22} & \varepsilon_{23} \\ \varepsilon_{31} & \varepsilon_{32} & \varepsilon_{33} \end{pmatrix}.$$

3. Physical meaning of the deformation velocity tensor components

To find out the physical meaning of the deformation velocity tensor components ε_{ik}, let's review vector $\bar{R}$ which is parallel to the Ox_1 axis. The directing cosines for this vector are $\alpha_1 = 1, \alpha_2 = \alpha_3 = 0$; in this case, using Eq. (3.18), $\varepsilon_R = \varepsilon_{11}$. Therefore, ε_{11} is the relative extension velocity vector for the vector parallel to the Ox_1 axis. Similarly one can show that ε_{kk} are the relative extension velocities along the corresponding coordinate axes.

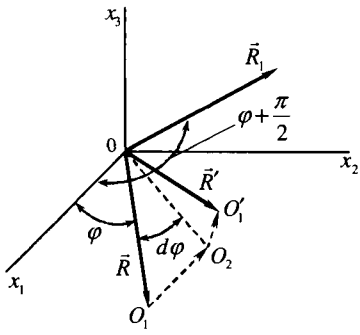

Fig. 3.2

Assume that both translational and rotational velocities of a fluid particle are zero. Let's consider vector $\bar{R}$ coplanar with x_1Ox_2 plane (Fig. 3.2). During time interval dt, this vector transforms into vector $\bar{R}'$ which may not be coplanar with the x_1Ox_2 plane. Then (Fig. 3.2), $O_1O_1 = v^* dt\, Fdt$. Let's expand vector $v^* dt$ into the vectors O_1O_2 and O_2O_1 such that the vector O_1O_2 is perpendicular to $\bar{R}$ and coplanar with x_1Ox_2. From Fig. 3.2 it can be concluded that $O_1O_2 = \vec{v}^*_1 dt$, and $\vec{v}^*$ is a component of vector $\vec{v}^*$ on the x_1Ox_2 plane.

Because $O_1O_2 = Rd\varphi = v'_1\, dt$, then:

$$\frac{d\varphi}{dt} = \frac{v^*_1}{R} = \frac{n\nabla F}{R} = \frac{1}{R}\frac{\partial F}{\partial n} = \frac{1}{R^2}\frac{\partial F}{\partial \varphi},$$

where $\bar{n}$ is a singular vector directed along O_1O_2.

The vector $\bar{R}$ coordinates on the x_1Ox_2 plane are $\xi_1 = R\cos\varphi$, $\xi_2 = R\sin\varphi$, $\xi_3 = 0$ and, according to Eq. (3.10):

$$F = \frac{1}{2}(\varepsilon_{11}\xi^2_1 + 2\varepsilon_{12}\xi_1\xi_2 + \varepsilon_{22}\xi_2{}^2) = \frac{R^2}{2}(\varepsilon_{11}\cos^2\varphi + \varepsilon_{12}\sin 2\varphi + \varepsilon_{22}\sin^2\varphi),$$

from where:

$$\frac{d\varphi}{dt} = \frac{1}{2}(\varepsilon_{22} - \varepsilon_{11}\xi)\sin 2\varphi + \varepsilon_{12}\cos 2\varphi). \qquad (3.23)$$

Now let's review vector $\bar{R}_1$, perpendicular to $\bar{R}$ and coplanar with the x_1Ox_2 plane. It can be seen that $\varphi_1 = \varphi + \frac{\pi}{2}$ and from Eq. (3.23) $d\varphi_1 = -d\varphi$. Therefore,

vectors $\bar{R}$ and $\bar{R}_1$ are either divergent or convergent, but always rotate in the opposite directions. The rate of $\dot{\gamma}$ of the angle variation between vectors $\bar{R}$ and $\bar{R}_1$ is equal to $\dot{\gamma} = 2\dfrac{d\varphi}{dt}$. If $\varphi = 0$, considering Eq. (3.23) results in $\dot{\gamma} = 2\varepsilon_{12}$.

So, ε_{12} represents one half of the coordinate angle skewing rate in the x_1Ox_2 plane. The $\varepsilon_{ik}(i \neq k)$ components have a similar meaning on the corresponding planes.

Let's review an example of flow with a velocity field $v_1 = 0$, $v_2 = kx_3$ and $v_3 = 0$. It is can be seen that in this case an infinitely small square $OABC$ (Fig. 3.3) over the time t with the second order accuracy to small variables will turn into a rhomb OA_1B_1C. According to Eq. (3.5), for the field of assigned velocities:

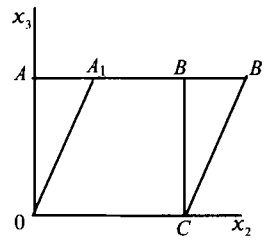

Fig. 3.3

$$\varepsilon_{11} = \varepsilon_{22} = \varepsilon_{33} = = \varepsilon_{12} = \varepsilon_{13} = 0,\ \varepsilon_{23} = \frac{k}{2}.$$

Therefore, the skewing velocity of the direct angle AOC is equal to $\gamma = 2\varepsilon_{23} = k$.

4. Tensor surface of a symmetric second rank tensor

Consider a second-order surface with the center in the origin of coordinates. Its equation is given by the analytical geometry:

$$a_{ij}x_ix_j = 1,\ a_{ij} = a_{ji}, \tag{3.24}$$

where x_i are Cartesian coordinates, a_{ij} are coefficients of the second-order surface. When changing from one coordinate system to the other, the Cartesian coordinates transform according to following rule $x_i = a_{ki}\,\tilde{x}_k$, $\tilde{x}_j = a_{ij}\,\tilde{x}_l$, and in the new coordinate system Eq. (3.24) can be written as follows:

$$a_{ij}a_{ki}\alpha_{lj}\,\tilde{x}_k\,\tilde{x}_l = \tilde{a}_{mn}\,\tilde{x}_m\,\tilde{x}_n = 1, \tag{3.25}$$

where $\tilde{a}_{mn}$ are the second-order surface coefficients in the new coordinate system.

Eq. (3.25) indicates that the second-order surface coefficients in the new and old coordinate systems are associated in the following way:

$$\tilde{a}_{mn} = a_{ij}\alpha_{mi}\alpha_{ni},$$

i. e., a_{ij} = second-order surface coefficients [Eq. (3.24)] represent a symmetric tensor of second-rank.

Thus, each symmetric tensor of the second rank may be put next to a second-order surface in Eq. (3.24), and any second-order surface in Eq. (3.24) may be placed next to a symmetric tensor of the second rank. The surface $a_{ij}x_ix_j = 1$ is called the *characteristic surface* of the second rank tensor or the *tensor surface*.

The analytical geometry proves that any second-order surface in Eq. (3.24) has at least three such mutually ortagonal directions which, if taken as coordinate axes, lead to the canonic form. These directions are called *main* or *own directions*, and the coordinate axes, the *main axes* of the tensor surface.

Tensor surface [Eq. (3.24)] in main axes has the following form:

$$(a_1x_1^2 + a_2x_2^2 + a_3x_3^2) = 1, \tag{3.26}$$

with the matrix of tensor a_{ik}:

$$\begin{pmatrix} a_1 & 0 & 0 \\ 0 & a_2 & 0 \\ 0 & 0 & a_3 \end{pmatrix}.$$

The components of the tensor a_{ij} written in main axes are called main components and are denoted by one subscript.

As follows from the Helmholtz theorem, in a general case the main axes of the tensor surface are rotating with the instantaneous angular velocity $\bar{\omega}$.

The deformation velocities of an infinitely small spherical particle are given by:

$$\frac{\xi_1^2 + \xi_2^2 + \xi_3^2}{R^2} = 1. \tag{3.27}$$

During the time period dt, it will transform into an ellipsoid:[2]

$$\frac{\xi_1'^2}{a^2} + \frac{\xi_2'^2}{b^2} + \frac{\xi_3'^2}{c^2} = 1. \tag{3.28}$$

As discussed earlier, the ellipsoid semi-axes are: $a = R(1 + \varepsilon_1 dt)$, $b = R(1 + \varepsilon_2 dt)$, $c = R(1 + \varepsilon_3 dt)$.

The velocity Θ of the particle's volume expansion is:

$$\Theta = \lim_{\Delta t \to 0} \frac{V' - V}{V} = \lim_{\Delta t \to 0} \frac{\frac{4}{3}abc - \frac{4}{3}\pi R^3}{\frac{4}{3}\pi R^3} = \varepsilon_1 + \varepsilon_2 + \varepsilon_3 = \frac{\partial v_i}{\partial x_i} = \bar{div}v,$$

where V' is the volume of the ellipsoid-Eq. (3.28), V is the volume of the sphere-Eq. (3.27). It can be concluded from the definition of the volume expansion velocity that Θ and $\bar{div}v$ are the invariants relative the coordinate transformation.

[2] Main axes of the ellipsoid may not coincide with the coordinate axes Ox_i due to the rotation deformation.

5. Velocity circulation. Potential motion of the liquid

Let's review a curve AB within a volume occupied by a fluid. Draw vectors $\bar{v}$ in each point of the line (Fig. 3.4). A scalar product $\bar{v} * d\bar{s}$, where $d\bar{s}$ is an element of the AB curve, does not depend on the coordinate selection. The corresponding value:

$$\Gamma = \int_{AB} \bar{v} d\bar{s} = \int_{AB} v_s ds \qquad (3.29)$$

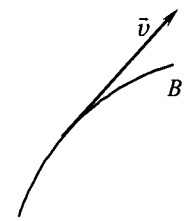

Fig. 3.4

is called the linear integral of vector $\bar{v}$ along the AB curve or the velocity circulation along this curve. When integrating from A to B or when the pass-around direction changes while integrating along the closed curve, the circulation sign changes to the opposite. It means that the circulation along the closed contour (Fig. 3.5) is equal to the sum of the circulations along contours I and II, because the integral Eq. (3.29) along the AB line is computed twice, and in the opposite directions.

According to the Stokes' law, circulation at velocity $\bar{v}$ along a closed contour L is equal to the doubled vortex flow of rotor $\bar{\omega}$ through surface S tightly pulled over this contour, i. e.:

$$\Gamma = \int_L \bar{v} d\bar{s} = 2 \int_S \bar{\omega} d\bar{s} = 2 \int_S \omega_n ds . \qquad (3.30)$$

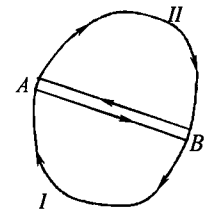

Fig. 3.5

If there is a function $\varphi(x_j,t)$ satisfying the following condition:

$$v_i = \frac{\partial \varphi}{\partial x_i}, \; v = \nabla \varphi , \qquad (3.31)$$

then the flow is called a potential flow, and the function φ is called the potential velocity. It is proven mathematically that for the potential velocity to exist, the following is necessary and sufficient:

$$\frac{\partial v_i}{\partial x_j} - \frac{\partial v_j}{\partial x_i} = 0, \; i \neq j. \qquad (3.32)$$

By definition, the rotor of velocity $\bar{\omega}$ is equal to:

$$\bar{\omega} = \frac{1}{2} rot \bar{v} = \begin{vmatrix} \bar{e}_1 & \bar{e}_2 & \bar{e}_3 \\ \dfrac{\partial}{\partial x_1} & \dfrac{\partial}{\partial x_2} & \dfrac{\partial}{\partial x_3} \\ v_1 & v_2 & v_3 \end{vmatrix}, \qquad (3.33)$$

and it follows from Eqs. (3.36) and (3.37) that if $\bar{v} = \nabla\varphi$ then $\bar{\omega} = 0$, and conversely, if $\bar{\omega} = 0$ then $\bar{v} = \nabla\varphi$. It means that the condition $\bar{\omega} = 0$, i. e., the absence of rotors, is necessary and sufficient for the existence of a potential flow.

As the AB curve's element $d\bar{s} = e_k dx_k$, the potential flow from Eqs. (3.31) and (3.32) forms the following format:

$$\Gamma = \int_{AB} \bar{v} d\bar{s} = \int_A^B e_i \frac{\partial\varphi}{\partial x_i} e_k dx_k = \int_A^B \frac{\partial\varphi}{\partial x_i} dx_i = \int_A^B \partial\varphi = \varphi(B) - \varphi(A). \qquad (3.34)$$

Therefore, in this case the velocity circulation depends only on the positions of the initial and final points of the AB curve and does not depend on the integration path.

If potential φ is non-univalent, the circulation along the closed contour L differs from zero. This case can happen if there are rotors within the area encircled by contour L.

Under a potential flow, the circulation along the closed contour L is not equal to zero only if contour L cannot be constricted to a point through a continuous transformation, i. e., if the area within L is multiloop (Fig. 3.6). Potential within a multiloop area may be non-univalent.

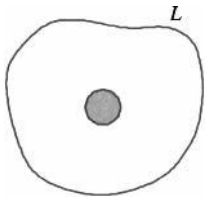

Fig. 3.6

Let's review the flow with the velocity potential as an example:

$$\varphi = \frac{J}{2\pi}\theta = \frac{J}{2\pi} arctg \frac{x_2}{x_1}. \qquad (3.35)$$

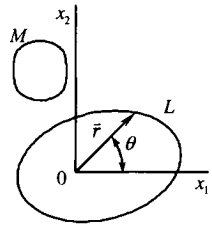

Fig. 3.7

Function φ is univalent on contour M and non-univalent, on contour L (Fig. 3.7). After a pass-around of point O, potential φ obtains an increment equal to $2\pi n$, where n is the number of pass around about point O. Point O (the origin) is a singularity. The corresponding potential within it maintains a finite value but this value depends on the pass along which the approach to point O is conducted.

Thus the following form of the velocity potential equation can be obtained:

$$v_1 = \frac{\partial\varphi}{\partial x_1} = -\frac{J}{2\pi_1}\frac{x_2}{r^2},\ v_2 = \frac{\partial\varphi}{\partial x_2} = -\frac{J}{2\pi_1}\frac{x_2}{r^2},\ v_3 = 0;\ v = \sqrt{v_1^2 + v_2^2} = \frac{J}{2\pi r},$$

$$r = \sqrt{x^2 + x_2^2}.$$

Vector $\bar{v} = \nabla\varphi$ is perpendicular to the line $\varphi = \text{const}$ and is directed toward the increase of function $\varphi = \varphi(\theta)$. The flow-lines are circles with the center at origin (Fig. 3.8).

When $r \to 0$, $v \to \infty$, i. e., the origin is a singularity region of the velocity field. At this point, derivatives $\frac{\partial\varphi}{\partial x_1}$ and $\frac{\partial\varphi}{\partial x_2}$ experience disruption; therefore, the Stokes' law conditions are violated. But if the point $r = 0$ is excluded, the area becomes multi-loop. A singularity may be considered as a concentrated rotor.

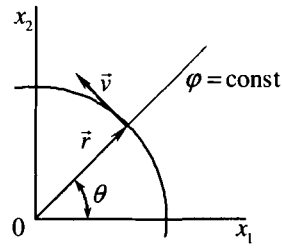

Fig. 3.8

Circulation along the circle C with the center at point O is equal to:

$$\Gamma = \int_C v dr = \int_0^{2\pi} v r d\varphi = 2\pi r v = J .$$

Circulation along any closed curve C_1 which contains the origin is equal to J. Indeed, $\Gamma_{C_1} = \Gamma_{BA} + \Gamma_C + \Gamma_{AB} = \Gamma_C$, where the subscripts correspond to the curves along which the integration is performed (Fig. 3.9).

Now consider the field of rotor $\bar{\omega}$. Vector lines[3] — rotor lines — may be constructed for this field. Similar to the flow-tube, rotor tubes may be constructed with their effective cross-sections (Fig. 3.10).

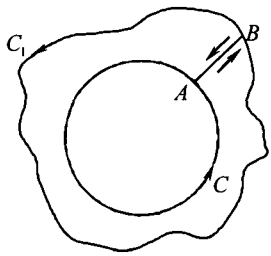

Fig. 3.9

It follows from Eq. (3.33) that $div\bar{\omega} = 0$ and, under the Gauss–Ostrogradsky theorem,

$$\int_V div\bar{\omega} dV = \int_S \bar{\omega}^* n dS = \int_S \omega_n dS = 0, \qquad (3.36)$$

i. e., vortex flow through a closed surface is equal to zero.

Take a rotor-tube limited by the cross-sections S_1 and S_2 and by the side-surface S_3 (Fig. 3.10). By definition, for a rotor-tube $\omega_n = 0$ at S_3, so from Eq. (3.36):

$$\int_S \omega_n dS = \int_{S_1} \omega_n dS + = 0 . \qquad (3.37)$$

[3] See Chapter I, Section 4.

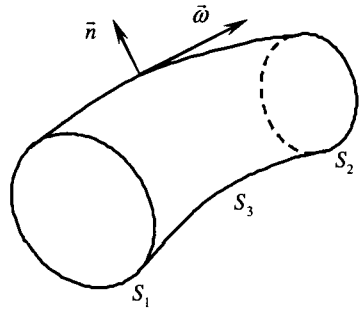

Fig. 3.10

Reversing on S_1 the direction of the normal[4] and using the Stokes' law Eq. (3.30), the following equation can be derived from Eq. (3.37):

$$\int_{S_1}\omega_n dS = \int_{S_2}\omega_n dS + = \frac{1}{2}\int_C \vec{v}d\vec{s} = \frac{1}{2}\Gamma . \tag{3.38}$$

Eq. (3.38) indicates that circulation along any closed contour C containing the rotor-tube is a constant value. This conclusion is the second Helmholtz theorem.

From Eq. (3.38), for an elementary rotor-tube:

$$2\omega_1\Delta S_1 = 2\omega_2\Delta S_2 = \Gamma , \tag{3.39}$$

where S_1 and S_2 are cross-section areas of the rotor-tube. The value $2\omega\Delta S$ is called the rotor-tube stress.

Eq. (3.39) shows that if the $\bar{\omega}$ value is finite within the entire volume of the fluid, the ΔS within this volume is also finite. Therefore, the rotor-tubes cannot end within the fluid volume. They are either closed onto themselves, or end up on the surface or stretch into infinity. Apparently, the same conclusion is valid also for the flow-tubes.

[4] When using the Stokes' law, the pass-around direction along the contours encircling the cross-sections S_1 and S_2 should be the same. That is why, if we take an external normal on S_2, it is necessary to take an internal normal on S_1.

CHAPTER IV

LIQUIDS

1. Mathematical model of ideal fluid

As it has already been discussed in Section 2.9, the system of equations of continuous medium Eq. (2.90) is unclosed. In order to close it, it is necessary to add the rheological equation of the continuous medium under consideration, or in other words, to assign the properties of this medium. The simplest continuous medium model is the ideal liquid.

The ideal fluid (gas) is such isotropic continuous medium where there are no tangent stresses, i.e., $p_{ik} = 0$ $(i \neq k)$. *At that, the normal stresses are compressing, their value depends only on the point within the continuous medium and does not depend on the direction.* Tangential stresses in liquid occur due to the friction. That is why it may be stated that the ideal fluid is fluid devoid of the internal friction.

Disregarding the internal (inner, viscous) friction significantly simplifies mathematical handling of hydrodynamic problems. In some cases it helps understand the physics of the processes under consideration. Besides, the ideal fluid model allows for a good enough description of such practically important phenomena as hydraulic shock, emergence of shock waves in gases, of the wing's lifting force, flow-around of smooth bodies, etc., etc.

For ideal fluid, by definition:

$$p_{nn} = p_1 = p_2 = p_3 = -p\,. \tag{4.1}$$

A positive scalar value p is called pressure. It is usually assumed that the introduced value p is identical to the pressure used in thermodynamics. This, however, needs additional substantiation.

The minus sign in front of p indicates that only compressing normal stresses are accepted in fluids. The stresses in ideal fluid are:

In a vector format,

$$\bar{p}_{nn} = -p\vec{n}, \tag{4.2}$$

in a tensor format,

$$p_{ij} = -p\delta_{ij}, \tag{4.3}$$

and in a matrix format,

$$\begin{pmatrix} -p & 0 & 0 \\ 0 & -p & 0 \\ 0 & 0 & -p \end{pmatrix},$$

where δ_{ij} is the Kronecker delta. The stress tensor in ideal fluid is often called spherical or isotropic. The reason for that is that the tensor surface corresponding to the stress tensor is a sphere, and physical properties assigned by such tensors are isotropic.

Eq. (2.83) includes such parameters as $\frac{\partial \bar{p}_i}{\partial x_i}$, $\frac{\partial(\bar{p}_i \bar{v})}{\partial x_i}$. Based on Eqs. (4.1) and (4.3):

$$\frac{\partial \bar{p}_i}{\partial x_i} = \frac{\partial \bar{e}_i p}{\partial x_i} = -\bar{e}_i \frac{\partial p}{\partial x_i} = -\nabla p, \tag{4.4}$$

$$\frac{\partial(\bar{p}_i \bar{v})}{\partial x_i} = -\frac{\partial(\bar{e}_i p \bar{e}_k v_k)}{\partial x_i} = \frac{\partial(p v_k)}{\partial x_k} = -div p\bar{v} - \bar{v}\nabla p. \tag{4.5}$$

Substituting Eqs. (4.4) and (4.5) into Eq. (2.83) results in an ideal fluid model:

$$\frac{\partial \rho}{\partial t} + \rho div \bar{v} = 0$$

$$\rho \frac{d\bar{v}}{dt} = \rho \bar{F} - \nabla p \tag{4.6}$$

$$\rho \frac{d}{dt}(u + \frac{v^2}{2}) = \rho \bar{F}\bar{v} - div p\bar{v} + \rho q_e.$$

The first equation is the continuity equation, the second one is the *Euler's motion equation*, and the third one represents the energy conservation law.

Systems of equation Eq. (4.6) includes five scalar equations and six variables (ρ, v_i, p, u). In order to close it, it is necessary to assign the equation of state:

$$p = p(\rho, T), \tag{4.7}$$

which associates the pressure, temperature and density, and the caloric equation of state:

$$u = u(\rho, T). \tag{4.8}$$

Eqs. (4.6), (4.7) and (4.8) include seven equations and seven variables and a closed system of equations describing the motion of an ideal compressible fluid (gas).

To derive the kinetic energy theorem in the ideal fluid, Eq. (4.5) should be substituted into Eq. (2.74). The result is:

$$\rho \frac{d}{dt}\left(\frac{v^2}{2}\right) = \rho \bar{F}\bar{v} - div p\bar{v} + \rho N^{(i)}. \tag{4.9}$$

According to the ideal fluid definition and Eq. (2.87), an expression for the internal forces $\rho N^{(i)}$ is:

$$\rho N^{(i)} = -p_{ik}\frac{\partial v_k}{\partial x_i} = p\frac{\partial v_i}{\partial x_i} = p div\bar{v} \tag{4.10}$$

or, by considering the continuity equation Eq. (2.32):

$$\rho N^{(i)} = -p div\bar{v} = -\frac{p}{\rho}\frac{\partial p}{\partial t}. \tag{4.11}$$

Considering Eqs. (4.10) and (4.11), the heat inflow equation Eq. (2.88) can be presented with the following format:

$$\frac{du}{dt} = q_e + \frac{p}{\rho^2}\frac{dp}{dt} \tag{4.12}$$

or

$$\frac{du}{dt} = q_e - \frac{p}{\rho} div\bar{v}. \tag{4.13}$$

Thus, considering Eqs. (4.12) and (4.13), internal energy variation in the ideal fluid can occur only due to the supply of external heat q_e and to changes in its density (volume).

2. Mathematical model of ideal incompressible fluid

At transient-free fluid flow as well as non-stationary flow with soft velocity changes, fluid's density variations are negligible and can be disregarded. The same argument is valid for the transient-free gas flow at a low velocity or a flow with soft velocity changes. In such cases, the non-compressible fluid model can be used.

A fluid is ***incompressible*** if ρ = const for a material particle or (under the definition of material derivative, see Eq. (1.14)) if:

$$\frac{d\rho}{dt} = \frac{\partial \rho}{\partial t} + v_i\frac{\partial \rho}{\partial x_i} = 0. \tag{4.14}$$

A fluid is ***incompressible*** and ***uniform*** if the density value is constant and is the same for all material points within the fluid volume under consideration. In such a case:

$$\frac{d\rho}{dt} = 0,\ \frac{\partial \rho}{\partial t} = 0 \text{ and } \frac{\partial \rho}{\partial x_i} = 0. \tag{4.15}$$

Here, density is not an unknown function but a known value assigned at the problem setting.

Eq. (4.14) (or (4.15)) is the equation of state of incompressible fluid.

As Eqs. (4.6), (4.14) and (4.15) show, regardless of whether the incompressible fluid is uniform or non-uniform, the system of motion equations has the following format:

$$div\bar{v} = 0,$$

$$\rho \frac{d\bar{v}}{dt} = \rho \bar{F} - \nabla p. \tag{4.16}$$

In the case of a uniform incompressible fluid, the system of above equation contains four unknown functions of the space and time (p,v_i), and, hence, it is a closed system. In the case of a non-uniform incompressible fluid, the system of equation [Eq. (4.16)] contains five unknowns, so to close it the application of Eq. (4.14) is necessary.

The closed system of equations describing the motions of an incompressible fluid is purely mechanical, i. e., it does not include any thermodynamic parameters.

The law of kinetic energy variation Eq. (4.9) for a incompressible fluid is:

$$\rho \frac{d}{dt}\left(\frac{v^2}{2}\right) = \rho \bar{F}\bar{v} - \bar{v}\nabla p, \tag{4.17}$$

as, according to Eqs. (4.10) and (4.11), in this case $N^{(i)} = 0$.

The heat-flow equation [Eq. (4.12) or (4.13)] then becomes:

$$\frac{du}{dt} = q_e. \tag{4.18}$$

Multiplying (scalar multiplication) the second equation of Eq. (4.6) by $\bar{v}$ and subtracting the result from the third equation of Eq. (4.6) results an incompressible fluid equation:

$$\frac{du}{dt} = q_e$$

which coincides with the heat-flow equation [Eq. (4.18)]. Thus, the use of the energy conservation law or heat-flow equation enables only a judgment of the internal energy, i. e., of changes of its temperature.

It is important to note that the temperature variations can have no effect on the flow of an incompressible ideal fluid.

The boundary condition at a hard wall for the Euler's equation is derived from the condition of non-leakage of fluid through the hard surface, i. e., the following condition must be valid at the points of the hard surface:

$$\bar{v} * \bar{n} = \bar{V} * \bar{n}, \tag{4.19}$$

where $\bar{V}$ is hard surface points motion velocity, and $\bar{n}$ is a normal to this surface. If the hard surface is stationary:

$$v_n = \bar{v} * \bar{n} = 0. \tag{4.20}$$

It is necessary to mention that due to the presence of non-linear terms such as:

$$\frac{dA}{dt} = \frac{\partial A}{\partial t} + v_i \frac{\partial A}{\partial x_i}, \ \rho div\bar{v} \text{ and } div p\bar{v}$$

Eqs. (4.6) and (4.16) are systems of nonlinear differential equations with partial derivatives. The nonlinearity makes it very difficult to come up with accurate solution of the hydromechanical equations even for an ideal fluid model.

3. Viscous fluid. Stress tensor in viscous fluid

A viscous fluid is a continuous medium with the following properties: (1) the fluid is an isotropic continuous medium, i. e., all directions within it are physically equivalent (properties do not depend on the direction); (2) the stress tensor in a viscous fluid has the following format:

$$\begin{pmatrix} p_{11} & p_{12} & p_{13} \\ p_{21} & p_{22} & p_{23} \\ p_{31} & p_{32} & p_{33} \end{pmatrix} + \begin{pmatrix} -p & 0 & 0 \\ 0 & -p & 0 \\ 0 & 0 & -p \end{pmatrix} + \begin{pmatrix} \tau_{11} & \tau_{12} & \tau_{13} \\ \tau_{21} & \tau_{22} & \tau_{23} \\ \tau_{31} & \tau_{32} & \tau_{33} \end{pmatrix} \text{ or } p_{ik} = -p\delta_{i\,k} + \tau_{ik}, \tag{4.21}$$

where τ_{ik} are viscous stresses which depend on ε_{ik}, δ_{ik} — Kronecker's delta. If in addition the correlation between tensors τ_{ik} and ε_{ik} is assumed to be ***linear*** then the viscous fluid is called the ***Newtonian viscous fluid***. In other words, Newtonian viscous fluid requires that each one of the nine components of the viscous stress tensor must be linearly associated with all nine components of the deformation velocity tensor. The most general format of this linear association is:

$$\tau_{11} = a_{1111}\varepsilon_{11} + a_{1122}\varepsilon_{22} + a_{1133}\varepsilon_{33} + \ldots + a_{1121}\varepsilon_{21},$$

$$\tau_{22} = a_{2211}\varepsilon_{11} + a_{2222}\varepsilon_{22} + a_{2233}\varepsilon_{33} + \ldots + a_{2221}\varepsilon_{21},$$

$$\ldots\ldots\ldots\ldots\ldots\ldots\ldots\ldots\ldots\ldots\ldots\ldots$$

$$\tau_{21} = a_{1211}\varepsilon_{11} + a_{2122}\varepsilon_{22} + a_{2133}\varepsilon_{33} + \ldots + a_{2121}\varepsilon_{21},$$

Or in a matrix format:

$$\begin{pmatrix}\tau_{11}\\ \tau_{22}\\ \tau_{33}\\ \tau_{23}\\ \tau_{13}\\ \tau_{12}\\ \tau_{32}\\ \tau_{31}\\ \tau_{21}\end{pmatrix} = \begin{pmatrix} a_{1111} & a_{1122} & a_{1133} & a_{1123} & a_{1113} & a_{1112} & a_{1132} & a_{1131} & a_{1121}\\ a_{2211} & a_{2222} & a_{2233} & a_{2223} & a_{2213} & a_{2212} & a_{2232} & a_{2231} & a_{2221}\\ a_{3311} & a_{3322} & a_{3333} & a_{3323} & a_{3313} & a_{3312} & a_{3332} & a_{3331} & a_{3321}\\ a_{2311} & a_{2322} & a_{2333} & a_{2323} & a_{2313} & a_{2312} & a_{2332} & a_{2331} & a_{2321}\\ a_{1311} & a_{1322} & a_{1333} & a_{1323} & a_{1313} & a_{1312} & a_{1332} & a_{1331} & a_{1321}\\ a_{1211} & a_{1222} & a_{1233} & a_{1223} & a_{1213} & a_{1212} & a_{1232} & a_{1231} & a_{1221}\\ a_{3211} & a_{3222} & a_{3233} & a_{3223} & a_{3213} & a_{3212} & a_{3232} & a_{3231} & a_{3221}\\ a_{3111} & a_{3122} & a_{3133} & a_{3123} & a_{3113} & a_{3112} & a_{3132} & a_{3131} & a_{3121}\\ a_{2111} & a_{2122} & a_{2133} & a_{2123} & a_{2113} & a_{2112} & a_{2132} & a_{2131} & a_{2121}\end{pmatrix}\begin{pmatrix}\varepsilon_{11}\\ \varepsilon_{22}\\ \varepsilon_{33}\\ \varepsilon_{23}\\ \varepsilon_{13}\\ \varepsilon_{12}\\ \varepsilon_{32}\\ \varepsilon_{31}\\ \varepsilon_{21}\end{pmatrix}$$

or, by using the summation convention:

$$\tau_{ij} = a_{ijkl}\varepsilon_{kl}.$$

For an isotropic continuous medium, the aggregate of components $\|a_{ijkl}\|$ forming the tensor, forth rank, should be such that at any orthogonal transformation of the coordinate system the matrix $\|a_{ijkl}\|$ would not change its form. This limitation allows for introducing the decisive form of the a_{ijkl} tensor and determination of a connection between the τ_{ik} and ε_{ik} tensors.

The a_{ijkl} coefficients must satisfy the symmetry conditions, the conditions that result from the symmetry of the stress and deformation velocity tensors. That is why the a_{ijkl} coefficients must satisfy conditions $a_{ijkl} = a_{jikl} = a_{jilk} = a_{ijlk}$. Besides, the exchangeability condition of ij and kl pairs is realized for a_{ijkl}. Therefore, this results in subscript symmetry:

$$a_{ijkl} = a_{jikl} = a_{jilk} = a_{ijlk} = a_{klij} = a_{lkij} = a_{lkji} = a_{klji}. \tag{4.22}$$

The symmetry condition [Eq. (4.22)] reduces the number of independent components of the a_{ijkl} tensor:

$$\begin{pmatrix}\tau_{11}\\ \tau_{22}\\ \tau_{33}\\ \tau_{23}\\ \tau_{13}\\ \tau_{12}\\ \tau_{32}\\ \tau_{31}\\ \tau_{21}\end{pmatrix} = \begin{pmatrix} a_{1111} & a_{1122} & a_{1133} & a_{1123} & a_{1113} & a_{1112} & a_{1132} & a_{1113} & a_{1112}\\ a_{1122} & a_{2222} & a_{2233} & a_{2223} & a_{2213} & a_{2212} & a_{2223} & a_{2213} & a_{2212}\\ a_{1133} & a_{2233} & a_{3333} & a_{3323} & a_{3313} & a_{3312} & a_{3323} & a_{3313} & a_{3312}\\ a_{2311} & a_{2223} & a_{3323} & a_{2323} & a_{2313} & a_{2312} & a_{2323} & a_{2313} & a_{2312}\\ a_{1113} & a_{2213} & a_{3313} & a_{1323} & a_{1313} & a_{1312} & a_{1323} & a_{1313} & a_{1312}\\ a_{1112} & a_{2212} & a_{3312} & a_{1223} & a_{1213} & a_{1212} & a_{1223} & a_{1213} & a_{1212}\\ a_{1123} & a_{2223} & a_{3323} & a_{2323} & a_{2313} & a_{2312} & a_{2323} & a_{2313} & a_{2312}\\ a_{1113} & a_{2213} & a_{3313} & a_{1323} & a_{1313} & a_{1312} & a_{1323} & a_{1313} & a_{1312}\\ a_{1112} & a_{2212} & a_{3312} & a_{1223} & a_{1213} & a_{1212} & a_{1223} & a_{1213} & a_{1212}\end{pmatrix}\begin{pmatrix}\varepsilon_{11}\\ \varepsilon_{22}\\ \varepsilon_{33}\\ \varepsilon_{23}\\ \varepsilon_{13}\\ \varepsilon_{12}\\ \varepsilon_{32}\\ \varepsilon_{31}\\ \varepsilon_{21}\end{pmatrix}.$$

As it can be seen, the last three lines in the matrix are the same as the previous three lines, so the matrix can be simplified:

$$\begin{pmatrix}\tau_{11}\\ \tau_{22}\\ \tau_{33}\\ \tau_{23}\\ \tau_{13}\\ \tau_{12}\end{pmatrix}\begin{pmatrix}a_{1111} & a_{1122} & a_{1133} & a_{1123} & a_{1113} & a_{1112}\\ a_{1122} & a_{2222} & a_{2233} & a_{2223} & a_{2213} & a_{2212}\\ a_{1133} & a_{2233} & a_{3333} & a_{3323} & a_{3313} & a_{3312}\\ a_{1123} & a_{2223} & a_{3323} & a_{2323} & a_{2313} & a_{2312}\\ a_{1113} & a_{2213} & a_{3313} & a_{1323} & a_{1313} & a_{1312}\\ a_{1112} & a_{2212} & a_{3312} & a_{1223} & a_{1213} & a_{1212}\end{pmatrix}\begin{pmatrix}\varepsilon_{11}\\ \varepsilon_{22}\\ \varepsilon_{33}\\ \varepsilon_{23}\\ \varepsilon_{13}\\ \varepsilon_{12}\end{pmatrix} \tag{4.23}$$

Thus, with the symmetry condition [Eq. (4.22)], in general case the linear association between the symmetric tensors, second rank, contains 21 independent coefficient (a constant) a_{ijkl}. Let's assume the matrix Eq. (4.23) is presented in the "old coordinate system" $Ox_1x_2x_3$ (Fig. 4.1) and perform a coordinate transformation $x'_1 = x_1$, $x'_2 = -x_2$, $x'_3 = x_3$ (the mirror reflection in plane Ox_1x_3) as assigned by the transformation matrix:

$$\alpha_{ij} = \begin{pmatrix}1 & 0 & 0\\ 0 & -1 & 0\\ 0 & 0 & 1\end{pmatrix}. \tag{4.24}$$

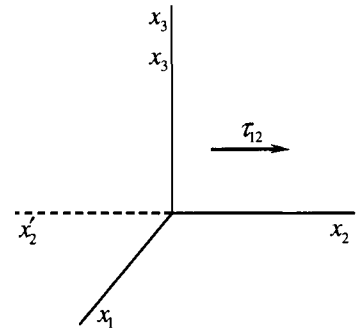

Fig. 4.1

Under the requirement imposed on the matrix of the coefficients a_{ijkl}, the matrix components should not change at any orthogonal transformation. So, the following equality:

$$a'_{ijkl} = \alpha_{in}\alpha_{jm}\alpha_{kt}\alpha_{lr}\alpha_{nmtr} = \alpha_{ijkl} \tag{4.25}$$

should be realized of the components in the new and old coordinate systems. Let's review the condition imposed by Eq. (4.25) on the matrix a_{ijkl} components by transformation Eq. (4.24). For example, by reviewing the component a_{1222}:

$$a_{1222} = \alpha_{1i}\alpha_{2j}\alpha_{2k}\alpha_{2l}\alpha_{ijkl},$$

then substituting the transformation matrix [Eq. (4.24)] components into this equation results:

$$a_{1222} = -a_{1222}.$$

This is the reason that the condition of Eq. (4.25) is valid only at $a_{1222} = 0$. It can be shown in a similar fashion that for the condition Eq. (4.25) on the transforma-

tion Eq. (4.24) to be valid, all a_{ijkl} matrix components containing the uneven number of subscripts 2 must be equal to zero. After reviewing the transformations:

$$\alpha_{ij} = \begin{pmatrix} -1 & 0 & 0 \\ 0 & 1 & 0 \\ 0 & 0 & 1 \end{pmatrix} \text{ and } \alpha_{ij} = \begin{pmatrix} 1 & 0 & 0 \\ 0 & 1 & 0 \\ 0 & 0 & -1 \end{pmatrix}$$

the matrix a_{ijkl} components have certain requirements "all components containing the uneven number of subscripts 1 and 3 must be equal to zero". Therefore, the Eq. (4.23) changes into the following format:

$$\begin{pmatrix} \tau_{11} \\ \tau_{22} \\ \tau_{33} \\ \tau_{23} \\ \tau_{13} \\ \tau_{12} \end{pmatrix} = \begin{pmatrix} a_{1111} & a_{1122} & a_{1133} & 0 & 0 & 0 \\ a_{1122} & a_{2222} & a_{2233} & 0 & 0 & 0 \\ a_{1133} & a_{2233} & a_{3333} & 0 & 0 & 0 \\ 0 & 0 & 0 & a_{2323} & 0 & 0 \\ 0 & 0 & 0 & 0 & a_{1313} & 0 \\ 0 & 0 & 0 & 0 & 0 & a_{1212} \end{pmatrix} \begin{pmatrix} \varepsilon_{11} \\ \varepsilon_{22} \\ \varepsilon_{33} \\ \varepsilon_{23} \\ \varepsilon_{13} \\ \varepsilon_{12} \end{pmatrix}.$$

New requirements of the matrix components can be derived upon reviewing the transformation matrices:

$$\alpha_{ij} = \begin{pmatrix} 0 & 1 & 0 \\ 0 & 0 & 1 \\ 1 & 0 & 0 \end{pmatrix}, \alpha_{ij} = \begin{pmatrix} 0 & 1 & 0 \\ 1 & 0 & 0 \\ 0 & 0 & -1 \end{pmatrix}, \alpha_{ij} = \begin{pmatrix} 0 & 0 & 1 \\ 1 & 0 & 0 \\ 0 & 1 & 0 \end{pmatrix}.$$

Reviewing condition of Eq. (4.25) for these transformations results in the following conditions:

$$a_{1111} = a_{2222} = a_{3333}, a_{1122} = a_{1133} = a_{3333}, a_{2323} = a_{1313} = a_{1212},$$

and the matrix equation:

$$\begin{pmatrix} \tau_{11} \\ \tau_{22} \\ \tau_{33} \\ \tau_{23} \\ \tau_{13} \\ \tau_{12} \end{pmatrix} = \begin{pmatrix} a_{1111} & a_{1122} & a_{1122} & 0 & 0 & 0 \\ a_{1122} & a_{1111} & a_{1122} & 0 & 0 & 0 \\ a_{1122} & a_{2222} & a_{1111} & 0 & 0 & 0 \\ 0 & 0 & 0 & a_{1212} & 0 & 0 \\ 0 & 0 & 0 & 0 & a_{1212} & 0 \\ 0 & 0 & 0 & 0 & 0 & a_{1212} \end{pmatrix} \begin{pmatrix} \varepsilon_{11} \\ \varepsilon_{22} \\ \varepsilon_{33} \\ \varepsilon_{23} \\ \varepsilon_{13} \\ \varepsilon_{12} \end{pmatrix} \quad (4.26)$$

Reviewing the transformation representing a rotation by 120° relative to Z-axis results:

$$\alpha_{ij} = \begin{pmatrix} -1/2 & \sqrt{3}/2 & 0 \\ -\sqrt{3}/2 & -1/2 & 0 \\ 0 & 0 & 1 \end{pmatrix},$$

and consequently results in the following condition:

$$a_{1212} = \frac{1}{2}(a_{1111} - a_{1122}).$$

Assuming $a_{1111} = \lambda + 2\mu$, $a_{1122} = \lambda$ results $a_{1212} = \mu$ (λ and μ are called Lame's constants). Rewriting in index format, the matrix of coefficients in Eq. (4.26):

$$a_{ijkl} = \lambda \delta ij \delta_{kl} + \mu(\delta_{ik}\delta_{jl} + \delta_{il}\delta_{jk}). \tag{4.27}$$

The substitution of Eq. (4.27) tensor into Eq. (4.21) results in the association between the τ_{ik} and ε_{ik} tensors for an isotropic viscous fluid. The viscous stress tensor in the matrix format is:

$$\begin{pmatrix} \tau_{11} & \tau_{12} & \tau_{13} \\ \tau_{21} & \tau_{22} & \tau_{23} \\ \tau_{31} & \tau_{32} & \tau_{33} \end{pmatrix} = \lambda div\bar{v} \begin{pmatrix} -1 & 0 & 0 \\ 0 & 1 & 0 \\ 0 & 0 & 1 \end{pmatrix} + 2\mu \begin{pmatrix} \varepsilon_{11} & \varepsilon_{12} & \varepsilon_{13} \\ \varepsilon_{21} & \varepsilon_{22} & \varepsilon_{23} \\ \varepsilon_{31} & \varepsilon_{32} & \varepsilon_{33} \end{pmatrix}, \tag{4.28}$$

and in the index (subscript) format:

$$\tau_{ij} = \lambda div\bar{v}\delta_{ij} + 2\mu\varepsilon_{ij}, \quad \varepsilon_{kk} = div\bar{v}. \tag{4.29}$$

Substituting Eq. (4.29) into Eq. (4.21), the final result is:

$$p_{ij} = -p\delta_{ij} + \left[\lambda\delta_{ij}\delta_{kl} + \mu(\delta_{ik}\delta_{jl} + \delta_{il}\delta_{jk})\right]\varepsilon_{ij} = -p\delta_{ji} + \lambda\delta_{ij}\varepsilon_{kk} + 2\mu\varepsilon_{ij}. \tag{4.30}$$

Eq. (4.29) shows that viscous properties of a fluid are defined by the λ and μ coefficients. If the fluid is not compressible, $div\bar{v} = 0$, and then only one coefficient, μ, exists for a incompressible fluid. It follows from Eq. (4.29) that μ affects not only the tangential stresses but also normal stresses.

The summation in the Eq. (4.30) is the expressions for normal stresses p_{kk}:

$$\frac{p_{11} + p_{22} + p_{33}}{3} = -p + \left(\lambda + \frac{2}{3}\mu\right) div\bar{v} = -p + \xi div\bar{v}. \tag{4.31}$$

The $\xi = \lambda + \frac{2}{3}\mu$ is the coefficient of the second or volume viscosity. The kinetic gas theory shows that for monoatomic gases $\xi = 0$, but in general $\xi \neq 0$.

A conclusion based on Eq. (4.31) is that for a incompressible fluid, the pressure is the arithmetic average of normal stresses.

For example, consider a transient-free flow with the velocity field of (Fig. 4.2):

$$v_1 = kx_2,\ v_2 = v_3 = 0. \tag{4.32}$$

From the equations stated earlier:

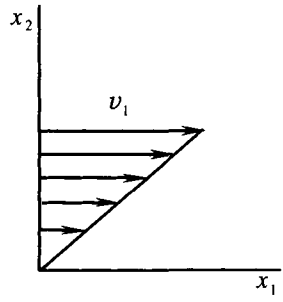

Fig. 4.2

$$div\bar{v} = \frac{\partial v_i}{\partial x_i} = 0,\ \varepsilon_{12} = \frac{1}{2}\frac{\partial v_i}{\partial x_2},$$

$$\varepsilon_{11} = \varepsilon_{22} = \varepsilon_{33} = \varepsilon_{13} = \varepsilon_{23} = 0.$$

From this, based on Eq. (4.29):

$$p_{12} = \mu\frac{\partial v_1}{\partial x_2},\ p_{11} = p_{22} = p_{33} = -p,\ p_{13} = p_{23} = 0.$$

Therefore, in this example only the angle skewing is occurring, and such a flow is called simple shear. The $2\varepsilon_{12} = \frac{\partial v_1}{\partial x_2}$, as proved earlier, is the velocity of the coordinate angle skewing and is called shear velocity.

Eq. (4.32) from Eq. (3.38), the flow lines – straight lines $x_2 = \text{const}$.

According to $\bar{\omega} = \frac{1}{2}rot\bar{v} = \begin{vmatrix} \bar{e}_1 & \bar{e}_2 & \bar{e}_3 \\ \frac{\partial}{\partial x_1} & \frac{\partial}{\partial x_2} & \frac{\partial}{\partial x_3} \\ kx_2 & 0 & 0 \end{vmatrix} = -\bar{e}_3 k$, e. i., the flow under consideration, despite the presence of straight flow-lines, is a rotor flow.

The equation $p_{12} = \mu\frac{\partial v_1}{\partial x_2}$ is a well known Newton's friction law where μ is the dynamic friction factor. For gases, μ is often determined from $\mu = \mu_0\sqrt{\frac{T}{T_0}}$ where T is temperature, °K. The more exact equation (Sutherland equation) is: $\mu = \mu_0\frac{1 + C/T_0}{1 + C/T}\sqrt{\frac{T}{T_0}}$, where C is a constant differing for various gases.

The above equations indicate that the gas viscosity increases with the temperature. For liquids it works the other way: their viscosity declines as temperature increases.

As in the fluid (gas) flow, the temperature depends on space and time, the viscosity factors are also functions of the space and time.

4. Motion equations of viscous fluids

The continuous matter motion equation is used to derive the fluid matter motion equation (2.43).

Considering $\lambda = \xi - \frac{2}{3}\mu$, from Eq. (4.29):

$$\frac{\partial p_{ij}}{\partial x_i} = \frac{\partial}{\partial x_i}\left\{\left[-p + (\xi - \frac{2}{3}\mu) div\bar{v}\right]\delta_{ij} + 2\mu\varepsilon_{ij}\right\} = \\ = \frac{\partial}{\partial x_i}\left[-p + (\xi - \frac{2}{3}\mu) div\bar{v}\right]\delta_{ij} + 2\frac{\partial(\mu\varepsilon_{ij})}{\partial x_i} \tag{4.33}$$

From Eq. (3.5):

$$2\frac{\partial(\mu\varepsilon_{ij})}{\partial x_i} = \frac{\partial\mu}{\partial x_i}\left(\frac{\partial v_i}{\partial x_j} + \frac{\partial v_j}{\partial x_i}\right) + \mu\frac{\partial}{\partial x_i}\left(\frac{\partial v_i}{\partial x_j} + \frac{\partial v_j}{\partial x_i}\right) = \mathrm{R} \tag{4.34}$$

$$\nabla\mu\nabla v_j + \nabla\mu\frac{\partial\bar{v}}{\partial x_j} + \mu\frac{\partial}{\partial x_j} div\bar{v} + \mu\Delta v_j,$$

where Δ is the Laplace operator.

Substituting Eqs. (4.33) and (4.34) into Eq. (2.43):

$$\rho\frac{\partial v_j}{\partial t} = \rho F_j - \frac{\partial p}{\partial x_j} + \mu\Delta v_j + \frac{\partial}{\partial x_j}\left[(\xi - \frac{2}{3}\mu) div\bar{v}\right] + \\ + \mu\frac{\partial}{\partial x_j} div\bar{v} + \nabla\mu\nabla v_j + \nabla\mu\frac{\partial\bar{v}}{\partial x_j} \tag{4.35}$$

Eq. (4.35) is called Navier–Stokes equations for a viscous compressible liquid. At $\mu = \zeta = 0$ they convert into Euler's Eq. (4.6). The Navier–Stokes equations, as as opposed to the Euler's equations, are nonlinear equations of the second order.

In order to derive the equation of the energy conservation law for the viscous compressible fluid, first the following equation should be computed:

$$\frac{\partial(\bar{p}_i\bar{v})}{\partial x_i} = \frac{\partial(pi_j v_j)}{\partial x_i} = p_{ij}\frac{\partial v_j}{\partial x_i} + v_j\frac{\partial p_{ij}}{\partial x_i}. \tag{4.36}$$

From Eqs. (3.5) and (4.29):

$$p_{ij}\frac{\partial v_j}{\partial x_i} = \left\{\left[-p + (\xi - \frac{2}{3}\mu) div\bar{v}\right]\delta_{ij} + 2\mu\varepsilon_{ij}\right\}\frac{\partial v_j}{\partial x_i} = \\ = \left[-p + (\xi - \frac{2}{3}\mu) div\bar{v}\right]\frac{\partial v_j}{\partial x_j} + 2\mu\varepsilon_{ij}\frac{\partial v_j}{\partial x_i} = \\ = \left[-p + (\xi - \frac{2}{3}\mu) div\bar{v}\right] div\bar{v} + 2\mu\varepsilon_{ij}\varepsilon_{ij}. \tag{4.37}$$

And, from Eqs. (4.33) and (4.34):

$$v_j \frac{\partial p_{ij}}{\partial x_i} = \bar{v}\nabla\left[-p + (\xi - \frac{2}{3}\mu) div\bar{v}\right] + \\ + v_j \nabla\mu\nabla v_j + v_j \nabla\mu \frac{\partial \bar{v}}{\partial x_j} + \mu\bar{v}\nabla(div\bar{v}) + \mu\bar{v}\Delta\bar{v} \tag{4.38}$$

Substituting Eqs. (4.237) and (4.38) into Eq.(2.65) and using a known equation of the vector analysis:

$$div\varphi\bar{v} = \varphi div\bar{v} + \bar{v}\nabla\varphi,$$

one obtains:

$$\rho\frac{d}{dt}(u + \frac{v^2}{2}) = \rho\bar{F}\bar{v} + div\left[-p + (\xi - \frac{2}{3}\mu) div\bar{v}\right]\bar{v} + v_j\nabla\mu\nabla v_j + v_j\nabla\mu\frac{\partial\bar{v}}{\partial x_j} + \\ \mu\bar{v}\nabla(div\bar{v}) + \mu\bar{v}\Delta\bar{v} + 2\mu\varepsilon_{ij}\varepsilon_{ij} + \rho q_\varepsilon. \tag{4.39}$$

Eq. (4.39) represents the energy conservation law for a viscous compressible fluid. When $\mu = \zeta = 0$, this equation changes into the equation for the ideal fluid-Eq. (4.6).

The systems of equations for a viscous compressible fluid includes 9 unknown variables (ρ, μ, ζ, u, p, v_i and T) and seven equations: the continuity equation-Eq. (2.32); equations of state-Eqs. (4.7) and (4.8); motion equations-Eq. (4.35); and the energy conservation law-Eq. (4.39). In order to lock it, it is necessary to add:

$$\mu = \mu(T), \quad \zeta = \zeta(T). \tag{4.40}$$

5. Mathematical model of a viscous incompressible fluid

The system of equation for a viscous incompressible fluid follows from Eqs. (2.25), (4.8), (4.14), (4.35), (4.39) and (4.40), and has the following format:

$$\frac{\partial\rho}{\partial t} = \frac{\partial\rho}{\partial t} + v_i\frac{\partial\rho}{\partial x_i} = 0$$

$$div\bar{v} = 0 \tag{4.41}$$

$$\rho\frac{dv_i}{dt} = \rho F_i - \frac{dp}{dx_i} + \mu\Delta v_i + \frac{dv_i}{dt}\nabla\mu\nabla v_i + \nabla\mu\frac{\partial v}{\partial x_i},$$

$$\rho\frac{d}{dt}(u + \frac{v^2}{2}) = \rho Fv - v\nabla p + + v_i\nabla\mu\nabla v_i + v_i\nabla\mu\frac{\partial\bar{v}}{\partial x_i} + \mu v\Delta v + 2\mu\varepsilon_{ij}\varepsilon_{ij} + \rho q_\varepsilon,$$

$$u = u(\rho, T), \mu = \mu(T).$$

This system of equations includes eight unknown variables (ρ, μ, u, p, v_i and T) and is closed.

For a uniform incompressible fluid, the first equation of the Eq. (4.41) becomes an identity, and density, as indicated, is a known constant.

As opposed to a incompressible ideal fluid, the Eq. (4.41) is not totally mechanical. Indeed, as viscosity is a function of temperature, the temperature affects the nature of the flow.

Under isothermal viscous incompressible fluid flow regime, the system Eq. (4.41) becomes much simpler:

$$div\bar{v} = 0$$

$$\rho\frac{dv_i}{dt} = \rho F_i - \frac{\partial p}{\partial x_i} + \mu\Delta v_i . \tag{4.42}$$

This system of equations contains four unknown variables and is closed. In a case of a non-uniform incompressible fluid, the first term of the Eq. (4.41) is added to Eq. (4.42). Thus, the problem of isothermal flow for an incompressible fluid, like the problem of the ideal incompressible fluid flow, is purely mechanical.

From the kinetic energy theorem at the isothermal motion of a viscous incompressible fluid and from Eqs. (2.74), (2.80) and (4.38):

$$\rho\frac{d}{dt}\left(\frac{v^2}{2}\right) = \rho\bar{F}\bar{v} + v_k\frac{\partial p_{ik}}{\partial x_i} = \rho\bar{F}\bar{v} - \bar{v}\nabla p + \mu\bar{v}\Delta\bar{v} . \tag{4.43}$$

As opposed to the Euler's equations, the Navier–Stokes equations are second-order equations. So, one more condition must be added to the boundary conditions Eqs. (4.19) or (4.20). The adhesion hypothesis is accepted accordingly. Its substance is: on a hard wall, the following conditions is assumed to be realized:

$$v_\tau = V_\tau \tag{4.44}$$

where v_τ and V_τ are tangential components of the fluid's and wall's velocities. Therefore, the boundary conditions for the Navier–Stokes equations are:

$$v_n = V_n,\ v_\tau = V_\tau \tag{4.45}$$

or, if the wall is stable,

$$v_n = v_\tau = 0 \tag{4.46}$$

The difference in the boundary conditions for ideal and viscous liquids has very significant results. Indeed, when viscosity tends to zero, the Navier–Stokes equations at the limit turn into the Euler's equations. However, the Navier–Stokes equations solutions at $\mu = 0$, $\zeta = 0$ do not turn into the Euler's equations solutions as they are derived under different boundary conditions, and the boundary conditions of Eq. (4.45) do not depend on viscosity.

A more detailed analysis indicates that viscosity substantially affects the flow nature only within a rather thin fluid layer next to the hard surface. This layer is called the boundary layer. Outside of the boundary layer, viscosity can be disregarded, and the fluid can be considered to be ideal.

These facts resulted in the emergence of a new hydromechanical division, i.e., the theory of the boundary layer.

6. The work of internal forces. Equation of the heat inflow

As shown in Section 2.7, the kinetic energy equation includes per-unit mass power of internal forces $N^{(i)}$. For this, the Eq. (2.80) was derived which is valid for any continuous medium. Substituting Eq. (4.37), results in the equation for a compressible viscous fluid:

$$\rho N^{(i)} = -\left[-p+\left(\zeta-\frac{2}{3}\mu\right)div\bar{v}\right]div\bar{v}-2\mu\varepsilon_{ij}\varepsilon_{ij} = pdiv\bar{v}-W, \qquad (4.47)$$

where:

$$-W=\left(\zeta-\frac{2}{3}\mu\right)(div\bar{v})^2-2\mu\varepsilon_{ij}\varepsilon_{ij} \qquad (4.48)$$

is per-unit volume power of internal forces caused by viscosity, or the power of dissipative forces.

Using the transformation:

$$2\mu\varepsilon_{ij}\varepsilon_{ij}-\frac{2}{3}\mu(div\bar{v})^2 = 2\mu(\varepsilon^2_{11}+\varepsilon^2_{22}+\varepsilon^2_{33})+4\mu(\varepsilon^2_{12}+\varepsilon^2_{23}+\varepsilon^2_{31})-\frac{2}{3}\mu(div\bar{v})^2 =$$

$$=2\mu\left[\left(\varepsilon_{11}-\frac{2}{3}\mu(div\bar{v})^2\right)+\left(\varepsilon_{22}-\frac{2}{3}\mu(div\bar{v})^2\right)+\left(\varepsilon_{33}-\frac{2}{3}\mu(div\bar{v})^2\right)\right]+$$

$$+4\mu(\varepsilon^2_{12}+\varepsilon^2_{23}+\varepsilon^2_{31})-\frac{2}{3}\mu(div\bar{v})^2$$

one can rewrite Eq. (4.48) as:

$$W=\zeta(div\bar{v})^2-2\mu\left[\left(\varepsilon_{11}-\frac{1}{3}div\bar{v}\right)^2+\left(\varepsilon_{22}-\frac{1}{3}div\bar{v}\right)^2+\left(\varepsilon_{33}-\frac{1}{3}div\bar{v}\right)^2\right]+ \qquad (4.49)$$
$$+4\mu(\varepsilon^2_{12}+\varepsilon^2_{23}+\varepsilon^2_{31})$$

As $\zeta > 0, \mu > 0$, according to Eqs. (4.47) and (4.49), $W > 0$, and the work of the dissipative forces is always negative. If fluid moves as a solid (i. e., if $\varepsilon_{ik} = 0$) then $W = 0$.

By substituting Eq. (4.47) into the general heat-flow equation [Eq. (2.88)] gives the heat-flow equation for a viscous compressible fluid:

$$\frac{du}{dt} = q_e - \frac{p}{\rho} div + \frac{W}{\rho}. \tag{4.50}$$

From the kinetic energy law [Eq. (2.14)] and from Eq. (4.47), in the absence of external forces:

$$\frac{dK}{dt} = \frac{d}{dt}\int_V \rho \frac{v^2}{2} dV = \int_V \rho N^{(i)} dV = \int_V \left(p\, div\, \bar{v} - W\right) dV, \tag{4.51}$$

i. e., the kinetic energy in this case varies only due to the work of the internal forces.

For a viscous incompressible fluid, based on Eq. (4.49), Eq. (4.51) changes into the following format:

$$\frac{dK}{dt} = -\int_V W dV = -\int_V 2\mu\varepsilon_{ij}\mu\varepsilon_{ij} dV.$$

As $W > 0$, the kinetic energy declines due to the work of internal forces. The limiting value $W = 0$ is reached at $\varepsilon_{ik} = 0$. Therefore, in the absence of external forces, the limiting motion of a viscous incompressible fluid will be the solid body motion at which $\frac{dK}{dt} = 0$.

Let's now review some specific forms of the heat-flow and dissipative force equation.

1. The liquid is ideal and in compressible, i.e., $\mu = 0$, $\zeta = 0$, $div\bar{v} = 0$. From Eqs. Eqs. (4.47), (4.48) and (4.50):

$$N^{(i)} = 0, \quad W = 0, \quad \frac{du}{dt} = q_e.$$

Therefore, the work of internal forces (including the dissipative) is equal to zero. The internal energy can change only due to the heat supply.

2. The fluid is ideal and compressible. From Eqs. (4.47), (4.48) and (4.50):

$$N^{(i)} = \frac{p}{\rho} div\bar{v}, \quad W = 0, \quad \frac{du}{dt} = q_e - \frac{p}{\rho} div\bar{v}$$

It follows from the continuity equation that $\frac{d\rho}{dt} = -div\bar{v}$. Then:

$$N^{(i)} = -\frac{p}{\rho^2}\frac{d\rho}{dt}, \quad \frac{du}{dt} = q_e + \frac{p}{\rho^2}\frac{d\rho}{dt}.$$

Under expansion, $\frac{d\rho}{dt} < 0$ and $N^{(i)} > 0$. Under compression, $\frac{d\rho}{dt} > 0$ and $N^{(i)} < 0$. In case of an adiabatic process (no external heat supply), $q_e = 0$. Under compression, $\frac{du}{dt} > 0$, and the fluid heats-up, under expansion it cools down.

3. The fluid is viscous and in compressible. From (4.47), (4.48) and (4.50):

$$N^{(i)} = \frac{W}{\rho}, \quad W = 2\mu\varepsilon_{ik}\varepsilon_{ik} = 2\mu(\varepsilon^2_{11} + \varepsilon^2_{22} + \varepsilon^2_{33}) + 4\mu(\varepsilon^2_{12} + \varepsilon^2_{21} + \varepsilon^2_{13}) > 0$$

(4.52)

$$\frac{du}{dt} = q_e + \frac{W}{\rho}$$

The work of internal forces is caused by dissipation only. At $q_e = 0$, the work of dissipative forces increases the internal energy, i. e., heats the fluid.

Some important conclusions based on the above examples:

The work (power) is equal to zero only at the motion of an ideal incompressible fluid. In case of a compressible ideal fluid this work may cause an increase as well as a decrease in internal energy. At motion of a viscous incompressible fluid, the work of internal forces boils down to the work of the forces of friction and is always negative. The presence of friction results in the fluid heating.

Mechanics of Fluid Flow
by Kaplan S. Basniev, Nikolay M. Dmitriev and George V. Chilingar

CHAPTER V

BASICS OF THE DIMENSIONALITY AND CONFORMITY THEORY

The dimensionality and conformity theory establishes conditions for modeling and identifies parameters defining the major effects and regimes of the processes.

1. Systems of units. Dimensionality

In order to quantitatively describe a physical phenomenon, parameters of that phenomenon should be expressed in the form of numbers. These numbers are obtained by way of measuring, i. e., comparing (directly or indirectly) the measured physical value with an accepted standard as a measurement unit. Obviously, the numerical value of the measurement depends on the measurement unit, i. e. on the size of the accepted standard. For instance, the duration of a day may be expresses as 1 day = 24 (hours) = 1,440 (minutes) = 86,400 (seconds).

If the numeric significance of a measured physical value depends on the measurement unit (the size of the standards), such value is called dimensional (velocity, time, length, etc.).

The values whose numeric significance does not depend on the measurement unit are called dimensionless (circle length to its radius ratio, the ratio of a substance density to the water density, etc.). If the standards of the measurement unit is selected, *independent from the other*, for a sufficient number of physical values (for instance, describing mechanical phenomena), then based on that and using physical laws and definitions it may be possible to establish the measurement unit for all values in the description of the phenomena of interest. For instance, under the Newton's Second law, force is equal to the product of mass and acceleration. Thus, describing force with the physical units can be done through the units of length, mass and time and introduction of new standard is not necessary.

The measurement unit introduced using the standards whose numerical significance, by definition, is equal to one, are called the basic units of measurement.

The measurement units derived for the physical values from the basic units using the corresponding laws of physics or from the definitions of these values, are called the derived measurement units.

The aggregation of basic measurement units sufficient for measuring all physical values used for the description of some class of physical phenomena is called a system of measurement units.

The selection of both the basic measurement units and the systems of measurement units is rather arbitrary. For instance, in mechanics and its applications are used such systems of units as CGS (centimeter-gram-second), international system SI (meter-kilogram-second), MKS (meter-kilogram-force-second). Heinrich Hertz proposed a system based on the units of length, mass and energy. For the mechanics, the system containing either more or fewer than three basic measurement units can be constructed. That is why the criterion for the selection of the basic units of measure and their number in the system of units is their practicality.

In the above examples of the SI and CGS systems the basic measurement units include the standards physical values of length, mass and time. They are different only by the value of the standards. The MKS and Hertz's systems include a different set of standards, length, force, time or length, mass, energy.

The aggregation of measurement units, different only in the value of their standards rather than in their physical nature, is called a class of the measurement units systems. Thus, the SI and CGS systems belong to the same class, and the SI and MKS systems, to the different classes. Let's denote length as L, mass as M, time as T, and force as F. Then the class which the SI and CGS systems belong to may be denoted as LMT, and the class where MKS belongs, as LFT.

The dimensionality of a physical unit φ is usually denoted as $[\varphi]$. It represents the expression of derived measurement units through the basic units.

Under the Newton's Second law, the dimensionality of mass m in the MKS class is $[m]=\frac{[F]}{[a]}=\frac{FT^2}{L}$ where F is force, a is acceleration, and in the MLT class $[m] = M$.

By definition, the density ρ of a substance is the ratio of its mass m to its volume V. Thus in MLT and MKS classes, respectively:

$$[\rho]=\frac{[m]}{[V]}=\frac{M}{L^3}, \quad [\rho]=\frac{[m]}{[V]}=\frac{FT^2}{L^4}.$$

It shows that the unit of mass is basic in the MLT class and derived in the MKS class. The dimensionality of the density looks differently in the MLT and MKS classes. Therefore, one may call measurement units basic or derived *only* as it is applicable to the measurement units class under consideration.

Dividing the mass unit by the factor α, and the time unit, by the factor β, the number for the density value, following from the dimensionality in the MLT class, will change by the factor of $\alpha\beta^{-3}$. The same can be done for any other physical value.

Therefore, the dimensionality of a physical value is a function which determines how its numerical significance will change when converting the source measurement units system to the other system of units within the same class.

2. Dimensionality formula

The starting point for the derivation of the dimensionality formula is a statement that within the assigned class all unit systems are equivalent. It follows from this that the ratio of two numerical expressions of any derived value does not depend on the scale of the basic measurement unit within given class of measurement units. For instance,

$$\frac{S_1 m^2}{S_2 m^2} = \frac{S_1 cm^2}{S_2 cm^2}, \quad \frac{\rho_1 kg/m^3}{\rho_2 kg/m^3} = \frac{\rho_1 g/cm^3}{\rho_2 g/cm^3},$$

where S_1, S_2 are areas of some geometric configurations; ρ_1, ρ_2 are densities of two different media.

Assume that $u = f(x,y,z)$ is a derived dimensional value, and x, y, z are numerical significances of basic measurement units, for instance, length, mass and time. Also assume that u' is the significance of u value corresponding to the significances of arguments x', y', z'. Multiplying the basic measurement units by the factors α, β, γ:

$$\frac{u}{u'} = \frac{f(x,y,z)}{f(x',y',z')} = \frac{f(\alpha x, \beta y, \gamma z)}{f(\alpha x', \beta y', \gamma z')},$$

where from:

$$\frac{f(\alpha x, \beta y, \gamma z)}{f(x,y,z)} = \frac{f(\alpha x', \beta y', \gamma z')}{f(x',y',z')} = \varphi(\alpha, \beta, \gamma). \tag{5.1}$$

Thus, the ratio of numerically derived values depends only on the ratio of these scales. According to the above definition, the function $\varphi(\alpha,\beta,\gamma)$ is the dimensionality of value u.

Following from Eq. (5.1):

$$\varphi(\alpha_1,\beta_1,\gamma_1) = \frac{f(\alpha_1 x, \beta_1 y, \gamma_1 z)}{f(x,y,z)}, \quad \varphi(\alpha_2,\beta_2,\gamma_2) = \frac{f(\alpha_2 x, \beta_2 y, \gamma_2 z)}{f(x,y,z)}$$

or

$$\frac{\varphi(\alpha_1,\beta_1,\gamma_1)}{\varphi(\alpha_2,\beta_2,\gamma_2)} = \frac{f(\alpha_1 x, \beta_1 y, \gamma_1 z)}{f(\alpha_2 x, \beta_2 y, \gamma_2 z)}. \tag{5.2}$$

Assuming $\alpha_2 x = x'$, $\beta_2 y = y'$, $\gamma_2 z = z'$, then, from Eqs. (5.1) and (5.2):

$$\frac{f(\alpha x, \beta y, \gamma z)}{f(x,y,z)} = \frac{f\left(\frac{\alpha_1}{\alpha_2}x', \frac{\beta_1}{\beta_2}y', \frac{\gamma_1}{\gamma_2}z'\right)}{f(x',y',z')} = \varphi\left(\frac{\alpha_1}{\alpha_2}, \frac{\beta_1}{\beta_2}, \frac{\gamma_1}{\gamma_2}\right). \tag{5.3}$$

Taking derivative of Eq. (5.3) with respect to α_1:

$$\frac{1}{\varphi(\alpha_2,\beta_2,\gamma_2)} \frac{\partial \varphi(\alpha_1,\beta_1,\gamma_1)}{\partial \alpha_1} = \frac{1}{\partial \alpha_2} \frac{\partial \varphi\left(\frac{\alpha_1}{\alpha_2}, \frac{\beta_1}{\beta_2}, \frac{\gamma_1}{\gamma_2}\right)}{\partial\left(\frac{\alpha_1}{\alpha_2}\right)}.$$

Assuming that $\alpha_1 = \alpha = \alpha$, $\beta_1 = \beta_2 = \beta$, $\gamma_1 = \gamma_2 = \gamma$, then:

$$\frac{1}{\varphi(\alpha,\beta,\gamma)}\frac{\partial\varphi(\alpha,\beta,\gamma)}{\partial\alpha} = \frac{m}{\alpha}, \tag{5.4}$$

where:

$$m = \left[\frac{\partial\varphi\left(\frac{\alpha_1}{\alpha_2},\frac{\beta_1}{\beta_2},\frac{\gamma_1}{\gamma_2}\right)}{\partial\left(\frac{\alpha_1}{\alpha_2}\right)}\right]_{\frac{\alpha_1}{\alpha_2},\frac{\beta_1}{\beta_2},\frac{\gamma_1}{\gamma_2}=1} = \text{const}$$

Integrating Eq. (5.4) with respect to α, results in $\ln\varphi = m\ln\alpha + \ln C_1(\beta,\gamma)$. Thus:

$$\varphi = \alpha^m C_1(\beta,\gamma). \tag{5.5}$$

Substituting Eq. (5.5) into Eq. (5.3):

$$\left(\frac{\alpha_1}{\alpha_2}\right)^m \frac{C_1(\beta_1,\gamma_1)}{C_1(\beta_2,\gamma_2)} = \left(\frac{\alpha_1}{\alpha_2}\right)^m C_1\left(\frac{\beta_1}{\beta_2}\frac{\gamma_1}{\gamma_2}\right), \tag{5.6}$$

i. e., the same equation in the form of Eq. (5.3) exists. Continuing along the same way, i. e., taking derivative of Eq. (5.6) with respect to β_1, etc., results:

$$\varphi = C\alpha^m\beta^n\gamma^l.$$

Following from Eq. (5.1) that if $\alpha = \beta = \gamma = 1$ then $\varphi = 1$. Therefore, $C = 1$, and the dimensionality equation has the following format:

$$\varphi = \alpha^m\beta^n\gamma^l. \tag{5.7}$$

Thus, it is proven that the equation of physical value dimensionality has the an exponential mononomial format.

Following from Eq. (5.7) that for dimensionless values $m = n = l = 0$, $\varphi = 1$.

3. Values with independent dimensionalities

Let's review two the dimensionality of these values: velocity v, pressure p, density ρ and viscosity μ, throughflow Q, length l in the class MLT:

$$[v] = \frac{L}{T},\quad [p] = \frac{M}{LT^2},\quad [\rho] = \frac{M}{L^3},\quad [\mu] = \frac{M}{LT},\quad Q = \frac{l^3}{T}, [l] = L,$$

and:

$$[p] = [\rho]^\alpha[v]^\beta \text{ or } \frac{M}{LT^2} = \left(\frac{M}{L^3}\right)^\alpha\left(\frac{l}{T}\right)^\beta. \tag{5.8}$$

As the units of length, mass and time are mutually independent, by equating the exponents of L, M, T in Eq. (5.8):

$$\alpha = 1, -3\alpha + \beta = -1, \quad -\beta = -2,$$

where from $\alpha = 1, \beta = 2$ and $[p] = [\rho][v]^2$.

Similarly, for μ, Q, l:

$$[\mu] = [Q]^{\alpha}[l]^{\beta} \text{ or } \frac{M}{LT} = \left(\frac{L^3}{T}\right)^{\alpha} L^{\beta}.$$

The latter equation cannot be fulfilled at no α and β.

Therefore, the dimensionality of pressure may be expressed through the dimensionalities of density and velocity, and the dimensionality of viscosity cannot be expressed through the dimensionalities of throughflow and length.

First let's introduce the following definition. Suppose the aggregation k is given of dimensional physical values a_1, a_2, ... a_k. If the dimension of neither of these values can be expressed through the dimensionalities of the remaining k-1 values, the aggregation a_1, a_2, ... a_k is called a parameter aggregation with independent dimensionalities.

Following from this definition results that μ, Q, l form a parameter aggregation with independent dimensionalities, and p, ρ, v, a parameter aggregation with dependent dimensionalities.

Suppose a system of measurement is given with m basic units. It can be shown that in this system the number k of units with independent dimensionalities cannot be greater than m, i. e., $k \leq m$.

To simplify the reasoning, assume that $m = 3$ and the basic units are L, M, T. Suppose a_1, a_2, a_3, a_4 are dimensional units and also assume:

$$[a_4] = [a_1]^x[a_2]^y[a_3]^z. \tag{5.9}$$

According to the dimensionality equation Eq. (5.7), $[a_i] = [M]^{m_i}[L]^{n_i}[T]^{l_i}$, and the Eq. (5.9) can be rewritten as:

$$M^{m_4}L^{n_4}T^{l_4} = (M^{m_1}L^{n_1}T^{l_1})(M^{m_2}L^{n_2}T^{l_2})(M^{m_3}L^{n_3}T^{l_3})^z,$$

Thus, equating the L, M and T exponents:

$$\begin{aligned} m_1x + m_2y + m_3z &= m_4, \\ n_1x + n_2y + n_3z &= n_4, \\ l_1x + l_2y + l_3z &= l_4. \end{aligned} \tag{5.10}$$

By stipulation, α_4, β_4, γ_4 are not equal to zero simultaneously ($[a_4] \neq 1$). Thus, Eq. (5.10) represent a non-uniform system of three linear equations relative the unknown variables x, y, z.

Let's review the determinant of this system:

$$\Delta = \begin{vmatrix} m_1 & m_2 & m_3 \\ n_1 & n_2 & n_3 \\ l_1 & l_2 & l_3 \end{vmatrix}.$$

If $\Delta \neq 0$, the system of Eq. (5.10) has a singular solution; therefore, the Eq. (5.9) is valid. Thus, the a_4 value is dimensionally-dependent, and $k = 3$.

If $\Delta = 0$, the determinant's columns are in linear correlation, such as:

$$\lambda m_1 = \lambda m_2 + \nu m_3,\ \lambda n_1 = \lambda n_2 + \nu n_3,\ \lambda l_1 = \lambda l_2 + \nu l_3$$

$$[a_1]^{\lambda} = [a_2]^{\mu}[a_3]^{\nu}.$$

The cases $\mu = \nu = 0$, $\mu = \lambda = 0$, $\lambda = \nu = 0$ are excluded as, by stipulation, a_1, a_2, a_3 are dimensional values. Therefore, at $\Delta = 0$, the a_1, a_2, a_3 values are dimensionally-dependent, and $k < 3$.

Apparently, the same procedure may be expanded to include the case $m > 3$.

Following from the above proof that if a_1, a_2, ... a_k at $k = m$ have independent dimensionalities, then the dimensionality of any dimensional value a_{k+1} may be expressed as:

$$[a_{k+1}] = [a_1]^{m+1}[a_2]^{m+2}...[a_k]^{m+k}. \tag{5.11}$$

Following from Eq. (5.11) that at $k = m$, the values a_1, a_2, ... a_k can be accepted as a new system of measurement units.

4. Π-theorem

The Π-theorem is the fundamental theorem of the dimensionality theory. To prove it, first it is necessary to review one auxiliary statement.

Suppose within a measurement unit system of a given class there is an aggregate of physical values a_1, a_2, ... a_k having independent dimensionalities. It will be shown that within the given class it is possible to switch to such a units of measure system where the numerical significance of any of the a_1, a_2, ... a_k values (for instance, a_1) will change by an arbitrary factor A, and the numerical significances of all other values will remain unchanged.

Suppose there are m basic units of measure P, Q, ... in the selected class. Then, according to the earlier proved therorem:

$$[a_1] = P^{\alpha_1}Q^{\beta_1}..., \quad [a_2] = P^{\alpha_2}Q^{\beta_2}..., \quad [a_k] = P^{\alpha_k}Q^{\beta_k}...,$$

where at least one of the α_i, β_i significances ($i = 1,2,... m$) is different from zero.

Change the scale of the basic measurement units by the factor P, Q, ... so that the numerical significance of the others remained unchanged. Then:

$$[P^{\alpha_1}Q^{\beta_1}... = A, \quad P^{\alpha_2}Q^{\beta_2}... = 1, \quad ..., \quad P^{\alpha_k}Q^{\beta_k}... = 1. \tag{5.12}$$

Taking the natural logarithm of Eq. (5.12):

$$\begin{aligned} \alpha_1 \ln P + \beta_1 \ln Q + ... &= \ln A, \\ \alpha_2 \ln P + \beta_2 \ln Q + ... &= 0, \\ &\cdots\cdots\cdots \\ \alpha_k \ln P + \beta_k \ln Q + ... &= 0, \end{aligned} \tag{5.13}$$

i. e., resulting in a system of k linear algebraic equations for the unknown transitional multipliers P, Q, ...

It is proved above that the number of parameters with independent dimensionalities k is less or equal to the number of the basic units of measure, i. e., $k \leq m$. Suppose $k = m$. The determinant of the Eq. (5.13) system is different from zero as otherwise a linear dependence would exist between its columns, and the a_1, a_2, ... a_k values would have dependent dimensionalities, which is contrary to the original statement. Hence, at $k = m$ the system Eq. (5.13) have a singular solution.

When $k < m$, the number of equations is less than the number of unknown variables, and the system Eq. (5.13) has an infinite multiplicity of solutions.

Thus, statement is proved.

Now it is important to prove the Π-theorem.

Suppose the function:

$$a = f(a_1, a_2, \ldots, a_k, a_{k+1}, \ldots, a_n), \tag{5.14}$$

whose arguments a_1, a_2, ... a_k have independent variables, represents a physical correlation. The mathematical form of this correlation is not important here.

Selecting various measurement units systems is possible to change arbitrarily the numerical significances of the function f arguments. It is clear, however, that the physical correlation, i. e., the format of the f function cannot depend on the applied measurement units system. In other words, the physical correlations must be invariant relative the applied measurement units systems.

As it was shown in Section 3, the dimensionalities of the a, a_{k+1}, ... a_n values can be expressed through the dimensionalities of values with independent dimensionalities, i. e.:

$$[a] = [a_1]^{\alpha}[a_2]^{\beta}\ldots[a_k]^{\gamma}, \quad [a_{k+1}] = [a_1]^{\alpha_{k+1}}[a_2]^{\beta_{k+1}}\ldots[a_k]^{\gamma_{k+1}},$$
$$[a_n] = [a_1]^{\alpha_n}[a_2]^{\beta_n}\ldots[a_k]^{\gamma_n}. \tag{5.15}$$

Consider the following parameters:

$$\Pi = \frac{a}{a_1^{\alpha} a_2^{\beta} \ldots a_k^{\gamma}}, \quad \Pi_i = \frac{a_{k+1}}{a_1^{\alpha_{k+1}} a_2^{\beta_{k+1}} \ldots a_k^{\gamma_{k+1}}}, \; i = 1,2, \ldots, n\text{-}k. \tag{5.16}$$

Following Eq. (5.15), the Eq. (5.16) values are dimensionless.

Substituting the Eq. (5.16) into Eq. (5.14):

$$\Pi a_1^{\alpha} a_2^{\beta} \ldots a_k^{\gamma} = f(a_1, a2, \ldots, ak, \quad \Pi a_1^{\alpha_1} a_2^{\beta_1} \ldots a_k^{\gamma_1}, \ldots, \quad \Pi_{n-k} a_1^{\alpha_n} a_2^{\beta_n} \ldots a_k^{\gamma_n} \text{ or}$$

$$\Pi = \Phi(a_1, a_2, \ldots, a_k, \quad \Pi_1, \Pi_2, \ldots, \Pi_{n-k}. \tag{5.17}$$

As it was proved above, by changing the scale of the basic measurement units it is possible to change an arbitrary factor the numeric significance of the a_1 value. Also it is possible to do it so that numerical values of the a_2, a_3,...a_k values remain unchanged. As the $\Pi, \Pi_1, \Pi_2, \ldots, \Pi_{n-k}$ parameters are dimensionless, their numerical values also do not change. This means that the function Φ does not depend on the argument a_1, and:

$$\Pi = \Phi(a_2, a_3, \ldots, a_k, \quad \Pi_1, \Pi_2, \ldots, \Pi_{n-k}).$$

Performing the same procedure consecutively for the parameters $a_2, a_3, ..., a_k$ from Eq. (5.17), results in:

$$\Pi = \Phi(\Pi_1, \Pi_2, ..., \Pi_{n-k}). \tag{5.18}$$

This result is the content of the Π theorem, or Buckingham's theorem. Suppose there is a physical pattern expressed as the correlation of some dimensional value on the dimensional determining parameters. This correlation can always be presented as a correlation of some dimensionless value on the dimensionless combination of the determining parameters. The number of these dimensionless combinations is less than the total number of the determining parameters with independent dimensionalities.

In other words, suppose the physical correlation Eq. (5.14) is established and suppose the $a_1, a_2, ..., a_k$ values have independent dimensionalities. In this case, Eq. (5.14) can be reduced to the Eq. (5.18) format where the dimensionless parameters $\Pi, \Pi_1, \Pi_2, ..., \Pi_{n-k}$ are computed from Eq. (5.16).

Following Eqs. (5.14) and (5.18) that when switching from the correlation Eq. (5.14) between the dimensional values to the dimensionless correlation Eq. (5.18), the number of arguments decreases by the number k of parameters with independent dimensionalities, and Eq. (5.18) is invariant relative to the applied measurement units systems.

The case $k = n$ is an important case. From Eqs. (5.16) and (5.18) that in such a case:

$$\Pi = \frac{a}{a_1^{\alpha} a_2^{\beta} ... a_k^{\gamma}} = C = \text{const} \quad \text{or} \quad a = C a_1^{\alpha} a_2^{\beta} ... a_k^{\gamma}. \tag{5.19}$$

It is critical to state that out of the total parameters $a_1, a_2, ..., a_n$ in Eq. (5.14), the parameter aggregate $a_1, a_2, ..., a_k$ with independent dimensionalities can be selected using various techniques. Thus, as it can be seen in Eq. (5.16), the dimensionless parameters $\Pi, \Pi_1, \Pi_2, ..., \Pi_{n-k}$ can have different formats at the same format of the Eq. (5.14).

Another point to be mentioned is that the substance of the Π-theorem is, in essence, in switching to the new units of measure system $a_1, a_2, ..., a_k$.

5. Conformity of physical phenomena, modeling

Let's review a description of a physical phenomenon in the assigned measurement units system. This system is denoted by the superscript (1). Now the scale of the basic measurement units is changed and the new system is denoted by the superscript (2). Then:

$$\Pi_i^{(1)} = \Pi_i^{(2)}, \quad \Pi^{(1)} = \Pi^{(2)}.$$

As defined by Robert Pohl, "a physical value is the product of the numerical significance and the unit of this value". In other words, $Y = y[y]$ where Y is a physical value, and y is its numerical significance in measurement units $[y]$. Changing

the Y parameter under the same rule as the measurement units $[y]$ is changed results in the same change in the y numerical significance. Indeed, the medium density ρ, as an example, is determined as the ratio of its mass m to volume V, i. e.:

$$\rho = \frac{m}{V}, \quad [\rho] = \frac{M}{L^3}.$$

Decreasing the unit of mass by the factor of 10 and increasing the unit of length by the factor of 10 results increasing the density's numerical value by the factor of $10/(10^{-1})^3 = 10^4$. Increasing the mass of the medium by the factor of 10 results in decreasing the linear dimensions of its volume by the factor of 10. The density's numerical value will also change by the factor of 10^4.

Now consider two similar physical phenomena (for instance, fluid flow in tubes). One of the physical phenomenon is called (N), for Nature, and the other one, (M), for Model. The physical parameters are selected in such a way that the following conditions are made:

$$\Pi_i^{(M)} = \Pi_i^{(N)}. \tag{5.20}$$

Then, as follows from the Π-theorem Eq. (5.18),

$$\Pi^{(M)} = \Pi^{(N)}. \tag{5.21}$$

When the conditions Eq. (5.20) are valid, the model and natural phenomena are called similar, and the Π_i values are called conformity criteria.

As stated by L. I. Sedov, "two phenomena are similar if from the parameters of one of them it is possible to derive the parameters of the second one using a simple computation resembling the transition from one measurement units system to another measurement units system".

From Eqs. (5.16) and (5.21) for the similar phenomena:

$$\left[\frac{a}{a_1^{\alpha} a_2^{\beta} \ldots a_k^{\gamma}}\right]^{(M)} = \left[\frac{a}{a_1^{\alpha} a_2^{\beta} \ldots a_k^{\gamma}}\right]^{(N)},$$

from where:

$$a^{(N)} = a^{(M)} \left(\frac{a_1^{(N)}}{a_1^{(M)}}\right)^{\alpha} \left(\frac{a_2^{(N)}}{a_2^{(M)}}\right)^{\beta} \ldots \left(\frac{a_k^{(N)}}{a_k^{(M)}}\right)^{\gamma}. \tag{5.22}$$

Therefore, when the conformity condition is observed, a model study of a physical phenomenon can be replaced for its the experimental study. On numerous occasions that is the only possibility.

The requirement to realize the Eq. (5.20) conditions shows which numerical significances of the process parameters should be selected in modeling, i. e., it determines the model parameters providing for the observation of the conformity.

Eq. (5.22) is a rule for the conversion of model results $a^{(M)}$ into the nature results $a^{(N)}$.

6. Parameters determining the class of phenomena

The mathematical correlation between the value a and the values $a_1, a_2, \ldots a_n$ in Eq. (5.14) can have different formats, i. e., it can describe different physical processes. Thus, the values $a_1, a_2, \ldots a_n$ are called parameters defining the class of phenomena. The a parameter is called definiendum.

In the cases when the mathematical model of a physical process is known, the table of parameters which define the class of phenomena is built from the equations and initial and boundary conditions defining the class. That is, an aggregation of dimensional and dimensionless values necessary and sufficient for the problem solution is written down. The dimensional constants are also included in the defining parameters.

If the mathematical model of a physical process is not known, the table of parameters can be prepared based on qualitative considerations and experimental data (if available).

The system of parameters defining the class of phenomena must have a property of *completeness*. It means that system must include parameters through the dimensionalities of the determining parameters.

For instance, it is not possible to state that the force F acting on a body from the liquid is a function only of its density ρ and flow velocity v, i. e., that $F = f(\rho,v)$. Indeed, as it is easy to see, the equality:

$$[F] = \frac{ML}{T^2} = \left(\frac{M}{L^3}\right)^{\alpha}\left(\frac{L}{T}\right)^{\beta}$$

is not possible at any numerical significances of α and β. It is possible to state, however, that $F = f(l,\rho,v)$ where l is a value with the dimensionality of length. Indeed, in this case:

$$[F] = \frac{ML}{T^2} = \left(\frac{M}{L^3}\right)^{\alpha}\left(\frac{L}{T}\right)^{\beta} L^{\gamma}.$$

From here it can be seen immediately that $\alpha = 1, \beta = 2, \gamma = 2$ and $F = \rho v^2 l^2$.

In a similar way, it cannot be stated that a tangential stress τ is a function of liquids' density and velocity gradient because:

$$[\tau] = \frac{M}{LT^2}, \quad [\nabla v] = \frac{1}{T} \quad \text{and} \quad \frac{M}{LT^2} \neq \left(\frac{M}{L^3}\right)^{\alpha}\left(\frac{1}{T}\right)^{\beta}.$$

At the same time, it is possible to state that $\tau = f(\rho,l,\nabla v)$ because:

$$[\tau] = \frac{M}{LT^2}[\rho][l]^2[\nabla v].$$

7. Examples of application of the Π-theorem

1. Weggling (oscillations) of a mathematical pendulum. The mathematical pendulum is a material point of mass m suspended by a weightless and unstretchable, immovable thread with length l attached at point O (Fig. 5.1). The equation of planar vibrations for such a pendulum is:

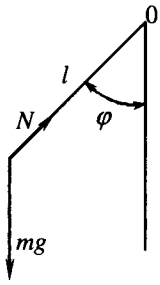

Fig. 5.1

$$\frac{d^2\varphi}{dt^2} = -\frac{g}{l}\sin\varphi, \quad m\left(\frac{d\varphi}{dt}\right)^2 l = N - mg\cos\varphi \qquad (5.23)$$

with the initial conditions:

$$\varphi = \varphi_0, \quad \frac{d\varphi}{dt} = 0 \quad \text{at } t = t_0, \qquad (5.24)$$

where φ is the angle between the thread and the vertical, N is thread tension and g is gravity acceleration. Following Eq. (5.23) and initial conditions [Eq. (5.24)] that the system of parameters defining the class of phenomena is:

$$\varphi_0, m, l, g, t.$$

Therefore,

$$\varphi = \varphi(\varphi_0, m, l, g, t), N = n(\varphi_0, m, l, g, t)$$

Assume as parameters with independent dimensionalities the m, g, l values. Then under the Π-theorem, i. e., Eqs. (5.16) and (5.18):

$$\Pi = \varphi(\Pi_1,\Pi_2), \Pi' = N(\Pi_1',\Pi_2'),$$

where:

$$\Pi = \varphi, \Pi_1 = \varphi_0, \Pi_2 = \frac{t}{m^\alpha l^\beta g^\gamma}, \Pi' = \frac{N}{m^{\alpha_1} l^{\beta_1} g^{\gamma_1}}, \quad ...\Pi_1' = \Pi_1, \quad \Pi_2' = \Pi_2, \quad (5.25)$$

as φ and φ_0 are dimensionless values and the "y" arguments of the functions φ and N are the same.

Based on Eq. (5.25):

$$[t] = [m]^\alpha [l]^\beta [g]^\gamma, \quad [N] = [m]^{\alpha_1} [l]^{\beta_1} [g]^{\gamma_1}$$

or:

$$T = M^\alpha L^\beta \left(\frac{L}{T^2}\right)^\gamma, \quad \frac{M}{LT^2} = M^{\alpha_1} L^{\beta_1} \left(\frac{L}{T^2}\right)^{\gamma_1}.$$

From this, equating the exponents of M, L and T:

$$\alpha = 0, \beta + \gamma = 0, \ -2\gamma = 1, \alpha_1 = 1, \beta_1 + \gamma_1 = 1, -2\gamma_1 = -2,$$

or:

$$\alpha = 0, \beta = \frac{1}{2}, \gamma = \frac{1}{2}, \alpha_1 = 1, \beta_1 = 0, \gamma_1 = 1,$$

and:

$$\Pi_2 = t\sqrt{\frac{g}{l}}, \quad \Pi' = \frac{N}{mg}.$$

Therefore:

$$\varphi = \varphi\left(\varphi_0, t\sqrt{\frac{g}{l}}\right), \quad \frac{M}{mg} = f\left(\varphi_0, t\sqrt{\frac{g}{l}}\right).$$

It is known from experience that the oscillations of a mathematical pendulum have period τ. Then:

$$\tau = \tau(\varphi_0, m, l, g)$$

or, after switching to dimensionless values:

$$\tau\sqrt{\frac{g}{l}} = \tau(\varphi_0).$$

The oscillations are symmetric, thus $\tau(\varphi_0) = -\tau(\varphi_0)$; therefore, the $\tau(\varphi_0)$ function is even. Expanding this function into a series, results:

$$\tau(\varphi_0) = C_1 + C_2\varphi_0^2 + C_3\varphi_0^4 + \ldots$$

Disregarding small oscillations ($\varphi_0 << 0$) the terms of the order φ_0^2 and higher, results:

$$\tau = C_1\sqrt{\frac{l}{g}}.$$

It is known from the theory, i. e., from the solutions of Eq. (5.23) at $\varphi_0 << 1$, that $C_1 = 2\pi$.

2. Clapeyron equation. Assume as a hypothesis that pressure p in gas is totally defined by its density ρ, its heat capacity c_v (or c_p) and Kelvin temperature Θ. Then:

$$p = f(\rho, c_v, \Theta).$$

The ρ, c_v and Θ values have the dimensionalities of:

$$[\rho] = \frac{M}{L^3}, \quad [c_v] = \frac{L^2}{T^2\,{}^oK}, \quad [\Theta] = {}^oK,$$

i. e., form the parameter system with independent dimensionalities. Then, according to Eq. (5.19):

$$p = C\rho^{\alpha}, c_v^{\beta}, \Theta^{\gamma}, \; C = \text{const}.$$

It is easy to see that $\alpha = \beta = \gamma = 1$, and:

$$p = C\rho c_v\Theta = R\rho\Theta, \; R = Cc_v.$$

Thus, the Clapeyron equation is based on the stated hypothesis.

The reviewed examples provide a good illustration to strengths and weaknesses of the dimensionality theory. Indeed, by analyzing dimensionalities we obtain the structure of equations for τ and p, but it is not possible to determine with this analysis the numerical significances of C_1 and C constants.

3. Darcy's filtration law. Consider the filtration rate velocity modulus w within a horizontal uniform layer depends only on the pressure gradient modulus $|\nabla p|$, viscosity μ, porosity m and module d. Then:[1]

$$\bar{v} = f(\nabla p, \mu, m, d). \tag{5.26}$$

The values ∇p, μ, m, d have dimensionalities:

$$[\nabla p] = \frac{M}{L^2T^2}, \quad [\mu] = \frac{M}{LT}, \quad [m] = 1, \quad [d] = L.$$

Therefore, $\nabla p, \mu, d$ form a parameter system with independent dimensionalities, and:

$$\frac{w}{(\nabla p)^\alpha \mu^\beta d^\gamma} = f(m).$$

Analyzing the dimensionalities similar to the example 1, results:

$$\frac{L}{T} = \left(\frac{M}{L^2T^2}\right)^\alpha \left(\frac{M}{LT}\right)^\beta L^\gamma, \quad \alpha + \beta = 0, \quad -2\alpha - \beta + \gamma = 1, \quad 2\alpha + \beta = 1,$$

from here $\alpha = 1$, $\beta = -1$, $\gamma = 2$, and:

$$w = -\frac{d^2}{\mu} f(m) |\nabla p|$$

or, in the vector format:

$$\bar{w} = -\frac{d^2}{\mu} f(m) \nabla p. \tag{5.27}$$

The minus sign is introduced in Eq. (5.27) because $\bar{v}$ and ∇p have opposite directions.

4. Darcy-Weisbach equation. Consider the liquid flow through a horizontal cylindrical tube, the pressure gradient per unit length of the tube $\Delta p / l$ depends on the average liquid's flow velocity v, liquid's viscosity μ, its density ρ, tube diameter d and the wall roughness Δ.

Then:

$$\frac{\Delta p}{l} = f(d, \Delta, \rho, \mu, v). \tag{5.28}$$

The ρ, v, d values form a parameter system with independent dimensionalities. Therefore, based on the Π-theorem Eq. (5.28) may be written as:

$$\Pi = \Phi(\Pi_1, \Pi_2), \tag{5.29}$$

where:

$$\Pi = \frac{\Delta p}{l} \rho^\alpha v^\beta d^\gamma, \quad \Pi_1 = \frac{\Delta}{d}, \quad \Pi_2 = \frac{\mu}{\rho^{\alpha_1} v^{\beta_1} d^{\gamma_1}}.$$

[1] Liquid's density enters the motion equations only as a multiplier of the acceleration. The acceleration is usually negligibly small at filtration. That is why it is possible to disregard in Eq. (5.26) possible correlation with density.

The dimensionality analysis results in $\alpha = 1, \quad \beta = 2, \quad \gamma = -1$. Therefore:

$$\Pi = \frac{\Delta p * d}{l\rho v^2}, \quad \Pi_2 = \frac{\mu}{\rho v d}.$$

Substituting it into Eq. (5.29), results:

$$\Delta p = \frac{l}{d}\rho v^2 \Phi\left(\frac{\Delta}{d}, \frac{\mu}{\rho v d}\right) = \frac{l}{d}\rho w^2 \Phi_1\left(\frac{\Delta}{d}, \frac{\rho v d}{\mu}\right).$$

Denoting, as it is customary:

$$\frac{\Delta}{d} = \varepsilon, \quad \frac{\rho v d}{\mu} = \mathrm{Re}, \quad \Phi\left(\frac{\Delta}{d}, \frac{\mu}{\rho v d}\right) = \frac{\lambda(\varepsilon, \mathrm{Re})}{2}$$

(where ε is relative roughness of the tube's walls, Re is the Reynolds number, λ is the hydraulic resistivity coefficient), gives the Darcy-Weisbach equation:

$$\Delta p = \lambda \frac{l}{d}\frac{\rho v^2}{2}. \tag{5.30}$$

The ε, Re coefficients in this case are obviously the conformity criteria. Therefore, having determined the $\lambda(\varepsilon, \mathrm{Re})$ value for a liquid flow, concludes that for the flow of a different liquid through a different tube, the hydraulic resistivity coefficient λ, on condition $\varepsilon^{(1)} = \varepsilon^{(2)}$, $\mathrm{Re}^{(1)} = \mathrm{Re}^{(2)}$, will have the same numerical significance.

When the flow is laminar, the acceleration is zero; hence, the ρ's numerical significance is negligible. The experience shows that in such a case the Δ's numerical significance is also negligible. So, the Eq. (5.28) for the laminar flow is given by:

$$\frac{\Delta p}{l} = f(d, \mu, v).$$

As the d, μ, v parameters have independent dimensionalities; then, according to Eq. (5.19):

$$\frac{\Delta p}{l} = C d^{\alpha} \mu^{\beta} v^{\gamma}).$$

It is easy to see that $\alpha = -2, \quad \beta = \gamma = 1$, and:

$$\Delta p = C \frac{1}{d^2} \mu v. \tag{5.31}$$

Equating the right parts of Eqs. (5.30) and (5.31), it can be found that the hydraulic resistivity factor at laminar flow is:

$$\lambda = \frac{2C\mu}{\rho v d} = \frac{2C}{\mathrm{Re}}, \quad C = \mathrm{const}.$$

Theoretical analysis comes up with a numerical significance for $C = 32$.

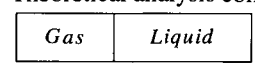

Fig. 5.2

5. Reservoir liquid displacement by gas. Consider a uniform horizontal layer from which the liquid is being displaced by a gas (Fig. 5.2). The displacement rate α is given by:

$\alpha = \frac{V_{gas}}{V}$ where V_{gas} is the volume of area I occupied by the gas, and V is the volume of all pores in this area.

It may be stated, based on qualitative considerations and experiments, that:

$$\alpha = \alpha(k, m, \sigma, \Theta, \Delta p, l, \mu_{gas}, \mu_{liquid}, h, \Delta\gamma, p, c, M, t), \qquad (5.32)$$

where k and m are layer's permeability and porosity; σ is liquid's surface tension; Θ is contact angle; $\Delta p = (p_1 - p_2)$ is pressure difference between the end of the layer section with the length l; μ_{gas}, μ_{liquid} are viscosities of gas and liquid; h is layer's thickness, $\Delta\gamma = \gamma_{gas} - \gamma_{liquid}$ is specific gravity difference between the liquid and gas; p is absolute pressure in any cross-section of the layer; c is the surfactant concentration; M is formation water salinity; and t is time.

The values in Eq. (5.32) have the following dimensionalities:

$$[k] = L^2, \quad [\sigma] = \frac{M}{T^2}, \quad [\Delta p] = [p] = \frac{M}{LT^2}, \quad [l] = [h] = L,$$

$$[\mu_{gas}] = [\mu_{liquid}] = \frac{M}{LT}, \quad [\Delta\gamma] = \frac{M}{L^2T^2}.$$

Assume that the l, Δp, μ_{gas} values have independent dimensionalities. Using Π-theorem, Eq. (5.32) can be written as:

$$\alpha = \alpha\left(\frac{k}{l^2}, m, \frac{\sigma}{l\Delta p}, \Theta, \frac{\mu_{liquid}}{\mu_{gas}}, \frac{h}{l}, \frac{l\Delta\gamma}{\Delta p}, \frac{p}{\Delta p}, c, M, \frac{t\Delta p}{\mu_{gas}}\right). \qquad (5.33)$$

Modeling the displacement process using natural fluids and porous media (physicochemical conformity) gives:

$$\mu_{gas}^{(natural)} = \mu_{gas}^{(model)}, \quad \Delta\gamma^{(natural)} = \Delta\gamma^{(model)}, \quad \sigma^{(natural)} = \sigma^{(model)}. \qquad (5.34)$$

To observe conformity, the following conditions in particular must be observed as Eq. (5.33) shows:

$$\left(\frac{l\Delta\gamma}{\Delta p}\right)^{(natural)} = \left(\frac{l\Delta\gamma}{\Delta p}\right)^{(model)}, \quad \left(\frac{\sigma}{l\Delta p}\right)^{(natural)} = \left(\frac{\sigma}{l\Delta p}\right)^{(model)},$$

from where, if the Eq. (5.34) conditions are observed, it follows that at the same time these equalities must be realized:

$$\frac{\Delta p^{(model)}}{\Delta p^{(natural)}} = \frac{l^{(model)}}{l^{(natural)}}, \quad \frac{\Delta p^{(model)}}{\Delta p^{(natural)}} = \frac{l^{(natural)}}{l^{(model)}}.$$

This is possible only if $l^{(model)} = l^{(natural)}$, so when working with natural media, it is impossible to observe a complete conformity between the model and nature, and it is necessary resort to partial modeling.

The partial modeling is such that only for some conformity criteria the equality is observed. The effect of nonobservance of other criteria equality is estimated

by different methods depending on the phenomenon under study. The problems of partial modeling are encountered in solving problems in aviation, shipbuilding and other disciplines.

In dealing with the displacement issues, the conformity criteria of the following format may be found in publications:

$$\Pi_1 = \frac{\sigma}{\sqrt{\frac{k}{m}}\Delta p}, \quad \Pi_2 = \frac{\sigma l}{k\Delta p}, \quad \Pi_3 = \frac{\sigma}{h\sqrt{\frac{k}{m}}\Delta\gamma}, \quad \Pi_4 = \cos\Theta.$$

Considering the conformity criteria in Eq. (5.33), respectively, as:

$$\Pi'_1 = \frac{k}{l^2}, \quad \Pi'_2 = m, \quad \Pi'_3 = \frac{\sigma}{l\Delta p}, \quad \Pi'_4 = \Theta, \quad \Pi'_5 = \frac{h}{l}, \quad \Pi'_6 = \frac{l\Delta\gamma}{\Delta p}.$$

As easy to see:

$$\Pi_1 = \Pi'_3\sqrt{\frac{\Pi'_2}{\Pi'_1}}, \quad \Pi_2 = \frac{\Pi'_3}{\Pi'_1}, \quad \Pi_3 = \frac{\Pi'_3}{\Pi'_5\Pi'_6}\sqrt{\frac{\Pi'_2}{\Pi'_1}}, \quad \Pi_4 = \cos\Pi'_4.$$

This example may serve an illustration to the note in Section 4. that the selection of dimensionless parameters when using the Π-theorem is not singular.

8. Contraction of equations to dimensionless format

When conducting numerical calculations, the corresponding equations and their analytical solutions are usually contracted to a dimensionless format. As follows from Π-theorem, it enables two things. First, it allows for a decrease in a number of arguments of the definiendum functions. Second, by selecting the corresponding modules of the process, it allows to find most convenient numerical ranges for dimensionless parameters.

Indeed, suppose the problem to be solved includes n defining parameters. For its comprehensive numerical study it is necessary to vary each parameter m times independently of the others. i. e., it is necessary to perform m^n computations. After contracting to the dimensionless format, the number of parameters will be m-k where k is the number of parameters with independent dimensionalities. Therefore, the number of the necessary calculations will be m^{n-k}.

Consider another example. One of the parameters in a problem of the pressure shock is the length of the tube l. The lengthwise coordinate x is within the $0 \le x \le l$. Assuming $x = \xi l$, regardless of the tube's length the dimensionless coordinate ξ varies within the $0 \le \xi \le 1$ range.

Now consider the problem of contracting to a dimensionless format using as the example of the motion equations system for a uniform viscous incompressible fluid [Eq. (4.42)]. The motion equations and the boundary conditions in this case have the following format:

$$\mathrm{div}\bar{v} = 0, \quad \rho\frac{d\bar{v}}{dt} = \rho\bar{F} - \nabla p + \mu\Delta\bar{v}, \quad \bar{v} = \bar{V} \quad \text{over} \quad S. \qquad (5.35)$$

Suppose $x_i = Lx'_i$ where L is linear module in the problem, and the geometric conformity is assumed in the problems of a similar class. Further assume $\bar{v} = V_0\bar{v}'$, $p = \Pi p'$, $t = \Theta t'$, where V_0, Π, Θ are characteristic velocity, pressure and time in the problem. For the fluid flow in a tube, for instance, its diameter is L, the average velocity at some moment in time may be the V_0, the pressure difference at the ends of the tube may be Π, and the time of the transitional process (at the non-stationary motion) may be Θ. Similarly, the characteristic parameters L, V_0, Π, Θ may be introduced in the study of any flow. Further assume, for certainty, that $\bar{F} = \bar{g}$. Substituting x_i, $\bar{v}$, p, t into Eq. (5.35) and unrolling the $\frac{dv}{dt}$ derivative, results:

$$\frac{\partial v'_i}{\partial x'_i} = 0, \quad \rho\left(\frac{V_0}{\Theta}\frac{\partial v'}{\partial x'} + \frac{V_0^2}{L}v'_i\frac{\partial v'}{\partial x'_i}\right) = \rho\bar{g} - \frac{\Pi}{L}\bar{e}_k\frac{\partial p'}{\partial x'} + \frac{\mu V_0}{L^2}\bar{e}_k\frac{\partial^2 v'_k}{\partial x'^2_k}, \quad \bar{v}' = \bar{V}'. \quad (5.36)$$

Eq. (5.36) shows that the continuity equation and the boundary condition maintain their format after the switch to dimensionless values. By dividing all terms of the Navier-Stokes equation by $\rho V_0^2/L$ results:

$$\frac{L}{V_0\Theta}\frac{\partial \bar{v}'}{\partial t'} + \frac{\partial \bar{v}'}{\partial x'_i} = \frac{gL}{V_0^2}\bar{g}^0 - \frac{\Pi}{\rho V_0^2}\bar{e}_i\frac{\partial p'}{\partial x'} + \frac{\mu}{\rho V_0 L}\bar{e}_i\frac{\partial^2 v'_i}{\partial x'^2_i},$$

where $\bar{g}^0$ is the basis vector of the $\bar{g}$ vector.

Let's introduce the following designations:

$\frac{L}{V_0\Theta} = \mathrm{Sh}$ is the Strouhal number; $\frac{V_0^2}{gL} = \mathrm{Fr}$ is the Froude number[2]; $\frac{\Pi}{\rho V_0^2} = \mathrm{Eu}$ is the Euler's number; $\frac{\rho V_0 L}{\mu} = \mathrm{Re}$ is the Reynolds number.

Using these designation, the Navier-Stokes equation can be written as follows:

$$\mathrm{Sh}\frac{\partial \bar{v}'}{\partial t'} + \frac{\partial \bar{v}'}{\partial x'_i} = \frac{g^0}{\mathrm{Fr}} - \mathrm{Eu}\bar{e}_i\frac{\partial p'}{\partial x'} + \frac{1}{\mathrm{Re}}\bar{e}_i\frac{\partial^2 v'_i}{\partial x'^2_i}.$$

If in two flows the conditions of the flow areas geometrical conformity and the relationships $\mathrm{Sh}_1 = \mathrm{Sh}_2$, $\mathrm{Fr}_1 = \mathrm{Fr}_2$, $\mathrm{Re}_1 = \mathrm{Re}_2$ are realized, these flows are conformable. The Eu number is often not important for the flow of an incompressible fluid. The reason is that the Navier Stokes equation includes not the pressure but pressure gradient. That is why a pressure change within the entire flow volume by a constant

[2] In publications, the $\frac{V_0}{\sqrt{2gL}}$ value is commonly taken for the Froude number.

numerical value (or, which is the same, a change in the characteristic pressure by a constant numerical value) does not affect the flow nature. That is why the Euler's number may be assigned any numerical value. In particular, assuming $\Pi = \rho V_0^2$, the Euler's number Eu = 1.

To find the physical meaning of the conformity criteria, let's review a parallelepiped within the fluid with the edges dx_i, and mass m. The following forces acting on the parallelepiped:

– gravitational force $Fg = mg = \rho g dx_1\, dx_2\, dx_3 \sim \rho g L^3$;

– local inertia force $F_{loc} = m\dfrac{\partial v}{\partial t} \sim \rho L^3 \dfrac{V_0}{\Theta}$;

– convective inertia force $F_{con} = mv\dfrac{\partial v}{\partial x} \sim \rho L^3 \dfrac{V_0^2}{L}$;

– and friction $F_{fric} = \dfrac{\partial \tau}{\partial x} dxdS = \mu \dfrac{\partial^2 v}{\partial x^2} dxdS \sim \mu \dfrac{V_0^2}{L^2} L^3$.

Then:

$$\frac{F_{loc}}{F_{con}} = \frac{L}{\Theta V_0} = \mathrm{Sh}, \frac{F_{con}}{F_g} = \frac{V_0^2}{gL} = \mathrm{Fr}, \frac{F_{con}}{F_{fric}} = \frac{\rho V_0 L}{\mu} = \mathrm{Re}.$$

PART II. HYDROMECHANICS

CHAPTER VI

HYDROSTATICS

1. Liquids and gas equilibrium equations

Hydrostatics deals with the equilibrium laws of fluids. If the fluid is static relative to the walls of the enclosing vessel, and the vessel is static or moving at a contant speed relative to the Earth, the quiescent state is called absolute. If the fluid is static relative to the walls of the enclosing vessel, and the vessel is moving relative to the Earth with acceleration, the quiescent state is called relative. The fluid motion in the case of relative quiescent state may be considered as translational.

These definitions indicate that under the absolute quiescent state liquid is acted upon by the force of gravity, and under the relative quiescent state it is acted upon by the force of gravity and the force of the translational motion.

The deformation rate $\varepsilon_{ik} = 0$ in a quiescent liquid; thus, from the rheologic equation for a viscous liquid Eq. (4.29):

$$p_{ik} = -p\delta_{ik}, \tag{6.1}$$

i. e., only normal compressing stress is acting in a quiescent liquid. L. Prandtl stated that "a liquid is such a body where in the state of equilibrium any resistance to deformation is zero". Following Prandtl statement, $p_{ik} = 0$ $(i \neq k)$ and, under Eq. (4.29), $\varepsilon_{ik} = 0$. The size of this stress does not depend on the direction and is called pressure. This pressure is called hydrostatic pressure.

Substituting Eq. (6.1) into the continuous medium motion equations in stresses [Eq. (2.42)], gives $\left(\frac{dv_j}{dt} = 0\right)$:

$$\frac{\partial p}{\partial x_j} = \rho F_j, \text{ or } \nabla p = \rho \overline{F}. \tag{6.2}$$

Eq. (6.2) is called the Euler's equation in hydrostatics.

By the scalar multiplication of Eq. (6.2) and singular vector $\overline{s}^0$:

$$\frac{\partial p}{\partial S} = \rho \overline{F}\overline{s}^0 = \rho F_s, \tag{6.3}$$

i. e., the pressure change in a direction $\bar{s}$ is determined by the projection of the mass force F_s in this direction.

Multiplying (scalar multiplication) Eq. (6.2) by dx_j and under equilibrium $p = p(x_j)$ then:

$$\frac{\partial p}{\partial x_j} dx_j = dp = \rho F_j dx_j, \text{ or } dp = \rho \bar{F} * d\bar{r}. \tag{6.4}$$

The surfaces along which $p = \text{const}$ are called isobars. Following from Eq. (6.4), the isobar equation has the following format:

$$F_j dx_j = 0, \text{ or } \bar{F} * d\bar{r} = 0, \tag{6.5}$$

where the vector $d\bar{r}$ lies on the plane tangential to the isobar. Following from Eq. (6.5), the mass force stress is normal to the isobar. The same conclusion directly follows from Eq. (6.2).

It is obvious that Eqs. (6.2)–(6.5) are equally valid for both compressible and incompressible fluids.

From Eq. (6.4):

$$\int_{p_0}^{p} \frac{dp}{\rho} = \int_{M_0}^{M} \bar{F} * d\bar{r}, \tag{6.6}$$

where M, M_0 are points where hydrostatic pressures are, respectively, p and p_0. If the mass force have potential (i. e., $\bar{F} = -\nabla\Pi$), Eq. (6.6) takes the format:

$$\int_{p_0}^{p} \frac{dp}{\rho} = \int_{M_0}^{M} d\Pi = \Pi(M) - \Pi(M_0). \tag{6.7}$$

2. Equilibrium of a liquid in the gravitational field

For reviewing the liquid equilibrium in the gravitational field it is necessary to introduce a coordinate system $0xyz$ where the $0z$ axis is directed against the gravity force $\bar{g}$ (Fig. 6.1). In this case, $\Pi = -gz$, $F_x = F_y = 0$, $Fz = -g$, and Eq. (6.4) looks as follows:

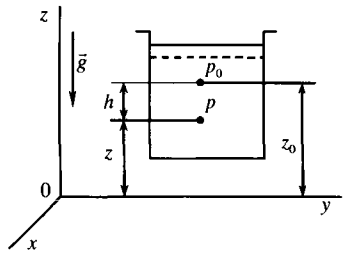

Fig. 6.1

$$dp = -\rho g dz. \tag{6.8}$$

In the case of a uniform incompressible fluid $\rho = \text{const}$, and from Eq. (6.8):

$$P = -\rho g z + C, \; C = \text{const}. \tag{6.9}$$

Eq. (6.9) is valid for any point within the liquid' volume. The isobar equation in this case has a format:

$$dz = 0, \text{ or } z = C = \text{const}. \tag{6.10}$$

Thus, when a fluid in the gravitational field is in the state of equilibrium, the isobar is a horizontal plane.

In order to determine the constant C in Eq. (6.9) it is necessary to assign boundary conditions. Assume that at $z = z_0$, $p = p_0$ (Fig. 6.1). Then:

$$p - p_0 = \rho g(z_0 - z), \tag{6.11}$$

or

$$\frac{p}{\rho g} + z = \frac{p_0}{\rho g} + z_0 . \tag{6.12}$$

Calling $z_0 - z = h$, Eq. (6.11) takes the following format:

$$p = p_0 + \rho g h, \tag{6.13}$$

where $\rho g h$ is pressure created by the liquid's column with the height h.

Eqs. (6.8), (6.12) are usually called the basic equation of hydrostatics. Following Eq. (6.13) that the force of the liquid's pressure on the vessel's bottom with base S does not depend on the vessel's shape (Fig. 6.2) and equals $(p_0 + \rho g h)S$. This result is called Pascal's paradox.

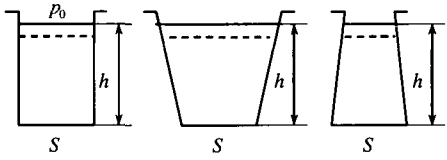

Fig. 6.2

The excess of the absolute pressure p_{abs} over the atmospheric pressure p_{atm}, i.e., the difference:

$$p_m = p_{abs} - p_{atm},$$

is called the manometric pressure. The value: $p_{vac} = p_{atm} - p_{abs}$ at $p_{atm} > p_{abs}$ is called vacuum.

Now it is desired to review some application examples of the hydrostatics equations.

1. Communicating vessels (Fig. 6.3). Pressure on the free surfaces with coordinates z_1 and z_2 is equal. Therefore, they are areas of a single isobaric surface and, in compliance with Eq. (6.9), $z_1 = z_2$. The same conclusion follows from the isobar Eq. (6.10).

2. Equilibrium of different liquids. Suppose two immiscible liquids with densities ρ_1 and ρ_2 are in a state of equilibrium. The pressure when crossing the separation remains continuous. At the separation surface, from Eq. (6.8): $dp = -\rho_1 g dz$, $dp = -\rho_2 g dz$, or $\rho_1 g dz = \rho_2 g dz$. Therefore, $dz = 0$, and the seperation boundary is a horizontal plane with z = const.

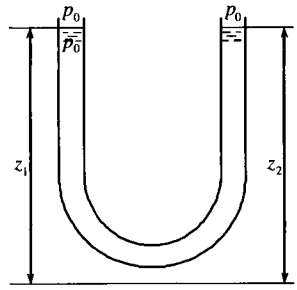

Fig. 6.3

3. Double-liquid manometer (Fig. 6.4). A manometer with the work liquid of density ρ_2 is used for the determination of pressure difference in the system filled-in with a liquid of density ρ_1. At the points 4 and 5 positioned on a horizontal plane within the same liquid, $p_4 = p_5$. According to Eq. (6.13), $p_5 = p_1 + \rho_1 g H$, $p_4 = p_3 + \rho_2 g H$, $p_3 = p_2 + \rho_1 g(H - h)$, wherefrom: $p_1 - p_2 = gh(\rho_2 - \rho_1)$.

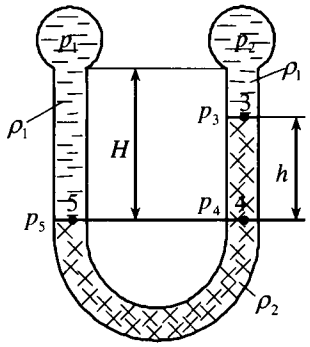

Fig. 6.4

4. Piezometric height (Fig. 6.5). The pressure within a incompressible liquid may be measured by the column height of the same liquid H_{piez} with a help of tube A. For the points 1 and 2, $p_{1abs} = p_0$, $p_{abs} = p_{atm} + \rho g H_{piez}$, $p_{1abs} = p_{2abs}$.

Then:

$$H_{piez} = \frac{p_0 - p_{atm}}{\rho g}. \qquad (6.14)$$

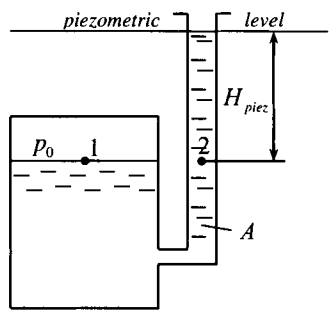

Fig. 6.5

Pressure at any point within the vessel is $p = p_0 + \rho g h = \rho g(H_{piez} + h)$.

The height H_{piez} iss called piezometric, and the surface running through the level in the piezometer is called a piezometric plane. If $p_0 > p_{atm}$, the piezometric plane is positioned above the free surface in the vessel, and if $p_0 < p_{atm}$, it is below it.

5. Heavy gas equilibrium. For a gas in equilibrium in the gravitational field from Eq. (6.7):

$$\int_{p_0}^{p} \frac{dp}{\rho} = g(z_0 - z). \qquad (6.15)$$

To calculate the integral in Eq. (6.15), it is necessary to assign the $p = p(\rho)$ correlation.

Let's limit the problem to isothermal equilibrium of an ideal gas at temperature T_0. Then:

$$\rho = \frac{p}{RT_0},$$

and, from Eq. (6.15):

$$\ln\frac{p}{p_0} = -\frac{g(z - z_0)}{RT_0},$$

or:

$$p = p_0 \exp\left[-\frac{g(z-z_0)}{RT_0}\right].$$

Expanding it into a series:

$$p = p_0\left\{1-\frac{g(z-z_0)}{RT_0}+\frac{1}{2}\left[\frac{g(z-z_0)}{RT_0}\right]^2-\ldots\right\}.$$

If $\frac{1}{2}\left[\frac{g(z-z_0)}{RT_0}\right] << 1$, then:

$$p = p_0\left[1-\frac{g(z-z_0)}{RT_0}\right] = \\ = p_0 - \frac{p_0 g(z-z_0)}{RT_0} = p_0 - \rho_0 g(z-z_0) \quad , \tag{6.16}$$

where ρ is gas density at pressure p_0 and temperature T_0. Following from Eq. (6.16) that if $z - z_0$ is small, the pressure distribution in gas is practically the same as within incompressible fluid.

For the air, the gas constant $R = 287 \ \frac{\text{J}}{\text{kg}^0\text{K}}$. Suppose $T_0 = 293°\text{K}$. In this case, at $z - z_0 \le 85$ m the error from the application of Eq. (6.16) is less than 1 %.

3. Relative quiescence of fluid

As indicated earlier, when analyzing relative quiescence of fluid, the mass force stress in Eq. (6.2) is understood as the resultant of gravitational force stress and of the translational motion inertia force.

Let's solve a problem of a liquid-filled vessel revolving at a constant angular velocity ω about the vertical axis Oz (Fig. 6.6). A liquid's element with the mass m is subjected to the gravitational force and centrifugal force whose stresses are:

$$\bar{F}_g = \bar{g}, \quad \bar{F}_{cent} = \bar{r}\omega^2,$$

where $\bar{r}$ is a vector directed along the beeline from the revolution axis toward the element under consideration. The projections of these stresses on the selected coordinate axes $Oxyz$ are:

$$F_x = r\omega^2\cos\varphi = x\omega^2, \ F_y = r\omega^2\sin\varphi = y\omega^2, \ F_z = -g.$$

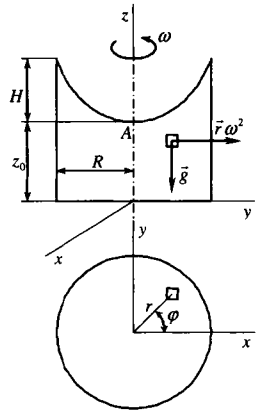

Fig. 6.6

Substituting into Eqs. (6.4) and (6.5), results:

$$dp = \rho(\omega^2 x dx + \omega^2 y dy - g dz),$$

$$\omega^2 x dx + \omega^2 y dy - g dz = 0.$$

Integrating these equation, gives:

$$p = \rho\left(\omega^2 \frac{x^2 + y^2}{2}\right) + C = \rho \frac{\omega^2 r^2}{2} - \rho g z + C, \tag{6.17}$$

$$\omega^2 \frac{x^2 + y^2}{2} - g z = \frac{\omega^2 r^2}{2} - g z + C_1. \tag{6.18}$$

Eq. (6.18) reflects the pressure distribution in the liquid, whereas Eq. (6.18) is equation of the isobar family, with the isobars being paraboloid of revolution.

In order to determine the C constant in Eq. (6.17) and in the free surface Eq. (6.18) the point A of the intersection between the free surface and $0z$ axis has chosen been. The point A's coordinates are $(0,0,z_0)$, and the pressure at the point is p_0. Then, from Eqs. (6.17) and (6.18), $C = p_0 + g z_0$, $C_1 = g z_0$, therefore:

$$p = \rho \frac{\omega^2 r^2}{2} - g(z - z_0), \tag{6.19}$$

$$\frac{\omega^2 r^2}{2} = g(z - z_0). \tag{6.20}$$

Let's determine the height H of the paraboloid. For this purpose, assume $r = R$ in Eq. (6.20), where R is the radius of the vessel. Then H is:

$$H = \frac{\omega^2 r^2}{2g}.$$

Eq. (6.20) can be written as follows:

$$\frac{\omega^2 r_1^2}{2} = g(z_1 - z_0),$$

where z_1 is the coordinate of the intersection point of the straight line $r = r_1 = \text{const}$ with the free surface. Substituting into Eq. (6.19) results:

$$p = p_0 + \rho g(z_1 - z). \tag{6.21}$$

Thus, if z coordinate from the free surface is considered, the vertical pressure distribution in a revolving vessel will be the same as in the quiescent liquid. The explanation is in that the force of inertia projection on the $0z$ axis equals zero.

This result also directly follows from Eq. (6.3). Indeed, in this case:

$$\frac{\partial p}{\partial z} = -\rho g,$$

Wherefrom, after integrating it, immediately follows Eq. (6.21).

Let's now analyze the motion of a closed and liquid-filled vessel down the inclined plane with the acceleration $\bar{a}$ (Fig. 6.7).

The mass forces' projections on the coordinate axes are:

$$F_x = j\cos\alpha,\ F_y = 0,$$

$$F_z = j\sin\alpha - g,$$

where α is the angle between the plane and the horizontal plane, $\bar{j} = -\bar{a}$. Substituting these expressions into Eqs. (6.4) and (6.5):

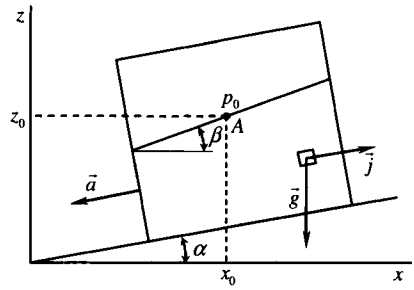

Fig. 6.7

$$dp = \rho[j\cos\alpha dx + (j\sin\alpha - g)dz, \tag{6.22}$$

$$j\cos\alpha dx + (j\sin\alpha - g)dz = 0 \tag{6.23}$$

Eq. (6.23) is the expression for the isobar family. From it:

$$\frac{\partial z}{\partial x} = \mathrm{tg}\beta = \frac{j\cos\alpha}{j - \sin\alpha} = \mathrm{const}, \tag{6.24}$$

i. e., the isobars are the planes inclined at angle β to a horizontal plane.

Integrating Eq. (6.22), gives the pressure distribution law:

$$p = \rho[xj\cos\alpha + z(g\sin\alpha - g)] + C,\ C = \mathrm{const}.$$

Let's assume, for the determination of the integration constant C, that pressure $p = p_0$ is known at some point $H(x_0,0,z_0)$. Then:

$$p - p_0 = \rho[(x - x_0)j\cos\alpha + (z - z_0)(g\sin\alpha - g)]. \tag{6.25}$$

Review of special cases.

(a) Descending a vertical wall, i. e., the case of $\alpha = \pi/2$. It follows from Eq. (6.24) that $\beta = 0$, $z = \mathrm{const}$. Isobars are horizontal planes. From Eq. (6.25):

$$p - p_0 = (j - g)(z - z_0).$$

During a free fall, $j = g$ and $p = p_0$, i. e., pressure is equal at all point of the fluids volume.

(b) Vessel sliding on the plane without friction. In this case the system is moving ("dropping") with the acceleration $j = g\sin\alpha$, and from Eq. (6.24), $\mathrm{tg}\beta = \mathrm{tg}\alpha$, i. e., the equipotentials are parallel to the plane of sliding. From Eq. (6.25):

$$p - p_0 = \rho g[(x - x_0)\sin\alpha - (z - z_0)\cos\alpha]\cos\alpha.$$

4. Static pressure of liquid on firm surfaces

Let's review within liquid a surface AB with area S (Fig. 6.8). Resultant $\bar{R}$ of pressure forces acting on this surface and their moment $\bar{L}$ are:

$$\bar{R} = -\int_S \bar{n} p dS, \tag{6.26}$$

$$\bar{L} = -\int_S \bar{r}_x * \bar{n} p dS, \tag{6.27}$$

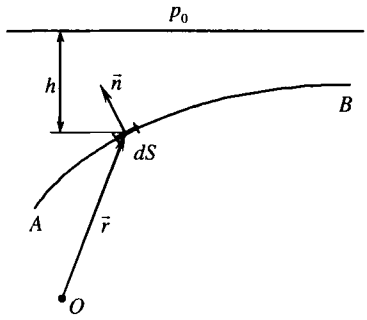

Fig. 6.8

where $\bar{n}$ is the normal external to the surface directed inside of the liquid volume, and $\bar{r}$ is the radius-vector of the point on AB.

In the case of a incompressible fluid, in the gravitational field the pressure at points of the AB surface, according to Eq. (6.13), is:

$$p - p_0 = \rho g h, \tag{6.28}$$

where p_0 is the pressure on the liquid's surface. With Eq. (6.14), the Eq. (6.28) can be written as follows:

$$p - p_{atm} \rho g (h + H_{piez}) \tag{6.29}$$

Suppose the AB surface is a plane inclined at the angle α to the horizon (Fig. 6.9). All vectors $\bar{n}$ are parallel to each other; so from Eqs. (6.26), (6.28) and (6.29):

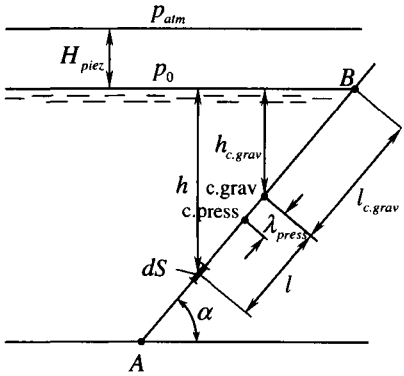

Fig. 6.9

$$\bar{R} = -\bar{n}\int_S (p_0 + \rho g h) dS = \\ = -\bar{n}\int_S \left[p_{atm} + \rho g h (h + H_{piez}) \right] dS. \tag{6.30}$$

And as:

$$\int_S h dS = h_{center} S,$$

where h_{center} is the distance from the fluid's surface to the AB plane center of gravity. Using Eq. (6.30):

$$\bar{R} = -\bar{n}(p_0 + \rho h_{c.grav}) S = -\bar{n}[p_{atm} + \rho g (h_{c.grav} + H_{piez})] S - \\ - \bar{n} p_{c.grav} S, \quad R = p_{c.grav} S, \tag{6.31}$$

where $p_{center} = p_0 + \rho g h_{c.grav} = p_{atm} + \rho g (h_{c.grav} + H_{piez})$ is the pressure in the center gravity of AB.

If the force $\overline{R}$ is calculated by manometric rather than absolute pressure, it is clear that:

$$\overline{R} = -\overline{n}(h_{c.grav} - p_{atm})]S, \quad R = (p_{c.grav} - p_{atm})S. \tag{6.32}$$

Now determining the position of the pressure center, i. e., the point of application of resultant $\overline{R}$. Moment M_x of this force relative to axis O_x, which is passing ing through the AB plane center of gravity (Fig. 6.9), is equal to:

$$M_x = \lambda_{press} R = \int_S lpdS = \int_S l(p_0 + \rho g h)dS, \tag{6.33}$$

where λ_{press} is the distance between the AB's center of gravity and the pressure center, l is the distance between the center of gravity and the element dS.

Fig. (6.9) shows that $h = (l_{c.grav} + l)\sin$. Inserting this expression into Eq. (6.33), results in:

$$\lambda_{press} R = (p_0 + \rho g l_{c.grav} \sin\alpha) \int_S l dS + \rho g \sin\alpha \int_S l^2 dS. \tag{6.34}$$

Keeping in mind that the static momentum of the S area relative to the axis passing through the center of gravity is equals to zero, i. e.:

$$\int_S l dS = 0$$

and:

$$\int_S l^2 dS = J,$$

where J is momentum of inertia of area S relative the same axis, from Eq. (6.34) (considering Eq. (6.31)):

$$\lambda_{press} = \frac{\rho g J}{R} \sin\alpha = \frac{\rho g J}{p_{c.grav}} \sin\alpha.$$

If the force R is calculated considering excess pressure, then from Eq. (6.32):

$$\lambda_{press} = \frac{\rho g J}{(p_{c.grav} - p_{atm})S} \sin\alpha.$$

If $p_{c.grav} > p_{atm}$, then $\lambda_{press} > 0$, and the pressure center is positioned lower than the center of gravity.

Consider the case of a curvilinear surface AB. By projecting Eq. (6.26) on the vertical axis $0z$ and any horizontal axis (for instance, $0x$), results:

$$R_{vert} = -\int_S p\cos(n,z)dS = -\int_{S_{horiz}} p dS_{horiz}, \tag{6.35}$$

$$R_{\text{horiz}} = -\int_S p\cos(n,x)dS = -\int_{S_{\text{horiz}}} pdS_{\text{vert}}, \tag{6.36}$$

where dS_{horiz}, dS_{vert} are dS projections on, respectively, a horizontal plane perpendicular to $0z$ and a vertical plane perpendicular to $0x$.

Substituting p value from Eq. (6.29) into Eqs. (6.35) and (6.36):

$$\begin{aligned} R_{\text{vert}} &= -\int_{S_{horiz}} [p_{atm} + \rho g(h + H_{piez})]dS_{horiz} = \\ &= -p_{atm}S_{horiz} - \rho g \int_{S_{\text{horiz}}} (h + H_{piez})dS_{\text{horiz}}, \end{aligned} \tag{6.37}$$

$$\begin{aligned} R_{\text{horiz}} &= -\int_{S_{vert}} [p_{atm} + \rho g(h + H_{piez})]dS_{vert} = \\ &= -p_{atm}S_{vert} - \rho g \int_{S_{\text{horiz}}} (h + H_{piez})dS_{\text{horiz}}, \end{aligned} \tag{6.38}$$

The integral:

$$\int_{S_{\text{horiz}}} (h + H_{piez})dS_{\text{horiz}} = V_{\text{pb}}$$

is the volume of pressure body V_{pb} formed by the surface AB, its projection on the piezometric plane and vertical generatrices. Eq. (6.37) can be written as follows:

$$R_{vert} = -(p_{atm}S_{horiz} + \rho g V_{pb}). \tag{6.39}$$

The integral:

$$\int_{S_{\text{vert}}} (h + H_{piez})dS_{\text{vert}} = (h_{c.grav} + H_{piez})S_{\text{vert}}$$

is the static momentum of the vertical projection S_{vert} relative the piezometric plane. Thus, from Eq. (6.38):

$$R_{\text{horiz}} = -\left[p_{atm} + \rho g(h_{c.grav} + H_{piez})\right]S_{vert} = -p_{c.grav}S_{vert}, \tag{6.40}$$

where p_{center} is pressure in the center of gravity of the area S_{vert}.

For the forces calculated using excess pressure instead of Eqs. (6.39) and (6.40):

$$R_{vert} = -\rho g V_{pb}, \quad R_{horiz} = \rho g(h_{c.grav} + H_{piez})S_{vert}.$$

Note that Eq. (6.31) converts to Eq. (6.40) if S_{vert} is replaced by S.

Examples of construction of pressure bodies are shown in Fig. 6.10. In Fig. 6a the volume of the pressure body constructed on the AB surface is within the liquid. In Fig. 6b, the volume of the pressure body is outside the liquid. Such a pressure body is called fictitious and is used with the minus sign. Fig. 6.10c shows a case where vertical generatrices intersect the ABC surface in more than one point. So the pressure bodies are constructed separately for the areas AB (the $ABED$ body) and BC (the $CBED$ body). The vertical component of the pressure forces on ABC is determined as the difference of the vertical components of forces acting on AB and AC.

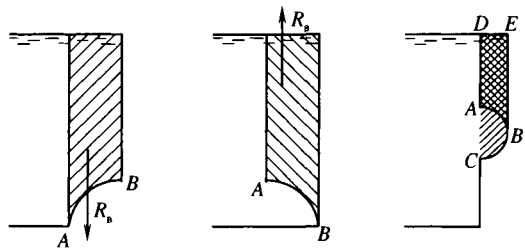

a) b) c)

Fig. 6.10

If the surface S is closed and totally submerged in the liquid, then in conformity with Eq. (6.26) and the Gauss–Ostrogradsky theorem:

$$\bar{R} = -\int_S \bar{n} p dS = -\int_V \nabla p dV , \tag{6.41}$$

where V is the fluid's volume bounded by the surface S. In the gravitational force and according to the Euler's Eq. (6.2), $\nabla p = -\rho \bar{g}$, from Eq. (6.41):

$$\bar{R} = -\bar{g} \int_V \rho dV = -\bar{G} , \tag{6.42}$$

where $\bar{G}$ is the weight of the fluid within the volume V. Eq. (6.42) expresses the Archimedes law: a body submerged in a fluid is acted upon by the expelling force $\bar{R}$ equal to the weight of the liquid in the volume of the submerged body. The force $\bar{R}$ is also called the hydrostatic lift.

From Eq. (6.27) and Gauss–Ostrogradsky theorem:

$$\bar{L} = -\int_S \bar{r} * \bar{n} p dS = -\int_V \mathrm{rot}(\bar{r} p) dV \tag{6.43}$$

Radius-vector $\bar{r} = \bar{i}x + \bar{k}z$, therefore:

$$\mathrm{rot}(\bar{r} p) = -\bar{r} * \nabla p .$$

Substituting this expression into Eq. (6.43) results in:

$$\bar{L} = -\int_V \bar{r} * \rho \bar{g} dV = -\int_V \bar{r} * \rho \frac{\bar{G}}{G} g dV = \frac{\bar{G}}{G} * \int_V \bar{r} \rho g dV . \tag{6.44}$$

The radius-vector of volume V's center of gravity is equal to:

$$\bar{r}_{c.grav} = \frac{1}{G}\int_V \bar{r}\rho g dV ,$$

And Eq. (6.44), considering Eq.(6.42), can be presented as follows:

$$\bar{L} = \bar{G} * \bar{r}_{c.grav} = \bar{r}_{c.grav} * \bar{R} , \qquad (6.45)$$

which indicates that the action line of hydrostatic lift $\bar{R}$ runs through the volume V's center of gravity.

5. Elements of buoyancy theory

Let us consider a body (ship) floating in a liquid.

The liquid volume displaced by the body is called its volume draught. The resultant of the pressure forces acting on the body, as shown in Section 4, is reduced to Archimedes force (also called the supporting force) directed straight up. As follows from Eq. (6.45), the supporting force's line of action runs through the center of gravity of the liquid volume being displaced (which is called the center of draught D). It is accepted that the supporting force is attached to the center of draught.

In a general case, center of gravity T of a floating body does not coincide with the pressure center D. It is clear that in a static situation these two points are located on one vertical line, which is called the buoyancy axis. It is also obvious that in a static situation the body weight G is equal in size to the supporting force R and that $\bar{G} = -\bar{R}$.

The liquid's free surface plane intersecting the buoyant body is called buoyancy plane. The cross-section perimeter of the buoyant body by the buoyancy plane is called waterline. The area enclosed by the waterline is called the waterline area.

Buoyancy of the body is its capacity to float at the given weight G. The measure of buoyancy is draught. The buoyancy margin is the acceptable overloading at which the body will not sink yet. As the body's submergence in a liquid results in its increased draught, the margin of buoyancy is determined by the height of *impermeable* portion of the emerced board over the buoyancy plane.

The capacity of a body to float in the normal position and return to normal position in a case when the normal position was disturbed due to listing, as soon as the forces that caused listing cease, is called the static stability of a buoyant body.

The weight of the body does not change at the static listing. Thus, its draught and the supporting force R also do not change. However, as the shape of the submerged portion changes, the center of draught is shifting relative to the body to a point D_1 (Fig. 6.11). The body's center of gravity maintains its position on the buoyancy axis. In this case movable loads or unbushed liquids is not considered. So, when listing occurs the body weight and the supporting force form a force couple. Depending on the mutual position of the body's center of gravity T and the center of draught D_1 this force couple may be either restoring or overturning.

The line DD_1 along which the center of draught moves during listing is called the center of draught line.

The point M where the restoring force R_1 intersects with the buoyancy axis at low listing angles α is called the initial metacenter. The listing angle α is the angle between the buoyancy axis and the vertical.

The H_M value (the distance between the center of gravity and the initial metacenter M) is called the initial metacentric height. The restoring momentum M_M generated by the G and R_1 force couple is equal to:

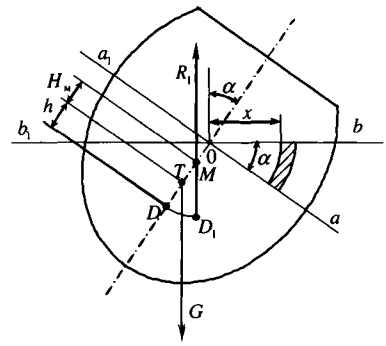

Fig. 6.11

$$M_M = R_1 H_M \sin\alpha = R H_M \sin\alpha \tag{6.46}$$

because at the static listing, the supporting force does not change and is equal to the weight of a buoyant body G.

Fig. 6.11 shows that if the point M is positioned higher than the point T, the momentum M_M tends to return the body to its initial position. So, if the point M is positioned higher than the point T, the initial metacentric height H_M is considered positive. Obviously, at $H_M < 0$ the M_M momentum will be overturning. In other words, it is necessary for the static metacentric stability of a buoyant body that the initial metacentric height is positive.

The distance $H_M + h$ between the initial metacenter and initial draught center (i. e., the length of the MD segment) is called the initial metacentric radius.

Consider a buoyant body listing at a small angle α from its normal position. The amount of the so submerged volume Oab is equal to:

$$V_1 = \int_{S_1} \alpha x dS, \tag{6.47}$$

where S_1 is the portion of the new waterline area, and x is the distance between the intersection line between the waterline and element dS. The body weight G and its supporting force R did not change, so the amount of the emersion volume is equal to:

$$V_2 = -\int_{S_2} \alpha x dS = -V_1, \quad S_2 = S - S_1, \tag{6.48}$$

were S is the waterline area.

The supporting force increases by:

$$\delta R_1 = -\rho g V_1$$

and decreases by:

$$\delta R_2 = -\rho g V_2 = \delta R_1 .$$

The momentums generated by these forces are equal to:

$$M_1 = \alpha\rho g \int_{S_1} x^2 dS, \; M_2 = \alpha\rho g \int_{S_2} x^2 dS. \tag{6.49}$$

According to Eqs. (6.47) and (6.48),

$$\int_{S_1} xdS + \int_{S_2} xdS = 0,$$

i. e., the static momentum of the new waterline's area relative to the intersection axis of the contiguous waterline areas is equal to zero, and this axis passes through the center of gravity of the new waterline area (Euler's theorem).

From Eqs. (6.48) and (6.49), the restoring momentum M_M is equal to:

$$M_M = M_1 + M_2 = \alpha\rho g \int_S x^2 dS = \alpha\rho g J, \qquad (6.50)$$

where J is the new waterline momentum of inertia relative the axis passing through its center of gravity (as seen in Fig. 6.11, M_1 and M_2 are directed in the same direction).

The restoring force R_1 may be presented as:

$$R_1 = R + \delta R_1 + \delta R_2.$$

Its momentum relative to the pressure center D is equal to the sum of momentums δR_1, δR_2, i. e., it is equal to M as the action line of the force R passes through D. On the other hand, the force R_1 momentum is equal to:

$$M_M = (H_M + h)\, R\sin\alpha \approx (H_M + h)\, R\alpha, \qquad (6.51)$$

as $R_1 = R$ and al low angles $\sin\alpha = \alpha$.

Equating Eqs. (6.51) and (6.50), results:

$$H_M = \frac{J}{W} - h, \qquad (6.52)$$

where $W = \dfrac{R}{\rho g}$ is the volume draught.

If the body's center of gravity T is lower that the draught center D, then $h < 0$, and the initial metacentric height H_M is always greater than zero.

Substituting Eq. (6.52) into Eq. (6.46) gives an equation for the restoring momentum M_M as follows:

$$M_M = R\left(\frac{J}{W} - h\right)\sin\alpha, \qquad (6.53)$$

which is the metacentric stability equation.

Eq. (6.53) is derived for low-listing angles (for high-board ships $\alpha \le 15 - 20^\circ$). At high listing angles, the correlation between M_M and α becomes more complex as the metacenter shift relative to its initial position.

Dynamic metacentric stability is the capacity of a buoyant body to oscillate under the action of forces generating the listing momentums within the assigned listing angle. The greater the initial metacentric height, the shorter the oscillation period.

Special studies showed that the dynamic listing range under a suddenly applied force is equal to the double static listing emerging under action of a force of the same numerical significance.

Static (and dynamic) metacentric stability issues have application in shipbuilding.

CHAPTER VII

FLOW OF IDEAL FLUID

1. Euler's equations in the Gromeko-Lamb format

The system of equations for the ideal fluid has the following format:

$$\frac{d\rho}{dt} + \rho \mathrm{div}\bar{v} = 0, \tag{7.1}$$

$$\rho \frac{d\bar{v}}{dt} = \rho \bar{F} - \nabla p, \tag{7.2}$$

$$\rho\left(u + \frac{v^2}{2}\right) = \rho \bar{F}\bar{v} - \mathrm{div}p\bar{v} + \rho q_e. \tag{7.3}$$

The heat-flow equation for the ideal fluid is:

$$\frac{du}{dt} = q_e - \frac{p}{\rho}\rho \mathrm{div}\bar{v} = q_e + \frac{p}{\rho^2}\frac{d\rho}{dt}. \tag{7.4}$$

To transform Euler's equation [Eq. (7.2)], let's review total derivative $\frac{d\bar{v}}{dt}$. According to Eq. (1.19):

$$\frac{d\bar{v}}{dt} = \frac{\partial \bar{v}}{\partial t} + (\bar{v} * \nabla)\bar{v} = \frac{\partial \bar{v}}{\partial t} + v_j \frac{\partial \bar{v}}{\partial x_j}. \tag{7.5}$$

Projecting vector $(\bar{v} * \nabla)\bar{v} = v_j \frac{\partial \bar{v}}{\partial x_j}$ onto the $0x_1$ coordinate axis:

$$[(v * \nabla)v]_{x_1} = v_j \frac{\partial \bar{v}}{\partial x_j} = v_1 \frac{\partial v_1}{\partial x_1} + v_2 \frac{\partial v_1}{\partial x_2} + v_3 \frac{\partial v_1}{\partial x_3}. \tag{7.6}$$

Eq. (7.6) can be written in the following format:

$$v_j\frac{\partial v_1}{\partial x_j}=v_1\frac{\partial v_1}{\partial x_1}+v_2\frac{\partial v_2}{\partial x_1}-v_2\frac{\partial v_2}{\partial x_1}+v_3\frac{\partial v_3}{\partial x_3}-v_3\frac{\partial v_3}{\partial x_3}+v_2\frac{\partial v_1}{\partial x_2}+v_3\frac{\partial v_1}{\partial x_3}=$$
$$=\frac{1}{2}\frac{\partial}{\partial x_1}(v_1^2+v_2^2+v_3^2)+v_2\left(\frac{\partial v_1}{\partial x_2}-\frac{\partial v_2}{\partial x_1}\right)+v_3\left(\frac{\partial v_1}{\partial x_3}-\frac{\partial v_3}{\partial x_1}\right). \tag{7.7}$$

According to Eq. (3.9):

$$2\bar{\omega}=\mathrm{rot}\bar{v}=\begin{vmatrix}\bar{e}_1 & \bar{e}_2 & \bar{e}_3\\ \dfrac{\partial}{\partial x_1} & \dfrac{\partial}{\partial x_2} & \dfrac{\partial}{\partial x_3}\\ v_1 & v_2 & v_3\end{vmatrix}, \tag{7.8}$$

and Eq. (7.7) can be presented in the following format:

$$v_j\frac{\partial v_1}{\partial x_j}=\frac{\partial}{\partial x_1}\left(\frac{v^2}{2}\right)-2v_2\omega_3+2v_3\omega_2. \tag{7.9}$$

The medium is isotropic so all coordinate axes are equivalent, and after the cyclic rearrangement of the subscript:

$$v_j\frac{\partial v_2}{\partial x_j}=\frac{\partial}{\partial x_2}\left(\frac{v^2}{2}\right)-2v_3\omega_1+2v_1\omega_3, \tag{7.10}$$

$$v_j\frac{\partial v_3}{\partial x_j}=\frac{\partial}{\partial x_3}\left(\frac{v^2}{2}\right)-2v_1\omega_2+2v_2\omega_1, \tag{7.11}$$

where ω_i is projection of vector $\bar{\omega}$ onto the $0x_i$ axes. Multiply Eqs. (7.9), (7.10) and (7.11), respectively, by $\bar{e}_1$, $\bar{e}_2$ and $\bar{e}_3$ results:

$$v_j\frac{\partial\bar{v}}{\partial x_j}=\nabla\frac{v^2}{2}+2\bar{\omega}*\bar{v}. \tag{7.12}$$

Substituting Eqs. (7.5) and (7.12) into Euler's equation, gives:

$$\frac{\partial\bar{v}}{\partial t}+\nabla\frac{v^2}{2}-2\bar{v}*\bar{\omega}=\bar{F}-\frac{1}{\rho}\nabla p. \tag{7.13}$$

Eq. (7.13) is Euler's equation in the Gromeko-Lamb format.

2. Bernoulli integral

Continuous medium motion equations in stresses Eq. (2.42) were derived from Newton's second law. Euler's equations are a particular case of the Eq. (2.42); therefore, they are a mathematical expression of the second law for the ideal fluid. Theoretical mechanics states that the motion equations under certain conditions have the first integral, which is the law of mechanical energy conservation. Hence, Euler's equations under certain conditions also must have the first integral. This integral is called Bernoulli's integral.

Bernoulli's integral is among the most important hydromechanical equations. In order to derive it, it is necessary to state the following assumptions:

(a) the flow is transient-free, $\frac{\partial \bar{v}}{\partial t} = 0$;

(b) the mass force stress has potential, $\bar{F} = \nabla\Pi$.

Under these assumptions, Eq. (7.13) assumes the following format:

$$\nabla\left(-\Pi + \frac{v^2}{2}\right) + \frac{1}{\rho}\nabla p = \bar{v} * \mathrm{rot}\,\bar{v}. \tag{7.14}$$

Flow-lines and rotor-lines at transient-free motion are immobile in the space, and the flow-lines coincide with trajectories of the fluid's particles. Along the flow-line, $\bar{v} = v\bar{s}_1^0$, and along the rotor-line, $\mathrm{rot}\bar{v} = |\mathrm{rot}\bar{v}|\bar{s}_2^0$, where $\bar{s}_1^0$ and $\bar{s}_2^0$ are basis vectors of tangents to the flow-line and rotor-line. Thus, sequential multiplying Eq. (7.14) by $\bar{s}_1^0$ and $\bar{s}_2^0$ or, which is the same, projecting this equation on the flow-line and rotor-line, results:

$$\frac{\partial}{\partial s_1}\left(-\Pi + \frac{v^2}{2}\right) + \frac{1}{\rho}\frac{\partial p}{\partial s_1} = 0, \tag{7.15}$$

$$\frac{\partial}{\partial s_2}\left(-\Pi + \frac{v^2}{2}\right) + \frac{1}{\rho}\frac{\partial p}{\partial s_2} = 0. \tag{7.16}$$

At the transient-free motion, all motion parameters (p, ρ, T, v) are function of s_1 coordinate counted along the spatially immobile flow-line. So, $p = p(s_1,L_1)$, $\rho = \rho(s_1,L_1)$, where L_1 is a mark of the flow-line of interest. Canceling s_1, we have $p = f_2(\rho,L_2)$, where L_2 is a mark of the corresponding rotor-line.

The presence of functions of type $p = f(\rho,L)$ enables the introduction of a pressure function:

$$d\mathrm{P} = \frac{dp}{\rho}, \text{ or } \mathrm{P} = \int\frac{dp}{\rho}, \tag{7.17}$$

where the integral is integrated along the flow-line (rotor-line). The pressure function P is determined with accuracy to the additive constant and in the general case

is a function of L, i. e., the function of the selected flow- (rotor-) line. Following from Eq. (7.17):

$$\frac{d\mathrm{P}}{dx_1}=\frac{1}{\rho}\frac{\partial \mathrm{P}}{\partial x_1},\quad \nabla \mathrm{P}=\frac{1}{\rho}\nabla p. \tag{7.18}$$

Substituting this equation into Eqs. (7.15) and (7.16):

$$\frac{\partial}{\partial s_1}\left(-\Pi+\mathrm{P}+\frac{v^2}{2}\right)=0, \tag{7.19}$$

$$\frac{\partial}{\partial s_2}\left(-\Pi+\mathrm{P}+\frac{v^2}{2}\right)=0, \tag{7.20}$$

where from, after integrating along the flow- (rotor-) line:

$$-\Pi+\mathrm{P}+\frac{v^2}{2}=C_1L_1, \tag{7.21}$$

$$-\Pi+\mathrm{P}+\frac{v^2}{2}=C_2L_2. \tag{7.22}$$

Beroulli's integral states that at the transient-free motion and in the presence of mass force stress potential, the trinomial:

$$-\Pi+\mathrm{P}+\frac{v^2}{2} \tag{7.23}$$

maintains constant numerical value along the flow- (rotor-) line. The $C_1(C_2)$ constant may have different numerical value on different flow- (rotor-) lines.

Eqs. (7.21) and (7.22) are valid, respectively, along any flow-line and rotor-line, and are called Bernoulli's integral.

By taking a rotor-line and pass flow-lines through its points forms the surface of a flow. As $C_2(L_2)$ = const along the locked rotor-line, then along all the flow-lines crossing it $C_1(L_1) = C_2(L_2)$ = const. Therefore, on the constructed surface a condition C_1 = const is realized.

Similarly, if rotor-lines carried through a flow-line, then the condition C_2 = const will be realized on the formed surface. In the case of a potential flow (i. e., $\bar{v}=\nabla\varphi$), from Eq. (7.8) that rot $\bar{v}=0$, and Eq. (7.14) looks as follows:

$$\nabla\left(-\Pi+\frac{v^2}{2}\right)+\frac{1}{\rho}\nabla p=0. \tag{7.24}$$

It is necessary to emphasize that at $\bar{v}=\nabla\varphi$, Eq. (7.24) is valid within the entire flow volume. Because of this:

$$\frac{1}{\rho}\nabla p=\nabla \mathrm{P}, \tag{7.25}$$

And the function P is obviously the same all over the flow volume. Therefore, as Eq. (7.18) shows, the pressure depends only on the density. The process at which the pressure depends only on the density is called *barotropic*.

Examples of barotropic processes are the flow of a incompressible fluid, and isothermal processes. Later, we'll review some other barotropic processes.

Substituting Eq. (7.25) into Eq. (7.24) results:

$$\nabla\left(-\Pi+\mathrm{P}+\frac{v^2}{2}\right)=0 \tag{7.26}$$

or

$$-\Pi+\mathrm{P}+\frac{v^2}{2}=C. \tag{7.27}$$

Eq. (7.27) is valid along any line drawn within the fluid, and the constant C has the same numerical value within the entire fluid's volume.

So, if the flow is transient-free, and the mass force stress has potential, the process becomes barotropic.

Conversely, it follows from Eqs. (7.13) and (7.25) that if the flow is transient-free, potential and barotropic then:

$$\nabla\left(\mathrm{P}+\frac{v^2}{2}\right)=\overline{F},$$

i. e., such flow may only exist if the mass force stress potential is present.

3. Particular forms of Bernoulli's integral

Let's analyze a transient-free flow of the ideal incompressible fluid in the gravitational field. In this case, ρ = const, $\overline{F}=\overline{g}$, $\Pi=-gz$ where z is the vertical coordinate.

From Eq. (7.17), the pressure function is $\mathrm{P}=\frac{p}{\rho}+\mathrm{const}$, and Bernoulli's integral Eq. (7.21) [or (7.22)] changes into the following format:

$$gz+\frac{p}{\rho}+\frac{v^2}{2}=\mathrm{const} \tag{7.28}$$

or

$$z+\frac{p}{\rho g}+\frac{v^2}{2g}=H=\mathrm{const}. \tag{7.29}$$

The terms of the Eq. (7.29) have the dimension of the length and are called: z — geometric (or leveling) height or geometric head; $\frac{p}{\rho g}$ — piezometric height or piezometric head; $\frac{v^2}{2g}$ — velocity height or velocity head; their sum H — total head.

Following from Eq. (7.29) at a transient-free flow of the ideal incompressible fluid in the gravitational field the total head maintains constant numerical value along any flow-line or rotor-line.

In an effective cross-section of the elementary flow-tube all flow parameters are constant by definition. So Eq. (7.29) is valid for the elementary flow-tube. Let's review a horizontal flow-tube, z = const. Then, following from Eq. (7.29) the pressure declines as the velocity increases.

As the flow velocity increases, the pressure may become sufficiently low to be equal to the saturated vapor pressure p_y. The fluid begins to boil, and caverns filled-up with its vapor form within it. This phenomenon is called cavitation.

From Eq. (7.28):

$$gz_0 + \frac{p_0}{\rho} + \frac{v_0^2}{2} = gz + \frac{p_y}{\rho} + \frac{v_0^{*2}}{2},$$

or:

$$v^{*2} = 2\frac{\rho g(z_0 - z) - p_0 - p_y}{\rho} + \frac{v_0^2}{2},$$

where v^* is velocity at which cavitation begins.

Cavitation is damaging for the operation of pumps, intake lines, siphons, propeller screws, etc., and may even cause their destruction. At the transient-free flow, the throughflow along the flow-tube is constant under Eq. (2.41) ($v_1S_1 = v_2S_2$). Therefore, if the tube narrows, the velocity increases, and the pressure declines. This principle is used in water-suction pumps, pulverizers and other devices.

Let's now review transient-free motion of an ideal non-viscous gas. Its equation of state (Clapeyron's equation) is:

$$\frac{p}{\rho} = RT, \tag{7.30}$$

where R is the gas constant and T is the absolute temperature.

Eqs. (7.17) and (7.30) demonstrate that the thermodynamic process must be assigned for derivation of the pressure function.

From the heat-flow Eq. (7.4):

$$q_e dt = du - \frac{p}{\rho^2} d\rho = du + pd\frac{1}{\rho} = du + pdV, \tag{7.31}$$

where $V = \frac{1}{\rho}$ is specific (per/unit) volume. Therefore, for a non-viscous gas the heat-flow equation is the same as the first law of thermodynamics.

At $\rho = \text{const}$, $V = \text{const}$, and:

$$q_e dt = C_v dT = du, \tag{7.32}$$

where C_v is heat capacity at constant volume. At $p = \text{const}$, we obtain from Eqs. (7.30) and (7.32):

$$q_e dt = C_p dT = du + d\frac{p}{\rho} = C_V dT + RdT,$$

and from here, Mayer's equation:

$$R = C_p - C_V, \tag{7.33}$$

where C_p is heat capacity at constant pressure.

Combining Eq. (7.31), the equation of state Eq. (7.30), and also Eqs. (7.32) and (7.33) results:

$$q_e dt = C_V dT + pd\frac{1}{\rho} = \frac{C_V}{C_P - C_V} d\frac{p}{\rho} + pd\frac{1}{\rho} = \frac{1}{k-1}\left(kpd\frac{1}{\rho} + \frac{dp}{\rho}\right) = \tag{7.34}$$

$$\frac{\rho^{k-1}}{k-1}\left(kpd\frac{1}{\rho^{k-1}}\frac{1}{\rho} + \frac{dp}{\rho^k}\right) = \frac{\rho^{k-1}}{k-1} d\frac{p}{\rho^k},$$

where $k = \frac{C_p}{C_V}$ is adiabatic exponent.

At adiabatic process (i. e., the absence of the external heat inflow) $q_e = 0$ and:

$$\frac{p}{\rho^k} = \Theta \quad \text{or} \quad \frac{p}{p_0} = \left(\frac{\rho}{\rho_0}\right)^k. \tag{7.35}$$

It is important to note that for the derivation of the *Poisson's adiabat* equation the heat-flow equation Eq. (7.31) is used for the ideal fluid. Therefore, the Poisson's adiabat is valid at adiabatic process without friction.

Now it is necessary to demonstrate that the adiabatic process without friction is iso-entropic, i. e., in this process entropy remains constant.

Entropy s can be determined as follows:

$$ds = \frac{dq}{T}. \tag{7.36}$$

Suppose the heat in the liquid volume under consideration comes only from the outside, i. e., $dq = q_e dt$. Then, from the equation of state and Eqs. (7.33), (7.34) and (7.36):

$$ds = \frac{q_e dt}{T} = C_V \frac{dT}{T} + \frac{p}{T} d\frac{1}{\rho} = C_V \frac{dT}{T} + (C_p - C_V)\rho d\frac{1}{\rho} =$$

$$= C_V \left[d\ln T + (k-1) d\ln \frac{1}{\rho} \right] = C_V d\ln \frac{T}{\rho^{k-1}}.$$

Then:

$$s_2 - s_1 = C_V \ln \left[\frac{T_2}{T_1} \left(\frac{\rho_1}{\rho_2} \right)^{(k-1)} \right] = C_V \ln \left[\frac{p_2}{p_1} \left(\frac{\rho_1}{\rho_2} \right)^{k} \right]. \tag{7.37}$$

At isentropic process, $s_2 = s_1$, and from Eq. (7.37):

$$\ln \left[\frac{p}{p_1} \left(\frac{\rho_1}{\rho_2} \right)^{k} \right] \quad 0 \text{ or } \frac{p_2}{p_1} = \left(\frac{\rho_2}{\rho_1} \right)^{k}. \tag{7.38}$$

Eqs. (7.35) and (7.38) show that the adiabatic process without friction is indeed isentropic.

For a general case of a non-adiabatic process, the heat-flow equation Eq. (7.31) can be transformed as follows considering Eqs. (7.30), (7.32) and (7.33)

$$q_e dt = CdT = C_V dT + pd\frac{1}{\rho},$$

or:

$$\frac{C - C_V}{C_P - C_V} d\frac{p}{\rho} - pd\frac{1}{\rho} = 0, \tag{7.39}$$

where C is heat capacity at the thermodynamic process under review. Calling:

$$\frac{C - C_V}{C_P - C_V} = \frac{1}{n-1}, \quad n \neq 1,$$

and from Eq. (7.39):

$$npd\frac{1}{\rho} + \frac{dp}{\rho} = \rho^{n-1} \left(\frac{np}{\rho^{n-1}} d\frac{1}{\rho} + \frac{dp}{\rho^n} \right) = \rho^{n-1} d\frac{p}{\rho^n} = 0,$$

wherefrom:

$$p = A\rho^n. \tag{7.40}$$

This is the equation of the polytropic process. In a general case, the numerical values of A and n (through heat capacity C) may vary from one particle to the next (for a non-uniform liquid). Therefore, A and n are functions of the particle's Lagrangian coordinates X_j and t. At the transient-free motion, the flow-line coincides with the trajectory; so, if A and n depended on X_j, the pressure at a locked point of

the flow-line (of space) would have changed with time, and the motion would be non-stationary. Therefore, A and n at transient-free motion may only depend on L.

If the A and n parameters have the same values within the entire fluid's volume, the polytropic process becomes barotropic.

Eqs. (7.17), (7.30), (7.33), (7.35) and (7.40) are used to derive pressure P function. For adiabatic process, with the accuracy for the constants of integration, one obtains:

$$\mathrm{P} = \frac{k}{k-1}\Theta\rho^{k-1} = \frac{k}{k-1}\Theta^{\frac{1}{k}} p^{\frac{k-1}{k}} = \frac{k}{k-1}\frac{p}{\rho} = C_p T, \tag{7.41}$$

and for polytropic process:

$$\mathrm{P} = \frac{n}{n-1}A\rho^{n-1} = \frac{n}{n-1}A^{\frac{1}{n}} p^{\frac{n-1}{n}} = \frac{n}{n-1}\frac{p}{\rho}. \tag{7.42}$$

For isothermal process:

$$\frac{p}{\rho} = \frac{p_0}{\rho_0} = RT_0 = \text{const}, \tag{7.43}$$

where p_0, ρ_0 are pressure and density at temperature T_0; so from Eqs. (7.17) and (7.43):

$$\mathrm{P} = \frac{p_0}{\rho_0}\ln\frac{p}{p_0} = \frac{p_0}{\rho_0}\ln\frac{\rho}{\rho_0}. \tag{7.44}$$

By substituting Eq. (7.41) into Eq. (7.21) and assuming $\Pi = -gz$, the following Bernoulli integral for the adiabatic process is obtained:

$$gz + \frac{k}{k-1}\frac{p}{\rho} + \frac{v^2}{2} = C = \text{const}, \tag{7.45}$$

$$gz + \frac{k}{k-1}\Theta^{\frac{1}{k}} p^{\frac{k-1}{k}} + \frac{v^2}{2} = C = \text{const}, \tag{7.46}$$

$$gz + \frac{k}{k-1}\Theta\rho^{k-1} + \frac{v^2}{2} = C = \text{const}, \tag{7.47}$$

$$gz + C_p T + \frac{v^2}{2} = C = \text{const}. \tag{7.48}$$

From the same Eqs. (7.21) and (7.42) for the polytropic process:

$$gz + \frac{n}{n-1}\frac{p}{\rho} + \frac{v^2}{2} = C = \text{const} \quad (n \neq 1), \tag{7.49}$$

$$gz + \frac{n}{n-1} A^{\frac{1}{n}} p^{\frac{n-1}{n}} + \frac{v^2}{2} = C = \text{const} \quad (n \neq 1), \tag{7.50}$$

$$gz + \frac{n}{n-1} A\rho^{n-1} + \frac{v^2}{2} = C = \text{const} \ (n \neq 1). \tag{7.51}$$

And for isothermal process from Eqs. (7.21) and (7.44),

$$gz + \frac{p_0}{\rho_0} \ln \frac{p}{p_0} + \frac{v^2}{2} = \text{const}, \tag{7.52}$$

$$gz + \frac{p_0}{\rho_0} \ln \frac{\rho}{\rho_0} + \frac{v^2}{2} = \text{const}. \tag{7.53}$$

Eqs. (7.45)–(7.51) show that the numerical values of the $\frac{p}{\rho}$, p and ρ values under adiabatic and polytropic processes decrease with increasing velocity. Under adiabatic process, absolute temperature T also decreases with the increase in velocity. Under the isothermal process, as Eqs. (7.43), (7.52) and (7.53) show, with increasing velocity p and ρ decrease, and $\frac{p}{\rho}$ remains constant.

4. Simple applications of Bernoulli's integral

First it is desired to review some simple examples of applying Bernoulli integral to the flow of ideal incompressible fluid in the gravitational field.

1. Fluid's flow through a small hole in a vessel. Suppose $S_0 >> S$ where S_0 is the area of the fluid's free surface, and S is the area of the vessel's hole (Fig. 7.1). In such a case the fluid's level change in the vessel can be disregarded and assume that z_0 = = const.

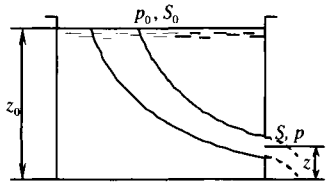

Fig. 7.1

From Eq. (7.28):

$$gz_0 + \frac{p_0}{\rho} = gz + \frac{p}{\rho} + \frac{v^2}{2}, \tag{7.54}$$

where p_0 is pressure on the free surface, z, p, v are parameters of the stream at the exit hole. Eq. (7.54) provides the flow velocity from the hole:

$$v = \sqrt{2gh + 2\frac{p_0 - p}{\rho}}, \tag{7.55}$$

where $h = z_0 - z$. When $p_0 = p$, from Eq. (7.55) emerges a well-known Torricelli's equation:

$$v = \sqrt{2gh},$$

i. e., the outflow velocity is equal to the velocity of a heavy body falling from the height h. As p = const on the surface of the outflow stream, following Bernoulli's integral, with lowering of the stream its velocity increases.

2. Velocity tube (Pitot's tube). Suppose an axisymmetric body is submerged in a fluid so that its axis' direction coincides with the direction of the flow velocity (Fig. 7.2). At the point A at a sufficient distance from the nozzle of the body B, the velocity is v_A, and pressure, p_A. At the point B, the velocity is $v_B = 0$, flow-lines branch-out. Thus, point B is a singularity. It is acceptable to believe that at point C also quite remote from point B the flow disturbance caused by the tube nozzle disappeared, so $v_C = v_A$, $p_C = p_A$ (to simplify the problem, the flow is considered to be horizontal).

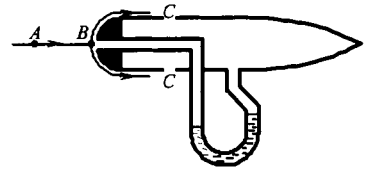

Fig. 7.2

From Eq. (7.28) for the flow-line AB:

$$\frac{p_A}{\rho} + \frac{v_A^2}{2} = \frac{p_B}{\rho},$$

and from this:

$$v_A = v_C = \sqrt{2\frac{p_B - p_A}{\rho}} = \sqrt{2\frac{p_B - p_C}{\rho}}. \qquad (7.56)$$

This way, by measuring pressure difference $p_B - p_C$ the velocity v_A can be determined.

In practice, a correction factor φ is introduced in Eq. (7.56) considering the flow distortion and the presence of friction. Factor φ is determined by calibration. For high-quality tubes, φ = 0.99 to 1.02.

3. Venturi meter. As demonstrated in Fig. 1.3, cross-sections I-I and II-II are selected and assumed that the velocities in these cross-sections are uniformly distributed, i. e., $\frac{\partial v_j}{\partial x_i} = 0$. Then, it follows from Euler's equation Eq. (7.2) that at transient-free flow in each of these cross-sections $\nabla p = \rho \bar{g}$, i. e., the pressure is distributed under the hydrostatic law:[1]

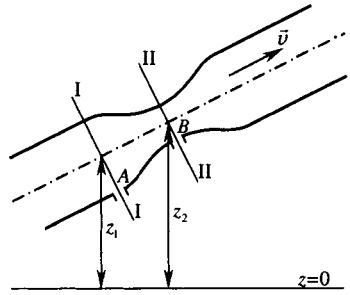

Fig. 7.3

$$\rho g z + p = \text{const}. \qquad (7.57)$$

[1] The same conclusion may be made from the Navier-Stockes equation (4.42).

Subscript 1 is ascribed to all values related to the cross-section I-I and a subscript 2, to all values related to the cross-section II-II. Let's write Bernoulli's integral

Eq. (7.28) for a flow-line passing along the tube's axis:

$$gz_1 + \frac{p_1}{\rho} + \frac{v_1^2}{2} = gz_2 + \frac{p_2}{\rho} + \frac{v_2^2}{2}. \tag{7.58}$$

As the velocities are distributed uniformly in the cross-sections, under the continuity equation Eq. (2.41):

$$v_1 S_1 = v_2 S_2 = Q. \tag{7.59}$$

From Eqs. (7.58) and (7.59) follows that:

$$\frac{Q^2}{2}\left(\frac{1}{S_2^2} - \frac{1}{S_1^2}\right) = g(z_1 - z_2) + \frac{p_1 - p_2}{\rho}. \tag{7.60}$$

On the other hand, from Eq. (7.57):

$$\rho g z_A + p_A = \rho g z_1 + p_1, \quad \rho g z_B + p_B = \rho g z_2 + p_2, \tag{7.61}$$

where subscripts A and B relate to holes A and B.

After substituting Eq. (7.61) into Eq. (7.60):

$$Q = S_1 S_2 \sqrt{\frac{2}{S_1^2 - S_2^2}\left| g(z_A - z_B) + \frac{p_A - p_B}{\rho} \right|}. \tag{7.62}$$

Eq. (7.62) shows that having measured the pressure difference $p_A - p_B$ it is possible to determine the throughput Q. In practice, a correction factor μ is introduced into Eq. (7.62). It accounts for a non-uniform velocity field in the cross-sections and the friction.

5. Cauchy-Lagrange's integral

Cauchy-Lagrange's integral is the Bernoulli's integral analog for the non-stationary motion and derived based on the following assumptions:

(a) the flow is potential, $\bar{v} = \nabla\varphi$;

(b) stress of the mass forces has potential, $\overline{F} = \nabla\Pi$;

(c) the process is barotropic, $p = p(\rho)$.

The third assumption is based on the fact that the flow-lines under a non-stationary motion do not coincide with trajectories. Therefore, it is not possible to assume that $p = p(L,s)$ and $\rho = \rho\,(L,s)$ and eliminate s as it was done when deriving Bernoulli's integral. Thus in a general case of a non-barotropic motion it is not possible to compute the pressure function P.

In the above assumptions $\mathrm{rot}\bar{v} = 0$, and Euler's equation in the Gromeko-Lamb format Eq. (7.63) looks as follows:

$$\frac{\partial \bar{v}}{\partial t} + \nabla \frac{v^2}{2} = \nabla \Pi - \nabla \mathrm{P}, \tag{7.63}$$

where the pressure function P is computed from Eq. (7.18).

As:

$$\frac{\partial \bar{v}}{\partial t} = \frac{\partial}{\partial t}(\nabla \varphi) = \nabla \frac{\partial \varphi}{\partial t},$$

Eq. (7.63) can be written in the following format:

$$\nabla\left(\frac{\partial \varphi}{\partial t} - \Pi + \mathrm{P} + \frac{v^2}{2}\right) = 0. \tag{7.64}$$

As the Hamilton's operator ∇ includes only the space derivatives, and the functions in Eq. (7.64) are in general case depends on time, and from Eq. (7.64):

$$\frac{\partial \varphi}{\partial t} - \Pi + \mathrm{P} + \frac{v^2}{2} = f(t). \tag{7.65}$$

This equation is called the Cauchy-Lagrange's integral. Following from its derivation that the function $f(t)$ has the same format within the entire volume occupied by the fluid. In the transient-free motion, Cauchy-Lagrange's integral converts into Bernoulli's integral Eq. (7.27) for the barotropic potential motion.

To determine function $f(t)$, it is necessary to know the motion at any one point of the fluid, for instance, at the volume's boundary.

Instead of the potential φ, the function φ_1 is introduced as follows:

$$\varphi_1 = \varphi + \int f(t)dt.$$

Then:

$$\frac{\partial \varphi_1}{\partial t} = \frac{\partial \varphi}{\partial t} + f(t), \quad \nabla \varphi_1 = \nabla \varphi,$$

and the Cauchy-Lagrange's integral may be written as follows:

$$\frac{\partial \varphi_1}{\partial t} - \Pi + \mathrm{P} + \frac{v^2}{2} = 0.$$

For an incompressible fluid in the gravitational field:

$$\frac{\partial \varphi_1}{\partial t} + gz + \frac{p}{\rho} + \frac{v^2}{2} = 0. \tag{7.66}$$

For an ideal gas under the iso-entropy process from Eq. (7.37):

$$\frac{\partial \varphi_1}{\partial t} + gz + \frac{k}{k-1}\frac{p}{\rho} + \frac{v^2}{2} = 0.$$

In many cases, it is more convenient to describe the considered motion in an immobile coordinate system using a movable coordinate system. Suppose beside the immobile system $Ox_1x_2x_3$ a movable coordinate system $Ox'_1x'_2x'_3$ exists (Fig. 7.4). Assigning numerical values to x'_j means setting the point M relative to the movable system.

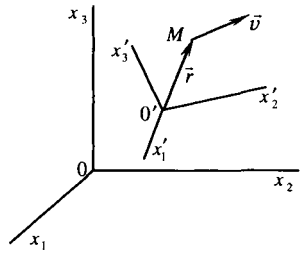

Fig. 7.4

If point M's motion relative to the immobile coordinate system is known, then:

$$x_i = x_i(x'_j,t)^2. \tag{7.67}$$

Then, setting numerical values of x'_j:

$$\frac{\partial x_i}{\partial t} = \frac{\partial x_i(x'_j,t)}{\partial t} = v_{i\,trans}, \tag{7.68}$$

where $v_{i\,trans}$ are the projections of the transfer motion velocity $\bar{v}_{i\,trans}$. From Euler's equation:

$$v_{trans} = v_{0'} + \omega * r,$$

where v_0 is the velocity of the origin 0', ω is the instantaneous angular velocity of rotation of the coordinate system $O'x'_1x'_2x'_3$, $\bar{r}$ is the point M's radius-vector in this system.

In the immobile system $Ox_1x_2x_3$ the velocity potential depends on x_i, t – φ = $= \varphi(x_i,t)$. Substituting the motion law Eq. (7.67) into this equation, the result is the potential $\varphi_1 = \varphi[x_i(x_j,t)]$ expressed through the coordinates of the mobile system. Then:

$$\frac{\partial \varphi_1}{\partial t} = \frac{\partial \varphi}{\partial t} + \frac{\partial \varphi}{\partial x_i}\frac{\partial x_i}{\partial t},$$

or, by taking Eq. (7.68) into account:

$$\frac{\partial \varphi_1}{\partial t} = \frac{\partial \varphi}{\partial t} + \bar{v}_{trans}\nabla\varphi = \frac{\partial \varphi}{\partial t} + \bar{v}_{trans}\bar{v}.$$

Now Cauchy-Lagranges integral may be presented as follows:

$$\frac{\partial \varphi_1}{\partial t} - \bar{v}_{trans}\bar{v} - \Pi + \mathrm{P} + \frac{v^2}{2} = f(t). \tag{7.69}$$

Assume the system $O'x'_1x'_2x'_3$ is moving relative to an immobile system $Ox_1x_2x_3$ at a speed $\bar{v}_{trans} = \bar{e}_1 V(t)$. Then, Eq. (7.69) changes into the following format:

$$\frac{\partial \varphi_1}{\partial t} - \bar{e}V\bar{v} - \Pi + \mathrm{P} + \frac{v^2}{2} = \frac{\partial \varphi_1}{\partial t} - V\frac{\partial \varphi}{\partial x} - \Pi + \mathrm{P} + \frac{1}{2}(\nabla\varphi)^2 = f(t)$$

[2] A reminder: $x_i(x'_j,t)$ means $x_i = x_i(x_1, x_2, x_3, t)$, $j = 1, 2, 3$.

6. Thomson's theorem

Select a line AB within the liquid and assume that all its points are moving together with the fluid, i. e., AB is a fluid line. Then equation representing the line AB can be written as $\bar{r} = \bar{r}(s,t)$ where s is a parameter changing along the line, for instance, the length of arc. If $s = \text{const}$ $\bar{r} = \bar{r}(t)$, which is the motion law of any point of the liquid line AB.

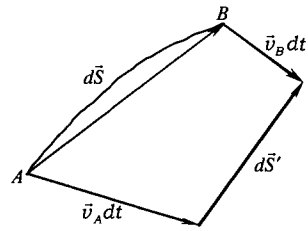

Fig. 7.5

The velocity circulation:

$$\Gamma = \int_{AB} \bar{v} d\bar{r}, \qquad (7.70)$$

is taken along AB, and computed by the derivative $\frac{d\Gamma}{dt}$. Remember, not only the velocity of the points forming the line AB but also the appearance of the line change with time. First the time derivative of the integral is taken along the fluid line. Using the integral definition, results:

$$\frac{d}{dt}\int_{AB} \varphi d\bar{r} = \frac{d}{dt} \lim_{\Delta r \to 0} \sum_{i=1}^{\infty} \varphi_i \Delta \bar{r}_i = \lim_{\Delta r \to 0} \left(\frac{d\varphi_i}{dt} \Delta \bar{r}_i + \varphi_i \frac{d\Delta \bar{r}_i}{dt} \right).$$

As $\Delta \bar{r}_i = \bar{s}^0 \Delta s$ (where $\bar{s}^0$ is a singular vector of the tangential to AB, Fig. 7.5), then:

$$\frac{d\Delta \bar{r}_i}{dt} = \bar{v}_{B_i} - \bar{v}_{A_i} = \frac{\partial \bar{v}}{\partial s} ds \qquad (7.71)$$

and:

$$\frac{d}{dt}\int_{AB} \varphi d\bar{r} = \int_{AB} \frac{\partial \varphi}{\partial t} d\bar{r} + \int_{AB} \varphi \frac{\partial \bar{v}}{\partial t} ds. \qquad (7.72)$$

Assuming in Eq. (7.72) $\varphi = \bar{v}$, from Eq. (7.70):

$$\frac{d\Gamma}{dt} = \int_{AB} \frac{dv}{dt} d\bar{r} + \int_{AB} \bar{v} \frac{\partial \bar{v}}{\partial s} ds = \int_{AB} \frac{d\bar{v}}{dt} dr + \int_{AB} \frac{1}{2} \frac{\partial v^2}{\partial s} ds = \int_{AB} \frac{d\bar{v}}{dr} dr + \frac{1}{2}\left(v_B^2 - v_A^2\right) \qquad (7.73)$$

Eq. (7.73) is purely cinematic, i. e., it is valid for any motion of any fluid.

If AB is a closed contour, the second term in Eq. (7.73) is disregarded:

$$\frac{d\Gamma}{dt} = \int_{AB} \bar{F} d\bar{r} - \int_{AB} \frac{1}{\rho} \nabla p d\bar{r} + \frac{1}{2}\left(v_B^2 - v_A^2\right). \qquad (7.74)$$

When the mass force potential is present ($\bar{F} = \nabla\Pi$), Eq. (7.74) changes its appearance:

$$\frac{d\Gamma}{dt} = \int_{AB} d\Pi - \int_{AB} \frac{1}{\rho} dp + \frac{1}{2}\left(v_B^2 - v_A^2\right), \tag{7.75}$$

where $d\Pi$, dp are differentials taken along the arc of the AB curve.

If the curve AB is closed, and the potential of Π is a univalent function, then following from Eq. (7.75):

$$\frac{d\Gamma}{dt} = -\oint \frac{1}{\rho} dp . \tag{7.76}$$

Under a barotropic process:

$$\frac{1}{\rho} dp = d\mathrm{P}, \quad \oint d\mathrm{P} = 0 ,$$

and from Eq. (7.76):

$$\frac{d\Gamma}{dt} = 0 . \tag{7.77}$$

Eq. (7.77) is the Thomson's theorem: in a case of ideal fluid, when the mass force stress has a univalent potential and the process is barotropic, the circulation along any closed fluid contour does not depend on time.

Let us pull an arbitrary surface S over a closed contour C. From the Stockes' law Eq. (3.35):

$$\Gamma = -\oint_C \bar{v} d\bar{r} = 2 \int_S \omega_n ds . \tag{7.78}$$

Following from Eqs. (7.77) and (7.78) that if the Thomson's theorem conditions are valid, the flow of rotor does not depend on time, or:

$$2 \int_S \omega_n ds = \int_S (\mathrm{rot}\,\bar{v})_n ds = \mathrm{const} , \tag{7.79}$$

Eqs. (7.78) and (7.79) are true for any contour C which can be continuously drawn tight into a point, and for any surface S pulled over this contour.

Suppose at initial time $t = 0$ there are no rotors in the entire volume occupied by the fluid ($\bar{\omega} = 0$). Then, according to Eq. (7.79):

$$\int_S (\mathrm{rot}\,\bar{v})_n ds = 0 ,$$

and as the surface S is arbitrary, for the entire fluid volume:

$$(\mathrm{rot}\bar{v})_n = 0. \tag{7.80}$$

The arbitrariness in the selection of surface S also means the arbitrariness in the selection of the direction for the normal n. So, from Eq. (7.80):

$$\mathrm{rot}\bar{v} = 2\omega = 0. \tag{7.81}$$

Eq. (7.81) gives rise to the Lagrange's theorem — on the following conditions: the fluid is ideal; the process is barotropic; mass force stresses have potential; the velocity rotor at some moment in time was equal to zero, — the motion will be vortex-free at any future time.

The condition Eq. (7.81) is a condition of a potential flow (Chapter III, Section 5). Thus in a fluid, satisfying the conditions of the Thomson's theorem, a potential flow remains potential forever if it were potential at some point in time. Similarly, the reverse statement can be shown: if the motion was vertical, it remains vertical in the future.

Lagrange's theorem shows that the motion that emerged continuously from the state of quiescence is potential. Remember, this is true only if Thomson's theorem conditions are valid. This statement is true particularly for a uniform ideal incompressible fluid in the gravitational field. In a viscous fluid and also when the barotropic nature is broken, the vortices (rotors) may emerge and disappear.

7. Helmholtz equation

Following is the ideal fluid motion equation in the Gromeko-Lamb format [Eq. (7.13)] under an assumption that the mass force stress has potential, and the process is barotropic:

$$\frac{\partial\bar{v}}{\partial t} + \nabla\left(-\Pi + \mathrm{P} + \frac{v^2}{2}\right) - 2\bar{v} * \bar{\omega} = 0, \tag{7.82}$$

where $\nabla\Pi = \bar{F}$, and P is a function of pressure: $\mathrm{P} = \int\frac{dp}{\rho}$.

Applying the rot operation to Eq. (7.82) and keeping in mind that $\mathrm{rot}(\nabla\varphi) = 0$, $\mathrm{rot}\bar{v} = 2\bar{\omega}$, results:

$$\frac{\partial\bar{\omega}}{\partial t} + \mathrm{rot}(\bar{\omega} * \bar{v}) = 0. \tag{7.83}$$

Projecting Eq. (7.83) on the axis $0x_1$:

$$\frac{\partial \omega_1}{\partial t}+\frac{\partial}{\partial x_2}(\bar{\omega}*\bar{v})_3-\frac{\partial}{\partial x_3}(\bar{\omega}*\bar{v})_2=\frac{\partial \omega_1}{\partial t}+\frac{\partial}{\partial x_2}(\omega_1 v_2-\omega_2 v_1)-\frac{\partial}{\partial x_3}(\omega_3 v_1-\omega_1 v_3)=$$

$$=\frac{\partial \omega_1}{\partial t}+\omega_1\frac{\partial v_2}{\partial x_2}+v_2\frac{\partial \omega_1}{\partial x_2}-\omega_2\frac{\partial v_1}{\partial x_2}-v_1\frac{\partial \omega_2}{\partial x_2}-\omega_3\frac{\partial v_1}{\partial x_3}-v_1\frac{\partial \omega_3}{\partial x_3}= \tag{7.84}$$

$$=\frac{\partial \omega_1}{\partial t}+v_1\frac{\partial \omega_1}{\partial x_1}+v_2\frac{\partial \omega_1}{\partial x_2}+v_3\frac{\partial \omega_1}{\partial x_3}+\omega_1\left(\frac{\partial v_1}{\partial x_1}+\frac{\partial v_2}{\partial x_2}+\frac{\partial v_3}{\partial x_3}\right)-v_1\left(\frac{\partial \omega_1}{\partial x_1}+\frac{\partial \omega_2}{\partial x_2}+\frac{\partial \omega_3}{\partial x_3}\right)-$$

$$-\omega_1\frac{\partial v_1}{\partial x_1}-\omega_2\frac{\partial v_1}{\partial x_2}-\omega_3\frac{\partial v_1}{\partial x_3}=\frac{d\omega_1}{dt}+\omega_1\mathrm{div}\bar{v}-v_1\mathrm{div}\bar{\omega}-\bar{\omega}\nabla v_1=0.$$

It is easy to check that div $\bar{\omega}=0$ using a direct substitution. Besides, following the continuity equation Eq. (7.1), div $v=-\frac{1}{\rho}\frac{d\rho}{dt}$. So, Eq. (7.84) can be written as:

$$\frac{d\omega_1}{dt}-\frac{\omega_1}{\rho}\frac{d\rho}{dt}=\bar{\omega}\nabla v_1,$$

or:

$$\frac{1}{\rho}\frac{d\omega_1}{dt}-\frac{\omega_1}{\rho^2}\frac{d\rho}{dt}=\frac{\omega}{\rho}\nabla v_1,$$

wherefrom:

$$\frac{d}{dt}\left(\frac{\omega_1}{\rho}\right)=\frac{\bar{\omega}}{\rho}\nabla v_1. \tag{7.85}$$

The Eq. (7.85) is the Helmholtz equation as projected onto the $0x_1$ axis and its vector format is:

$$\frac{d}{dt}\left(\frac{\bar{\omega}}{\rho}\right)=\left(\frac{\bar{\omega}}{\rho}*\nabla\right)\bar{v}\ . \tag{7.86}$$

Helmholtz equation Eq. (7.85) or (7.86) provides an opportunity to find a change in the vortex field with time.

Eqs. (7.83) and (7.86) are purely kinematic and it is apparent from Eq. (7.83). Eq. (7.86) is a direct consequence of Eq. (7.84), which, considering $\mathrm{div}\bar{\omega}=0$, takes the following vector format:

$$\frac{d\bar{\omega}}{dt}+\bar{\omega}\mathrm{div}\bar{v}=\left(\bar{\omega}*\nabla\right)\bar{v}.$$

Consider a vortex line in a fluid. Now it is important to review its element $d\bar{s}=\varepsilon\frac{\bar{\omega}}{\rho}$ (by definition of a vortex line, $d\bar{s}\|\bar{\omega}$) where ε is a small constant. Lets

denote both ends of the $d\bar{s}$ vector A and B (Fig. 7.5). Fluid's particles (material points) which formed $d\bar{s}$ at the time t form the $d\bar{s}'$ element at the time $t + dt$.

Then:

$$d\bar{s}' = d\bar{s} + \bar{v}_B dt - \bar{v}_A dt . \tag{7.87}$$

It is important to note the fact that Eq. (7.87) in its meaning is in agreement with Eq. (7.71).

In accordance with Eq. (3.3) and with the definition of vector $d\bar{s}$:

$$\bar{v}_B - \bar{v}_A = (d\bar{s} * \nabla)\bar{v} = \left(\varepsilon \frac{\bar{\omega}}{\rho} * \nabla\right)\bar{v},$$

and Eq. (7.87) takes the format of :

$$d\bar{s}' = \left[\frac{\bar{\omega}}{\rho} + \left(\frac{\bar{\omega}}{\rho} * \nabla\right)\bar{v}dt\right]. \tag{7.88}$$

Now take the vector of vortex $d\bar{s} = \varepsilon \frac{\bar{\omega}}{\rho}$. At the time $t + \Delta t$ it is equal to:

$$d\bar{s}'' = \varepsilon \frac{\bar{\omega}'}{\rho'} = d\bar{s} + \frac{d\bar{s}}{dt}dt = \varepsilon \frac{\bar{\omega}}{\rho} + \varepsilon \frac{d}{dt}\left(\frac{\bar{\omega}}{\rho}\right)dt . \tag{7.89}$$

It is critical to remember that a total derivative is taken in Eq. (7.89). For this reason, the second term of this equation (with the accuracy to the terms of higher order of smallness) is an addition of a fluid vortex element $d\bar{s} = \varepsilon \frac{\bar{\omega}}{\rho}$ for the time period dt.

Using Helmholtz equation Eq. (7.86), Eq. (7.89) can be written as follows:

$$d\bar{s}'' = \varepsilon\left[\frac{\bar{\omega}}{\rho} + \left(\frac{\bar{\omega}}{\rho} * \nabla\right)\bar{v}dt\right]. \tag{7.90}$$

Vector $d\bar{s}'$ is the element of the liquid line into which the $d\bar{s}$ element will transform over time period dt. Vector $d\bar{s}''$ is the element of the fluid line at the time period $dt + t$. It can be seen from Eqs. (7.88) and (7.90), that $d\bar{s}' = d\bar{s}''$. Therefore, the vortex line elements always coincide with the fluid line elements from which this vortex line is composed. Thus, if the mass force stress has potential, the fluid is ideal and the process is barotropic (the conditions under which Helmholtz equation is valid), the vortices move together with the fluid's particles (the second Helmholtz theorem).

Now consider an elementary vortex tube with the cross-section $d\sigma$. Its stress is equal to $\omega d\sigma$. During the time interval dt it converts into a vortex tube with the cross-section $d\sigma'$. It is proved earlier that the vortex tube consists of the same particles at all times. Therefore, from the mass conservation law:

$$\rho d\sigma ds = \rho' d\sigma' ds'.$$

Replacing ds with $\varepsilon\frac{\omega}{\rho}$ and ds' with $\varepsilon\frac{\omega'}{\rho'}$, results:

$$\omega d\sigma = \omega' d\sigma',$$

meaning that the stress of the vortex tube remains unchanged in time.

Following from Helmholtz equation Eq. (7.86) that if at some moment in time $\bar{\omega}=0$, then $\frac{d}{dt}\left(\frac{\bar{\omega}}{\rho}\right)=0$, i. e., if there were no vortices, they cannot emerge in the future.

This statement is not true for a viscous fluid.

The viscous incompressible fluid's motion equation at μ = const is Eq. (4.42). When the mass force potential is present, this equation can be written as:

$$\frac{d\bar{v}}{dt}=\frac{\partial\bar{v}}{\partial t}+\Delta\frac{v^2}{2}-2\bar{v}*\bar{\omega}=\Delta\Pi-\Delta p+\frac{\mu}{\rho}\Delta\bar{v}. \tag{7.91}$$

Applying to this equation the same procedure as to Eq. (7.82), and considering $\mathrm{rot}(\Delta\bar{\alpha}) = \Delta\,\mathrm{rot}\bar{\alpha}$, the result is:

$$\frac{d\bar{\omega}}{dt}=(\bar{\omega}*\nabla)\bar{v}+\frac{\mu}{\rho}\Delta\bar{\omega}. \tag{7.92}$$

Due to the presence of the additional term $\frac{\mu}{\rho}\Delta\bar{\omega}$, the vortex lines will not be the fluid lines, and the vortices can spread from one particle to the next.

When the interruptions are small, the terms $v_i\frac{\partial\bar{\omega}}{\partial x_i}$ and $(\bar{\omega}*\nabla)\bar{v}$ in Eq. (7.92) are negligible second-order numerical values, and the equation can be written as follows:

$$\frac{d\bar{\omega}}{dt}=\frac{\mu}{\rho}\Delta\bar{\omega},$$

this equation is the same as heat-conductivity equation. Therefore, under small interruptions vorticity in a viscous fluid behave the same way as temperature of a non-uniformly-heated body. Its tendency is to spread all over the heated body. The vortex diffusion occurs.

8. Potential flow of a incompressible fluid

The Cauchy-Lagrange's integral Eq. (7.66) for the potential flow of a uniform incompressible fluid can be written as follows:

$$\frac{\partial\varphi}{\partial t}-\Pi+\frac{p}{\rho}+\frac{1}{2}(\nabla\varphi)^2=0. \tag{7.93}$$

From the continuity equation and a condition of the flow potentiality:

$$\operatorname{div}\bar{v} = \operatorname{div}(\nabla\varphi) = \Delta\varphi = 0, \tag{7.94}$$

where Δ is the Laplace operator.

Considering Eq. (7.94) that φ is a harmonic function, and Eq. (7.93), when φ is known, allows to find the pressure distribution. Eq. (7.93) does not impose limitations on the solution of the Laplace equation. So, each potential flow of a incompressible fluid has its corresponding harmonic function φ, and any harmonic function has its corresponding potential flow of a incompressible fluid. Thus, study of the potential motion of a uniform incompressible fluid is reduced to the study of the Laplace equation solutions, i. e., to a search of its solutions with the assigned boundary conditions.

Let's review a space volume where any harmonic function is assigned. From Gauss—Ostrogradsky theorem and Eq. (7.94):

$$\int_V \operatorname{div}\bar{v}\,dV = \int_V \operatorname{div}(\nabla\varphi)\,dV = \int_S \bar{n}\nabla\varphi\,dS = \int_S \frac{\partial\varphi}{\partial n}dS = 0. \tag{7.95}$$

Suppose the harmonic function φ comes up to a maximum at the internal point M of the volume D. Surrounding the point M with an infinitely small surface S, as φ comes to a maximum at the point M, there must be $\frac{\partial\varphi}{\partial n} < 0$ at the points of the surface S, and Eq. (7.95) is not valid. Therefore, the function φ cannot have a maximum at the internal point of the volume D. Using the same approach, it is easy to prove that the function φ cannot have a minimum at the internal point of the volume D. Thus, the harmonic function may come to a maximum or minimum only at the volume D boundary.

Suppose the flow velocity reaches to a maximum at the internal point of the volume and is equal to v_M. The coordinate axes at this point is selected so that $v_M = \frac{\partial\varphi}{\partial x_1}$. As φ is a harmonic function, $\frac{\partial\varphi}{\partial x_1}$ is also a harmonic function, so it cannot reach a maximum at point M. Then within a small neighborhood of the point M, it is possible to find such a point N where:

$$\left(\frac{\partial\varphi}{\partial x_1}\right)_N > \left(\frac{\partial\varphi}{\partial x_1}\right)_M,$$

and from here:

$$\sqrt{\left(\frac{\partial\varphi}{\partial x_1}\right)_N^2 + \left(\frac{\partial\varphi}{\partial x_2}\right)_N^2 + \left(\frac{\partial\varphi}{\partial x_3}\right)_N^2} > \left(\frac{\partial\varphi}{\partial x_1}\right)_N > \left(\frac{\partial\varphi}{\partial x_1}\right)_M = v_M. \tag{7.96}$$

Eq. (7.96) shows that the flow velocity cannot reach maximum at the internal point of a volume. Using the same approach, it is easy to prove that it cannot have a minimum at the internal point of the volume. Thus, the potential flow velocity of a

incompressible fluid can come to a maximum or minimum only at the volume D boundary.

Now it is beneficial to review some examples of the potential flow of incompressible fluids.

Suppose:

$$\varphi = -\frac{Q(t)}{4\pi r},\ r = \sqrt{(x_1 - x_{10})^2 + (x_2 - x_{20})^2 + (x_3 - x_{30})^2}. \tag{7.97}$$

In this case:

$$\frac{\partial \varphi}{\partial x_1} = \frac{Q(t)}{4\pi r} * \frac{x_i - x_{i0}}{r^3},\ \frac{\partial^2 \varphi}{\partial x^2{}_1} = \frac{Q(t)}{4\pi r} * \frac{r^2 - 3(x_i - x_{i0})^2}{r^5},$$

and it follows from here that:

$$\Delta\varphi = \frac{\partial^2 \varphi}{\partial x^2{}_1} + \frac{\partial^2 \varphi}{\partial x^2{}_2} + \frac{\partial^2 \varphi}{\partial x^2{}_3} = 0.$$

Therefore, φ is a harmonic function describing the flow of a incompressible fluid.

Equipotential surfaces φ =const are spheres with the center at point (x_{10}, x_{20}, x_{30},). The flow velocity $\bar{v} = \nabla\varphi$ is directed along the normals to these spheres, i. e., along the radii, which are also the flow lines. Then:

$$v_r = \frac{\partial \varphi}{\partial r} = \frac{Q(t)}{4\pi r^2}, \tag{7.98}$$

with r = const and v_r = const.

At $r \to 0$, $v_r \to \infty$, i. e., the center of the sphere is a singularity where infinite number of flow lines intersect.

The throughflow through the surface of a sphere of an arbitrary radius is equal to:

$$\int_S v_r d\sigma = v_r \int_S d\sigma = 4\pi r^2 v_r = Q(t).$$

If $Q(t) > 0$, the flow velocities are directed away from the sphere, there is a fluid's source with the intensity $Q(t)$ in the center. If $Q(t) < 0$, there is a drain.

Eq. (7.98) indicates that if the source (drain) intensity changes in time, the velocities in the entire fluid's occupied volume simultaneously change. i. e., the disturbances in a incompressible fluid are translated at infinitely large velocity (instantaneously).

Thus, Eq. (7.97) determines the velocity potential from the source (drain) in the space.

Laplace equation is linear; thus, the function:

$$\varphi = -\frac{1}{4\pi}\sum \frac{Q_k(t)}{r_k},\ r_k = \sqrt{(x_1 - x_{1k})^2 + (x_2 - x_{2k})^2 + (x_3 - x_{3k})^2}$$

is also its solution and describes the flow emerging in the presence of n sources (drains).

Consider some volume V_0 positioned outside of the moving fluid-occupied volume D. In this case the function:

$$\varphi = -\frac{1}{4\pi}\int_{V_0}\frac{q(x_{i0},t)}{r}dV_0,\ r_k = \sqrt{(x_1-x_{10})^2+(x_2-x_{20})^2+(x_3-x_{30})^2},$$

is harmonic an describes the flow in volume D from the sources with density q, continuously distributed in volume V_0. Similarly, it is possible to determine potentials for the surface S_0 and line l_0, which do not belong to D:

$$\varphi = -\frac{1}{4\pi}\int_{S_0}\frac{m(x_{i0},t)}{r}dS_0,\ \varphi = -\frac{1}{4\pi}\int_{l_0}\frac{n(x_{i0},t)}{r}dl_0,$$

where m and n are distribution densities of the surficial and linear sources.

2. Suppose there is a sink at the point $N(x_{i0})$ and the source at the point $N_1(x_{i0}+dx_i)$. Assume that the source's and drain's intensities are equal and consider point $M(x_j)$ (Fig. 7.6) immobile. Potential at this point from the combination of the source and drain is:

$$\varphi = -\frac{Q}{4\pi r_1}+\frac{Q}{4\pi r} = -\frac{Q\Delta s}{4\pi\Delta s}\left(\frac{1}{r_1}-\frac{1}{r}\right),\ r = \sqrt{(x_1-x_{10})^2+(x_2-x_{20})^2+(x_3-x_{30})^2}. \quad (7.99)$$

Suppose the point N_1 approaches point N with no limit, and the product $Q\Delta s$ remains constant. Then, from Eq. (7.99):

$$\varphi = -\frac{m}{4\pi}\lim_{\Delta s\to 0}\frac{1}{\Delta s}\left(\frac{1}{r_1}-\frac{1}{r}\right) = -\frac{m}{4\pi}\frac{\partial}{\partial s}\left(\frac{1}{r}\right) = -\frac{m}{4\pi}\bar{s}^0\nabla\left(\frac{1}{r}\right),$$

where $\bar{s}^0$ is a singular vector of the straight line connecting the points N and N_1. The value $\nabla\left(\frac{1}{r}\right)$ is computed at the point $N(x_{i0})$, and as the point M is immobile, the differentiation is performed with respect to coordinates x_{i0}, and:

$$\nabla\left(\frac{1}{r}\right) = \bar{e}_k\frac{\partial}{\partial x_{k0}}\left(\frac{1}{r}\right) = \bar{e}_k\frac{x_k-x_{k0}}{r^3} = \frac{\bar{r}}{r^3}.$$

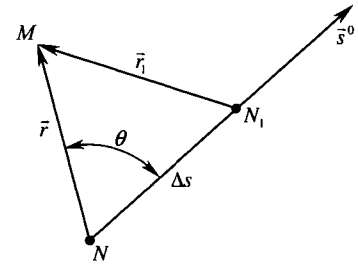

Fig. 7.6

In this case:

$$\varphi = -\frac{m}{4\pi}\frac{\bar{r}*\bar{s}^0}{r^3} = -\frac{m}{4\pi}\frac{\cos\theta}{r^2}. \quad (7.100)$$

Such combination of the source and drain is called dipole, the value m is called the dipole momentum, and the axis passing through the points N and N_1 is called the dipole axis.

Superposing the dipole axis with one of the coordinate axes, it is easy to show that the function φ defined by Eq. (7.100) is harmonic.

9. Flow around the sphere

Let's review the motion of a sphere within the infinite incompressible ideal fluid. Assume that the fluid at infinity is at rest. There is some disturbed volume near the sphere. If the motions of both the sphere and the fluid emerged continuously from the state of rest then, under Thomson theorem, the fluid's motion is potential.

Now it is important to put together the conditions for the determination of the potential of this motion. Under Eq. (7.94), $\Delta\varphi = 0$ within the fluid. As the fluid is at rest at infinity, $\nabla\varphi = 0$ there. From the fluid's non-leakage condition [Eq. (4.20)], $v_n = u_n$ where u_n, is the normal component of the sphere velocity u at the points of its surface. As $\bar{v} = \nabla\varphi$, this condition acquires the following format: $\frac{\partial\varphi}{\partial u} = u_n$.

Thus, the problem of finding the velocity potential at flowing around the sphere is reduced to the solution of Laplace equation when a normal derivative is established at the boundary. This is a classical Neumann's problem.

Suppose a sphere with the radius a is in the translational motion at the velocity U. It is important to introduce a coordinate system $0x_1y_1z_1$ rigidly attached to the sphere, and will direct axis $0x_1$ parallel to the velocity U (Fig. 7.7). Now, take a dipole with the axis parallel to $0x_1$ and place it into the origin. Eq. (7.101) is valid in a stationary coordinate system at the time when the center of the sphere is at the origin. At any other time t_0 in the stationary coordinate system $\varphi = -\frac{m}{4\pi}\frac{\cos\theta}{(r-r_0)^2}$, where r_0 is the sphere's center coordinate at $t = t_0$.

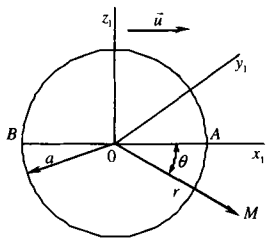

Fig. 7.7

$$\varphi = -\frac{m}{4\pi}\frac{\cos\theta}{r^2}. \tag{7.101}$$

At any point M of the space:

$$\frac{\partial\varphi}{\partial r} = \frac{m}{2\pi}\frac{\cos\theta}{r^3},$$

and at $\theta = 0$ (Fig. 7.7) at the point A of the sphere:

$$\frac{\partial\varphi}{\partial r} = U = \frac{m}{2\pi a^3},$$

and from this:

$$\varphi = -\frac{Ua^3\cos\theta}{2r^2} = -\frac{Ua^3x_1}{2r^3}. \tag{7.102}$$

It is easy to see that the potential φ as defined by Eq. (7.102) responds to all set conditions.

Now assign a velocity to the entire system opposite to the sphere's velocity, i. e., $-U$. This motion has the potential $-Ux_1$. The relative motion's potential (the sphere is quiescent, and the liquid overruns it at a velocity of $-U$) is obtained by adding the potentials of the absolute and translational motion together:

$$\varphi_{rel} = -\frac{Ua^3 x_1}{2r^3} - Ux_1 = -\left(1 + \frac{a^3}{2r^3}\right) Ux_1 = -U\left(r + \frac{a^3}{2r^2}\right)\cos\theta . \qquad (7.103)$$

Following from Eq. (7.103), the normal component of the fluid's velocity v_n on the sphere's surface is equal to:

$$v_n = -\left(\frac{\partial \varphi_{rel}}{\partial r}\right)_{r=a} = 0 ,$$

i. e., the immobile sphere is the surface of the flow. That is why the fluid's velocity v_s tangential to this surface is the total value of the velocity, and:

$$v = v_s = -\frac{\partial \varphi_{rel}}{\partial s}\Big|_{r=a} = \frac{\partial \varphi_{rel}}{r\partial\theta}\Big|_{r=a} = \frac{3}{2} U \sin\theta . \qquad (7.104)$$

As this equation shows, at points A and B (Fig. 7.7) $v = 0$, and at $\theta = \frac{\pi}{2}$ (at the equator) $v = \frac{3}{2}U$. Therefore, the velocity of flowing-around the sphere is 50 % greater at the equator than the velocity of the overrunning flow.

At a transient-free motion, disregarding the mass forces, and from Bernoulli's integral Eq. (7.28):

$$p = p_0 + \rho \frac{U^2 - v^2}{2} , \qquad (7.105)$$

where p_0 and U are pressure and velocity at infinity. Substituting the velocity value at the equator in Eq. (7.105), results:

$$p = p_0 - \frac{5}{8}\rho U^2$$

The velocities are symmetrically distributed relative the equator. Therefore, pressures are also symmetrically distributed, and the resistance to the sphere motion and the lift are equal to zero. This result is a specific case of Dalamber's paradox (see below).

The theory of a potential continuous motion of the ideal fluid results in Dalamber's paradox. Still, it can be used to compute the close-to-actual velocity distribution for flow-around bodies. This enables also a computation of the friction forces using the theory of boundary layer where the viscous friction forces appear (see Chapter XIV).

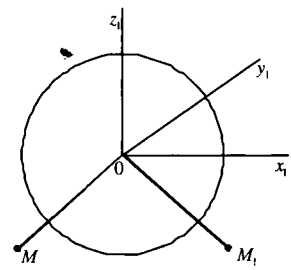

Fig. 7.8

Now it is important to review the non-stationary motion of the sphere. Suppose a sphere with the radius a is in the translational motion at a speed $U = U(t)$

parallel to axis $0x$. For a movable coordinate system tied-in with the sphere, the flow potential has the format of Eq. (7.102). Assuming the fluid is incompressible and that the mass forces may be disregarded, Cauchy-Lagrange's integral in this case is:

$$\frac{\partial \varphi_1}{\partial t} - \frac{\partial \varphi}{\partial x} U + \frac{p}{\rho} + \frac{v^2}{2} = \frac{p_0}{\rho} = \text{const}, \tag{7.106}$$

as the fluid is quiescent at infinity, the pressure is equal to p_0 (φ_1 is potential in a moving coordinate system).

From Eq. (7.102):

$$\frac{\partial \varphi}{\partial x_1} = -\frac{Ua^3}{2} \frac{r^2 - 3x_1^2}{r^5}, \quad \frac{\partial \varphi}{\partial y_1} = \frac{3}{2} \frac{Ua^3}{r^5} x_1 y_1, \quad \frac{\partial \varphi}{\partial z_1} = \frac{3}{2} \frac{Ua^3}{r^5} x_1 z_1.$$

Therefore, at points M and M_1 symmetric relative to the $y_1 0 z_1$ plane (Fig. 7.8):

$$\left(\frac{\partial \varphi}{\partial x_1}\right)_M = \left(\frac{\partial \varphi}{\partial x_1}\right)_{M_1}, \quad \left(\frac{\partial \varphi}{\partial y_1}\right)_M = \left(\frac{\partial \varphi}{\partial y_1}\right)_{M_1}, \quad \left(\frac{\partial \varphi}{\partial z_1}\right)_M = \left(\frac{\partial \varphi}{z y_1}\right)_{M_1}, \tag{7.107}$$

so:

$$v^2{}_M = v^2{}_{M_1}, \quad \left(U \frac{\partial \varphi}{\partial x_1}\right)_M = \left(\frac{\partial \varphi}{\partial x_1}\right)_{M_1}. \tag{7.108}$$

The following hydrodynamic force will be acting on the moving sphere:

$$\bar{R} = -\int_\sigma p \bar{n} d\sigma, \tag{7.109}$$

where σ is the surface of the sphere. The area of an elementary spherical belt is:

$$d\sigma = 2\pi a^2 \sin\theta d\theta, \tag{7.110}$$

$$\int_\sigma p_0 \cos\theta d\sigma = 2\pi a^2 p_0 \int_0^\pi \cos\theta \sin\theta d\theta = 0. \tag{7.111}$$

Projecting Eq. (7.109) onto $0x$ axis and considering Eqs. (7.109) and (7.111) gives:

$$R_x = -2\pi a^2 \int_0^\pi (p - p_0) \cos\theta \sin\theta d\theta. \tag{7.112}$$

Substituting into Eq. (7.108) the difference $(p - p_0)$ from Cauchy-Lagrange's integral [Eq. (7.106)], and considering Eqs. (7.107) and (7.108), one obtains:

$$R_x = -2\pi a^2 \rho \int_0^\pi \left(-\frac{\partial \varphi_1}{\partial t}\right) \cos\theta \sin\theta d\theta, \tag{7.113}$$

where, in integrating it is necessary to assume $r = a$ as p is pressure at points of the sphere.

From equation for the potential in a moving coordinate system Eq. (7.98) at $r = a$ and $x_1 = r\cos\theta$:

$$\frac{\partial \varphi_1}{\partial t} = -\frac{a}{2} \frac{dU}{dt} \cos\theta.$$

Substituting this equation into Eq. (7.109), results:

$$R_x = -2\pi a^3 \rho \frac{dU}{dt} \int_0^{\pi} \cos^2\theta \sin\theta d\theta = -\frac{3}{2}\pi a^3 \rho \frac{dU}{dt}.$$

If $\frac{dU}{dt} > 0$, the resistance force R_x is negative, i. e., it impedes the increase in velocity U. If $\frac{dU}{dt} < 0$, R_x obstructs the drag. The ideal fluid is as if increasing the body's inertia.

Indeed, the sphere motion equation in the ideal fluid can be written in the following format:

$$m\frac{dU}{dt} = F^{(e)} - \frac{2\pi}{3}\rho a^3 \frac{dU}{dt} \text{ or } \left(m + \frac{2\pi}{3}\rho a^3\right)\frac{dU}{dt} = F^{(e)},$$

and in vacuum:

$$m\frac{dU}{dt} = F^{(e)}.$$

The value $\frac{2\pi}{3}\rho a^3$ is called the attached mass. For a sphere it is equal to a half of the fluid mass within its volume.

For a body moving in a viscous fluid the problem in a general case cannot be reduced to the computation of the attached masses. However, for a body with good flow-around and moving at a high velocity, viscosity may be disregarded, and the effect from the action of a variable velocity will be the same as in the ideal fluid.

10. Applications of the of momentum law

1. Flat immobile wall at which a jet-stream is directed (Fig. 7.9). The transient-free motion is disregarded by the mass forces. Under these conditions, the momentum law [Eq. (2.51)] is:

$$\int_{\Sigma} \rho \bar{v} v_n d\Sigma = -\int_{\Sigma} \bar{p}_n d\Sigma, \tag{7.114}$$

where Σ is a closed surface limited by cross-sections S_1, S_2, S_3, by the jet surface S_4 and the surface of the wall σ. It is also necessary to assume that the pressure at the jet surface is constant ($p = p_0 = \text{const}$) and that the velocity is uniformly distributed in the cross-sections S_1, S_2, S_3. Based on this and using Bernoulli's integral, a conclusion is that the velocity at the jet surface is constant, and using Euler's equations, the pressure in cross-sections S_1, S_2, S_3 is also constant and is equal to $p = p_0$.

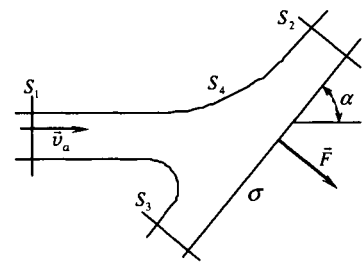

Fig. 7.9

For an incompressible ideal fluid $\rho = \text{const}$, and $\bar{p}_n = -p\bar{n}$, where $\bar{n}$ is a normal to the surface Σ; thus Eq. (7.114) can be written as follows:

$$\rho \int_{\Sigma} \bar{v} v_n d\Sigma = -\int_{\Sigma} (p - p_0)\bar{n} d\Sigma \tag{7.115}$$

because for a closed surface Σ, under Gauss–Ostrogradsky theorem:

$$\int_{\Sigma} p_0 \bar{n} d\Sigma = 0$$

As $p \neq p_0$ only at the points of the surface σ, considering Eq. (7.115) gives:

$$\rho \int_{\Sigma} \bar{v} v_n d\Sigma = -\int_{\sigma} (p - p_0)\bar{n} d\sigma = -\bar{F} = F\bar{n}, \tag{7.116}$$

where $\bar{F}$ is the force at which the jet is acting on the wall. Because the fluid is ideal, this force is perpendicular to the wall.

Project Eq. (7.116) onto the axis $0x$, which is perpendicular to the wall. Remember that $v_n = 0$ S_4 and σ, $v_x = 0$ on S_2 and S_3, and on $S_1 v_n = -v_0 = \text{constant}$, $= v_x = v_0 \sin\alpha$, where α is the angle between the wall and the jet direction. In this case:

$$F = \rho \int_{S_1} v_0^2 \sin\alpha dS = \rho v_0^2 S \sin\alpha.$$

As the force $\bar{F}$ emerges due to change in momentum of the jet, i. e., due to a rotation of the velocity vector, the cross-sections S_2, S_3 should be selected where the jet surface and, therefore, its velocity, become parallel to the wall.

2. Horizontal segment of the tube bent at 90° (the "knee") where a liquid (or gas) is flowing (Fig. 7.10); Assume the motion is transient-free and using the law of variation in momentum [Eq. (2.58)] in the following format:

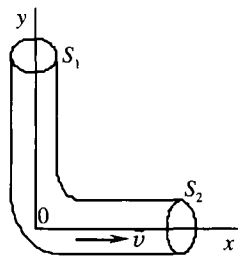

Fig. 7.10

$$Q_m = \left(\bar{v}_2^{(avg)} - \bar{v}_1^{(avg)}\right) = \bar{G} + \bar{P} + \bar{R} \tag{7.117}$$

where $\bar{R} = \bar{N} + \bar{T}$ is the force with which the knee is acting upon the liquid.

Assuming $\bar{p}_n = -p\bar{n}$ and projecting Eq. (7.117) onto axes $0x$ and $0y$, and considering Eq. (2.54) gives:

$$Q_m = \left(v_{2x}^{(avg)} - v_{1x}^{(avg)}\right) = \bar{P}_x + \bar{R}_x = -p_2 S_2 + R_x,$$

$$Q_m = \left(v_{2y}^{(avg)} - v_{1y}^{(avg)}\right) = \bar{P}_y + \bar{R}_y = -p_1 S_1 + R_y. \tag{7.118}$$

In the cross-section S_1, $v_{1x}^{(avg)} = 0$, $v_{1y}^{(avg)} = -v_1^{(avg)}$. In the cross-section S_2, $v_{2x}^{(avg)} = v_2^{(avg)}$, $v_{2y}^{(avg)} = 0$. Then, the Eq. (7.118) takes the following format:

$$\bar{F}_x = -\bar{R}_x = -Q_m v_2^{(avg)} - p_2 S_2,$$

$$\overline{F}_y = -\overline{R}_y = -Q_m v_1^{(avg)} - p_1 S_1,$$

where F_x, F_y are components of the force with which the liquid acts upon the knee.

Note that due to the presence of a term $\overline{T}$, this conclusion is valid also for a viscous medium.

3. Infinitely-long tube filled-up with an ideal liquid. Suppose a body is moving within the tube at a constant velocity v_0 (Fig. 7.11). Assuming the hypothesis that far behind the body and far ahead of it the liquid is not disturbed, i. e., its velocity is equal to zero. Reversing the problem by attributing the velocity $-\bar{v}_0$ to the entire system, in such a case, the body is immobile, the velocity at infinity behind and ahead of the body is $-\bar{v}_0$, and the flow is transient-free.

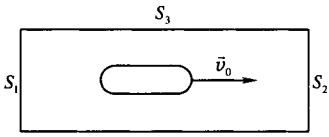

Fig. 7.11

Due to the law of variation in momentum [Eq. (2.44)], disregarding the mass forces, results:

$$\int_S \rho \bar{v} v_n dS = \int_S \overline{p}_n dS. \tag{7.119}$$

The body under consideration is within the flow-tube limited by cross-sections S_1 and S_2 (with $S_1 = S_2$) and the side surface S_3. Thus, the closed surface bounding the liquid is:

$$S = S_1 + S_2 + S_3 + \sigma \text{ where } \sigma \text{ is the surface of the body.}$$

Now it is important to review the distribution of the velocity's normal component v_n on the S surface. On S_3, $v_n = 0$ by definition of the flow-tube. On σ, $v_n = 0$ from the condition of impermeability of the body's surface. In the section S_1 far ahead of the body, $v_n = v_0$. In the section S_2 far beyond the body, $v_n = -v_0$. Besides, in the sections S_1 and S_2, $\bar{v} = -\bar{v}_0$. Then:

$$\int_S \rho \bar{v} v_n dS = -\int_{S_1} \rho \bar{v}_0 v_0 dS + \int_{S_2} \rho \bar{v} v_0 dS. \tag{7.120}$$

The liquid by definition is ideal, so $\overline{p}_n = -\overline{pn}$, and:

$$\int_S \overline{p}_n dS = -\int_{S_1} \overline{pn} dS - \int_{S_2} \overline{pn} dS - \int_{S_3} \overline{pn} dS - \overline{R}, \tag{7.121}$$

where $\overline{R} = \int_\sigma \overline{pn} d\sigma$ is the force with which the flow acts upon the body.

Suppose either the liquid is incompressible or the process is adiabatic. As the velocities in the cross-sections S_1 and S_2 are of equal numerical value, then following Bernoulli's integral Eq. (7.28) or from Eqs. (7.46) and (7.47), $p_1 = p_2 = p_0$, $\rho_1 = \rho_2 = \rho_0$,

where p_1, p_2, ρ_1, ρ_2 are pressures and densities in cross-sections S_1 and S_2. Under these conditions and from Eq. (7.120):

$$\int_S \rho \bar{v} v_n dS = 0,$$

and from Eqs. (7.119) and (7.121):

$$\bar{R} = \int_{S_3} p \bar{n} dS, \tag{7.122}$$

because $S_1 = S_2$, and the normals on these surfaces are oppositely directed.

The normal on the surface S_3 is perpendicular to the direction of velocity $\bar{v}_0$. So, by projecting Eq. (7.122) onto the direction of the velocity, results:

$$R = 0$$

Thus, if: a body of arbitrary shape is moving within a liquid at a constant velocity, the liquid is ideal and does not have a free surface, it is incompressible, and the process is adiabatic; the motion of the liquid is continuous, the liquid at infinity behind and in front of the body is not disturbed — then the resistance to the body motion is equal to zero. This statement is the Dalamber's paradox.

The paradox appears to suggest that far in front of and far behind the body the liquid is quiescent, that the liquid is ideal and its flow os continuous. In real life, these conditions are not maintained, so the Dalamber's paradox is not observed.

Mechanics of Fluid Flow
by Kaplan S. Basniev, Nikolay M. Dmitriev and George V. Chilingar

CHAPTER VIII

PARALLEL-PLANE FLOWS OF IDEAL INCOMPRESSIBLE FLUID

1. Complex-valued potential of flow

The flow whose parameters are the same in parallel planes, i. e., depends only on the two spatial coordinates and time, is called parallel-plane flow. Such a flow is usually considered in the $x0y$ plane. Each line drawn in this plane is actually a directrix of a cylindrical surface with the generatrix perpendicular to the $x0y$ plane. All numerical values of the fluid's throughflow, of forces attached to the bodies, are related to the unit height of the corresponding cylindrical surfaces.

Taking a parallel-plane flow of a incompressible fluid, based on the continuity equation Eq. (2.25):

$$\operatorname{div}\bar{v} = \frac{\partial v_x}{\partial x} + \frac{\partial v_y}{\partial y} = 0. \tag{8.1}$$

Suppose:

$$v_x = \frac{\partial \psi}{\partial x}, \quad v_y = \frac{-\partial \psi}{\partial x}. \tag{8.2}$$

Function $\psi = \psi(x,y,t)$ is in accordance with the continuity equation Eq. (8.1), and:[1]

$$\partial \psi = \frac{\partial \psi}{\partial x}dx + \frac{\partial \psi}{\partial y}dy = v_x dy - v_y dx. \tag{8.3}$$

Function $\psi = \psi(x,y,t)$ is called the flow function. At $d\psi = 0$ and from Eq. (8.3):

$$\frac{dx}{v_x} = \frac{dy}{v_y}. \tag{8.4}$$

[1] Time t is considered as a parameter here.

As can be seen from Eq. (7.122), Eq. (8.4) is the equation of the flow-lines at which ψ = const.

Taking the flow-lines $\psi(x,y) = \psi_0$ and $\psi(x,y) = \psi_1$ (Fig. 8.1) the throughflow Q over the line S is equal to:

$$Q = \int_S \bar{v} * \bar{n} ds = \int_S [v_x \cos(n,x)dx + v_y \cos(n,y)]dS .$$

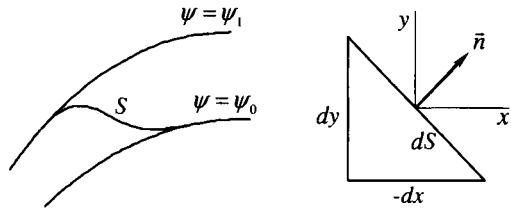

Fig. 8.1

As $\cos(n,x) = \frac{dy}{dS}$, $\cos(n,y) = \frac{dx}{dS}$, then, under Eq. (8.3):

$$Q = \int_S v_y dx - v_x dy = \int_S d\psi = \psi_1 - \psi_0 , \tag{8.5}$$

i. e., the difference $\psi_1 - \psi_0$ is the fluid throughflow between the flow-lines ψ_0 = const and ψ_1 = const.

At a potential flow:

$$v_x = \frac{\partial \varphi}{\partial x}, \quad v_y = \frac{\partial \varphi}{\partial y}. \tag{8.6}$$

Following Eqs. (8.2) and (8.6), at a potential flow:

$$\frac{\partial \varphi}{\partial x} = \frac{\partial \psi}{\partial x}, \quad \frac{\partial \varphi}{\partial y} = -\frac{\partial \psi}{\partial x}. \tag{8.7}$$

The Eq. (8.7) ratios are Cauchy-Riemann conditions. If they are valid, the function of a complex variable z:

$$W(z) = \varphi(x,y) + i\psi(x,y), \quad z = x + iy \tag{8.8}$$

is an analytical function. The function $W(z)$ is called a complex potential.

From the continuity equation Eqs. (8.1), (8.6) ratios and the Cauchy-Riemann conditions Eq. (8.7), $\Delta\varphi = 0$, $\Delta\psi = 0$, i. e., both the velocity potential and the flow function are harmonic functions.

The relations:

$$\varphi(x,y)=\text{const}, \quad \psi(x,y)=\text{const}$$

are, respectively, equations of equipotential lines and flow-lines. From Eqs. (8.2) and (8.6):

$$\nabla\varphi\nabla\psi=\frac{\partial\varphi}{\partial x}\frac{\partial\psi}{\partial x}+\frac{\partial\varphi}{\partial y}\frac{\partial\psi}{\partial y}=-v_x v_y+v_y v_x\equiv 0,$$

i. e., the vectors $\nabla\varphi$ and $\nabla\psi$ are mutually perpendicular. Therefore, the equipotential lines and flow-lines form a family of mutually orthogonal lines.

By differentiating a complex potential Eq. (8.7) and considering Eqs. (8.2) and (8.7)[2], results:

$$\frac{\partial W}{\partial z}=\frac{\partial\varphi}{\partial x}+i\frac{\partial\psi}{\partial x}=v_x-iv_y=ve^{-i\theta}, \tag{8.9}$$

and from this:

$$\left|\frac{dW}{dz}\right|=v, \quad \arg\frac{dW}{dz}=-\theta, \tag{8.10}$$

where θ is the angle between the velocity direction and $0x$ axis.

Thus, the modulus of the complex potential's derivative is equal to the numerical value of the velocity, and the argument is equal to the velocity argument with the opposite sign. In other words, the derivative of a complex potential is the value of the complex-conjugate with the flow velocity (Fig. 8.2).

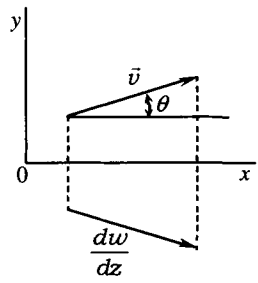

Fig. 8.2

So, it is possible to construct a complex potential for a parallel-plane potential flow that represent an analytical function. Conversely, any analytical function has corresponding parallel-plane potential flow of an ideal incompressible fluid. So, the entire apparatus of the analytical function theory may be used to study such flows.

2. Examples of parallel-plane potential flows

First it is critical to examine the simplest analytical function of complex variables and the corresponding flows.

1. $W(z)=(a+ib)z=(a+ib)(x+iy)=\varphi+i\psi, \quad a>0, \quad b>0.$

From Eqs. (8.8), (8.9) and (8.10):

$$\varphi=ax-by, \quad \psi=bx+ay, \quad \frac{dW}{dz}=a+ib=ve^{-i\theta}, \quad \arg\frac{dW}{dz}=\operatorname{arctg}\frac{b}{a}=-\theta,$$

$$v=\sqrt{a^2+b^2}.$$

[2] *Sic* in the original

Flow-lines $\psi = \text{const}$ and equipotentials $\varphi = \text{const}$ form a family of mutually orthogonal curves. The complex potential W describes the motion at a velocity directed at angle $\theta = \text{arctg}\dfrac{b}{a}$ to the axis $0x$ (Fig. 8.3).

2. $W(z) = z^2 = (x+iy)^2 = \varphi + i\psi$.

In this case:

$$\varphi = x^2 - y^2, \quad \psi = 2xy, \quad \frac{dW}{dz} = 2z = 2(x+iy)ve^{-i\theta},$$

$$\arg\frac{dW}{dz} = \text{arctg}\frac{y}{x} = -\theta, \quad v = \sqrt{a^2+b^2}.$$

The flow-lines $\psi = \text{const}$ are equilateral hyperboles with the asymptotes $x = 0$, $y = 0$; the equipotentials are equilateral hyperboles with the asymptotes $x = y$, $y = -x$. At the point of origin, flow-lines $x = 0$, $y = 0$ intersect, i. e., the origin is a singularity where $v = 0$.

As in the ideal fluid flow the flow-lines may be replaced with hard walls, the complex potential may be interpreted as the flow-around of a direct angle (Fig. 8.4).

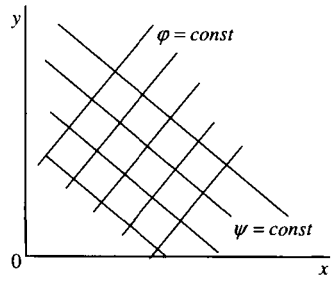

Fig. 8.3

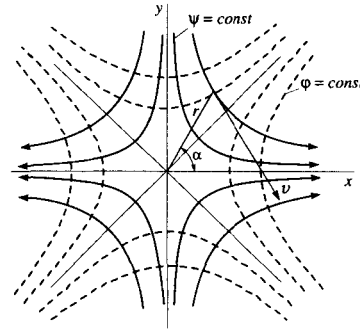

Fig. 8.4

3. $W(z) = z^n$, where n is any real number. From the De Moivre's relationship:

$$z^n = r^n e^{in\alpha} = r^n(\cos n\alpha + i\sin n\alpha),$$

where from:

$$\varphi = r^n \cos n\alpha, \quad \psi = i\sin n\alpha,$$

$$\frac{dW}{dz} = z^{n-1}.$$

Suppose $\psi = r^n \sin n\alpha = 0$. As $r \neq 0$, then $\alpha = \dfrac{k\pi}{n}$, where k is an integer, and the flow-lines are straight lines passing through the origin, which is a singularity.

At $\psi = \text{const} \neq 0$ results the flow-lines within the angle α. This flow (Fig. 8.5) may be interpreted as the flow-around of an angle $\alpha = \dfrac{\pi}{n}$. Fig. 8.3 reflects a case with $n = 3$.

The flow corresponding to the function $W(z) = z^n$ can be considered for any $n \geq \dfrac{1}{2}$. If it is a flow in the entire plane, the condition $\dfrac{k\pi}{n} = 2\pi$ should be realized. Otherwise points exist within the fluid where the velocity is multivalued, which is a physical impossibility. Such points may exist only at the volume's boundary.

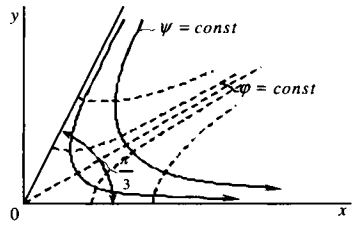

Fig. 8.5

Considering a case with $n = \dfrac{1}{2}$. Then:

$$\frac{\pi}{n} = 2\pi, \quad \frac{dW}{dz} = \frac{1}{2\sqrt{z}} = \frac{1}{2\sqrt{r}} e^{-i\frac{\alpha}{2}}, \quad \theta = \frac{\alpha}{2}.$$

At point P_1 of the $0x$ axis (Fig. 8.6), $\alpha = 0$, $\theta = 0$, $v = \dfrac{1}{2\sqrt{r}}$, i. e., the velocity is directed along the $0x$ axis. At $r \to 0$, $v \to \infty$; at $r \to \infty$, $v \to 0$. At the point P_2, $\alpha = 2\pi$, $\theta = \pi$, and the velocity is directed along the $0x$ axis but in the opposite direction. The velocity undergoes a disruption along the $0x$ axis: its modulus is maintained but its direction changes to the opposite. The flow represents a flow around an infinitely-thin plate (Fig. 8.6).

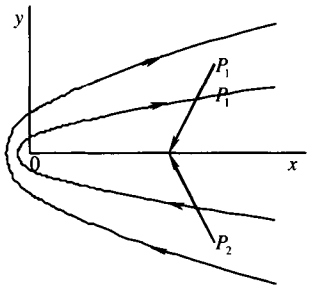

Fig. 8.6

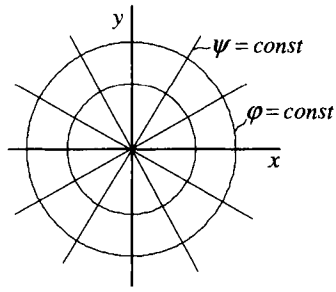

Fig. 8.7

4. $W(z) = \dfrac{\Gamma}{2\pi} \ln z = \dfrac{\Gamma}{2\pi} \ln(re^{i\alpha}) = \dfrac{\Gamma}{2\pi}(\ln r + i\alpha) = \varphi + i\psi$.

Therefore:

$$\varphi = \frac{\Gamma}{2\pi} \ln r, \quad \psi = \frac{\Gamma}{2\pi}\alpha, \quad \frac{dW}{dz} = \frac{\Gamma}{2\pi z} = \frac{\Gamma}{2\pi r} e^{-i\alpha}, \quad v = \frac{\Gamma}{2\pi r}, \quad \theta = \alpha.$$

The flow-lines $\psi = \text{const}$ (Fig. 8.7) are straight lines passing through the origin, the equipotentials $\varphi = \text{const}$ are circles with the center at the origin. The origin is a singularity. At $r \to 0$, $v \to \infty$; at $r \to \infty$, $v \to 0$. The throughflow through a circle with radius $r = \text{const}$ (as well as through any closed curve passing through the origin) is $Q = 2\pi r v = \Gamma$. At $\Gamma > 0$, there is a source at the origin, at $\Gamma < 0$, there is a drain.

5. $W(z) = \dfrac{\Gamma}{2\pi i}\ln z = \dfrac{\Gamma}{2\pi i}\ln re^{i\alpha} = \dfrac{\Gamma}{2\pi}(\alpha - i\ln r) = \varphi + i\psi$.

Then:

$$\varphi = \frac{\Gamma\alpha}{2\pi}, \quad \psi = -\frac{\Gamma}{2\pi}\ln r, \quad \frac{dW}{dz} = \frac{\Gamma}{2\pi i z} = \frac{\Gamma}{2\pi r}e^{-i\left(\alpha+\frac{\pi}{2}\right)}, \quad v = \frac{\Gamma}{2\pi r}, \quad \theta = \alpha + \frac{\pi}{2}.$$

The flow-lines $\psi = \text{const}$ are circles with the center at the origin, the equipotentials $\varphi = \text{const}$ are straight lines passing through the origin. Compared with Fig. 8.7, the flow-lines and equipotentials switched places. As $\dfrac{1}{i}W(z) = W(z)e^{-i\frac{\pi}{2}}$, and the flow-lines and equipotentials are mutually orthogonal, the flow-lines for the flow $W(z)$ always turn into equipotentials for the flow $\dfrac{1}{i}W(z)$, and the equipotentials, into the flow-lines.

The circulation along the flow-line $r = \text{const}$ is:

$$\int v dr = \int_0^{2\pi} v r d\varphi = 2\pi r \frac{\Gamma}{2\pi r} = \Gamma,$$

i. e., there is a vortex at the origin with vorticity Γ.

6. $W = \dfrac{-m^2}{z} = \dfrac{-m^2\bar{z}}{z\bar{z}} = \dfrac{m^2(x-iy)}{x^2+y^2} = \varphi + i\psi$.

In this case:

$$\varphi = \frac{m^2 x}{x^2+y^2}, \quad \psi = \frac{m^2 y}{x^2+y^2}, \quad \frac{dW}{dz} = -\frac{m^2}{z} = +\frac{m^2}{r^2}e^{i(2\alpha+\rho)}, \quad v = \frac{m^2}{r^2}, \quad \theta = 2\alpha + \pi.$$

Assuming $\varphi = \dfrac{1}{C}$, $\psi = \dfrac{1}{2C_1}$, results:

$$x^2 + y^2 + 2Cm^2 y = 0, \quad x^2 + y^2 - 2C_1 m^2 x = 0.$$

Thus, the flow-lines are circles with the centers at the $0y$ axis and radii $R = |C|m^2$; the equipotentials are circles with the centers at the $0x$ axis and radii

$R = |C_1| m^2$ (Fig. 8.8). The $0x$ axis is also a flow-line $\varphi = 0$. In this example, the function $W = m^2 z^{-1}$ is a complex potential of a flat dipole with the axis $0x$.

Combining the described simple cases, it is possible to derive more complex flows.

Let's review a combination of the translational motion parallel to the axis $0x$, the dipole and vortex, i. e., the following equation:

$$W = -V\left(z + \frac{R^2}{z}\right) + \frac{\Gamma}{2\pi i} \ln z = \\ = -V\left(re^{i\alpha} + \frac{R^2}{r} e^{-i\alpha}\right) + \frac{\Gamma}{2\pi i}(\ln r + i\alpha) \qquad (8.11)$$

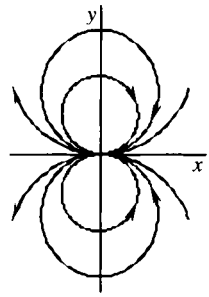

Fig. 8.8

Obviously, the translational motion velocity is equal to $-V$, the dipole momentum is equal to $m^2 = -VR^2$, and the circulation is equal to Γ. According to Eq. (8.11):

$$\varphi = -\left(r + \frac{R^2}{r}\right) V \cos\alpha + \frac{\Gamma\alpha}{2\pi}, \quad \psi = -\left(r - \frac{R^2}{r}\right) V \sin\alpha - \frac{\Gamma}{2\pi} \ln r, \qquad (8.12)$$

$$\frac{dW}{dz} = -V\left(1 - \frac{R^2}{z^2}\right) + \frac{\Gamma}{2\pi i z} = -V\left(1 - \frac{R^2}{r^2} e^{-2i\alpha}\right) + \frac{\Gamma}{2\pi r} e^{-i\left(\alpha + \frac{\pi}{2}\right)}. \qquad (8.13)$$

Following Eq. (8.12) that at $r = R$, $\psi = -\dfrac{\Gamma}{2\pi} \ln r = \text{const}$, i. e., the circle of the radius R with the center at the origin is a flow-line. From Eq. (8.13), $\left(\dfrac{dW}{dz}\right)_{z=\infty} = -V$. Thus, the complex potential Eq. (8.11) describes a flow-around of the circle (a cylinder with the axis perpendicular to the $x0y$ plane) by a flow whose velocity at infinity is $-V$ (Fig. 8.9).

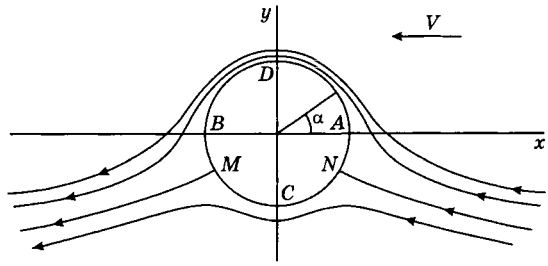

Fig. 8.9

According to Eq. (8.13), the squared velocity v at the circle points $r = R$ is equal to:

$$v^2 = \left(\frac{dW}{dz}\overline{\frac{dW}{dz}}\right)_{r=R} = \left(2v\sin\alpha + \frac{\Gamma}{2\pi r}\right)^2.$$

As the velocity induced by the circulation $\left(\theta = \alpha + \frac{\pi}{2}\right)$ is directed counter clockwise, then in the upper half-plane:

$$v = -2v\sin\alpha - \frac{\Gamma}{2\pi r} \quad (\alpha < \pi), \tag{8.14}$$

and in the lower half-plane:

$$v = 2v\sin\alpha + \frac{\Gamma}{2\pi r} \quad (\alpha > \pi). \tag{8.15}$$

At a no-circulation flow-around, the velocity at the points A ($\alpha = 0$) and B ($\alpha = \pi$) is equal to zero, and these points are singularities. At $\Gamma \neq 0$ the velocity at these points is different from zero. As can be seen from Eqs. (8.14) and (8.15), the maximum value of the velocity modulus is reached at the point D and is:

$$|v| = 2V + \frac{\Gamma}{2\pi r}.$$

The position of the critical points M and N as follows from Eq. (8.14) is determined from the condition:

$$2V\sin\alpha^* = \frac{\Gamma}{2\pi R} \text{ or } \sin\alpha^* = -\frac{\Gamma}{4\pi VR}, \ \sin\alpha^* \geq -1. \tag{8.16}$$

At $\Gamma = 4\pi VR$, the points M and N coincide with the point C. As Γ further increases, the critical point leaves the circle.

At the potential flow of a incompressible fluid, the Cauchy-Lagrange's integral Eq. (7.65) looks as follows:

$$\frac{\partial\varphi}{\partial t} - \Pi + \frac{\pi}{\rho} + \frac{v^2}{2} = f(t). \tag{8.17}$$

If $\Gamma = \Gamma(t)$, then, as follows from Eq. (8.12), a term $\frac{\alpha}{2\pi}\frac{d\Gamma}{dt}$ enters Eq. (8.17). Therefore, at $\Gamma = \Gamma(t)$ pressure is no longer a univalent function of the coordinates (r,α), which is physically impossible. Therefore, the potential flow-around is only possible at $\Gamma = \text{const}$.

At $V = \text{const}$, $\frac{\partial\varphi}{\partial t} = 0$, and the pressure in the flow is calculated using the flow velocity and conditions at infinity (or any other conditions allowing for the determination of the constant in Bernoulli's integral). As it can be seen from Eqs. (8.14) and (8.15), the velocity above the cylinder is higher than below it. As a

result, pressure above the cylinder is lower than below it. Due to this, lift is generated during a circulation flow-around of a cylinder. The resistance is absent as the flow is symmetrical relative the 0*y* axis.

Thus, for a circulation flow-around of a cylinder the ideal fluid's model allows for the computation of lift operating on the cylinder (and not necessarily only the cylinder). Experiments show that it may be done with a high accuracy.

3. Conformous reflection of flows

Let's take complex variable function $\zeta = F(z)$. Using this function, each point in a complex plane z is associated with a point in a complex plane ζ. Thus, function $\zeta = F(z)$ can be viewed as a reflection of some area D in the plane z onto some area D_1 in the plane ζ (Fig. 8.10).

A reflection where the angles between curves at the points of their intersection are preserved and infinitely small elements are transformed in a conformous way is called conformal. In order for the function $F(z)$ to realize a conformal reflection of the plane D, it is necessary and sufficient for it to be biunique, analytical, and for the derivative $F'(z)$ to be different from zero and from infinity in the plane D. The importance of conformal reflections for the hydromechanics is in that if complex potentials of simple flows are known, then it is possible using these reflections to construct the complex potentials of more complex flows.

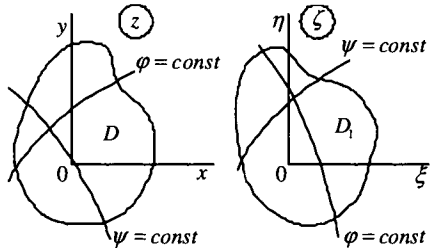

Fig. 8.10

Suppose a flow with the complex potential $W = W(z)$ is given in the plane z. As at the conformal reflection the function $\zeta = \xi + i\eta = F(z)$ must be biunique, it is always possible to find a function $z = f(\zeta)$. Then:

$$W(z) = \varphi(x, y) + i\psi(x, y) = W(f(\zeta)) = W^*(\zeta) = \varphi(\xi,\eta) + i\psi(\xi,\eta). \quad (8.18)$$

Following from Eq. (8.18) that at $\varphi(x, y) = \text{const}$ and $\varphi = \varphi(\xi,\eta) = \text{const}$ and at $\psi(x, y) = \text{const}$, $\psi(\xi,\eta) = \text{const}$. Thus, the equipotentials and flow-lines in the plane z turn, correspondingly, into equipotentials and flow-lines in the plane ζ. (Fig. 8.10).

Now it is important to review the following equation:

$$W(z) = \int \frac{dW}{dz} dz = \int (v_x - iv_y)(dx + idy) = \int v dx + v dy + i \int v_x dy - v_y dx. \quad (8.19)$$

According to Eqs. (3.39), (8.3), (8.5) and (8.6):

$$\int v_x dx + v_y dy = \int d\varphi = \Gamma, \quad \int v_x dy - v_y dx = Q,$$

i. e., the real part of the Eq. (8.19) integral is the velocity circulation along the curve, and the imaginary part is the liquid throughflow through this curve and:

$$W(z) = \int \frac{dW}{dz} dz = \Gamma + iQ. \tag{8.20}$$

Replacing the variables $z = f(\zeta)$ in Eq. (8.19), results:

$$W(z) = W[f(\zeta)] = \int \frac{dW}{d\zeta}\frac{d\zeta}{dz} dz = \int \frac{dW}{d\zeta} d\zeta = \Gamma + iQ. \tag{8.21}$$

Eqs. (8.20) and (8.21) show that the velocity circulation along any line on the z plane and along the velocity circulation along the corresponding line in the ζ plane coincide.

Establish association between the flow velocities at corresponding points of the planes z and ζ. From (8.9):

$$\frac{dW}{dz} = v_z e^{-i\theta_z} = \frac{dW}{d\zeta}\frac{d\zeta}{dz} = \frac{dW}{d\zeta} F'(z), \tag{8.22}$$

where v_z, θ_z are velocity's modulus and argument in the plane z. As:

$$\frac{dW}{d\zeta} = v_\zeta e^{-i\theta_\zeta},$$

$$v_z = v_\zeta |F'(z)|, \quad \theta_z = \theta_\zeta - \arg F'(z). \tag{8.23}$$

Eq. (8.23) provides a connection between the flow velocities in planes z and ζ. From the condition $F'(z) \neq 0$ and $F'(z) \neq \infty$, the critical points at conformal formal transformation convert to the critical points, and no new critical points may emerge.

The $W = W(z)$ correlation can be considered as a reflection of the area D in the plane z into the area D^* in the W plane (Fig. 8.11). The function $W(z)$ is analytical so wherever $\frac{dW}{dz} \neq 0$ and $\frac{dW}{dz} \neq \infty$, this reflection is conformal. The flow-lines ψ = const in the plane W are straight lines parallel to the 0ψ axis. Therefore, $W = W(z)$ is a reflection of the flow in the plane z onto the straight-linear translational motion in the plane W.

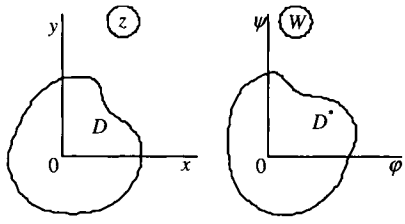

Fig. 8.11

Suppose there is a flow-line $\psi = \text{const}$ with the corner points A and B in the plane z (Fig. 8.12). Suppose $W(z)$ is the complex potential of this flow. All straight lines in the plane W will turn into flow-lines, i. e., the conformity will be broken at points A and B.

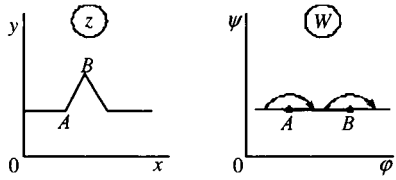

Fig. 8.12

It is demonstrated in Example 3 that the complex potential:

$$W - W_0 = (z - z_0)^n \tag{8.24}$$

is describing a flow-around of the angle $\alpha = \dfrac{\pi}{n}$ with the apex at the point $z = z_0$. At point A, $\alpha < \pi$, $n > 1$, and at point B, $\alpha > \pi$, $n < 1$. Then, from Eq. (8.24), $\dfrac{dW}{dz} = 0$ at $z = z_A$, and $\dfrac{dW}{dz} = \infty$ at $z = z_B$, i. e., at flow-around of the incurrent angle $v = 0$, and at flow-around of the pointed end, $v = \infty$.

It follows from the Cauchy-Lagrange's integral that at $v = \infty$ $p = -\infty$. Therefore, potential flow-around the pointed end is physically impossible.

4. Zhukovsky's transform

Take a complex potential:

$$W = k\left(z + \frac{R^2}{r}\right) = \varphi + i\psi, \tag{8.25}$$

describing a symmetric flow-around the cylinder with the radius R (Fig. 8.13). The flow area is the entire plane z external with respect to the cylinder. Now it is important to find the corresponding area in the plane W.

The flow-lines $\psi = \text{const}$ in the plane W are straight lines. From Eq. (8.25):

$$\varphi = k\left(z + \frac{R^2}{r}\right)\cos\theta, \quad \psi = k\left(z - \frac{R^2}{r}\right)\sin\theta.$$

A circle with the radius R and the center at the origin, and the half-segments $[R \le x < \infty)$ and $(-\infty < x \le -R]$ correspond to the flow-line $\psi = 0$ in the plane z. The points A_1, B_1 on the axis $\psi = 0$ with the coordinates $\varphi_{A_1} = -2kR$, $\varphi_{B_1} = 2kR$ in the plane W correspond to the points A and B with the coordinates $z_A = -R$, $z_B = R$ (Fig. 8.13).

For the point C with the coordinates $z_C = Re^{i\theta}$, we have: $\psi = 0$, $\varphi = 2kR\cos\theta$, i. e., the point C in reflected on the W plane into the inside of segment $[-2kR, 2kR]$.

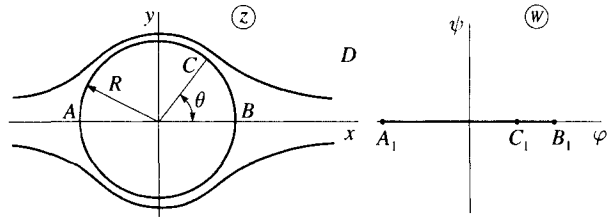

Fig. 8.13

Thus, Eq. (8.25) is the reflection of the plane z onto the plane W at which the cylinder's external appearance is reflected onto the external appearance of the one-dimensional simplex A_1B_1, and the flow-around the cylinder is transformed into the flow-around the one-dimensional simplex A_1B_1.

At $z = \pm R$, the derivative:

$$\frac{dW}{dz} = k\left(1 - \frac{R^2}{z^2}\right)$$

turns into zero, i. e., the reflection's conformance is disrupted at points A and B. An infinitely remote point in the plane z turns into an infinitely remote point in the plane W. The direction of the velocity at infinity is maintained as $\left(\frac{dW}{dz}\right)_\infty = k$, and $k > 0$ is a real number.

The transformation such as (8.25) is called the Zhukovsky's transform.

Suppose there is in the plane z a circle with the center at the origin and the radius $r > R$. Then $z = re^{i\theta}$, and under Eq. (8.25):

$$\varphi = k\left(r + \frac{R^2}{r}\right)\cos\theta, \quad \psi = k\left(r - \frac{R^2}{r}\right)\sin\theta, \tag{8.26}$$

i. e., the Zhukovsky's transform reflects the external appearance of the circle in the plane z onto the external appearance of an ellipse in the plane W, with the points A_1 and B_1 being the ellipse's foci. Eq. (8.26) are parametric equations of the ellipse with the half-axes $a = k\left(r + \frac{R^2}{r}\right)$, $b = k\left(r - \frac{R^2}{r}\right)$ and the foci at the points $\varphi = \pm 2kR$.

It may be shown that the circle with the center at the point $(x,0)$ has a corresponding symmetric winged profile C in the plane W (Zhukovsky's rudder); the circle with the center at the point $(0,y)$ has a corresponding arc of the circle; the circle with the center at the point (x,y) has a corresponding asymmetric winged profile G (Zhukovsky's profile) (Fig. 8.14). The angle at the back-edge of the Zhukovsky's profiles is 2π, which is their distinctive feature.

5. Flow-around of an arbitrary profile

Suppose a contour C is given in a complex plane ζ. It is required to construct its potential flow-around so that at infinity the motion would be translational at a velocity V_ζ directed at the angle α to axis 0ζ. The angle α is called the incidence angle (Fig. 8.15).

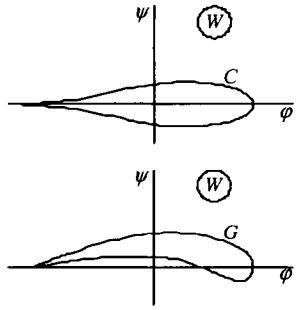

Fig. 8.14

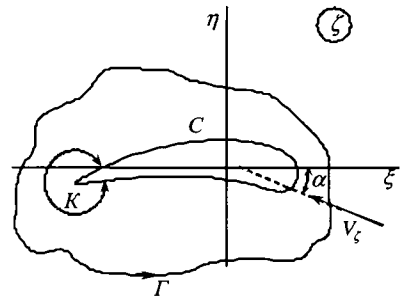

Fig. 8.15

To solve this problem, it is necessary to find a complex potential $W(\zeta) = \varphi(\xi,\eta) + i\psi(\xi,\eta)$. Consider, together with the plane ζ, the plane z of a complex varible and a circle with the radius R in the plane z (Fig.8.16). Function $\zeta = F(z)$ gives a reflection of the external appearance of the circle S onto the external appearance of the profile C so that a point $z = \infty$ has a corresponding point $\zeta = \infty$, and the derivative $\left(\frac{dS}{dz}\right)_\infty = k$ is real and positive. Under these conditions, the function $\zeta = F(z)$ exists for any contour C and is uniquely determined.

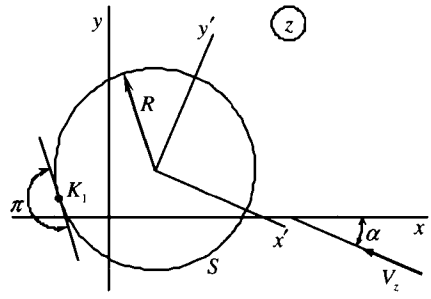

Fig. 8.16

Suppose the function $\zeta = F(z)$ is given. As the contour C is a flow-line, the circle S is also a flow-line. According to Eqs. (8.20) and (8.21), the circulation Γ in the planes z and ζ has the same value.

From Eqs. (8.22) and (8.23):

$$\left|\frac{dW}{dz}\right|_\infty = \left|\frac{dW}{d\zeta}\right|_\infty \left|\frac{d\zeta}{dz}\right|_\infty = k\left|\frac{dW}{d\zeta}\right|_\infty, \quad V_z = kV_\zeta .$$

Because, by proviso, k is a real number and $k > 0$, then:

$$\arg\left(\left|\frac{dW}{dz}\right|\right)_{\infty} = \arg\left(\left|\frac{dW}{d\zeta}\right|\right)_{\infty}.$$

Therefore, at infinity the velocity V_z has the same angle α with the axis $0x$.

Now select a coordinate system $x'0y'$ so that its origin coincides with the center of the circle S, and the axis $0x'$ is parallel to the velocity V_z. The, Eq. (8.11) for a circulation flow-around the circle S:

$$W(z') = -V_z\left(z' + \frac{R^2}{z'}\right)_{\infty} + \frac{\Gamma}{2\pi i}\ln z'.$$

The function $W(z')$ describes the flow-around in the coordinate system $x'0y'$. Stepping from z' to z by turning the coordinate system at the angle α, results in a complex potential $W(z)$.

As the function $\zeta = F(z)$ is biunique, the function $z = f(\zeta)$ can be found:

$$W(z) = W(f(z)) = W'(\zeta),$$

i. e., if the complex potential $W(z)$ and the function $\zeta = F(z)$ are known, complex potential of the flow-around of the contour C can be constructed.

Suppose the flow-around contour C has the angle point K (Fig. 8.15). The point K_1 on the circle S corresponds to this point (Fig. 8.16). As the angle at the point K_1 equals π, and at the point K is greater than π, the reflection conformity at point K is disrupted, and at that point $\zeta' = F'(z) = 0$.

Under Eq. (8.22), velocity modulus at any point of the profile C is:

$$\left|\frac{dW}{d\zeta}\right| = \left|\frac{dW}{dz}\right| * \frac{1}{F'(z)},$$

which shows that at $\frac{dW}{dz} \neq 0$, the velocity at point K turns into infinity. It is demonstrated above that it is typical of a pointed end and is physically impossible. If so, the condition $\frac{dW}{dz} = 0$ must be realized at point K_1, i.e., the point K_1 must be a critical point.

By selecting the circulation Γ, it is possible to make any point of the circle S into a critical point, and to make it so that the condition $\frac{dW}{dz} = 0$ is realized at this point. This requirement was formulated in the Chaplygin–Zhukovsky postulate: a circulation must be defined so that the velocity at an angle point K has a finite value.

As can be seen from Eq. (8.16), critical points at the circulating flow-around of a circle are located in such a way that their contracting bisectant is parallel to V_z (Fig. 8.17) and:

$$\Gamma = 4\pi R V_z |\sin \alpha^*| = 4\pi R V k(\sin(\alpha + \gamma)). \tag{8.27}$$

The values k, R, γ are constants determined by the selected circle and by the conform reflection. The incidence angle α and the velocity at infinity V_ζ can be assigned arbitrarily[3], and the circulation Γ is determined from Eq. (8.27).

6. Forces acting on a profile under the stationary flow-around

Suppose there is a contour C in the plane z (Fig. 8.18). The contour is being flowed-around by the fluid's flow. The complex potential of the flow $W(z) = \phi + i\psi$ is known. The pressure acting on the contour C, under Bernoulli's integral Eq. (7.28), disregarding the mass forces, is:

$$p = p_0 - \rho \frac{v^2}{2},$$

where p_0 is pressure at $v = 0$.

As:

$$v^2 = (v_x - iv_y)(v_x + iv_y) = \frac{dW}{dz}\frac{\overline{dW}}{dz},$$

then:

$$p = p_0 - \frac{\rho}{2}\frac{dW}{dz}\frac{\overline{dW}}{dz}. \tag{8.28}$$

The elementary force with the following projections acts on the element of the contour dz:

$$dX = -pdy,\ dY = pdx$$

(the contour C pass-around occurs counterclockwise, and the pressure is directed in the inside of the contour). Then, taking Eq. (8.28) into account, results:

$$dX - idY = -ip(dx - idy) = -ipd\bar{z} = -i\left(p_0 - \frac{\rho}{2}\frac{dW}{dz}\frac{\overline{dW}}{dz}\right)d\bar{z}. \tag{8.29}$$

Integrating Eq. (8.29) with respect to the closed contour C, gives:

$$X - iY = -\frac{i\rho}{2}\int_C \frac{dW}{dz}\frac{\overline{dW}}{dz}d\bar{z}. \tag{8.30}$$

[3] There is certain value of the incidence angle beyond which the flow-around breaks-down. So, the incidence angle must be assigned so that this critical value is not exceeded.

For a transformation of Eq. (8.30):

$$\overline{\frac{dW}{dz}}d\bar{z} = v_x dx + v_y dy + i(v_y dx - v_x dy), \text{ and}$$

$$\frac{dW}{dz}dz = v_x dx + v_y dy + i(v_y dx - v_x dy).$$

The flow-around contour C is a flow-line. As is known, along the flow-line $v_x dy - v_y dx = 0$. So, along the contour C:

$$\overline{\frac{dW}{dz}}d\bar{z} = \frac{dW}{dz}dz. \tag{8.31}$$

So, Eq. (8.30) can be presented in the following format:

$$X - iY = i\frac{\rho}{2}\int_C \left(\frac{dW}{dz}\right)^2 dz. \tag{8.32}$$

This equation is the first Chaplygin's equation.

The elementary momentum of a force relative to the origin (Fig. 8.18) is given by the following equation:

$$dM = xdY - ydX = Reiz(dX - idY),$$

wherefrom, in consideration of Eqs.(8.29) and (8.31), and upon integrating along the closed contour C, gives:

$$M = \frac{\rho}{2}\mathrm{Re}\int_C z\left(\frac{dW}{dz}\right)^2 dz. \tag{8.33}$$

In order to be able to compute the integrals in Eqs. (8.32) and (8.33), it is necessary to keep in mind that the function $\frac{dW}{dz}$ near an infinitely remote point is a univalent analytical function, so it may be expanded into a Laurent's series, and as at $z = \infty$ it has a finite value, the expansion looks as follows:

$$\frac{dW}{dz} = C_0 + \frac{C_1}{z} + \frac{C_2}{z^2} + \ldots \tag{8.34}$$

Assuming $z = \infty$:

$$\left(\frac{dW}{dz}\right)_{z=\infty} = C_0.$$

On the other hand, under Eq. (8.9):

$$\left(\frac{dW}{dz}\right)_{z=\infty} = V_z e^{-i\theta},$$

where V_z is modulus of the flow velocity at infinity; therefore:

$$C_0 = V_z e^{-i\theta}. \tag{8.35}$$

Under theorem of residues, integrals along the closed contour are:

$$\int_C \frac{dz}{z} = 2\pi i, \quad \int_C \frac{dz}{z^n} = 0, \quad n > 1.$$

Therefore, from Eqs. (8.34) and (8.20):

$$\int_C \frac{dW}{dz} dz = 2\pi i C_1 = \Gamma + iQ.$$

The throughflow of a incompressible fluid through a closed contour in the absence of sources is equal to zero. Therefore:

$$C_1 = \frac{\Gamma}{2\pi i}. \tag{8.36}$$

By squaring Eq. (8.34):

$$\left(\frac{dW}{dz}\right)^2 = C_0^{\,2} + 2\frac{C_0 C_1}{z} + (C_1^{\,2} + 2C_0 C_2)\frac{1}{z^2} + \ldots,$$

or, including Eqs. (8.35) and (8.36):

$$\left(\frac{dW}{dz}\right)^2 = V_z^{\,2} e^{-2i\theta} + \frac{\Gamma}{\pi i z} V_z e^{-i\theta} + \left(-\frac{\Gamma^2}{4\pi^2} + V_z C_2 e^{-i\theta}\right)\frac{1}{z^2} + \ldots. \tag{8.37}$$

Substituting Eq. (8.37) into Eq. (8.32) and integrating along the closed contour C, gives:

$$X - iY = i\rho\Gamma V_z e^{-i\theta},$$

or:

$$X - iY = -i\rho\Gamma V_z e^{-i\theta} = \rho\Gamma V_z e^{i\left(\theta + \frac{\pi}{2}\right)}. \tag{8.38}$$

This equation is an expression of Zhukovsky theorem: the resultant of pressure forces is equal to the product of density ρ, circulation Γ and velocity of the overrunning flow V_z and is aimed at direct angle to this velocity. Thus:

$$P = |X + iY| = \rho\Gamma V_z \tag{8.39}$$

is called lift.

At the continuous flow-around, the circulation in Eqs. (8.38) and (8.39) is determined from Eq. (8.27).

After the substitution of the Eq. (8.37) series into Eq. (8.33) and transformations, results:

$$M = 2\pi\rho \operatorname{Re}(iC_2 V_z e^{-i\theta}), \tag{8.40}$$

and this is the equation of the lift momentum relative the origin.

Eqs. (8.38) and (8.40) show that in order to compute the lift and its momentum it is sufficient to know V_z, Γ and C_2, i. e., it is sufficient to know three first terms of the expansion Eq. (8.34).

It is important to note that at the circulation flow-around the contour, i. e., at $\Gamma \neq 0$, the model of an ideal fluid allows for the lift computation, and the results are well supported by experiments. At $\Gamma = 0$ and $P = 0$, the Dalamber's paradox occurs.

CHAPTER IX

FLOW OF VISCOUS INCOMPRESSIBLE FLUID IN PRISMATIC TUBES

It is well known that there are two fluid flow regimes. First fundamental studies of the issue have been published by a German scientist G. Gagen in 1839 and 1854. He showed that as water flows within the tubes, there is a regime when liquid's particles move parallel to the tube's wall, i. e., the liquid is moving in immiscible layers. Under the other regime, the liquid's particles mix in a direction across the tube's axis. Later on, these regimes have been named, respectively, laminar and turbulent.

The laminar flow is such that the trajectories of fluid's particles are smooth curves. The shape of these curves is defined by the geometry of the flow area. In particular flow in prismatic tubes, the trajectories are straight lines parallel to the tube's generatrix. Thus, at laminar fluid flow in prismatic tubes the vector of the velocity must be parallel to the tube's axis.

The condition for a laminar flow has been defined by O. Reynolds in 1883. The laminar regime takes place if the Reynolds number "Re" satisfies the following condition:

$$\mathrm{Re} = \frac{\rho w l}{\mu} < \mathrm{Re}_{\mathrm{crit}},$$

where w is the characteristic velocity of a flow, l is the characteristic size, μ is dynamic viscosity of fluid, and $\mathrm{Re}_{\mathrm{crit}}$ is the critical Reynolds number. The numeric value of $\mathrm{Re}_{\mathrm{crit}}$ is greatly dependent on the geometry of the flow area.

1. Equations descring straight-line motion of a viscous incompressible fluid in prismatic tubes

General equation of isothermal motion of a viscous noncompressible fluid is:

$$\rho \frac{d\bar{v}}{dt} = \rho \bar{F} - \nabla p + \mu \Delta \bar{v}, \ \mathrm{div}\, \bar{v} = 0. \tag{9.1}$$

Introducing a coordinate system $0xyz$ and directing the $0z$ axis along the axis of prismatic tube (Fig. 9.1) and assuming that the flow velocity vector is parallel to the tube's axis, i. e.,

$$v_x = v_y = 0, \ v_z = u, \ \bar{v} = \bar{k}u, \tag{9.2}$$

where $\bar{k}$ is the singular vector of the 0z axis. Following the continuity equation Eq. (9.1) and from Eq. (9.2):

$$\frac{\partial u}{\partial z} = 0, \quad u = u(x, y, t).$$

So, for a viscous noncompressible fluid in prismatic tubes:

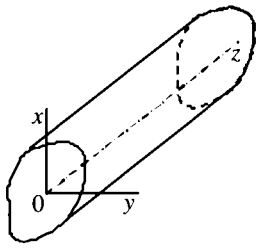

Fig. 9.1

$$\frac{d\bar{v}}{dt} = \frac{\partial \bar{v}}{\partial t} + v_x \frac{\partial \bar{v}}{\partial x} + v_y \frac{\partial \bar{v}}{\partial y} + v_z \frac{\partial \bar{v}}{\partial z} = \frac{\partial \bar{v}}{\partial t} = \bar{k} \frac{\partial u}{\partial t},$$

and the motion equation can be presented in the following format:

$$\bar{k}\rho \frac{\partial u}{\partial t} = \rho \bar{F} - \nabla p + \bar{k}\mu \Delta \bar{v}. \tag{9.3}$$

Please note that there are no convective terms in Eq. (9.3) resulting in linear simplified equation. Projecting Eq. (9.3) onto the coordinate axes results:

$$\rho F_x = \frac{\partial p}{\partial x}, \quad \rho F_y = \frac{\partial p}{\partial y}, \quad \rho = \frac{\partial u}{\partial t} = \rho F_z - \frac{\partial p}{\partial z} + \mu \Delta u. \tag{9.4}$$

Assuming $\bar{F} = \bar{g} = \text{const}$, the two first equations in Eq. (9.4) coincide with Eq. (6.2). Therefore, the hydrostatic pressure distribution lies on the plane x0y perpendicular to the tube's axis.

As $u = u(x,y,t)$, and following from the last equation of Eq. (9.4) :

$$\frac{\partial p}{\partial z} = f(x, y, t).$$

It can be seen from the first two equations of Eq. (9.4) and the above equation that pressure at any given time is linearly associated with the coordinates, i. e.:

$$p = \rho F_x x + \rho F_y y + C(t)z + D(t), \quad \frac{\partial p}{\partial z} = C(t). \tag{9.5}$$

The boundary condition for Eq. (9.4) is:

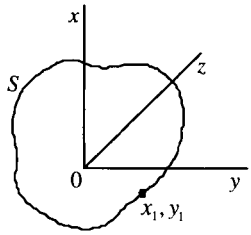

Fig. 9.2

$$u(x_1, y_1, t) = V, \tag{9.6}$$

where x_1, y_1 are coordinates of the points within the tube S (Fig. 9.2), and V is the velocity of its motion along the 0z axis. If the tube is motionless, $V = 0$.

Consider the following equation:

$$\tilde{u} = u - \int_0^t \left(F_z - \frac{1}{\rho} \frac{\partial p}{\partial z} \right) dt. \tag{9.7}$$

F_z = const and $\frac{\partial p}{\partial z} = C(t)$. Therefore, substituting Eq. (9.7) into Eq. (9.4) and using the boundary condition Eq. (9.6), results in:

$$\frac{\partial \tilde{u}}{\partial t} = \frac{\mu}{\rho}\left(\frac{\partial^2 \tilde{u}}{\partial x^2} + \frac{\partial^2 \tilde{u}}{\partial y^2}\right), \tag{9.8}$$

$$\tilde{u}(x_1, y_1, t) = V - \int_0^t \left(F_z - \frac{1}{\rho}\frac{\partial p}{\partial z}\right)dt, \quad \frac{\partial p}{\partial z} = C(t). \tag{9.9}$$

Thus, the problem of a non-stationary motion of viscous incompressible fluid in a prismatic tube may be reduced to the solution of Eq. (9.8), which has the format of the heat-conductivity equation with the boundary conditions [Eq. (9.9)]. In the case of a transient-free motion $\frac{\partial p}{\partial z}$ = const, Eq. (9.4) has the following format:

$$\Delta u = \frac{1}{\mu}\left(\frac{\partial p}{\partial z} - \rho F_z\right) = \text{const}, \tag{9.10}$$

i. e., the motion equation is reduced to the Poisson's equation.

The new function ψ is introduced through the following equation:

$$u = \psi + \frac{1}{4\mu}\left(\frac{\partial p}{\partial z} - \rho F_z\right)(x^2 + y^2).$$

Substituting this equation into Eq. (9.10) and the boundary condition [Eq. (9.6)], gives:

$$\frac{\partial^2 \psi}{\partial x^2} + \frac{\partial^2 \psi}{\partial y^2} = 0, \ \psi(x_1, y_1) = V - \frac{1}{4\mu}\left(\frac{\partial p}{\partial z} - \rho F_z\right)(x^2 + y^2). \tag{9.11}$$

As it can be seen, the problem of a transient-free motion of viscous incompressible fluid in a prismatic tube can be reduced to the solution of the Laplace equation on the boundary, i. e., the Dirichlet problem.

Consider parallel-plane, vortex-free motion of an ideal incompressible fluid within a contour S (Fig. 9.2), restricting the transversal cross-section of a prismatic tube. Suppose this contour is revolving at the angular velocity ω about the $0z$ axis. The projections of contour S velocities points are:

$$v_x = -\omega y_1, \ v_y = -\omega x_1. \tag{9.12}$$

On the other hand, considering Eqs. (8.2) and (8.7):

$$\frac{\partial^2 \psi}{\partial x^2} + \frac{\partial^2 \psi}{\partial y^2} = 0, \tag{9.13}$$

$$v_x = \frac{\partial \psi}{\partial y}, \quad v_y = \frac{\partial \psi}{\partial x}, \tag{9.14}$$

where ψ is the flow function. Following Eqs. (9.12) and (9.14) that at the points of the contour S:

$$d\psi = -v_y dx + v_x dy = -\omega(x_1 dx + y_1 dy),$$

and from here:

$$\psi_1 = -\frac{\omega}{2}(x_1^2 + y_1^2) + C. \tag{9.15}$$

At $C = V$ and $\omega = \frac{1}{2\mu}\left(\frac{\partial p}{\partial z} - \rho F_z\right)$, Eqs. (9.13) and (9.15) are the same as Eq. (9.11). Therefore, the study of the transient-free motion of an ideal incompressible fluid within prismatic tubes may be replaced by a review of the parallel-plane potential flow of an ideal incompressible fluid within a revolving contour, and *vice versa*. It is also important to remark here that equations such as Eq. (9.13), with the boundary conditions-Eq. (9.15), describe twisting of prismatic rods.

2. Straight-line flow between two parallel walls

A flow within a narrow slit (notch) can be modeled as a motion between two parallel walls.

Consider a transient-free flow between two motionless parallel planes located at a distance of $2h$ from one another (Fig. 9.3). As previously discussed, the flow velocity is $\bar{u} = \bar{k}u$. The boundary conditions are:

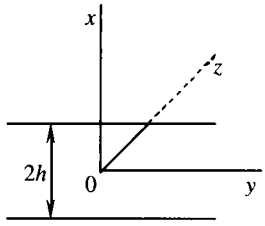

Fig. 9.3

$$at\ x = h,\ u = 0;\ at\ x = -h,\ u = 0. \tag{9.16}$$

Due to the symmetry, the motion in the planes parallel to the $x0z$ plane is similar, so $u = u(x)$. Thus, the motion equation Eq. (9.10) becomes:

$$\frac{\partial^2 u}{\partial x^2} = \frac{1}{\mu}\left(\frac{\partial p}{\partial z} - \rho F_z\right) = \text{const},$$

and from this:

$$u = \frac{1}{2\mu}\left(\frac{\partial p}{\partial z} - \rho F_z\right)x^2 + C_1 x + C_2. \tag{9.17}$$

After substituting the Eq.(9.17) into the boundary conditions Eq. (9.16):

$$C_1 = 0, \quad C_2 = -\frac{1}{2\mu}\left(\frac{\partial p}{\partial z} - \rho F_z\right)h^2$$

and:

$$u = \frac{1}{2\mu}\left(\frac{\partial p}{\partial z} - \rho F_z\right)(x^2 - h^2) = -\frac{h^2}{2\mu}\left(\frac{\partial p}{\partial z} - \rho F_z\right)\left(1 - \frac{x^2}{h^2}\right). \quad (9.18)$$

Considering the above equation, the maximum flow velocity $u_{\max}$ is:

$$u_{\max} = -\frac{h^2}{2\mu}\left(\frac{\partial p}{\partial z} - \rho F_z\right) \quad (9.19)$$

and:

$$u = u_{\max}\left(1 - \frac{x^2}{h^2}\right), \quad (9.20)$$

i. e., a parabolic velocity distribution occurs in the slit between the planes under review. In dimensionless coordinates $\frac{u}{u_{\max}}$, $\frac{x}{h}$, this distribution is universal (Fig. 9.4) and does not depend on either pressure gradient or on the fluid's properties. The fluid's throughflow Q per unit of the slit width is

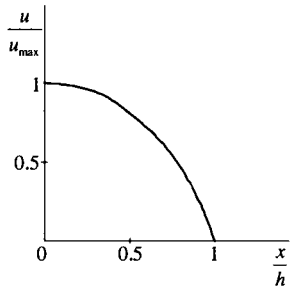

Fig. 9.4

$$Q = \int_{-h}^{h} u dx = -\frac{2h^3}{3\mu}\left(\frac{\partial p}{\partial z} - \rho F_z\right) = \frac{4h}{3}u_{\max}. \quad (9.21)$$

The average flow velocity u_{avg} is:

$$u_{\text{avg}} = \frac{Q}{2h} = -\frac{h^2}{3\mu}\left(\frac{\partial p}{\partial z} - \rho F_z\right) = \frac{2}{3}u_{\max}. \quad (9.22)$$

The friction stresses for a incompressible fluid, considering Eqs. (4.8) and (3.5), are:

$$\tau_{ik} = 2\mu\varepsilon_{ik}, \quad \varepsilon_{ik} = \frac{1}{2}\left(\frac{\partial v_i}{\partial x_k} + \frac{\partial v_k}{\partial x_i}\right). \quad (9.23)$$

In this case, the velocity vector has a single nonzero component $v_3 = v_z = u$, and from Eq. (9.18):

$$\varepsilon_{zx} = \frac{1}{2}\frac{\partial u}{\partial x} = \left(\frac{\partial p}{\partial z} - \rho F_z\right)\frac{x}{\mu}, \quad (9.24)$$

and other components of the deformations velocity tensor are equal to zero. By denoting the friction's tension at the wall as τ_h:

$$\tau_h = \left(\frac{\partial p}{\partial z} - \rho F_z\right)h. \quad (9.25)$$

Substituting Eq. (9.25) into Eqs. (9.18), (9.19), (9.21) and (9.22), gives:

$$u = -\frac{h}{2\mu}\tau_h\left(1-\frac{x^2}{h^2}\right),\quad u_{\max} = -\frac{h}{2\mu}\tau_h,\quad Q = -\frac{2h^2}{3\mu}\tau_h,\quad u_{\text{avg}} = -\frac{h}{3\mu}\tau_h. \tag{9.26}$$

The positive direction of the $0z$ axis is selected so that $u > 0$ and from Eq. (9.26), $\tau_h < 0$.

3. Straight-line flow within axisymmetric tubes

Let's review the transient-free, untwisted axisymmetric flow of an incompressible viscous fluid. Consider a cylindrical coordinate system $0rz\theta$ such that the $0z$ axis coincides with the flow axis of symmetry. Suppose the positive direction on the $0z$ axis coincides with the direction of the flow velocity. Then $\bar{u} = \bar{k}u(r)$, and the Lagrange's operator becomes:

$$\Delta u = \frac{1}{r}\frac{\partial}{\partial r}\left(r\frac{\partial u}{\partial r}\right). \tag{9.27}$$

Substituting this equation into Eq. (9.10):

$$\frac{\mu}{r}\frac{\partial}{\partial r}\left(r\frac{\partial u}{\partial r}\right) = \frac{\partial p}{\partial z} - \rho F_z = \text{const}.$$

Upon integrating this equation:

$$u = \left(\frac{\partial p}{\partial z} - \rho F_z\right)\frac{r^2}{4\mu} + C_1 \ln + C_2. \tag{9.28}$$

The solution of Eq. (9.28) is valid for any untwisted axisymmetric flow within cylindrical tubes. To determine the integration constants C_1 and C_2, it is necessary to assign the boundary conditions.

Taking a flow within a circular cylindrical tube of radius R, at $r = 0$ the velocity is finite; therefore, $C_1 = 0$. According to the adhesion hypothesis, at $r = R$, $u = 0$:

$$C_2 = -\left(\frac{\partial p}{\partial z} - \rho F_z\right)\frac{r^2}{4\mu},$$

and:

$$u = -\frac{1}{4\mu}\left(\frac{\partial p}{\partial z} - \rho F_z\right)(R^2 - r^2) = -\frac{R^2}{4\mu}\left(\frac{\partial p}{\partial z} - \rho F_z\right)\left(1-\frac{r^2}{R^2}\right). \tag{9.29}$$

The above equation demonstrates that maximum velocity value $u_{\max}$ is reached along the tube's axis:

$$u_{\max} = -\frac{R^2}{4\mu}\left(\frac{\partial p}{\partial z} - \rho F_z\right). \tag{9.30}$$

Accordingly, Eq. (9.29) can be written as follows:

$$u = u_{\max}\left(1 - \frac{r^2}{R^2}\right),$$

i. e., same as in the case of a flow between parallel planes — see Eq. (9.20) — the velocities are parabolically distributed, and this pattern is universal for dimensionless coordinates $\frac{u}{u_{\max}}$, $\frac{r}{R}$.

Let's now turn to the fluid's throughflow. For this purpose, it is important to consider a ring in the transversal cross-section of the tube with the area of $dS = 2\pi r dr$. Then, according to Eqs. (9.29) and (9.30), the throughflow Q is:

$$Q = \int_S u\,dS = 2\pi \int_0^R u r\,dr = \frac{\pi R^4}{8\mu}\left(\frac{\partial p}{\partial z} - \rho F_z\right) = \frac{\pi R^2}{2} u_{\max}. \qquad (9.31)$$

Average flow velocity u_{avg} is equal to:

$$u_{\text{avg}} = \frac{Q}{\pi R^2} = -\frac{R^2}{8\mu}\left(\frac{\partial p}{\partial z} - \rho F_z\right) = \frac{u_{\max}}{2}. \qquad (9.32)$$

Eq. (9.31) is the well-known Poiseuille's equation for laminar flow regime in round tubes.

At $u = u(r)$, the deformation velocity tensor has a single nonzero component:

$$\varepsilon_{rz} = \frac{1}{2}\frac{\partial u}{\partial r},$$

and, from Eq.(9.23), the friction stress is:

$$\tau_{rz} = \mu \frac{\partial u}{\partial r}. \qquad (9.33)$$

By substituting Eq. (9.29) into Eq. (9.33):

$$\tau_{rz} = \frac{r}{2}\left(\frac{\partial p}{\partial z} - \rho F_z\right). \qquad (9.34)$$

Eq. (9.34) shows that the friction stress is linearly associated with the radius. Assuming $r = R$ in Eq. (9.34), the friction stress on the tube's wall is:

$$\tau_R = \frac{R}{2}\left(\frac{\partial p}{\partial z} - \rho F_z\right). \qquad (9.35)$$

After substituting Eq. (9.35) into Eqs. (9.29)–(9.32):

$$u = -\frac{R\tau_R}{2\mu}\left(1 - \frac{r^2}{R^2}\right),\ u_{\max} = -\frac{R\tau_R}{2\mu},\ Q = -\frac{\pi R^3}{4\mu}\tau_R,\ u_{\text{avg}} = -\frac{R\tau_R}{4\mu}.$$

In a horizontal tube $F_z = 0$, and from Eq. (9.32):

$$u_{\text{avg}} = -\frac{R^2}{8\mu}\frac{\partial p}{\partial z}. \qquad (9.36)$$

Taking an l-length segment of the tube, as $\frac{\partial p}{\partial z} = \text{const}$, then:

$$\frac{\partial p}{\partial z} = \frac{p_2 - p_1}{l} = \frac{p_1 - p_2}{l} = -\frac{\Delta p}{l}, \tag{9.37}$$

where p_1, p_2 are pressures in the beginning and at the end of the tube segment under consideration. After substituting Eqs. (9.36) and (9.37) into the Darcy-Weisbach equation Eq. (5.30), the hydraulic resistivity λ is obtained:

$$\lambda = \frac{64\mu}{\rho u_{avg} d} = \frac{64}{\mathrm{Re}}, \quad d = 2R.$$

It is important to note that from the dimensionality and conformance theory:

$$\lambda = \frac{2C}{\mathrm{Re}}, \; C = \text{const},$$

i. e., the exact solution produces $C = 64$.

Now consider the flow in a canal formed by two round coaxial cylinders with radii R_1 (external) and. R_2 (internal). See Fig. 9.5.

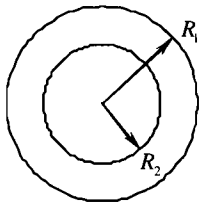

Fig. 9.5

The boundary conditions in this case are:

at $r = R_1$ $u = 0$, and at $r = R_2$ $u = 0$. (9.38)

Substituting the boundary conditions into the solution Eq. (9.28), gives:

$$C_1 = -\frac{1}{4\mu}\left(\frac{\partial p}{\partial z} - \rho F_z\right)\frac{R_1^2 - R_2^2}{\ln R_1 / R_2},$$

$$C_2 = -\frac{1}{4\mu}\left(\frac{\partial p}{\partial z} - \rho F_z\right)\frac{R_2^2 \ln R_1 - R_1^2 \ln R_2}{\ln R_1 / R_2}$$

and:

$$u = \frac{1}{4\mu}\left(\frac{\partial p}{\partial z} - \rho F_z\right)\left(r^2 - \frac{R_1^2 - R_2^2}{\ln R_1 / R_2}\ln r - \frac{R_2^2 \ln R_1 - R_1^2 \ln R_2}{\ln R_1 / R_2}\right) = \tag{9.39}$$

$$= \frac{1}{4\mu}\left(\frac{\partial p}{\partial z} - \rho F_z\right)\left[r^2 - R_2^2 - (R_1^2 - R_2^2)\frac{\ln r/R_2}{\ln R_1/R_2}\right].$$

The throughflow Q through the ring-tube cross-section is equal to:

$$Q = \int_{R_2}^{R_1} u r\, dr = \frac{\pi}{8\mu}\left(\frac{\partial p}{\partial z} - \rho F_z\right)(R_1^2 - R_2^2)\left[\frac{R_1^2 - R_2^2}{\ln R_1 / R_2} - (R_1^2 + R_2^2)\right]. \tag{9.40}$$

Now consider a narrow ring opening when, $R_2 \to R_1$. Suppose:

$$r = R_2 + y, \; R_1 = R_2 + h, \; \frac{h}{R_2} << 1.$$

Truncating terms not higher than second order, results in:

$$\ln\frac{r}{R_2}=\ln\left(1+\frac{y}{R_2}\right)\approx\frac{y}{R_2}\left(1-\frac{1}{2}\frac{y}{R_2}\right),\quad \ln\frac{R_1}{R_2}=\ln\left(1+\frac{h}{R_2}\right)\approx\frac{h}{R_2}\left(1-\frac{1}{2}\frac{h}{R_2}\right).$$

Further,

$$r^2-R_2^2-(R_1^2-R_2^2)\frac{\ln r/R_2}{\ln R_1/R_2}=\frac{2y(y-h)}{1-\frac{1}{2}\frac{h}{R_2}}\approx 2y(y-h)\left(1+\frac{1}{2}\frac{h}{R_2}\right)\approx 2y(y-h).$$

By substituting this expression into Eq. (9.39):

$$u=\frac{1}{2\mu}\left(\frac{\partial p}{\partial z}-\rho F_z\right)(y^2-hy). \tag{9.41}$$

Note that if the boundary conditions are assigned as:

at $x = 0$ $u = 0$, and at $x = 2h = h_1$ $u = 0$,

Eq. (9.18) takes the following format:

$$u=\frac{1}{2\mu}\left(\frac{\partial p}{\partial z}-\rho F_z\right)(x^2-h_1 y). \tag{9.42}$$

This equation with accuracy to subscripts is the same as Eq. (9.41). Therefore, the solution of Eq. (9.41) is also a solution of viscous fluid motion between two motionless parallel planes positioned at a distance $h = 2h$ from one another.

4. Equation of transient-free circular motion of a viscous fluid

Equation of transient-free motion of a viscous fluid in cylindrical coordinates $0r\varphi z$ has the following format:

$$v_r\frac{\partial v_r}{\partial r}+\frac{v_\varphi}{r}\frac{\partial v_r}{\partial \varphi}+v_z\frac{\partial v_r}{\partial z}-\frac{v_\varphi^2}{r}=$$

$$=F_r-\frac{1}{\rho}\frac{\partial p}{\partial r}+\frac{\mu}{\rho}\left(\frac{\partial^2 v_r}{\partial \varphi^2}+\frac{1}{r^2}\frac{\partial^2 v_r}{\partial \varphi^2}+\frac{\partial^2 v_r}{\partial z^2}+\frac{1}{r}\frac{\partial v_r}{\partial r}-\frac{2}{r^2}\frac{\partial v_\varphi}{\partial \varphi}-\frac{v_r}{r^2}\right),$$

$$v_r\frac{\partial v_\varphi}{\partial r}+\frac{v_\varphi}{r}\frac{\partial v_\varphi}{\partial \varphi}+v_z\frac{\partial v_\varphi}{\partial z}+\frac{v_r v_\varphi}{r}= \tag{9.43}$$

$$=F_\varphi-\frac{1}{\rho r}\frac{\partial p}{\partial \varphi}+\frac{\mu}{\rho}\left(\frac{\partial^2 v_\varphi}{\partial r^2}+\frac{1}{r^2}\frac{\partial^2 v_\varphi}{\partial \varphi^2}+\frac{\partial^2 v_\varphi}{\partial z^2}+\frac{1}{r}\frac{\partial v_\varphi}{\partial r}+\frac{2}{r^2}\frac{\partial v_r}{\partial \varphi}-\frac{v_\varphi}{r^2}\right),$$

$$v_r\frac{\partial v_z}{\partial r}+\frac{v_\varphi}{r}\frac{\partial v_z}{\partial \varphi}+v_z\frac{\partial v_z}{\partial z}=F_z-\frac{1}{\rho}\frac{\partial p}{\partial z}+\frac{\mu}{\rho}\left(\frac{\partial^2 v_z}{\partial r^2}+\frac{1}{r^2}\frac{\partial^2 v_z}{\partial \varphi^2}+\frac{\partial^2 v_z}{\partial z^2}+\frac{1}{r}\frac{\partial v_Z}{\partial r}\right),$$

$$\frac{\partial v}{\partial r}+\frac{1}{r}\frac{\partial v_\varphi}{\partial \varphi}+\frac{\partial v_z}{\partial z}+\frac{v_r}{r}=0. \tag{9.44}$$

Assuming that 0z axis is directed vertically upward and only one mass force (the gravitational force) is acting on the system, then:

$$F_r = F_\varphi = 0,\ F_z = -g = \text{const.} \tag{9.45}$$

It is also assumed that:

$$v_r \equiv 0,\ v_z \equiv 0, \tag{9.46}$$

i. e., studying a flow where the trajectories of all particles are concentric circles with the center on the axis 0z.

Based on the continuity equations Eq. (9.44) and conditions of Eq. (9.46) that:

$$\frac{\partial v_\varphi}{\partial \varphi} \equiv 0, \tag{9.47}$$

i. e., the velocity modulus along the circular trajectory maintains its numerical value.

Considering Eqs. (9.45), (9.46) and (9.47), the motion equations [Eq. (9.43)] take the following format:

$$\begin{gathered} \frac{v_\varphi^2}{r} = \frac{1}{\rho}\frac{\partial p}{\partial r}, \\ \mu\left(\frac{\partial^2 v_\varphi}{\partial r^2} + \frac{\partial^2 v_\varphi}{\partial z^2} + \frac{1}{r}\frac{\partial v_\varphi}{\partial r} - \frac{v_\varphi}{r^2}\right) \frac{v_\varphi^2}{r} = \frac{1}{\rho}\frac{\partial p}{\partial \varphi}, \\ 0 = \rho g + \frac{\partial p}{\partial z}. \end{gathered} \tag{9.48}$$

From the first and third equations of Eq. (9.48):

$$2\frac{v_\varphi}{r}\frac{\partial v_\varphi}{\partial z} = \frac{1}{\rho}\frac{\partial^2 p}{\partial z \partial r} = \frac{1}{\rho}\frac{\partial g}{\partial z},$$

from which:

$$\frac{\partial v_\varphi}{\partial z} = 0. \tag{9.49}$$

Thus, the circular motion under review is parallel-plane, and from Eqs. (9.47) and (9.49):

$$v_\varphi = v_\varphi(r). \tag{9.50}$$

Following from Eqs. (9.45) and (9.47) that the flow is axisymmetric:

$$\frac{\partial p}{\partial \varphi} = 0. \tag{9.51}$$

Based on Eqs. (9.50) and (9.51), the second equation of Eq. (9.48) can be presented in the following format:

$$\frac{\partial^2 v_\varphi}{\partial r^2}+\frac{1}{r}\frac{\partial v_\varphi}{\partial r}-\frac{v_\varphi}{r^2}=\frac{d}{dr}\left(\frac{dv_\varphi}{dr}+\frac{v_\varphi}{r^2}\right)=\frac{d}{dr}\left[\frac{1}{r}\frac{d}{dr}(rv_\varphi)\right]=0. \qquad (9.52)$$

By integrating Eq. (9.52):

$$v_\varphi = C_1\frac{r}{2}+\frac{C_2}{r},\ C_1, C_2 = \text{const}. \qquad (9.53)$$

From the first term in Eq. (9.48):

$$p=\rho\int\frac{v^2_\varphi}{r}dr+C_3,\ C_3 = \text{const}. \qquad (9.54)$$

5. Flow between two revolving cylinders

Let's review transient-free flow of a viscous incompressible fluid between two round cylinders. The cylinders are coaxial and have the vertical axis $0z$ of unlimited length.

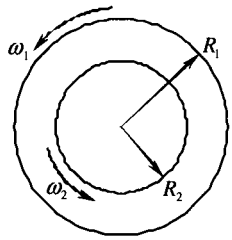

Fig. 9.6

Suppose the internal cylinder has radius R_2 and is revolving at an angular velocity ω_2, and the external cylinder has radius R_1 and is revolving at an angular velocity ω_1 (Fig. 9.6). Clearly, the boundary conditions are:

at $r = R_1$ $v_\varphi = R_1\omega_1$; at $r = R_2$ $v_\varphi = R_2\omega_2$. (9.55)

Substituting Eq. (9.55) into Eq. (9.53) results:

$$C_1 = 2\frac{R_1^2\omega_1 - R_2^2\omega_2}{R_1^2 - R_2^2},\ C_2 = \frac{R_1^2R_2^2(\omega_2-\omega_1)}{R_1^2-R_2^2}.$$

Therefore, Eq. (9.53) for velocity v_φ acquires the following format:

$$v_\varphi = \frac{R_1^2\omega_1 - R_2^2\omega_2}{R_1^2-R_2^2}r+\frac{R_1^2R_2^2(\omega_2-\omega_1)}{(R_1^2-R_2^2)r} = \frac{(R_1^2\omega_1 - R_2^2\omega_2)r^2+R_1^2R_2^2(\omega_2-\omega_1)}{(R_1^2-R_2^2)r}. \qquad (9.56)$$

Substituting Eq. (9.56) into Eq. (9.54) and performing simple transformations, results:

$$p=\frac{\rho}{(R_1^2-R_2^2)^2}\text{x}\left[(R_1^2\omega_1-R_2^2\omega_2)^2\frac{r^2}{2}+\right.$$

$$\left.+2R_1^2R_2^2(R_1^2\omega_1-R_2^2\omega_2)(\omega_2-\omega_1)\ln r-\frac{R_1^4R_2^4(\omega_2-\omega_1)^2}{2r^2}\right]+C_3$$

At $v_r = v_z = 0$, and $v_\varphi = v_\varphi(r)$, the tensor of velocities deformation has a single nonzero component:

$$\varepsilon_r\varphi = \frac{1}{2}\left(\frac{\partial v_\varphi}{\partial r} - \frac{v_\varphi}{r}\right),$$

and, according to Eq. (9.23), the friction stress $\tau_{r\varphi}$ is equal to:

$$\tau_{r\varphi} = \mu\left(\frac{\partial v_\varphi}{\partial r} - \frac{v_\varphi}{r}\right). \tag{9.57}$$

Substituting Eq. (9.56) into Eq. (9.57), gives:

$$\tau_{r\varphi} = -2\mu\frac{R_1^2 R_2^2(\omega_2 - \omega_1)}{(R_1^2 - R_2^2)r^2}. \tag{9.58}$$

The above equations show that friction stress decreases inversely to the radius squared $\left(\frac{\text{constant}}{r^2}\right)$ as the radius increases.

The friction force at the cylinder's surface (the cylinder's radius is r, and its height is H) is defined by $2\pi rH\tau_{r\varphi}$, and its momentum relative to the $0z$ axis is equal to:

$$M = 2\pi r^2 H\tau_{r\varphi} = -4\pi\mu H\frac{R_1^2 R_2^2}{R_1^2 - R_2^2}(\omega_2 - \omega_1). \tag{9.59}$$

Therefore, friction force momentum does not depend on the cylinder's radius.

In computing the stress tensor components, the normal is considered to be external toward the volume under consideration. Thus, Eqs. (9.58) and (9.59) provide the values of friction force stress and momentum on the surface of radius r when it experiences friction at the surface of radius $r + dr$. When the surface of radius r exposes to friction at the surface of radius $r - dr$, the external normal has the direction of $-r$ and the sign in Eqs. (9.58) and (9.59) must be reversed.

Following from this argument, the momentum of friction forces on the cylinders of the radii R_1 and R_2 have the same numerical value with the opposite sign.

A special case exists when the internal cylinder is motionless, i. e., $\omega_2 = 0$. From Eq. (9.59):

$$M = 4\pi\mu H\frac{R_1^2 R_2^2}{R_1^2 - R_2^2}\omega_1. \tag{9.60}$$

This Eq. (9.60) is utilized for the determination of viscosity using rotation viscosimeters with coaxial cylinders. Indeed, by measuring angular velocity ω_1 of the external cylinder and the momentum M on the internal cylinder, Eq. (9.60) enables the computation of viscosity μ.

Mechanics of Fluid Flow
by Kaplan S. Basniev, Nikolay M. Dmitriev and George V. Chilingar

CHAPTER X

TURBULENT FLOW OF FLUIDS IN PIPES

The theory of turbulent flow is an independent and vast hydrodynamic discipline. This chapter deals with the simplest and very important issues.

1. Reynolds' experiments

The classical studies of the fluid flow within circular tubes have been conducted in 1876–1883 by a British physicist Osborn Reynolds. See Fig. 10.1 for the schematics of his experimental equipment. A thin stream of paint was supplied through a nozzle of a long glass tube *B* into the fluid's flow exiting a large tank *A*.

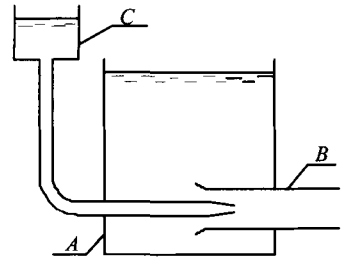

Fig. 10.1

It turned out that at a low flow velocity the colored stream is extended along the tube *B*'s axis: the flow occurs without any transverse mixing. Fluid's layers move parallel to one another. As previously mentioned, such flow is called laminar.

At a high flow velocity the colored stream was fuzzy and washed over the entire cross-section of the tube. The flow experienced intense intermixing of clearly unstable nature. Such a flow is called turbulent. A typical feature of turbulent flow is the presence of incoherent crosswise components of the velocity vector. Thus, turbulent flow is in its essence non-stationary.

Experimental studies showed that the transition from a laminar to a turbulent flow is defined neither by the tube's diameter d, average flow velocity w, viscosity μ or density ρ individually but rather by a dimensionless value $\mathrm{Re} = \frac{\rho w d}{\mu}$, called "the Reynolds number".

The Re value at which the transition from the laminar to turbulent flow occurs is called critical ($\mathrm{Re_{crit}}$). When $\mathrm{Re} < \mathrm{Re_{crit}}$, the flow is laminar, and when $\mathrm{Re} > \mathrm{Re_{crit}}$, the flow is turbulent.

Reynolds believed, and it was later proved, that the Re_{crit} value is growing with the decrease in disturbance of the flow. For tubes with well rounded intake, he obtained Re_{crit} values on the order of 12,000 to 13,000. Later studies by other physicists, with the application of special measures to decrease the initial disturbances, reached the Re_{crit} values of about 50,000. However, even a slightest disturbance resulted in the flow immediately becoming turbulent.

At the same time, experiments showed that at Reynolds numbers on the order of 2,200 the disturbances present or artificially caused in the flow tended to decay, and the flow became laminar.

There are always some disturbances in technical equipment. That is why for calculating flows within the round cylindrical tubes it is customary to assume $Re_{crit} = 2{,}320$.

2. Averaging the parameters of turbulent flow

When measuring at some point of a turbulent flow using an inertia-free sensor, a resulting velocity *vs.* time graph looks like in Fig. 10.2 where v_x, v_y and v_z are component vectors of the velocity. I. e., the velocity fluctuates around the average value. Reynolds proposed to take the instantaneous velocity and all other turbulent flow parameters value as the sum of time-averaged values and pulsation components.

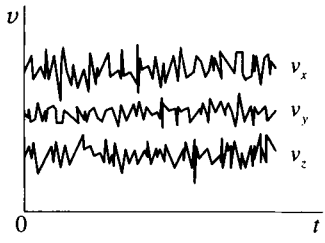

Fig. 10.2

Suppose $\varphi(x,y,z,t)$ is any parameter of the turbulent flow (velocity, pressure, etc.). Its instantaneous value is:

$$\varphi = \overline{\varphi} + \varphi', \qquad (10.1)$$

where $\overline{\varphi}$ is the time-averaged value and φ' is the pulsation. The averaged $\overline{\varphi}$ value is found as:

$$\overline{\varphi}(x,y,z,t) = \frac{1}{T}\int_{t-\frac{T}{2}}^{t+\frac{T}{2}} \varphi(x,y,z,\tau)d\tau, \qquad (10.2)$$

where the T averaging period is much longer than the characteristic fluctuation period but much shorter than the characteristic process time.

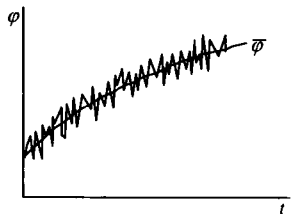

Fig. 10.3

If $\overline{\varphi}$ estimated for different t values has the same numerical value, the turbulent flow is called quasi-stationary (or stationary). If $\overline{\varphi}$ value depends on time (Fig. 10.3), the turbulent flow is non-stationary.

For a stationary flow, the repeated averaging of the φ parameter results, based on Eq. (10.2), in:

$$\bar{\varphi} = \frac{1}{T}\int_{t-\frac{T}{2}}^{t+\frac{T}{2}} \bar{\varphi}(x, y, z, \tau)d\tau = \bar{\varphi}. \tag{10.3}$$

For non-stationary processes the Eq. (10.3) is postulated.
It directly follows from Eq. (10.2) that:

$$\overline{\overline{\varphi} + \overline{\psi}} = \bar{\varphi} + \bar{\psi}. \tag{10.4}$$

According to Eqs. (10.1), (10.3) and (10.4):

$$\bar{\varphi} = \overline{\bar{\varphi} + \varphi'} = \bar{\bar{\varphi}} + \bar{\varphi'} = \bar{\varphi} + \bar{\varphi'}, \quad \bar{\varphi'} = 0, \tag{10.5}$$

i. e., average value of the pulsation is equal to zero.

In the case of a quasi-stationary flow, as follows from the averaging definition Eq. (10.2),

$$\overline{\bar{\varphi}\bar{\psi}} = \frac{1}{T}\int_{t-\frac{T}{2}}^{t+\frac{T}{2}} \bar{\varphi}(x, y, z, \tau)d\tau = \bar{\varphi}\bar{\psi}. \tag{10.6}$$

For non-stationary processes the Eq. (10.6) is postulated.
Following from Eqs. (10.5) and (10.6) that:

$$\overline{\bar{\varphi}\psi} = \bar{\varphi}\bar{\psi'} = 0. \tag{10.7}$$

Under the rule of differentiating an integral with variable limits:

$$\frac{\partial \bar{\varphi}}{\partial t} = \frac{1}{T}\frac{\partial}{\partial t}\int_{t-\frac{T}{2}}^{t+\frac{T}{2}} \varphi(x, y, z, \tau)d\tau = \frac{1}{T}\left[\varphi\left(x, y, z, t + \frac{T}{2}\right) - \varphi\left(x, y, z, t - \frac{T}{2}\right)\right] \tag{10.8}$$

$$= \frac{1}{T}\frac{\partial}{\partial t}\int_{t-\frac{T}{2}}^{t+\frac{T}{2}} \frac{\partial \varphi}{\partial \tau}d\tau = \frac{\overline{\partial \varphi}}{\partial \tau},$$

i. e., the time derivative of the averaged value is equal to the averaged value of the derivative:

$$\frac{\partial \bar{\varphi}}{\partial x_i} = \frac{\overline{\partial \varphi}}{\partial x_i} \tag{10.9}$$

3. Reynolds' equations

Reynolds' equations are motion equations of a viscous incompressible fluid for the averaged flow parameters.

Let's review the motion equation of a viscous incompressible fluid (4.42) or:

$$\frac{\partial v_i}{\partial x_i} = 0, \quad \rho \frac{\partial v_i}{\partial t} = \rho F_i - \frac{\partial p}{\partial t} + \mu \Delta v_i. \tag{10.10}$$

Suppose, according to Reynolds' hypothesis, that:

$$p = \bar{p} + p', \quad v_i = \bar{v}_i + v_i'. \tag{10.11}$$

To make the further transformation easier, for a incompressible fluid:

$$\frac{\partial v_i}{\partial t} = \frac{\partial v_i}{\partial t} + v_i \frac{\partial v_j}{\partial x_j} = \frac{\partial v_i}{\partial t} = \frac{\partial v_i}{\partial t} + v_j \frac{\partial v_i}{\partial x_j} + v_i \frac{\partial v_j}{\partial x_j} = \frac{\partial v_i}{\partial t} + \frac{\partial (v_i v_j)}{\partial x_j}. \tag{10.12}$$

By substituting Eq. (10.11) for velocity into Eq. (10.12), based on the averaging rules [Eqs. (10.3)–(10.9)] and considering the continuity equation:

$$\overline{\frac{\partial v_i}{\partial t}} = \frac{\partial \bar{v}_i}{\partial t} + \frac{\partial (\bar{v}_i \bar{v}_j)}{\partial x_j} + \frac{\partial \overline{v_i' v_j'}}{\partial x_j} = \frac{\partial \bar{v}_i}{\partial t} + \frac{\partial \overline{v_i' v_j'}}{\partial x_j}. \tag{10.13}$$

Further, it is clear that under the averaging rules:

$$\overline{\frac{\partial v_i}{\partial t}} = \frac{\partial \bar{v}_i}{\partial t}, \quad \overline{\Delta v_i} = \Delta \bar{v}_i, \quad \overline{\frac{\partial p}{\partial x_i}} = \frac{\partial \bar{p}_i}{\partial x_i}. \tag{10.14}$$

Finally, from Eqs. (10.13), (10.14) and (10.10):

$$\frac{\partial \bar{v}_i}{\partial x_i} = 0, \quad \rho \frac{\partial \bar{v}_i}{\partial t} = \rho F_i - \frac{\partial \bar{p}_i}{\partial x_i} + \mu \Delta \bar{v}_i - \rho \frac{\partial (\bar{v}_i \bar{v}_j)}{\partial x_i}, \tag{10.15}$$

or, in the vector format:

$$\operatorname{div} \bar{\vec{v}} = 0, \quad \rho \frac{d \bar{\vec{v}}}{dt} = \rho \bar{F} - \nabla \bar{p} + \mu \Delta \bar{\vec{v}} - \rho \frac{\partial (\overline{\bar{v}_i \bar{v}_j})}{\partial x_i}. \tag{10.16}$$

Thus, as a result of the averaging, the continuity equation maintains its format, and the motion equations acquired additional terms for the $\rho \overline{v_i' v_j'}$ format.

In order to understand the obtained result, consider the continuous medium motion equations [Eq. (2.49)]:

$$\rho \frac{\partial \bar{v}}{\partial t} = \rho \bar{F} + \frac{\partial \bar{p}_i}{\partial x_i} \tag{10.17}$$

or:

$$\rho\frac{\partial v_j}{\partial t}=\rho F_j+\frac{\partial p_{ij}}{\partial x_i}. \tag{10.18}$$

Averaging Eqs. (10.17) and (10.18) over time, and considering Eq. (10.13):

$$\rho\frac{d\bar{\vec{v}}}{dt}=\rho\vec{F}+\frac{\partial}{\partial x_i}\left(\bar{\vec{p}}_i-\rho\overline{\vec{v}'v_i'}\right), \tag{10.19}$$

$$\rho\frac{d\bar{v}_j}{dt}=\rho F_j+\frac{\partial}{\partial x_i}\left(\bar{p}_{ij}-\rho\overline{v_j'v_i'}\right). \tag{10.20}$$

Eqs. (10.15), (10.16), (10.19), (10.20) are different ways to write the Reynolds equations. Following from the Reynolds equations that at averaging a turbulent flow over time, in addition to the tensor of the averaged viscous stresses:

$$\bar{p}_{ji}=-\bar{p}\delta_{ji}+2\mu\bar{\varepsilon}_{ji}$$

a symmetric tensor of the turbulent stresses arises:

$$\begin{pmatrix}-\rho\overline{v_1'v_1'} & -\rho\overline{v_1'v_2'} & -\rho\overline{v_1'v_3'}\\ -\rho\overline{v_2'v_1'} & -\rho\overline{v_2'v_2'} & -\rho\overline{v_2'v_3'}\\ -\rho\overline{v_3'v_1'} & -\rho\overline{v_3'v_2'} & -\rho\overline{v_3'v_3'}\end{pmatrix}. \tag{10.21}$$

Thus, the Reynolds equations include 6 additional variables – components of the turbulent tensor stresses Eq. (10.21)-and, therefore, they are unclosed. The issue of their closing, i. e., the issue of finding an association between the tensor of turbulent stresses and the averaged flow parameters is until this day one of the major problems of the turbulency theory.

4. Semi-empiric turbulency theory by L. Prandtl

Semi-empiric theories of turbulency are based on hypotheses, which associate the turbulent stresses with the averaged velocity field. Such hypotheses are formulated based on generalization of the experimental data and the introduction of the empirical constants in the obtained expressions.

In generating the semi-empirical theories, the Reynolds' concept is used for the representation of the turbulent flow velocity field as a sum of the averaged velocity $\bar{\vec{v}}$ field and the fluctuating components $\vec{v}'$. The averaged motion's flow lines are introduced such that they are impermeable to the averaged velocities and permeable to the fluctuating components enabling the crosswise mixing in the turbulent flow.

The fluctuating velocity components transfer through the averaged flow lines. Thus, under the Newton's 2nd law turbulent flow results in the emergence of additional (turbulent) stresses.

Now consider quasi-stationary turbulent flow between the stationary planes $y=0$ and $y=h$ (Fig. 10.4). It is clear that here $\overline{v}_y=0$ due to the wall impermeability, and $\overline{v}_z=v_z'=0$ by definition of the plane flow. The averaged flow flow-lines are the straight lines parallel to the $0x$ axis. Clearly, the different from zero components of the turbulent stress tensor are $-\rho\overline{v_x'v_x'}, -\rho\overline{v_y'v_y'}$, $-\rho\overline{v_x'v_y'}=-\rho\overline{v_y'v_x'}$. Experiments showed that the $\rho\overline{v_x'v_x'}$ and $\rho\overline{v_y'v_y'}$ values can be disregarded.

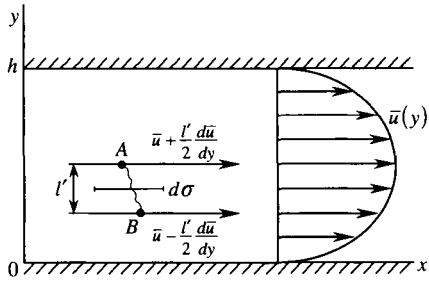

Fig. 10.4

Introducing the following parameters:

$$\overline{v}_x=\overline{u},\quad v_y'=v',\quad -\rho\overline{v_x'v_y'}=\tau.$$

assume that the friction is acting on the upper layer and the lower one, (Fig. 10.4). Clearly, the downward momentum transfer must be taken with the «+» sign, and upward, with the «–» sign. Due to the presence of the fluctuating component v', the the fluid particle located at point A with the coordinate $y+\frac{l'}{2}$ will be transferred through the elementary area $d\sigma$ (normal to the $0x_1$ axis) to the point B with the coordinate $y-\frac{l'}{2}$.

The particle under consideration has averaged velocity $\overline{u}=\overline{u}\left(y+\frac{l'}{2}\right)$ at point A. According to Prandtl's hypothesis, the particle's velocity does not change along the way l', and becomes equal to $\overline{u}=\overline{u}\left(y-\frac{l'}{2}\right)$ at point B. The mass flow through the $d\sigma$ area equals $\rho v'd\sigma$; the change of the time averaged momentum for the lower layer is equal to:

$$\overline{\rho v'\left[\overline{u}\left(y+\frac{l'}{2}\right)-\overline{u}\left(y-\frac{l'}{2}\right)\right]}d\sigma$$

Therefore, the time-averaged force of turbulent friction $\tau d\sigma$ is equal to:

$$\overline{\tau d\sigma} = \rho \overline{v' \left[\bar{u}\left(y + \frac{l'}{2} \right) - \bar{u}\left(y - \frac{l'}{2} \right) \right]} d\sigma . \tag{10.22}$$

The l' value is called the agitation length.

The numerical value of l' is assumed to be small, thus:

$$\bar{u}\left(y \pm \frac{l'}{2} \right) = \bar{u}(y) \pm \frac{l'}{2} \frac{d\bar{u}}{dy} . \tag{10.23}$$

After Substituting Eq. (10.23) into Eq. (10.22):

$$\tau = \rho \overline{v' l'} \frac{d\bar{u}}{dy} = A \frac{d\bar{u}}{dy} , \tag{10.24}$$

where $A = \rho \overline{v' l'}$ is dynamic turbulent viscosity.

The expression $\tau = A \frac{d\bar{u}}{dy}$ is the additional turbulent stress obtained from analogy with Newton's friction law for laminar flow introduced in 1887 by J. Boussinesq. It is important to emphasize that turbulent viscosity A, as opposed to dynamic viscosity μ, is not a constant value for the fluids, but depends on y coordinate and flow parameters.

In the thin near-wall fluid layer, $A << \mu$. This case is called "viscous sublayer"; its thickness is about 1 % of the canal's crosswise dimension. Outside of this sublayer, within the so-called "turbulent core", $A >> \mu$.

The total time-averaged tangential stress $\bar{p}_{xy}$ has the following format:

$$\bar{p}_{xy} = (\mu + A) \frac{d\bar{u}}{dy} . \tag{10.25}$$

In order to determined the agitation length, Prandtl proposed a hypothesis, under which:

$$v' \sim l' \frac{d\bar{u}}{dy} . \tag{10.26}$$

Substituting Eq. (10.26) into Eq. (10.24), results:

$$A = \rho l^2 \left| \frac{d\bar{u}}{dy} \right| , \quad \tau = \left| \frac{d\bar{u}}{dy} \right| \frac{d\bar{u}}{dy} , \tag{10.27}$$

where the modulus sign is used to underline that $A > 0$, and τ is and alternating-sign value. The proportionality factor, which should be presented in Eq. (10.26), is included into l value, which is also called the agitation length.

A theory built based on the concept of the agitation length is called the semi-empirical Prandlt theory.

5. Application of the dimensionality theory to the construction of semi-empirical turbulence theories

In constructing his theory, Prandtl assumed that the turbulent viscosity depends on fluid's density and the average velocity $\bar{u}$ distribution law in the canal's cross-section. This distribution, as the first approximation, is determined by the derivative $\frac{d\bar{u}}{dy}$. Therefore:

$$A = f\left(\rho, \frac{d\bar{u}}{dy}\right). \tag{10.28}$$

The dimensionality of the values in Eq. (10.28) are:

$$[A] = \frac{M}{LT}, \quad [\rho] = \frac{M}{L^3}, \quad \left[\frac{d\bar{u}}{dy}\right] = \frac{1}{T},$$

so the parameter system that determines the class of phenomena, i. e., ρ and $\frac{d\bar{u}}{dy}$, does not have the property of completeness. Thus, the equation such as Eq. (10.28) is physically impossible and requires to consider l' as independent variable:

$$A = f\left(\rho, \frac{d\bar{u}}{dy}, l'\right). \tag{10.29}$$

It is easy to see that the parameters ρ, $\frac{d\bar{u}}{dy}$, and l' have independent dimensionalities. So, under the Π-theorem of the dimensionality theory from Eq. (10.29):

$$A = C\rho^{\alpha}\left(\frac{d\bar{u}}{dy}\right)^{\beta} l'^{\gamma}, \quad C = \text{const}.$$

Following the calculations described in detail in Chapter V:

$$A = Cl'^2 \rho\left|\frac{d\bar{u}}{dy}\right| = \rho l^2\left|\frac{d\bar{u}}{dy}\right|, \quad \tau = A\frac{d\bar{u}}{dy} = \rho l^2\left|\frac{d\bar{u}}{dy}\right|\frac{d\bar{u}}{dy}, \tag{10.30}$$

which is exactly the same as Eq. (10.27).

The shape of the curve $\bar{u} = \bar{u}(y)$ is defined not only by the first derivative but also by higher order derivatives. Thus:

$$A = f\left(\rho, \frac{d\bar{u}}{dy}, \frac{d^2\bar{u}}{dy^2}\right).$$

Parameters ρ, $\frac{d\bar{u}}{dy}$, $\frac{d^2\bar{u}}{dy^2}$ have independent dimensionalities. Therefore, based on the Π-theorem:

$$A = C\rho^{\alpha}\left(\frac{d\bar{u}}{dy}\right)^{\beta}\left(\frac{d^2\bar{u}}{dy^2}\right)^{\gamma}.$$

Performing the necessary transformations, results in:

$$A = k^2\rho\frac{\left|\frac{d\bar{u}}{dy}\right|^3}{\left(\frac{d^2\bar{u}}{dy^2}\right)^2}, \quad \tau = k^2\rho\frac{\left|\frac{d\bar{u}}{dy}\right|^3}{\left(\frac{d^2\bar{u}}{dy^2}\right)^2}\frac{d\bar{u}}{dy}, \tag{10.31}$$

where k = const is an empirical constant.

A German hydro-mechanicist T. von Carman derived Eq. (10.31) in 1930 using a more complex thinking.

As shown above, Prandtl's equations [Eq. (10.30)] have been derived by analyzing two points in a turbulent flow. However, Carman's equations [Eq. (10.31)] do not include the linear dimension.

Eqs. (10.30) and (10.31) demonstrate the different rheological models for the turbulent flow of a viscous fluid.

These equations have been derived based on the assumption that the averaged velocity field depends only on one coordinate crosswise to the direction of the flow. Because of this assumption, they are valid for a flat as well as for a round tube (assuming the axisymmetric flow).

6. Logarithmic law of velocity distribution

Let's analyze, using Prandtl's concept, a quazi-stationary turbulent flow within a circular cylindrical tube of radius α. In this case:

$$\frac{d\bar{u}}{dy} = -\frac{d\bar{u}}{dr}$$

(y is measured from the tube's wall to its axis). From Eqs. (10.25) and (10.27), the total tangential stress $\bar{p}_{xy}$ is equal to:

$$\bar{p}_{xy} = -(\mu + A)\frac{du}{dy} = -\left(\mu + \rho l^2\left|\frac{d\bar{u}}{dy}\right|\right)\frac{d\bar{u}}{dy}.$$

Within the flow's core $A >> \mu$, so that the following assumption in valid:

$$\overline{p}_{xy} \approx \tau = -\rho l^2 \left|\frac{d\bar{u}}{dy}\right| \frac{d\bar{u}}{dy}. \tag{10.32}$$

Assuming, for the sake of the simplicity, that the tube is horizontal, and considering its element of radius r and length L (Fig. 10.5). The flow is transient-free, so the sum of forces acting on the identified element is equal to zero, i. e.,

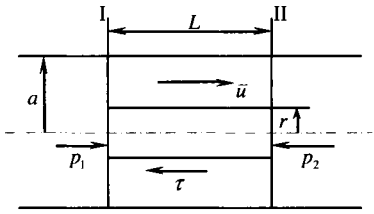

Fig. 10.5

$$\pi r^2(p_1 - p_2) - 2\pi r L\tau = 0,$$

where:

$$\tau = \frac{p_1 - p_2}{2L} r = \frac{\Delta p}{2L}. \tag{10.33}$$

Then the friction stress at the tube's wall is:

$$\tau_a = \frac{\Delta p}{2L} a \tag{10.34}$$

or, from Darcy-Weisbach equation Eq. (5.30):

$$\tau_a = \frac{\lambda \rho |w|}{8} w. \tag{10.35}$$

From Eqs. (10.33) and (10.34):

$$\tau = \tau_a \frac{r}{a},$$

and Eq. (10.32) can be presented in the following format:

$$\frac{\tau_a}{\rho} \frac{r}{a} = -l^2 \left|\frac{d\bar{u}}{dy}\right| \frac{d\bar{u}}{dy}. \tag{10.36}$$

Eq. (10.36) is the differential equation required to determine of the averaged velocity $\bar{u}$.

It is apparent that the displacement length l near the tube's wall and at the flow's axis (out of axial symmetry considerations) must be zero. A. Satkevich proposed the following equation for the displacement length:

$$l = k\sqrt{\frac{r}{a}}(a - r), \tag{10.37}$$

where k is an empirical constant.

Substituting Eq. (10.37) into Eq. (10.36), results:

$$\frac{\tau_a}{\rho} = -k^2 (a - r)^2 \left|\frac{d\bar{u}}{dy}\right| \frac{d\bar{u}}{dy}. \tag{10.38}$$

The value $v_* = \sqrt{\frac{\tau_a}{\rho}}$ has the dimensionality of velocity and is called dynamic velocity. As $v_* > 0$ and $\frac{d\bar{u}}{dr} < 0$, from Eq. (10.38):

$$\sqrt{\frac{\tau_a}{\rho}} = v_* = -k(a-r)\frac{d\bar{u}}{dy}. \tag{10.39}$$

Integrating Eq. (10.39) and considering that the velocity $\bar{u}$ has maxima at the tube's axis (i. e., at $r = 0$), results:

$$\frac{\bar{u}}{v_*} = \frac{\bar{u}_{\max}}{v_*} + \frac{1}{k}\ln\frac{a-r}{a}. \tag{10.40}$$

The Eq. (10.40) demonstrates that under the above assumptions the velocity distribution within the tube is logarithmic. Next to the wall, at $r \to a$, $\bar{u} \to \infty$, which does not make physical sense. The reason is that in deriving Eq. (10.40), the molecular viscosity μ relation relative to A is disregarded, and it is not valid for the near-wall layer.

Calling $a - r = y$, now it is possible to present Eq. (10.40) as follows:

$$\frac{\bar{u}}{v_*} = \frac{\bar{u}_{\max}}{v_*} + \frac{1}{k}\ln\frac{yvv_*}{avv_*} = \frac{\bar{u}_{\max}}{v_*} - \frac{1}{k}\ln\frac{av_*}{v} + \frac{1}{k}\ln\frac{yv_*}{v} = B + \ln\frac{yv_*}{v}, \tag{10.41}$$

where $v = \frac{\mu}{\rho}$ is kinematic viscosity, and B = const for the flow under consideration (i. e., for the tube of given radius r and given pressure gradient $\frac{\Delta p}{L}$).

Considering a small thickness of the near-wall layer and the fact that at $x \to 0$, the value $x\ln x \to 0$, from Eq. (10.41):

$$\begin{aligned} \frac{w}{v_*} &= \frac{Q}{\pi a^2 v_*} = \frac{1}{\pi a^2 v_*}\int_0^a 2\pi a\bar{u}(r)dr = \\ &= \frac{2}{a^2}\int_0^a r\left(B + \frac{1}{k}\ln\frac{yv_*}{v}\right)dr = B + \frac{1}{k}\ln\frac{av_*}{v} - \frac{2}{3}k, \end{aligned} \tag{10.42}$$

where w is average flow velocity and Q is throughflow.

From the definition of the dynamic velocity v_*, Eq. (10.34) and the Darcy-Weisbach equation Eq. (5.30) — or directly from Eq. (10.35):

$$v_* = \sqrt{\frac{\tau_a}{\rho}} = \sqrt{\frac{\lambda}{8}} w . \tag{10.43}$$

Substituting Eq. (10.43) into Eq. (10.42), results in:

$$\sqrt{\frac{8}{\lambda}} = B - \frac{3}{2k} + \frac{1}{k} \ln \frac{1}{2} \mathrm{Re} \sqrt{\frac{\lambda}{8}} , \tag{10.44}$$

where Reynolds number is determined as:

$$\mathrm{Re} = \frac{2aw}{\nu} = \frac{wd}{\nu} ,$$

where d is the tube's diameter.

In conclusion, the velocity distribution law [Eq. (10.41)] enables the derivation of equation for the determination of hydraulic resistivity λ. Some experimental data determined the numerical values of $B \approx 5.5$ and $k \approx 0.4$.

Substituting these values into Eq. (10.44) and switching to decimal logarithms:

$$\frac{1}{\sqrt{\lambda}} = 2.035 \lg \mathrm{Re} \sqrt{\lambda} - 0.913 .$$

A more precise description of the results can be derived using the following equation:

$$\frac{1}{\sqrt{\lambda}} = 2 \log (\mathrm{Re} \sqrt{\lambda}) - 0.8 = 2 \log \frac{\mathrm{Re} \sqrt{\lambda}}{2.51} .$$

Note that when deriving Eq. (10.44), the tube walls' roughness is not considered. Thus, the equation is valid only for smooth tubes.

It is also important that currently empirical rather than analytical equations are preferred for the λ calculation.

7. Experimental studies of hydraulic resistivity

Experimental studies of pressure *vs.* fluid's throughflow were conducted beginning at least 200 years ago. Individual results significantly varied because the scientists did not observe Reynolds conformity law and different roughness of the walls.

First systematic experimental studies of hydraulic resistivity λ *vs.* Re and roughness were conducted in the Gottingen University in 1920's-1039's by Nikuradze. The tubes involved were smooth brass tubes and the tubes with uniform artificial roughness. The results in log Re – log λ coordinates are shown in Fig. 10.6 where $\varepsilon = \Delta/d$. He concluded that there were five hydraulic resistivity zones.

Zone one (curve I): Re < 2,300; the flow regime is laminar, λ depends on Re but does not depend on ε.

Zone two is under transition from the laminar to turbulent regime. λ is increasing and depends only on Re.

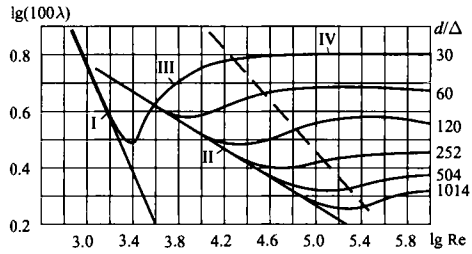

Fig. 10.6

Zone three (curve III) is so-called zone of hydraulically-smooth tubes. Tubes of different roughness behave as if they were smooth, i. e., λ depends only on Re.

Zone four is the area of a mixed friction. λ depends on Re and on ε.

Zone five is the quadratic friction area. λ depends only on ε.

The experiments conducted in 1940's in Moscow by Murin with naturally rough steel tubes (Fig. 10.7) also identified five hydraulic resistivity zones. Contrary to Nikuradze's experiments, the results showed monotonous decline of hydraulic resistivity λ with the increasing Re number.

There are many empirical and semi-empirical equations for the determination of hydraulic resistivity λ in round tubes. In this chapter the most common equations are reviewed.

The laminar flow regime:

$$\lambda = \frac{64}{\mathrm{Re}}, \quad \mathrm{Re} < 2{,}300.$$

The equation was analytically derived and experimentally confirmed.

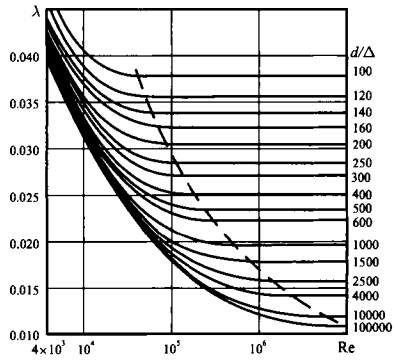

Fig. 10.7

The turbulent flow regime, hydraulically smooth tubes:

$$\lambda = \frac{1}{\sqrt[4]{100\,\mathrm{Re}}}, \quad \mathrm{Re} < 10^5 \text{ (Blasius equation).}$$

$$\lambda = \frac{1}{(1.8\log \mathrm{Re} - 1.5)^2} \text{ (Konakov's equation).}$$

Both equations have been derived based on processing the experimental results. Konakov's equation does not have limitations in terms of the Reynolds number.

The mixed flow zone:

$\lambda = 0.11\left(\frac{\Delta}{d} + \frac{68}{\mathrm{Re}}\right)^{0.25}$, $10\frac{d}{\Delta} < \mathrm{Re} < 500\frac{d}{\Delta}$ (Altschul equation). The equation was derived by modifying the empirical Colebrooke's equation.

Quadratic friction zone:

$$\lambda = 0.11\left(\frac{\Delta}{d}\right)^{0.25}, \mathrm{Re} > 500\frac{d}{\Delta} \text{ (Shifrinson's equation).}$$

At small values of $\frac{\Delta}{d}$, Altschul's equation turns into the Blasius equation, and at high Re numbers, into the Shifrinson's equation.

A more complex equation valid for any Re value, including the laminar flow regime, is:

$$\lambda = 8\left[\left(\frac{8}{\mathrm{Re}}\right)^{12} + \frac{1}{(A+B)^{\frac{3}{2}}}\right]^{\frac{1}{12}},$$

where

$$A = \left\{2.457\ln\left[\frac{1}{(7/\mathrm{Re})^{0.9} + 0.27(\Delta/d)}\right]\right\}^{16}, \quad B = \left(\frac{37{,}530}{\mathrm{Re}}\right)^{16}.$$

CHAPTER XI

HYDRAULIC CALCULATION FOR PIPELINES

1. Bernoulli's equation for a viscous fluid flow

Bernoulli's Eq. for a viscous fluid flow is one of the main equations used at hydraulic design of pipelines. In order to derive it, the following assumptions are required:

(a) the flow is transient-free;

(b) the fluid is incompressible, density $\rho = \text{const}$;

(c) only one mass force, the gravitational force, is active, $\overline{F} = \overline{g}$.

Under these assumptions, the law of variations in the kinetic energy [Eq. (2.82)] has the following format:

$$\int_S \rho \frac{v^2}{2} v_n dS = \int_V \rho \overline{g}\,\overline{v} dV = + \int_S \overline{p}_n \overline{v} dS + \int_V \rho N^{(i)} dV, \tag{11.1}$$

where for incompressible fluids, according to Eq. (4.50):

$$\rho N^{(i)} = -2\mu\varepsilon_{ik}. \tag{11.2}$$

The flow is transient-free, so $\operatorname{div} \rho\overline{v} = 0$, and:

$$\rho \overline{g}\,\overline{v} = -\rho g v_z - gz \operatorname{div} \rho\overline{v} = -\operatorname{div} \rho g z \overline{v}.$$

Then, based on Gauss–Ostrogradsky theorem:

$$\int_V \rho \overline{g}\,\overline{v} dV = -\int_V \operatorname{div} \rho g z \overline{v}\, dV = -\int_S \rho g z v_n\, dS. \tag{11.3}$$

Furthermore, under Eqs. (1.31), (4.21) and (4.28) for a incompressible fluid:

$$p_n = \overline{e}_k p_{ik} \alpha_{ni} = \overline{e}_k (-p\delta_{ik} + \tau_{ik}) \alpha_{ni} = -p\overline{n} + \overline{e}_k \tau_{ik} \alpha_{ni}, \quad \tau_{ik} = 2\mu\varepsilon_{ik}$$

and:

$$\int_V \overline{p}_n \overline{v} dS = -\int_S p\overline{n}\,\overline{v} dS + \int_S \overline{e}_k \overline{v} \tau_{ik} \alpha_{ni} dS = -\int_S \rho v_n\, dS + \int_S 2\mu v_k \varepsilon_{ik} \alpha_{ni} dS. \tag{11.4}$$

Following Eqs. (11.2) and (11.4) that the sum of terms:

$$\int_S 2\mu v_k \varepsilon_{ik} \alpha_{ni} dS + \int_V \rho N^{(i)} dV = -N_{\text{fr}} \tag{11.5}$$

is the capacity of the friction forces. As this capacity is always negative, $N_{\text{fr}} > 0$.

Substituting Eqs. (11.3) and (11.4) into Eq. (11.1) and considering Eq. (11.5) results in:

$$\int_{S_1} \left(z + \frac{p}{\rho g} + \frac{v^2}{2g} \right) g\rho v \, dS = -N_{\text{fr}}. \tag{11.6}$$

Consider the flow in a tube limited by cross-sections S_1 and S_2 and the tube's wall S_3. It is clear that $v_n = -v$ on S_1, $v_n = v$ on S_2 and $v_n = 0$ on S_3. In this case, for the tube segment under consideration, Eq. (11.6) takes the following format:

$$\int_{S_1} \left(z + \frac{p}{\rho g} + \frac{v^2}{2g} \right) g\rho v \, dS = \int_{S_2} \left(z + \frac{p}{\rho g} + \frac{v^2}{2g} \right) g\rho v \, dS + N_{\text{fr}}. \tag{11.7}$$

It is also required to assume that the pressure in the cross-sections S_1 and S_2 is distributed hydrostatically:

$$z + \frac{p}{\rho g} = \text{const}. \tag{11.8}$$

It was shown in Section 9.1 that such pressure distribution occurs at the laminar flow in prismatic tubes. This pattern can be approximated by the averaged straight-linear turbulent flow and the smoothly-changing flows, i. e., to the flows where the area and shape of the cross-section changes little along the tube's length.

According to Eq. (11.8):

$$\int_S \left(z + \frac{p}{\rho g} \right) g\rho v \, dS = \left(z + \frac{p}{\rho g} \right) g \int_S \rho v \, dS = \left(z + \frac{p}{\rho g} \right) g Q_m. \tag{11.9}$$

The product of the gravity acceleration g and the mass through-flow Q_m is the weight of the fluid flowing through the cross-section per unit time, called the *weight throughflow*.

In order to calculate the integral:

$$\int_S \frac{v^2}{2g} g\rho v \, dS = g \int_S \frac{\rho v^2}{2} v \, dS$$

it is important to review fluid flow with the same mass throughflow Q_m but with the uniform velocity distribution in the tube's cross-section. Clearly, the velocity of such flow is equal to the *average flow velocity* w, i. e.:

$$w = \frac{Q_m}{\rho S}.$$

Kinetic energy K of such flow carried per unit time through the tube's cross-section (the kinetic energy flow) is equal to:

$$K = \int_S \rho \frac{w^2}{2} w\, dS = \frac{w^2}{2} \rho w S = \frac{w^2}{2} Q_m.$$

The kinetic energy flow of a real flow is equal to:

$$\int_S \rho \frac{v^2}{2} v\, dS = \alpha K = \alpha \frac{w^2}{2} Q_m, \tag{11.10}$$

where α is the correction factor for a non-uniform velocity distribution in the cross-section (the so called *Coriolis coefficient*).

Substituting Eqs. (11.9) and (11.10) into Eq. (11.7) and considering that at a transient-free flow $Q_m = \text{const}$:

$$z_1 + \frac{p_1}{\rho g} + \alpha_1 \frac{w_1^2}{2g} = z_2 + \frac{p_2}{\rho g} + \alpha_2 \frac{w_2^2}{2g} + h_{1-2}, \tag{11.11}$$

where:

$$h_{1-2} = \frac{N_{\text{fr}}}{g Q_m}$$

is *the work of the friction forces per unit weight, or the specific capacity of these forces* expended in the tube's segment between the cross-sections S_1 and S_2.

Eq. (11.11) is Bernoulli's equation for a viscous incompressible fluid flow.

Following Eq. (11.8), p_1, p_2 are pressures at the arbitrarily selected points of the cross-sections S_1 and S_2 with the respective coordinates z_1 and z_2. In other words, p and z values must correspond with the same point in the S section.

For the laminar flow regime within a round tube of radius R, according to Eqs. (11.29), (11.30) and (11.32):

$$v = 2w\left(1 - \frac{r^2}{R^2}\right).$$

Then:

$$\int_S \rho \frac{v^2}{2} v\, dS = 2\pi \int_0^R \rho \frac{v^2}{2} v\, r\, dr = 8\pi\rho w^3 \int_0^R \left(1 - \frac{r^2}{R^2}\right) r\, dr = \pi R^2 \rho w^3,$$

and from Eq. (11.10):

$$\alpha = \frac{2\pi R^2 \rho w^3}{w^2 Q_m} = \frac{2\pi R^2 \rho w^3}{w^2 \rho w \pi R^2} = 2 .$$

For the turbulent flow regime $\alpha \approx 1.1$ to 1.2.

The flow regime in pipelines is generally turbulent, and $\frac{w^2}{2g} << \frac{p}{\rho g}$; so usually in calculations the accepted value of $\alpha \approx 1$.

The terms of Bernoulli's equation (exactly as the terms of Bernoulli's integral-Eq. (7.29)) have the dimensionality of length and are called:

z, *geometric head or geometric height;*

$\frac{p}{\rho g}$, *piezometric head, or piezometric height;*

$\alpha \frac{w^2}{2g}$, *velocity head, or velocity height;*

$h_{1\text{-}2}$, *head loss in the 1-2 segment;*

$H = z + \frac{p}{\rho g} + \alpha \frac{w^2}{2g}$, *total head.*

There is a simple graphic interpretation of Bernoulli's equation. Consider a graph with distance along x-axis and the heads, on the y-axis. Curve A in Fig. 11.1 describes the position of the flow's axis relative to the plane of reference $z = 0$. The distance between curve B and x-axis is equal to $z + \frac{p}{\rho g}$, and between curve C and x-axis is equal to the total head H.

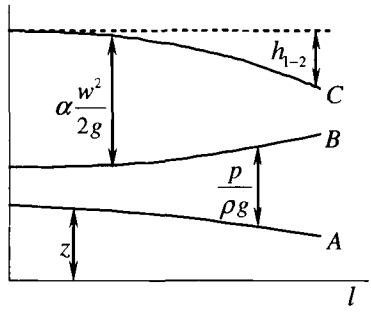

Fig. 11.1

Depending on the flow geometry and its spatial position, the sum $z + \frac{p}{\rho g}$ may decline or increase in the direction of the flow. Due to the friction, the total head is always declining. Eq. (11.11) shows that if the flow cross-section 1-1 is set, and the distance l to 2-2 cross-section is variable, then:

$$H_1 = H + h = \text{const},$$

and from this:

$$i = \frac{dh}{dl} = -\frac{dH}{dl} . \tag{11.12}$$

Value i is called *hydraulic grade.*

2. Types of head loss

Two kinds of friction are distinguished in a fluid flowing through a pipeline: length loss h_τ and loss to local resistances h_{loc}.

Local resistances are small segments (compared to the tube's length) in which velocity drastically changes in size and/or direction. Such segments are various locks, turns, valves, etc.

The length losses (*friction losses*) occur due to friction within the flow. They are linearly dependent on the tube's length. Losses to the local resistances are caused by strong fluid's agitation which is accompanied by vortex formation and large velocity gradients.

Consider a horizontal segment of a cylindrical tube with diameter d and length l located between cross-sections 1-1 and 2-2. As the cross-sections are equal, the velocity heads are also equal, and from Bernoulli's equation, Eq. (11.11):

$$\Delta p = p_1 - p_2 = \rho g h_\tau$$

then it is possible to write (in accordance with Eq. (5.30)):

$$h_\tau = \lambda \frac{l}{d} \frac{w^2}{2g}. \tag{11.13}$$

This equation is a form of the Darcy-Weisbach equation. The length of the local resistances is small, so the pressure loss does not depend on the length and roughness, so:

$$\Delta p = f(d,\mu,\rho,w). \tag{11.14}$$

After applying Π-theorem and simple transformations:

$$\Delta p = \zeta(\mathrm{Re}) \frac{\rho w^2}{2}, \quad h_{loc} = \frac{\Delta p}{\rho g} = \zeta \frac{w^2}{2g}. \tag{11.15}$$

Eq. (11.15) is called Weisbach equation, and $\zeta(\mathrm{Re})$ is called local resistivity factor.

Total loss in a pipeline between the cross-sections 1-1 and 2-2 is usually determined based on the loss superposition concept, i. e.:

$$h_{1-2} = \sum_{i=1}^{n} h_{li} + \sum_{j}^{m} h_{locj}, \tag{11.16}$$

where n is the number of straight-line segments of the tubes, and m is the number of local resistances. When applying the superposition concept, it is important to note that the size of loss due to the local resistances depends on the velocity distribution in front of them.

Vortex formation behind a local resistance deforms the velocity profile. Then velocity profile recovery to the original format, typical of a straight-line segment of a long tube, occurs in the stabilization segment. The length of this segment l_{st}, based on experiments, is 30 to 40 diameters of the supply pipeline (under the turbulent flow regime). If the distance between the adjacent local resistances is smaller than l_{st}, interference occurs between them. As a result the local resistance factors ζ and hydraulic resistance factors λ of the connecting tubes will be different from the values obtained for the local resistivities at a significant distance from one another.

In conclusion if the distance between local resistivities is smaller than l_{st}, the use of the superposition concept is not valid.

3. Designing simple pipelines

A pipeline is called simple if it has constant diameter with no branching lines. All other pipelines are called complex. In this section three main procedures of designing simple pipelines reviewed are:

Determination of pressure p_1 when the fluid's throughflow Q and pressure p_2 (Fig. 11.2) are given.

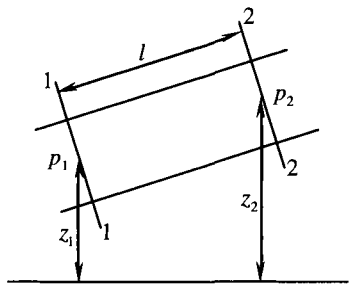

Fig. 11.2

1. Determination of throughflow Q when pressures p_1 and p_2 are given.
2. Determination of the pipeline diameter d when the throughflow Q and pressures p_1 and p_2 are given.

It is assumed in all these cases that the elevations z_1 and z_2, length l, tube roughness Δ, fluid's density ρ and viscosity μ are given.

The first step is deploying the Bernoulli's equation for the segment between cross-sections 1-1 and 2-2. As d = const, $w_1 = w_2$, and Eq. (11.11), considering the Eq. (11.13), with no local resistances, is:

$$p_1 = p_2 + \rho g(z_2 - z_1) + \rho g h_r = p_2 + \rho g(z_2 - z_1) + \rho g \lambda \frac{1}{d}\frac{w^2}{2g}. \quad (11.17)$$

Average velocity, w is equal to:

$$w = \frac{4Q}{\pi d^2}.$$

Reynolds' number Re and relative roughness ε are:

$$\mathrm{Re} = \frac{\rho w d}{\mu}, \quad \varepsilon = \frac{\Delta}{d}.$$

After calculating the Re and relative roughness values, the flow regime, flow area and proper equation for the calculation of hydraulic resistance λ can be determined. Then, by using the Darcy-Weisbach Eq. (11.13) the losses h_τ can be found and, subsequently, from Eq. (11.17), pressure p_1. Thus, the calculation procedure is a chain, which may be schematically represented as follows:

$$Q \rightarrow w \rightarrow \mathrm{Re} \rightarrow \text{flow area} \rightarrow \lambda \rightarrow h_\tau \rightarrow p_1 . \qquad (11.18)$$

The second procedure is based on the solution of Eq. (11.17) relative to the velocity w. A form of the $\lambda = \lambda(\varepsilon,\mathrm{Re})$ function is not known in advance, so it may be selected either by step-by-step approximation or analytical graphs.

To utilize the latter technique, let's assign a series of the throughflow values Q_1, Q_2, ... Q_n. Using the flow-chart (11.18), the head losses $h_{\tau 1}$, $h_{\tau 2}$, ... $h_{\tau n}$ can be calculated; then, a throughflow profile of the pipeline is estimated (Fig. 11.3). The values p_1, p_2, z_1, z_2 are known, so it is possible to determine the losses h_τ from Eq. (11.17). Placing this value on the y-axis (Fig. 11.3), it is possible to find the corresponding value of the sought-for fluid's throughflow.

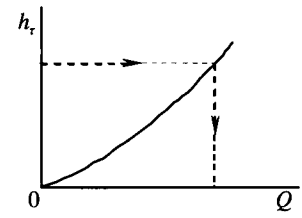

Fig. 11.3

The variable to be determined in the third procedure is the pipeline diameter d. Without knowing pipeline diameter, calculating the average velocity w, Reynolds number Re and λ factor are not possible. The solution of Eq. (11.17) can be derived either by step-by-step approximation or analytical graphs.

Let's assign a series of pipeline diameters d_1, d_2, ... d_n and for each of them, knowing the throughflow Q, calculate velocities w_1, w_2, ... w_n. Then by using the flow-chart (11.18), for each d_i the head loss $h_{\tau i}$ and the correlation plot $h_\tau = h_\tau(d)$ can be estimated (Fig. 11.4). Because the values of p_1, p_2, z_1, z_2 are known, the losses h_τ can be calculated from Eq. (11.17). Placing this value on Fig. 11.4, the corresponding value of the pipeline diameter d is found.

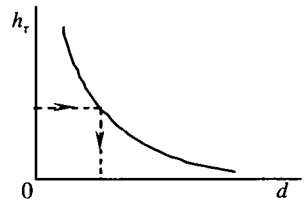

Fig. 11.4

4. Designing complex pipelines

The pipelines with local resistances or composed of tubes with different diameters or having branches are called complex pipelines.

Let's review the calculating procedure of most typical complex pipelines. First, starting with the serial connection, this is a complex pipeline including serially

connected tubes with local resistances between them. The tubes can have the same diameter or of different diameters (Fig. 11.5).

The pipeline is designed as a system composed of simple pipelines with local resistances. The fluid's throughflow is the same at any segment. The loss within the segment is calculated the same way as for a simple pipeline. The total losses of the segment between the cross-sections 1-1 and 2-2 are calculated from Eq. (11.16). It is assumed that all geometrical elements of the pipeline and properties of the fluid are known.

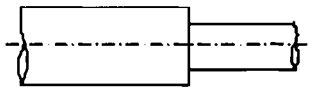

Fig. 11.5

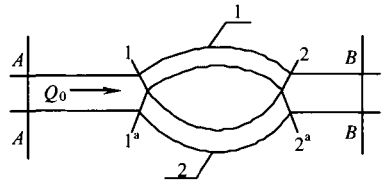

Fig. 11.6

The throughflow profile for a serial connection can be constructed using the calculation procedure for a simple pipeline. The throughflow profile enables, same as a simple pipeline design, finding the fluid's throughflow if the pressures in the beginning and at the end of the pipeline are given.

For a number of purposes (such as increase in throughput capacity, reliability increase of a river crossing, etc.) parallel connections are used. A parallel connection is a pipeline comprising several tubes with the common beginning and common end (Fig. 11.6).

Consider a parallel connection of two tubes, and deploy the Bernoulli's equation Eq. (11.11) for each of them between the cross-sections 1-2 and 1a-2a, respectively. As previously mentioned, $\alpha = 1$ is usually assumed for technical calculations.

$$z_1^{(1)} + \frac{p_1^{(1)}}{\rho g} + \frac{(w_1^{(1)})^2}{2g} = z_2^{(1)} + \frac{p_2^{(1)}}{\rho g} + \frac{(w_2^{(1)})^2}{2g} + h_r^{(1)},$$

$$z_1^{(2)} + \frac{p_1^{(2)}}{\rho g} + \frac{(w_1^{(2)})^2}{2g} = z_2^{(2)} + \frac{p_2^{(2)}}{\rho g} + \frac{(w_2^{(2)})^2}{2g} + h_r^{(2)}, \qquad (11.19)$$

where superscripts are tube numbers.

The cross-section 1 and 1a, and 2 and 2a are located close to one another. Therefore, it is possible to assume:

$$z_1^{(1)} = z_1^{(2)},\ z_2^{(1)} = z_2^{(2)},\ p_1^{(1)} = p_1^{(2)},\ p_2^{(1)} = p_2^{(2)}. \tag{11.20}$$

Besides, because the tubes' diameters are constant:

$$w_1^{(1)} = w_2^{(1)},\ w_1^{(2)} = w_2^{(2)}. \tag{11.21}$$

Following Eqs. (11.19), (11.20) and (11.21):

$$h_\tau^{(1)} = h_\tau^{(2)} = h_\tau. \tag{11.22}$$

Let's now determine the head loss in the *A-B* segment (Fig. 11.6). Using the Bernoulli's equation is not possible because the segment has branches. It is possible to maintain, however, that the energy loss ΔE within the *A-B* segment is:

$$\Delta E^{(A-B)} = \Delta E^{(A-1)} + \Delta E^{(1)} + \Delta E^{(2)} + \Delta E^{(2-B)}, \tag{11.23}$$

where the superscripts denote the respective pipeline segments.

As h_τ is losses per unit weight, then:

$$\Delta E = h_\tau \rho g Q\, dt,$$

and Eq. (11.23) may be rewritten in the following format:

$$h_\tau^{(A-B)} \rho g Q_0\, dt = h_\tau^{(A-1)} \rho g Q_0\, dt + h_\tau^{(1)} \rho g Q_1\, dt + h_\tau^{(2)} \rho g Q_2\, dt + h_\tau^{(2-B)} \rho g Q_0\, dt. \tag{11.24}$$

The fluid's throughflow Q_0 before the branching is equal to the sum of the throughflows in the branches, i. e.:

$$Q_0 = Q_1 + Q_2.$$

After substituting this equation into Eq. (11.24), and considering Eq. (11.22), gives:

$$h_\tau^{(A-B)} = h_\tau^{(A-1)} + h_\tau + h_\tau^{(2-B)}.$$

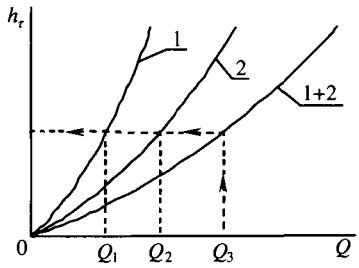

Fig. 11.7

Similar conclusions may be derived for the branching pipelines with any number of parallel branches.

Therefore, a design of parallel connections with n branches can be reduced to the solution of the following system of Eq.s:

$$Q_0 = \sum_{i=1}^{n} Q_i,\ h_\tau = h_\tau^{(1)} = h_\tau^{(2)} = ... = h_\tau^{(n)}. \qquad (11.25)$$

The system Eq. (11.25) can be easily solved by analytical graphs. For example, Let's review a case of n = 2. Given a series of the throughflow values $Q_1^{(1)}$, $Q_2^{(1)}$,..., $Q_n^{(1)}$ for the branch 1 and using the calculation procedure (11.18), it is possible to compute the losses $h_\tau^{(1)}$, $h_\tau^{(2)}$,...$h_\tau^{(n)}$ for each of these values. Based on the computation results, the throughflow profile can be built (curve 1 in Fig. 11.7). Similarly, the throughflow profile for the branch 2 is constructed (curve 2 in Fig. 11.7). By summing-up the x-axis readings for curves 1 and 2, the summary profile is constructed (curve 1+2). Putting the total throughflow Q_0 on the x-axis, the head loss at the intersection with curve 1+2 is estimated. It is clear that $h_\tau^{(1)} = h_\tau^{(2)}$, $Q_1 + Q_2 = Q_0$, i. e., the system Eq. (11.25) is solved.

It is important to stress again that when determining the head in the A-B segment the losses within only one of the tubes forming the parallel connection is considered.

5. Pipelines performing under vacuum

Pipelines performing under vacuum (i. e., with pressure below the atmospheric pressure) are quite common. They include pump intake lines, siphon pipelines, etc.

If pressure in any cross-section of such pipeline becomes equal to pressure of the saturated vapor of the pumped fluid, the fluid begins to boil , resulting the formation of vapor-saturated voids (caverns). As mentioned, this phenomenon is called cavitation.

Following Bernoulli's equation that if the velocity increases in any cross-section of a flow, pressure in this cross-section declines. Therefore, cavitation may occur in any narrow flow segments; for instance, within local resistances or within flow channels of hydraulic machinery.

The formation of cavitation results in increased head loss, decreases the throughflow and subsequently the head loss, i. e., in pressure increase in the location where cavitations occurred. This phenomenon is accompanied by shocks (pressure in the cavern's center at its collapse can reach 50 MPa), which cause the pipeline to vibrate.

Thus, pressure decline in any pipeline cross-section to the saturated vapor pressure p_y results in an unstable flow regime and may cause the pipeline destruction. Similar phenomena can occur within the hydraulic equipment. Therefore, the

main concept in designing pipelines performing under vacuum is the following requirement:

$$p_{min} > p_y, \tag{11.26}$$

where p_{min} is the minimum absolute pressure within the pipeline.

Let's review designing of a siphon with a constant diameter (Fig. 11.8). It is clear that the lowest pressure occurs in the cross-section $k - k$. Assuming that the plane of the 0 – 0 cross-section (free water surface in the left tank) is the reference plane $z = 0$. In this case, Bernoulli's equation for the segment between the cross-sections 0 – 0 and $k - k$ is:

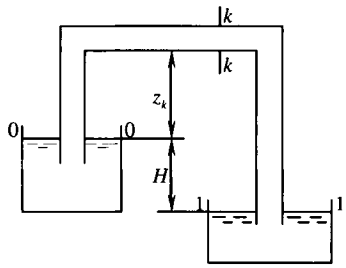

Fig. 11.8

$$\frac{p_{atm}}{\rho g} + \frac{w_0^2}{2g} = z_k + \frac{p_k}{\rho g} + \frac{w_k^2}{2g} + h_{0-k}, \quad h_{0-k} = \left(\lambda \frac{l}{d} + \zeta\right)\frac{w_k^2}{2g}, \tag{11.27}$$

where p_{atm} is atmospheric pressure, and ζ is the sum of all local resistances within the $0 - k$ segment. Because the free surface area in the tank is much larger than the tube's cross-section, then:

$$\frac{w_0^2}{2g} << \frac{w_k^2}{2g},$$

and Eq. (11.27) can be reformatted assuming the tank diameter $D = 10d$. As $\frac{\pi D^2}{4} w_0 = \frac{\pi D^2}{4} w_k$, $\frac{w_0^2}{w_k^2} = \frac{d^4}{D^4} = 10^{-4}$:

$$\frac{p_{atm}}{\rho g} = z_k + \frac{p_k}{\rho g} + \frac{w_k^2}{2g}\left(1 + \lambda \frac{l}{d} + \zeta\right). \tag{11.28}$$

The pipeline length from its beginning to the cross-section $k - k$ is:

$$l + L + z_k,$$

where L does not change when z_k changes. Then, from Eq. (11.28) and considering Eq. (11.26):

$$\frac{p_k}{\rho g} = \frac{p_{atm}}{\rho g} - \left(1 + \lambda \frac{l}{d}\frac{w_k^2}{2g}\right) z_k - \left(1 + \lambda \frac{L}{d}\frac{w_k^2}{2g} + \zeta\right)\frac{w_k^2}{2g} > \frac{p_y}{\rho g},$$

and:

$$z_k < \frac{\frac{p_{atm} - p_y}{\rho g} - \left(1 + \lambda \frac{L}{d} + \zeta\right) \frac{w_k^2}{2g}}{1 + \lambda \frac{l}{d} \frac{w_k^2}{2g}}. \qquad (11.29)$$

Thus, the acceptable fluid's raise height in the siphon is *a priori* less than $\frac{p_{atm}}{\rho g}$. The acceptable suction lift of a pump is calculated in the same way.

Let's write Bernoulli's equation for the segment between the fluid's free surfaces in the tanks 0 – 0 and 1 – 1. Disregarding the velocity heads $\frac{w_0^2}{2g}$, $\frac{w_1^2}{2g}$ and considering that on free surfaces $p_0 = p_1 = p_{atm}$ results:

$$-H + h_{1\text{-}2} = 0. \qquad (11.30)$$

Therefore, the head loss in siphon is equal to the difference of geometrical elevations H of the free surfaces in the tanks.

Eq. (11.30) provides an opportunity to compute the throughflow under the second procedure of the simple pipeline design.

Mechanics of Fluid Flow
by Kaplan S. Basniev, Nikolay M. Dmitriev and George V. Chilingar

CHAPTER XII

FLUID'S OUTFLOW FROM ORIFICES AND NOZZLES

The issue of fluid's outflow through orifices and nozzles of various shapes is a common occurrence when dealing with numerous technical issues.

1. Outflow from a small orifice

Consider a tank with a round orifice of radius d at the bottom (Fig. 12.1). The theoretical mechanics states that in the absence of shock forces material particles cannot move along the trajectories with angular points. It is assumed that particles' velocities at those points are different from zero. Thus, the surface of a stream flowing out of the orifice adjoin the orifice's edge; then, the stream is constricted and at some distance l acquires the cross-sectional area ω_c, which is smaller than that of the orifice (ω, Fig. 12.2).

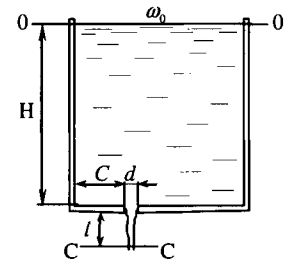

Fig. 12.1

The value:

$$\varepsilon = \frac{\omega_c}{\omega} < 1 \tag{12.1}$$

is called the stream contraction factor.

Unless the tank's walls affect the stream formation, the compression is called *perfect*. Otherwise it is called *imperfect*. Experiments show that in order for contraction to be perfect the distance C from the tank's wall must be greater than $3d$. I. e., a condition $C > 3d$ must be observed (Fig. 12.1). If there are flow deflectors along part of the orifice's perimeter (Fig. 12.2), the contraction is called *incomplete*. When there are no deflectors, it is called *complete*.

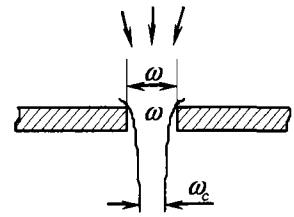

Fig. 12.2

In order to determine the outflow velocity from the orifice cross-section, $O-O$ is drawn through the fluid's free surface in the tank and $C-C$ at the level where stream's contraction is ended (Fig. 12.1). Let's now write Bernoulli's equation for the segment between these cross-sections, taking the $C-C$ cross-section for a reference plane. Then:

$$l + H + \frac{p_o}{\rho g} + \alpha_o \frac{w_o^2}{2g} = \frac{p_c}{\rho g} + \alpha_c \frac{w_c^2}{2g} + h_{o-c}. \tag{12.2}$$

Besides, following the continuity equation that:

$$\omega_o w_o = \omega_c w_c = \varepsilon \omega w_c, \tag{12.3}$$

where ω_o is the tank's area in the $O-O$ cross-section.

Experiments showed that the distance l at which the stream contraction ends is approximately equal to the orifice's diameter d, i. e., $l \approx d$. Thus in most cases it may be assumed that $l << H$, and the effect of l in Eq. (12.2) may be disregarded.

The flow velocity in the orifice is much higher than that in the tank. Thus, it can be assumed that all head losses are concentrated within the orifice which is the local resistance. Therefore, according to Eq. (11.5):

$$h_{o-c} = h_{loc} = \zeta \frac{w_c^2}{2g}. \tag{12.4}$$

By eliminating w_o from Bernoulli's equation using Eq. (12.3), disregarding l and considering Eq. (12.4), gives:

$$H + \frac{p_0}{\rho g} + \alpha_o \left(\varepsilon \frac{\omega}{\omega_o} \right) \frac{w_c^2}{2g} = \frac{p_C}{\rho g} + \alpha_c \frac{w_c^2}{2g} + \zeta \frac{w_c^2}{2g},$$

or:

$$H + \frac{p_o - p_c}{\rho g} = \left[\alpha_c + \zeta + \alpha_o \left(\varepsilon \frac{\omega}{\omega_o} \right) \right] \frac{w_c^2}{2g}. \tag{12.5}$$

Following Eq. (12.15) that the outflow velocity w_c is equal to:

$$w_c = \frac{1}{\sqrt{\alpha_c + \zeta + \alpha_o \left(\varepsilon \frac{\omega}{\omega_o} \right)^2}} \sqrt{2g \left(H + \frac{p_o - p_c}{\rho g} \right)}. \tag{12.6}$$

The value H_{outflow}:

$$H_{\text{outflow}} = H + \frac{p_o - p_c}{\rho g} \tag{12.7}$$

is called *the outflow head.*

The value φ:

$$\varphi = \frac{1}{\sqrt{\alpha_c + \zeta + \alpha_o \left(\varepsilon \frac{\omega}{\omega_o}\right)^2}} \tag{12.8}$$

is called *the velocity factor.*

Using notations in Eq. (12.7) and (12.8), Eq. (12.6) may be written as:

$$w_c = \varphi \sqrt{2gH_{\text{outflow}}} . \tag{12.9}$$

The values α_o and α_c are different from one, and the ζ value is greater than zero due to fluid's viscosity. $\varepsilon < 1$ due to inertia. Thus, it is possible to state that the velocity factor φ takes into account the viscosity and inertia properties of the fluid.

As shown on p. 182, $\alpha_o > 1$ and $\alpha_c > 1$. Besides, it is clear that $\zeta > 0$. If the ratio of the orifice area ω and the free surface area in the reservoir ω_o is low, i. e., if $\left(\frac{\omega}{\omega_o}\right)^2 << 1$, the orifice is called *small.*

Eq. (12.9) preserves its format for the small orifice but, as opposed to Eq. (12.8), the velocity factor is:

$$\varphi = \frac{1}{\sqrt{\alpha_c + \zeta}},$$

And, as $\alpha_c > 1$ and $\zeta > 0$, $\varphi < 1$.

There is no friction in the ideal fluid flow, so $\alpha_c = 1$ and $\zeta = 0$. Then $\varphi = 1$, and Eq. (12.9) becomes:

$$w_{Th} = \sqrt{2gH_{\text{outflow}}} . \tag{12.10}$$

The velocity defined by Eq. (12.10) is called the *theoretical* outflow velocity. Thus, as Eq.s (12.9) and (12.10) demonstrate, the velocity factor is the ratio of the actual and theoretical outflow velocities.

Fluid's throughflow through the orifice is the product of the stream velocity and its cross-sectional area, i. e.:

$$Q = w_c \omega_c = \varepsilon w_c \omega,$$

or, by considering Eq. (12.9):

$$Q = \omega\varepsilon\varphi\sqrt{2gH_{\text{outflow}}} \tag{12.11}$$

or :

$$Q = \omega\mu\sqrt{2gH_{\text{outflow}}} \,. \tag{12.12}$$

The value $\mu = \varepsilon\varphi$ is called the *throughflow factor.*

Thus, the compression factor ε, velocity factor φ and the throughflow factor μ are not independent, but are linked through Eq. (12.12). So, it is sufficient only to know one of them to calculate the outflow from an orifice.

Let's recall the value:

$$Q_{Th}\omega w_{Th} = \omega\sqrt{2gH_{\text{outflow}}} \tag{12.13}$$

the *theoretical throughflow.*

Following Eqs. (12.11) and (12.13), the throughflow factor is the ratio of the actual to theoretical throughflow.

The factors ε, φ and μ are determined experimentally and are functions of the Reynolds' number (Fig. 12.3).

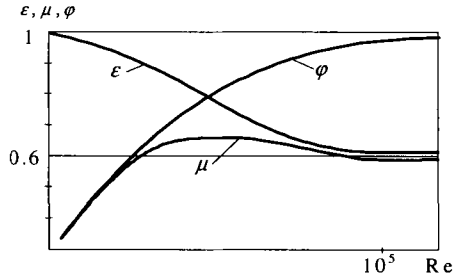

Fig. 12.3

It is easy to show with Bernoulli's equation that for a small orifice Eqs. (12.9) and (12.12) are valid for the orifice located on the side wall of a tank. H in such a case is the distance between the orifice's axis and the free surface.

2. Outflow through nozzles

A short tube connected to the orifice is called a *nozzle.* The length of the nozzle is 3 to 5 orifice's diameters. The nature of fluid's outflow through the nozzle strongly depends on the nozzle's shape. It is clear from the derivation of Eqs. (12.9) and (12.12) that these equations are valid also for a nozzle. However, φ and μ factors are different for different nozzles.

Fig. 12.4 illustrates various nozzles: 1.external cylindrical; 2.internal cylindrical; 3.conical converging; 4. conical diverging; 5.conoidal.

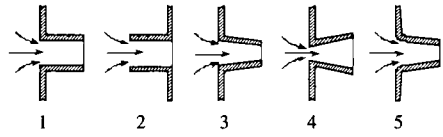

Fig. 12.4

The values of the velocity factor φ and throughflow factor μ for the quadratic outflow law are listed in the following Table. The flow regime at outflow through orifices and nozzles, same as at flow through the tubes, is quadratic, i. e., φ and μ do not depend on the Reynolds' number.

Type of nozzle	μ	φ
Round orifice	0.62	0.97
External cylindrical	0.82	0.82
Internal cylindrical	0.71	0.71
Conical convergent (13°24')	0.95	0.96
Conical divergent (5°)	0.48	0.48
Conoidal	0.98	0.98

The Table indicates that for some nozzles $\mu = \varphi$, i. e., $\varepsilon = 1$. The reason is that the constriction occurs inside the nozzles, and the μ and φ values are listed for the output cross-sections. It also shows that, the throughflow through the external cylindrical nozzle is 30 % greater that through a round orifice of the same diameter.

In this section the fluid's outflow through the external cylindrical nozzle are reviewed in more detail.

In order for the stream to be able to fill-up the nozzle cross-section completely its length, as experiments showed, must be equal to at least three diameters (see Fig. 12.5) for the the stream schematics. Fig. 12.5 shows that stream stream is compressed on entry of the nozzle, and then expands. A stagnation zone forms in the constriction area filled-up with vortices.

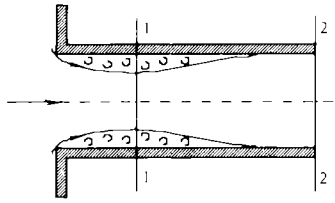

Fig. 12.5

Let's draw the cross-sections 1–1 and 2–2 within the nozzle (Fig. 12.5) and write Bernoulli's equation for the segment between the cross-sections. (To simplify the problem, the nozzle is considered horizontal). Then:

$$\frac{p_1}{\rho g} + \frac{w_1^2}{2g} = \frac{p_2}{\rho g} + \frac{w_2^2}{2g} + h_{1-2}. \qquad (12.14)$$

The distance between the cross-sections is small so it is possible to disregard the loss along the nozzle length. Therefore, the loss along the 1–2 segment is determined by the loss due to a sudden stream expansion. In order to determine the head loss due to such expansion of the stream, consider the variation of momentum law Eq. (2.51), i. e.:

$$Q_m(\bar{v}_2^{(mean)} - \bar{v}_1^{(mean)}) = \overline{G} + \overline{\mathrm{P}} + \overline{N} + \overline{T}. \qquad (12.15)$$

The gravitational force $\overline{G}$, pressure force $\overline{\mathrm{P}}$, the force of normal reactions $\overline{N}$ applied to stream's side surface, and the friction force $\overline{T}$ are determined, respectively, from Eqs. (2.53), (2.54) and (2.55).

Projecting Eq. (12.15) onto the nozzle's horizontal axis $0x$ and disregarding, due to its small length, the friction force $\vec{T}$, gives:

$$Q_m(w_2 - w_1) = \mathrm{P}_x + N_x. \qquad (12.16)$$

Assuming the pressure distribution in the cross-sections 1–1 and 2–2 is hydrostatic:

$$\mathrm{P}_x = p_1\omega_1 - p_2\omega_2, \quad N_x = p_1(\omega_2 - \omega_1), \qquad (12.17)$$

where ω_1, ω_2 are stream cross-section areas 1–1 and 2–2, respectively. The mass throughput Q_m can be formatted as $Q_m = \rho w_2 \omega_2$; then, substituting Eq. (12.17) into Eq. (12.16):

$$\rho w_2(w_2 - w_1) = p_1 - p_2. \qquad (12.18)$$

Canceling the pressure differences $p_1 - p_2$ from Eqs. (12.14) and (12.18), and after simple transformations:

$$h_{1-2} = \frac{(w_1 - w_2)^2}{2g}. \qquad (12.19)$$

This expression is called Bord equation.

Following the stream continuity equation that:

$$w_1 = \frac{\omega_2}{\omega_1} w_2 = \frac{1}{\varepsilon_{\text{input}}} w_2, \qquad (12.20)$$

where $\varepsilon_{\text{input}} = \dfrac{\omega_1}{\omega_2}$ is the stream contraction factor at the input to the nozzle.

Substituting Eqs. (12.19) and (12.20) into the Bernoulli equation Eq. (12.14), results in:

$$\frac{p_1}{\rho g} = \frac{p_2}{\rho g} - \frac{1-\varepsilon_{input}}{\varepsilon_{input}} \frac{w_2^2}{2g}. \tag{12.21}$$

As $\varepsilon_{input} < 1$, it can be observed from Eq. (12.21) that $p_1 < p_2$, i. e., a pressure drawdown occurs in the cross-section 1–1, and that results in the throughput increase compared with the round orifice. Using Eq. (12.9) it is possible to reformat Eq. (12.21) as follows:

$$\frac{p_1}{\rho g} = \frac{p_2}{\rho g} - 2\varphi^2 \frac{1-\varepsilon_{input}}{\varepsilon_{input}} H_{outflow}. \tag{12.22}$$

At the outflow to the atmosphere, $p_2 = p_{atm}$, and vacuum forms in the cross-section 1-1. The value of this vacuum ($p_{vac} = p_{atm} - p_1$) is equal to:

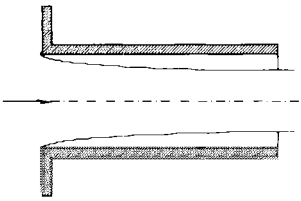

Fig. 12.6

$$\frac{p_{vac}}{\rho g} = \frac{p_{atm} - p_1}{\rho g} = 2\varphi^2 \frac{1-\varepsilon_{input}}{\varepsilon_{input}} H_{outflow}$$

and it increases with the increase in the outflow head $H_{outflow}$. There is, however, a critical value $H_{outflow}=H_{crit}$, above which the nozzle performance is disrupted, the stream detaches from its walls, and the throughput drastically declines (Fig. 12.6). The outflow now is occurring the same way as through the orifice. The phenomenon is called the *outflow detachment.* For the water, $H_{crit} = 14.5$ m.

As the nozzle length increases, the losses along its length raise. From Darcy-Weisbach equation, the friction loss h_τ is equal to:

$$h_\tau = \lambda \frac{l}{d} \frac{w^2}{2g}.$$

and following Bernoulli's equation Eq. (12.5), for a nozzle:

$$\varphi = \sqrt{\alpha_c + \zeta + \lambda \frac{l}{d}}. \tag{12.23}$$

Eq. (12.23) enables to determine the $\frac{l}{d}$ value at which the throughflow through the nozzle is equal to the throughflow through the orifice.

3. Outflow of fluid at variable level

Let's analyze the fluid's outflow through a small orifice or nozzle with changing fluid's level in the tank. The flow is non-stationary as the outflow head, (hence velocity) changes with time. Suppose the area of the tank's cross-wise section Ω depends on the height, i. e., $\Omega = \Omega(z)$ (Fig. 12.7). The fluid's level in the tank will decline by dz over the time interval dt. Therefore, the outflowing volume will be $V = -\Omega dz$. On the other hand, during time interval dt the volume $V = Qdt$ outflows through the orifice (nozzle). Clearly:

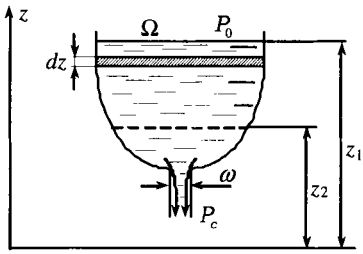

Fig. 12.7

$$Qdt = -\Omega(z)dz. \tag{12.24}$$

Assuming that Eq. (12.12) is valid for non-stationary flow, Eq. (12.24) can be written as:

$$dt = -\frac{\Omega(z)dz}{\omega\mu\sqrt{2gH_{\text{outflow}}}} \tag{12.25}$$

or, as in this case:

$$H_{\text{outflow}} = z + \frac{p_o - p_c}{\rho g},$$

as:

$$dt = -\frac{\Omega(z)dz}{\omega\mu\sqrt{2g\left(z + \frac{p_o - p_c}{\rho g}\right)}}. \tag{12.26}$$

Following Eq. (12.26), the time t of the level's drop in the tank from elevation z_1 to z_2 is equal to:

$$t = -\int_{z_1}^{z_2} \frac{\Omega(z)dz}{\omega\mu\sqrt{2g\left(z + \frac{p_o - p_c}{\rho g}\right)}} = \int_{z_2}^{z_1} \frac{\Omega(z)dz}{\omega\mu\sqrt{\left(z + \frac{p_o - p_c}{\rho g}\right)}}. \tag{12.27}$$

Suppose the throughflow factor μ at the outflow with the constant level is the same as at the outflow with variable level. Also suppose that μ = const. Experience shows that all these assumptions cause only very small errors. Thus, it is possible to rewrite Eq. (12.27) as follows:

$$t = \frac{1}{\omega\mu\sqrt{2g}} \int_{z_2}^{z_1} \frac{\Omega(z)dz}{\sqrt{z + \frac{p_o - p_c}{\rho g}}}. \tag{12.28}$$

Let's now review some examples assuming for the simplicity's sake that $p_o = p_c$.

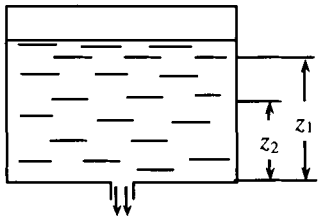

Fig. 12.8

1. Outflow from a vertical cylinder (Fig. 12.8). In this case Ω = const, and from Eq. (12.28):

$$t = \frac{2\Omega\left(\sqrt{z_1} - \sqrt{z_2}\right)}{\omega\mu\sqrt{2g}}.$$

2. Outflow from a horizontal round cylinder (Fig. 12.9).

It may be seen from Fig. 12.9 that:

$$b = 2\sqrt{R^2 - (z-R)^2} = 2\sqrt{2Rz - z^2}, \tag{12.29}$$

and the area of free surface is equal to:

$$\Omega = bL = 2L\sqrt{2Rz - z^2}.$$

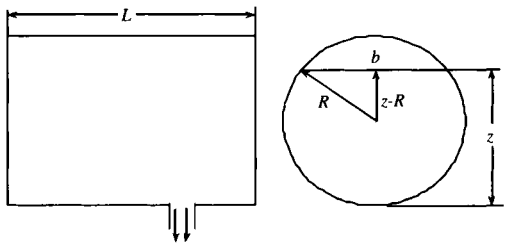

Fig. 12.9

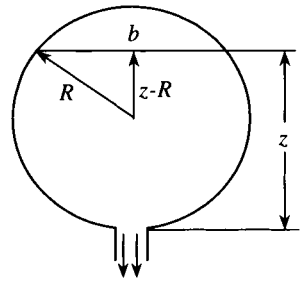

Fig. 12.10

Then, from Eq. (12.28) at $p_o = p_c$:

$$t = \frac{2L}{\omega\mu\sqrt{2g}} \int_{z_2}^{z_1} \frac{\sqrt{2Rz - z^2}}{\sqrt{z}} dz = \frac{2L}{\omega\mu\sqrt{2g}} \int_{z_2}^{z_1} \sqrt{2Rz - z} dz =$$

$$= \frac{4L}{3\omega\mu\sqrt{2g}} \left(\sqrt{2Rz - z_2} - \sqrt{2Rz - z_1} \right).$$

3. Outflow from a spherical tank (Fig. 12.10). In this case:

$$\Omega = \frac{\pi b^2}{4},$$

where b value is determined from Eq. (12.29). Then:

$$\Omega = \pi(2Rz - z^2),$$

and from Eq. (12.28):

$$t = \frac{\pi}{\omega\mu\sqrt{2g}} \int_{z_2}^{z_1} \frac{2Rz - z^2}{\sqrt{z}} dz = \frac{2\pi}{\omega\mu\sqrt{2g}} \left[\frac{2}{3} R \left(z_1^{3/2} - z_2^{3/2} \right) - \frac{1}{5} \left(z_1^{5/2} - z_2^{5/2} \right) \right].$$

CHAPTER XIII

NON-STATIONARY FLOW OF VISCOUS FLUID IN PIPES

A wide class of engineering problems such as designing pipelines of various designations causes the need to study the non-stationary fluids' flow in the tubes. However, the techniques using models of incompressible fluids and non-deformable pipelines result in substantial discrepancies with the experimental data especially in case of long pipelines and fast-going processes.

Indeed, as Eq. (2.41) shows the above models cannot as a matter of principle describe wave processes occurring in the tubes. For such description, the fluid's elasticity and tube walls' ductility must be accounted for.

This resulted in the separation of the theory of non-stationary fluid's flow in pipes, as more or less independent section of hydromechanics.

A complete theory of non-stationary flow of ideal incompressible fluid in pipes was constructed by Zhukovsky. Subsequently, other scientists developed various approximate techniques for the inclusion of friction forces as corrections introduced into the solutions for ideal fluid. Based on the quasi-stationary hypothesis by Christiansen. I. Charny implemented the inclusion of friction forces directly into the fluids' motion equations.

Currently, the theory based on the quasi-stationary hypothesis is commonly accepted. It was shown in experimental studies, however, that the quasi-stationary hypothesis is just a first approximation and has limited application.

1. Equations of the non-stationary fluid's flow in pipes

In order to derive equations of non-stationary fluid's flow in pipes, the continuity equations [Eq. (2.34)] and variation in momentum law [Eq. (2.51)] are used:

$$\int_V \frac{\partial p}{\partial v} dV + \int_S \rho v_n dS = 0, \tag{13.1}$$

$$\int_V \frac{\partial(\rho \bar{v})}{\partial t} dV + \int_S \rho \bar{v} v_n dS = \int_V \rho \bar{F} dV + \int_S \bar{p}_n dS. \tag{13.2}$$

Assuming:

$$\bar{p}_n = -p\bar{n} + \bar{\tau}_n,$$

where $\bar{\tau}_n$ is the friction stress, and using Gauss–Ostrogradsky theorem, Eq. (13.2) can be presented as follows:

$$\int_V \frac{\partial(\rho\bar{v})}{\partial t} dV + \int_S \rho\bar{v}v_n dS = \int_V (\rho\bar{F} - -\nabla p) dV + \int_S \bar{\tau}_n dS. \qquad (13.3)$$

Let's take a volume V of the tube segment with a straight-line axis $0x$ (hydraulic axis). The volume is limited by cross-sections f and f_1 positioned at a distance dx from one another (Fig. 13.1). Thus, $f = f(x,t)$, i. e., the area of the tube's cross-wise section depends on the coordinate and time. As in the cross-section f, $v_n = -v_x$, and in the cross-section f_1, $v_n = v_x$, Eq. (13.1) for the identified volume V can be written as:

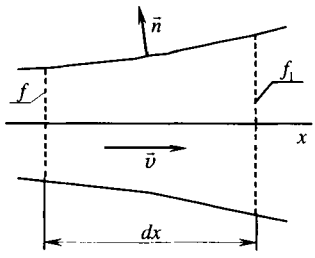

Fig. 13.1

$$\int_V \frac{\partial\rho}{\partial t} dV - \int_f \rho v_x df + \int_{f_1} \rho v_x df + \int_\omega \rho v_n d\omega = 0, \quad (13.4)$$

where ω is the side surface of volume V.

Eq. (13.3) projected onto axis $0x$ becomes:

$$\int_V \frac{\partial(\rho\bar{v})}{\partial t} dV - \int_f \rho v_x^2 df + \int_{f_1} \rho v_x^2 df + \int_\omega \rho v_x v_n d\omega =$$

(13.5)

$$\int_V \left(\rho F_x - \frac{\partial p}{\partial x}\right) dV - \int_f \tau_{xx} df + \int_{f_1} \tau_{xx} df + \int_\omega \tau_{nx} d\omega.$$

Clearly, for the object under consideration:

$$\int_V \varphi dV = \int_f \varphi df\, dx, \quad \int_{f_1} \varphi df - \int_f \varphi df = \frac{\partial}{\partial x} \int_f \varphi df dx. \qquad (13.6)$$

Let's also assume that the shape and cross-section of the tube are changing relatively smoothly, i. e. (Fig. 13.1):

$$\cos^2(n,x) << 1$$

In this case:

$$\lim_{\Delta x \to 0} \frac{1}{dx} \int_\omega \varphi d\omega = \int_\chi \varphi d\chi, \qquad (13.7)$$

where χ is the flow cross-section's perimeter. Using Eqs. (13.6) and (13.7) and using the same transformation in Eqs. (13.4) and (13.5) to the limit at $dx \to 0$ results:

$$\int_f \frac{\partial \rho}{\partial t} df + \frac{\partial}{\partial x} \int_f \rho v_x df + \int_\chi \rho v_n d\chi, \tag{13.8}$$

$$\int_f \frac{\partial (\rho v_x)}{\partial t} df + \frac{\partial}{\partial x} \int_f \rho v^2{}_x df + \int_\chi \rho v_x v_n d\chi = \int_f \left(\rho F_x - \frac{\partial p}{\partial x} \right) df + \frac{\partial}{\partial x} \int_f \tau_{xx} df + \int_\chi \tau_{nx} d\chi. \tag{13.9}$$

To be able to further transform Eqs. (13.8) and (13.9), it is necessary to compute the value:

$$\frac{\partial}{\partial t} \int_f \varphi df,$$

where $\varphi(x,y,z,t)$ is some differentiable function of the coordinates and time.

As $f = f(x,t)$, $df = v'_n d\chi \Delta t$, where v'_n is the velocity $\bar{v}$ projection onto the external normal $\bar{n}'$ to the flat contour χ (Fig. 13.2). Then:

$$\frac{\partial}{\partial t} \int_f \varphi df = \lim \left[\int_{f(x,t+\Delta t)} \frac{\varphi(x,y,z,t+\Delta t)}{\Delta t} df - \int_{f(x,t)} \frac{\varphi(x,y,z,t)}{\Delta t} df \right] =$$

$$= \lim \int_{f(x,t)} \frac{\varphi(t+\Delta t) - \varphi(t)}{\Delta t} df + \lim_{\Delta t \to 0} \int_{f(x,t+\Delta t)} \frac{\varphi(t+\Delta t)}{\Delta t} df = \tag{13.10}$$

$$\int_f \frac{\partial \varphi}{\partial t} df + \int_f \varphi v'_n \, d\chi.$$

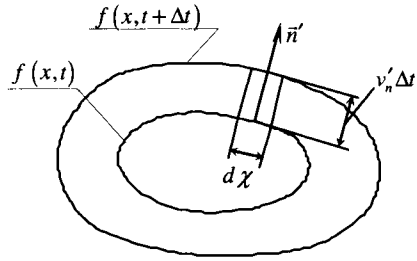

Fig. 13.2

In viscous fluid flow, the tangential component of velocity v_τ at its side surface ω is equal to zero ($v_\tau = 0$), and the normal component $v_n = \pm|\bar{v}|$. The normal $\bar{n}'$ lies in the surface perpendicular to $0x$, and $\cos^2(n,x) << 1$ by proviso, then:

$$v_n' = v_n \cos(\bar{v},\bar{n}') = v_n\sqrt{1-\cos^2(n,x)} \approx v_n,$$

and Eq. (13.10) can be rewritten as:

$$\frac{\partial}{\partial t}\int_f \varphi df = \int_f \frac{\partial \varphi}{\partial t} + \int_\chi \varphi v_n d\chi . \tag{13.11}$$

Substituting Eq. (13.11) into Eqs. (13.8) and (13.9), gives:

$$\int_f \rho df + \frac{\partial}{\partial x}\int_f \rho v_x df = 0, \tag{13.12}$$

$$\frac{\partial}{\partial t}\int_f \rho v_x df + \frac{\partial}{\partial x}\int_f \rho v_x^2 df = \int_f \left(\rho F_x - \frac{\partial p}{\partial x}\right)df + \frac{\partial}{\partial x}\int_f \tau_{xx} df + \int_\chi \tau_{nx} d\chi . \tag{13.13}$$

Assume further that the only operating mass force is the gravitational force, i. e., $\rho F_x = -\rho g \frac{\partial z_1}{\partial x}$, where z_1 is the coordinate of a point in the fluid measured from an arbitrary horizontal plane vertically up. Then:

$$\int_f \left(\rho F_x - \frac{\partial p}{\partial x}\right)df = -\int_f \left(\rho g \frac{\partial z_1}{\partial x} + \frac{\partial p}{\partial x}\right)df = -\frac{\partial}{\partial t}\int_f \left[\frac{\partial}{\partial x}(p + \rho g z_1) - g z_1 \frac{\partial p}{\partial x}\right]df .$$

Both for gases and for slightly compressible fluids, the $g z_1 \frac{\partial p}{\partial x}$ value is small compared with $\frac{\partial p}{\partial x}$, so:

$$\int_f \left(\rho F_x - \frac{\partial p}{\partial x}\right)df \approx -\int_f \frac{\partial}{\partial x}(p + \rho g z_1)df = -f\frac{\partial}{\partial x}(p + \rho g z_1), \tag{13.14}$$

because for a smoothly-changing flow ($\cos^2(n,x) << 1$), as Navier-Stokes equations indicate, $p + \rho g z_1 \approx$ const in the cross-wise section f.

Further, it is clear that:

$$\int_\chi \tau_{nx} d\chi = \tau_\chi \chi , \tag{13.15}$$

where τ_χ is average over the cross-section perimeter of flow value of τ_{nx}. It is customary to disregard the:

$$\frac{\partial}{\partial x}\int_f \tau_{xx} df$$

value in hydraulic computations. This statement is based on the following. According to Eqs. (4.21) and (4.28) for a slightly compressible fluid, $p_{xx} = -p + \tau_{xx} = -p + \mu\frac{\partial v}{\partial x}$, and under regular circumstances $\mu\frac{\partial v}{\partial x} << p$. Besides, it is assumed that the fluid's density changes negligibly in the flow cross-section.

Considering and substituting Eqs. (13.14) and (13.15) into Eq. (13.13), and from Eqs. (13.12) and (13.13):

$$\frac{\partial(\rho f)}{\partial t} + \frac{\partial M}{\partial x} = 0,$$

(13.16)

$$\frac{\partial M}{\partial t} + \frac{\partial J}{\partial x} = -f\frac{\partial}{\partial x}(p + \rho g z_1) + \chi\tau_\chi,$$

where $M = \int_f \rho v_x df = \rho w f$ is the fluid's mass throughflow; $J = \int_f \rho v_x^2 df = \beta\rho w^2 f = \beta\rho M w$ is projection onto the $0x$ axis of momentum of the mass M; w is average (in the cross-section) fluid's velocity; and β is Coriolis's correction for a non-uniform density and velocity distribution in the flow's momentum equations. For turbulent flow, $\beta \approx 1.03$ to 1.1, for laminar flow $\beta = 1.33$. When deriving Eq. (13.16), no assumptions are made about the format of the friction law. Thus, these equations are valid for any liquid or gas flow (either Newtonian or non-Newtonian) provided $\cos^2(n,x) << 1$. Eq. (13.16) includes five unknown variables: p, ρ, w, f, τ_χ β (β is considered to be a known function of w, fluids properties, type of nonstationarity and geometry of pipe). In order for the system to be closed, it is necessary to add to Eq. (13.16) τ_χ as a function of w, liquid's (gas) equation of state and the connection between the tube cross-section area and pressure.

It is assumed that the pipe's walls are elastic and the area of cross-section depends on pressure under Hooke's law, i. e.:

$$f = f_0\left(1 + e\frac{p - p_0}{E}\right), \qquad (13.17)$$

where $f_0 = f_0(x)$ is the area of the pipe's cross-section at pressure p, E_0 is Young's modulus of the pipe's material, e is a dimensionless factor depending on the pipe's cross-section shape and wall material. Also, the effect of the lengthwise elasticity forces and inertia forces of the pipe's walls are ignored. For a case of a slightly compressible fluid, it is also assumed that Hooke's law is valid, i. e.:

$$\rho = \rho_0\left(1 + e\frac{p - p_0}{K_{liq}}\right), \tag{13.18}$$

where ρ_0 is density at pressure p_0, K_{liq} is fluid's bulk modulus of compression.

Eqs. (13.17) and (13.18) are only valid when:

$$e\frac{p - p_0}{E} << 1, \quad \frac{p - p_0}{K_{liq}} << 1, \tag{13.19}$$

so:

$$\rho f = \rho_0 f_0\left[1 + \left(1 + \frac{1}{K_{liq}} + \frac{e}{E}\right)(p - p_0)\right] = \rho_0 f_0\left(1 + \frac{p - p_0}{K}\right). \tag{13.20}$$

where:

$$K = \frac{K_{liq}}{1 + e\dfrac{K_{liq}}{E}}$$

is *normalized bulk modulus of compression*, which considers elasticity of both the fluid and the pipe. For a thin-walled round pipe:

$$e = \frac{d}{h},$$

where d is the internal diameter, h is the thickness of pipe's wall. By definition, sound velocity[1] in a system "elastic fluid flowing in the elastic pipe" is equal to:

$$c = \sqrt{\frac{K}{\rho}} \approx \sqrt{\frac{K}{\rho_0}}. \tag{13.21}$$

According to Eqs. (13.20) and (13.21):

$$\frac{\partial(\rho f)}{\partial t} = \frac{\rho_0 f_0}{K}\frac{\partial p}{\partial t} = \frac{f_0}{c^2}\frac{\partial p}{\partial t}. \tag{13.22}$$

[1] Under the sound velocity, the propagation velocity of small disturbances is understood, i. e., for which the conditions of Eq. (13.19) are fulfilled.

On the other hand, under Hooke's law Eq. (13.18),

$$\frac{\partial \bar{p}}{\partial t} = \frac{\partial}{\partial t}(p + \rho g z_1) = \frac{\partial p}{\partial x} + g z_1 \frac{\partial \rho}{\partial t} = \frac{\partial p}{\partial t} + \frac{g z_1 \rho_0}{K_{liq}} \frac{\partial p}{\partial t} \approx \frac{\partial p}{\partial t}, \qquad (13.23)$$

where $\bar{p} = p + \rho g z_1$ is normalized pressure.

By substituting Eqs. (13.22) and (13.23) into Eq. (13.16):

$$\frac{f_0}{c^2}\frac{\partial \bar{p}}{\partial t} + \frac{\partial M}{\partial x} = 0,$$

$$\frac{\partial M}{\partial t}\frac{\partial J}{\partial x} = -f\frac{\partial \bar{p}}{\partial x} + \chi\tau_\chi. \qquad (13.24)$$

For a gas flowing in a pipe, $\frac{\partial f}{\partial t} = 0$, i. e., disregard changes in the pipe's cross-section area. In such a case, using a known equation $\frac{\partial f}{\partial \rho} = c_0^{\,2}$, where c_0 is sound velocity of gas, results in:

$$\frac{\partial \rho}{\partial t} = \frac{1}{c_0^{\,2}}\frac{\partial p}{\partial t}, \quad \frac{\partial(\rho f)}{\partial t} = \frac{f}{c_0^{\,2}}\frac{\partial p}{\partial t},$$

$$\frac{\partial \bar{p}}{\partial t} = \frac{\partial}{\partial t}(p + \rho g z_1) = \frac{\partial p}{\partial t} g z_1 \frac{\partial \rho}{\partial t} = \frac{\partial p}{\partial t} + \frac{g z_1}{c_0^{\,2}}\frac{\partial p}{\partial t} \approx \frac{\partial p}{\partial t} \qquad (13.25)$$

Consequently, Eqs. (13.24) are valid also for the gas. Thus, different notations for c and c_0 are not used.

In order to establish the correlation between τ_χ and fluid's properties and flow parameters, the quasi-stationary hypothesis is used, i. e., the assumption that the flow parameters established for a stationary flow are also valid for a non-stationary flow. Then, under Eq. (10.35):

$$\tau_\chi = -\lambda\frac{|w|}{8}\rho w,$$

and Eq. (13.24) becomes:

$$\frac{f_0}{c^2}\frac{\partial \bar{p}}{\partial t} + \frac{\partial M}{\partial x} = 0,$$

$$\frac{\partial M}{\partial t} + \frac{\partial J}{\partial x} = -f\frac{\partial \bar{p}}{\partial x} - \chi\lambda\frac{|w|}{8}\rho w. \qquad (13.26)$$

2. Equation of non-stationary flow for slightly-compressible fluid in pipes

Integrating the second equation Eq. (13.26) with respect to x, results in:

$$\int_0^x \frac{\partial M}{\partial t} dx + J(x) - J(0) = -f_{\text{avg}}\left[\bar{p}(x) - \bar{p}(0)\right] + \int_0^x \chi\lambda \frac{|w|}{8} \rho w dx_1,$$

where f_{avg} is average value of area f over the segment $[0,x]$. Following the definition of J that:

$$\frac{J}{f} = \beta\rho w^2$$

is dynamic pressure corresponding to the doubled velocity head. Clearly, when dealing with the flow of a slightly compressible fluid it is possible to disregard the changes of this pressure compared with the changes of the normalized pressure $\bar{p}(x) - \bar{p}(0)$. The latter is equivalent to disregarding the term $\frac{\partial J}{\partial x}$ in Eq. (13.26). Further, according to Eqs. (13.20) and (13.21):

$$\frac{\partial M}{\partial x} = \frac{\partial(\rho f w)}{\partial x} = \rho f \frac{\partial w}{\partial x} + w\frac{\partial(\rho f)}{\partial x} = \rho f \frac{\partial w}{\partial x} + \frac{f_0 w}{c^2}\frac{\partial p}{\partial x} \approx \rho f \frac{\partial w}{\partial x},$$

$$\frac{\partial M}{\partial t} = \frac{\partial(\rho f w)}{\partial t} = \rho f \frac{\partial w}{\partial t} + w\frac{\partial(\rho f)}{\partial t} = \rho f \frac{\partial w}{\partial t} + \frac{f_0 w}{c^2}\frac{\partial p}{\partial t} \approx \rho f \frac{\partial w}{\partial t}. \tag{13.27}$$

By substituting Eq. (13.27) into Eq. (13.26), disregarding the term $\frac{\partial J}{\partial x}$ and assuming $f \approx f_0$, $\rho \approx \rho_0$, the equations for flow of a viscous slightly-compressible fluid are obtained:

$$-\frac{\partial \bar{p}}{\partial t} = \rho c^2 \frac{\partial w}{\partial x},$$

$$-\frac{\partial \bar{p}}{\partial x} = \rho\left(\frac{\partial w}{\partial t} + \frac{\lambda|w|}{8\delta} w\right), \tag{13.28}$$

where $\delta = \frac{f}{\lambda}$ is hydraulic radius of the flow. To evaluate the results, let's review the Navier-Stokes equation [Eq. (9.3)] describing the flow of an incompressible fluid in a prismatic tube. Assuming the tube has a circular cross section (the flow is axisymmetric) and $\bar{F} = \bar{g}$, and from Eq. (9.3) as projected onto the axis $0x$:

$$\rho\frac{\partial u}{\partial t} = -\frac{\partial}{\partial x}(\rho g z_1 + p) + \frac{\mu}{r}\frac{\partial}{\partial r}\left(r\frac{\partial u}{\partial r}\right). \tag{13.29}$$

Average flow velocity in this case is equal to:

$$w = \frac{1}{\pi R^2}\int_0^R 2\pi r u\, dr = \frac{2}{R^2}\int_0^R r u\, dr, \tag{13.30}$$

where R is the tube's radius. By multiplying Eq. (13.29) by $2\pi r\, dr$ and integrating with respect to the radius from 0 to R, and considering Eq. (13.30):

$$-\frac{\partial \bar{p}}{\partial x} = \rho\frac{\partial w}{\partial t} - \frac{2\mu}{R}\frac{\partial u}{\partial r}\bigg|_{r=R},$$

or, as for a round tube $\delta = \frac{R}{2}$, $\tau_\chi = \mu\frac{\partial u}{\partial r}\Big|_{r=R}$,

$$-\frac{\partial \bar{p}}{\partial x} = \rho\frac{\partial w}{\partial t} - \frac{\tau_k}{\delta}. \tag{13.31}$$

Continuity equation for an incompressible fluid has the following format:

$$\frac{\partial w}{\partial x} = 0. \tag{13.32}$$

Comparing Eqs. (13.31) and (13.32) with the Eq. (13.28), shows that the fluid's compressibility and tube walls' elasticity are considered in Eq. (13.28), as opposed to an incompressible fluid, $w = w(x,t)$, and the sound velocity has a finite value. These distinctions, however, have conceptual importance. Indeed, the system Eq. (13.28) is hyperbolic, i. e., enabling wave solutions (as opposed to equations for incompressible fluid). Therefore, Eq. (13.28) provides description of the wave processes arising in the pipes at a non-stationary flow. In a general case, Eq. (13.28) includes a nonlinear term $\lambda\frac{|w|}{8\delta}w$, which complicates integration operations. Various linearization techniques, which can be reduced to the representation of the nonlinear term, such as:

$$\lambda\frac{|w|}{8\delta}w = 2aw,\ 2a = \left(\frac{\lambda|w|}{8\delta}\right)_{\text{avg}} = \text{const} > 0, \tag{13.33}$$

are analyzed in various publications (see References), which also analyze error as a result of linearization. At a laminar flow regime, $\lambda = \frac{A}{\text{Re}}$, and from that:

$$\lambda\frac{|w|}{8\delta} = \frac{A|w|\mu}{\rho|w|4\delta * 8\delta} = \frac{A|w|\mu}{32\rho\delta^2} = 2a.$$

For round pipes, $A = 64$, $\delta = \frac{d}{4}$ and $2a = \frac{32\mu}{\rho d^2}$ where d is tube's diameter. By substituting Eq. (13.33) into Eq. (13.28):

$$-\frac{\partial \bar{p}}{\partial t} = \rho c^2 \frac{\partial w}{\partial x},$$

$$-\frac{\partial \bar{p}}{\partial x} = \rho\left(\frac{\partial w}{\partial t} + 2aw\right). \tag{13.34}$$

Once again, it is assumed in these equations that $\rho = \text{const}$.

3. Equations of non-stationary gas flow in pipes at low subsonic velocities

When dealing with gas flow it is necessary to supply Eq. (13.26) with equation of state, for instance:

$$\frac{p}{\rho} = ZRT, \tag{13.35}$$

where Z is super-compressibility, R is the gas constant, and T is temperature, K.

Substituting Eq. (13.35) into $\bar{p} = p + \rho g z_1$ results in:

$$\bar{p} = p + \rho g z_1 = p\left(1 + \frac{g z_1}{ZRT}\right),$$

which shows that even at relatively large z_1 ($z_1 < 200$ m) it is possible to assume $\bar{p} \approx p$. As the evaluations show, for the gas flow in long gas lines at low subsonic velocities it is possible to disregard dynamic pressure, which corresponds to doubled velocity head, and even more so it is possible to disregard its changes, i. e., the term $\frac{\partial J}{\partial x}$ in Eq. (13.24).

Considering and assuming $f = f_0$, and from Eq. (13.26):

$$-\frac{\partial p}{\partial t} = c^2 \frac{\partial(\rho w)}{\partial t},$$

$$-\frac{\partial p}{\partial x} = \frac{\partial(\rho w)}{\partial t} + \frac{\lambda |w|}{8\delta}\rho w = \frac{\partial(\rho w)}{\partial t} + \frac{\lambda |\rho w|}{8\delta}\frac{\rho w}{\rho}. \tag{13.36}$$

Hydraulic resistance depends on Re number, so:

$$\lambda = \lambda(\mathrm{Re}) = \lambda\left(\frac{4\delta\rho w}{\mu}\right),$$

viscosity depends on temperature, $\mu = \mu(\mathrm{T})$, so the system of Eqs. (13.35) and (13.36) includes four unknown variables, p, ρ, w, T. For the gas flow in long gas lines it is

usually assumed that the flow regime is isothermal, i. e., $T = T_0 = \text{const}$. In this, case, the system Eqs. (13.35) and (13.36) becomes closed.

To linearize the second equation of Eq. (13.36), Eq. (13.33) is used. Then:

$$-\frac{\partial p}{\partial t} = c^2 \frac{\partial(\rho w)}{\partial t}$$

$$-\frac{\partial p}{\partial x} = \frac{\partial(\rho w)}{\partial t} + 2a\rho w, \tag{13.37}$$

where at low subsonic velocities it can be assumed that $c = \text{const}$. Then the linearization of Eq. (13.37) coincides with Eq. (3.34) for fluids when $\rho = \text{const}$. Such linearization is cruder than that for the fluids, as in long pipelines velocity can significantly change along the length of the pipe, in contrast with the fluids.

Now, other linearization techniques of Eq. (13.36) are indicated. Considering Eq. (13.25), let's rewrite Eq. (13.36) as follows:

$$-\frac{\partial p}{\partial t} = \rho\frac{\partial w}{\partial x} + w\frac{\partial \rho}{\partial x} = \rho\frac{\partial w}{\partial x} + \frac{w}{c^2}\frac{\partial p}{\partial x},$$

$$-\frac{\partial p}{\partial x} = \rho\frac{\partial w}{\partial t} + w\frac{\partial \rho}{\partial t} + \frac{\lambda|\rho w|}{8\delta}\rho w. \tag{13.38}$$

Cancelling $\frac{\partial \rho}{\partial t}$ from the second equation Eq. of (13.38):

$$-\left(1 - \frac{w^2}{c^2}\right)\frac{\partial p}{\partial x} = \rho\frac{\partial w}{\partial t} - \rho\frac{\partial}{\partial x}\left(\frac{w^2}{2}\right) + \frac{\lambda|\rho w|}{8\delta}\rho w. \tag{13.39}$$

It is discussed earlier to review low subsonic velocities and disregard the velocity head and its derivatives. So it is possible to rewrite the first equation of Eq. (13.37) and Eq. (13.39) as follows, considering Eq. (13.25) and the equation of state [Eq. (13.35)]:

$$-\frac{1}{c^2}\frac{\partial p}{\partial t} = \rho\frac{\partial w}{\partial x} = \frac{p}{ZRT}\frac{\partial w}{\partial x},$$

$$-\frac{\partial p}{\partial x} = \rho\left(\frac{\partial w}{\partial t} + \frac{\lambda|\rho w|}{8\delta}w\right) = \frac{p}{ZRT}\left(\frac{\partial w}{\partial t} + \frac{\lambda|\rho w|}{8\delta}w\right),$$

or

$$-\frac{\partial \ln p}{\partial t} = \frac{c^2}{ZRT}\frac{\partial w}{\partial x}$$

$$-\frac{\partial \ln p}{\partial t} = \frac{1}{ZRT}\left(\frac{\partial w}{\partial t} + \frac{\lambda|\rho w|}{8\delta}w\right). \tag{13.40}$$

Eq. (13.40) coincide with Eq. (13.28) for the fluid if $\bar{p}$ is replaced by $\ln p$, and ρ, by $1/(ZRT)$. Linearization of Eq. (13.40) can be done using Eq. (13.33).

4. Integrating equations of non-stationary fluids and gas flow using the characteristics technique

The following systems of equations:

(a) Nonlinear –

$$-\frac{\partial p}{\partial t}=\rho c^2\frac{\partial w}{\partial x},$$

$$-\frac{\partial p}{\partial x}=\rho\left(\frac{\partial w}{\partial t}+\frac{\lambda|\rho w|}{8\delta}w\right) \tag{13.41}$$

and (b) Linearized –

$$-\frac{\partial p}{\partial t}=\rho c^2\frac{\partial w}{\partial x},$$

$$-\frac{\partial p}{\partial x}=\rho\left(\frac{\partial w}{\partial t}+2aw\right) \tag{13.42}$$

belong to hyperbolic type. Subsequently, discussing the fluid flow, as follows from Eqs. (13.28) and (13.34), p is normalized pressure $\overline{p}=p+\rho g z_1$. When discussing the gas flow, according to Eq. (13.40), p is considered as $\ln p$, and ρ as $\rho-\frac{1}{ZRT}=\text{const}$.

The method of characteristics is highly convenient for the numerical integration of the nonlinear system Eq. (13.41). Using standard methodology, it is shown that the equations of characteristics and the correlations in them have the following format:

$$x-ct=\text{const},\ dp+\rho c\,dw+\rho\frac{\lambda|\rho w|}{8\delta}w\,dx=0,$$

$$x+ct=\text{const},\ dp-\rho c\,dw+\rho\frac{\lambda|\rho w|}{8\delta}w\,dx=0. \tag{13.43}$$

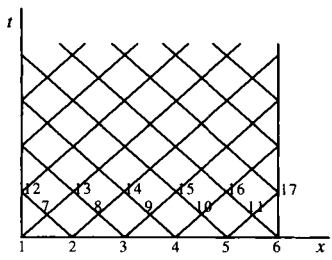

Fig. 13.3

In this case, equations of characteristics do not depend on the solution. It means that their grid can be constructed before beginning to solve them, which significantly simplify the numerical integration procedure. The characteristic described by equation $x-ct$ = const is is called direct, and by equation $x+ct$ = const is called inverse. Replacing the dirrerentials in in the differential functions Eq. (13.43) by finite differences, the system of equations for the

approximation of p and w values at point 7 are obtained (Fig. 13.3) denoted by p_7, w_7. The System has the following format:

$$p_7 - p_1 + \rho c d(w_7 - w_1) + \rho \frac{\lambda_1 |w_1|}{8\delta} w_1 (x_7 - x_1) = 0,$$

$$p_7 - p_2 + \rho c d(w_7 - w_2) + \rho \frac{\lambda_2 |w_2|}{8\delta} w_2 (x_7 - x_2) = 0, \tag{13.44}$$

where p_1, p_2, w_1, w_2, λ_1, λ_2 are p, w, λ values, at the points 1 and 2, respectively. In order to find these values, it is necessary to assign the initial conditions:

$$w(x,0) = f_1(x),\ p(x,0) = f_2(x),\ 0 \le x \le l,$$

where l is tube's length. The p and w values at the points 8, 9, 10 and 11 are calculated similarly. The p_7, w_7 values derived using Eq. (13.44) are the first approximation of the p and w functions at the point 7. To increase accuracy, conventional iteration techniques can be employed. Another way of increasing accuracy is decreasing the size of the characteristic grid cell. Thus, it is only one relationship to consider from Eq. (13.44):

$$p_{12} - p_7 + \rho c(w_{12} - w_7) + \rho \frac{\lambda_7 |w_7|}{8\delta} w_7 (x_{12} - x_7) = 0,$$

which includes two unknown variables, p_{12} and w_{12}. To produce the second equation, it is necessary to assign the boundary conditions at $x = 0$, i. e., one of the functions of the kind:

$$w = w(t),\ p = p(t),\ f(p,w) = 0 \text{ at } x = 0,\ t > 0. \tag{13.45}$$

The solution at the boundary point 17 is derived similarly. For this, it is necessary to write the finite-difference relationship for the characteristic and assign the boundary condition of Eq. (13.45) type but at $x = l$. Clearly, the characteristics technique can be used also for the numerical integration of the linearized system of Eq. (13.42).

5. Integrating linearized equations of non-stationary flow using Laplace transform

The Laplace representations of a function of two variables $u(x,t)$ and its partial derivatives are, respectively:

$$U(x,s) = \int_0^\infty u(x,t) e^{-st} dt,\ \frac{dU}{dx} \int_0^\infty \frac{\partial u(x,t)}{\partial x} e^{-st} dt,$$

$$sU(x,s) - u(x,0) = \int_0^\infty \frac{\partial u(x,t)}{\partial t} e^{-st} dt, \tag{13.46}$$

where $u(x,0)$ is the initial condition for function $u(x,t)$, s is a complex parameter, and $\mathrm{Re}(s) > 0$. It is assumed that the integrals in Eq. (13.46) do exist, the integration and differentiation operations with respect to the coordinate are commutative and:

$$\lim_{t\to\infty} u(x,t)e^{-st}dt = 0, \quad \lim_{t\to\infty} \frac{\partial u(x,t)}{\partial t}e^{-st} = 0, \quad \lim_{t\to\infty} \frac{\partial u(x,t)}{\partial x}e^{-st} = 0.$$

The transition from the representation to the original format is performed using the conversion equation:

$$u(x,t) = \frac{1}{2\pi i}\int_{\gamma-i\infty}^{\gamma+i\infty} e^{st}U(x,s)ds, \tag{13.47}$$

and the straight line $\gamma - i\infty$, $\gamma + i\infty$ is drawn in such a way that all singularities of the representation $U(x,s)$ are to the left of it.

Let's now review the application of Laplace integral conversion to the solution of a system of linearized Eq. (13.42).

One preliminary note.

Suppose at $t \le 0$ the flow is stationary. Then following Eq. (13.42):

$$w_0 = w(x,0) = \text{const}, \; p_0 = p(x,0) = p(0,0) - 2a\rho w_0 x,$$

where w_0, p_0 are velocity and pressure at stationary flow.

Let's assume that:

$$w(x,t) = w_0 + w^*(x,t), \; p(x,t) = p_0 + p^*(x,t),$$

where w^*, p^* are disturbances of velocity and pressure (their deviations off the stationary values). It is easy to see that w^*, p^* satisfy Eq. (13.42). Any non-stationary motion can be considered as if it emerged from the stationary motion so the initial conditions for the disturbances are:

$$t \le 0, \quad w^*(x,0) = 0, \quad p^*(x,0) = 0, \quad (0 \le x \le l). \tag{13.48}$$

So in the future, Eq. (13.42) is considered at initial conditions Eq. (13.48) and, dropping the superscript *, $w(x,t)$, $p(x,t)$ represent the velocity and pressure *disturbances*. It is obvious that the boundary conditions also must be formulated for the disturbances.

Applying the Laplace conversion with respect to variable t to Eq. (13.42), and using Eq. (13.46) and the initial conditions [Eq. (13.48)], results in:

$$\begin{aligned} \frac{dV(x,s)}{dx} + \frac{s}{\rho c^2}\mathrm{P}(x,s) &= 0, \\ \frac{d\mathrm{P}(x,s)}{dx} + \rho(s+2a)V(x,s) &= 0, \end{aligned} \tag{13.49}$$

where:

$$\mathrm{P}(x,s)=\int_0^\infty p(x,t)e^{-st}dt,\ V(x,s)=\int_0^\infty w(x,t)e^{-st}dt,$$

are the Laplace representations of pressure $p(x,t)$ and velocity $w(x,t)$. A general solution of the system of conventional differential Eq. (13.49) has the following format:

$$\mathrm{P}(x,s)=Ae^{\lambda x}+Be^{-\lambda x},\ V(x,s)=-\frac{1}{Z(s)}(Ae^{\lambda x}-Be^{-\lambda x}), \qquad (13.50)$$

where:

$$\lambda=\frac{s}{c}\sqrt{1+\frac{2a}{s}},\ Z(s)=\rho c\sqrt{1+\frac{2a}{s}}. \qquad (13.51)$$

Assuming in Eq. (13.50) sequentially $x = 0$ and $x = l$:

$$\mathrm{P}(0,s)=A+B,\ V(0,s)=-\frac{1}{Z(s)}(A-B),$$

$$\mathrm{P}(l,s)=Ae^{\lambda l}+Be^{-\lambda l},\ V(l,s)=-\frac{1}{Z(s)}(Ae^{\lambda l}-Be^{-\lambda l}). \qquad (13.52)$$

Canceling the integration constants A and B from Eq. (13.52):

$$\mathrm{P}(0,s)\mathrm{ch}\lambda l-\mathrm{P}(l,s)-V(0,s)Z(s)\mathrm{sh}\lambda l=0$$

$$\mathrm{P}(0,s)\frac{\mathrm{sh}\lambda l}{Z(s)}+V(0,s)Z(s)\mathrm{ch}\lambda l-V(l,s)=0. \qquad (13.53)$$

Two equations in Eq. (13.53) are equations of hydraulic quadruple, connecting the pressure and velocity representations at the ends of the pipeline. To emphasize, the format of Eq. (13.53) does not depend on the boundary conditions of the problem under consideration.

In order to obtain the solutions of Eq. (13.42) as representations, it is necessary to determine the constants A and B at arbitrary boundary conditions. Eq. (13.52) shows that it is necessary to know any pair of the values $\mathrm{P}(0,s)$, $V(0,s)$, $\mathrm{P}(l,s)$, $V(l,s)$. Following Eq. (13.53) it is sufficient to have two more independent interrelations for these values. They can be obtained from additional conditions linking the numeric values of pressure, velocity and their derivatives at the end of the pipeline.

Subsequently, only the linear additional conditions are considered. According to Eq. (13.42), derivatives with respect to a coordinate can be expressed through

velocity and derivatives with respect to time. Thus, any linear additional conditions for these equations can be reduced to the following format:

$$\alpha_{11}p(0,t)+\alpha_{12}\frac{\partial p(0,t)}{\partial t}+\alpha_{13}w(0,t)+\alpha_{14}\frac{\partial w(0,t)}{\partial t}+$$
$$+\beta_{11}p(l,t)+\beta_{12}\frac{\partial p(l,t)}{\partial t}+\beta_{13}w(l,t)+\beta_{14}\frac{\partial w(l,t)}{\partial t}=\varphi(t),$$
$$\alpha_{21}p(0,t)+\alpha_{22}\frac{\partial p(0,t)}{\partial t}+\alpha_{23}w(0,t)+\alpha_{24}\frac{\partial w(0,t)}{\partial t}+ \tag{13.54}$$
$$+\beta_{21}p(l,t)+\beta_{22}\frac{\partial p(l,t)}{\partial t}+\beta_{23}w(l,t)+\beta_{24}\frac{\partial w(l,t)}{\partial t}=\psi(t),$$

where α_{ij}, β_{ij}, φ, ψ are known functions of time.

Assuming in Eq. (13.54):

$$\alpha_{2j}=\beta_{1j}=0,\quad j=1,2,3,4,$$

a general rerepresentation of the linear edge problem is obtained. Assuming:

$$\beta_{1j}=\beta_{2j}=0 \text{ or } ,\ \alpha_{1j}=\alpha_{2j}=0,\quad j=1,2,3,4,$$

a general representation of the linear Cauchy problem at $x = 0$ or $x = l$, respectively, is obtained.

Now, the only stationary additional conditions are considered, i. e., factors α_{ij}, β_{ij} are assumed to be constants. Applying the Laplace transform with respect to time and imposing the initial conditions [Eq. (13.48)] to the Eq. (13.54):

$$\alpha_1\mathrm{P}(0,s)+\beta_1\mathrm{P}(l,s)+\alpha_2V(0,s)+\beta_2V(l,s)=\Phi(s),$$
$$\alpha_3\mathrm{P}(0,s)+\beta_3\mathrm{P}(l,s)+\alpha_4V(0,s)+\beta_4V(l,s)=\Psi(s), \tag{13.55}$$

where:

$$\alpha_1=\alpha_{11}+\alpha_{12}s,\quad \beta_1=\beta_{11}+\beta_{12}s,$$
$$\alpha_2=\alpha_{13}+\alpha_{14}s,\quad \beta_2=\beta_{13}+\beta_{14}s,$$

$$\alpha_3=\alpha_{21}+\alpha_{22}s,\quad \beta_3=\beta_{12}+\beta_{22}s, \tag{13.56}$$
$$\alpha_4=\alpha_{23}+\alpha_{24}s,\quad \beta_4=\beta_{23}+\beta_{24}s,$$
$$\Phi(s)=\int_0^\infty\varphi(t)e^{-st}dt,\quad \Psi(s)=\int_0^\infty\psi(t)e^{-st}dt.$$

Eqs. (13.53) and (13.56) form a closed system of four linear algebraic equations, from which:

$$\mathrm{P}(0,s)=\frac{\Delta_1(s)}{\Delta(s)},\quad V(0,s)=\frac{\Delta_3(s)}{\Delta(s)}, \tag{13.57}$$

where :

$$\Delta(s)=\begin{vmatrix} \operatorname{ch}\lambda l & -1 & Z(s)\operatorname{sh}\lambda l & 0 \\ \dfrac{\operatorname{sh}\lambda l}{Z(s)} & 0 & \operatorname{ch}\lambda l & -1 \\ \alpha_1 & \beta_1 & \alpha_2 & \beta_2 \\ \alpha_3 & \beta_3 & \alpha_4 & \beta_4 \end{vmatrix},$$

$$\Delta_1(s)=\begin{vmatrix} 0 & -1 & Z(s)\operatorname{sh}\lambda l & 0 \\ 0 & 0 & \operatorname{ch}\lambda l & -1 \\ \Phi(s) & \beta_1 & \alpha_2 & \beta_2 \\ \Psi(s) & \beta_3 & \alpha_4 & \beta_4 \end{vmatrix}, \qquad (13.58)$$

$$\Delta_3(s)=\begin{vmatrix} \operatorname{ch}\lambda l & -1 & 0 & 0 \\ \dfrac{\operatorname{sh}\lambda l}{Z(s)} & 0 & 0 & -1 \\ \alpha_1 & \beta_1 & \Phi(s) & \beta_2 \\ \alpha_3 & \beta_3 & \Psi(s) & \beta_4 \end{vmatrix}.$$

From the first equation of Eq. (13.52) and considering Eq. (13.57):

$$A=\frac{\Delta_1(s)-Z(s)\Delta_3(s)}{2\Delta(s)},\quad B=\frac{\Delta_1(s)-Z(s)\Delta_3(s)}{2\Delta(s)}. \qquad (13.59)$$

Substituting Eq. (13.59) into Eq. (13.50), results in:

$$\mathrm{P}(x,s)=\frac{\Delta_1(s)}{\Delta(s)}\operatorname{ch}\lambda s-\frac{\Delta_3(s)}{\Delta(s)}Z(s)\operatorname{sh}\lambda x,$$

$$V(x,s)=\frac{\Delta_1(s)}{\Delta(s)}\frac{\operatorname{sh}\lambda x}{Z(s)}+\frac{\Delta_3(s)}{\Delta(s)}\operatorname{ch}\lambda x. \qquad (13.60)$$

Back transform Eq. (13.60) from Laplace domain to time domain, $\mathrm{P}(x,s)$, $V(x,s)$ to $p(x,t)$, $w(x,t)$, the solution of Eq. (13.42) with initial condition [Eq. (13.48)] and additional conditions [Eq. (13.54)] is obtained. This change can be performed either with correspondence table or with the conversion Eq. (13.47).

The presentation, after Laplace, of function $f(t)$, i. e., $L[f(t)]$ and its representation after Laplace-Carson are connected through the following equation:

$$K[f(t)]=sL[f(t)].$$

This equation enables the determination of $[f(t)]$, if its representation $L[f(t)]$ is known, using the conversion tables for the Laplace conversion.

Let's review some examples using to Eq. (13.47).

6. Examples of computing non-stationary flow in pipelines

Computing non-stationary flow in pipelines, in particular, computing the hydraulic shocks is often reduced to solving the problems where pressure and velocity as a function of time are assigned at the end of the tube. The following cases are considered:

$$\begin{aligned} &A.\ t \geq 0,\ p(0,t) = \varphi_1(t),\ w(l,t) = \psi_2(t), \\ &B.\ t \geq 0,\ p(0,t) = \varphi_1(t),\ p(l,t) = \varphi_2(t), \\ &C.\ t \geq 0,\ w(0,t) = \psi_1(t),\ w(l,t) = \psi_2(t), \\ &D.\ t \geq 0,\ w(0,t) = \psi_1(t),\ p(l,t) = \varphi_2(t). \end{aligned} \tag{13.61}$$

The initial conditions in all cases are assumed to be zero, i. e., determined from Eq. (13.48).

Clearly, case D is reduced to case A by replacing $y = l - x$, $\varphi_2(t) = \varphi_1(t)$, $\psi_1(t) = -\psi_2(t)$. It is assumed that the boundary functions $\varphi_i(t)$, $\psi_i(t)$ can have disruptions at $t = +0$. From Eqs. (13.54), (13.56) and (13.51):

$$\begin{aligned} &\text{in case } A,\ \alpha_1 = 1, \beta_4 = 1, \\ &\text{in case } B,\ \alpha_1 = 1, \beta_3 = 1, \\ &\text{in case } C,\ \alpha_2 = 1, \beta_4 = 1. \end{aligned}$$

The remaining α_i, β_i in all three cases are equal to zero.

Upon having these relationships calculated, the determinant Eq. (13.58) is obtained from Eq. (13.60):

Case A

$$\begin{aligned} P(x,s) &= [s\Phi_1(s) - \varphi_1(+0) + \varphi_1(+0)]F_1(l-x,s) - \\ &\quad -\rho c^2[s\Psi_2(s) - \psi_2(+0) + \psi_2(+0)]F_1(x,s) \\ V(x,s) &= \frac{1}{\rho c^2}[s\Phi_1(s) - \varphi_1(+0) + \varphi_1(+0)]F_3(l-x,s) + \\ &\quad +[s\Psi_2(s) - \psi_2(+0) + \psi_2(+0)]F_1(x,s) \end{aligned}, \tag{13.62}$$

Case B

$$\begin{aligned} P(x,s) &= [s\Phi_1(s) - \varphi_1(+0) + \varphi_1(+0)]F_4(l-x,s) - \\ &\quad -[s\Phi_2(s) - \varphi_2(+0) + \varphi_2(+0)]F_4(x,s) \\ V(x,s) &= \frac{1}{\rho c^2}[s\Phi_1(s) - \varphi_1(+0) + \varphi_1(+0)]F_5(l-x,s) - \\ &\quad -\frac{1}{\rho c^2}[s\Phi_2(s) - \varphi_2(+0) + \varphi_2(+0)]F_5(x,s) \end{aligned}; \tag{13.63}$$

Case C

$$\begin{aligned} P(x,s) &= \rho c^2[s\Psi_1(s) - \psi_1(+0) + \psi_1(+0)]F_6(l-x,s) - \\ &\quad -\rho c^2[s\Psi_2(s) - \psi_2(+0) + \psi_2(+0)]F_6(x,s) \end{aligned}, \tag{13.64}$$

$$V(x,s) = [s\Psi_1(s) - \psi_1(+0) + \psi_1(+0)]F_4(l-x,s) + [s\Psi_2(s) - \psi_2(+0) + \psi_2(+0)]F_4(x,s),$$

where:

$$\Phi_i(s)=\int_0^\infty \varphi_i(t)e^{-st}dt,\quad \Psi_i(s)=\int_0^\infty \psi_i(t)e^{-st}dt,\quad i=1,2,$$

$$F_1(y,s)=\frac{\operatorname{ch}\lambda y}{s\operatorname{ch}\lambda l},\quad F_2(y,s)=\frac{\lambda\operatorname{sh}\lambda y}{s^2\operatorname{ch}\lambda l},\quad F_3(y,s)=\frac{\operatorname{sh}\lambda y}{\lambda\operatorname{ch}\lambda l},$$
$$F_4(y,s)=\frac{\operatorname{sh}\lambda y}{s\operatorname{sh}\lambda l},\quad F_5(y,s)=\frac{\operatorname{ch}\lambda y}{\lambda\operatorname{sh}\lambda l},\quad F_6(y,s)=\frac{\lambda\operatorname{ch}\lambda y}{s^2\operatorname{ch}\lambda l}. \tag{13.65}$$

While deriving Eq. (13.65), the following expression [from Eq. (13.51)] is used:

$$Z(s)=\frac{\rho c^2}{s}\lambda,$$

As the expression $s\Phi(s)-\varphi(+0)$ is a representation of function $\frac{\partial\varphi}{\partial t}$, then according to the convolution theorem and Eqs. (13.62), (13.63) and (13.64):

Case *A*

$$p(x,t)=\int_0^t[\varphi'_1(\theta)N_1(l-x,t-\theta)-\rho c^2\psi'_2(\theta)N_2(x,t-\theta)]d\theta+$$
$$+\varphi_1(+0)N_1(l-x,t)-\rho c^2\psi_2(+0)N_2(x,t),$$

$$w(x,t)=\int_0^t[\frac{1}{\rho c^2}\varphi'_1(\theta)N_3(l-x,t-\theta)-\psi'_2(\theta)N_1(x,t-\theta)]d\theta+ \tag{13.66}$$
$$+\frac{1}{\rho c^2}\varphi_1(+0)N_3(l-x,t)-\psi_2(+0)N_1(x,t);$$

Case *B*

$$p(x,t)=\int_0^t[\varphi'_1(\theta)N_4(l-x,t-\theta)+\varphi'_2(\theta)N_4(x,t-\theta)]d\theta+$$
$$+\varphi_1(+0)N_4(l-x,t)+\varphi_2(+0)N_4(x,t),$$

$$w(x,t)=\frac{1}{\rho c^2}\int_0^t[\varphi'_1(\theta)N_5(l-x,t-\theta)-\varphi'_2(\theta)N_5(x,t-\theta)]d\theta+ \tag{13.67}$$
$$+\frac{1}{\rho c^2}[\varphi_1(+0)N_5(l-x,t)-\varphi_2(+0)N_5(x,t)];$$

Case *C*

$$p(x,t) = \rho c^2 \int_0^t [\psi'_1(\theta) N_6(l-x,t-\theta) + \psi'_2(\theta) N_6(x,t-\theta)] d\theta + \\ + \rho c^2 [\psi_1(+0) N_6(l-x,t) + \psi_2(+0) N_6(x,t),$$

$$w(x,t) = \int_0^t [\psi'_1(\theta) N_4(l-x,t-\theta) + \psi'_2(\theta) N_4(x,t-\theta)] d\theta + \\ + \psi_1(+0) N_4(l-x,t) - \psi_2(+0) N_4(x,t)], \tag{13.68}$$

where, according to Eq. (13.47):

$$N_i(y,t) = \frac{1}{2\pi i} \int_{\gamma-i\infty}^{\gamma+i\infty} F_i(y,s) e^{st} ds, \quad i = 1,2,...,6. \tag{13.69}$$

Functions F_1, F_2, F_3 have simple poles s_n corresponding to roots of equation:

$$\text{ch } \gamma l = \cos i\gamma l = 0, \tag{13.70}$$

and functions F_4, F_5, F_6 have simple poles s_m corresponding to roots of equation:

$$\text{sh } \gamma l = -i \sin i\gamma l = 0. \tag{13.71}$$

Besides, functions F_1, F_2, F_4 have simple pole $s_0 = 0$, function F_5 — simple poles $s_0 = 0$ and $s_0^{(1)} = -2a$, and function F_6 — pole $s_0 = 0$ of the second order.

From Eqs. (13.70), (13.71) and (13.51) follows that simple poles s_n and s_m are determined from:

$$s_n = -a \pm i\nu_n, \; s_m = -a \pm i\gamma_n, \; m = 1, 2, 3, \ldots,$$

$$\nu_n = \sqrt{\left(\frac{n-1}{2}\frac{\pi c}{l}\right)^2 - a^2}, \; \gamma_m = \sqrt{\left(\frac{m\pi c}{l}\right)^2 - a^2}, \tag{13.72}$$

i. e., two poles correspond to each m and each n.

All roots s_n and s_m correspond to the conditions Re $s_n < 0$, Re $s_m < 0$; therefore, in Eq. (13.69) it is possible to assume $\gamma = 0$.

To close the integrating contour in Eq. (13.69), let's consider, when computing functions N_1, N_2, N_3, the arc sequence of radius:

$$R_n = \frac{\pi c}{l} n,$$

and when computing N_4, N_5, N_6, of radius:

$$R_m = \frac{\pi c}{l} \frac{2m-1}{2}$$

with the centers at the origin and located left of the imaginary axis of plane s. Eq. (13.72) indicates that not a single pole s_n lies on arcs of radius R_n, and not a single pole s_m lies on arcs of radius R_m. It is shown that on the arc of radius R_n at $n \to \infty$ the value:

$$A = \left| \frac{\operatorname{ch} \lambda x}{\operatorname{ch} \lambda l} \right|$$

is limited. On the arc of radius R_n:

$$s = R_n e^{i\theta}, \quad \frac{\pi}{2} \le \theta \le \frac{3\pi}{2}.$$

Then, according to Eq. (13.51), the value of λ_n on this arc will be:

$$\lambda_n = \alpha_n + \beta_n = \frac{R_n}{c} \sqrt{e^{i\theta} \left(e^{i\theta} + \frac{2a}{R_n} \right)},$$

where from, after simple transformations:

$$\alpha_n^2 = \frac{R_n^2}{2c^2} \left(\sqrt{1 + 4\frac{a^2}{R_n^2} + 4\frac{a}{R_n}\cos\theta} + 2\cos^2 - 1 + 2\frac{a}{R_n}\cos\theta \right),$$

$$\beta_n^2 = \frac{R_n^2}{2c^2} \left(\sqrt{1 + 4\frac{a^2}{R_n^2} + 4\frac{a}{R_n}\cos\theta} - 2\cos^2 + 1 - 2\frac{a}{R_n}\cos\theta \right). \tag{13.73}$$

The first sub-equation in Eq. (13.73) shows that at $n \to \infty$ (and, therefore, $R_n \to \infty$) $-\infty < \alpha_n < +\infty$.

As:

$$\left| \frac{\operatorname{ch} \lambda_n x}{\operatorname{ch} \lambda_n l} \right| = \left| \frac{e^{-\lambda_n (l-x)} + e^{-\lambda_n (l+x)}}{1 + e^{-2\lambda_n l}} \right| = \left| \frac{e^{\lambda_n (l+x)} + e^{\lambda_n (l-x)}}{1 + e^{2\lambda_n l}} \right| = \sqrt{\frac{\operatorname{sh}^2 \alpha_n x + \cos^2 \beta_n x}{\operatorname{sh}^2 \alpha_n l + \cos^2 \beta_n l}} = A,$$

then at $x < 1$, Re $\lambda_n = \alpha_n \to \pm\infty$ $A \to 0$. When α_n is finite, A is a finite value. As Eq. (13.73) shows, the condition $\alpha_n = 0$ is only realized when $\cos\theta = -\frac{a}{R_n}$. Thus, $\beta_n = \pm\frac{R_n}{c}$ and $\cos^2 \beta_n l = \cos^2 \pi n = 1$, i. e., in this case A has a finite value. Similarly, it can be shown that on arcs of radius R_n with $n \to \infty$ the value:

$$\left| \frac{\operatorname{ch} \lambda x}{\operatorname{ch} \lambda l} \right|,$$

and on arcs of radius R_m with $m \to \infty$, the values:

$$\left|\frac{\operatorname{sh}\lambda x}{\operatorname{sh}\lambda l}\right|, \left|\frac{\operatorname{ch}\lambda x}{\operatorname{sh}\lambda l}\right|$$

are limited. Following the proven (as Eq. (13.65) shows) that with $R_n \to \infty$ values F_1, F_2, F_3 uniformly tend to zero, and with $R_m \to \infty$, values F_4, F_5, F_6 monotonously tend to zero. Now, according to Jordan's lemma, for $t > 0$ the integral Eq. (13.69), based on Cauchy's integral theorem, can be written as follows:

$$N_i(y,t) = \frac{1}{2\pi i}\oint_{\Gamma_k} F_j(y,s)e^{st}ds = \sum_0^\infty \operatorname{Re} s\left[F_j(y,s)e^{st}\right]_{s=s_n},$$

where Γ_k ($k = n, m$) is a closed contour formed by the arc of the radius R_k and by the imaginary axis of the complex plane s. Applying a standard procedure of finding residue, and after corresponding transformations:

$$N_1(y,t) = 1 + \frac{4}{\pi} i^{-at} \sum_1^\infty \frac{(-1)^n}{2n-1}\left(\operatorname{ch} iv_n t + \frac{a}{iv_n}\operatorname{sh} iv_n t\right)\cos\frac{2n-1}{2}\frac{\pi y}{l},$$

$$N_2(y,t) = \frac{2ay}{c^2} + \frac{8l}{\pi^2 c^2}e^{-at}\sum_1^\infty \frac{(-1)^n}{(2n-1)^2}\left(\frac{a^2 - v_n^2}{iv_n}\operatorname{sh} iv_n t + 2a\operatorname{ch} iv_n t\right)\sin\frac{2n-1}{2}\frac{\pi y}{l},$$

$$N_3(y,t) = -2\frac{c^2}{l}e^{-at}\sum_1^\infty \frac{(-1)^n}{iv_n}\operatorname{sh} iv_n t \sin\frac{2n-1}{2}\frac{\pi y}{l}, \qquad (13.74)$$

$$N_4(y,t) = \frac{y}{l} + \frac{2}{\pi}e^{-at}\sum_1^\infty \frac{(-1)^m}{m}\left(\operatorname{ch} i\gamma_m t + \frac{a}{i\gamma_m}\operatorname{sh} i\gamma_m t\right)\sin m\pi\frac{y}{l},$$

$$N_5(y,t) = \frac{c^2}{2al}(1 - e^{-2at}) + \frac{2c^2}{l}e^{-at}\sum_1^\infty \frac{(-1)^m}{i\gamma_m}\operatorname{sh} i\gamma_m t \cos m\pi\frac{y}{l},$$

$$N_6(y,t) = \frac{t}{l} - \frac{al}{3c^2} + \frac{iy^2}{c^2 l} - \frac{2l}{\pi^2 c^2}\sum_1^\infty \frac{(-1)^m}{m^2}\left(\frac{a^2 - \gamma_m^2}{i\gamma_m}\operatorname{sh} i\gamma_m t + 2a\operatorname{ch} i\gamma_m t\right)\cos m\pi\frac{y}{l}.$$

Eqs. (13.66)–(13.68) and (13.74) provide a solution of problems of Eq. (13. 61) It is important that when the pipeline is long, for small n values:

$$\frac{2n-1}{2}\frac{\pi c}{l} < a.$$

In such a case, the value v_n will be imaginary, and:

$$iv_n = -v_n^* = \sqrt{a^2 - \left(\frac{2n-1}{2}\frac{\pi c}{l}\right)^2}, \quad \operatorname{sh} iv_n t = -\operatorname{sh} v_n^* t, \quad \operatorname{ch} iv_n t = \operatorname{ch} v_n^* t.$$

when:

$$\frac{2n-1}{2}\frac{\pi c}{l} > a,$$

ν_n is a real value, and:

$$\mathrm{sh}\, i\nu_n t = i \sin \nu_n t, \quad \mathrm{ch}\, i\nu_n t = \cos \nu_n t.$$

Similar observations are valid for the cases:

$$\frac{m\pi c}{l} < a \quad \text{and} \quad \frac{m\pi c}{l} > a.$$

7. Hydraulic shock

A drastic velocity change in a pipeline (such as shutting the valve) is followed by the corresponding change in pressure. This is called hydraulic shock. This phenomenon in an ideal fluid was first studied in detail by Zhukovsky (1898).

In this section, the application of the equations derived in par. 6 to a classical problem of the hydraulic shock is reviewed. At $x = 0$, there is a high-capacity reservoir where pressure is considered to be constant. At $x = l$, the velocity change under a specified rule is occurring. At the instantaneous flow stoppage, the boundary conditions for disturbances have the following format:

$$t \geq 0,\ p(0,t) = \varphi_1(t) = 0,\ w(l,t) = \psi_2(t) = -w_0,$$

where w_0 is the velocity of the stationary flow.

Using the boundary conditions with Eq. (13.65), results in:

$$p(x,t) = \rho c^2 w_0 N_2(x,t),$$
$$w(x,t) = -w_0 N_1(x,t). \tag{13.75}$$

Following Eqs. (13.74) and (13.75), the solution of the problem under consideration has the appearance of slowly converging series. When $a = 0$ (ideal fluid):

$$\nu_n = \frac{2n-1}{2}\frac{\pi c}{l}, \quad \mathrm{sh}\, i\nu_n t = i \sin \nu_n t,$$

and at $x = l$, according to Eq. (13.74),

$$N_2(y,t) = \frac{4}{\pi c}\sum_{1}^{\infty}\frac{1}{2n-1}\sin\frac{2n-1}{2}\frac{\pi c}{l}t = \frac{1}{c}, \quad 0 < t < \frac{2l}{c}, \tag{13.76}$$

and from this:

$$p(l,t) = \rho c w_0, \quad 0 < t < \frac{2l}{c}. \tag{13.77}$$

Eq. (13.77) is the classical Zhukovsky equation for hydraulic shock in the ideal fluid. A correlation curve $\Pi = \frac{p(l,t)}{\rho c w_0}$ *vs.* $\tau = \frac{ct}{l}$ (i. e., in dimensionless coordinates) is presented in Fig. 13.4. Correlation curves $\Pi = \frac{p(l,t)}{\rho c w_0}$ *vs.* $\tau = \frac{ct}{l}$ at $a = 0.125\frac{c}{l}$, $a = 0.25\frac{c}{l}$, and $a = 0.5\frac{c}{l}$ are presented in Figs. 13.5, 13.6 and 13.7.

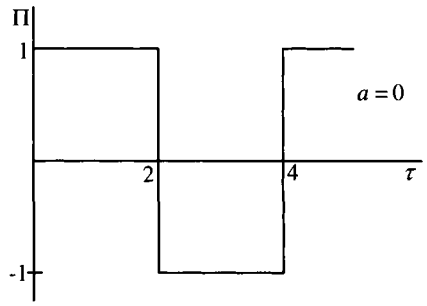

Fig. 13.4

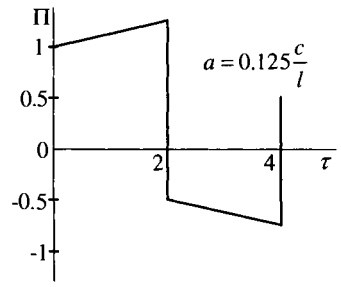

Fig. 13.5

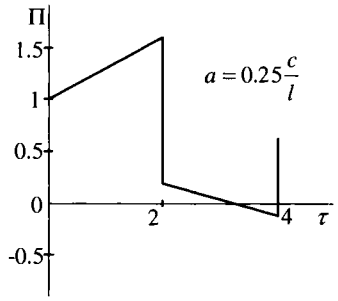

Fig. 13.6

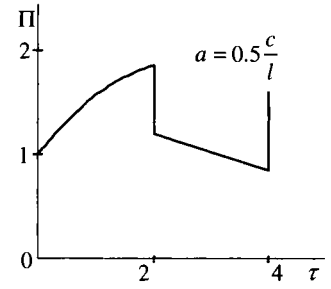

Fig. 13.7

Note that the $\frac{2a\rho c w_0 l}{\rho c w_0 c}$ value is the ratio of the pressure loss along the length l to the shock pressure (after Zhukovsky). The graphs indicate that when friction is present, pressure in cross-section $x = l$ continues to increase till the time $t = \frac{2l}{c}$, i. e., to the arrival of the wave reflected from the cross-section $x = 0$. That was established by Charny. At $a \geq c/l$, wave phenomena disappear for all practical purposes.

Let's now review hydraulic shock with the boundary conditions:

$$t \geq 0,\ p(0,t) = \varphi_1(t) = 0,\ w(l,t) = \begin{cases} \dfrac{-w_0 t}{T}, & 0 \leq t \leq T, \\ -w_0, & t \geq T, \end{cases} \tag{13.78}$$

where T is time of the flow slow-down.

From Eqs. (13.66) and (13.78), at $0 \leq t \leq T$:

$$p(l,t) = \frac{\rho c^2 w_0}{T} \int_0^t N_2(l, t-\theta)\, d\theta = \frac{\rho c^2 w_0}{T} \int_0^t N_2(l,\theta)\, d\theta,$$

at $t > T$:

$$p(l,t) = \frac{\rho c^2 w_0}{T} \int_0^T N_2(l, t-\theta)\, d\theta = \frac{\rho c^2 w_0}{T} \int_{t-T}^t N_2(l,\theta)\, d\theta.$$

For the simplicity, it is assumed $a = 0$. Then, by considering Eq. (13.76):

$$p(l,t) = -\frac{8\rho w_0 l}{\pi^2 T} \sum_{n=1}^{\infty} \frac{1}{(2n-1)^2} \cos\frac{2n-1}{2}\frac{\pi c}{l} t \Big|_{t_1}^{t}, \tag{13.79}$$

where at $t \leq T$ $t_1 = 0$, and at $t \geq T$ $t_1 = t - T$.

The sum of the series Eq. (13.79) is known and is equal to:

$$\sum_{n=1}^{\infty} \frac{1}{(2n-1)^2} \cos\frac{2n-1}{2} t = \frac{\pi}{4}\left(\frac{\pi}{2} - \left|\frac{\pi c t}{2l}\right|\right), \quad -\pi \leq \frac{\pi c t}{2l} \leq \pi. \tag{13.80}$$

Considering periodicity, Eq. (13.80) can be presented in a more convenient format:

$$\sum_{n=1}^{\infty} \frac{1}{(2n-1)^2} \cos\frac{2n-1}{2}\frac{\pi}{l} t = \frac{\pi^2}{8} F(t),$$

where:

$$F(t) = \begin{cases} 1 - \dfrac{ct}{l} + 4k, & 4k \leq \dfrac{ct}{l} \leq 4k+2, \\ & k = 1, 2, 3 \ldots. \\ 1 + \dfrac{ct}{l} - 4k - 4, & 4k+2 \leq \dfrac{ct}{l} \leq 4k+4, \end{cases} \tag{13.81}$$

Then Eq. (13.79) becomes:

$$p(l,t) = -\frac{\rho w_0 l}{T}[F(t) - F(t_1)]. \tag{13.82}$$

To illustrate the application of Eqs. (13.81) and (13.82), the case when $T = l/c$ is considered.

When $t \le T$, $0 \le \frac{ct}{l} \le 1$, $k = 0$, $F(t) = 1 - \frac{ct}{l}$, $F(t_1) = F(0) = 1$ and $p = \rho c w_0 \frac{t}{T}$.

When $t \ge T$, the range of the values $\frac{ct}{l}$ and $\frac{ct_1}{l} = \frac{c}{l}(t - T) = \frac{ct}{l} - 1$ are subdivided into the following segments:

$$1 \le \frac{ct}{l} \le 2,\ k = 0,\ F(t) = 1 - \frac{ct}{l};\ 0 \le \frac{ct_1}{l} \le 1,\ k = 0,\ F(t_1) = 2 - \frac{ct}{l},\ p_c = \rho c w_0;$$

$$2 \le \frac{ct}{l} \le 3,\ k = 0,\ F(t) = 1 + \frac{ct}{l} - 4;\ 1 \le \frac{ct_1}{l} \le 2,\ k = 0,$$

$$F(t_1) = 2 - \frac{ct}{l},\ p = -\rho c w_0 \left(2\frac{ct}{l} - 5\right);$$

$$3 \le \frac{ct}{l} \le 4,\ k = 0,\ F(t) = 1 + \frac{ct}{l} - 4;\ 2 \le \frac{ct_1}{l} \le 3,\ k = 0,$$

$$F(t_1) = -4 + \frac{ct}{l},\ p = -\rho c w_0;$$

$$4 \le \frac{ct}{l} \le 5,\ k = 1,\ F(t) = 5 - \frac{ct}{l};\ 3 \le \frac{ct_1}{l} \le 4,\ k = 0,$$

$$F(t_1) = -4 + \frac{ct}{l},\ p = -\rho c w_0 \left(9 - 2\frac{ct}{l}\right),$$

etc. The correlation $\Pi = \frac{p}{\rho c w_0}$ *vs.* $\tau = (ct)/l$ is shown in Fig. 13.8. Correlations Π *vs.* τ at $T = \frac{2l}{c}$ and $T = \frac{3l}{c}$ are displayed in Figs. 13.9 and 13.10, respectively.

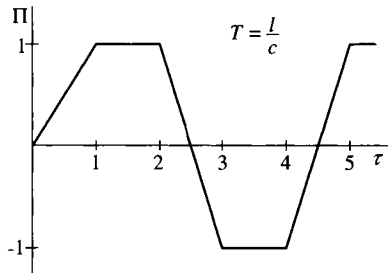

Fig. 13.8

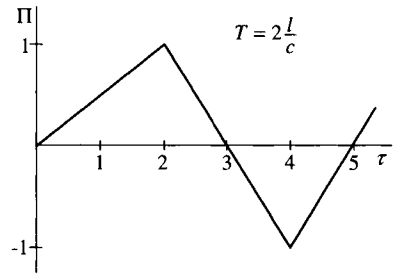

Fig. 13.9

Of a particular interest is the case of $T = \frac{4l}{c}$. When $0 \le \frac{ct}{l} \le 2$, $F(t) = 1 - \frac{ct}{l}$, $F(t_1) = F(0) = 1$, $p = \rho c w_0 \frac{t}{T}$. When $2 \le \frac{ct}{l} \le 4$, $F(t) = 1 + \frac{ct}{l} - 4$, $F(t_1) = F(0) = -1$, $p = \frac{\rho c w_0}{4}\left(4 - \frac{ct}{l}\right)$. When $t > T$, $t_1 = \frac{ct}{l} - 4$, on segment $4 \le \frac{ct}{l} \le 6$, $k = 1$, $F(t_1) = 5 - \frac{ct}{l}$; on segment $0 \le \frac{ct_1}{l} \le 2$, $k = 0$ and $F(t) = 5 - \frac{ct}{l}$, from where it follows that $p(l,t) = 0$.

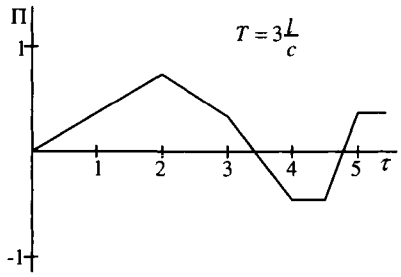

Fig. 13.10

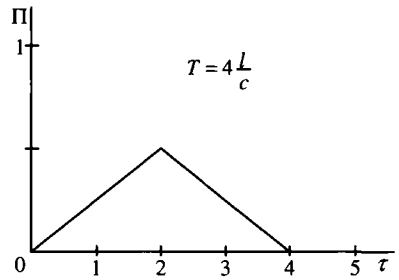

Fig. 13.11

It is easy to see that when $6 \le \frac{ct}{l} \le \infty$, $p(l,t) = 0$. The correlation $\Pi = \frac{p}{\rho c w_0}$ *vs.* $\tau = (ct)/l$ when $T = 4l/c$ is shown in Fig. 13.11. It is possible to show that if $T = 4n\frac{l}{c}$, $p(l,t) = 0$. Note that the $\frac{l}{c}$ value is the travel time of the hydraulic shock wave along the entire length of the pipe l.

8. Effect of flow instability on force of friction

The equations for non-stationary flow in pipes derived in par. 1, e.g., Eq. (13.24), link the average in the cross-section velocity w, density ρ, pressure p and average over the tube's perimeter tangential stress τ_χ. To close this system of equation, the quasi-stationarity hypothesis is usually employed. The computation results are usually in a good agreement with experimental data. In some cases, however, significant discrepancies with theoretical results were observed, for example in cases of steep pressure (velocity) fronts of non-Newtonian fluid flow.

This casts a shadow over the validity of the stationarity hypothesis. Indeed, τ_χ is function of fluid's rheological parameters and local velocity distribution in the

flow cross-section. At the same time, the velocity distribution at non-stationary flow is highly different from that at stationary flow. For a laminar non-stationary flow of an incompressible fluid was theoretically substantiated by Gromeka, Lambossi, etc., and experimentally established by Richardson and Tayler. It is evident that the equations for averaged values do not allow for the estimation of non-stationarity effect on the size of friction force. In order to fine-tune the association between τ_χ and averaged flow parameters, it is necessary to analyze differential equation for local values, i. e., Navier-Stokes equation.

Under the same assumption as for the derivation of Eq. (13.28), i. e., disregarding the fluid's compressibility and the tube elasticity in the motion equation, let's write down Navier-Stokes equation in the following format:

$$\rho\frac{\partial\bar{v}}{\partial t}=\rho\bar{F}-\nabla p+\mu\Delta\bar{v}. \tag{13.83}$$

Let's review axisymmetric flow in a round cylindrical tube under assumption that the only operating mass force is force of gravity. In this case Eq. (13.83), projected on the tube's axis $0x$, has the Eq. (13.29) format:

$$\rho\frac{\partial u}{\partial t}=-\frac{\partial}{\partial x}(\rho g z_1+p)+\frac{\mu}{r}\frac{\partial}{\partial r}\left(r\frac{\partial u}{\partial r}\right),\ u=v_x. \tag{13.84}$$

Assuming $p(x,t) = p_0(x) + p^*(x,t)$, $u(x,r,t) = u_0(x,r) + u^*(x,r,t)$, where u_0, p_0 are stationary values of the velocity and pressure, and u^*_0, p^*_0 are their disturbances, Eq. (13.84) can be reformatted in the following structure:

$$\rho\frac{\partial u^*}{\partial t}=-\frac{\partial p^*}{\partial x}+\frac{\mu}{r}\frac{\partial}{\partial r}\left(r\frac{\partial u^*}{\partial r}\right). \tag{13.85}$$

The initial conditions for the disturbances are:

$$t\le\ ,\ u^*(x,r,0)=0,\ p^*(x,t)=0. \tag{13.86}$$

Subsequently, superscript * is omitted and as a result, p and u are pressure and velocity disturbances.

Applying Laplace's transform with respect to time to Eq. (13.85) and initial conditions [Eq. (13.86)], results in:

$$\frac{\partial^2U(x,r,s)}{\partial r^2}+\frac{1}{r}\frac{\partial U(x,r,s)}{\partial r}-\frac{s}{v}\left[U(x,r,s)+\frac{1}{\rho s}\frac{d\mathrm{P}(x,s)}{dx}\right]=0. \tag{13.87}$$

where:

$$U(x,r,s)=\int_0^\infty u(x,r,t)e^{-st}dt,\ \ \mathrm{P}(x,s)=\int_0^\infty p(x,t)e^{-st}dt,\ \ v=\frac{\mu}{\rho}. \tag{13.88}$$

Let's introduce a function:

$$\Phi(x,r,s) = U(x,r,s) + \frac{1}{\rho s}\frac{d\mathrm{P}(x,s)}{dx}. \tag{13.89}$$

By multiplying Eq. (13.87) by r^2 and substituting the variable:

$$z = \sqrt{\frac{s}{\nu}}r, \tag{13.90}$$

results in:

$$z^2\frac{\partial^2\Phi}{\partial z^2} + z\frac{\partial\Phi}{\partial z} - z^2\Phi = 0. \tag{13.91}$$

Eq. (13.91) is a regular zero-order Bessel equation with solution limited at $r = z = 0$:

$$\Phi(x,z,s) = C(x,s)I_0(z), \tag{13.92}$$

where $I_0(z)$ is Bessel function of the first order imaginary argument.

Substituting Eq. (13.92) into Eq. (13.89) and considering Eq. (13.90):

$$U(x,r,s) = C(x,s)I_0\left(\sqrt{\frac{s}{\nu}}r\right) - \frac{1}{\rho s}\frac{d\mathrm{P}(x,s)}{dx}, \tag{13.93}$$

Function $U(x,r,s)$ must satisfy the condition of fluid's adhesion to the pipe's wall, i. e., at $r = R$:

$$U(x,R,s) = 0,$$

and from here, according to Eq. (13.93):

$$\frac{1}{\rho s}\frac{d\mathrm{P}(x,s)}{dx} = C(x,s)I_0\left(\sqrt{\frac{s}{\nu}}R\right), \tag{13.94}$$

Canceling $C(x,s)$ in Eqs. (13.93) and (13.94), results in:

$$U(x,r,s) = \frac{1}{\rho s}\left[\frac{I_0\left(\sqrt{\frac{s}{\nu}}r\right)}{I_0\left(\sqrt{\frac{s}{\nu}}R\right)} - 1\right]\frac{d\mathrm{P}(x,s)}{dx}. \tag{13.95}$$

Multiply Eq. (13.95) by $\frac{2\pi r dr}{\pi R^2}$ and integrate the result from 0 to R, i. e., averages the solution with respect to the radius. When deriving Eq. (13.96), the known relationships for Bessel functions are used:

$$\int zI_0(z)dz = I_1(z),\ I_2(z) = I_0(z) - \frac{2I_1(z)}{z}.$$

The result is:

$$\frac{d\mathrm{P}(x,s)}{dx} = -\rho s V(x,s)\frac{I_0\left(\sqrt{\frac{s}{\nu}}R\right)}{I_2\left(\sqrt{\frac{s}{\nu}}R\right)} = -\rho s V(x,s)\frac{I_0\left(2\sqrt{\frac{s}{a}}\right)}{I_2\left(2\sqrt{\frac{s}{a}}\right)}, \qquad (13.96)$$

where I_2 is Bessel function of the second order imaginary argument:

$$V(x,s) = \frac{2}{R^2}\int_0^R rU(x,r,s)dr, \quad a = \frac{4\nu}{R^2}. \qquad (13.97)$$

Following Eqs. (13.30), (13.88) and (13.97):

$$V(x,s) = \frac{2}{R^2}\int_0^R r\int_0^\infty U(x,r,t)e^{-st}dt\,dr = \int_0^\infty \frac{2}{R^2}\int_0^R ru(x,r,t)e^{-st}dr\,dt = \int_0^\infty w(x,t)e^{-st}dt,$$

i. e., $V(x,s)$ is a representation after Laplace of average velocity $w(x,t)$.

Applying Laplace transform to the first equation in Eq. (13.41) (i. e., to the continuity equation) and considering the initial conditions of Eq. (13.86), results in:

$$\frac{dV(x,s)}{dx} = -\frac{s}{\rho c^2}\mathrm{P}(x,s). \qquad (13.98)$$

Eqs. (13.96) and (13.98) are written as representations after performing Laplace transformation and they are equations of a laminar non-stationary flow of a viscous slightly compressible fluid in a round cylindrical tube. They are valid for the average in the cross-section values of velocity and pressure at initial conditions [Eq. (13.86)].

The link between the average velocity w and tangential stress τ_χ is now to be determined. By averaging Eq. (13.85) over the tube's cross-section:

$$\rho\frac{\partial v}{\partial t} = -\frac{\partial p}{\partial x} + \frac{2\mu}{R}\frac{\partial u}{\partial r}\bigg|_{r=R} = -\frac{\partial p}{\partial x} + \frac{2\tau_\chi}{R}, \qquad (13.99)$$

and after applying Laplace transform to this equation and considering the initial conditions [Eq. (13.86)]:

$$\frac{2T}{R} = \frac{d\mathrm{P}(x,s)}{dx} + \rho x V(s,x), \qquad (13.100)$$

where:

$$T = \int_0^\infty \tau_\chi(x,t)e^{-st}dt.$$

Substituting $\frac{d\mathrm{P}(x,s)}{dx}$ value from Eq. (13.96) into Eq. (13.100), results in:

$$T=\frac{\rho R}{2}SV(x,s)\left[1-\frac{I_0\left(2\sqrt{\frac{s}{a}}\right)}{I_2\left(2\sqrt{\frac{s}{a}}\right)}\right], \tag{13.101}$$

i. e., now a link between the representations of tangential stress T and average velocity $V(x,s)$ exists. And because:

$$sV(x,s)=\int_0^{\infty}\frac{\partial w}{\partial t}e^{-st}dt,$$

according to the convolution theorem, from Eq. (13.101):

$$\tau_x=\frac{\rho R}{2}\int_0^{t}\frac{\partial w(x,\theta)}{\partial\theta}k(t-\theta)d\theta, \tag{13.102}$$

where:

$$k(t)=\frac{1}{2\pi i}\int_{\gamma-i\infty}^{\gamma+i\infty}\left[1-\frac{I_0\left(2\sqrt{\frac{s}{a}}\right)}{I_2\left(2\sqrt{\frac{s}{a}}\right)}\right]e^{st}ds,$$

or, as $I_0(z)=J_0(iz)$, $I_2(z)=J_2(iz)$:

$$k(t)=\frac{1}{2\pi i}\int_{\gamma-i\infty}^{\gamma+i\infty}\left[1-\frac{J_0\left(2i\sqrt{\frac{s}{a}}\right)}{J_2\left(2i\sqrt{\frac{s}{a}}\right)}\right]e^{st}ds.$$

As a result:

$$k(t)=-2a-a\sum_{k=1}^{\infty}\exp\left(-\frac{az_k^2}{4}t\right), \tag{13.103}$$

where z_k $(k\neq 0)$ are roots of equations $J_2(z)=J_2\left(2i\sqrt{\frac{s}{a}}\right)=0$. Substituting Eqs. (13.103) and (13.103) into Eq. (13.99) and using continuity equation from Eq. (13.41) or Eq. (13.42) (which, clearly, remains unchanged):

$$\begin{aligned}-\frac{\partial p}{\partial t}&=\rho c^2\frac{\partial w}{\partial x},\\ -\frac{\partial p}{\partial x}&=\rho\left(\frac{\partial w}{\partial x}+2wa\right)+\rho a\int_0^{t}\frac{\partial w(x,\theta)}{\partial\theta}W(t-\theta)d\theta,\end{aligned} \tag{13.104}$$

where:

$$W(\bar{t}) = \sum_{k=1}^{\infty} \exp\left(-\frac{az_k^2}{4}\bar{t}\right), \quad \bar{t} = at.$$

The graph of $W(t)$ function is shown in Fig. 13.12. The parameter $2a$, as Eq. (13.33) shows, at the laminar flow in a round tube is equal to:

$$2a = \frac{\lambda|w|}{8\delta} = \frac{64|w|}{\mathrm{Re}8\delta} = \frac{8\nu}{R^2} = \mathrm{const},$$

which coincides with Eq. (13.97). Therefore, under laminar flow regime there is no need in linearization of Eq. (13.41), i. e., Eq. (13.42) is valid. The rejection of the quasi-stationarity hypothesis results in the appearance of the following integral term in the motion equation:

$$a\rho \int_0^t \frac{\partial w(x,\theta)}{\partial \theta} W(t-\theta)d\theta.$$

This term accounts, with certain weight assigned, the entire previous history of a non-stationary process.

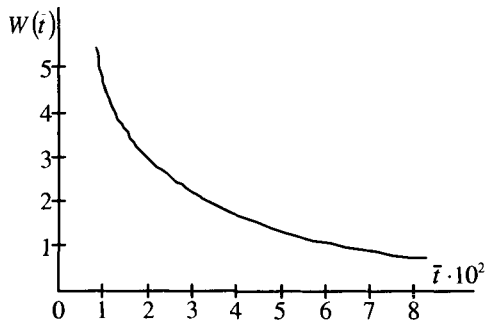

Fig. 13.12

Analysis of solutions of Eq. (13.104) showed that under periodic processes the attenuation factor of high-frequency harmonics is directly proportional to square root of frequency. This results in smoothing of the pressure (velocity) impulses and "smearing" of steep fronts. These facts were experimentally confirmed. At the same time, following the solutions of Eq. (13.42) the attenuation factor of high-frequency harmonics is practically not dependent on frequency.

The use of the quasi-stationarity hypothesis does not allow taking the above phenomena into account. Behind the hydraulic shock front, the pressure increase curves computed from Eqs. (13.42) and (13.104) gradually become closer. So the pressure computation behind the front, including maximum pressure increase, can be performed with sufficiently high accuracy using equations derived on the assumption that the quasi-stationarity hypothesis is valid.

Mechanics of Fluid Flow
by Kaplan S. Basniev, Nikolay M. Dmitriev and George V. Chilingar

CHAPTER XIV

LAMINAR BOUNDARY LAYER

Let's consider a case of the fluid flow-around an immobile wall. If the fluid is ideal, the process is described by Euler's equations:

$$\rho \frac{dv_i}{dt} = \rho F_i - \frac{\partial p}{\partial x_i} \tag{14.1}$$

and the boundary condition:

$$v_n|_C = 0. \tag{14.2}$$

For a incompressible viscous fluid, Navier-Stokes equation must be used:

$$\rho \frac{dv_i}{dt} = \rho F_i - \frac{\partial p}{\partial x_i} + \mu \Delta v_i \tag{14.3}$$

and the boundary conditions:

$$v_n|_C = 0, \ v_\tau|_C = 0. \tag{14.4}$$

Clearly, at $\mu \to 0$, Navier-Stokes Eq. (14.3) at the limit coincides with the Euler's Eq. (14.1). However, the solution of Navier-Stokes equation does not tend to Euler's equation solution because the boundary conditions Eq. (14.4) do not depend on the viscosity and cannot tend to the boundary condition [Eq. (14.2)].

These considerations and some experimental results made Prandtl believe that at low viscosity (or, which is the same, at high Reynolds numbers), viscosity is active only within a thin layer next to the wall (called the boundary layer). Outside the boundary layer viscosity effects are negligible, and the fluid can be considered to be ideal.

Navier-Stokes equations for the boundary layer flow, considering its small thickness, can be substantially simplified.

1. Equations of the boundary layer

In order to derive equations of the boundary layer let's review, disregarding mass forces, the parallel-plane flow-around a thin cylindrical body by a viscous incompressible fluid (Fig. 14.1). The flow around the wall is considered to be planar along the $0x$ axis and the $0y$ axis normal to the $0x$ axis.

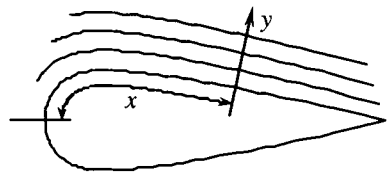

Fig. 14.1

Following Eq. (4.42), the flow equations in this case will have the following format:

$$\rho\left(\frac{\partial v_x}{\partial t}+v_x\frac{\partial v_x}{\partial x}+v_y\frac{\partial v_x}{\partial y}\right)=-\frac{\partial p}{\partial x}+\mu\left(\frac{\partial^2 v_x}{\partial x^2}+\frac{\partial^2 v_x}{\partial y^2}\right),$$

$$\rho\left(\frac{\partial v_y}{\partial t}+v_x\frac{\partial v_y}{\partial x}+v_y\frac{\partial v_y}{\partial y}\right)=-\frac{\partial p}{\partial y}+\mu\left(\frac{\partial^2 v_y}{\partial x^2}+\frac{\partial^2 v_y}{\partial y^2}\right), \qquad (14.5)$$

$$\frac{\partial v_x}{\partial x}+\frac{\partial v_y}{\partial y}=0.$$

To reduce Eq. (14.5) to the dimensionless format, it is required to assume:

$$x=L\xi,\ \ y=L\eta,\ \ v_x=Vu,\ \ v_y=Vu,\ \ p=\rho V^2\bar{p},\ \ t=\frac{L}{V}\bar{t},$$

where L is the characteristic length of the flowed-around body, V is the characteristic velocity of the flow. Substituting these terms into Eq. (14.5) and dropping (for convenience) the bars over the dimensionless time and pressure:

$$\frac{\partial u}{\partial t}+u\frac{\partial u}{\partial \xi}+v\frac{\partial u}{\partial \eta}=-\frac{\partial p}{\partial \xi}+\frac{1}{\mathrm{Re}}\frac{\partial^2 u}{\partial \xi^2}+\frac{1}{\mathrm{Re}}\frac{\partial^2 u}{\partial \eta^2}, \qquad (14.6)$$

1 1.1 $\bar{\delta}\frac{1}{\bar{\delta}}$ 1 $\frac{1}{\bar{\delta}^2}$

$$\frac{\partial v}{\partial t}+u\frac{\partial v}{\partial \xi}+v\frac{\partial v}{\partial \eta}=-\frac{\partial p}{\partial \eta}+\frac{1}{\mathrm{Re}}\frac{\partial^2 v}{\partial \xi^2}+\frac{1}{\mathrm{Re}}\frac{\partial^2 v}{\partial \eta^2}, \qquad (14.7)$$

$\bar{\delta}$ $1.\bar{\delta}$ $\bar{\delta}.1$ $\bar{\delta}$ $\frac{1}{\bar{\delta}}$

$$\frac{\partial u}{\partial \xi}+\frac{\partial v}{\partial \eta}=0, \qquad (14.8)$$

1 1

where $\bar{\delta} = \frac{\delta}{L}$, $\mathrm{Re} = \frac{\rho V L}{\mu}$, δ is the thickness of the boundary layer, and the values underneath the two equations are their estimates within the boundary level by the $\bar{\delta}$ value.

Let's now review the accuracy of these estimates. Suppose velocity v_x changes by V over the length L. Then $u \sim 1$, and:

$$\frac{\partial v_x}{\partial x} = \frac{V}{L}\frac{\partial u}{\partial \xi} \sim \frac{V}{L}, \quad \frac{\partial u}{\partial \xi} \sim 1.$$

Similarly, it is possible to show that $\frac{\partial^2 u}{\partial \xi^2} \sim 1$.

From the continuity equation Eq. (14.8):

$$\frac{\partial v}{\partial \eta} = -\frac{\partial u}{\partial \xi} \sim 1.$$

Further:

$$v = -\int_0^{\eta} \frac{\partial u}{\partial \xi} \partial \eta \sim \bar{\delta}.,$$

because within the boundary level $0 < \mu < \bar{\delta}$. Also from this inequality:

$$\frac{\partial^2 v}{\partial \eta^2} \sim \frac{1}{\bar{\delta}}, \quad \frac{\partial u}{\partial \eta} \sim \frac{1}{\bar{\delta}}, \quad \frac{\partial^2 v}{\partial \eta^2} \sim \frac{1}{\bar{\delta}^2}.$$

As $v \sim \bar{\delta}$, then:

$$\frac{\partial v}{\partial \xi} \sim \bar{\delta}, \quad \frac{\partial^2 v}{\partial \xi^2} \sim \bar{\delta}.$$

It is also assumed that $\frac{\partial u}{\partial t} \sim 1$, meaning that the sudden acceleration events like the hydraulic shock are not considered. Then:

$$\frac{\partial v}{\partial t} = \sim \bar{\delta}.$$

Thus, the validity of the above estimates of individual terms in Eqs. (14.6), (14.7) and (14.8) is confirmed. Considering these estimates that enable viscosity effect in Eq. (14.6) results in the definition of the term $\frac{1}{\mathrm{Re}}\frac{\partial^2 u}{\partial \dot{\eta}^2}$ So the relationship between the friction forces and the inertia forces can be represented by:

$$u\frac{\partial u}{\partial \eta} : \frac{1}{\mathrm{Re}}\frac{\partial^2 u}{\partial \eta^2}.$$

Prandtl suggested that within the boundary layer the relationship between inertia forces and friction forces is the value on the order of 1, i. e.:

$$\mathrm{Re} \sim \frac{1}{\bar{\delta}^2}. \tag{14.9}$$

This relationship enables the boundary layer thickness estimate as:

$$\bar{\delta} \sim \frac{1}{\sqrt{\mathrm{Re}}}. \tag{14.10}$$

For example, suppose the characteristic size of a flow around body L = 1 m, the characteristic flow velocity V = 1 m/s, and the dynamic viscosity $\mu = 10^{-3} \frac{kg}{m*s}$ (water, 20 °C), density $\rho = 10^3 \frac{kg}{m^3}$. Then:

$$\mathrm{Re} = \frac{\rho VL}{\mu} = 10^6,$$

and under Eq. (14.10):

$$\bar{\delta} \sim \frac{1}{\sqrt{\mathrm{Re}}} = 10^{-3},$$

or $\delta \sim$ 1 mm. This is the thickness of the layer in which velocity v_x changes in value from zero to its value in the external flow.

Now, the problem is the nature of the flow within the boundary layer at such Re number values. Observations show that the flow along the tablet remains laminar at $\mathrm{Re} = \frac{\rho VL}{\mu} < (5*10^5 \text{ to } 10^6)$.

Disregarding small terms in Eqs. (14.6), (14.7) and (14.8) and considering Eq. (14.9) results in:

$$\begin{aligned} &\frac{\partial u}{\partial t} + u\frac{\partial u}{\partial \xi} + v\frac{\partial u}{\partial \eta} = -\frac{\partial p}{\partial \xi} + \frac{1}{\mathrm{Re}}\frac{\partial^2 u}{\partial \eta^2}, \\ &\frac{\partial p}{\partial \eta} = 0, \quad \frac{\partial u}{\partial \xi} + \frac{\partial v}{\partial \eta} = 0. \end{aligned} \tag{14.11}$$

Eq. (14.11) is the Prandtl's equation for the boundary layer in a dimensionless format. Back transforming into the dimensional format:

$$\begin{aligned} &\frac{\partial v_x}{\partial t} + v_x\frac{\partial v_x}{\partial x} + v_y\frac{\partial v_x}{\partial y} = -\frac{1}{\rho}\frac{\partial p}{\partial x} + \frac{\mu}{\rho}\frac{\partial^2 v_x}{\partial^2 y}, \\ &\frac{\partial p}{\partial y} = 0, \quad \frac{\partial v_x}{\partial x} + \frac{\partial v_y}{\partial y} = 0. \end{aligned} \tag{14.12}$$

These equations indicate that pressure in the cross-wise direction to the boundary layer can be considered to be constant and equal to pressure at its external borders. The external flow in relation to the boundary layer, as already indicated, can be described using the model for ideal fluid.

As was shown, at the external boundary of the boundary layer, $v \sim \bar{\delta}$ or $v_y \sim \frac{V}{L}\delta$. The derivative $\frac{\partial v_x}{\partial y}$, due to disregarding viscosity in the external cross-section at this boundary is also small, and the lengthwise velocity v_x turns to velocity of the external flow $U(x,t)$. Thus the motion equation at the boundary of the boundary layer can be written as follows:

$$\frac{\partial U}{\partial t} + U\frac{\partial U}{\partial x} = -\frac{1}{\rho}\frac{\partial p}{\partial x}. \tag{14.13}$$

In a case of the transient-free flow, from Eq. (14.13):

$$p + \frac{\rho}{2}U^2 = \text{const}. \tag{14.14}$$

As the boundary layer is thin and $v_y \sim \frac{V}{L}\delta$, the boundary conditions for the external flow can be assumed as being the same as at the direct flow-around of a body by ideal fluid. In other words, in order to compute the external flow it is possible to take the ideal fluid's flow-around of the body and disregard the boundary layer's thickness.

Thus, the system of equations of Eq. (14.12) becomes:

$$\begin{aligned} &\frac{\partial v_x}{\partial t} + v_x\frac{\partial v_x}{\partial x} + v_y\frac{\partial v_x}{\partial y} = -\frac{1}{\rho}\frac{\partial p}{\partial x} + \frac{\mu}{\rho}\frac{\partial^2 v_x}{\partial y^2}, \\ &\frac{\partial v_x}{\partial x} + \frac{\partial v_y}{\partial y} = 0, \end{aligned} \tag{14.15}$$

where $p = p(x,t)$ should be considered as a known function and in the case of transient-free flow it can be determined from Eq. (14.14). Eqs. (14.15) are Prandtl's equations for the boundary layer.

The boundary conditions for the Eq. (14.15) have the following format:

$$v_x = v_y = 0 \quad \text{at} \quad y = 0, \quad v_x = U(x,t) \quad \text{at} \quad y \to \infty.$$

The last condition should be understood so that v_x asymptotically tends to the $U(x,t)$ function which is believed to be assigned in advance.

Eq. (14.10) provides only an approximate estimate of the boundary layer thickness. In reality, the separation between the boundary layer and external flow is rather tentative, so various criteria are used to refine it. The simplest case is that the velocity at the boundary layer's external border is equal to 99 % of the external flow velocity.

2. Blasius problem

To illustrate the application of the boundary layer's Eq. (14.15), the flow around a thin immobile tablet is analyzed (Fig. 14.2). The origin is placed at the edge of the tablet and place $0x$ axis along the tablet and parallel to the velocity of the overrunning flow. The tablet's length is considered infinite, and the flow is considered stationary. It is also assumed that the overrunning flow velocity is U_0. The mentioned assumptions and model gives the Blasius problem.

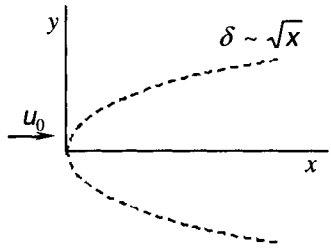

Fig. 14.2

The external flow velocity is constant, $\frac{dp}{dx} = 0$, so Eq. (14.15) becomes:

$$\begin{aligned} u\frac{\partial u}{\partial x} + v\frac{\partial u}{\partial y} &= v\frac{\partial^2 u}{\partial y^2}, \\ \frac{\partial u}{\partial x} + \frac{\partial u}{\partial y} &= 0, \end{aligned} \tag{14.16}$$

where:

$$u \equiv v_x, \quad v \equiv v_y \quad v = \frac{\mu}{\rho}.$$

The boundary conditions for Eq. (14.16) are:

$$u = v = 0 \text{ at } y = 0; \; u = U_0 \;\; at \;\; y \to \infty. \tag{14.17}$$

Let's now solve the Blasius problem. Eq. (14.16) and boundary conditions of Eq. (14.17) include the following parameters:

$$x, y, v, U_0,$$

of which only two have independent dimensionalities. Therefore, two dimensionless combinations can be formed based on this system, such as:

$$\frac{y}{x}, \quad y\sqrt{\frac{U_0}{vx}}.$$

In this case, functions $u(x,y)$, $v(x,y)$ can be represented through dimensionless functions f and Φ as:

$$u = U_0 f\left(\frac{y}{x}, \; y\sqrt{\frac{U_0}{vx}}\right), \quad v = \sqrt{\frac{vU_0}{x}}\Phi\left(\frac{y}{x}, \; y\sqrt{\frac{U_0}{vx}}\right). \tag{14.18}$$

Let's replace variables in Eq. (14.16) and boundary conditions of Eq. (14.17):

$$x = lx_1, \quad y = \sqrt{\frac{\nu l}{U_0}} y_1, \quad u = U_0 u_1, \quad v = \sqrt{\frac{\nu U_0}{l}} v_1, \tag{14.19}$$

where l is some linear dimension value.

By substituting Eq. (14.19) into Eq. (14.16) and boundary conditions Eq. (14.17):

$$u_1 \frac{\partial u_1}{\partial x_1} + v_1 \frac{\partial u_1}{\partial y_1} = \frac{\partial^2 u_1}{\partial y_1^2}, \tag{14.20}$$

$$\frac{\partial u_1}{\partial x_1} + \frac{\partial v_1}{\partial y_1} = 0, \tag{14.21}$$

$$U_1 = v_1 = 0 \text{ at } y_1 = 0; \; u_1 = 1 \;\; at \;\; y_1 \to \infty. \tag{14.22}$$

Considering Eq. (14.19):

$$\frac{y}{x} = \sqrt{\frac{\nu}{lU_0}} \frac{y_1}{x_1}, \quad y\sqrt{\frac{U_0}{\nu x}} = \sqrt{\frac{l}{x}} y_1 = \frac{y_1}{\sqrt{x_1}}, \quad v\sqrt{\frac{\nu}{\nu U_0}} = v_1 \sqrt{\frac{x}{l}} = v_1 \sqrt{x_1},$$

Eq. (14.18) can be presented as follows:

$$u_1 = f\left(\sqrt{\frac{\nu}{lU_0}} \frac{y_1}{x_1}, \; \frac{y_1}{\sqrt{x_1}}\right), \quad v_1 = \frac{1}{\sqrt{x_1}} \Phi\left(\sqrt{\frac{\nu}{lU_0}} \frac{y_1}{x_1}, \; \frac{y_1}{\sqrt{x_1}}\right).$$

At the same time, Eqs. (14.20), (14.21) and boundary conditions [Eq. (14.22)] do not include length l. Therefore, solution of these equations cannot depend on l, i. e., on the argument $\sqrt{\frac{\nu}{lU_0}}$, so:

$$u_1 = f\left(\frac{y_1}{\sqrt{x_1}}\right), \quad v_1 = \frac{1}{\sqrt{x_1}} \Phi\left(\frac{y_1}{\sqrt{x_1}}\right),$$

or:

$$u_1 = f(\xi), \quad v_1 = \frac{1}{\sqrt{x_1}} \Phi(\xi), \quad \xi = \frac{y_1}{\sqrt{x_1}} = y\sqrt{\frac{U_0}{\nu x}}. \tag{14.23}$$

Following continuity Eq. (14.21) that there is a flow function $\psi(x,y)$ such that:

$$u_1 = \frac{\partial \psi}{\partial y_1}, \quad v_1 = \frac{\partial \psi}{\partial x_1}.$$

Suppose:

$$u_1 = \frac{\partial \psi}{\partial y_1} = f(\xi) = \varphi'(\xi) = \varphi'\left(\frac{y_1}{\sqrt{x_1}}\right). \tag{14.24}$$

Then:

$$\psi = \int u_1 dy_1 = \int \varphi'(\xi) dy_1 = \sqrt{x_1} \int \varphi'(\xi) d\xi = \sqrt{x_1}\varphi(\xi),$$
$$v_1 = -\frac{\partial \psi}{\partial x_1} = \frac{1}{2\sqrt{x_1}}\varphi(\xi) - \sqrt{x_1}\frac{d\varphi}{d\xi}\frac{d\xi}{dx_1} = \frac{1}{2\sqrt{x_1}}[\xi\varphi'(\xi) - \varphi(\xi)]. \quad (14.25)$$

Substituting Eqs. (14.24) and (14.25) into Eq. (14.20) gives:

$$\varphi' \frac{d'\varphi}{d\xi}\frac{d\xi}{dx_1} + \frac{1}{2\sqrt{x_1}}(\xi\varphi' - \varphi)\frac{d\varphi'}{d\xi}\frac{d\xi}{dy_1} = \frac{d}{d\xi}\left(\frac{d\varphi'}{d\xi}\frac{d\xi}{dy_1}\right)\frac{d\xi}{dy_1},$$

or, after differentiating and reduction of similar terms:

$$2\varphi''' - \varphi\varphi'' = 0. \quad (14.26)$$

Following the boundary conditions [Eqs. (14.22)], and Eqs. (14.24), and (14.25), that the boundary conditions for Eq. (14.26) are:

$$\varphi(0) = 0, \quad \varphi'(0) = 0, \quad \varphi'(\infty) = 1. \quad (14.27)$$

Thus, partial derivative Eq. (14.16) with boundary conditions [Eq. (14.17)] is reduced to a regular nonlinear differential Eq. (14.26) with marginal conditions [Eq. (14.27)]. This problem had long ago been numerically solved with a high degree of accuracy.

From Eqs. (14.19), (14.23), (14.24) and (14.25):

$$\frac{u}{U_0} = \varphi'\left(y\sqrt{\frac{U_0}{\nu x}}\right), \quad \frac{v}{U_0} = \frac{1}{2}\sqrt{\frac{\nu}{U_0 x}\left[y\sqrt{\frac{U_0}{\nu x}}\varphi'\left(y\sqrt{\frac{U_0}{\sqrt{x}}}\right) - \varphi\left(y\sqrt{\frac{U_0}{\sqrt{x}}}\right)\right]}. \quad (14.28)$$

The graphs of lengthwise and crosswise velocity component distribution within the boundary layer are presented in Figs.14.3 and 14.4, respectively.

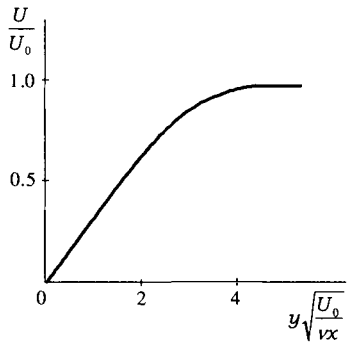

Fig. 14.3

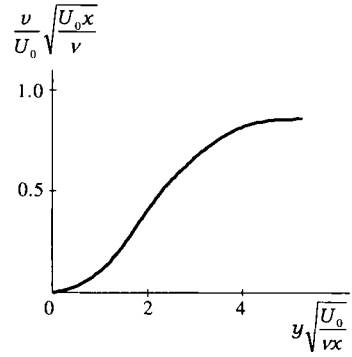

Fig. 14.4

Assuming that at the external boundary of the boundary layer $\frac{u}{U_0} = 0.99$, from the first equation in Eq. (14.28):

$$0.99 = \varphi'\left(y\sqrt{\frac{U_0}{\nu x}}\right).$$

Then, using the function $\varphi'(\xi)$ table:

$$y = \delta \approx 5\sqrt{\frac{\nu x}{U_0}}.$$

Substituting this value into the second equation of Eq. (14.28) and using the tables of functions $\varphi(\xi)$, $\varphi'(\xi)$, at the external boundary of the boundary layer:

$$\frac{u}{U_0} = \frac{1}{2}\sqrt{\frac{\nu}{U_0 x}[5\varphi'(5) - \varphi(5)]}y \approx 0.837\sqrt{\frac{\nu}{U_0 x}}.$$

This solution for the velocity component distribution within the boundary layer enables the calculation of friction stress τ_0 on the tablet.

At laminar flow:

$$\tau_0 = \mu\left(\frac{\partial u}{\partial y}\right)_{y=0}.$$

Substituting the first equation of Eq. (14.28) results in:

$$\tau_0 = \mu\left[\frac{\partial}{\partial y}\varphi'\left(y\sqrt{\frac{U_0}{\nu x}}\right)\right]_{y=0} = \mu U_0\sqrt{\frac{U_0}{\nu x}}\varphi''(0).$$

From the table of function $\varphi''(\xi)$ numerical values, $\varphi''(0) = 0.332$, and:

$$\tau_0 = 0.332\rho\sqrt{\frac{\nu U_0^3}{x}}. \qquad (14.29)$$

From Eq. (14.29), the friction forces W on one side of the plate per unit width are:

$$W = \int_0^x \tau_0 dx = 0.664\rho\sqrt{\nu U_0^3 x}.$$

3. Detachment of the boundary layer

It was shown in par. 8.2 that under the stationary flow around a circle by an ideal fluid, first the flow velocity along the arc increases, and then decreases. According to the Bernoulli's integral, the pressure is also increases first, and then

decreases. A similar phenomenon occurs at the flow around any concave contour. The fluid flow in a diffuser also occurs under the positive pressure gradient.

Under the ideal fluid flow, the kinetic energy is sufficient to overcome the positive pressure gradient. Due to the viscosity, the flow slows down within the boundary layer. Because of this phenomenon, the fluid's kinetic energy is insufficient for the particle to move far enough into the elevated pressure area. As a result, a reverse flow and the associated vortex formation occurs. Thus, the boundary layer thickness drastically increases, and the conditions under which Prandtl's equations were derived are not valid any longer.

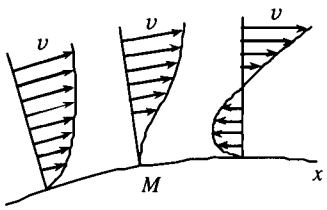

Fig. 14.5

Let's analyze the flow around a curvilinear contour C. The coordinate x is considered along this contour (Fig. 14.5). According to the previously mentioned theories, there is a point M with the coordinate x_M that at $x < x_M$, $\frac{\partial p}{\partial x} < 0$, and at $x > x_M$, $\frac{\partial p}{\partial x} > 0$.

At any point of the contour C (i. e., $y = 0$) $v_x = v_y = 0$.

Therefore, according to Eq. (14.15):

$$\mu \frac{\partial^2 v_x}{\partial y^2} = \frac{\partial p}{\partial x} < 0 \quad \text{at} \quad x < x_M,$$
$$\mu \frac{\partial^2 v_x}{\partial y^2} = \frac{\partial p}{\partial x} > 0 \quad \text{at} \quad x > x_M, \tag{14.30}$$

and at point M:

$$\frac{\partial^2 v_x}{\partial y^2} = 0. \tag{14.31}$$

As the curvature k of the curve $y = l(x)$ is:

$$k = \frac{d^2 y}{dx^2}\left[1 + \left(\frac{dy}{dx}\right)^2\right]^{-\frac{3}{2}},$$

then, following Eqs. (14.30) and (14.31) that the velocity $v_x = v_x(x)$ profile curvature at point M changes its sign (Fig. 14.5). Therefore, the backflow occurs at $x > x_M$ and, as a result, the detachment of the boundary layer occurs.

It is clear that if everywhere within the flow $\frac{\partial p}{\partial x} \le 0$, there is no detachment of the boundary layer.

Mechanics of Fluid Flow
by Kaplan S. Basniev, Nikolay M. Dmitriev and George V. Chilingar

CHAPTER XV

UNIDIMENSIONAL GAS FLOW

Review of unidimensional flow provides an opportunity to study major patterns regarding gases moving at high velocity. Unidimensional gas (liquid) flow is such that the flow parameters (velocity v, density ρ, pressure p, temperature T) depends only on one coordinate and time. An example of the unidimensional flow is the flow in a flow-tube providing the velocity, density, pressure and temperature are uniformly distributed over the flow cross-section. In this case:

$$v = v(l,t),\ \rho = \rho(l,t),\ p = p(l,t),\ T = T(l,t),$$

where l is the coordinate counted along the tube's length.

For the simplicity and demonstration, the gas is considered to be ideal, i. e., with the following equation of state:

$$\frac{p}{\rho} = RT. \tag{15.1}$$

1. Sound velocity

The velocity of the sound propagation in gas is one of the most important concepts of the gas dynamics. To analyze this type of flow, a long cylindrical tube closed on one side by a piston and filled-up with gas is considered (Fig. 15.1). It is assumed that at the initial time the gas in the tube is immobile, and pressure p_0 and density ρ_0 are equal in all cross-sections of the tube.

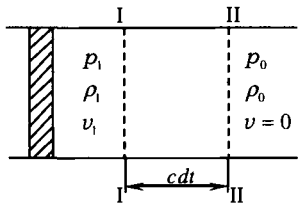

Fig. 15.1

Let's move the piston along the tube. The gas in front of the piston will begin to compress and move at the velocity v, and then disturbance propagates left-to-right along the tube at some velocity c.

Suppose at the time t the disturbance reached cross-section I-I, and at the moment in time $t + dt$, it reached cross-section II-II. During the time period dt between the cross-sections the gas-flow parameters change, i. e., this flow is

non-stationary. The mass conservation law [Eq. (2.29)] and the variation in momentum law [Eq. (2.49)] are used.

During the time interval dt gas velocity, pressure and density in the cross-section I-I change and reach the values v_1, p_1, ρ_1; in the cross-section II-II velocity is equal to zero, and gas pressure and density are constant (p_0, ρ_0) as the disturbance did not have time to reach this cross-section. Therefore, at the time $t + dt$ (i. e., by the end of the time interval under consideration) Eqs. (2.29) and (2.49) by projecting on the tube's axis $0x$ become:

$$\int_V \frac{\partial \rho}{\partial t} dV = \int_{S_1} \rho_1 v_1 dS, \tag{15.2}$$

$$\int_V \frac{\partial (\rho v)}{\partial t} dV - \int_{S_1} \rho_1 v_1^2 dS = P_x + T_x, \tag{15.3}$$

where S_1 is the tube's cross-sectional area. The projection of the main vector $\overline{N}$ of the normal components of tube's walls reaction onto its axis is equal to zero, and the gas weight is ignored.

The pressure force acting on the gas volume between the I-I and II-II cross-sections at the moment in time $t + dt$ is:

$$\mathrm{P}_x = \int_{S_1} (p_1 - p_0) dS_1, \tag{15.4}$$

and the friction force is:

$$T_x = -\tau_{avg} \chi c dt, \tag{15.5}$$

where τ_{avg} is the average friction on the tube's wall over time interval dt and length cdt; χ is the wetted perimeter of the tube. Over the time interval dt, the gas density over the tube's segment in question varies within the ρ_0 and ρ_1 values, and velocity changes from 0 to v_1. So, over the dt segment:

$$\frac{\partial \rho}{\partial t} dt \approx \left(\frac{\partial \rho}{\partial t} \right)_{\mathrm{avg}} dt = \rho_1 - \rho_0, \quad \frac{\partial (\rho v)}{\partial t} dt = \left(\frac{\partial (\rho v)}{\partial t} \right)_{\mathrm{avg}} = \rho_1 v_1, \tag{15.6}$$

where the subscript $_{\mathrm{avg}}$ also means average value over the time interval dt and volume V.

The volume element dV can be represented as:

$$dV = cdtdS. \tag{15.7}$$

Substituting Eqs. (15.4)–(15.7) into Eqs. (15.2) and (15.3) approximately (because of the difference between the average and exact values) results in:

$$\int_{S_1} [(\rho_1 - \rho_0) c - \rho_1 v_1] dS = 0, \tag{15.8}$$

$$\int_{S_1}(\rho_1 v_1 c - \rho_1 v_1^2)dS = (p_1 - p_0)S - \tau_{avg}\chi c\,dt. \tag{15.9}$$

Considering that the flow is unidimensional (i. e., all parameters are distributed uniformly over the tube's length) and the gas is ideal ($\tau = \tau_{avg} = 0$), by taking the limit at $dt \to 0$, and from Eqs. (15.8) and (15.9):

$$(\rho_1 - \rho_0)c = \rho_1 v_1, \quad \rho_1 v_1 c - \rho_1 v_1^2 = p_1 - p_0. \tag{15.10}$$

Canceling velocity v_1 from Eq. (15.10), the result is:

$$c^2 = \frac{\rho_1}{\rho_0} * \frac{p_1 - p_0}{\rho_1 - \rho_0}. \tag{15.11}$$

The sound velocity a is the velocity of infinitely small disturbances:

$$a = \lim_{\substack{p_1 \to p_0 \\ \rho_1 \to \rho_0}} c,$$

so, according to Eq. (15.11):

$$a^2 = \lim_{\substack{p_1 \to p_0 \\ \rho_1 \to \rho_0}} \frac{\rho_1}{\rho_0}\frac{p_1 - p_0}{\rho_1 - \rho_0} = \frac{dp}{d\rho}. \tag{15.12}$$

It is important to note that in deriving Eq. (15.12) the medium under consideration can be either gas or liquid. Therefore, this equation is valid for any compressible medium. As gas pressure p and density ρ are associated through equation of state [Eq. (15.1)], then to compute the sound velocity a, it is necessary to assign a type of the thermodynamic process associated with the sound propagation.

Suppose the process is isothermal, i. e., T = const. The sound velocity can be computed based on this assumption as a_T. Then, from Eqs. (15.1) and (15.2):

$$a_T = \sqrt{\frac{dp}{d\rho}} = \sqrt{RT}. \tag{15.13}$$

Gas constant for the air is $R = 287\frac{\text{m}^2}{\text{c}^2\,\text{deg}}$, so for the temperature $T = 293°\text{K}$ sound velocity is $a_T = 290$ m/s. This is significantly different from the experimental results, and Eq. (15.13) is unsuitable for the sound velocity determination. So, we will assume now that the sound propagation process is isentropic, i. e., Eq. (7.38) is valid:

$$\frac{p}{p_0} = \left(\frac{\rho}{\rho_0}\right)^k. \tag{15.14}$$

Then, considering equation of state Eq. (15.1):

$$a_s^2 \frac{dp}{d\rho} = kp_0 \frac{\rho^{k-1}}{\rho_0^k} = k \frac{p_0}{\rho_0} \frac{\rho^k}{\rho} = \frac{kp}{\rho} = kRT, \tag{15.15}$$

where a_s the sound velocity computed under the assumption of the isentropic process. For the air, the adiabatic exponent $k = 1.4$, and at $R = 287 \frac{\text{m}^2}{\text{c}^2 \text{deg}}$ and $T = 293^\circ\text{K}$. Thus, from Eq. (15.15), the sound velocity $a = 343$ *m/s*, which agrees well with experimental results. Thus, in the future Eq. (15.15) for the sound velocity computation will be used.

2. Energy conservation law

In this section, the energy conservation law is derived for the transient-free unidimensional flow of an ideal (i. e., nonviscous) gas. For this purpose Eqs. (2.70) and (4.3) are used, according to which for an ideal gas $\bar{p}_n = p_{nn}\bar{n} = -p\bar{n}$. In this case, $\bar{p}_n * \bar{\tau}_1 = 0$, and Eq. (2.70) becomes:

$$\int_{S_2} \left(-\Pi + u + \frac{p}{\rho} + \frac{v^2}{2} \right) \rho v \, dS - \int_{S_1} \left(-\Pi + u + \frac{p}{\rho} + \frac{v^2}{2} \right) \rho v \, dS = \int_V \rho q_e dV. \tag{15.16}$$

The flow is unidimensional by definition; therefore, expressions in parentheses can be removed from the integral. Besides, at transient-free flow:

$$\int_{S_2} \rho v \, dS - \int_{S_1} \rho v \, dS = Q_m. \tag{15.17}$$

Considering Eq. (15.17), Eq. (15.16) can be rewritten as:

$$\left(-\Pi + u + \frac{p}{\rho} + \frac{v^2}{2} \right)_2 - \left(-\Pi + u + \frac{p}{\rho} + \frac{v^2}{2} \right)_1 = \frac{1}{Q_m} \int_V \rho q_e dV. \tag{15.18}$$

Eq. (15.18) is an expression of the energy conservation law for the unidimensional transient-free flow of an ideal gas. In the future, when analyzing gas flow, the mass force effect (in particular, weight) is ignored, i. e., $\Pi = 0$.

At adiabatic process, $q_e = 0$; thus, from Eq. (15.18):

$$u + \frac{p}{\rho} + \frac{v^2}{2} = \text{const}. \tag{15.19}$$

The heat function enthalpy i by definition is equal to:

$$i = u + \frac{p}{\rho}. \tag{15.20}$$

Substituting it into Eq. (15.19) results in:

$$i + \frac{v^2}{2} = \text{const}. \tag{15.21}$$

The unit internal energy u for a gas governed by Eq. (15.1) is proportional to its absolute temperature T and is equal to:

$$u = C_v T. \tag{15.22}$$

Besides, such gas is subordinated to Mayer's Eq. (7.33):

$$C_p - C_V = R. \tag{15.23}$$

Following Eqs. (15.22) and (15.23):

$$i = C_V T + RT = C_p T, \tag{15.24}$$

Thus, the energy conservation law Eq. (15.21) can be formatted as follows:

$$C_p T \frac{v^2}{2} = \text{const}. \tag{15.25}$$

From Mendeleyev-Clapeyron's Eq. (15.1) and Mayer's equation:

$$C_p T = \frac{C_p}{R}\frac{p}{\rho} = \frac{C_p}{C_p - C_v}\frac{p}{\rho} = \frac{k}{k-1}\frac{p}{\rho}, \quad k = \frac{C_p}{C_v}. \tag{15.26}$$

Substituting Eq. (15.26) into Eq. (15.25), results in:

$$\frac{k}{k-1}\frac{p}{\rho} + \frac{v^2}{2} = \text{const}. \tag{15.27}$$

Note that accurate to the gz term (which we disregard), Eq. (15.27) is the same as Bernoulli's Eq. (7.45). It means that Bernoulli's integral is a particular case of the energy conservation law.

A concept of drag parameters is now introduced. Drag parameters in a given crosswise section of a unidimensional flow (a flow-tube) are parameters of the gas if *mentally* reduced to isoentropical state, i. e., with the preservation of the energy which the flowing gas has in this cross section. Temperature, pressure, drag enthalpy, and density of the dragged gas are denoted, respectively, as T_0, p_0, i_0, ρ_0.

Using the drag parameters, Eqs. (15.21), (15.25) and (15.27), i. e., various forms for the energy conservation law, can be written as follows:

$$1+\frac{v^2}{2}=i_0, \tag{15.28}$$

$$C_pT+\frac{v^2}{2}=C_pT_0, \tag{15.29}$$

$$\frac{k}{k-1}\frac{p}{\rho}+\frac{v^2}{2}=\frac{k}{k-1}\frac{p_0}{\rho_0}. \tag{15.30}$$

According to Eqs. (15.28), (15.29) and (15.30), at adiabatic flow of an ideal gas, its temperature, enthalpy and $\frac{p}{\rho}$ ratio decrease. Eqs. (7.46) and (7.47) show also that p and ρ also decrease ($k > 1$). It is important to note that if entropy changes along the flow, the drag parameters in various cross-sections, generally speaking, will be different. Another comment is that adiabatic flow of a nonviscous gas is isentropic.

3. Mach number. Velocity factor

The energy conservation law [Eq. (15.29)] shows that in the adiabatic flow the flow velocity changes from one cross-section to the next resulting in the corresponding temperature changes. On the other hand, from Eq. (15.15), temperature changes result in the sound velocity changes. Thus, the sound velocity at any place within the flow depends on the gas flow velocity at the same place; increase in the local sound velocity v results in the local sound velocity a decrease.

The ratio M between the velocity v of the gas flow at a given point in the flow and the sound velocity at the same point:

$$M=\frac{v}{\alpha} \tag{15.31}$$

is called Mach number. When:

$v < a$, or $M < 1$, the regime is called subsonic;

$v > a$, or $M > 1$, the regime is called supersonic;

$v = a$, or $M = 1$, the regime is called critical.

Parameters of gas flows under the critical regime are called critical parameters and are denoted by v_{cr}, p_{cr}, ρ_{cr}, T_{cr}, α_{cr}.

The ratio between local gas velocity v and the critical velocity $v_{cr} = \alpha_{cr}$, i. e., λ:

$$\lambda=\frac{v}{a_{cr}}=\frac{v}{v_{cr}}, \tag{15.32}$$

is called velocity factor.

Following the energy conservation law Eq. (15.29), the maximum possible velocity of adiabatic flow v_{max} is reached at $T = 0$ and:

$$v_{max} = \sqrt{2c_p T_0} \tag{15.33}$$

From Eq. (15.15), sound velocity at $T = 0$ is also equal to zero. Thus, the Mach number can range between zero and infinity:

$$0 \le M < \infty.$$

Substituting sound velocity Eq. (15.31) into the energy conservation law Eq. (15.30) results in:

$$\frac{a^2}{k-1} + \frac{v^2}{2} = \frac{a_0^{\,2}}{k-1}, \tag{15.34}$$

where $a_0 = \sqrt{k\frac{p_0}{\rho_0}} = \sqrt{kRT_0}$ is sound velocity at drag temperature $T = T_0$.

Assuming in Eq. (15.34) $a = v = a_{cr}$:

$$a_{cr} = v_{cr} = \sqrt{\frac{2}{k+1}}a_0 = \sqrt{\frac{2k}{k+1}RT_0} = \sqrt{\frac{2k}{k+1}\frac{p_0}{\rho_0}}. \tag{15.35}$$

It can be seen that in the adiabatic flow with the drag temperature T_0 critical velocity is a constant value for the entire flow. Assuming $a = 0$ in Eq. (15.34), one more equation for v_{max} is obtained:

$$v_{max} = \sqrt{\frac{2}{k-1}}a_0. \tag{15.36}$$

According to the a_0 definition and Mayer's Eq. (15.23), Eqs. (15.33) and (15.36) are identical. Eqs. (15.32), (15.35) and (15.36) show that the velocity factor λ can range between the following limits:

$$0 \le \lambda < \sqrt{\frac{k+1}{k-1}}.$$

In order to establish the correlation between the flow parameters and Mach number and drag parameters, the energy conservation law is used in the Eq. (15.34). From this equation:

$$1 + \frac{k-1}{2}\frac{v^2}{a^2} = \frac{a_0^{\,2}}{a^2},$$

or, considering Eqs. (15.15) and (15.31):

$$\frac{T_0}{T} = 1 + \frac{k-1}{2}M^2. \tag{15.37}$$

According to the Mendeleyev–Clapeyron's equation of state [Eq. (15.1)] and Poisson's adiabatic Eq. (15.14):

$$\frac{p_0}{p}=\frac{\rho_0 T_0}{\rho T}=\left(\frac{\rho_0}{\rho}\right)^k,\quad \frac{\rho_0}{\rho}=\left(\frac{T_0}{T}\right)^{\frac{1}{k-1}},\quad \frac{p_0}{p}=\left(\frac{T_0}{T}\right)^{\frac{k}{k-1}}. \tag{15.38}$$

Substituting this Eq. (15.38) into Eq. (15.37) results in:

$$\frac{\rho_0}{\rho}=\left(1+\frac{k-1}{2}M^2\right)^{\frac{1}{k-1}} \tag{15.39}$$

$$\frac{p_0}{p}=\left(1+\frac{k-1}{2}M^2\right)^{\frac{k}{k-1}}. \tag{15.40}$$

Eqs. (15.37), (15.39) and (15.40) are necessary correlations between the flow parameters and Mach number. Note, that if the values p, ρ, T and p_0, ρ_0, T_0 are taken in the same cross-section, then, as follows from the definition of the drag parameters, Eqs. (15.37), (15.39) and (15.40) are valid for non-adiabatic processes as well.

Assuming $M = 1$ in Eqs. (15.37), (15.39) and (15.40):

$$\frac{T_{cr}}{T_0}=\frac{2}{k+1},\quad \frac{\rho_{cr}}{\rho_0}=\left(\frac{2}{k+1}\right)^{\frac{1}{k-1}},\quad \frac{p_{cr}}{p_0}=\left(\frac{2}{k+1}\right)^{\frac{k}{k-1}}. \tag{15.41}$$

For methane, $k = 1.3$, for the air, $k = 1.4$. So for methane:

$$\frac{T_{cr}}{T_0}=0.870,\quad \frac{\rho_{cr}}{\rho_0}=0.628,\quad \frac{p_{cr}}{p_0}=0.546.$$

For the air:

$$\frac{T_{cr}}{T_0}=0.833,\quad \frac{\rho_{cr}}{\rho_0}=0.634,\quad \frac{p_{cr}}{p_0}=0.528.$$

This example shows that the critical flow can occur at relatively small pressure gradient.

According to Eqs. (15.15), (15.31`), (15.32), (15.35) and (15.37):

$$\lambda^2=\frac{v^2}{a_{cr}^2}=\frac{v^2}{a^2}\frac{a^2}{a_0^2}\frac{a_0^2}{a_{cr}^2}=M^2\frac{T}{T_0}\frac{k+1}{2}=\frac{k+1}{2}M^2\left(1+\frac{k-1}{2}M^2\right)^{-1}, \tag{15.42}$$

and therefrom:

$$M^2=\frac{2\lambda^2}{k+1-(k-1)\lambda^2}.$$

Substituting this into Eqs. (15.37), (15.39) and (15.40) results in:

$$\tau(\lambda) = \frac{T}{T_0} = 1 - \frac{k-1}{k+1}\lambda^2, \tag{15.43}$$

$$\varepsilon(\lambda) = \frac{\rho}{\rho_0} = \left(1 - \frac{k-1}{k+1}\lambda^2\right)^{\frac{1}{k-1}}, \tag{15.44}$$

$$\pi(\lambda) = \frac{p}{p_0} = \left(1 - \frac{k-1}{k+1}\lambda^2\right)^{\frac{k}{k-1}}, \tag{15.45}$$

and these are equations linking the flow parameters, drag parameters and velocity factor.

4. Linkage between the flow tube's cross-sectional area and flow velocity

Continuity equation Eq. (2.30) or (5.17) for the not-transient unidimensional gas flow is:

$$Q_m = \rho v S = \text{const}. \tag{15.46}$$

Differentiating this equation, results in:

$$vS\,d\rho + \rho S\,dv + \rho v\,dS = 0,$$

or:

$$\frac{dS}{S} = -\left(\frac{d\rho}{\rho} + \frac{dv}{v}\right). \tag{15.47}$$

Differentiating the energy conservation law Eq. (15.30), results in:

$$\frac{k}{k-1}\frac{\rho\,dp - p\,d\rho}{\rho^2} + v\,dv = 0, \tag{15.48}$$

and as in accordance with Eqs. (15.12) and (15.15):

$$dp = a^2 d\rho, \quad p = \frac{1}{k}\rho a^2,$$

then, Eq. (15.48) can be formatted as follows:

$$a^2\frac{d\rho}{\rho} + v\,dv = 0. \tag{15.49}$$

Cancelling $\frac{d\rho}{\rho}$ from Eqs. (15.47) and (15.49), results in:

$$\frac{dS}{S} = -\left(\frac{dv}{v} - \frac{vdv}{a^2}\right) = -\frac{dv}{v}\left(1 - \frac{v^2}{a^2}\right) = -\frac{dv}{v}\left(1 - M^2\right). \qquad (15.50)$$

Eq. (15.50) shows that at $M = 1$, $dS = 0$. Therefore, extrema of the function $S = S(x)$, where x coordinate is considered along the axis of the flow tube, corresponds to the critical regime. At $M < 1$, $1 - M^2 > 0$, and the signs at dv and dS are opposite. It means that under the subsonic regime the flow velocity increases as the tube cross-section decreases. In a supersonic flow $M > 1$, $1 - M^2 < 0$, and the signs at dv and dS coincide. Therefore, in this case, the flow velocity increases as the tube cross-section increases. Thus, extrema S is a minimum, and the critical regime ($M = 1$) can occur only in the narrowest, so-called critical cross-section of the flow-tube. The condition $dS = 0$ cannot correspond to a maximum at subsonic flow; approaching to S_{max} results in decrease in flow velocity, i. e., the Mach number, which is smaller than one, will further decrease. If $M > 1$, then approaching to S_{max} results in acceleration of flow velocity. Therefore, the critical flow ($M = 1$) is possible only when $S = S_{min}$.

Following Eq. (15.46), at $S = S_{min} = S_{cr}$ the mass velocity ρv reaches its maximum. An example of the S/S_{min} graph is presented in Fig. 15.2.

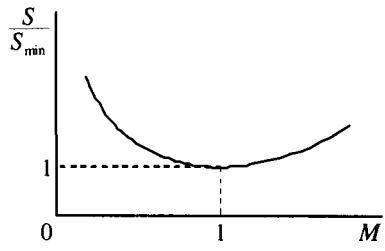

Fig. 15.2

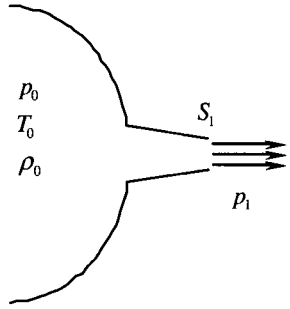

Fig. 15.3

Eq. (15.39) indicates that at supersonic flow the increase in Mach number is accompanied by a drastic decrease in the gas density. So, in order for the mass conservation law [Eq. (15.46)] to be fulfilled it is necessary to increase the flow-tube cross-sectional area. A special note is that under the subsonic flow the correlation velocity *vs.* cross-sectional area is qualitatively similar to the incompressible fluid flow. Under a supersonic flow, this correlation is conceptually totally different.

5. Gas outflow through a convergent nozzle

Let's review the stationary adiabatic gas outflow from a tank through a convergent nozzle (Fig. 15.3). As mentioned, adiabatic flow of a nonviscous gas is isentropic so that the immobile gas parameters in the tank (p_0, T_0, ρ_0) can be considered as the drag parameters. From the energy conservation law [Eq. (15.30)], the gas velocity in any cross-section of the nozzle is:

$$v = \sqrt{\frac{2k}{k-1}\frac{p_0}{\rho_0}\left(1 - \frac{p}{p_0}\frac{\rho_0}{\rho}\right)},$$

or, considering Poisson's adiabatic equation Eq. (15.14):

$$v = \sqrt{\frac{2k}{k-1}\frac{p_0}{\rho_0}\left[1 - \left(\frac{p}{p_0}\right)^{\frac{k-1}{k}}\right]}. \tag{15.51}$$

The mass through-flow in the cross-section under review, under Eqs. (15.1), (15.14) and (15.51), is:

$$Q_m = \rho v S = \frac{\rho}{\rho_0}\rho_0 v S = \left(\frac{p}{p_0}\right)^{\frac{1}{k}}\rho_0 v S = \\ = \frac{S p_0}{\sqrt{RT_0}}\sqrt{\frac{2k}{k-1}\left[\left(\frac{p}{\rho_0}\right)^{\frac{2}{k}} - \left(\frac{p}{p_0}\right)^{\frac{k-1}{k}}\right]}. \tag{15.52}$$

This equation can be rewritten after naming the nozzle's output cross-section area as S_1 and pressure outside the tank as p_1:

$$Q_m = \frac{S_1 p_0}{\sqrt{RT_0}}\sqrt{\frac{2k}{k-1}\left[\left(\frac{p_1}{\rho_0}\right)^{\frac{2}{k}} - \left(\frac{p_1}{p_0}\right)^{\frac{k-1}{k}}\right]}. \tag{15.53}$$

For a study of Eq. (15.53) it is assumed:

$$\frac{p_1}{\rho_0} = x, \quad \left(\frac{p_1}{\rho_0}\right)^{\frac{2}{k}} - \left(\frac{p_1}{p_0}\right)^{\frac{k-1}{k}} = x^{\frac{2}{k}} - x^{\frac{k-1}{k}} = y.$$

Clearly, $0 \le p_1 \le p_0$ or $0 \le x \le 1$. Inside this interval $y > 0$ because $(k+1)/k > 2k$, and at its end, $y = 0$. Therefore, the $y(x)$ function has a maximum within the [0,1] segment. Equating first derivative to zero, results in:

$$\frac{dy}{dx} = \frac{2}{k}x^{\frac{2}{k}-1} - \frac{k+1}{k}x^{\frac{1}{k}} = 0,$$

from where the mass throughflow Q_m will reach its maximum at:

$$x = \frac{p_1}{p} = \left(\frac{2}{k+1}\right)^{\frac{k}{k-1}} \tag{15.54}$$

and:

$$Q_m^{\max} = \frac{S_1 p_0}{\sqrt{RT_0}} \sqrt{k\left(\frac{2}{k+1}\right)^{\frac{k+1}{k-1}}}. \tag{15.55}$$

Comparing Eqs. (15.54) and (15.41):

$$\left(\frac{2}{k+1}\right)^{\frac{k}{k-1}} = \frac{p_{cr}}{p}.$$

Thus, as the external pressure p_1 declines, the mass throughflow Q_m increases from $Q = 0$ at $p = p_0$ to $Q_m^{\max}$ at $p = p_{cr}$. At $p = p_{cr}$ the gas velocity in the nozzle's output cross-section is critical, i. e., $v = v_{cr} = a_{cr}$. Such an outflow is called critical. Any further decline in pressure p_1 must, according to Eq. (15.53), result in a decline in mass throughflow contradicting the physical meaning of the process. Experience shows that at $0 \le p_1 \le p_{cr}$, the mass throughflow remains constant, pressure and velocity in the output orifice remain equal ($p = p_{cr}$, $v = v_{cr}$) and the flow on exiting the nozzle expands. Thus, there is a break between the pressure in the output cross-section p_{cr} and the pressure in the ambient space p_1.

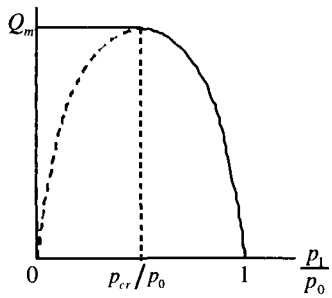

Fig. 15.4

Therefore, the mass throughflow through the convergent nozzle at $p_{cr} \le p_1 \le p_0$ is determined by Eq. (15.53), and at $0 \le p_1 \le p_{cr}$, by Eq. (15.55). The correlation graph Q_m *vs.* $\frac{p_{cr}}{p}$ is shown in Fig. 15.4. The dashed line corresponds to that part of Eq. (15.53) solution which does not have any physical meaning. The throughput consistency in the $0 \le p_1 \le p_{cr}$ area can be explained as follows. When the gas flow velocity in the nozzle's outflow cross-section becomes equal to the sound velocity, pressure changes in the outside medium cannot penetrate within the nozzle. Indeed, these changes (pressure changes) propagate at sound velocity. Therefore, it cannot penetrate the cross-section where velocity is critical. A dynamic barrier is created which isolates the internal portion of the nozzle from external disturbances, and that is exactly what results in the consistency of the mass throughflow.

6. De Laval's nozzle

The Laval's nozzle is composed of the narrowing and expanding portions and is used for achieving supersonic gas velocities. In analyzing the operation of De Laval's nozzle, the flow is considered as stationary and isentropic. Then, along the nozzle the mass conservation law is fulfilled in the format of Eq. (15.46), and the mass velocity in anycross-section, according to Eq. (15.52), is:

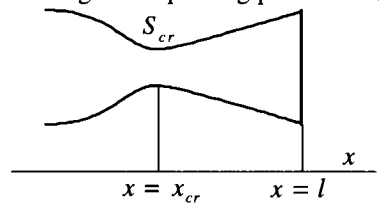

Fig. 15.5

$$\rho v = \frac{Q_m}{S(x)} = \frac{p_0}{\sqrt{RT_0}} \sqrt{\frac{2k}{k-1}\left[\left(\frac{p_1}{\rho_0}\right)^{\frac{2}{k}} - \left(\frac{p_1}{p_0}\right)^{\frac{k+1}{k}}\right]}. \qquad (15.56)$$

This equation shows that $\rho v = f\left(\frac{p}{\rho_0}\right)$, i. e., mass velocity depends only on the pressure distribution along the nozzle (flow-tube) and is not clearly dependent on its geometry. In other words, mass velocity is a universal function of pressure. Based on the analysis in the previous paragraph, $\max(\rho v)$ is achieved at $p = p_{cr}$, i. e., under the critical regime, and:

$$\max(\rho v) = \rho_{cr} v_{cr} = \frac{p_0}{\sqrt{RT_0}} \sqrt{k\left(\frac{2}{k+1}\right)^{\frac{k+1}{k-1}}}.$$

Schematic of the correlation graph $\frac{\rho v}{\rho_{cr} v_{cr}} = f\left(\frac{p}{\rho_0}\right)$ is shown in Fig. 15.6.

Therefore, if the area distribution law $S(x)$ and mass throughflow Q_m are given, it is possible to use Eq. (15.56) to find $\frac{p}{\rho_0} = f(x)$, i. e., pressure distribution along de Laval's nozzle. Let's use the graph of Fig. 15.6 to find the solution. Suppose the shape of de Laval's nozzle (i. e., the $S = S(x)$ function) is known. Suppose also that the mass throughflow Q_m is also known. Let's take any nozzle's cross-section x_1 left of the cross-section $x = x_{cr}$ (Fig. 15.5).

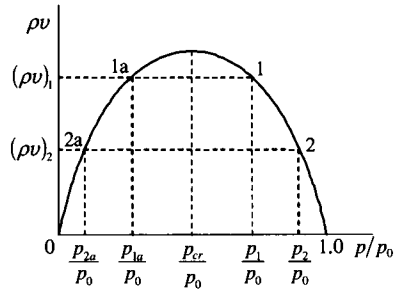

Fig. 15.6

Then, according to Eq. (15.56), the value:

$$(\rho v)_1 = \frac{Q_m}{S(x_1)}$$

is also known. In the correlation Eq. (15.56), this value of mass velocity has corresponding points 1 and 1a. At point 1, $\frac{p_1}{\rho_0} > \frac{p_{cr}}{\rho_0}$, and at point 1a, $\frac{p_{1a}}{\rho_0} < \frac{p_{cr}}{\rho_0}$. Therefore, point 1 corresponds to the subsonic flow, and point 1a, to the supersonic flow. In the narrowing part of the nozzle the flow is speeding-up, and at $x = x_{cr}$ the flow cannot be supersonic. Thus, at $x = x_{cr}$ only subsonic flow can exist in which only one value of $\frac{p_1}{\rho_0}$ is realized.

Let's now take a nozzle's cross-section x_2 right of the cross-section $x = x_{cr}$. Mass velocity in this cross-section is:

$$(\rho v)_2 = \frac{Q_m}{S(x_2)}.$$

In Fig. 15.6, to the value $\rho v = (\rho v)_2$ correspond the points 2 ($\frac{p_2}{\rho_0} > \frac{p_{cr}}{\rho_0}$ — subsonic regime) and 2a ($\frac{p_{2a}}{\rho_0} < \frac{p_{cr}}{\rho_0}$ — supersonic regime).

The flow can experience either increase or drag within the expanding portion of the nozzle, i. e., either subsonic or supersonic regimes can exist. Either one's occurring in reality depends on the pressure at the exit of the nozzle. Conducting these calculations for various cross-sections, it is possible to plot the pressure distribution curves along de Laval's nozzle length.

The above discussion indicates that at $p_e = p_0$ (where p_e is pressure of the outside space) the gas in the nozzle is immobile. Decreasing p_e results in the increase in the flow at the narrowing part of the nozzle and drag at the expanding part. In the process, velocity everywhere remains subsonic, and the pressure distribution is shown by the dashed-line in Fig. 15.7. As p_e further declines ($p_e > p_c$), velocity in all cross-sections and mass throughflow increase. At $p_e = p_c$, the flow velocity in cross-section $x = x_{cr}$ equals to the sound velocity $a_{cr} = v_{cr}$ and gradually decreases in the expanding part of the nozzle. Mass throughflow reaches its maximum value $Q_m^{max} = \rho_{cr} v_{cr} S_{cr}$, pressure in the expanding portion increases from $p = p_{cr}$ to $p = p_c$ (curve A in Fig. 15.7). A further decrease in p_e ($p_p = p_e = p_c$) results in the emergence of pressure jumps in the expanding portion of the nozzle (curve B in Fig. 15.7). In the segment $x_{cr} < x < x_c$ the flow is supersonic, and at $x_c < x < l$, subsonic.

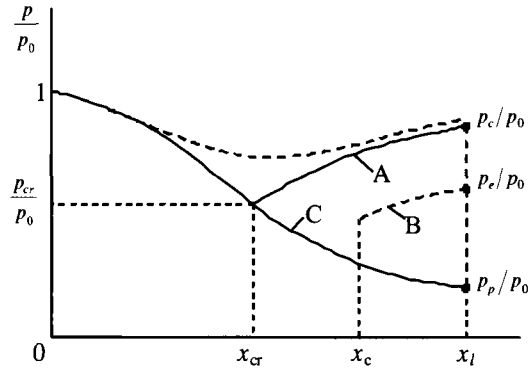

Fig. 15.7

At $p = p_p$ the flow anywhere in the expanding portion of the nozzle is supersonic, and the pressure distribution is described by the curve C in Fig. 15.7.

At $p_e < p_p$, the gas parameters (v, p, ρ, T) in the output cross-section of the nozzle are the same as at $p = p_p$, and upon leaving the nozzle, the gas flow will expand. Leveling the pressure from the value p_p to the value p_e is accompanied by numerous expansions and contractions of the flow with the occurrence of oblique jumps. What results from the construction of curves A and C is that at $Q_m + Q_m^{\max}$ the pressures p_c and p_p at the butt of the nozzle are determined only by the nozzle geometry and do not depend on backpressure.

The regimes under which $p_c = p_e$ and $p_p = p_e$ are called computable regimes, the former being a regime of adiabatic compression, the latter, expansion. All other operating regimes of de Laval nozzle are not computable regimes.

7. Gas-dynamic functions

Eqs. (15.43), (15.44) and (15.45), i. e., $\tau(\lambda)$, $\varepsilon(\lambda)$ and $\pi(\lambda)$ are called gas-dynamic functions. Detailed tables have been compiled for these functions which makes it much easier to conduct gas-dynamic computations.

There are clear connections between gas-dynamic functions $\tau(\lambda)$, $\varepsilon(\lambda)$ and $\pi(\lambda)$:

$$\frac{T}{T_0} = \tau(\lambda) = \frac{\pi(\lambda)}{\varepsilon(\lambda)}, \quad \frac{\rho}{\rho_0} = \varepsilon(\lambda) = [\tau(\lambda)]^{\frac{1}{k-1}}, \quad \frac{p}{p_0} = \pi(\lambda) = [\tau(\lambda)]^{\frac{k}{k-1}}[\varepsilon(\lambda)]^k. \quad (15.57)$$

Using gas-dynamic function, the mass throughflow can be represented by:

$$Q_m = \rho v S = \frac{\rho}{\rho_0}\rho_0 \frac{v}{a_{cr}} a_{cr} S = \rho a_{cr} S \lambda \varepsilon(\lambda). \quad (15.58)$$

Let's introduce a new gas-dynamic function:

$$q(\lambda) = C\lambda\varepsilon(\lambda) \quad (15.59)$$

and define the constant C so that $q(1) = 1$. Following Eqs. (15.54) and (15.59):

$$C = \frac{q(1)}{\varepsilon(1)} - \frac{1}{\varepsilon(1)} = \left(\frac{k+1}{2}\right)^{\frac{1}{k-1}},$$

and Eq. (15.59) then becomes:

$$q(\lambda) = \left(\frac{k+1}{2}\right)^{\frac{1}{k-1}} \lambda\varepsilon(\lambda). \tag{15.60}$$

Considering that $\varepsilon(1) = \frac{\rho_{cr}}{\rho_0}$, let's now present the $q(\lambda)$ function as:

$$q(\lambda) = \frac{\lambda\varepsilon(\lambda)}{\varepsilon(1)} = \frac{v}{v_{cr}} \frac{\rho}{\rho_{cr}} \frac{\rho}{\rho_0} = \frac{\rho v}{\rho_{cr} v_{cr}}. \tag{15.61}$$

This equation shows that $q(\lambda)$ is a ratio of mass velocity and critical mass velocity.

The $q(\lambda)$ graph is shown in Fig. 15.8. It is important to note that for each value of $q(\lambda) \neq 1$ corresponds two λ values: one, under the subsonic regime, and another one under the supersonic regime.

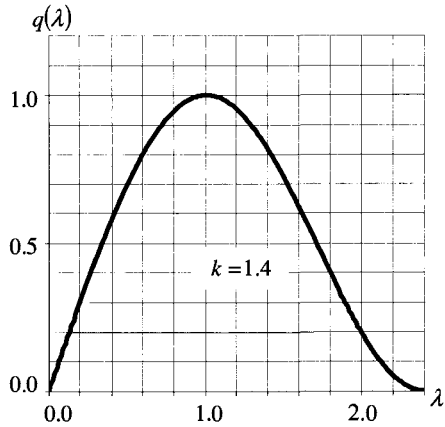

Fig. 15.8

With the introduction of the $q(\lambda)$ function, Eq. (15.58) can be rewritten as follows:

$$Q_m = \frac{p_0 S}{\sqrt{RT_0}} \sqrt{k\left(\frac{2}{k+1}\right)^{\frac{k+1}{k-1}}} q(\lambda). \tag{15.62}$$

The $q(\lambda)$ value in Eq. (15.62) should be taken in the same cross-section as S. For instance, when de Laval's nozzle is working under the design regime at $x = x_{cr}$, $\lambda = 1$, one should assume $S = S_{cr}$. To illustrate possible applications of gas-dynamic functions, let's review de Laval's nozzle operation under the design regime. In this case:

$$Q_m = \rho_{cr} v_{cr} S_{cr} = \rho_{output} v_{output} S_{output}, \tag{15.63}$$

where ρ_{output}, v_{output} are density and velocity in the nozzle's output cross-section, and S_{output} is the area of this cross-section. Following Eqs. (15.62) and (15.63):

$$\frac{\rho_{output} v_{output}}{\rho_{cr} v_{cr}} = q(\lambda_{output}) = \frac{S_{cr}}{S_{output}}. \tag{15.64}$$

Let's assume that $p_0 = 10^7$ Pa, $S_{cr} = 0.5$ cm^2, $R = 287$ m^2/s^2*deg, adiabatic exponent $k = 1.4$. It is required to determine λ, M, p, T in the output cross-section of the nozzle. From Eq. (15.64), $q(\lambda_{output}) = 0.25$. from the gas dynamic function tables for $k = 1.4$, $q(\lambda) = 0.25$ value:

$\lambda_1 = 0.16$; $M_1 = 0.146$; $\tau(\lambda_1) = 0.996$; $\pi(\lambda_1) = 0.985$;
$\lambda_2 = 1.95$; $M_2 = 2/94$; $\tau(\lambda_2) = 0.366$; $\pi(\lambda_2) = 0.0297$.

As $\lambda_1 < 1$ and $\lambda_2 > 1$, the first regime corresponds to the adiabatic compression, and the second one, to adiabatic expansion.

Using Eq. (15.57), results in:

$T_1 = \tau(\lambda_1) T_0 = 292°K$, $p_1 = \pi(\lambda_1) p_0 = 9.85*10^6$Pa;
$T_2 = \tau(\lambda_2) T_0 = 107°K$, $p_2 = \pi(\lambda_2) p_0 = 2.97*10^5$Pa.

And from Eq. (15.62):

$$Q_m = \frac{p_0 S}{\sqrt{R T_0}} \sqrt{k \left(\frac{2}{k+1} \right)^{\frac{k+1}{k-1}}} q(1) = 1.18 \text{ kg/s}.$$

8. Shock waves

In the previous sections, flows where the distribution of all variables (ρ, v, h, T) is continuous in the gas are studied. There are, however, such situations where the flow variables experience discontinuity. These discontinuities occur along certain surfaces called the rupture surfaces. Intersecting the rupture surface, the flow variables experience a leap, otherwise called a shock wave.

In order to explain why such leaps occur, it is necessary to review a tube closed on one end by a piston and filled with a gas (Fig. 15.1). At the initial time, both the piston and the gas are immobile. When the piston begins to enter the tube, a disturbance (gas compression) arises in front of it. It is possible to consider the disturbance propagation velocity in each cross-section to be equal to the local sound

velocity. The propagation of the piston-created disturbances can be considered as a sequence of sound waves continuously following one another where each subsequent wave is spreading in the gas disturbed by the previous waves. The gas compression is accompanied by heating, and the disturbance propagation velocity increases with increase in temperature. Thus each subsequent wave will move relative to the tube's walls faster than the previous one. The waves will catch up with one another, pile up and form one strong compression wave – the shock wave.

When the piston is moving within the tube, the under-pressured waves emerge behind it. But in this case the waves will not emerge with one another as a subsequent wave will be in a gas cooled-down region as a result of the previous wave, so the propagation velocity of the subsequent wave will be lower than that of the preceding wave. Thus, the under-pressured waves cannot form shock waves.

Direct compression leap

Spatially immobile shock wave whose front is perpendicular to the flow velocity is called a direct leap (Fig. 15.9). In order to compute the direct leap, i. e., to establish a connection between the gas parameters before and after the leap, the mass conservation law, momentum law and energy conservation law are used. The motion is considered as stationary, and the process as adiabatic. Assuming the tube's cross-section is constant ($S = 1$):

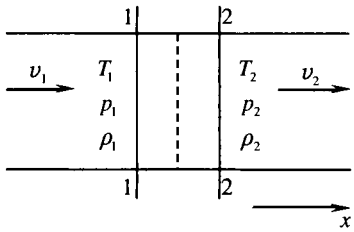

Fig. 15.9

$$\rho_1 v_1 = \rho_2 v_2 = m. \tag{15.65}$$

Here, m is mass throughflow per unit area of the tube; the subscript 1 relates to the gas parameters before the leap, and the subscript 2 relates to the gas parameters after the leap. The kinetic momentum law Eq. (2.58) in this case (i. e., when the gravitational force and friction are disregarded), as projected on $0x$ axis, is:

$$m(v_2 - v_1) = P_x = p_1 - p_2. \tag{15.66}$$

From the energy conservation law:

$$\frac{k}{k-1}\frac{p_1}{\rho_1} + \frac{v_1^2}{2} = \frac{k}{k-1}\frac{p_2}{\rho_2} + \frac{v_2^2}{2} = \frac{k}{k-1}\frac{p_0}{\rho_0}. \tag{15.67}$$

From Eq. (15.65):

$$v_1 = \frac{m}{\rho_1},\ v_2 = \frac{m}{\rho_2},$$
$$\frac{k}{k-1}\left(\frac{p_1}{\rho_1} - \frac{p_2}{\rho_2}\right) = \frac{m^2}{2}\left(\frac{1}{\rho_2^2} - \frac{1}{\rho_1^2}\right). \tag{15.68}$$

Canceling m from Eq. (15.68), results in:

$$\frac{k}{k-1}\left(\frac{p_1}{\rho_1}-\frac{p_2}{\rho_2}\right)=\frac{1}{2}\frac{p_1-p_2}{\frac{1}{\rho_2}-\frac{1}{\rho_1}}\left(\frac{1}{\rho_2^2}-\frac{1}{\rho_1^2}\right)=\frac{p_1-p_2}{2}\left(\frac{1}{\rho_2}+\frac{1}{\rho_1}\right). \quad (15.69)$$

Multiplying Eq. (15.69) by $\frac{\rho_2}{p_2}$:

$$\frac{k}{k-1}\left(\frac{p_1}{p_2}\frac{\rho_2}{\rho_1}-1\right)=\frac{1}{2}\left(\frac{p_1}{p_2}-1\right)\left(\frac{\rho_2}{\rho_1}-1\right),$$

or, after the reduction of the similar terms:

$$\frac{k+1}{k-1}\frac{p_1}{p_2}\frac{\rho_2}{\rho_1}=\frac{k+1}{k-1}+\frac{p_1}{p_2}-\frac{\rho_2}{\rho_1}. \quad (15.70)$$

Solving Eq. (15.70) relative to $\frac{p_2}{p_1}$ results:

$$\frac{p_1}{p_2}=\frac{\frac{k+1}{k-1}\frac{\rho_2}{\rho_1}-1}{\frac{k+1}{k-1}-\frac{\rho_2}{\rho_1}}, \quad (15.71)$$

or, solving it relative to $\frac{\rho_2}{\rho_1}$:

$$\frac{\rho_2}{\rho_1}=\left(\frac{k+1}{k-1}\frac{p_2}{p_1}+1\right)\Big/\left(\frac{k+1}{k-1}\frac{p_2}{p_1}\right). \quad (15.72)$$

The Eq. (15.71) or (15.72) functions are called the shock adiabatic or Gugonio's adiabatic impact. Following Eq. (15.71):

$$\frac{p_2}{p_1}\to\infty \text{ when } \frac{\rho_2}{\rho_1}\to\frac{k+1}{k-1} \text{ and}$$

$$\frac{p_2}{p_1}\to-\frac{k+1}{k-1} \text{ when } \frac{\rho_2}{\rho_1}\to\infty.$$

Fig. 15.10 displays both the Gugonio's adiabatic impact and Poisson's adiabatic impact. When reviewing these adiabatic shock waves, a number of questions arise.

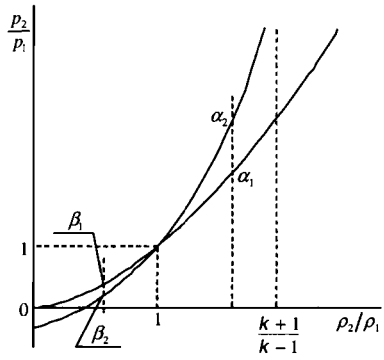

Fig. 15.10

First, at $\rho_2/\rho_1 = 0$, the ratio p_2/p_1, under Eq. (15.71), becomes negative, which has no physical meaning. Second, why $\rho_2/\rho_1 \to \infty$ at $p_2/p_1 \to \infty$ according to Poisson's adiabatic but according to Gugonio's adiabatic impact the maximum compression is limited to $\frac{k+1}{k-1}$?

Let's consider the points α_1 and α_2 in Fig. 15.10 (they correspond to a value $\frac{\rho_2}{\rho_1}>1$) and β_1 and β_2 (they correspond to a value $\frac{\rho_2}{\rho_1}<1$). According to Eq. (7.37), the entropy change is:

$$s_2 - s_1 = C_V \ln\left[\frac{p_2}{p_1}\left(\frac{\rho_1}{\rho_2}\right)^k\right]. \tag{15.73}$$

It is evident in Fig. 15.10 that at $\frac{\rho_2}{\rho_1}>1$:

$$\left(\frac{p_2}{p_1}\right)_\Gamma > \left(\frac{p_2}{p_1}\right)_\Pi, \tag{15.74}$$

where $\left(\frac{p_2}{p_1}\right)_\Gamma$ is pressure ratio as determined from the Gugonio's adiabatic impact, and $\left(\frac{p_2}{p_1}\right)_\Pi$ is pressure ratio as determined from the Poisson's adiabatic impact. Therefore, according to inequality Eq. (15.74):

$$\left(\frac{p_2}{p_1}\right)_\Gamma\left(\frac{\rho_1}{\rho_2}\right)^k > \left(\frac{p_2}{p_1}\right)_\Pi\left(\frac{\rho_1}{\rho_2}\right)^k = 1. \tag{15.75}$$

From Eqs. (15.73) and (15.75) at $\frac{\rho_2}{\rho_1} > 1$:

$$s_2 - s_1 = C_V \ln\left[\left(\frac{p_2}{p_1}\right)_\Gamma\left(\frac{\rho_1}{\rho_2}\right)^k\right] > 0. \tag{15.76}$$

Repeating the similar procedure for points β_1 and β_2 (i. e., $\frac{\rho_2}{\rho_1} < 1$), results in:

$$S_2 - S_1 = C_V \ln\left[\left(\frac{p_2}{p_1}\right)_\Pi\left(\frac{\rho_1}{\rho_2}\right)^k\right] < 0. \tag{15.77}$$

The inequalities Eqs. (15.76) and (15.77) show that the compression under the Gugonio's adiabatic impact is accompanied by entropy increase, and the under-pressured process, by entropy decrease. Thus, entropy growth and irreversible transformation of the mechanical energy into heat occur in the compression shock wave. This prevents the unlimited increase of the $\frac{\rho_2}{\rho_1}$ value.

Entropy decline occurs in the under-pressured shock wave. This is physically impossible as it contradicts the second law of thermodynamics. I. e., the under-pressured shock waves are impossible, and the part of Gugonio's adiabatic impact corresponding to $\frac{\rho_2}{\rho_1}<1$ does not have physical meaning.

Let's now return to Eqs. (15.65), (15.66) and (15.67) and cancel pressures and densities from them.

From Eq. (15.65):

$$\rho_1 = \frac{m}{v_1},\ \rho_2 = \frac{m}{v_2}.$$

Substituting these expressions into Eq. (15.66), results in:

$$m(v_2 - v_1) = \frac{p_1}{\rho_1}\rho_1 - \frac{p_2}{\rho_2}\rho_2 = m\left(\frac{p_1}{\rho_1}\frac{1}{v_1} - \frac{p_2}{\rho_2}\frac{1}{v_2}\right). \tag{15.78}$$

Using Eq. (15.67), excluding $\frac{p_1}{\rho_1}$ and $\frac{p_2}{\rho_2}$ values from Eq. (15.78) and, after simple transformations:

$$v_1 v_2 = \frac{2k}{k+1}\frac{p_0}{\rho_0} \tag{15.79}$$

or, considering Eq. (15.35):

$$v_1 v_2 = a_{cr}^2. \tag{15.80}$$

Eq. (15.80) connecting the velocity values before and after the leap is called the Prandtl's ratio. It can be represented differently by:

$$\frac{v_1}{a_{cr}} * \frac{v_2}{a_{cr}} = \lambda_1 \lambda_2 = 1. \tag{15.81}$$

Considering this equation, the following cases are technically possible:

$$(1)\ \lambda_1 > 1, \lambda_2 < 1;\ (2)\ \lambda_2 = \lambda_2;\ (3)\ \lambda_1 < 1, \lambda_2 > 1.$$

According to the continuity equation Eqs. (15.65) and (15.80):

$$\frac{\rho_2}{\rho_1} = \frac{v_1}{v_2} = \frac{v_1^2}{v_1 v_2} = \frac{v_1^2}{a_{cr}^2} = \lambda_1^2 . \tag{15.82}$$

Case (3) corresponds to the condition $\frac{\rho_2}{\rho_1} < 1$, i. e., the under-pressured leap. As it was shown before, this case is a physical impossibility. Case (2), $\rho_1 = \rho_2$, there is no leap. Case (1) corresponds to the condition $\frac{\rho_2}{\rho_1} > 1$, i. e., the compression shock wave.

The conditions $\lambda_1 > 1$, $\lambda_2 < 1$ mean that the flow in front of the leap is supersonic, and behind the leap is subsonic.

Thus, compression leaps (direct shock waves) can occur only in a supersonic flow. When crossing through the direct shock wave, a supersonic flow converts to a subsonic flow. The inverse case is impossible.

Let's analyze the changes in the gas parameters when it is crossing through a direct compression leap.

Because the process is adiabatic, the drag temperature T_{01} before the leap is equal to the drag temperature T_{02} after the leap, i. e.:

$$T_{01} = T_{02} = T_0 . \tag{15.83}$$

Therefore:

$$a_{01} = \sqrt{kRT_{01}} = a_{02} = \sqrt{kRT_{02}} = a_0 .$$

To determine the pressure change, the Gugjnio's adiabatic impact Eqs. (15.71) and (15.82) are used. Then:

$$\frac{\Delta p}{p_1} = \frac{p_2 - p_1}{p_1} = \frac{p_2}{p_1} - 1 = \frac{\frac{k+1}{k-1}\frac{\rho_2}{\rho_1} - 1}{\frac{k+1}{k-1} - \frac{\rho_2}{\rho_1}} - 1 = 2k\frac{\lambda_1^2 - 1}{k+1-(k-1)\lambda_1^2} . \tag{15.84}$$

Replacing λ_1 in Eq. (15.84) using Eq. (15.42), results in:

$$\frac{\Delta p}{p_1} = \frac{2k}{k+1}\left(M_1^2 - 1\right). \tag{15.85}$$

When $M \to \infty$ or $\lambda \to \sqrt{\frac{k+1}{k-1}}$, $\frac{\Delta p}{p_1} \to \infty$.

The density change, as follows from Eq. (15.82), is:

$$\frac{\Delta\rho}{\rho_1} = \frac{\rho_2 - \rho_1}{\rho_1} = \lambda_1^2 - 1.$$

Now Eqs. (15.433) and (15.83) are used to determine temperature changes. Then, considering Prandtl's Eq. (15.81), results in:

$$\frac{T_2}{T_1} = \frac{T_2}{T_0}\frac{T_0}{T_1} = \frac{\tau(\lambda_2)}{\tau(\lambda_1)} = \frac{1 - \frac{k-1}{k+1}\lambda_2^2}{1 - \frac{k-1}{k+1}\lambda_1^2} = \frac{1 - \frac{k-1}{k+1}\frac{1}{\lambda_1^2}}{1 - \frac{k-1}{k+1}\lambda_1^2}.$$

When $\lambda_1 \to \sqrt{\frac{k+1}{k-1}}$, i. e., $v \to v_{max}$, $\frac{T_2}{T_1} \to \infty$. This does not mean, however, that $T_2 \to \infty$, because at $v \to v_{max}$ $T_1 \to 0$. When gas is crossing the shock wave, entropy increases. Thus, this process is accompanied by a change in the drag pressure. As the drag temperature is maintained, then under the Mendeleyev-Clapeyron equation of state:

$$\frac{p_{02}}{\rho_{02}} = \frac{p_{01}}{\rho_{01}},$$

and:

$$\sigma = \frac{p_{02}}{p_{01}} = \frac{\rho_{02}}{\rho_{01}} = \frac{\rho_{02}}{\rho_2}\frac{\rho_2}{\rho_1}\frac{\rho_1}{\rho_{01}}.$$

Using Eqs. (15.44), (15.81) and (15.82), the latter equation can be presented as:

$$\sigma = \lambda_1^2 \frac{\varepsilon(\lambda_1)}{\varepsilon(\lambda_2)} = \frac{\rho_{02}}{\rho_{01}} = \lambda_1^2 \left(\frac{1 - \frac{k-1}{2}\lambda_1^2}{1 - \frac{k-1}{2}\frac{1}{\lambda_1^2}} \right)^{\frac{1}{k-1}}. \qquad (15.86)$$

This equation shows that at $\lambda_1 > 1$, always $\sigma < 1$, i. e., $p_{02} < p_{01}$. Therefore, the mechanical energy irreversibly turns into heat, exactly as it should with increasing entropy.

Oblique compression leap

When the gas flow direction changes, for instance, at flow around a wedge (Fig. 15.11), so-called oblique compression leaps occur. The front of such leaps is inclined toward the direction of the overrunning flow. Clearly, in this case the mass throughflow through unit area of the frontal surface OA is equal to:

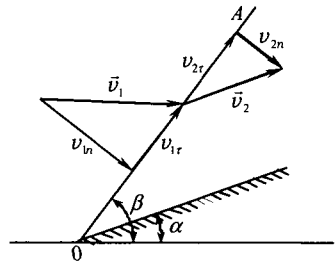

Fig. 15.11

$$\rho_1 v_{n1} = \rho_2 v_{n2} = m, \qquad (15.87)$$

where v_{n1}, v_{n2} are velocity projections onto the normal to the leap plane.

Let's write the law of kinetic momentum Eq. (2.54) in the following format:

$$m(\bar{v}_2 - \bar{v}_1) = \bar{n}(p_1 - p_2), \qquad (15.88)$$

where $\bar{n}$ is singular vector to the normal OA.

The energy conservation law maintains its format-Eq. (15.67).

Projecting Eq. (15.88) onto the plane of the OA leap and onto its normal, results in:

$$v_{2\tau} - v_{1\tau} = 0, \quad m(v_{2n} - v_{1n}) = p_1 - p_2, \qquad (15.89)$$

where $v_{2\tau}$, $v_{1\tau}$ are the velocity projections onto the leap plane.

According to the Eq. (15.89) intersecting the leap plane, the tangential component of velocity v_τ does not experience disruption, i. e.:

$$v_{1\tau} = v_{2\tau} = v_\tau.$$

As:

$$v_1^2 = v_{1n}^2 + v_\tau^2, \quad v_2^2 = v_{2n}^2 + v_\tau^2,$$

then, substituting these functions into the energy conservation law [Eq. (15.67)], results in:

$$\frac{k}{k-1}\frac{p_1}{\rho_1} + \frac{v_{1n}^2}{2} = \frac{k}{k-1}\frac{p_2}{\rho_2} + \frac{v_{2n}^2}{2} = \frac{k}{k-1}\frac{p_0}{\rho_0} - \frac{v_\tau^2}{2} = \frac{k}{k-1}\left(\frac{p_0}{\rho_0} - \frac{k-1}{2k}v_\tau^2\right). \qquad (15.90)$$

Comparing the equation groups [Eqs. (15.65), (15.66), (15.67) and Eqs. (15.87), (15.89) and (15.90)], these systems of equations are identical if the velocities v_1, v_2 in equations of the direct leap Eqs. (15.65), (15.66), (15.67) are replaced by v_{1n}, v_{2n}, and the value $\frac{k}{k-1}\frac{p_0}{\rho_0}$ by $\frac{k}{k-1}\left(\frac{p_0}{\rho_0} - \frac{k-1}{2k}v_\tau^2\right)$. I. e., all equations for the direct leap remain valid provided the indicated replacement is done.

The Gugonio's adiabatic impact, i. e., Eqs. (15.71) and (15.72), maintains its format as these equations do not include velocities. Pradtl's Eq. (15.80), considering Eqs. (15.79) and (15.89), takes the following format:

$$v_{1n}v_{2n} = \frac{2k}{k+1}\left(\frac{p_0}{\rho_0} - \frac{k-1}{2k}v_\tau^2\right) = a_{cr}^2 - \frac{k-1}{k+1}v_\tau^2. \qquad (15.91)$$

Analyzing Eq. (15.91) shows that at an oblique leap always $v_1 > v_2$, but cases $v_1 > a_{cr}$, $v_2 > a_{cr}$ can be realized. Therefore, as opposed to the direct leap, velocity behind the oblique leap can remain supersonic. Eq. (15.85) for the oblique leap takes the following format (see Fig. 15.11):

$$\frac{\Delta p}{p_1} = \frac{2k}{k+1}\left(\frac{v_{1n}^2}{a^2} - 1\right) = \frac{2k}{k+1}\left(\frac{v_1}{a^2}\sin^2\beta - 1\right) = \frac{2k}{k+1}\left(M_1^2\sin^2\beta - 1\right),$$

i. e., pressure change for the oblique leap is smaller than for the direct one. The smaller β, the weaker the leap.

9. Computation of gas ejector

Gas ejectors use a property of a gas stream moving in a gas medium to carry along with it the particles of this medium. Thus, gas ejectors are a kind of pump widely used in industry. In an ejector, a high-velocity gas stream (the active gas) and a lower-velocity gas stream (the passive gas) are introduced through the separate nozzles into a mixing chamber. The mixing goes as far as to create an almost uniform flow at the end of the mixing chamber. The flow from the mixing chamber is directed to the output diffuser. The simplest case is when both active and passive gases have the same (or almost the same) composition. In other cases, both gas flows can have different physicochemical properties. These differences can result in chemical reactions at mixing of the flows (such as burning). An ejector (Fig. 15.12) includes four major elements: the nozzle 1 of the high-pressure gas (the active gas); the nozzle 2 of the low-pressure gas (the passive gas); the mixing chamber 3, and the diffuser 4.

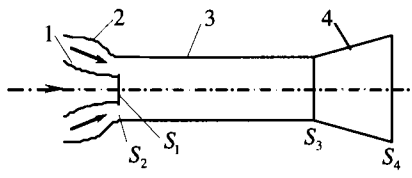

Fig. 15.12

In this section the subscripts: 1 is used for the active gas parameters at the output of the nozzle; 2, for the passive gas in the same cross-section; 3, for the mixture parameters at the output of the mixing chamber, and 0, as usual, for the drag parameters in the cross-sections under consideration.

At the exit of the high-pressure gas stream from the nozzle 1, pressure p_2 is set up in the entry cross-section of the mixing chamber. This pressure is always lower than the low-pressure gas drag pressure p_{02}. Under this pressure difference, the

low-pressure gas enters the mixing chamber through the nozzle 2. The ratio of mass throughflows Q_{m1} and Q_{m2} of the ejecting and ejected gases depends on the ratio of nozzles' areas, gas densities and ejector operating regime. The ejection factor n:

$$n = \frac{Q_{m2}}{Q_{m1}}, \tag{15.92}$$

can vary within a wide range depending of the ejector's geometric configuration.

The mass conservation law in this case clearly has the following format:

$$Q_{m3} = Q_{m1} + Q_{m2},$$

or, according to Eq. (15.92):

$$\frac{Q_{m3}}{Q_{m1}} = 1 + n. \tag{15.93}$$

The energy conservation law (disregarding the heat transfer through the ejector's walls) can be written as:

$$Q_{m1}\left(c_{p1}T_1 + \frac{v_1^2}{2}\right) + Q_{m2}\left(c_{p2}T_2 + \frac{v_2^2}{2}\right) = Q_{m3}\left(c_{p3}T_3 + \frac{v_0^2}{2}\right). \tag{15.94}$$

It is assumed from this point on that the thermodynamic parameters of the active and passive gases, and their mixture, are the same, i. e., $c_{p1} = c_{p2} = c_{p3}$, $k_1 = k_2 = k_3$. Then, changing to the drag temperatures in Eq. (15.94):

$$Q_{m1}T_{01} + Q_{m2}T_{02} = Q_{m3}T_{03}. \tag{15.95}$$

Taking Eq. (15.92) and (15.93) into consideration, Eq. (15.95) can be written in the following format:

$$T_{01} + nT_{02} = (1+n)T_{03}. \tag{15.96}$$

Let's introduce a following parameter:

$$\frac{T_{02}}{T_{01}} = \theta.$$

Then:

$$\frac{a_{2cr}}{a_{1cr}} = \sqrt{\frac{T_{02}}{T_{01}}} = \sqrt{\theta}, \tag{15.97}$$

and, according to Eq. (15.96):

$$\frac{a_{3cr}}{a_{1cr}} = \sqrt{\frac{T_{03}}{T_{01}}} = \sqrt{\frac{1+n\theta}{1+n}}. \tag{15.98}$$

Disregarding friction about the cylindrical wall of the mixing chamber, the momentum law can be written as follows:

$$Q_{m3}v_3 - Q_{m1}v_1 - Q_{m2}v_2 = p_1S_1 + p_2S_2 - p_3S_3 . \tag{15.99}$$

Let's review the following equation:

$$Q_m v + pS = Q_m\left(v + \frac{p}{\rho v}\right).$$

Using Eqs. (15.1), (15.32), (15.35) and (15.43):

$$\frac{p}{\rho_0} = RT = RT_0\tau(\lambda) = \frac{k-1}{2k}a_{cr}^2\left(1 - \frac{k-1}{k+1}\lambda^2\right), \quad v = a_{cr}\lambda .$$

Then:

$$Q_m v + pS = Q_m a_{cr}\frac{k+1}{2k}\left(\lambda + \frac{1}{\lambda}\right). \tag{15.100}$$

From Eqs. (15.99) and (15.100):

$$Q_{m1}a_{1cr}\left(\lambda_1 + \frac{1}{\lambda_1}\right) + Q_{m2}a_{2cr}\left(\lambda_2 + \frac{1}{\lambda_2}\right) = Q_{m3}a_{3cr}\left(\lambda_3 + \frac{1}{\lambda_3}\right).$$

Dividing this equation by $Q_{m1}a_{1cr}$ and considering Eqs. (15.92), (15.93), (15.97) and (15.98), results in:

$$\lambda_1 + \frac{1}{\lambda_1} + n\sqrt{\theta}\left(\lambda_2 + \frac{1}{\lambda_2}\right) = \sqrt{(1+n)(1+n\theta)}\left(\lambda_3 + \frac{1}{\lambda_3}\right). \tag{15.101}$$

The second equation, which together with Eq. (15.101) is used in the ejector design, is obtained assuming the cylindrical shape of the mixing chamber, i.e., from equation:

$$S_3 = S_1 + S_2 . \tag{15.102}$$

According to Eq. (15.62), the mass throughflow of the gas Q_m is:

$$Q_m = \frac{p_0 S}{\sqrt{RT_0}}\sqrt{k\left(\frac{2}{k+1}\right)^{\frac{k-1}{k+1}}}\,q(\lambda) . \tag{15.103}$$

Solving this equation relative to S, substituting the result into Eq. (15.102), and considering Eqs. (15.92), (15.93), (15.97) and (15.98), results in:

$$\frac{\sqrt{(1+n)(1+n\theta)}}{p_{03}q(\lambda_3)} = \frac{1}{p_{01}q(\lambda_1)} + \frac{n\sqrt{\theta}}{p_{02}q(\lambda_2)}, \tag{15.104}$$

According to Eqs. (15.92), (15.97) and (15.103):

$$n = \frac{1}{\alpha\sqrt{\theta}} \frac{p_{02}}{p_{01}} \frac{q(\lambda_2)}{q(\lambda_1)}, \tag{15.105}$$

where $\alpha = \frac{S_1}{S_2}$.

Five Eqs. (15.97), (15.98), (15.101), (15.104) and (15.105), with 12 variables: p_{01}, p_{02}, p_{03}, T_{01}, T_{02}, T_{03}, λ_1, λ_2, λ_3, n, α, θ, are required to design gas ejector. Therefore, if the parameters at the input of the mixing chamber are supplied, i. e., the p_{01}, p_{02}, T_{01}, T_{02}, λ_1, λ_2 values, and the n (or α) value, the indicated equations enable to determine the mixture parameters at the output from the mixing chamber, i. e., p_{03}, T_{03}, λ_3 values as well as θ and α (or n) values. Using the mixing chamber stream output parameters, it is possible to determine the stream parameters at the output from the diffuser. To perform this, it is necessary to know the diffuser's ratio of the output to input cross-section areas $\beta = \frac{S_4}{S_3}$ and the drag pressure loss factor within the diffuser $\sigma = \frac{p_{04}}{p_{03}}$.

As $T_{04} = T_{03}$, from the condition $Q_{m3} = Q_{m4}$ and Eq. (15.103):

$$p_{04} S_4 q(\lambda_4) = p_0 S_3 q(\lambda_3),$$

or:

$$q(\lambda_4) = \frac{1}{\beta\sigma} q(\lambda_3).$$

Having determined λ_4 from this equation and knowing p_{04}, T_{04}, all remaining flow parameters at the diffuser's output can be determined.

10. Transient-free gas flow in tubes[1]

In order to derive equations describing gas transient-free flow in tubes the in kinetic energy law Eq. (2.75) should be employed, i. e.:

$$\int_V \frac{\partial}{\partial t}\left(\frac{\rho v^2}{2}\right) dV + \int_S \frac{\rho v^2}{2} v_n dS = \int_V \rho \vec{F} \cdot \vec{v} dV + \int_S \vec{p}_n \vec{v} dS + \int_V \rho N_i dV, \tag{15.106}$$

where, according to Eq. (4.43):

$$\rho N_i = p \operatorname{div} \bar{v} - W. \tag{15.107}$$

[1] For the reader's convenience, some derivations presented in Ch. XI are repeated here.

The product $\bar{p}_n \bar{v}$ can be presented as:

$$\bar{p}_n \bar{v} = (-p\bar{n} + \bar{\tau}_n)\bar{v} = -- pv_n + \tau^*. \tag{15.108}$$

The values W and τ^* are the terms caused by the gas viscosity or, which is the same, by friction. Substituting Eqs. (15.107) and (15.108) into Eq. (15.106) and considering that under the Gauss–Ostrogradsky theorem:

$$\int_S p v_n dS = \int_S \operatorname{div} p\bar{v} dV,$$

$$\int_V \frac{\partial}{\partial t}\left(\frac{\rho v^2}{2}\right) dV + \int_S \frac{\rho v^2}{2} v_n dS = \int_V \left(\rho \vec{F} \cdot \vec{v} - \operatorname{div} p\bar{v} + p \operatorname{div} \bar{v}\right) dV - \frac{dA}{dt}, \tag{15.109}$$

where:

$$\frac{dA}{dt} = \int_V W dV = \int_S \tau^* dS$$

is friction force capacity.
Let's introduce a function:

$$\mathrm{P} = \frac{dp}{\rho} \quad \text{or} \quad \nabla \mathrm{P} = \frac{1}{\rho} \nabla p. \tag{15.110}$$

In this case:

$$p \operatorname{div} \bar{v} - \operatorname{div} p\bar{v} = -\bar{v} \nabla p = -\rho \bar{v} \nabla \mathrm{P},$$

and Eq. (15.109) can be rewritten as:

$$\int_V \frac{\partial}{\partial t}\left(\frac{\rho v^2}{2}\right) dV + \int_S \rho \frac{v^2}{2} v_n dS = \int_V \left(\rho \vec{F} \cdot \vec{v} - \rho \bar{v} \nabla \mathrm{P}\right) dV - \frac{dA}{dt}. \tag{15.111}$$

Let's assume that:

(1) the flow is transient-free, i. e.,

$$\frac{\partial}{\partial t} \equiv 0, \quad \operatorname{div} \rho \bar{v} = 0;$$

(2) mass force has potential, $\bar{F} = \nabla \Pi$.

Based on these assumptions:

$$(\bar{F} - \nabla \mathrm{P})\rho\vec{v} = \nabla(\Pi - \mathrm{P})\rho\bar{v} = \nabla(\Pi - \mathrm{P})\rho\vec{v} + (\Pi - \mathrm{P}) \operatorname{div} \rho\vec{v} = \operatorname{div}[\rho(\Pi - \mathrm{P})\bar{v}],$$

and Eq. (15.111) takes the following format:

$$\int_S \rho \frac{v^2}{2} v_n \, dS = \int_V \mathrm{div}[\rho(\Pi - \mathrm{P})\bar{v}] dV - \frac{dA}{dt}, \tag{15.112}$$

or, based on Gauss–Ostrogradsky theorem:

$$\int_S \left(\frac{v^2}{2} - \Pi + \mathrm{P} \right) \rho v_n \, dS = -\frac{dA}{dt}. \tag{15.113}$$

Now consider a tube's segment constrained between the cross-sections S_1 and S_2 and tube's side surface S_3. Because:

$$\text{on } S_1,\ v_n = -v;\ \text{on } S_2,\ v_n = v;\ \text{and on } S_3,\ v_n = 0,$$

Eq. (15.113) can be rewritten as:

$$\int_{S_2} \left(\frac{v^2}{2} - \Pi + \mathrm{P} \right) \rho v_n \, dS - \int_{S_1} \left(\frac{v^2}{2} - \Pi + \mathrm{P} \right) \rho v_n \, dS = -\frac{dA}{dt}. \tag{15.114}$$

According to the uniform mean value theorem:

$$\int_S \left(\frac{v^2}{2} - \Pi + \mathrm{P} \right) \rho v_n \, dS = \left(\frac{v^2}{2} - \Pi + \mathrm{P} \right)_{\mathrm{avg}} \int_S \rho v_n \, dS = \left(\frac{v^2}{2} - \Pi + \mathrm{P} \right)_{\mathrm{avg}} Q_m. \tag{15.115}$$

The mass throughflow Q_m is:

$$Q_m = \frac{dm}{dt}, \tag{15.116}$$

where dm is mass of the gas that flowed through the cross-section during time dt. Under transient-free flow, $Q_{m1} = Q_{m2}$.

From Eqs. (15.114), (15.115) and (15.116)[2]:

$$\left(\frac{v^2}{2} - \Pi + \mathrm{P} \right)_2 - \left(\frac{v^2}{2} - \Pi + \mathrm{P} \right)_1 = -\frac{1}{Q_m} \frac{dA}{dt} = -\frac{dA}{dm} = -\bar{h}_{1\text{-}2}, \tag{15.117}$$

where $\bar{h}_{1\text{-}2}$ is the work of friction forces *per unit mass*.

Suppose distance between the cross-sections S_1 and S_2 is dx. Then at $dx \to 0$ following Eq. (15.115):

$$d\left(\frac{v^2}{2} - \Pi + \mathrm{P} \right) + d\bar{h} = -d\Pi + \frac{dp}{\rho} + v dv + d\bar{h} = 0. \tag{15.118}$$

Eq. (15.118) is called the mechanical format of the energy equation or expanded Bernoulli's equation. In order to use this equation, it is necessary to assign the $p(\rho)$ function, i. e., it is necessary to assign a type of thermodynamic process

[2] For the convenience's sake, the subscript$_{\mathrm{avg}}$ is dropped.

that occurs while the gas is flowing in the pipeline. The process is assumed polytropic with a constant polytropic curve exponent n = const, i. e:

$$\frac{p}{\rho^n} = \text{const} \quad \text{or} \quad \frac{p}{p_1} = \left(\frac{\rho}{\rho_1}\right)^n . \tag{15.119}$$

According to Darcy-Weisbach equation [Eq. (11.13)], the head loss along the dx length is equal to:

$$d\bar{h} = \lambda \frac{dx}{D} \frac{v^2}{2g}, \tag{15.120}$$

where D is the tube's diameter.

Experiments showed that the correlations between λ and Re, and also between λ and relative roughness ε identified for fluids can be applied to the gas flow by disregarding the first approximation by the correlation λ *vs.* Mach number M. For turbulent flow it is acceptable to consider $\lambda \approx \text{const}$. Indeed, the dynamic viscosity μ depends on the temperature as follows:

$$\mu = \mu_0 \sqrt{\frac{T}{T_0}},$$

where $\mu = \mu_0$ at $T = T_0$. Then, as $Q_m = \frac{\pi D^2}{4}$:

$$\text{Re} = \frac{\rho v D}{\mu} = \frac{\rho v D \sqrt{T_0}}{\mu_0 \sqrt{T}} = \frac{4 Q_m \sqrt{T_0}}{\pi D \mu_0 \sqrt{T}} = \frac{A}{\sqrt{T}},$$

and A = const.

The correlation λ *vs.* Re in the turbulent flow is at its strongest in hydraulically smooth tubes where λ is determined from Blasius equation:

$$\lambda = \frac{1}{\sqrt[4]{\text{Re}}} = \frac{T^{\frac{1}{8}}}{\sqrt{100A}} \approx T^{\frac{1}{8}}.$$

When the gas temperature changes by ±30 °C, the absolute temperature changes by ±10 %; therefore, λ changes by ±2 %. So, indeed, it is possible to consider λ = const. Substituting Eq. (15.120) into Eq. (15.118) and, as usual, disregarding mass forces, results in:

$$\frac{dp}{\rho} + v dv + \lambda \frac{dx}{D} \frac{v^2}{2} = 0. \tag{15.121}$$

Multiplying Eq. (15.121) by the ρ^2 and expressing ρ through p using Eq. (15.119):

$$\rho_1 \left(\frac{p}{p_1}\right)^{\frac{1}{n}} dp + (\rho v)^2 \frac{dv}{v} + \lambda \frac{dx}{D} \frac{(\rho v)^2}{2} = 0.$$

As ρv = const when D = const, then, integrating this equation in full differentials with respect to x from $x = 0$ to x, with respect to v from $v = v_1$ to v, and with respect to p from p_1 to p results:

$$\frac{n}{n+1}\frac{\rho_1}{\rho_1^{1/n}}\left(p^{\frac{n+1}{n}} - p_1^{\frac{n+1}{n}}\right) + (\rho v)^2 \ln\frac{v}{v_1} + \lambda\frac{x}{D}\frac{(\rho v)^2}{2} = 0. \qquad (15.122)$$

As at D = const, $\rho v = \rho_1 v_1$, then:

$$\frac{v}{v_1} = \frac{\rho}{\rho_1} = \left(\frac{p_1}{p}\right)^{\frac{1}{n}},$$

and Eq. (15.122) can be rewritten as:

$$\frac{n}{n+1}\frac{\rho_1}{\rho_1^{1/n}}\left(p^{\frac{n+1}{n}} - p_1^{\frac{n+1}{n}}\right) + \frac{(\rho v)^2}{n}\ln\frac{p_1}{p} + \lambda\frac{x}{D}\frac{(\rho v)^2}{2} = 0. \qquad (15.123)$$

For the gas trunk-lines:

$$\frac{1}{n}\ln\frac{p_1}{p} << \lambda\frac{x}{2D}.$$

Let's review the following typical example. Suppose D = 1 m, $x = l = 10^5$ m, $\lambda = 1.5*10^{-2}$, n = 1.2, $p = p_2$, $\frac{p_1}{p_2} = 2$. Then:

$$\lambda\frac{l}{2D} = 0.75*10^{-3}, \quad \frac{1}{n}\ln\frac{p_1}{p_2} = 0.58.$$

Thus, the term with the logarithm in Eq. (15.123) can be disregarded compared to the other terms. Assuming $x = l$, $p = p_2$, from Eq. (15.123):

$$\frac{n}{n+1}\frac{\rho_1}{\rho_1^{1/n}}\left(p_1^{\frac{n+1}{n}} - p_2^{\frac{n+1}{n}}\right) = \lambda\frac{l}{d}\frac{(\rho v)^2}{2}. \qquad (15.124)$$

And the mass throughflow is:

$$Q_m = \frac{\pi}{4}D^2\rho v = \frac{\pi}{4}\sqrt{\frac{2n}{n+1}\frac{\rho_1 D^5}{\rho_1^{1/n}\lambda l}\left(p_1^{\frac{n+1}{n}} - p_2^{\frac{n+1}{n}}\right)}. \qquad (15.125)$$

This equation shows that $Q \sim D^{2.5}$, i. e., the mass throughflow is strongly dependent on the pipeline diameter. If $n = k$ in Eqs. (15.124) and (15.125), it is possible to obtain equations for pressure and throughflow in adiabatic flow. In long gas

pipelines the flow is usually isothermal. In this case, $n = 1$, and the condition for λ is realized exactly rather than approximately.

Substituting $n = 1$ into Eqs. (15.124) and (15.125):

$$\frac{\rho_1}{p_1}\left(p_1^2 - p^2\right) = \lambda \frac{1}{d}(\rho v)^2,$$
$$Q_m = \frac{\pi}{4}\sqrt{\frac{\rho_1}{p_1}\frac{D^5}{\lambda l}\left(p_1^2 - p^2\right)} \tag{15.126}$$

Eq. (15.126) indicates that pressure in an isothermal flow changes along the gas pipeline length under the parabolic law.

11. Shukhov's equation

If at the gasline intake temperature T_1 differs from the ambient temperature T_{amb}, the gas flow will be nonisothermal.

Let's review a pipeline segment (Fig. 15.13). Disregarding mass forces and considering Eqs. (15.20) and (15.24) and from the energy conservation law Eq. (4.18):

$$\left(C_p T + \frac{v^2}{2}\right)_2 - \left(C_p T + \frac{v^2}{2}\right)_1 = \frac{1}{Q_m}\int_V \rho q_e dV \tag{15.127}$$

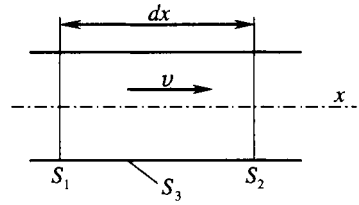

Fig. 15.13

The value $\int_V \rho q_e dV$ is the external heat supplied during unit time to the gas between the cross-sections S_1 and S_2. Disregarding the gas heat-conductivity, assuming the heat is conducted only through the side surface S_3, then:

$$\int_V \rho q_e dV = \int_{S_3} q_e^* dS = \int_x q_e^* d\chi dx, \tag{15.128}$$

where q_e^* is heat supplied during unit time through unit area of the surface S_3, and $\chi = \pi D$ is the gasline perimeter.

Substituting Eq. (15.127) into Eq. (15.126) and assuming $dx \to 0$, results in:

$$d\left(C_p T + \frac{v^2}{2}\right) = \frac{q_e^*}{Q_m}\pi D dx. \tag{15.129}$$

The value q_e^* can be represented as:

$$q_e^* = \alpha(T_{amb} - T_1), \tag{15.130}$$

where α is heat conductivity factor, and $T = T(x)$ is gas temperature in the gasline.

Disregarding changes in the velocity head along the gasline, from Eqs. (15.129) and (15.130):

$$C_p dT = \frac{\pi D}{Q_m} \alpha (T_{amb} - T) dx . \tag{15.131}$$

Integrating Eq. (15.130) on the condition that at the gasline intake at $x = 0$ $T = T_1$:

$$C_p Q_m \log \frac{(T - T_{amb})}{(T_1 - T_{amb})} = -\alpha \pi D x \tag{15.132}$$

or:

$$T = T_{amb} + (T_1 - T_{amb}) \exp\left(- \frac{\alpha \pi D}{C_p Q} x \right) . \tag{15.133}$$

Eq. (15.133) is Shukhov's equation. It was derived for calculating the cooling of heated oil pumped through a pipeline without considering heat released due to the hydraulic resistance. Shukhov's equation is totally accurate for ideal gas flowing in the tube at a subsonic velocity. Following Eq. (15.132) at $x \to \infty$ $T \to T_{amb}$. The value $x = x_1$ at which the gas temperature in the pipeline differs from T_{amb} by less than 1 °C, is determined from Eq. (15.132) as:

$$x_1 > \frac{c_p Q_m}{\alpha \pi D} \ln \frac{(T_1 - T_{amb})}{0.01 T_{amb}} .$$

The estimations using this inequality show that the x value is small, i. e., the flow in the gas pipeline can be considered as isothermal.

CHAPTER XVI

LAMINAR FLOW OF NON-NEWTONIAN FLUIDS

The preceding chapters dealt with the flow of viscous fluids, i. e., fluids for which the association between the stress tensors and deformation velocity tensors has this format:

$$p_{ik} = (-p + \lambda \operatorname{div} \bar{v})\delta_{ik} + 2\mu\varepsilon_{ik}, \tag{16.1}$$

or for an incompressible fluid:

$$p_{ik} = -p + \lambda \operatorname{div} \bar{v} + 2\mu\varepsilon_{ik}. \tag{16.2}$$

Thus, one major distinction of a viscous fluid is a linear correlation between the stress tensors and deformation velocity tensors. However, there exists a broad class of various media whose common property is the deviation from the generalized Newton's law Eqs. (16.1) or (16.2). Such fluids are called non-Newtonian fluids.

Non-Newtonian fluids are very common in the petroleum industry. They include many heavy crudes, fuel oils, drilling muds and cement slurries, and polymer solutions. Many non-Newtonian fluids, such as drilling muds, have internal spatial structure. They can be composed of paraffin crystals in oil, clay particles in drilling muds, etc. Increased stress destroys these structures and the medium properties change. As a reminder, a mathematical function connecting stress and deformation type of a continuous medium is called rheological equation, and its coefficients are called rheological constants. For instance, Eq. (16.1) is a rheological equation for a linearly-viscous compressible fluid, and the λ and μ are rheological constants.

Depending on the pressure, temperature and other parameters, the same fluid can behave as Newtonian or non-Newtonian. Thus, the selection of a model (rheological equation) for a given medium is a difficult problem.

1. Simple shear

Let's review the deformation velocity tensor:

$$\varepsilon_{ik} = \begin{pmatrix} \varepsilon_{11} & \varepsilon_{12} & \varepsilon_{13} \\ \varepsilon_{21} & \varepsilon_{22} & \varepsilon_{23} \\ \varepsilon_{31} & \varepsilon_{32} & \varepsilon_{33} \end{pmatrix}.$$

Suppose $\varepsilon_{11} = \varepsilon_{22} = \varepsilon_{33} = 0$, and out of the values $\varepsilon_{12} = \varepsilon_{21}$, $\varepsilon_{23} = \varepsilon_{32}$, $\varepsilon_{13} = \varepsilon_{31}$ only one is different from zero. Such a deformation is called *simple shear*, and the corresponding flow is called the flow with a simple shear. Clearly, the simple shear is the simplest kind of a deformation. It was shown in par. 3.3 that the velocity $\dot{\gamma}$ of skewing a direct angle between the axes x_i and x_k is equal to $2\varepsilon_{ik}$. Thus, the skewing of the direct angle between the two mutually ortagonal axes occurs in the flow with a simple shear, and the volume of the fluid particle under consideration does not change as $\varepsilon_{11} + \varepsilon_{22} + \varepsilon_{33} = \operatorname{div} v = 0$.

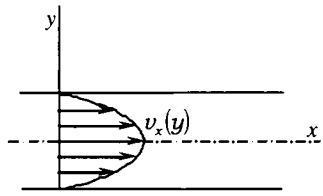

Fig. 16.1

Now some examples of flows with a simple shear are reviewed.

1. Laminar parallel-plane incompressible fluid flow between two parallel planes (Fig. 16.1). In this case:

$$v_x = v_x(y),\ v_y = v_z = 0. \tag{16.3}$$

Thus:

$$\varepsilon_{xx} = \frac{\partial v_x}{\partial x} = 0,\ \varepsilon_{yy} = \frac{\partial v_y}{\partial y} = 0,\ \varepsilon_{zz} = \frac{\partial v_z}{\partial z} = 0,\ \varepsilon_{xy} = \frac{1}{2}\left(\frac{\partial v_x}{\partial y} + \frac{\partial v_y}{\partial x}\right) = \frac{1}{2}\frac{\partial v_x}{\partial y},$$

$$\varepsilon_{yz} = \frac{1}{2}\left(\frac{\partial v_y}{\partial z} + \frac{\partial v_z}{\partial y}\right) = 0,\ \varepsilon_{zx} = \frac{1}{2}\left(\frac{\partial v_z}{\partial y} + \frac{\partial v_y}{\partial z}\right) = 0.$$

Therefore, the flow in question is a flow with a simple shear. The velocity of skewing the direct angle $x0y$, or the shear velocity is $\dot{\gamma} = 2\varepsilon_{xy} = \frac{\partial v_x}{\partial y}$. The tangential stress in the linearly-viscous fluid will be:

$$\tau = 2\mu\varepsilon_{xy} = \mu\frac{\partial v_x}{\partial y} = \mu\dot{\gamma}. \tag{16.4}$$

2. Laminar incompressible fluid flow in a circular tube. Let's introduce a cylindrical coordinate system $0xr\varphi$ so that $0x$ axis is coincident with the tube's axis. Then:

$$v_x = v_x(r),\ v_r = v_\varphi = 0. \tag{16.5}$$

Deformation velocity tensor components in a cylindrical coordinate system have the following format:

$$\varepsilon_{xx} = \frac{\partial v_x}{\partial x},\ \varepsilon_{rr} = \frac{\partial v_r}{\partial r},\ \varepsilon_{\varphi\varphi} = \frac{1}{r}\frac{\partial v_\varphi}{\partial \varphi} + \frac{v_r}{r},\ \varepsilon_{xr} = \frac{1}{2}\left(\frac{\partial v_x}{\partial r} + \frac{\partial v_r}{\partial x}\right),$$

$$\varepsilon_{r\varphi} = \frac{1}{2}\left(\frac{1}{r}\frac{\partial v_r}{\partial \varphi} + \frac{\partial v_\varphi}{\partial r} - \frac{v_\varphi}{r}\right),\ \varepsilon_{\varphi x} = \frac{1}{2}\left(\frac{\partial v_\varphi}{\partial x} + \frac{1}{r}\frac{\partial v_x}{\partial \varphi}\right). \tag{16.6}$$

Substituting Eq. (16.5) into Eq. (16.6), results in:

$$\varepsilon_{xx} = \varepsilon_{rr} = \varepsilon_{\varphi\varphi} = 0, \quad \varepsilon_{xr} = \frac{1}{2}\frac{\partial v_x}{\partial r}, \quad \varepsilon_{r\varphi} = \varepsilon_{\varphi x} = 0,$$

i. e., flow with the simple shear. The skewing velocity of the direct angle $x0r$ is equal to:

$$\dot{\gamma} = 2\varepsilon_{xr} = \frac{\partial v_x}{\partial r}, \tag{16.7}$$

and the tangential stress in the linearly-viscous fluid is equal to:

$$\tau = 2\mu\varepsilon_{xr} = \mu\frac{\partial v_x}{\partial r} = \mu\dot{\gamma}. \tag{16.8}$$

3. Laminar parallel-plane rotational flow between two coaxial cylinders (Fig.16.2). In a cylindrical coordinate system $0xr\varphi$:

$$v_x = v_r = 0, \; v_\varphi = \omega r, \tag{16.9}$$

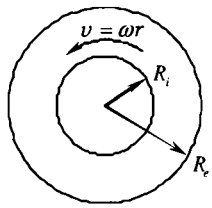

Fig. 16.2

where, $\omega = \omega(r)$ is angular velocity of the rotational flow. Substituting the velocity values of Eq. (16.9) into Eq. (16.6), results in:

$$\varepsilon_{xx} = \varepsilon_{rr} = \varepsilon_{\varphi\varphi} = 0, \quad \varepsilon_{xr} = \frac{1}{2}\frac{\partial v_x}{\partial r}, \quad \varepsilon_{\varphi x} = \varepsilon_{xr} = 0,$$
$$\varepsilon_{r\varphi} = \frac{1}{2}\left(\frac{\partial v_\varphi}{\partial r} - \frac{v_\varphi}{r}\right) = \frac{1}{2}\left(\frac{\partial(\omega r)}{\partial r} - \omega\right) = \frac{1}{2}r\frac{\partial\omega}{\partial r}, \tag{16.10}$$

i. e., the simple shear again. According to Eq. (16.10), the skewing velocity of the direct angle is:

$$\dot{\gamma} = 2\varepsilon_{r\varphi} = r\frac{\partial\omega}{\partial r}, \tag{16.11}$$

and the tangential stress in the linearly-viscous fluid is:

$$\tau = 2\mu\varepsilon_{r\varphi} = \mu r\frac{\partial\omega}{\partial r} = \mu\dot{\gamma}. \tag{16.12}$$

Eqs. (16.4), (16.8) and (16.12) represented Newton's law of viscous friction, and at $T = \text{const}$, $\mu = \text{const}$, where T is absolute temperature. The value $\varphi = \frac{1}{\mu}$ is fluidity.

As indicated earlier, the flows with simple shear are the simplest flows. Thus, they are commonly used in viscosimetric studies, i. e., for the experimental confirmation of a fluid model and for the determination of its rheological parameters.

2. Classification of non-Newtonian fluids

The classification of non-Newtonian fluids is usually based on a type of shear velocity $\dot{\gamma}$ correlation with the size of the tangential stress τ. All non-Newtonian fluids can be subdivided in three classes.

(1). The systems in which the shear velocity depends only on the size of the tangential stress, i. e.:

$$\dot{\gamma} = f(\tau). \tag{16.13}$$

These are non-Newtonian viscous fluids or nonlinearly-viscous fluids.

(2). The systems for which the shear velocity depends on the size of the tangential stress as well as on time, i. e.: $\dot{\gamma} = f(\tau, t)$.

If at a given $\dot{\gamma}$ value, stress in the fluid decreases with time, the fluid is called thixotropic, and if it increases, it is called rheopectic. The corresponding flow curves (correlations of tangential stress *vs.* shear velocity) are presented in Fig. 16.3. The arrows indicate the direction of the process (loading).

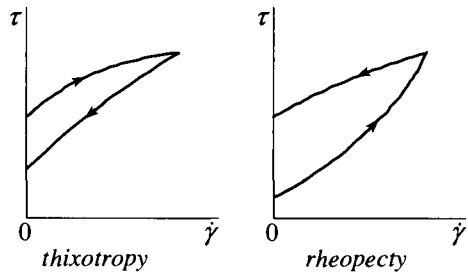

Fig. 16.3

(3). The systems possessing properties of both solids and fluids and partially demonstrating elastic restoration of the shape after the stress removal (visco-elastic fluids):

$$f_1(\gamma, \gamma', \gamma'', \ldots, \gamma^{(n)}) = f_2(\tau, \tau', \tau'', \ldots \tau^{(m)}).$$

In their turn, non-Newtonian viscous fluids can be subdivided into two groups:

(a) fluids with the initial shear stress τ_0, i. e., fluids which begin to flow (to deform) only after the tangential stress exceeds certain limit τ_0;

(b) fluids that do not have the threshold (initial) tangential stress τ_0.

For non-Newtonian fluids, exactly the same way as for the Newtonian fluids, the concepts of viscosity and fluidity can be formally introduced, namely:

$$\mu_a = \frac{\tau}{\dot{\gamma}}, \quad \varphi_a = \frac{\dot{\gamma}}{\tau} = \frac{1}{\mu_a}. \tag{16.14}$$

As opposed to the Newtonian fluids, the values μ_a and φ_a are not constants but functions of the tangential stress τ. Thus, these values are called apparent viscosity and apparent fluidity.

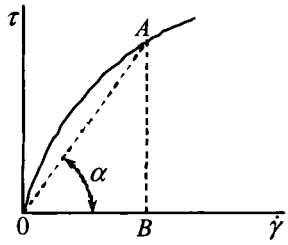

Fig. 16.4

If the flow curve (Fig. 16.4) is known, it is easy to find apparent viscosity μ_a graphically. Indeed, at point A:

$$\mu_a = \frac{\tau}{\dot{\gamma}} = \frac{AB}{OB} = \tan\alpha.$$

Following Eqs. (16.13) and (16.14):

$$\varphi_a = \varphi_a(\tau) = \frac{f(\tau)}{\tau}. \tag{16.15}$$

The sign of the shear velocity must change at the change of the stress sign, i. e.:

$$f(\tau) = -f(-\tau).$$

It means that the function $f(\tau)$ is an uneven function. Then, according to Eq. (16.15), the function $\varphi_a(\tau)$ is even.

A viscous-plastic fluid or the Bingham-Shvedov fluid is an example of fluids with the initial shear stress. Its rheological equation is:

$$\dot{\gamma} = \begin{cases} 0, & \tau \le \tau_0 \\ \dfrac{\tau - \tau_0}{\eta}, & \tau \ge \tau_0 \end{cases}, \tag{16.16}$$

where τ_0 is the initial shear stress, η is the plastic viscosity factor. The visco-plastic model is very common in descriptions of the behavior of drilling muds.

Examples of fluids without the initial shear stress are so-called "exponential fluids", i. e., fluids whose rheological equation is:

$$\tau = k\dot{\gamma}^n. \tag{16.17}$$

The k value is called "consistency", and the n is the flow exponent.

For the fluids with different flow exponents n, the k value has different dimensionality. It means that k does not have clear physical meaning, and Eq. (16.17) is just a convenient approximation. When $n < 1$, the fluid is called pseudoplastic, and when $n > 1$, it is called dilatant. At $n = 1$, Eq. (16.15) turns into Newton's law of friction, i. e., into the usual equation for the Newtonian viscous fluid, and k coincides with the dynamic viscosity factor. The flow curves are shown in Fig. 16.5, where curve 1 corresponds to the Newtonian fluid, curve 2, to a dilatant fluid, 3, to a pseudoplastic fluid and 4, to a visco-plastic fluid.

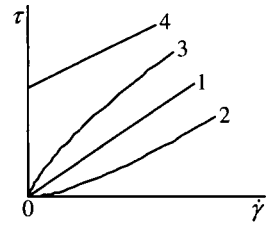

Fig. 16.5

In the following discussion only the non-Newtonian viscous fluids are discussed.

3. Viscosimetry

Viscosimetry (or viscometry) is a combination of techniques for the determination of fluids' viscosity properties, i. e., plotting the flow curve. Viscosimetry of Newtonian fluids is just the determination of their viscosity factor. For non-Newtonian fluids viscosimetry determines the type of correlation between the shear velocity and the tangential stress, and numerical values of constants (rheological parameters) of this correlation.

Most common methods to determine viscosity of fluids are capillary and rotational viscosimeters.

A conceptual scheme of the capillary viscosimeter is shown in Fig. 16.6. There, 1 is the reservoir containing the studied fluid; 2 is the calibration measuring tube; 3 is the pressure sensor. By changing the fluid's height in the reservoir or pressure p_0 over the free fluid's surface (if the reservoir is hermetically closed), it is possible to record the experimental correlation of the pressure gradient Δp_l within the l-length tube and the throughflow Q, i. e., the correlation $\Delta p_l = f(Q)$. The gradient is the sum of the gradient Δp_m over the measurement segment l_m and the gradient Δp_{inp} over the input segment of the length l_{inp} ($l_m = l - l_{inp}$)

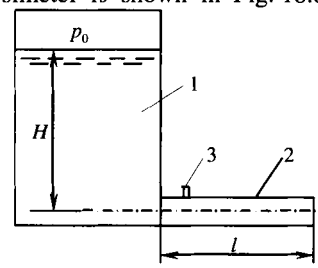

Fig. 16.6

$$\Delta p_l = \Delta p_{inp} + \Delta p_m.$$

Repeating the experiment with the same diameter tube of the length L gives the curve $\Delta p_L = f(Q)$, and again:

$$\Delta p_L = \Delta p_{inp}^{(1)} + \Delta p_m^{(1)},$$

where $\Delta p_{inp}^{(1)}$ is pressure gradient over the l-long input segment of the tube l_{inp}, and $\Delta p_m^{(1)}$ is pressure gradient over the length $L - l_{inp}$. The diameters of both tubes and conditions of the fluid's entering these tubes are the same. Thus, at equal throughflows, $\Delta p_{inp} = \Delta p_{inp}^{(1)}$, and the value:

$$\Delta p = \Delta p_L - \Delta p_l = \Delta p_m^{(1)} - \Delta p_m$$

is pressure gradient over the $L - l$ segment for an infinitely long tube. A segment of an infinitely long tube is a segment of the real tube where the end effects are not noticeable.

A conceptual scheme of the rotational viscosimeter is shown in Fig. 16.7. When the external cylinder 1 rotates at the angular velocity Ω, tangential stresses arise in fluid 2. Rotations generate torque M on the internal cylinder 3. Acted upon by this torque, the cylinder 3 rotates at the angle θ. This angle depends on M and on the elastic parameters of the thread 4. Measuring this angle, the acting torque M is determined. Experimenting with different Ω values, the correlation $M = f(\Omega)$ can be derived. As in the case of the capillary viscosimeter, end effects arise near the fluid's free surface and cylinder's bottom 2. To eliminate them, the experiment can be repeated with different fluid's level h. The subsequent procedure is similar to that for the capillary viscosimeter.

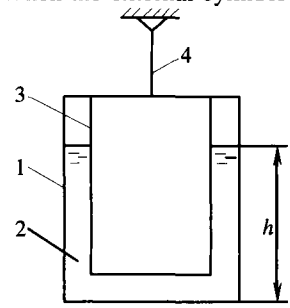

Fig. 16.7

Thus, using the capillary viscosimeter, the function:

$$\Delta p_L = f(Q) \tag{16.18}$$

can be derived, and using the rotational viscosimeter, the function:

$$\Omega = f_2(M). \tag{16.19}$$

Both functions are good for an infinitely-long tube and an infinitely-high gap. In order to find rheological parameters of a fluid from Eqs. (16.18) and (16.19), it is necessary to have the theoretical format of these expressions for various types of non-Newtonian fluids.

4. Fluid flow in an infinitely-long round tube

Let's review transient-free laminar fluid flow in the segment of an infinitely-long tube of the length l and radius a. The tangential stress distribution along the tube's radius is given by Eqs.[1] (10.33) and (10.34), i. e.:

$$\tau = \frac{r}{a}\tau_a, \quad \tau_a = \frac{p_1 - p_2}{2l}a. \tag{16.20}$$

[1] The derivation of (10.33) and (10.34) shows that the result does not depend on the viscosity parameters; therefore, they are valid also for the non-Newtonian liquids.

In our case, $v_x = v = v(r)$ and $\frac{dv}{dr} < 0$; therefore, from Eqs. (16.7) and (16.19):

$$\dot{\gamma} = \frac{dv}{dr} = -f(\tau). \tag{16.21}$$

With this sign selection $f(\tau) > 0$. Substituting Eq. (16.20) into Eq. (16.21), results in:

$$\frac{dv}{dr} = -f(\tau_a \frac{r}{a}), \tag{16.22}$$

which is a differential equation for the determination of the fluid's velocity $v(r)$.

In order to be able to use Eq. (16.22), the following needs to be kept in mind. In a non-Newtonian fluid flow, the presence of the tube's wall can cause the emergence in the fluid of special directions although the fluid is isotropic at a distance from the wall. For instance, a potential distribution of the colloidal particles' orientation or the orientation of long polymer chains is affected by the presence of the wall. Anomalous flow next to the wall can also occur due to a physico-chemical interaction between the fluid and wall material. The flow anomaly arising near the wall is called wall-adjacent sliding. The substance of the anomaly is in a drastic change of the $\frac{dv}{dr}$ value in the wall-adjacent layer at the continuous velocity distribution along the radius.

When the wall-adjacent sliding is present, Eq. (16.22) is valid only within the $0 \le r \le a - h$, where h is the thickness of the wall-adjacent layer where anomalous flow is occurring. Usually, $h << a$; so, instead of studying the wall-adjacent layer flow it is possible to assign the value $v(a) = v(a - h)$ on the tube's wall, i. e., velocity value different from zero and equal to velocity at the boundary of the wall-adjacent layer.

It is possible to show that the introduced fictional velocity is a function of the tangential stress τ_a. Velocity $v(a) = v(\tau_a) = s(\tau_a)$ is called the sliding velocity. By integrating Eq. (16.22):

$$\int_a^r dv = v(r) - s(\tau_a) = -\int_a^r f\left(\tau_a \frac{r}{a}\right) dr = \frac{a}{\tau_a} \int_\tau^{\tau_a} f(\tau) d\tau. \tag{16.23}$$

The fluid's throughflow through the tube's cross-section is equal to:

$$Q = 2\pi \int_0^a v(r) r \, dr.$$

Following Oldroyd, let's integrate this expression partially. Then, considering Eqs. (16.22) and (16.23):

$$Q = 2\pi\left[\frac{r^2}{2}v(r)\right]_0^a - \pi\int_0^a r^2\frac{dv}{dr}dr = \pi a^2 s(\tau_a) + \pi\int_0^a r^2 f\left(\tau_a\frac{r}{a}\right)dr = \\ = \pi a^2 s(\tau_a) + \frac{\pi a^3}{\tau_a^3}\int_\tau^{\tau_a}\tau^2 f(\tau)d\tau \tag{16.24}$$

Eq. (16.24) is the main relationship for the determination of the slip velocity. The presence of the slip velocity and the type of $s(\tau_a)$ correlation can be experimentally established with a capillary viscosimeter. For this purpose, correlations $\Delta p(Q)$ should be determined for several tubes of different diameters. The results are plotted in coordinates $\frac{Q}{\pi a^3}$, $\tau_a = \frac{\Delta p}{2l}a$ (Fig. 16.8). Different curves relate to experiments with the tubes of different diameters.

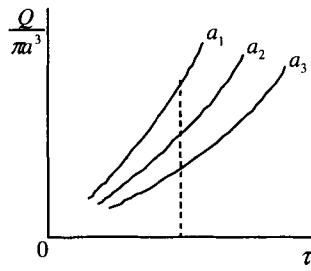

Fig. 16.8

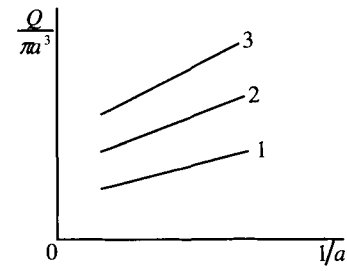

Fig. 16.9

Following Eq. (16.24):

$$\frac{Q}{\pi a^3} = \frac{s(\tau_a)}{a} + \frac{1}{\tau_a^3}\int_0^{\tau_a}\tau^2 f(\tau)d\tau = \frac{s(\tau_a)}{a} + F(\tau_a). \tag{16.25}$$

If $s(\tau_a) = 0$, the slippage is absent, $\frac{Q}{\pi a^3} = F(\tau_a)$, and the curves in Fig. 16.8 plotted for the tubes of different diameters should coincide. If $s(\tau_a) \neq 0$ ($\frac{Q}{\pi a^3}$ depends on $F(\tau_a)$ and a), Fig. 16.8 is valid. Drawing in Fig. 16.8 cross-sections by the curves (τ_a) = const, it is possible to plot the graph of Fig. 16.9, where the lines 1, 2 and 3 correspond to different τ_a values. Eq. (16.25) indicates that at (τ_a) = const, the value $\frac{Q}{\pi a^3}$ is linearly dependent on $\frac{1}{a}$; at that, $s(\tau_a)$ is the tangent

of inclination angle of lines 1, 2 and 3. After the function $s(\tau_a)$ is determined, Eq. (16.25) is used to determine the function:

$$F(\tau_a) = \frac{1}{\tau_a^3} \int_0^{\tau_a} \tau^2 f(\tau) d\tau,$$

wherefrom, after differentiation:

$$f(\tau_a) = \frac{1}{\tau_a^2} \frac{d\left[\tau_a^3 F(\tau_a)\right]}{d\tau_a}.$$

Therefore, the function τ_a can be experimentally determined by a capillary viscosimeter. This, however, requires extended experimentation and differentiating the function derived from the experiments. As it will be shown later, the task of determining parameters of the $f(\tau)$ function is significantly simplified if the analytical type of the function is known.

5. Rotational fluid flow within an annulus

Let's analyze the transient-free laminar rotational flow of a fluid between two coaxial cylinders of an infinite height. The fluid is flowing along the circular trajectories whose planes are perpendicular to the axis of the cylinder (Fig. 16.2). It was shown in section 1 that such flow is a flow with a simple shear, and the shear velocity is determined from Eq. (16.11). Let's identify within the flow an element of radius r, thickness dr and height h. The force attached to a cylindrical surface of the radius r is clearly:

$$F_1 = 2\pi r h \tau,$$

and the force attached to a cylindrical surface of the radius $r + dr$ is:

$$F_2 = 2\pi(r + dr)h(\tau + d\tau).$$

The identified element is revolving at a time-constant angular velocity ω. Therefore, the sum of the force momentums attached to this element is equal to zero, i. e.:

$$F_2(r + dr) - F_1 r = 2\pi h[(r + dr)^2(\tau + d\tau) - r^2\tau] = 0. \qquad (16.26)$$

After simple transformations and switching to the limit at $dr \to 0$ from Eq. (16.26):

$$\frac{d\tau}{\tau} = -2\frac{dr}{r}, \qquad (16.27)$$

or, after integrating:

$$\tau = \frac{C}{r^2}. \qquad (16.28)$$

To determine the integration constant C, M is denoted as the friction force momentum on the internal cylinder of radius R_i and of the unitary height. Then:

$$M = 2\pi R_i \tau_i R_i, \qquad (16.29)$$

where τ_i is the friction stress at the radius R_i.

From Eqs. (16.28) and (16.29):

$$\tau_i = \frac{C}{R_i^2} = \frac{M}{2\pi R_i^2},$$

and from there $C = \frac{M}{2\pi}$, Eq. (16.28) assumes the following format:

$$\tau = \frac{M}{2\pi r^2}. \tag{16.30}$$

Substituting Eqs. (16.10), (16.11) and (16.30) into Eq. (16.13), results in:

$$r\frac{d\omega}{dr} = f\left(\frac{M}{2\pi r^2}\right), \tag{16.31}$$

i. e., the differential equation of the fluid's rotational flow in a ring gap is obtained.

For integrating Eq. (16.31), the internal cylinder is assumed to be immobile, and the external one is revolving at an angular velocity Ω. Then, taking the wall-adjacent slippage into account, it is possible to present the flow velocity on the surface of the internal cylinder of the radius R_i:

$$v(R_i) = s(\tau_i), \tag{16.32}$$

and for the flow velocity on the surface of the external cylinder of the radius R_e:

$$v(R_e) = \Omega R_e - s(\tau_e), \tag{16.33}$$

where τ_e is the friction force stress on the surface of the external cylinder. As the angular velocity $\omega = \frac{v}{r}$, then from Eq. (16.31):

$$\int_{\frac{v_i}{R_i}}^{\frac{v}{R}} d\frac{v}{r} r = \frac{v}{r} - \frac{v_i}{R_i} \int_{R_i}^{r} f\left(\frac{M}{2\pi r^2}\right)\frac{dr}{r},$$

or, accounting for Eqs. (16.27), (16.30) and (16.32):

$$\frac{v}{r} = s\frac{\tau_i}{R_i} + \frac{1}{2}\int_{\tau}^{\tau_i} f(\tau)\frac{d\tau}{\tau}. \tag{16.34}$$

Eq. (16.34) gives the velocity distribution law with respect to the radius. Based on that equation and Eq. (16.33):

$$\Omega = \frac{s(\tau_e)}{R_e} + \frac{s(\tau_i)}{R_i} + \frac{1}{2}\int_{\tau_e}^{\tau_i} f(\tau)\frac{d\tau}{\tau}. \tag{16.35}$$

6. Integral technique in viscosimetry

The integral technique in viscosimetry involves the beforehand advance assignment of the functions of type $f(\tau)$ and $s(\tau_a)$ based on some physical assumptions.

It enables the computation of integrals in Eqs. (16.24) and (16.35) and derive, considering Eqs. (16.20) and (16.30), theoretical functions of the type:

$$Q = Q(\Delta p, \alpha_1, \alpha_2, \ldots, \alpha_n) \tag{16.36}$$

for the flow in a tube and:

$$\Omega = \Omega(M, \alpha_1, \alpha_2, \ldots, \alpha_n) \tag{16.37}$$

for the flow in an annulus, where $\alpha_1, \alpha_2, \ldots, \alpha_n$ are rheological parameters [the constants in functions $f(\tau)$ and $s(\tau_a)$] of the fluid under consideration.

Suppose the experiments with capillary viscosimeters produced n pairs of values Q_j, Δp_j. Substituting these values into Eq. (16.36), results in n equations for the determination of the numerical values of n rheological parameters $\alpha_1, \alpha_2, \ldots, \alpha_n$. Similarly, having obtained with rotational viscosimeter n pairs of values Ω_j, M_j and substituting them into Eq. (16.37) results in n equations for the determination of the fluid's rheological parameters. Clearly, the numerical values of the rheological parameters produced using either viscosimeter type must be similar. If this is not so, it means that the assumed $f(\tau)$ and $s(\tau_a)$ values do not describe the behavior of the fluid under consideration.

Several simple examples:

I. A viscous Newtonian fluid. Under Eq. (16.12), for such a fluid:

$$\dot{\gamma} = f(\tau) = \frac{\tau}{\mu}, \quad s(\tau_a) = 0. \tag{16.38}$$

Substituting these expressions into Eq. (16.23), and considering Eq. (16.20), results in:

$$v(r) = \frac{a}{\mu\tau_a}\int_{\tau}^{\tau_a} \tau d\tau = \frac{a}{\mu\tau_a}\left(1 - \frac{\tau^2}{\tau_a^2}\right) = \frac{a\Delta p}{4\mu l}\left(1 - \frac{r^2}{a^2}\right). \tag{16.39}$$

From Eqs. (16.23), (16.38) and (16.20):

$$Q = \frac{\pi a^3}{\mu\tau_a^3}\int_0^{\tau_a} \tau^3 d\tau = \frac{\pi a^3 \tau_a}{4\mu} = \frac{\pi a^4}{8\mu l}\Delta p. \tag{16.40}$$

As at the flow in a horizontal tube $\frac{\partial p}{\partial x} - \rho F_x = -\frac{\Delta p}{l}$, then it is easy to see that Eqs. (16.39) and (16.40) are identical with the earlier-derived Eqs. (9.29) and (9.31). The a and l values for the capillary viscosimeter are known, so following Eq. (16.40), in order to determine the value of the dynamic viscosity factor, it is sufficient to make one measurement of Δp and Q values.

For the rotational viscosimeter, under Eqs. (16.30), (16.34) and (16.38), the velocity distribution law within a ring gap is obtained as follows:

$$\frac{v}{r}=\frac{1}{2\mu}\int_{\tau}^{\tau_i}d\tau=\frac{\tau_i-\tau}{2\mu}=\frac{M}{4\pi\mu}\left(\frac{1}{R_i^2}-\frac{1}{r^2}\right). \tag{16.41}$$

Taking Eqs. (16.30), (16.35) and (16.38) or assuming $r = R_e$ in Eq. (16.41), gives:

$$\frac{v_e}{R_e}=\Omega=\frac{M}{4\pi\mu}\left(\frac{1}{R_i^2}-\frac{1}{R_e}\right).$$

The R_i and R_e radii are known, so, as with the capillary viscosimeter, it is sufficient to make one measurement of the M and Ω pair of values to determine μ.

II. Bingham-Shvedov fluid. For such a fluid, according to Eq. (16.16),

$$f(\tau)=\begin{cases}0, & \tau\le\tau_0\\ \dfrac{\tau-\tau_0}{\eta}, & \tau\ge\tau_0,\ s(\tau_a)=0.\end{cases} \tag{16.42}$$

Substituting this equations into Eq. (16.23), results in:

$$\begin{aligned}v(r)&=\frac{a}{\tau_a}\int_{\tau}^{\tau_0}f(\tau)d\tau+\frac{a}{\tau_a}\int_{\tau_0}^{\tau_a}f(\tau)d\tau=\frac{a}{\tau_a}\int_{\tau_0}^{\tau_a}\frac{\tau-\tau_0}{\eta}d\tau+\frac{a}{\tau_a}\int_{\tau}^{\tau_a}f(\tau)d\tau=\\&=\frac{a(\tau_a-\tau_0)^2}{2\eta\tau_a}+\frac{a}{\tau_a}\int_{\tau}^{\tau_0}f(\tau)d\tau.\end{aligned} \tag{16.43}$$

According to Eq. (16.42):

$$\text{when } \tau\le\tau_0,\ \frac{a}{\tau_a}\int_{\tau}^{\tau_0}f(\tau)d\tau=0, \tag{16.44}$$

$$\text{and when } \tau\ge\tau_0,\ \frac{a}{\tau_a}\int_{\tau}^{\tau_0}f(\tau)d\tau=\frac{a}{\tau_a}\int_{\tau}^{\tau_0}\frac{\tau-\tau_0}{\eta}d\tau=-\frac{a(\tau_a-\tau_0)^2}{2\eta\tau_a}. \tag{16.45}$$

Following Eq. (16.20):

$$\frac{\tau}{\tau_a}=\frac{r}{a},\ \frac{\tau_0}{\tau_a}=\frac{r_0}{a}, \tag{16.46}$$

where r_0 is the radius at which $\tau=\tau_0$. Then, from Eqs. (16.43), (16.44), (16.45) and (16.46):

$$v(r)=\frac{a\tau_a}{2\eta}\left(1-\frac{r_0}{a}\right)^2 \quad \text{when} \quad 0\le r\le r_0,$$

$$v(r)=\frac{a\tau_a}{2\eta}\left[\left(1-\frac{r_0}{a}\right)^2-\frac{r_0^2}{a^2}\left(1-\frac{r}{r_0}\right)^2\right] \quad \text{when} \quad r_0\le r\le a.$$

Thus, when $0\le r\le r_0$, $v(r)$ = const, i. e., there is a "flow core" where all particles are moving at the same speed, i. e., as a solid (Fig. 16.10).

It can be shown that the presence of the flow core is the property of any fluid with the initial shear stress and not only of Bingham-Shvedov fluid. By substituting Eq. (16.42) into Eq. (16.24):

$$Q = \frac{\pi a^3}{\mu \tau_a^3} \int_{\tau_0}^{\tau_a} \tau^2 \frac{\tau - \tau_0}{\eta} d\tau = \frac{\pi a^3 \tau_a}{4\eta} \left(1 - \frac{4}{3}\frac{\tau_0}{\tau_a} + \frac{1}{3}\frac{\tau_0^4}{\tau_a^4} \right) \quad (16.47)$$

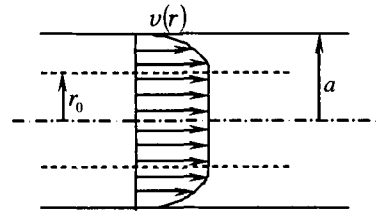

Fig. 16.10

or, considering Eqs. (16.20) and (16.46):

$$Q = \frac{\pi a^4 \Delta p}{8\eta l} \left(1 - \frac{4}{3}\frac{r_0}{a} + \frac{1}{3}\frac{r_0^4}{a^4} \right). \quad (16.48)$$

Eqs. (16.47) and (16.48) are different formats of Buckingham equation. At $\tau_0 = r_0 = 0$, it becomes Poiseuillle's Eq. (16.40). Eqs. (16.47) and (16.48) indicate that to determine the constants τ_0 and η, two pairs of Δp and Q numerical values must be measured.

Let's now turn to Bingham-Shvedov fluid flow in the ring gap of a rotational viscosimeter. As $R_i < R_e$, then under Eq. (16.30) always $\tau_e < \tau_i$. Thus, until $\tau_e \le \tau_i$, i. e., according to Eq. (16.30) $M \le 2\pi R_i^2 \tau_0 = M_0$, there is no shear, $\Omega = 0$, and the fluid between the cylinders is immobile. Suppose now $\tau_i > \tau_0 > \tau_e$. As along the radius, M = const, following Eq. (16.30):

$$R_i^2 \tau_i = r_0^2 \tau_0 = R_e^2 \tau,$$

where r_0 is the radius at which $\tau = \tau_0$. Then, it is evident that at $R_i < r < r_0$ $\tau > \tau_0$, and at $r_0 < r < R_e$, $\tau < \tau_0$. Therefore, in the interval $R_i < r < r_0$ there will be the shear flow, and at $r_0 < r < R_e$, the fluid will behave as a solid, i. e., it will be revolving at a constant angular velocity. Substituting Eq. (16.42) into Eq. (16.34) and considering Eq. (16.30), gives:

$$\frac{v}{r} = \frac{1}{2} \int_{\tau}^{\tau_i} \frac{\tau_a - \tau_0}{\eta} d\tau = \frac{M}{4\pi\eta} \left(\frac{1}{R_i^2} - \frac{1}{r^2} - \frac{2}{r_0^2} \log \frac{R_i}{r} \right), \text{ at } R_i \le r \le r_0,$$

$$\frac{v}{r} = \Omega = \frac{M}{4\pi\eta} \left(\frac{1}{R_i^2} - \frac{1}{r_0^2} - \frac{2}{r_0^2} \log \frac{R_i}{r} \right) = \text{const at } r_0 \le r \le R_e.$$

According to Eq. (16.30), $r_0 = \sqrt{\frac{M}{2\pi\tau_0}}$, i. e., with the increase in M, the r_0 value (hence, the volume involved in the shear flow), increase. At $\tau_0 > \tau_e$, the shear flow involves the entire interval $R_i < r < R_e$, and under Eqs. (16.30) and (16.35) the external cylinder angular velocity is:

$$\Omega = \frac{1}{2}\int_{\tau_e}^{\tau_i} \frac{\tau - \tau_0}{\eta}\frac{d\tau}{\tau} = \frac{M}{4\pi\eta}\left(\frac{1}{R_i^2} - \frac{1}{R_e^2}\right) - \frac{\tau_0}{\eta}\log\frac{R_i}{R_e}. \tag{16.49}$$

It can be seen from Eq. (16.49) that in order to determine the η and τ constants, it is necessary to have two pairs of M, Ω values.

III. Exponential fluid. According to Eq. (16.17), for an exponential fluid:

$$\dot{\gamma} = f(\tau) = \left(\frac{\tau}{k}\right)^{\frac{1}{n}}, \quad s(\tau_a) = 0. \tag{16.50}$$

Substituting Eq. (16.50) into Eqs. (16.23) and (16.24), and considering Eq. (16.20), respectively:

$$\frac{v}{r} = \frac{n}{n+1}a\left(\frac{\tau}{k}\right)^{\frac{1}{n}}\left[1 - \left(\frac{\tau}{\tau_a}\right)^{\frac{1+n}{n}}\right] = \frac{n}{n+1}a^{\frac{n+1}{n}}\left(\frac{\Delta p}{2kl}\right)^{\frac{1}{n}}\left[1 - \left(\frac{r}{a}\right)^{\frac{n+1}{n}}\right],$$

$$Q = \frac{n}{3n+1}\pi a^3\left(\frac{\tau}{k}\right)^{\frac{1}{n}} = \frac{n}{3n+1}\pi a^{\frac{3n+1}{n}}\left(\frac{\Delta p}{2kl}\right)^{\frac{1}{n}}, \tag{16.51}$$

i. e., the equation for the velocity and throughflow distribution for the flow in a round tube.

For the rotational viscosimeter, according to Eqs. (16.30), (16.34) and (16.38):

$$\frac{v}{r} = \frac{n}{2}\left(\frac{\tau_i}{k}\right)^{\frac{1}{n}}\left[1 - \left(\frac{\tau}{\tau_i}\right)^{\frac{1}{n}}\right] = \frac{n}{2}\left(\frac{M}{2\pi k R_i^2}\right)^{\frac{1}{n}}\left[1 - \left(\frac{R_i}{r}\right)^{\frac{2}{n}}\right],$$

$$\Omega = \frac{n}{2}\left(\frac{\tau_i}{k}\right)^{\frac{1}{n}}\left[1 - \left(\frac{\tau_e}{\tau_i}\right)^{\frac{1}{n}}\right] = \frac{n}{2}\left(\frac{M}{2\pi k R_i^2}\right)^{\frac{1}{n}}\left[1 - \left(\frac{R_i}{R_e}\right)^{\frac{2}{n}}\right].$$

IV. Reyner's series. It is assumed that for a fluid with the initial shear stress τ_0, the function $f(\tau - \tau_0)$ can be expanded into an exponential series. As this function is uneven, the series can include only uneven exponents of $(\tau - \tau_0)$. Therefore:

$$\dot{\gamma} = f(\tau - \tau_0) = \begin{cases} 0, & \tau \le \tau_0, \\ \sum_{k=0}^{n} b_k (\tau - \tau_0)^{2k+1}, & \tau \ge \tau_0,\ s(\tau_a) = 0 \end{cases} \tag{16.52}$$

where b_k, τ_0 are the fluid's rheological parameters.

Substituting Eq. (16.52) into Eq. (16.23) and applying the procedure identical to that used with Bingham-Shvedov fluid, results in:

$$v(r) = \frac{a}{2\tau a} \sum_{k=0}^{n} \frac{b_k}{k+1} (\tau_a - \tau_0)^{2k+2} = \frac{a}{2} \sum_{k=0}^{n} \frac{b_k}{k+1} \tau_a^{2k+1} \left(1 - \frac{r_0}{a}\right)^{2k+2} = \text{const},\ 0 \le r \le r_0,$$

$$v(r) = \frac{a}{2\tau a} \sum_{k=0}^{n} \frac{b_k}{k+1} \left[(\tau_a - \tau_0)^{2k+2} - (\tau - \tau_0)^{2k+2} \right] =$$

$$= \frac{a}{2} \sum_{k=0}^{n} \frac{b_k}{k+1} \tau_a^{2k+1} \left[\left(1 - \frac{r_0}{a}\right)^{2k+2} - \left(\frac{r_0}{a}\right)^{2k+2} \left(1 - \frac{r}{r_0}\right)^{2k+2} \right],\ r_0 \le r \le a.$$

These equations show that the velocity distribution along the radius is qualitatively similar to that shown in Fig. 16.10; i. e., in this case there is the flow core of the radius r_0 too.

Substituting Eq. (16.52) into Eq. (16.24), gives:

$$Q = \frac{\pi a^3}{3\tau_a} \sum_{k=0}^{n} b_k (\tau_a - \tau_0)^{2k+2} \left[\frac{(\tau_a - \tau_0)^2}{2k+4} + \frac{2\tau_0 (\tau_a - \tau_0)}{2k+3} + \frac{\tau_0^2}{2k+2} \right]. \tag{16.53}$$

In the case of a flow within the ring gap, as with Bingham-Shvedov fluid, when $\tau_i < \tau_0$, there is no flow. At $M > M_0 = 2\pi R_i^2 \tau_0$, the shear flow occurs in the gap:

$$R_i < r < r_0 = \sqrt{\frac{M}{2\pi\tau_0}},$$

and at $r_0 < r < R_e$, the fluid revolves at a constant angular velocity, i.e., as a solid. At $M \ge 2\pi R_e^2 \tau_0$, the shear flow involves the entire area $R_i < r < R_e$. According to Eqs. (16.34) and (16.49), at $\tau_i > \tau > \tau_e$:

$$\frac{v}{r} = \frac{1}{2} \sum_{k=0}^{n} b_k \int_{\tau}^{\tau_i} \frac{(\tau - \tau_0)^{2k+1}}{\tau} d\tau,\ R_i < r < r_0,$$

$$\frac{v}{r} = \Omega = \frac{1}{2}\sum_{k=0}^{n} b_k \int_{\tau}^{\tau_i} \frac{(\tau - \tau_0)^{2k+1}}{\tau} d\tau = \text{const}, \quad r_0 < r < R_e. \tag{16.54}$$

At $\tau_e > \tau_0$ the velocity distribution within the entire range ($R_i < r < R_e$) is determined from Eq. (16.54), where the interval must be taken within the τ_0, τ_i range, and the external cylinder's rotation angular velocity is:

$$\Omega = \frac{1}{2}\sum_{k=0}^{n} b_k \int_{\tau_e}^{\tau_i} \frac{(\tau - \tau_0)^{2k+1}}{\tau} d\tau. \tag{16.55}$$

The rheological Eq. (16.52) includes $n + 2$ rheological parameters: τ_0, b_0, b_1, ... , b_n. It is clear from Eqs. (16.53) and (16.55) that to determine these parameters, $n+2$ measurements of Δp, Q or M, Ω pairs' values must be made.

7. Hydraulic resistance factor

Let's take a fluid with the rheological equation:

$$\dot{\gamma} = f(\tau, \alpha_1, \alpha_2, ..., \alpha_n), \tag{16.56}$$

where, as previously, $\alpha_1, \alpha_2, ..., \alpha_n$ are the rheological parameters. Similarly to the considerations utilized in the derivation of Darcy-Weisbach's Eq. (5.30), the pressure gradient Δp is maintained over the length l within the tube of diameter d represented by the equation having the following format:

$$\Delta p = \varphi(l, d, \rho, w, \alpha_1, \alpha_2, ..., \alpha_n). \tag{16.57}$$

Assuming that the parameters d, ρ, w have independent dimensionalities, using the procedure similar to that utilized in the derivation of Eq. (5.30), from Eq. (16.57) we obtain:

$$\Delta p = \lambda \frac{l}{d} \frac{\rho w^2}{2},$$

where:

$$\lambda = \lambda(\Pi_1, \Pi_2, ..., \Pi_n), \tag{16.58}$$

and the values:

$$\Pi_i = \frac{\alpha_i}{d^{\beta} \rho^{\gamma} w^{\delta}}$$

are the conformity criteria. Eqs. (16.56) and (16.58) indicate that the number of the conformity criteria is equal to the number of the fluid's rheological parameters.

Let's for example study the Bingham-Shvedov fluid. In this case, Eq. (16.57) becomes:

$$\Delta p = \varphi(l, d, \rho, \eta, \tau_0, w),$$

and Eq. (16.58):

$$\lambda = \lambda(\Pi_1, \Pi_2), \tag{16.59}$$

where:

$$\Pi_1 = \frac{\rho w d}{\eta}, \quad \Pi_2 = \frac{\tau_0}{\rho w^2}. \tag{16.60}$$

To arrive at an analytical representation of Eq. (16.59), Eq. (16.47) is first analyzed. Using Eq. (16.20), it can be written as follows:

$$Q = \pi a^2 w = \frac{\pi a^4 \Delta p}{8 \eta l}\left[1 - \frac{4}{3}\frac{2l}{a}\frac{\tau_0}{\Delta p} + \frac{1}{3}\left(\frac{2l}{a}\frac{\tau_0}{\Delta p}\right)^4\right] \tag{16.61}$$

or:

$$w = \frac{d^2 \Delta p}{32 \eta l}\left[1 - \frac{4}{3}\frac{4l}{d}\frac{\tau_0}{\Delta p} + \frac{1}{3}\left(\frac{4l}{d}\frac{\tau_0}{\Delta p}\right)^4\right]. \tag{16.62}$$

It is evident that in order to arrive at an equation of the Eq. (16.37) format, Eq. (16.62) must be solved relative to Δp. Suppose:

$$\Delta p = \frac{4 l \tau_0}{d} z$$

and substitute this expression into Eq. (16.62). After performing some simple transformation

$$z^4 - \frac{4}{3}\alpha z^3 + \frac{1}{3} = 0, \tag{16.64}$$

where:

$$\alpha = 1 + \frac{6}{A}, \quad A = \frac{\tau_0 d}{\eta w}. \tag{16.65}$$

Using a standard technique for the solution of biquadratic equations, the roots of Eq. (16.64) are:

$$z_{1,2} = \frac{c}{3}\left[1 \pm \sqrt{1 - \frac{3b}{c(c-\alpha)}}\right], \tag{16.66}$$

$$z_{3,4} = \frac{c-2\alpha}{3}\left[1 \pm \sqrt{1 - \frac{3b}{(c-\alpha)(c-2\alpha)}}\right], \tag{16.67}$$

where:

$$b = \sqrt[3]{\alpha^2 + \sqrt{\alpha^4 - 1}} + \sqrt[3]{\alpha^2 - \sqrt{\alpha^4 - 1}} = \alpha^{\frac{2}{3}}\left(\sqrt[3]{1 + \sqrt{1 - \alpha^{-4}}} + \sqrt[3]{1 - \sqrt{1 - \alpha^{-4}}}\right) = \alpha^{\frac{2}{3}}\beta, \tag{16.68}$$

$$c = \alpha + \sqrt{\frac{3}{2}b + \alpha^2}\,. \tag{16.69}$$

Let's take the square root in Eq. (16.67). According to Eq. (16.69):

$$3b = 2(c-\alpha)^2 - 2\alpha^2,$$

and, after simple transformations:

$$1 - \frac{3b}{(c-\alpha)(c-2\alpha)} = \frac{(c+\alpha)}{(c-\alpha)}.$$

According to Eq. (16.65), $\alpha > 1$; so, following Eqs. (1.68) and (1.69), b and and c are real numbers, and $b > c$ and $c > \alpha$. Therefore:

$$1 - \frac{3b}{(c-\alpha)(c-2\alpha)} = \frac{(c+\alpha)}{(c-\alpha)} < 0,$$

and the roots $z_{3,4}$ are complex quantities.

Now let's take the roots $z_{1,2}$. A direct check with Eq. (16.68) shows that:

$$b^3 - 3b - 2\alpha^2 = 0,$$

and from Eq. (16.69):

$$c = \alpha + \sqrt{\frac{b^3}{2}}. \tag{16.70}$$

Substituting this into Eq. (16.66), provides:

$$z_{1,2} = \frac{c}{3}\left(1 \pm \sqrt{1 - \frac{6}{c\sqrt{2b}}}\right). \tag{16.71}$$

Following Eqs. (16.68) and (16.69), when $\alpha = 1$, $b = 2$, $c = 3$ and:

$$\frac{db}{d\alpha} = \frac{2\alpha}{3\sqrt{a^4 - 1}}\left(\sqrt[3]{\alpha^2 + \sqrt{a^4 - 1}} - \sqrt[3]{\alpha^2 - \sqrt{a^4 - 1}}\right),$$

where from, $\frac{db}{d\alpha} > 0$ when $\alpha > 0$. Thus, the functions $b(\alpha)$ and $c(\alpha)$ monotonously increase as α increases and $\frac{6}{c\sqrt{2b}} < 1$.

Thus, the roots $z_{1,2}$ are real numbers. To further analyze them, let's rewrite Eq. (16.71) using Eqs. (16.63), (16.65), (16.68) and (16.70):

$$\frac{\Delta pd}{4l} = \frac{1}{3}\left(\tau_0 + \frac{6\eta w}{d}\right)\left(1 + \sqrt{\frac{\beta^3}{c}}\right)\left(1 \pm \sqrt{1 - \frac{6}{c\sqrt{2b}}}\right). \tag{16.72}$$

Passing to limit in Eq. (16.72) at $\tau_0 \to 0$, results in:

$$\frac{\Delta pd}{4l} = 4\frac{\eta w}{d}\frac{1}{3}(1 \pm 1).$$

Eq. (16.61) shows that such passing to limit must result in Poiseuillle's equation. Therefore, in Eqs. (16.71) and (16.72) the "+" sign should be selected; so finally:

$$z = \frac{c}{3}\left(1 + \sqrt{1 - \frac{6}{c\sqrt{2b}}}\right),$$

or, considering Eq. (16.63):

$$\Delta p = \frac{4}{3}\frac{l}{d}\tau_0 c\left(1 + \sqrt{1 - \frac{6}{c\sqrt{2b}}}\right). \tag{16.73}$$

As follows from Eqs. (16.65), (16.68) and (16.69), $c = c(A)$. Comparing Eq. (16.73) with Darcy-Weisbach equation, results in:

$$\lambda = \frac{8}{3}B\varphi(A),$$

where $B = \frac{\tau_0}{\rho w^2}$ is a dimensionless parameter:

$$\varphi(A) = c\left(1 + \sqrt{1 - \frac{6}{c\sqrt{2b}}}\right).$$

Therefore, the hydraulic resistance factor at the Bingham-Shvedov fluid flow is a function of two independent conformity criteria A and B. At that, B coincides with Π_2 in Eq. (16.60) and $A = \Pi_1\Pi_2$.

The numerical values of the $\varphi(A)$ function are listed in the following Table. It can be shown that at $\frac{1}{A}=\frac{\eta w}{\tau_0 d}\geq 0.1$, the $\varphi(A)$ function can be approximated with the accuracy of below 2 % by the following equation:

$$\varphi(A)=4\left(1+\sqrt{1-\frac{6}{A}}\right).$$

1/A	$\varphi(A)$	1/A	$\varphi(A)$	1/A	$\varphi(A)$	1/A	$\varphi(A)$
0.0000	3.00	0.0060	3.53	0.0250	4.25	0.0700	5.52
0.0005	3.14	0.0080	3.63	0.0300	4.40	0.0800	5.78
0.0010	3.20	0.0100	3.71	0.0350	4.55	0.1000	6.29
0.0020	3.29	0.0120	3.79	0.0400	4.70	0.1500	7.54
0.0030	3.36	0.0140	3.87	0.0450	4.84	0.2000	8.76
0.0040	3.42	0.0160	3.94	0.0500	4.98	0.2500	9.97
0.0050	3.48	0.0200	4.08	0.0600	5.25	0.3000	11.18

The next example will be an exponential fluid. For such a fluid, Eq. (16.54) has the following format:

$$\Delta p=\varphi(l,d,\rho,k,n,w).$$

Accepting the d,ρ,w values as parameters with independent dimensionality, using Π-theorem, and considering that under Eq. (16.17) $[k]=MT^{n-2}L^{-1}$, the result is:

$$\Delta p=f\left(n,\frac{d^n\rho w^{2-n}}{k}\right)\frac{l}{d}\rho w^2\ ,$$

and from there:

$$\lambda=2f\left(n,\frac{d^n\rho w^{2-n}}{k}\right).$$

The non-dimensional conformity criteria are the values:

$$n,\ \frac{d^n\rho w^{2-n}}{k}=\mathrm{Re}',$$

where Re' is an equivalent of Reynolds' number for a linearly-viscous fluid. To find out the type of the $\lambda=2f(n,\mathrm{Re}')$ function, let's review Eq. (16.51) or:

$$w=\frac{n}{3n+1}\left(\frac{d}{2}\right)^{\frac{n+1}{n}}\left(\frac{\Delta p}{2kl}\right)^{\frac{1}{n}}. \qquad (16.74)$$

And, solving this equation relative to Δp:

$$\Delta p = 2klw^n\left(\frac{3n+1}{n}\right)^n\left(\frac{2}{d}\right)^{n+1}.$$

Comparing this equation with that of Darcy-Weisbach, results in:

$$\lambda = 2^{n+3}\left(\frac{3n+1}{n}\right)^n\frac{k}{\rho w^{2-n}d}.$$

8. Additional remarks to the calculation of non-Newtonian fluids flow in pipes

The main equation describing the transient-free flow of viscous fluids in pipes are:
continuity equation:

$$Q = wS = \text{const}, \tag{16.75}$$

Bernoulli's equation:

$$z_1 + \frac{p_1}{\rho g} + \alpha_1\frac{w_1^2}{2g} = z_2 + \frac{p_2}{\rho g} + \alpha_2\frac{w_2^2}{2g} + h_{1-2}, \tag{16.76}$$

Darcy-Weisbach and Weisbach equations:

$$h_r = \lambda\frac{l}{d}\frac{w^2}{2g},\quad h_m = \zeta\frac{w^2}{2g}. \tag{16.77}$$

The continuity equation does not include viscosity parameters of the fluid; so it is identical for both linearly-viscous and any non-Newtonian fluid. Bernoulli's equation, which is the mechanical energy conservation law, also preserves its format, although the Coriolis' factors α and loss amounts h_{1-2} will differ from those of the linearly-viscous fluids. Indeed, the α value is determined by the velocity distribution law along the tube's radius, whereas the loss h_{1-2} depends on the medium viscosity parameters. The Darcy-Weisbach's and Weisbach's equation are derived based on the general concepts of the dimensionality theory. Thus, the format is preserved, but the correlation of the hydraulic resistance factor λ and local resistance factor ζ *vs.* the conformity criteria are distinct for each type of the non-Newtonian fluid.

Thus, all techniques of the pipeline designing based on Eqs. (16.65)–(16.77) can be used for computing the flow of non-Newtonian viscous fluids in consideration of the above remarks.

Mechanics of Fluid Flow
by Kaplan S. Basniev, Nikolay M. Dmitriev and George V. Chilingar

CHAPTER XVII

TWO-PHASE FLOW IN PIPES

The flow of two-phase (multi-phase) fluids in pipes is very common for almost any branches of oil and gas industry. In drilling, this is the flow of aerated drilling muds and cement slurries, and removal of the cuttings. In oil and gas production, this is the gas lift, the flow of gas-condensate, water-oil and gas-water mixtures in the well. Multi-phase flows can also be present in the field gathering lines.

The phase is a portion of the uniform system bounded by a separation surface. For instance, a mixture of the oil and water is a two-phase system: liquid-liquid. Mixtures of the gas and condensate or the gas and oil are two-phase systems: gas-liquid. The mixture of the water, oil, and gas is a three-phase system.

The phase can consist of one substance, such as the water. Such a phase is called a single-component phase. If the phase comprises several chemical substances, for instance, a mixture of hydrocarbon gases, it is called multicomponent.

True solutions (salts in water, gas mixtures, etc.) are single-phase multicomponent systems.

The following assumptions are usually made when describing the motions of multiphase media:

(1) The size of inclusions or nonuniformities in a mixture (individual parts of a nonuniform system) are much larger than distances between molecules, lengths of the molecular free pass, etc. In other words, the inclusion sizes are such that the techniques of the mechanics of continuous medium are applicable to each individual part of a nonuniform system.

(2) The sizes of the above inclusions are much smaller than the distances over which macroscopic parameters of the mixture or phases significantly change, i. e., these sizes are much smaller than the characteristic sizes of the system under consideration.

These assumptions enable a description of the multiphase media motions using the multispeed continuum model. The multispeed continuum is an aggregation of N continuums, each of which is related to its component (phase) and fills-up one and the same volume occupied by the mixture. Therefore, at each point of the multispeed continuum there are N densities, N velocities, etc.

1. Equations of the conservation laws

The general concepts used in Chapter II to derive the conservation law equations for a single-phase medium, and the models of a multispeed continuum can be utilized for writing the equations of the mass conservation law, momentum law and energy conservation law for each component of the mixture.

The integral representation of these laws is as follows:

The mass conservation law:

$$\int_V \frac{\partial(\alpha_i \rho_i)}{\partial t} dV + \int_S \alpha_i \rho_i v_{in} dS = \int_V \sum_{j=1}^{N} J_{ji} dV, \quad i = 1, 2, ..., N \tag{17.1}$$

The momentum law:

$$\int_V \frac{\partial(\alpha_i \rho_i \bar{v}_i)}{\partial t} dV + \int_S \alpha_i \rho_i \bar{v}_i v_{in} dS = \\ = \int_V \alpha_i \rho_i \bar{F}_i dV + \int_S \bar{p}_{ni} dS + \int_V \sum_{j=1}^{N} \bar{P}_{ji} dV, \quad i = 1, 2, ..., N \tag{17.2}$$

The energy conservation law:

$$\int_V \frac{\partial(\alpha_i \rho_i E_i)}{\partial t} dV + \int_S \alpha_i \rho_i E_i v_{in} dS = \\ = \int_V \alpha_i \rho_i \bar{F}_i \bar{v}_i dV + \int_S \bar{p}_{ni} \bar{v}_i dS + \int_V \sum_{j=1}^{N} E_{ji} dV - \int_S q_i^{(n)} dS, \quad i = 1, 2, ..., N, \tag{17.3}$$

$$E_i = u_i + \frac{v_i^2}{2}.$$

In Eqs. (17.1)–(17.3), i is the number of a phase (component), $\alpha_i \geq 0$ is the fraction of the mixture's volume occupied by the phase at a given point, and the rest of the symbols are the same as in Chapter II. It is clear that:

$$\sum_{j=1}^{N} \alpha_i = 1. \tag{17.4}$$

The J_{ji} value is (due to the possibility of phase transformations) the intensity of mass transfer from the j^{th} to i^{th} component per unit of the mixture volume per unit time.

The $\bar{P}_{ji}$ is the impulse exchange intensity between the j^{th} and i^{th} components of the mixture. The E_{ji} is the energy exchange intensity between the j^{th} and i^{th} components of the mixture.

Following the conservation laws:

$$J_{ji} = -J_{ij}, \; J_{ii} \equiv 0, \; \bar{P}_{ji} = \bar{P}_{ij}, \; \bar{P}_{ii} \equiv 0, \; E_{ji} = -E_{ij}, \; E_{ii} \equiv 0. \tag{17.5}$$

It is necessary to note here that i is the phase number.

By summing up Eqs. (17.1)–(17.3) according to i and considering Eq. (17.5):

$$\int_V \frac{\partial}{\partial t}\sum_{i=1}^{N}\alpha_i\rho_i dV + \int_S \sum_{i=1}^{N}\alpha_i\rho_i v_{in} dS = 0, \tag{17.6}$$

$$\int_V \frac{\partial}{\partial t}\sum_{i=1}^{N}\alpha_i\rho_i \bar{v}_i dV + \int_S \sum_{i=1}^{N}\alpha_i\rho_i \bar{v}_i v_{in} dS = \int_V \sum_{i=1}^{N}\alpha_i\rho_i \bar{F}_i dV + \int_S \sum_{i=1}^{N}\bar{p}_{ni} dS, \tag{17.7}$$

$$\begin{aligned}\int_V \frac{\partial}{\partial t}\sum_{i=1}^{N}\alpha_i\rho_i E_i dV + \int_S \sum_{i=1}^{N}\alpha_i\rho_i E_i v_{in} dS = \int_V \sum_{i=1}^{N}\alpha_i\rho_i \bar{F}_i \bar{v}_i dV + \\ + \int_S \sum_{i=1}^{N}\bar{p}_{ni}\bar{v}_i dS - \int_S \sum_{i=1}^{N} q_i^{(n)}\bar{v}_i dS.\end{aligned} \tag{17.8}$$

The mixture density ρ_m is determined as:

$$\rho_m = \sum_{i=1}^{N}\alpha_i\rho_i, \tag{17.9}$$

and the mass- averaged velocity, from equation:

$$\bar{v} = \frac{1}{\rho_m}\sum_{i=1}^{N}\alpha_i\rho_i\bar{v}_i . \tag{17.10}$$

2. Equations of two-phase mixture flow in pipes

To derive these equations, we will make the following assumptions:

(a) The flow is transient-free;
(b) Pressure and temperature of both phases are the same and are constant in the tube's cross-section;
(c) Relative motions of the components within the phase can be disregarded;
(d) In each cross-section, the conditions of local thermodynamic equilibrium are maintained for a mixture volume crossing the cross-section per unit time;
(e) Only one mass force (the gravitational force) is active.

With these assumptions, Eqs. (17.6)–(17.8), by considering Eqs. (17.9) and (17.10), become:

$$\int_V \sum_{i=1}^{N}\alpha_i\rho_i\bar{v}_i v_{in} dS = 0, \tag{17.11}$$

$$\int_S \sum_{i=1}^{N}\alpha_i\rho_i\bar{v}_i v_{in} dS = \int_V \sum_{i=1}^{N}\rho\bar{g} dV + \int_S \sum_{i=1}^{N}\bar{p}_{ni} dS, \tag{17.12}$$

$$\int_S \sum_{i=1}^{N}\alpha_i\rho_i E_i v_{in} dS = \int_V \rho_m \bar{\bar{v}}\bar{g} dV + \int_S \sum_{i=1}^{N}\bar{p}_{ni}\bar{v}_i dS - \int_S \sum_{i=1}^{N} q_i^{(n)} dS. \tag{17.13}$$

Let's take as the surface S the tube's segment inclined at angle θ to the vertical and delimited by the cross-sections S_1, S_2, and the side surface S_3 (Fig. 17.1). To make the derivation more general it is assumed that the surface S_3 is permeable and

that continuously distributed gas-liquid mixture is entering the tube through this surface. According to Fig. 17.1, in the cross-sections S_1, S_2, S_3:

$$\begin{aligned}
&\text{at } S_1: \ \bar{v}_i = -\bar{n}v_i, \ \bar{n} = -\bar{e}_3, \ \alpha_{n1} = \alpha_{n2} = 0, \ \alpha_{n3} = -1, \ i = 1, \ 2; \\
&\text{at } S_2: \ \bar{v}_i = \bar{n}v_i, \ \bar{n} = \bar{e}_3, \ \alpha_{n1} = \alpha_{n2} = 0, \ \alpha_{n3} = 1, \ i = 1, \ 2; \\
&\text{at } S_3: \ \bar{v}_i = -\bar{n}v_i, \ \bar{n} = -\bar{e}_1\alpha_{n1} + \bar{e}_2\alpha_{n2}, \ \alpha_{n3} = 0, \ i = 3, \ 4.
\end{aligned} \tag{17.14}$$

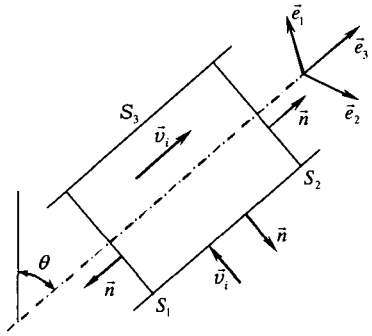

Fig. 17.1

Here and thereafter, the subscripts "3" and "4" indicate, respectively, the gas and liquid phases of the mixture entering the tube through the S_3 surface, $\bar{e}_m$ are basis vectors of the coordinate axes, $\alpha_{nm} = \bar{n}\bar{e}_m$ are cosines of the angles between the coordinate axes and the normal.

Substituting Eq. (17.14) into Eq. (17.11), results in:

$$\int_{S_2}(\alpha_1\rho_1v_1 + \alpha_2\rho_2v_2)dS - \int_{S_1}(\alpha_1\rho_1v_1 + \alpha_2\rho_2v_2)dS = \int_{S_3}(\alpha_3\rho_3v_3 + \alpha_4\rho_4v_4)dS\,. \tag{17.15}$$

To transform Eq. (17.12), the tensor of the surface stresses should be analyzed. It is assumed that:

$$p_i^{kl} = -\alpha_i p\delta_{kl} + \tau_i^{kl}, \ \tau_i^{kl} = \tau_i^{lk}, \ \tau_i^{kk} = 0. \tag{17.16}$$

And, considering Eq. (1.31), from Eq. (17.16):

$$\bar{p}_{ni} = -\alpha_i p\bar{n} + \bar{\tau}_{ni}, \ \bar{\tau}_{ni} = \bar{e}_m\tau_i^{km}\alpha_{nk}, \tag{17.17}$$

where τ_i^{km} are components of the tensor of additional stresses applied to the i^{th} phase.

It is assumed earlier that pressures within the phases are the same. Therefore, from Eq. (17.17) and considering Eq. (17.4), results in:

$$\begin{aligned}
&\bar{p}_n = \sum_{i=1}^{N}\bar{p}_{ni} = -p\bar{n} + \bar{\tau}_n, \ \bar{\tau}_n = \bar{e}_m\tau^{km}\alpha_{nk}, \\
&\tau^{km} = \sum_{i=1}^{N}\tau_i^{km}, \ \tau^{km} = \tau^{mk}, \ \tau^{kk} = 0.
\end{aligned} \tag{17.18}$$

Note that the summing-up on the repeating subscript is assumed in Eq. (17.18).

From Eqs. (17.14) and (17.18):

$$\begin{aligned}
&\text{at } S_1: \ \bar{p}_n = \bar{e}_3 p - \bar{e}_1 \tau^{31} - \bar{e}_2 \tau^{32};\\
&\text{at } S_2: \ \bar{p}_n = -\bar{e}_3 p + \bar{e}_1 \tau^{31} + \bar{e}_2 \tau^{32};\\
&\text{at } S_3: \ \bar{p}_n = -(\bar{e}_1 \alpha_{n1} + \bar{e}_2 \alpha_{n2}) p + \bar{e}_1 \tau^{21} \alpha_{n2} + \bar{e}_2 \tau^{12} \alpha_{n1} + \bar{e}_3 (\tau^{13} \alpha_{n1} + \tau^{23} \alpha_{n2}).
\end{aligned} \tag{17.19}$$

By projecting Eq. (17.12) onto the tube's axis $0x$, and considering Eqs. (17.14) and (17.19):

$$\begin{aligned}
&\int_{S_2} (\alpha_1 \rho_1 v_1^2 + \alpha_2 \rho_2 v_2^2) dS - \int_{S_1} (\alpha_1 \rho_1 v_1^2 + \alpha_2 \rho_2 v_2^2) dS =\\
&= \int_V \rho_m \vec{g} \cdot \vec{e}_3 dV + \int_{S_1} p dS - \int_{S_2} p dS + \int_{S_3} \tau dS,
\end{aligned} \tag{17.20}$$

where:

$$\tau = \tau^{13} \alpha_{n1} + \tau^{23} \alpha_{n2}$$

is a projection of additional stresses onto the axis $0z$.

To transform Eq. (17.13) functions similar to $\bar{p}_{ni} * \bar{v}_i$ are reviewed. From Eqs. (17.14) and (17.17):

$$\begin{aligned}
&\text{at } S_1: \ \bar{p}_{ni} * \bar{v}_i = \alpha_i p v_i, \ i = 1, \ 2;\\
&\text{at } S_2: \ \bar{p}_{ni} * \bar{v}_i = -\alpha_i p v_i, \ i = 1, \ 2;\\
&\text{at } S_3: \ \bar{p}_{ni} * \bar{v}_i = \alpha_i p v_i - 2\alpha_{n1} \alpha_{n2} \tau_i^{12} v_i, \ \alpha_{n1}^2 + \alpha_{n2}^2 = 1, \ i = 3, \ 4.
\end{aligned} \tag{17.21}$$

Now substituting Eqs. (17.14) and (17.21) into Eq. (17.13) and assuming that the heat inflow through cross-sections S_1 and S_2 can be disregarded, yields:

$$\begin{aligned}
&\int_{S_2} (\alpha_1 \rho_1 E_1 v_1 + \alpha_2 \rho_2 E_2 v_2) dS - \int_{S_1} (\alpha_1 \rho_1 E_1 v_1 + \alpha_2 \rho_2 E_2 v_2) dS -\\
&- \int_{S_3} (\alpha_3 \rho_3 E_3 v_3 + \alpha_4 \rho_4 E_4 v_4) dS = \int_V \rho_m \vec{v} \cdot \vec{g} dV + \int_{S_1} p(\alpha_1 v_1 + \alpha_2 v_2) dS -\\
&\int_{S_1} p(\alpha_1 v_1 + \alpha_2 v_2) dS + \int_{S_3} [(\alpha_3 v_3 + \alpha_4 v_4) p - 2\alpha_{n1} \alpha_{n2} (\tau_3^{12} v_3 + \tau_4^{12} v_4)] dS -\\
&- \int_{S_3} \sum_{i=1}^{N} q_i^{(n)} dS.
\end{aligned} \tag{17.22}$$

Eqs. (17.15), (17.20) and (17.22) include the following integrals:

$$\int_{S_1} f_1 dS, \ \int_{S_2} f_1 dS, \ \int_{S_3} f_2 dS, \ \int_V f_3 dV.$$

Taking limit between cross-sections $S_1 = S(z)$ and $S_2 = S(z + dz)$, gives:

$$\lim\left(\int_{S_2} f_1 dS - \int_{S_1} f_1 dS\right) = \frac{d}{dz}\int_S f_1 dS dz,$$
$$\lim \int_{S_3} f_2 dS = \int_\chi f_2 d\chi dz, \quad \lim \int_V f_3 dV = \int_S f_3 dS dz, \tag{17.23}$$

where χ is the wetted perimeter of tube's cross-section S.

Switching in Eqs. (17.15), (17.20) and (17.22) to limit at $dz \to 0$ and considering Eq. (17.23), results in:

$$\frac{d}{dz}\int_S (\alpha_1\rho_1 v_1 + \alpha_2\rho_2 v_2)dS = \int_\chi (\alpha_3\rho_3 v_3 + \alpha_4\rho_4 v_{42})d\chi, \tag{17.24}$$

$$\frac{d}{dz}\int_S (\alpha_1\rho_1 v_1^2 + \alpha_2\rho_2 v_2^2)dS = \int_S \rho_m \overline{\overline{g}}\, e_3 dS - \frac{d}{dz}\int_S p dS + \int_\chi \pi d\chi, \tag{17.25}$$

$$\frac{d}{dz}\int_S (\alpha_1\rho_1 E_1 v_1 + \alpha_2\rho_2 E_2 v_2)dS - \int_\chi (\alpha_3\rho_3 E_3 v_3 + \alpha_4\rho_4 E_4 v_4)d\chi =$$
$$= \int_S \rho_m \overline{\overline{v}}\, \overline{\overline{g}} dS - \frac{d}{dz}\int_S (\alpha_1 v_1 + \alpha_2 v_2) p dS + \int_\chi (\alpha_3 v_3 + \alpha_4 v_4) p d\chi - \tag{17.26}$$
$$-2\int_\chi (\tau_2^{12} v_3 + \tau_4^{12} v_4)\alpha_{n1}\alpha_{n2} d\chi - \int_\chi q^{(n)} d\chi,$$

where:

$$q(n) = \sum_{i=1}^{N} q_1(n).$$

It is assumed when calculating $\int_\chi q^{(n)} d\chi$ and $\int_\chi \pi d\chi$ that χ is the perimeter of the tube's cross-section.

Let's review the integrals in Eqs. (17.24)–(17.26). It is clear that:

$$\int_S \alpha_i\rho_i v_i dS = G_i, \quad i = 1, 2, \quad \int_\chi \alpha_i\rho_i v_i d\chi = J_i, \quad i = 3, 4, \tag{17.27}$$

where G_i is the mass throughflow of the i^{th} phase, J_i is the mass inflow of the i^{th} phase through the surface S_3 per unit length.

Further:

$$\int_S \alpha_i\rho_i v_i^2 dS = \bar{v}_i \int_\chi \alpha_i\rho_i v_i dS = \bar{v}_i G_i, \quad i = 1, 2, \tag{17.28}$$

where $\bar{v}_i$ is some average value of velocity v_i.

Following the assumption (b), the pressure, density and internal energy of a phase are uniformly distributed over the tube's cross-section. So, considering Eqs (17.9) and (17.27):

$$\int_S \rho_m \overline{g}\overline{e}_3 dS = g_z \rho_m S, \quad \rho_m S = \rho_1 \int_S \alpha_1 dS + \rho_2 \int_S \alpha_2 dS, \quad \int_S p dS = pS, \quad (17.29)$$

$$\int_S \alpha_i \rho_i E_i v_i dS = \int_S \alpha_i \rho_i \left(u_i + \frac{v_i^2}{2} \right) v_i dS = \left(u_i + \frac{v_{i\text{avg}}^2}{2} \right) G_i, \quad i = 1, 2, \quad (17.30)$$

$$\int_S \alpha_i v_i p dS = \int_S \alpha_i \rho_i v_i \frac{p}{\rho_i} dS = \frac{p}{\rho_i} G_i, \quad i = 1, 2, \quad (17.31)$$

where g_z is the projection of the g-force acceleration onto the tube's axis, $v_{i\,\text{avg}}$ is some averaged value of the velocity v_i different from $\bar{v}_i$.

According to Eqs. (17.10) and (17.27):

$$\int_S \rho_m \overline{v}\overline{g} dS = \overline{g}\overline{e}_3 \int_S (\alpha_1 \rho_1 v_1 + \alpha_2 \rho_2 v_2) dS = g_z (G_1 + G_2). \quad (17.32)$$

Assuming the inflow through the surface S_3 is axisymmetric, and taking Eq. (17.27) into account, results in:

$$\int_\chi \alpha_i \rho_i E_i v_i d\chi = E_i \int_\chi \alpha_i \rho_i v_i d\chi = \left(u_i + \frac{v_i^2}{2} \right) J_i, \quad i = 3, 4, \quad (17.33)$$

$$\int_\chi \alpha_i \rho_i p d\chi = \int_\chi \alpha_i \rho_i v_i \frac{p}{\rho_i} d\chi = \frac{p}{\rho_i} \int_\chi \alpha_i \rho_i v_i d\chi = \frac{p}{\rho_i} J_i, \quad i = 3, 4, \quad (17.34)$$

$$\int_\chi \tau_i^{12} v_i \alpha_{n1} \alpha_{n2} d\chi = \tau_i^{12} v_i \int_\chi \alpha_{n1} \alpha_{n2} d\chi = \tau_i^{12} v_i \int_0^{2\pi} \sin\gamma \cos\gamma R d\gamma = 0, \quad i = 3, 4, \quad (17.35)$$

where R is tube's radius, γ is the angle between the normal $\bar{n}$ to the surface S_3 and the basis vector $\bar{e}_1$ (Fig. 17.2).

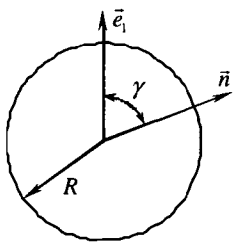

Fig. 17.2

It is also evident that:

$$\int_\chi \tau d\chi = \tau_{\text{avg}} \chi, \quad \int_\chi q^{(n)} d\chi = q_{\text{avg}}^{(n)} \chi, \quad (17.36)$$

where τ_{avg}, $q_{\text{avg}}^{(n)}$ are average over the perimeter τ and $q^{(n)}$ values.

Let's now denote S_i part of the tube's cross-section area occupied by the i^{th} phase. Then:

$$S_i = \int_S \alpha_i dS, \quad i = 1, 2, \quad (17.37)$$

and the mass throughflow G_i can be presented as :

$$G_i = \int_S \alpha_i \rho_i v_i dS = \rho_i w_i \int_S \alpha_i dS = \rho_i w_i S_i = \rho_i Q_i, \quad i = 1, 2, \quad (17.38)$$

where w_i, Q_i are average over the section velocity and volume throughflow of the i^{th} phase.

Supposing the phase velocity changes slightly over the tube's cross-section, it is possible to assume that:

$$\overline{v_i^2} = v_{i\text{avg}}^2 = w_i^2, \quad i = 1, \ 2. \tag{17.39}$$

Under the assumption (b) that the pressure and temperature are uniformly distributed over the tube's cross-section. So:

$$\rho_1 = \rho_3 = \rho_g, \ \rho_2 = \rho_4 = \rho_l, \ u_1 = u_3 = u_g, \ u_2 = u_4 = u_l, \tag{17.40}$$

where the subscript "g" denotes the gas phase, and the subscript "l" denotes the liquid phase. Besides, let's denote:

$$G_1 = G_g, G_2 = G_l, J_4 = J_l, w_1 = w_g, w_2 = w_l. \tag{17.41}$$

From Eq. (17.37):

$$S_1 = S_g = \int_S \alpha_i \, dS = \varphi S. \tag{17.42}$$

The value φ is called *true gas-content.*

But as, under Eq. (17.4), $\alpha_2 = 1 - \alpha_1$, then:

$$S_2 = S_l = \int_S \alpha_2 \, dS = (1-\varphi)S. \tag{17.43}$$

From Eqs. (17.38), (17.40)–(17.43), average velocities of the phases can be represented as follows:

$$w_g = \frac{G_g}{\varphi \rho_g S}, \quad w_l = \frac{G_l}{(1-\varphi)\rho_l S}. \tag{17.44}$$

Following Eqs. (17.29), (17.40), (17.42) and (17.43):

$$\rho_m = \varphi \rho_g + (1-\varphi)\rho_l. \tag{17.45}$$

The tangential stress on the tube's wall is assigned as[1]:

$$\tau_{\text{avg}} = -\frac{\lambda_m}{8}[\varphi \rho_g w_g^2 + (1-\varphi)\rho_l w_l^2] = -\frac{\lambda_m}{8S^2}\left[\frac{G_g^2}{\varphi \rho_g} + \frac{G_l^2}{(1-\varphi)\rho_l}\right], \tag{17.46}$$

and the heat inflow is assigned as:

$$q_{\text{avg}}^{(n)} = k(T - T_{\text{amb}}), \tag{17.47}$$

[1] The format of equation Eq. (17.46) is determined by the fact that it is used in this format for the laboratory determinations of λ_m.

where T_{amb} is ambient temperature, λ_m is hydraulic resistance of the mixture, k is heat transmissibility through the tube's wall, T is mixture's temperature in the tube, and T_{amb} is ambient temperature. Substituting integrals in Eqs. (17.27)–(17.36) and Eqs. (17.46) and (17.47) into Eqs. (17.24)–(17.26) and considering Eqs. (17.39)–(17.41) and (17.45) and after simple transformations results:

$$\frac{dG_m}{dz} = J_m,$$

$$\frac{dp}{dz} = \rho_m g_z - \frac{1}{S^2}\frac{dI}{dz}\left[\frac{G_g^2}{\varphi\rho_g} + \frac{G_l^2}{(1-\varphi)\rho_l}\right] - \frac{\chi\lambda_m}{8S^3}\left[\frac{G_g^2}{\varphi\rho_g} + \frac{G_l^2}{(1-\varphi)\rho_l}\right], \tag{17.48}$$

$$\frac{dp}{dz}\left[\left(h_g + \frac{w_g^2}{2}\right)G_g + \left(h_l + \frac{w_l^2}{2}\right)G_l\right] = \left(h_g + \frac{v_3^2}{2}\right)J_g + \left(h_l + \frac{v_4^2}{2}\right)J_l +$$

$$g_z G_m - \chi k(T - T_{amb}),$$

where:

$$G_m = G_g + G_l,\ J_m = J_g + J_l$$

are total mass throughflow and inflow:

$$h_g = u_g + \frac{p}{\rho_g},\ h_l = u_l + \frac{p}{\rho_l} \tag{17.49}$$

are enthalpy of gas and liquid phases.

Together with true gas-content φ, which, according to Eq. (17.42), is equal to:

$$\varphi = \frac{S_l}{S} = \frac{S_g}{S}, \tag{17.50}$$

the theory of two-phase flow employs the througflow gas-content β, which is by definition equal to:

$$\beta = \frac{Q_g}{Q_g + Q_l}, \tag{17.51}$$

where Q_g and Q_l are volume throughflows of the gas and liquid phases. From Eq. (17.44):

$$Q_g = \frac{G_g}{\rho_g} = \varphi w_g S,\ Q_l = \frac{G_l}{\rho_l} = (1-\varphi)w_l S. \tag{17.52}$$

Following Eqs. (17.51) and (17.52):

$$\frac{1-\varphi}{\varphi}=\frac{1-\beta}{\beta}\frac{w_g}{w_l}.$$

By substituting Eq. (17.52) into Eq. (17.52):

$$\beta=\frac{G_g}{\rho_g}\left(\frac{G_g}{\rho_g}+\frac{G_l}{\rho_l}\right)^{-1}.$$

As the mixture composition entering the tube through the side surface S_3 is the same as that flowing in the tube, then following the condition (d) of the local thermodynamic equilibrium that:

$$\frac{J_g}{\rho_g}\left(\frac{J_g}{\rho_g}+\frac{J_l}{\rho_l}\right)^{-1}=\beta=\frac{G_g}{\rho_g}\left(\frac{G_g}{\rho_g}+\frac{G_l}{\rho_l}\right)^{-1}. \tag{17.53}$$

$G_m = G_g + G_l$, $J_m = J_g + J_l$. Therefore, it is possible to obtain from Eq. (17.53) after simple transformations that:

$$G_g=\frac{\beta\rho_g G_m}{\beta\rho_g+(1-\beta)\rho_l},\quad G_l=\frac{\beta\rho_l G_m}{\beta\rho_g+(1-\beta)\rho_l},$$

$$J_g=\frac{\beta\rho_g J_m}{\beta\rho_g+(1-\beta)\rho_l},\quad J_l=\frac{\beta\rho_g J_m}{\beta\rho_g+(1-\beta)\rho_l}, \tag{17.54}$$

and from Eqs. (17.44) and (17.54):

$$w_g=\frac{\beta G_m}{S\varphi\left[\beta\rho_g+(1-\beta)\rho_l\right]},\quad w_l=\frac{(1-\beta)G_m}{S(1-\varphi)\left[\beta\rho_g+(1-\beta)\rho_l\right]}. \tag{17.55}$$

The densities of the gas and liquid phases are found from equations of state:

$$\rho_g=\rho_g(p,T),\quad \rho_l=\rho_l(p,T). \tag{17.56}$$

The true gas-content φ and hydraulic resistance factor λ_m are found from empirical equations. Suppose:

$$\varphi = \varphi(\beta, \mathrm{Re}_m, \mathrm{Fr}_m, \mathrm{We}_m, \bar{\rho}, \bar{\mu}), \tag{17.57}$$

$$\lambda_m = \lambda_m(\varphi, \mathrm{Re}_m, \mathrm{Fr}_m, \mathrm{We}_m, \bar{\rho}, \bar{\mu}, \varepsilon), \tag{17.58}$$

where Re_m, Fr_m, We_m are Reynolds, Frud's and Weber's numbers for the mixture calculated from these equations:

$$\mathrm{Re}_m = D\frac{\beta\rho_g w_g + (1-\beta)\rho_l w_l}{\beta\mu_g + (1-\beta)\mu_l},$$

$$\mathrm{Fr}_m = \frac{[\varphi w_g + (1-\varphi)w_l]^2}{gD},$$

$$\mathrm{We}_m = 2D[\varphi w_g + (1-\varphi)w_l]^2\frac{\rho_l - \rho_g}{\sigma}.$$

The above nomenclature is as follows: ratio of phase densities $\bar{\rho} = \rho_g / \rho_l$; dynamic viscosity factors of gas and liquid media μ_g, μ_l; normalized viscosity of the fluid phase $\bar{\mu} = \mu_l / \mu_w$; water viscosity μ_w; surface tension σ; tube's diameter D; relative roughness of the tube's walls ε.

In order to determine the inflow J_m, a function of the following format needs to be assigned:

$$J_m = J_m(p, p_{\mathrm{amb}}), \tag{17.59}$$

where p_{amb} is ambient pressure.

The system of 15 Eqs. (17.45), (17.48), (17.54)–(17.59) — called thereafter "system A" — includes 23 unknown variables: G_m, G_g, G_l, J_m, J_g, J_l, p, T, ρ_m, ρ_g, ρ_l, w_g, w_l, v_4, v_3, λ_m, β, φ, h_g, h_l, μ_g, μ_l, σ.

The values β, h_g, h_l, μ_g, μ_l, σ can be computed using the corresponding thermodynamic procedures as functions of p, T and the composition of the two-phase mixture. Squared velocities v_4, v_3 are usually much smaller than the corresponding enthalpies and can be disregarded. So, the system A is a closed system and contains 15 equations with 15 unknown variables.

Utilizing Eqs. (17.45) and (17.54)–(17.59), it is possible to cancel from Eq. (17.48) 12 unknown variables G_g, G_l, J_m, J_g, J_l, ρ_m, ρ_g, ρ_l, w_g, w_l, λ_m, φ, which are

decisively on indecisively enter the equations. Therefore, the system A can be reduced to the system Eq. (17.48), which includes p, T, G_m values as unknown variables.

3. Transformation of equations of two-phase flow in pipes

For the transformation of the equation system Eq. (17.48), it is necessary to introduce the following functions:

$$\Phi_1 = \frac{1}{S^2}\left[\frac{G_g^2}{\varphi\rho_g} + \frac{G_l^2}{(1-\varphi)\rho_l}\right], \quad \Phi_2 = \rho_m g_z - \frac{\lambda_m}{2D}\Phi_1 \quad \left(\chi = \pi D, \quad S = \frac{1}{4}\pi D^2\right),$$

$$\Phi_3 = \left(h_g + \frac{w_g^2}{2}\right)G_g + \left(h_l + \frac{w_l^2}{2}\right)G_l, \quad \Phi_4 = h_g J_g + h_l J_l, \tag{17.60}$$

$$\Phi_5 = g_z G_m - \pi D k (T - T_{amb}).$$

Using Eqs. (17.54)–(17.57), it is possible to represent Eq. (17.60) as:

$$\Phi_1 = G_m^2 \Psi_1(p, T, G_m), \quad \Psi_1 = \rho_m g_z - \frac{(1-\varphi)\beta^2\rho_g + \varphi(1-\beta)^2\rho_l}{S^2\left[\beta\rho_g + (1-\beta)\rho_l\right]},$$

$$\Phi_3 = G_m \Psi_3(p, T, G_m), \quad \Psi_3 = \tag{17.61}$$

$$= \frac{1}{\beta\rho_g + (1-\beta)\rho_l}\left[\beta\rho_g\left(h_g + \frac{w_g^2}{2}\right) + (1-\beta)\rho_l\left(h_l + \frac{w_l^2}{2}\right)\right].$$

Substituting Eqs. (17.60) and (17.61) Eq. into Eq. (17.48) ($v_3^2 << h_g$, $v_4^2 << h_l$):

$$\frac{dp}{dz} = \Phi_2 - \frac{d\Phi_1}{dz} = \Phi_2 - \frac{d}{dz}(G_m^2 \Psi_1),$$

$$\frac{d\Phi_3}{dz} = \frac{d}{dz}(G_m \Psi_3) = \Phi_4 + \Phi_5,$$

wherefrom, upon differentiating and substituting $\frac{dG_m}{dz} = J_m$, gives:

$$\left(1+G_m^2\frac{\partial\Psi_1}{\partial p}\right)\frac{dp}{dz}+G_m^2\frac{\partial\Psi_1}{\partial T}\frac{dT}{dz}=\Phi_2-G_mJ_m\left(2\Psi_1+G_m\frac{\partial\Psi_1}{\partial G_m}\right),$$

$$G_m\frac{\partial\Psi_3}{\partial p}\frac{dp}{dz}+G_m\frac{\partial\Psi_3}{\partial T}\frac{dT}{dz}=\Phi_4+\Phi_5-J_m\left(\Psi_3+G_m\frac{\partial\Psi_3}{\partial G_m}\right). \tag{17.62}$$

Solving the system Eq. (17.62) for $\frac{dp}{dz}$ and $\frac{dT}{dz}$, and taking the first Eq. (17.48) into consideration, yields:

$$\frac{dG_m}{dz}=J_m,$$

$$\frac{dp}{dz}=\frac{1}{\Delta}\left\{\left[\Phi_2-G_mJ_m\left(2\Psi_1+G_m\frac{\partial\Psi_1}{\partial G_m}\right)\right]\frac{\partial\Psi_3}{\partial T}-\right.$$

$$\left.-\left[\Phi_4+\Phi_5-J_m\left(\Psi_3+G_m\frac{\partial\Psi_3}{\partial G_m}\right)G_m\frac{\partial\Psi_1}{\partial T}\right]\right\}, \tag{17.63}$$

$$\frac{dT}{dz}=\frac{1}{G_m\Delta}\left\{\left[\Phi_4+\Phi_5-J_m\left(\Psi_3+G_m\frac{\partial\Psi_3}{\partial G_m}\right)\right]\left(1+G_m^2\frac{\partial\Psi_1}{\partial p}\right)-\right.$$

$$\left.-\left[\Phi_2-G_mJ_m\left(2\Psi_1+G_m\frac{\partial\Psi_3}{\partial G_m}\right)\right]G_m\frac{\partial\Psi_3}{\partial p}\right\},$$

where:

$$\Delta=\left(1+G_m^2\frac{\partial\Psi_1}{\partial p}\right)\frac{\partial\Psi_3}{\partial T}-G_m^2\frac{\partial\Psi_1}{\partial T}\frac{\partial\Psi_3}{\partial p}. \tag{17.64}$$

Within the constraints of our assumptions, Eqs. (17.63) describe the flow of two-phase mixtures within perforated tubes. The tube's inclination angle is accounted for in these equations by the term g_z and by the format of the functions of Eqs. (17.57), (17.58). If the tube's wall is impermeable, J_m = 0, and the system Eqs. (17.63) becomes much simpler. At $G_l = J_l = 0$, Eq. (17.63) describe the single-phase liquid flow, and at $G_g = J_g = 0$, the single-phase gas flow.

4. Flow regimes

As indicated earlier, a distinguishing feature of two-phase (multi-phase) flows is the presence of the interphase separation boundaries. These boundaries may have various shapes. The phase dispersion may also significantly vary. Because of these, a concept of the flow regime is introduced to classify the two-phase flows. Experimental studies discovered numerous regimes, which have been named and classified in many different ways. The following classification is most common for the vertical flows:

Bubble flow. The gas bubbles are distributed in the liquid more or less uniformly (Fig. 17-3-*1*).

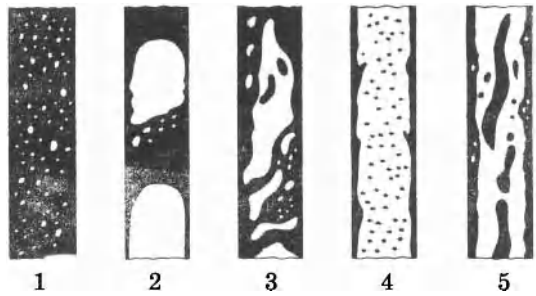

Fig. 17.3

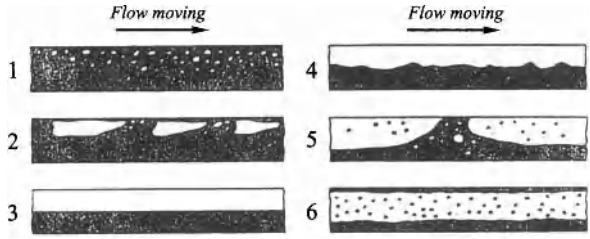

Fig. 17.4

Shell flow. When the bubbles are highly concentrated, they merge, their diameter becomes close to the channel diameter, and the bubbles themselves acquire a shell-like shape (Fig. 17-3-*2*).

Foam flow. As the gas phase flow velocity grows, the shell flow becomes unstable. The channel's wall becomes covered with a liquid film, and the gas-liquid core becomes a foam (Fig. 17-3-*3*).

Ring flow. The liquid flows along the tube's wall as a continuous film, and the gas phase moves in the center. Usually the gas core contains some liquid droplets (Fig. 17-3-*4*).

Flocky ring regime. The gas flow carries liquid droplets (Fig. 17-3-*5*).

A somewhat different classification is applicable to the horizontal flows:

Bubble flow. The gas bubbles are moving next to the upper generatrix of the tube (Fig. 17-4-*1*).

Plug flow. The shell-shaped gas bubbles are moving next to the upper generatrix of the tube (Fig. 17-4-*2*).

Laminated flow. The flow is gravitationally laminated. The liquid is flowing at the bottom of the channel, and the gas is flowing above it (Fig. 17-4-*3*).

Wavy flow. As the gas flow velocity increases, waves form on the free surface of the liquid (Fig. 17-4-*4*).

Shell flow. The waves on the liquid's surface increase so much that they reach the tube's upper generatrix. The gas phase is flowing along the upper generatrix as individual inclusions (Fig. 17-4-*5*).

Ring flow. Observed at large gas throughflow. Some amount of liquid is moving within the gas phase as individual droplets (Fig. 17-4-*6*).

The format of (17.57), (17.58) equations, i. e., true gas-content φ and hydraulic resistivity factor λ are strongly dependant on the flow regime.

5. Absolute open flow of a gas-condensate well

To kill an emergency gusher, it is necessary to know the absolutely open flow of the well. It is very important to be able to forecast such a flow in a specific field. The forecast rate of a gushing gas-condensate well can be calculated using the equation system Eq. (17.63).

Suppose that the penetrated thickness of the productive interval is much smaller that the depth of the well so that the flow can be considered concentrated. Then $J_m = 0$, and Eq. (17.63) for a vertical well assumes the following format:

$$\begin{aligned} &G_m = \text{const}, \\ &\frac{dp}{dz} = \frac{1}{\Delta}\left(\Phi_2 \frac{\partial \Psi_3}{\partial T} - \Phi_5 G_m \frac{\partial \Psi_1}{\partial T}\right), \\ &\frac{dT}{dz} = \frac{1}{G_m \Delta}\left[\Phi_5\left(1 + G_m^2 \frac{\partial \Psi_1}{\partial p}\right) - \Phi_2 G_m \frac{\partial \Psi_3}{\partial p}\right], \end{aligned} \tag{17.65}$$

where Δ is found from Eq. (17.64).

To account for the interaction between the well and the reservoir, the binomial equation of the fluid inflow is used from the reservoir to the well instead of Eq. (17.59):

$$p_{\text{res}}^2 - p_{\text{bh}}^2 = AQ_m + BQ_m^2, \tag{17.66}$$

where p_{res}, p_{bh} are, respectively, formation and bottomhole pressures, A and B are filtration resistance factors as determined during the regime testing of gas-condensate wells, Q_m is total volume throughflow reduced to standard conditions.

The system of equations Eq. (17.65) in conjunction with Eqs. (17.45) and (17.54)–(17.58) enables calculation of the distribution of pressure, temperature and other characteristic parameters of flow through the well under the commercial regime, i. e., when the value of the mass throughflow G_m is known. As the system includes two first-order differential equations, two boundary conditions are necessary for its solution. Such conditions can be the bottomhole temperature and pressure, i. e., $p_0 = p_{bh}$, $T_0 = T_{bh}$, or the wellhead temperature and pressure, i. e., $p(H) = p_{wh}$, $T(H) = T_{wh}$, where H is depth of the well. The conditions of the following format can also be assigned: $p(0) = p_{bh}$, $T(H) = T_{wh}$ or $p(h) = p_{bh}$, $T(0) = T_{bh}$.

In a case of the emergency flow (gusher), the G_m value is unknown. In such a case, Eq. (17.66) expressing the interaction between the well and the reservoir must be added to Eqs. (17.45), (17.54)–(17.58).

The emergency flow regime can be either critical (the flow velocity at the wellhead equals to the local speed of sound) or subcritical depending on the total resistance of the reservoir and the well. Under the subcritical flow, the wellhead pressure is equal to atmospheric pressure, i. e., $p_{wh} = p_{atm}$. Besides, it is necessary to assign T_{wh} or T_{bh}.

Under the critical flow a disruption between pressure and temperature occurs at the wellhead. Mathematically, it means that at $z \to H$, $\frac{dp}{dz} \to \infty$ and $\frac{dT}{dz} \to \infty$. Following Eqs. (17.63) and (17.64) it is necessary to have:

$$\Delta = \left(1 + G_m^2 \frac{\partial \Psi_1}{\partial p}\right)\frac{\partial \Psi_3}{\partial T} - G_m^2 \frac{\partial \Psi_1}{\partial T}\frac{\partial \Psi_3}{\partial p} = 0 \text{ at } z = H. \qquad (17.67)$$

Aside from the condition (17.67), it is necessary to assign $T(0) = T_{wh}$.

The rate determined by the condition Eq. (17.67) is called *critical*.

For different flow regimes of the two-phase mixture, the empiric functions Eqs. (17.57) and (17.58) have different formats.

To calculate the true gas-content φ and hydraulic resistance factor λ_m, we can use experimental results by VNIIGaz Institute. They showed that depending on the average volume velocity of the mixture flow (which is equal to: $w_m = \frac{Q_g + Q_l}{S} = \varphi w_m + (1-\varphi)w_l)$, four mixture flow regimes are identified: (1). Bubbly and shell regime ($w_m < w_a$); (2). Ring regime ($w_a \le w_m < w_r$); (3). Dispersion-ring regime ($w_r \le w_m < w_{cr}$); (4). Dispersion regime ($w_{cr} < w_m$). The w_a and w_{cr} values are computed as follows:

$$w_a = \frac{0.86\exp[9(1-\beta)]w_r}{3.3(1+0.0027(\overline{\mu}-1))} = \varphi w_m + (1-\varphi)w_l,$$

$$w_r = 3.3\sqrt{\frac{\rho_l}{\rho_g}}\left(\frac{\sigma g}{\rho_l - \rho_g}\right)^{0.25}.$$

The w_{cr} value is assumed to be 5 m/s. True gas-content for the above regimes is calculated from the following equations:

$$\varphi = \begin{cases} A\beta f_1(\mathrm{Fr}_m) & \text{at } w_m < w_a, \\ A\beta f_1(\mathrm{Fr}_m) + f_2(\beta) & \text{at } w_a \le w_m < w_r, \\ A\beta f_1(\mathrm{Fr}_m) - f_3(\beta) & \text{at } w_r \le w_m < w_{cr}, \\ \beta & \text{at } w_{cr} \le w_m, \end{cases}$$

where:

$$a = 0.5 + 0.3\exp[0.067(1-\bar{\mu})],$$

$$f_1(\mathrm{Fr}_m) = 1 - \exp(-4.4\sqrt{\mathrm{Fr}_m / \mathrm{Fr}^*}),$$

$$f_2(\beta) = \left[\frac{(1-A)(w_m - w_a^*)}{w_r - w_a^*} - 2(1-\beta)\right]\exp\left(-7.5\sqrt{1-\beta}\right),$$

$$f_3(\beta) = (1 + A - 2\beta)\exp\left(-7.5\sqrt{1-\beta}\right),$$

$$w_a^* = \frac{0.86}{1 + 0.00275(\bar{\mu} - 1)}\sqrt{\frac{\rho_l}{\rho_g}}\left(\frac{\sigma g}{\rho_l - \rho_g}\right)^{0.25},$$

$$\mathrm{Fr}^* = 4[1 - \exp(0.1\bar{\mu})] - 3[1 - \exp(0.05\bar{\mu})].$$

Hydraulic resistance factor is found as follows:

$$\lambda_m = \psi\lambda(\mathrm{Re}_m, \varepsilon),$$

where $\lambda_m(\mathrm{Re}_m, \varepsilon)$ is hydraulic resistance factor computed for a single-phase flow, ψ is the correction factor for double-phasiness determined as:

$$\psi = \begin{cases} f_4(\beta) & \text{at } w_m < w_a, \\ E[f_4(\beta) - f_5(k)] & \text{at } w_a \le w_m < w_r, \\ 1 & \text{at } w_{cr} \le w_m, \end{cases}$$

where:

$$E = 1 + 0.03\bar{\mu},$$

$$f_4(\beta) = \frac{1 - 0.78\beta f_1(\mathrm{Fr}_m) - 0.22\beta[1 - \exp(-15\bar{p})]}{1 - \beta + 0.03\exp[-1{,}350(1-\beta)^3]},$$

$$f_5(k) = \left(\frac{\rho_l - \rho_g}{g\sigma}\right)^{0.25}.$$

Phase densities ρ_l, ρ_g are calculated using the equations of state, such as Peng-Robinson's equation. The values of enthalpy, throughflow gas-content, surface tension, i. e., h_g, h_l, μ_g, μ_l, β, σ, are found with the help of corresponding thermodynamic equations.

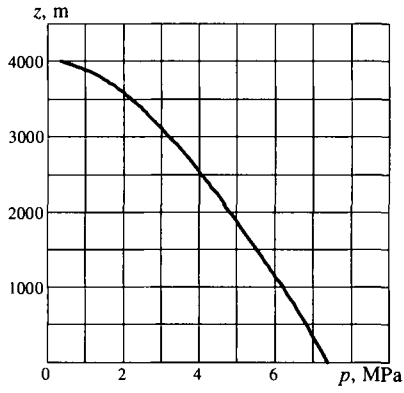

Fig. 17.5

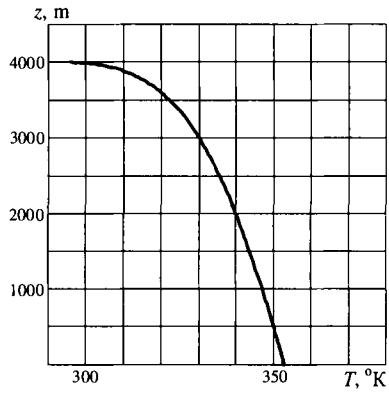

Fig. 17.6

To calculate viscosity of the gas phase, Dean's and Steel's correlation was utilized. Viscosity of the liquid phase was found using the Little and Kennedy technique. Ideal gas enthalpy for the pure components were determined by Passat and Donner's correlation, and for the fractions, by Kessler-Lee's correlation. The increment of enthalpy as a function of p and T was found using the known techniques. For the computation of the interphase tension factor, McLeod-Sugden correlation was applied. Typical pressure and temperature distribution curves in the well under the critical flow are presented in Figs. 17-5, 17-6.

Mechanics of Fluid Flow
by Kaplan S. Basniev, Nikolay M. Dmitriev and George V. Chilingar

PART III. OIL AND GAS SUBSURFACE HYDROMECHANICS

CHAPTER XVIII

MAIN DEFINITIONS AND CONCEPTS OF FLUID AND GAS FLOW. DARCY'S LAW AND EXPERIMENT

1. Specifics of fluid flow in natural reservoirs

The porous and permeable rocks which contain subsurface oil and gas accumulations and can release them in the process of development are called reservoirs. Depending on the origin and shape of the voids, the reservoirs are subdivided into the porous and fractured ones.

The natural fluids (oil, gas, underground water and their mixtures) are found in the voids (i. e., in pores and fractures) of reservoirs. The fluid in a reservoir can be quiescent or moving. The fluid flow through solid bodies (deformable or undeformable) along the communicating pores and/or fractures is called flow in underground rocks. Filtration can be caused by the action of various forces: pressure, concentration, temperature gradients as well as gravitational, capillary, electromolecular and other forces. For instance, the motion (filtration) of the melted wax within a candle's wick or of kerosene in an oil-lamp's wick is caused by capillary forces. Thereafter, however, we will be reviewing the flows caused by the action of the pressure gradient and/or gravitational force.

The flow in underground structures theory underwent a significant development due to the needs of the economy. In the petroleum industry, the flow in underground structures theory forms the theoretical base for the hydrocarbon field development. Due to its specifics, it is called "subsurface hydromechanics". The subsurface hydromechanics is a special branch of hydromechanics dealing with the fluid equilibrium and/or flow within a specific medium, a solid matrix comprised of cemented or loose particles of various shape and size. Thus, the petroleum subsurface hydromechanics is dealing with the laws of fluids' quiescence and flow within the oil- and gas-saturated reservoirs, as it applies to the technological processes of their recovery from the subsurface.

The particulars of the fluids' flow within the natural reservoirs are caused both by the specifics of the reservoir rocks and by the hydrocarbon development techniques.

Pore spaces of sedimentary rocks are a complex system of communicating and isolated intergranular voids where it is difficult to identify individual pore channels

(Fig. 18.1). The pore sizes of the sands are usually a few to few tens of a micrometer (μm).

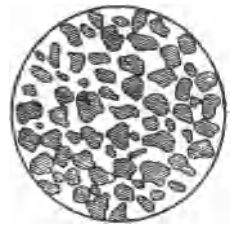

Fig. 18.1 Thin section of oil-saturated sandstone

The fluids' flow within reservoirs occurs at a very low velocity, usually micrometers per second (such flows are called "creeping flows" in hydromechanics). The heat-dispersal surfaces are large. Thus, the filtration process to a high degree of accuracy can be considered isothermal. At the same time, a substantial friction force emerges during filtration within the rocks.

When fluid flows through reservoirs' void spaces, the contact between the rock matrix and the fluid occurs on a huge surface area. As an example, the surface area of the void spaces within 1 m^3 of the porous medium (sandstone) can reach 10^4 m^2. Thus the main fluid property affecting the filtration is its viscosity. The viscosity is taken into account even for the gas filtration, and as the force of friction is uniformly distributed in the entire reservoir volume, it was proposed by Zhukovsky to include the force of friction among the mass forces.

The structure of oil and gas accumulations is complicated by substantial lithologic non-uniformity of the reservoirs, their lamination, faults, and stratigraphic unconformities. Appraisal and commercial testing of the accumulations, recovery of oil and gas is conducted through wells with diameter of 10 to 20 cm and greater, spaced by hundreds, sometimes thousands of meters.

Some other specifics of the oil and gas flow within the natural reservoirs are:

- An impossibility to study the fluids' flow within reservoirs through a direct application of the classical methods of hydromechanics, i. e., the solution of viscous fluid flow equations for the area encompassing the entire pore spaces.
- A combination of very diverse scales of the filtration processes. They are defined by characteristic sizes differing by many orders of magnitude: pore size (a few to a few tens of micrometers); well diameter (tens of centimeters); field size (tens of kilometers); the reservoir variability along its dip and strike can be of any value.
- The limited amount and imprecision of information about the reservoir and reservoir fluids properties, which often hampers the generation of a unique model of the fluid-saturated accumulation.

The listed specifics of the subsurface petroleum hydrodynamics result in the formulation of modeling concepts and the development of methodologies directed to the primary identification of qualitative process patterns and generation of models with low sensitivity to the source data accuracy. A cognitive and practical value of the results is to a significant degree determined by the clearness of the problem setting and depth of the preliminary data analysis.

2. Basic model concepts of the subsurface liquid and gas hydrodynamics

As earlier indicated, the subsurface petroleum hydromechanics is a special branch of hydromechanics. It means that the continuity hypothesis will be used in defining the physical values describing the flow process, and in formulating the conservation laws. Under this hypothesis the studied objects (such as the moving fluid) are considered to be continuously filling the entire area (the space wherein the problem is set and being solved). However, the porous medium is understood as a multitude of solid particles in close contact with one another, cemented or not. The spaces between them (pores, fractures) are filled with a liquid and/or gas.

Thus, the filtration flow of the reservoir fluids is an aggregation of individual micro-motions within an erratic system of the pore channels (Fig. 18.2). Therefore, the true filtration flow is not "continuous" so that the effective (fictitious) values are introduced in defining the physical parameters. These values are "smeared", spread over the entire volume in a continuous way (Fig. 18.3). The effective velocities, pressures, etc., are replaced for the real ones. These effective parameters are represented in Fig. 18-3 as a uniform square grid.

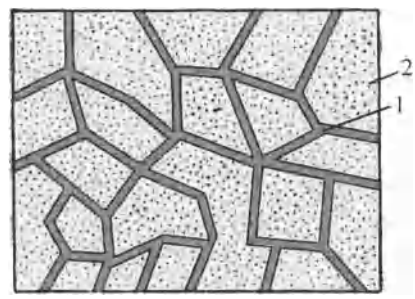

Fig. 18.2 Idealized porous medium. 1. pore channels, 2. matrix

It is known from statistical physics that the systems of the porous medium type can be described as continuous media whose effective properties are expressed not through the properties of individual component elements, but represent averaged parameters of sufficiently large volumes of that medium.

The transition to a macroscopic description of the processes in the subsurface hydromechanics means that all introduced parameters used for the problem setting and solving are in the general case functions of the *porous medium points*. The term is italicized because thereafter the concept of the porous medium and porous medium points will be used in the modeling sense. This means a mathematical model and its characteristics as used for the description of a physical process (in this case, the filtration).

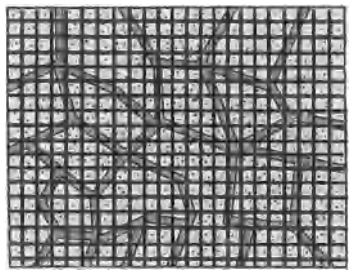

Fig. 18.3. Scheme of effective discription

The concept of a physical and mathematical points relate to totally different objects. If any volume of the porous medium is selected and the coordinate system associated with the sample is introduced, orderly triplets of numbers can be attributed to each infinitely small volume. These numbers assign the "mathematical point" of the porous medium. However, the volume of a "mathematical point" is so small that it always will be positioned entirely within the pore (then, for instance, the fluid velocity is different from zero) or within the solid matrix (then the fluid velocity is equal to zero).

Thus a "physical point" is used for description of model parameters in the subsurface hydromechanics.

The "physical point" is such volume of a porous rock, which is large enough so that the introduced physical parameter does not depend on the volume of the sample but small enough compared with the entire volume where this parameter is introduced. This latter circumstance (the sample smallness relative to the entire volume of interest) allows maintaining an infinitely small volume, the "physical point".

The volume of a porous medium which can be considered a physical point is called the elementary or representative volume. All characteristics and parameters introduced thereafter are defined over the elementary volumes and for the elementary volumes.

This situation with the introduction of the physical and material parameters in the subsurface hydromechanics is usual for all models in the mechanics of continuous medium. For instance, a gas similarly to a liquid is composed of individual molecules and atoms. Thus, in introducing physical parameters in hydromechanics and gas dynamics, they also relate to physical points, but the sizes of elementary volumes are much smaller than they are in subsurface hydromechanics. Indeed, an air cube with the edge of 10^{-3} mm under normal conditions contains $27*10^6$ molecules, so the elementary volume is fractions of a cubic millimeter. In subsurface hydromechanics sand grains can replace the molecules, so the elementary volume can be on the order of cubic centimeters, and in some reservoir types, tens of cubic centimeters and even meters. However, compared with the accumulation volume the elementary volume is still very small.

3. Reservoir properties of porous rocks. Porosity and clearance specific surface area.

Filtration is naturally determined by the properties of the fluid and of the void space (type of the reservoir) wherein it is occurring. So the reservoir properties of the porous medium are defined consequently. One of the most important properties of the porous medium is porosity denoted by a symbol m.

Porosity of a uniform porous space is the ratio of volume of pores V_c in the porous medium sample to the entire sample volume V:

$$\varnothing = \frac{V_c}{V}. \tag{18.1}$$

The porosity so defined is constant for all points of a uniform porous medium. In the case of a non-uniform porous medium, Eq. (18.1) defines the average porosity value for the sample. The porosity value at a physical point M for a non-uniform porous medium will be determined from equation:

$$\varnothing(M) = \lim_{\Delta V \to 0} \frac{\Delta V_c}{\Delta V} = \frac{dV_c}{dV}. \tag{18.2}$$

Therefore, in a general case porosity is a scalar function of the point (physical point).

There are concepts of the total and effective porosity. The effective porosity includes only the intercommunicating pores which can be filled with fluid from the outside. In studying the filtration processes, only this kind of porosity is meaningful. Thus thereafter, when dealing with porosity, the active or effective porosity will be considered.

Another important property of the porous medium is clearance or plane porosity, denoted by s. The clearance of a plane cross-section in a uniform porous medium is the ratio between the area of the pores in the cross-section to the area S of the entire cross-section:

$$s(\mathrm{n}) = \frac{S_{clear}}{S}. \tag{18.3}$$

In a case of a non-uniform porous medium, Eq. (18.3) defines the average clearance value for a cross-section. The clearance value at a physical point M for such a medium will be determined from equation:

$$s(M, \mathrm{n}) = \lim_{\Delta S \to 0} \frac{\Delta S_{clear}}{\Delta S} = \frac{dS_{clear}}{dS}. \tag{18.4}$$

Clearly, both porosity and clearance can range between 0 and 1. The end values of this range are, of course, purely model ones.

In Eqs. (18.3) and (18.4), "n" is the vector of a normal to the cross-section plane. The mentioned ratios and definitions indicate that clearance at a point in the porous medium depends not only on the point, but also on the cross-section orientation. Therefore, clearance in the above definition is a scalar function of the vector argument. Even taken by its own, this shows that porosity and clearance are different

mathematical objects, although connected. But the usual equating of these objects is a mistake. The clearance concept is more complex than that usually believed.

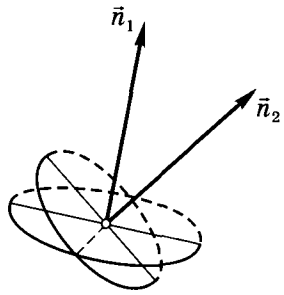

Fig. 18.4. Changing of section orientation and normal vector

Indeed, after the concept of clearance is introduced by Eq. (18.3), a statement usually follows that the average clearance value over all directions is equal to porosity. This is a correct statement but it is usually followed by an incorrect one: "therefore, thereafter there will be no distinctions made between the two". However, the quoted definition of clearance has more complex physical meaning than what is usually believed. The fact that the average clearance value over all directions is equal to porosity is no reason to identify these concepts. Later, when discussing the results of Darcy's experiment and the determination of the filtration velocity, the concept of clearance will be expanded and proved that it is impossible to identify it with porosity.

One more frequently used important parameter of the porous medium is the specific surface area per unit of porous medium's volume. The specific surface Σ per unit of porous medium's volume is the ratio of the void space's surface area of the S_{clear} medium to the total volume of the porous medium V:

$$\Sigma = \frac{S_{clear}}{V}. \tag{18.5}$$

By the definition Eq. (18.5), the specific pore surface, as opposed to the dimensionless porosity and clearance, has a dimensionality of m^{-1}.

4. Darcy's experiment and Darcy's law. Permeability. The concept of "true" average flow velocity and flow velocity

Let's now turn to the description of a fluid flowing within a porous medium. The first experiments with water flowing in sand-filled tubes were conducted by Darcy (1856) and Dupui (1848–1863). These experiments initiated the beginning of the filtration theory.

Darcy studied water flowing through the vertical sand filters (Fig. 18.5). The result of the experiment was the widely known law:

$$Q = k_f \frac{H_1 - H_2}{L} S = k_f \frac{\Delta H}{L} S, \tag{18.6}$$

where Q is volume throughflow of the liquid through an L-long sand filter with the cross-section area S, $\Delta H = H_1 - H_2$ is the difference of hydraulic water heads over the filter and at its base, and k_f is the proportionality factor. This factor was first called the water-permeability factor then filtration factor, which depends on the nature of the porous medium as well as on the filtering liquid's properties. As men-

tioned, the filtration velocities are very low, on the order of 10^{-4} to 10^{-5} m/s and even smaller. That allows disregarding the velocity heads when calculating the hydraulic head in Eq. (18.6):

$$H = \frac{\alpha v^2}{2g} + \frac{p}{\rho g} + z \approx \frac{p}{\rho g} + z. \qquad (18.7)$$

Here, v_α are the average velocities within the capillary, α_i are Coriolis' coefficients (in this case, $\alpha_1 = \alpha_2 = 2$), p is pressure, z is the geometric head, ρ is liquid's density, g is gravity acceleration.

As follows from Eq. (18.6), the filtration factor has the dimensionality of velocity and describes the velocity of flow through the unit of the cross-section area perpendicular to the flow under the action of a unit of the head gradient.

The filtration factor k_f is usually utilized for hydrotechnical designs where the only fluid is water. When analyzing filtration of the gas, oil and their mixtures, it is necessary to separate the effect of the porous medium from that of the fluid. For this purpose, Eq. (18.6) is formatted differently:

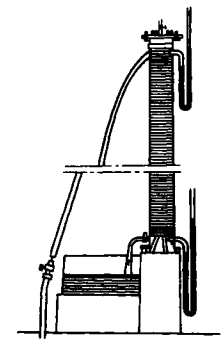

Fig. 18.5. Darcy laboratory unit water flow through vertical sandstone cores.

$$Q = \frac{k}{\mu} \rho g \frac{\Delta H}{L} S \qquad (18.8)$$

or:

$$Q = \frac{k}{\mu} \frac{p_1^* - p_2^*}{L} S, \qquad (18.9)$$

where μ is fluid's dynamic viscosity factor, $p^* = \rho g H = p + \rho g z$ is normalized pressure, k is permeability factor which does not depend on fluid's properties and is a dynamic parameter of the porous medium only. The permeability factor dimensionality is determined from the following formula:

$$[k] = \frac{[Q][\mu][L]}{[\Delta p^*][\Omega]} = \frac{\text{M}^3\text{C}^{-1}\Pi\text{a}\text{C}\text{M}}{\Pi\text{a}\text{M}^2} = \text{M}^2$$

It is the dimensionality of area, i. e., in the SI system, it is the square meter. Permeability of most of the rocks are very low, 10^{-12} to 10^{-13} m^2 (1 to 0.1 μm^2) for coarse-grained sandstones, 10^{-14} m^2 (0.01 μm^2) for tight sandstones. A commonly used permeability unit in the petroleum industry is 1 D (1 Darcy) = $1.02*10^{-12}$ m^2.

Following Eqs. (18.6) and (18.8) the filtration and permeability factors are related as follows:

$$k_f = \frac{\rho g}{\mu} k. \qquad (18.10)$$

The filtration factor k_f or permeability k is experimentally determined with a permeameter that contains a sample of the rock (Fig. 18.6). The total throughflow Q of the flow is maintained constant, the heads H_1 and H_2 are measured by two piezometers connected with the porous medium in the cross-sections 1 and 2. Elevations of the cross-sections' centers over the datum are equal to z_1 and z_2, pressures are p_1 and p_2, the distance between the cross-sections along the cylinder's axis is L.

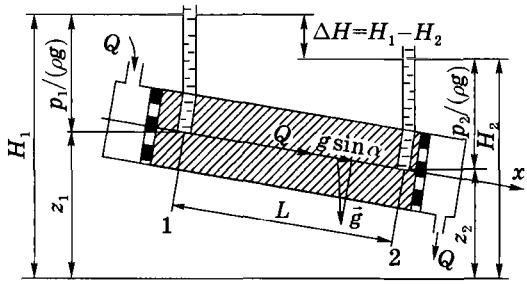

Fig. 18.6. Scheme of permeameter

From Eqs. (18.6) or (18.8):

$$k_f = \frac{Q}{S(\Delta H / L)} \text{ or } k = \frac{\mu Q}{S\rho g(\Delta H / L)},$$

where the head gradient per unit length (the pressure gradient modulus) can be formatted as follows:

$$\frac{\Delta H}{L} = \frac{z_1 - z_2}{L} + \frac{p_1 - p_2}{\rho g L} = \frac{p_1^* - p_2^*}{\rho g L}.$$

In the field, the permeability factor is determined by testing of wells. In the test, the experimentally found correlation between well's pressure and its flow rate is also used.

Eqs. (18.6) and (18.9) are usually called Darcy's law. In actuality, however, they are derived relations of Darcy's law and the solution of one of the simplest problems of unidimensional flow as it is implemented in the permeameter or a Darcy device. The Darcy's law is the correlation between the filtration velocity vector and the filtration pressure gradient. After a concept of the filtration velocity is introduced, the filtration pressure gradient concept will be reviewed.

Let's divide both parts of Eq. (18.9) by the cross-section area S:

$$w = \frac{Q}{S} = \frac{k}{\mu}\frac{\Delta p}{L}. \tag{18.11}$$

Expression $w = Q/S$ has the dimensionality of velocity and determines the modulus of the filtration velocity vector. When determining the throughflow, it is assumed that the filtration velocity vector is perpendicular to the plane (gallery) through which the fluid is filtering (Fig. 18.7). Therefore, if the unit (basis) vector perpendicular to this plane is defined (or parallel to velocity) as $\bar{n}$, then $\bar{w} = w\bar{n}$. The difference between the vector $\bar{w}$ and a regular velocity is in that the filtration velocity is a fictitious velocity as in its substance it is determined at any point within the porous medium (in the pores and in the matrix), whereas in actuality the flow occurs only through the pore channels at some "true average velocity" v. Of course, the w and v velocities are related, which is obvious from the equality of the throughflow at the true velocity through the clearance area and through the entire cross-section area at the filtration velocity:

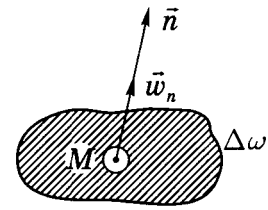

Fig. 18.7. Scheme for determination of filtration rate

$$wS = vS_{clear} = Q$$

This relation resulting from the above equality is:

$$\bar{w} = w\bar{n} = s\bar{v} = sv\bar{n}. \qquad (18.12)$$

Thus, filtration velocity is equal to true average velocity multiplied by the clearance. But it is illegitimate to replace porosity by clearance in Eq. (18.12).

Let's now prove this statement. Eq. (18.12) is valid on the assumption that the filtration properties of porous medium are isotropic and uniform, i. e., permeability is independent on the direction and is constant for all points. It is possible to perform an experiment on the assumption that the porous medium is uniform but anisotropic. Let's cut a cube with the facets perpendicular to the main directions of permeability (i. e., when applying pressure gradient perpendicular to cube's faces, the filtration velocity vectors will also be perpendicular to these faces). Now it is necessary to introduce a Cartesian coordinate system with the axes directed parallel to cube's edges, and conduct a series of experiments, sequentially directing filtration along each axis. As a result, for each experiment:

$$w_x = \frac{Q_x}{S} = \frac{k_x}{\mu}\frac{\Delta p}{L}, \quad w_y = \frac{Q_y}{S} = \frac{k_y}{\mu}\frac{\Delta p}{L}, \quad w_z = \frac{Q_z}{S} = \frac{k_z}{\mu}\frac{\Delta p}{L},$$

where w_x, w_y and w_z are component of the filtration velocity, Q_x, Q_y and Q_z, and k_x, k_y and k_z are throughflow and permeability values along the corresponding coordinate axes. Therefore, at the equal pressure gradients and sample (gallery) cross-section areas, in the general case it is necessary to input different clearance values for constructing the connection between the filtration velocities and true velocities, i. e., accept the equalities:

$$w_x S = w_x S_{xpor}, \quad w_y S = w_y S_{ypor}, \quad w_z S = w_z S_{zpor}$$

or:

$$w_x = s_x v_x, \quad w_y = s_y v_y, \quad w_z = s_z v_z, \qquad (18.13)$$

where v_x, v_y, v_z and s_x, s_y, s_z are true average velocity and clearance values along the respective coordinate axes. Indeed, Eq. (18.12) provides the linear correlation between two vectors. In the most general format, written for the main axes, it can be presented as:

$$\begin{pmatrix} w_1 \\ w_2 \\ w_3 \end{pmatrix} = \begin{pmatrix} s_1 & 0 & 0 \\ 0 & s_2 & 0 \\ 0 & 0 & s_3 \end{pmatrix} \begin{pmatrix} v_1 \\ v_2 \\ v_3 \end{pmatrix}. \tag{18.14}$$

A particular case of Eq. (18.14,) $s_1 = s_2 = s_3 = s$ results in Eq. (18.12), and in the general case results a matrix with the clearance factor.

Therefore, transiting from average true velocities to filtration velocities, it is necessary to use not the scalar function of a vector argument (defined above as clearance) but the matrix.

The transition from experimental Eq. (18.9) to Eq. (18.11) shows that in Darcy's experiment is a linear correlation identified between the two vector parameters: the filtration velocity vector and the filtration pressure gradient vector in a uniform, isotropic, non-deformable reservoir (porous medium). However, Eq. (18.11) is represented in a scalar format, so it must be restored to the vector format.

In the case of isotropic filtration properties, the filtration velocity vector and the filtration pressure gradient vector are positioned on the same straight line. So, multiplying Eq. (18.9) by the unit vector **n** (which gives the direction of filtration) gives:

$$\bar{w} = w\bar{n} = \frac{k}{\mu}\frac{\Delta p^*}{L}\bar{n}. \tag{18.15}$$

Here, the multiplier $\Delta p^* / L$ is the pressure gradient modulus under the linear pressure distribution law. Therefore, the further generalizations of the experimental result gives the vector equation of the following format:

$$\bar{w} = -\frac{k}{\mu}\operatorname{grad} p^*. \tag{18.16}$$

Vector equation Eq. (18.16) is Darcy's law for an isotropic porous medium. The minus sign in the right portion is due to the fact that filtration velocity is directed toward the decreased pressure. So, the filtration velocity vector and the filtration pressure gradient vector are oppositely directed (a reminder: the gradient is directed toward the growing pressure; therefore, filtration velocity is oppositely directed from the higher to the lower pressure).

Eq. (18.16) is the universal format of Darcy's law. It is valid for any coordinate system. The Cartesian format is as follows:

$$w_x\mathbf{i} + w_y\mathbf{j} + w_z\mathbf{k} = -\frac{k}{\mu}\left(\frac{\partial p}{\partial x}\mathbf{i} + \frac{\partial p}{\partial y}\mathbf{j} + \frac{\partial p}{\partial z}\mathbf{k} + \rho g\mathbf{k}\right), \tag{18.17}$$

where **i, j** and **k** are unit vectors of the Cartesian coordinate system; the z axis is directed upward. This vector equation can be projected onto the coordinate axes and rewritten as a system of equations:

$$w_x = -\frac{k}{\mu}\frac{\partial p}{\partial x},\ w_y = -\frac{k}{\mu}\frac{\partial p}{\partial y},\ w_z = -\frac{k}{\mu}\left(\frac{\partial p}{\partial z} + \rho g\right). \qquad (18.18)$$

However, Darcy's law has limitations which will be discussed in the following section.

5. Applicability limits of Darcy's law. Analysis and interpretation of experimental data

Numerous studies found that Darcy's law has the upper and lower applicability limits. The upper boundary is due to a number of reasons associated with the inertia forces at high filtration velocities. The lower boundary is caused by non-Newtonian rheological properties of fluids, by their interactions with the solid matrix of porous medium at low enough filtration velocities.

In this section both marginal cases resulting in the appearance of non-linearity in the filtration law will be reviewed.

The upper limit of Darcy's law applicability. This case is the most studied case. The upper limit of Darcy's law applicability is associated with some critical (cutoff) value of Reynolds' number Re:

$$\mathrm{Re} = \frac{wd}{\nu},$$

where d is some characteristic parameter of the porous medium, ν is kinematic viscosity factor of the fluid ($\nu = \mu/\rho$).

Numerous experimental studies (Fanchler; Lewis and Burns; Lindquist, Trebin, Zhavoronkov, Aerov and others) attempted to find a universal correlation for the porous medium (analogous to the tubular hydraulics) between the hydraulic resistance factor λ and Re number. However, due to variations in the porous media composition and structure, these attempts failed.

Significant care in processing the experimental results was taken to select such a characteristic parameter of the pore structure that the deviations from Darcy's law would occur at the same Reynolds' number values, and the filtration law within the nonlinear area would allow for a universal representation.

The first quantitative estimate of the upper limit for Darcy's law applicability was obtained by Pavlovsky. Using Slichter's results for a model of the ideal rock and assuming that the characteristic linear parameter d is equal to the effective diameter d_{eff} of the particles, he derived the following equation for Reynolds' number:

$$\mathrm{Re} = \frac{wd_{eff}}{(0.75\varnothing + 0.23)\nu}. \qquad (18.19)$$

Using this equation and the experimental results, Pavlovsky found that the critical value of Reynolds' number is:

$$7.5 < \mathrm{Re}_{cr} < 9.$$

The narrow range of Re's variability is due to the fact that the porous media used in the experiments were not too diverse. To facilitate the processing of massive experimental data acquired by various scientists, Shchelkachev proposed to use the following dimensionless parameter (he called it Darcy's parameter):

$$\mathrm{Da} = \frac{w\mu/k}{\Delta p/L} = \frac{w\mu L}{k\Delta p}. \tag{18.20}$$

Eq. (18.20) indicates that Darcy's parameter is the ratio of the force of viscous friction to force of pressure. If Darcy's law is realized, Darcy's parameter value must be equal to one:

$$\mathrm{Da} = 1. \tag{18.21}$$

The introduction of the Da parameter simplifies the study of the linear filtration law applicability limit. Indeed, if the log Re is depicted on the x-axis, and log Da, on the y-axis, then, as log Da = 0, the correlation graph log Re *vs.* log Da at $\mathrm{Re} < \mathrm{Re}_{cr}$ is a straight line coinciding with the x-axis while $\mathrm{Re} < \mathrm{Re}_{cr}$. As soon as the graph shows deviation from the x-axis, it indicates the deviation from Darcy's law (this corresponds to Da < 1, log Da < 0). The Re value at which the deviation occurs, is the critical value.

The above statements are illustrated by Fig. 18.8 showing a processing result of the experimental log Da *vs.* log Re measurements using Shchelkachev equation (Table 18.1). The graph reflects the nonlinear filtration area for various porous rocks.

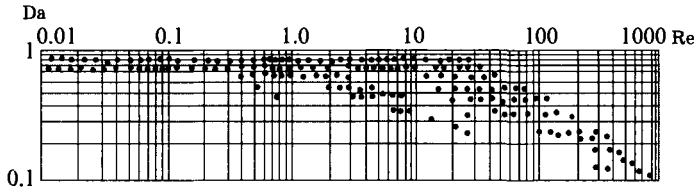

Fig. 18.8. lgDa versus lg Re on logarifmic grid

Using these data, he analyzed the results obtained by various scientists for Re determinations in the subsurface hydromechanics and evaluation of possible critical values of Re number for the upper Darcy's law applicability limit. See Table 18.1 for his comparison results. The first two lines are, respectively, Re number equations and hydraulic resistance factors obtained by various scientists. Lines four and five are, respectively, critical values of Reynolds' number obtained by these scientists, and their refined values.

Line 3 in the Table lists the $\mathrm{Re}\lambda$ values. Eq. (18.21) is valid for the linear filtration law area ($\mathrm{Re} < \mathrm{Re}_{cr}$). Therefore, if the product $\mathrm{Re}\lambda$ depends only on Darcy's parameter (see Table 18.1, columns 5-8) it is constant (i. e., does not depend on the properties of the porous medium) when $\mathrm{Re} < \mathrm{Re}_{cr}$. Only in this case it is possible to obtain the "universal" straight-line graph with coordinates (log Re, log λ), corresponding to filtration of different fluids through porous media having different properties. Experimental results support this conclusion.

Table 18.1.

Determinations of upper Darcy's law applicability limit by various scientists

No	Parameter	N.N. Pavlovsky	Fancher, Lewis, Burns	V.N. Shchelka-chev	M.D. Millionsh-chikov	F.I. Kotyakov (Trebin) G.F.	E.M. Minsky	A.I. Abdulvagabov
1	2	3	4	5	6	7	8	9
1	Re	$\frac{wd_{eff}}{(0.75\varnothing+0.23)\nu}$	$\frac{wd_{eff}}{\nu}$	$\frac{10}{\varnothing^{2.3}}\frac{w\sqrt{k}}{\nu}$	$\frac{10}{\varnothing^{3/2}}\frac{w\sqrt{k}}{\nu}$	$\frac{4\sqrt{2}w\sqrt{k}}{\varnothing^{3/2}\nu}$	$\frac{w\sqrt{k}}{\nu}$	$\frac{12(1-\varnothing)w\sqrt{k}}{\varnothing^{2}\nu}$
2	λ	–	$\frac{d_{eff}\Delta p}{2L\rho w^2}$	$\frac{2\varnothing^{2.3}\sqrt{k}\Delta p}{2L\rho w^2}$	$\frac{\varnothing^{3/2}\sqrt{k}\Delta p}{2L\rho w^2}$	$\frac{2\varnothing^{3/2}\sqrt{k}\Delta p}{L\rho w^2}$	$\frac{\sqrt{k}\Delta p}{2L\rho w^2}$	$\frac{4.6(1-\varnothing)\varnothing^{2}\sqrt{k}\Delta p}{2L\rho w^2}$
3	Reλ	–	$\frac{0.5}{f(\varnothing)\,\mathrm{Da}}$	$\frac{20}{\mathrm{Da}}$	$\frac{0.5}{\mathrm{Da}}$	$\frac{8\sqrt{2}}{\mathrm{Da}}$	$\frac{0.5}{\mathrm{Da}}$	$\frac{55.2(1-\varnothing)^{2}}{\mathrm{Da}}$
4	Re_{cr} by authors (from equations	7.5–9	1–4	1–12	0.022–0.29	0.3	–	0.019–8.1
5	Re_{cr} (refined values)	–	–	0.032–14	0.0015–0.60	0.0085–3.4	–	0.019–8.1

The following conclusions can be drawn from data listed in Table 18.1.

1. Despite some drawbacks in Pavlovsky's results, there are reasons to compare them with the corresponding results of the tubular hydraulics. What is important is that the critical Reynolds' number values calculated from Eq. (18.19) are much lower than those corresponding in the tubular hydraulics to the transition from the laminar to turbulent flow. It may indicate that the causes of deviations from Darcy's law at high filtration velocities (increase in the inertial forces effect with increases in Reynolds' number) should not be linked with the turbulent flow. The absence of turbulence with deviations from Darcy's law was proven by direct experiments by Schnobeli.

Fancher, Lewis and Burns equations were derived by way of introducing the effective diameter d_{eff} as the characteristic internal linear dimension of the porous medium into the equation for Reynolds' number. They do not compare with the results of the tubular hydraulics, result in too narrow a range for Re_{cr} (see column 4 in Table 18.1) and are not well substantiated.

2. All other formulae in Table 18.1 (columns 5–8) include as the characteristic linear dimension values proportionate to $\sqrt{k}$ (k is rock permeability factor) whose determination methods are well known. All these formulae are about equally convenient for the practical application. Their distinguishing feature is a very wide range of the resulting Re_{cr} values for the porous media. This appears to be quite natural considering wide variety of the tested porous media. Besides, it indicates that neither of the formulae proposed for the determination of Re_{cr} includes a complete set of parameters allowing for the description of the complex structure of porous media. It is quite insufficient to use for this purpose porosity and permeability factors. At the same time, the wide range of the Re_{cr} values can be subdivided into relatively narrow sub-ranges corresponding to different groups of porous rocks. Thus, this means that the upper limit of applicability of the Darcy's law is possible for fluid flow in a porous medium. The results of such subdivision for Shchelkachev formula (Table 18.1, line 1, column 5) are included in Table 18.2.

Table 18.2.

Critical Re values for porous rocks samples

No	Porous rock sample	Range of critical values
1	Uniform shots	13–14
2	Uniform coarse-grained sand	3–10
3	Nonuniform fine-grained sand dominated by less han 0.1 mm fractions	0.34–0.23
4	Cemented sandstone	0.05–1.4

6. Nonlinear laws of filtration

As was shown, Darcy's law, the major equation of the filtration theory, has the upper and lower applicability limits. The first expansion at $Re \geq Re_{cr}$ was suggested by Dupois. The law was named after Forchheimer who independently intro-

duced the law somewhat later. This binomial law solved relative to the pressure gradient in the vector format is:

$$\operatorname{grad} p = -\frac{\mu}{k}\bar{w} - \beta\frac{\rho}{\sqrt{k}}|w|\bar{w}, \tag{18.22}$$

where $|w|$ is modulus of the filtration velocity vector, β is the porous medium constant determined experimentally, ρ is fluid density. For the unidimensional flow where the pressure gradient modulus does not change along the flow (see Eq (18.15)), this equation can be projected onto a coordinate axis and presented in the scalar format:

$$\frac{\Delta p}{L} = \frac{\mu}{k}|w| + \beta\frac{\rho}{\sqrt{k}}|w|^2. \tag{18.23}$$

It is clear from this equation why it is usually interpreted as Taylor's series expansion by exponents of the filtration velocity vector.

It is important to emphasize that the representation of the nonlinear filtration law in the Eq. (18.22) format is not unique. Publications give another representation with the quadratic term. For instance, instead of the constant β and permeability factor, the macro-roughness factor l was introduced by Minsky:

$$\operatorname{grad} p = -\frac{\mu}{k}\bar{w} - \frac{\rho}{l}|w|\bar{w}$$

or another permeability factor (heavy fluid permeability factor):

$$\operatorname{grad} p = -\frac{\mu}{k_\mu}\bar{w} - \frac{\rho}{k_\rho}|w|\bar{w},$$

where k_μ is the viscous fluid permeability factor, and k_ρ is the heavy fluid permeability factor.

All these representations of the nonlinear filtration laws provide just one variant of Darcy's law expansion at high filtration velocity. Another common variant solved relative to filtration velocity is:

$$\bar{w} = c|\operatorname{grad} p|^{\frac{1-n}{n}}\operatorname{grad} p, \tag{18.24}$$

where $\operatorname{grad} p$ is modulus of filtration pressure gradient vector; c, n are material constants of the porous medium determined experimentally. The n constant usually ranges between 1 and 2. At $n = 2$, Eq. (18.24) is called Krasnopolsky's equation (this scientist suggested that the correlation between pressure gradient and filtration velocity when deviating from Darcy's law is quadratic). For a unidimensional flow, Eq. (18.24) can be projected onto a coordinate axis and written in the scalar format:

$$|w| = c|\operatorname{grad} p|^{\frac{1}{n}},$$

wherefrom at $n = 2$ we obtain:

$$|w|^2 = c|\text{grad } p|.$$

Eq. (18.22) appears to be more universal than Eq. (18.24). It is usually believed that it can be used at any filtration velocity. At a low velocity, the second component is negligible (with respect to filtration velocity) and can be disregarded. At the same time, the exponential law of filtration Eq. (18.24) can be used only in conditions when Darcy's law is deviated from (i. e., when $\text{Re} \geq \text{Re}_{cr}$).

The multiplier representation at the squared filtration velocity in Eq. (18.22) a multiplier ρ follows from the dimensionality theory as well as from the physical meaning of the cause of the filtration law deviation from linearity (density ρ is the mass per unit volume, i. e., the measure of inertia).

It is easy to produce the general format of the nonlinear filtration law for isotropic porous media. Let's first multiply (scalar multiplication) Eq. (18.16) by the unit vector directed along the filtration velocity. The result is:

$$|w| = \frac{k}{\mu}|\text{grad } p|.$$

Solving this equation relative to k:

$$k = \frac{\mu|w|}{|\text{grad } p|}. \qquad (18.25)$$

Experiments showed that $|w| = Q/S = F(|\text{grad } p|)$. *So, by selecting the class of functions where the approximation* $F(|\text{grad } p|)$ *is defined, it is possible to produce the expression of a nonlinear filtration law.*

In a similar fashion it is possible to have the filtration law solved relative to the filtration pressure gradient. Eq. (18.25) for the filtration resistance ratio has the following format:

$$r = \frac{|\text{grad } p|}{\mu|w|}.$$

In this case, the experimentally obtained Eq is formatted as:

$$|\text{grad } p| = \Psi(|w|).$$

Let's now go back to the previously mentioned deviation from Darcy's law experimentally observed at low filtration velocity (as the velocities are very low, these deviations are close to zero). As mentioned, the deviations at low filtration velocity have different physical nature and are caused by non-Newtonian properties of fluids and by the action of significant surface forces (forces of interaction between the fluid and the rock matrix). At a very low filtration velocity, even Newtonian fluids can acquire non-Newtonian properties in a porous medium. As velocity increases, however, this effect rapidly disappears.

In the petroleum industry, fluids displaying non-Newtonian properties include so-called anomalous oils and drilling muds.

A classic example of the filtration law expression for non-Newtonian fluids is the filtration law with the initial gradient. This filtration law is valid for Bingham-Shvedov visco-plastic fluids as follows:

$$w_i = -\frac{k}{\mu}\left(1 - \frac{\gamma}{|\text{grad } p|}\right)\frac{\partial p}{\partial x_i} \quad \text{at } |\text{grad } p| \geq \gamma, \tag{18.26}$$

$$w_i = 0 \quad \text{at } |\text{grad } p| \leq \gamma.$$

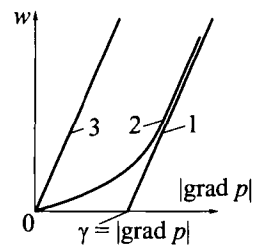

Fig. 18.9. Dependence diagram w from $|\text{grad } p|$: 1 — visco-plastic fluid with limit gradient; 2 — for real non-Newtonian oil; 3 — for Darcy law

As Eqs. (18.26) show, the filtration flow is only possible at pressure gradients exceeding some value γ which is called the initial gradient. At lower pressure gradient values the filtration flow is absent. The value of the initial gradient depends on the fluid's initial shear stress τ_0 and the effective diameter of the capillary d_{eff}. Fig. 18.9 displays graphs of the filtration velocity *vs.* filtration pressure gradient for the linear and nonlinear filtration laws.

7. Structural model of porous media

Real hydrocarbon reservoirs have very complex void space formed by pore channels of drastically changing diameters and direction, composed by particles of different shape and size, etc. Thus there is no practical possibility to generate analytical solutions considering all the above properties of real porous media, and simplified models are used in the subsurface hydromechanics. Such models include ideal (capillary) and fictitious (corpuscular) rocks (media). In the corpuscular models, the porous medium is modeled by balls, in the capillary models, by capillary tubules.

In the simplest corpuscular model, the porous medium is modeled by the constant diameter ball packing. It is called fictitious rock (or fictitious porous medium). In the simplest capillary model, the porous medium is modeled by capillary tubules of constant diameter laid at a constant interval. It is called ideal rock (or ideal porous medium).

Most common fictitious rock models are those with the most tight ball packing. Two basic packing, cubic and hexagonal, are produced as follows: the first flat layer is laid so that each ball touches six adjacent balls; each ball of the second layer is placed in the hollow between three balls of the first layer (Fig. 18.10, 18.11).

The third layer can be laid in two ways. The first one (the cubic packing): each third-layer ball lies over the three balls from the second layer so that there is no first-layer ball under the third-layer ball (Fig. 18.12). The second one (the hexagonal packing): each third-layer ball lies over the three balls from the second layer but there is a first-layer ball under the each third-layer ball.

Besides the mentioned tight packing with the cubic symmetry, the packing where each ball in the first layer touches only four balls, and all subsequent layers are identical with the first one, is also considered. It can be called a loose cubic packing.

Fig. 18.10. Layer of spheres, closely packed

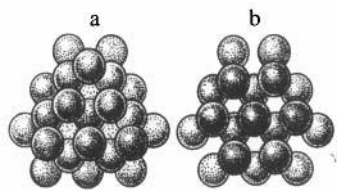

Fig. 18.11. Two main, the most compact packages of spheres: a — cubic, b — hexagonal

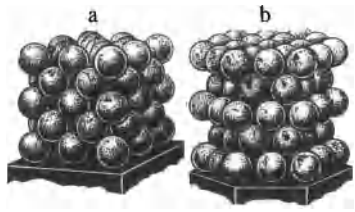

Fig. 18.12. The most compact packages of spheres: cubic (a) and hexagonal (b)

The simplest capillary rock models are formed at the perpendicular positioning of the capillaries.

The above ideal and fictitious rocks and resulting simplification of the pore space structure enables finding analytical equations associating between themselves reservoir properties of such simplified porous media and further expansion of the derived equations to the real porous media.

First the major relationships for the fictitious rock will be examined.

It is relatively simple to derive for the fictitious rock the relationship between per-unit volume surface with the packing porosity $\varnothing$ and ball diameter D. Suppose we have a volume containing n balls. The entire volume is the sum of void and solid volumes:

$$V_{\text{pore}} + \frac{\pi D^3}{6} n = V .$$

Porosity then is equal to:

$$\varnothing = 1 - \frac{\pi D^3 n}{6V} . \tag{18.27}$$

The per-unit volume surface is equal to the surface area of a single ball multiplied by the number of balls in the package:

$$\Sigma = \frac{\pi D^2 n}{V} . \tag{18.28}$$

Following Eqs. (18.27) and (18.28):

$$\Sigma = \frac{6(1-\varnothing)}{D}. \tag{18.29}$$

Slichter simplified the tightest ball packings and introduced the elementary ball-packing cell (Fig. 18.13). He also derived analytical equations for porosity and clearance:

$$\varnothing = 1 - \frac{\pi}{6(1-\cos\theta)\sqrt{1+2\cos\theta}} \tag{18.30}$$

and:

$$s = 1 - \frac{\pi}{4\sin\theta}, \tag{18.31}$$

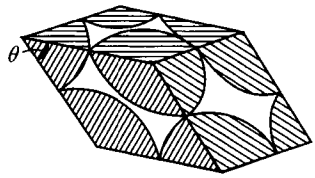

Fig. 18.13. Elementary box of spheres package

where θ is the acute angle of the side facet in the elementary rhombohedral cell of the ball packing. Slichter found that the value of this angle ranges between 60° and 90°, therefore, porosity and clearance range as follows: $0.259 \le \varnothing \le 0.476$ and $0.0931 \le s \le 0.2146$. As Eqs. (18.30) and (18.31) show, neither porosity nor clearance depend on the ball diameter and are determined only by the angle θ. Therefore, eliminating the angle from these equations it would be possible to derive the relationship between porosity and clearance. Regretfully, this equation system is transcendental and is not solvable in a decisive format, so this relationship is given approximately:

$$s = 0.61\varnothing^{1.4} \text{ or } s = 0.56\varnothing - 0.052, \tag{18.32}$$

with an error of less than 2 % within the aforementioned porosity range of the ball packings.

Later Kozeny and Carman proposed the following equation for the fictitious rock permeability:

$$k = \frac{\varnothing^3}{c\Sigma^2}, \tag{18.33}$$

where c is Carman's number. Experiments showed that for the ball packings Karman's number is approximately 5.

Substituting Eq. (18.29) into Eq. (18.33) results the following expression of permeability for the fictitious rock:

$$k = \frac{\varnothing^3 D^2}{36c(1-\varnothing)^2}. \tag{18.34}$$

For the ideal rock, the pore space structure allows for an analytical determination of major filtration and capacity parameters. Various types of the elementary cells (unidimensional, Fig. 18.14 and three-dimensional, Fig. 18.15) were used for the representation of the ideal rock.

The porosity, clearance, per-unit volume area and permeability for the ideal rock formed will be derived by the three systems of mutually perpendicular capillaries with a diameter $d_\alpha = 2r\alpha$ and the laying spacing of a_α, $\alpha = 1, 2, 3$.

All computations can be conducted for an elementary cell formed by three mutually perpendicular laying systems (Fig. 18.15).

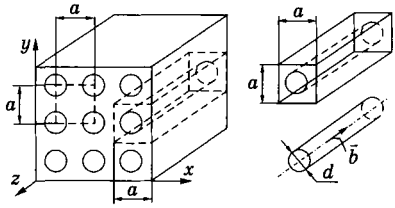

Fig. 18.14. Scheme of packing and elementary box of unidirectional permeability of perfect rock

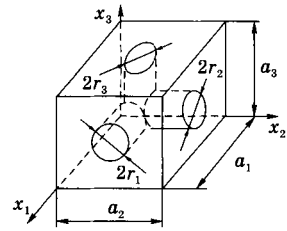

Fig. 18.15. Elementary box of three — dimensional model of perfect rock

Let's introduce a coordinate system with the axes parallel to the capillaries' axes of symmetry, which in turn are parallel to the laying systems. The subscript at denotations of the diameters and systems corresponds to the coordinate axis number to which the capillary and system are parallel. Then the following expressions is obtained for, respectively, porosity, clearance, per-unit volume area and permeability:

$$\varnothing = \frac{\pi d_i^2 a_i}{4a_1a_2a_3}, \quad s = \frac{\pi d_\alpha^2}{4a_\beta a_\gamma}, \quad \Sigma = \frac{\pi d_i a_i}{a_1a_2a_3}, \quad k_\alpha = \frac{\pi d_\alpha^4}{128a_\beta a_\gamma} = \frac{d_\alpha^2}{32} s_\alpha. \quad (18.35)$$

In Eqs. (18.35), the subscript i means summation, and the subscripts α, β and γ form cyclical permutation of numbers 1, 2 and 3. The calculations of porosity, clearance and per-unit volume area are purely geometric so they are omitted. The only remark is that in calculating porosity and per-unit volume area it was assumed that the "node" (capillaries' intersection) volume is small and can be disregarded.

To compute permeability, the fluid's flow within a capillary will be analyzed. The Bernoulli's equation is used for a viscous fluid flow and Darcy-Weisbech's equation for the head loss determination:

$$\frac{\alpha_1 v_1^2}{2g} + \frac{p_1}{\rho g} + z_1 = \frac{\alpha_2 v_2^2}{2g} + \frac{p_2}{\rho g} + z_2 + h_{1-2}, \quad h_\tau = \lambda \frac{l}{d} \frac{v^2}{2g},$$

where h_{1-2} is the head loss between cross-sections 1 and 2; h_τ is head loss along the length; λ is hydraulic resistivity factor; and l is length of the capillary between cross-sections 1 and 2.

The flow velocities at filtration are very low, so the velocity heads are ignored. Thus, for laminar flow in round pipe:

$$\lambda = \frac{64}{\mathrm{Re}} = \frac{64\mu}{vd\rho}.$$

To simplify the calculations we will assume that the capillaries are horizontal, i. e., the hydraulic resistivity factor with equation for the laminar flow within a round $z_1 = z_2$. We can also assume that the head loss is determined only by the loss for the friction along the length, so $h_{1-2} = h_\tau$. After simple transformations, the result is:

$$\frac{\Delta p}{\rho g} = \frac{64\mu}{vd\rho}\frac{l}{d}\frac{v^2}{2g}.$$

Solving this relative to the average fluid velocity within the capillary (the true average velocity of the fluid flow), results:

$$v = \frac{d^2}{32\mu}\frac{\Delta p}{l}.$$

In order to switch to the filtration velocity w, the definition Eq. (18.12) is used, i. e., the throughflow corresponding to velocity v is computed, and then "spread" it over the entire cross-section of the sample. By multiplying v by the capillary cross-section area $\pi d^2/4$ the volume throughflow Q is obtained. Then volume throughflow is divided by the elementary cell area a^2 resulting the filtering fluid's flow equation:

$$w = \frac{d^2}{32}\frac{\pi d^2}{4a^2}\frac{1}{\mu}\frac{\Delta p}{l}, \tag{18.36}$$

which in its format is identical to Darcy's law Eq. (18.15).

The structure of the numerical factor in the right portion of Eq. (18.36) is preserved for a purpose of emphasizing the physical meaning of its multipliers. Comparing it with the Darcy's law Eq. (18.15) — $\bar{w} = w\bar{n} = \frac{k}{\mu}\frac{\Delta p^*}{L}\bar{n}$ — it is easy to observe that the resulting factor $\pi d^4/128a^2$ is permeability of a "unidimensional" ideal rock. The first multiplier, $d^2/32$, gives the conductivity of the capillaries. Its format is defined by the shape of channels' crosswise section. The replacement of the cylindrical tubes with a round cross-section (used in our example) by flat slits or elliptically-shaped capillaries will not alter the proportionality between this multiplier and the squared characteristic size of the cross-section. The numerical factor, however, will be different. The second multiplier, $\pi d^2/4a^2$, is the clearance which serves as the averaging scale.

Therefore, permeability is a complex parameter of porous medium. It takes into account the pore channels' shape and cross-section size, and their concentration within the medium. Permeability computation equations commonly include the sinuosity α, which is equal to the ratio of the conducting pore channel (the "true" path of the fluid) to the sample (such as core) length. Various models of the unidimensional ideal rock can include α ranging between 1 and 3.

Eq. (18.36) was derived for a unidimensional model of the ideal rock. Clearly, it will stand for a 3D model as well except the subscripts will have to be added to indicate which capillary the equation corresponds to. Then Eq. (18.36) changes as following:

$$w_\alpha = \frac{d_\alpha^2}{32}\frac{\pi d_\alpha^2}{4a_\beta a_\gamma}\frac{1}{\mu}\frac{\Delta p}{l}, \tag{18.37}$$

where the subscripts α, β and γ form a cyclic permutation.

From Eq. (18.37) the permeability factor is derived for a 3D model of the ideal porous medium:

$$k = \frac{\pi d_\alpha^4}{128 a_\beta a_\gamma}. \tag{18.38}$$

Following Eq. (18.35) that $\varnothing = s_1 + s_2 + s_3$, and clearance is equal to porosity only when $s_2 = s_3 = 0$. Therefore, the equality $\varnothing = s$ is valid only for a unidimensional model of the ideal rock.

When dealing with applied problems, it is often necessary to determine the characteristic linear size, which is interpreted as the effective pore diameter or the capillary diameter in the model of the ideal rock. In the general case, the following can be derived from Eq. (18.38) for the capillary diameter:

$$d_\alpha = \sqrt{\frac{32k}{s_\alpha}}. \tag{18.39}$$

Usually, due to the identification of porosity and clearance, porosity is used in Eq. (18.39):

$$d_\alpha = \sqrt{\frac{32k}{\varnothing}}. \tag{18.40}$$

As indicated earlier, this equation is valid only for the unidimensional model when $\varnothing = s$ and is not valid for the three-dimensional model. To transit from clearance to porosity, a structural factor $\varphi_\alpha = \varnothing / s_\alpha$ can be suggested. Then Eq. (18.39) can be rewritten as follows:

$$d_\alpha = \sqrt{\frac{32\varphi_\alpha k}{\varnothing}}. \tag{18.41}$$

If we assume for a three-dimensional model that $d_1 = d_2 = d_3 = d$ and $s_1 = s_2 = s_3 = s$ then $\varnothing = 3s$, and therefore $\varphi = 3$, and the capillary diameter equation becomes as:

$$d = \sqrt{\frac{96k}{\varnothing}}. \tag{18.42}$$

In the general case, only the lower end of φ is limited ($\varphi \geq 1$), so the structural factor can change the effective capillary diameter within a wide range.

A final note: we reviewed only the simplest structural model of the porous medium. For these models reservoir properties can be easily calculated using geometric relationships and hydraulic Eqs without involving stochastic and other techniques. Currently porous media are modeled using statistical structural models with chaotically laid spheres, random grids and complex geometry of the capillary channels.

8. Darcy's law for anisotropic media

In this section the specifics of the filtration flow within media of a complex pore space geometry and anisotropy of the filtration properties will be discussed.

Depending on the pore space structural specifics and geometry, there are uniform and non-uniform, isotropic and anisotropic media. Anisotropy of properties

(including filtration properties) relates to different physical and geometrical properties in different directions. Anisotropy in actual oil and gas reservoirs can be caused by fracturing, lamination, the presence of inclusions. For instance, filtration properties of the laminated porous media are different along the lamination from those across the lamination. The filtration flows in fractured-porous media within the fractures are well in excess of those in some other directions.

The generalized Darcy's law is used for the description of the hydrocarbons flows within anisotropic reservoirs. The law's validity was confirmed by numerous experimental and theoretical studies. The expansion of Darcy's law for the case of anisotropic media is done mathematically formally. As Darcy's law postulates the linear correlation between two vector fields (filtration velocity vector and filtration pressure vector), then Eqs. (18.16)–(18.18) define the simplest relationship when both vectors are positioned on the same straight line and are different from one another in their direction and length. Such a correlation defines and assigns isotropic filtration properties. In the general case, the linear correlation between two vector fields is defined so that each component of one vector depends on all components of the other vector. Thus in the most general case the linear correlation between the filtration velocity vector and the filtration pressure gradient (the most general case of Darcy's law for anisotropic media) is formatted as follows:

$$\begin{aligned} w_1 &= -\frac{1}{\mu}\left(k_{11}\frac{\partial p^*}{\partial x_1} + k_{12}\frac{\partial p^*}{\partial x_2} + k_{13}\frac{\partial p^*}{\partial x_3}\right), \\ w_2 &= -\frac{1}{\mu}\left(k_{12}\frac{\partial p^*}{\partial x_1} + k_{22}\frac{\partial p^*}{\partial x_2} + k_{33}\frac{\partial p^*}{\partial x_3}\right), \\ w_3 &= -\frac{1}{\mu}\left(k_{13}\frac{\partial p^*}{\partial x_1} + k_{21}\frac{\partial p^*}{\partial x_2} + k_{23}\frac{\partial p^*}{\partial x_3}\right), \end{aligned} \tag{18.43}$$

where w_i are the components of the filtration velocity vector, $\partial p^*/\partial x_i$ are the components of the normalized pressure velocity vector, k_{ij} are the components of a symmetric matrix (tensor), which is called the permeability factors matrix (tensor). The tensor in Eq. (18.43) defines and assigns the filtration properties of the porous medium, which can be isotropic or anisotropic with different types of anisotropy. The decisive format of the permeability factors' matrix depends on the anisotropy type and the coordinate system in which the expanded Darcy's law is written. It is always possible to select at least one coordinate system $0x_1\, x_2\, x_3$ in which the format of the expanded Darcy's law is the simplest:

$$w_1 = -\frac{k_1}{\mu_1}\frac{\partial p^*}{\partial x_1}, \quad w_2 = -\frac{k_2}{\mu}\frac{\partial p^*}{\partial x_2}, \quad w_3 = -\frac{k_3}{\mu}\frac{\partial p^*}{\partial x_3}. \tag{18.44}$$

The Eqs. (18.43) can be represented in a matrix format:

$$\begin{pmatrix} w_1 \\ w_2 \\ w_3 \end{pmatrix} = \begin{pmatrix} k_{11} & k_{121} & k_{13} \\ k_{12} & k_{22} & k_{23} \\ k_{13} & k_{23} & k_{33} \end{pmatrix} \begin{pmatrix} \partial p^*/\partial x_1 \\ \partial p^*/\partial x_2 \\ \partial p^*/\partial x_3 \end{pmatrix}. \tag{18.45}$$

Rearranging Eq. (18.43) under summation of subscripts results:

$$w_i = -\frac{1}{\mu} k_{ij} \frac{\partial p^*}{\partial x_j}, \tag{18.46}$$

where i and j assume values of 1, 2 and 3.

A coordinate system where the permeability factor matrix has the diagonal format, and where the expanded Darcy's law is written in the Eq. (18.44) format is called the main coordinate system, and the value of the diagonal permeability factors k_i is called the main values of the permeability tensor. The matrix components in the main coordinate system have one subscript, and if the system is not main coordinate system, they have two subscripts. The first subscript corresponds to the line number, and the second one, to the column number.

Eq. (18.46) is the most general expression of Darcy's law for anisotropic porous media. By decreasing the number of non-zero matrix components of the permeability factor, it is possible to produce isotropy and all possible types of anisotropy. Indeed, if it is assumed that all non-diagonal matrix elements are equal to zero, and all diagonal elements are equal to one another, the porous media is isotropic. All other options will assign different types of anisotropy. Before classifying them, Let's first define the most common case of permeability.

By definition, permeability of the porous medium (directional permeability) is the value:

$$k(\bar{n}) = -\frac{\mu w_i n_i}{|\text{grad } p|}, \tag{18.47}$$

where n_i is a unit vector assigning the direction in the porous medium, along which directional permeability is determined, $w_i n_i = (\bar{w} * n)$ is a scalar product of the filtration velocity vector and unit vector, and $|\text{grad } p|$ is modulus of the filtration pressure gradient. As follows from the definition, in the general case permeability can depend on the direction.

The definition Eq. (18.47) has a transparent physical meaning: by definition, permeability is a scalar value which is calculated along certain direction. So, in order to calculate it, it is necessary to find the ratio of the scalar values defined along the direction in a special way. In Eq. (18.47), the direction of application of the pressure gradient ($\text{grad } p = |\text{grad } p|\bar{n}$) is assumed to be the direction along which the property is determined, and the scalar values are determined by projecting of the filtration velocity vector and filtration pressure gradient vector $\text{grad } p$, we obtain $w_i n_i$ and $|\text{grad } p|$. Their ratio multiplied by viscosity and taken with onto this direction. By projecting the vectors $\bar{w}$ and the opposite sign is equal to permeability. Minus sign is taken because the scalar product $w_i n_i$ is negative (the angle between $\bar{w}$ and n_i is obtuse). The definition of the directional permeability is illustrated by Fig. 18.16.

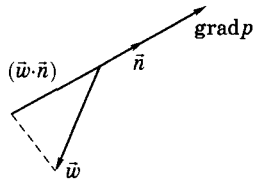

Fig. 18.16. Sheme to dimension of directional permeability

Substituting the Darcy's law expanded for anisotropic media Eq. (18.46) into Eq. (18.47):

$$k(\bar{n}) = -\frac{\mu w_i n_i}{|\text{grad } p|}\left(-\frac{k_{ij} n_i n_j}{\mu}|\text{grad } p|\right) = k_{ij} n_i n_j . \qquad (18.48)$$

Eq. (18.48) is a general rule for finding permeability valid for both anisotropic and isotropic porous media. Indeed, for isotropic porous media, under the definition Eq. (18.47) and rule Eq. (18.48) for calculating permeability at the linear filtration law:

$$k(\bar{n}) = k n_i n_i = k .$$

Therefore, permeability of isotropic media does not depend on the direction (it is the same for all directions and is equal to k).

Eq. (18.48) also clarifies the meaning of a statement that the permeability factor matrix k_{ij} defines and assigns the filtration properties of porous medium. The matrices define the type of the properties (isotropic or anisotropic), and the numeric values of its elements define values which characterize them.

As was shown, isotropic filtration properties are assigned by the matrix of the type:

$$k_{ij} = \begin{pmatrix} k & 0 & 0 \\ 0 & k & 0 \\ 0 & 0 & k \end{pmatrix}, \qquad (18.49)$$

therefore, all other types of matrices assign anisotropic filtration properties. It is possible to show using the linear algebra apparatus that all possible versions of the "anisotropic" matrices have the following format:

$$k_{ij} = \begin{pmatrix} k_1 & 0 & 0 \\ 0 & k_1 & 0 \\ 0 & 0 & k_3 \end{pmatrix}, \; k_{ij} = \begin{pmatrix} k_1 & 0 & 0 \\ 0 & k_2 & 0 \\ 0 & 0 & k_3 \end{pmatrix}, \; k_{ij} = \begin{pmatrix} k_{11} & k_{12} & 0 \\ k_{12} & k_{22} & 0 \\ 0 & 0 & k_3 \end{pmatrix},$$

$$k_{ij} = \begin{pmatrix} k_{11} & k_{12} & k_{13} \\ k_{12} & k_{22} & k_{23} \\ k_{13} & k_{23} & k_{33} \end{pmatrix}. \qquad (18.50)$$

The first type of Eq. (18.50) matrices assigns filtration properties, for example, of laminated (usually sedimentary) porous media for which permeability at the tops

of the layers is equal (a plane with isotropic filtration properties) and is different from permeability in the direction perpendicular to the lamination planes. The matrix has a diagonal format. Therefore, main directions of the permeability factors' tensor for this type of porous media are known *a priori*: one main direction is perpendicular to lamination, and the other two lie in the plane. As represented by the permeability factors' matrix Eq. (18.50), the direction perpendicular to lamination corresponds to the coordinate axis $0x_3$.

The first type of anisotropy assigns a porous or fractured medium where, as in the first case, the directions of all main k_{ij} matrix axes are known *a priori* but permeabilities along all main directions differ. Such anisotropy can be pertinent to fractured reservoirs with the three mutually perpendicular fracture systems or already mentioned sedimentary rocks formed by elongated grains.

These two types of anisotropy have proper names: the first one is called transverse isotropic, the second one, orthotropic.

For the remaining two types of anisotropy the position of the main axes is not known *a priori*. For type three, the position of the two main axes is unknown, and for the last type, the position of all three main axes in unknown. Apparently, the real-life fractured and porous media as a regular rule belong with these types but in solving the problems the two first types are usually considered. There are no proper names for these two types. By substituting the matrices Eq. (18.50) into Eqs. (18.45) or (18.46) the decisive representation of Darcy's law for all types of anisotropy is obtained.

Eq. (18.43) is a system of linear algebraic equations. It can be solved relative to the grad p component and rewritten like follows:

$$\frac{\partial p^*}{\partial x_j} = -\mu r_{ij} w_j .$$

In this case, filtration properties are defined and assigned by the symmetric matrix of filtration resistivity factors r_{ij}. The decisive format of r_{ij} matrices for all reviewed cases of anisotropy and isotropy is the same as for permeability factor matrices accurate to substituting corresponding components r_α, $r_{\alpha\beta}$ for k_α, $k_{\alpha\beta}$.

All Eqs. (18.49) and (18.50) given in the matrix format can be represented in the subscript format. For an index representation of the filtration laws in the anisotropic porous media the concept of a diad product for two vectors is introduced (see Attachment П.68).

$$\overline{\overline{ab}} \equiv a_i b_j \equiv \begin{pmatrix} a_1 b_1 & a_1 b_2 & a_1 b_3 \\ a_2 b_1 & a_2 b_2 & a_2 b_3 \\ a_3 b_1 & a_3 b_3 & a_3 b_3 \end{pmatrix}, \qquad (18.51)$$

Where a_i, b_i are the components of the vectors $\bar{a}$ and $\bar{b}$.

Further, as the vectors $\bar{a}$ and $\bar{b}$ are taken in the Cartesian basis vectors $\mathbf{e_1}$, $\mathbf{e_2}$, $\mathbf{e_3}$, whose coordinates we will denote $e_i^{(1)}$, $e_i^{(2)}$,$e_i^{(3)}$, respectively. It is easy to see that it is possible, using basis tensors, to put together nine diads which will represent nine special matrices of the Eq. (2.9) format. All components in these matrices besides one will be equal to zero. The only component different from the zero will occupy the "ij^{th} position" in multiplying the i_{th} basis vector by the j_{th} basis vector.

Let's review, as an example, the diad product of $\mathbf{e_1}$ and $\mathbf{e_2}$. Then, we have $e_i^{(1)} = (1,0,0)$, $e_i^{(2)} = (0,1,0)$, and in accordance with the definition Eq. (18.51), the matrix for this diad will be defined as:

$$\mathbf{e}_1\mathbf{e}_2 = e_i^{(1)}e_j^{(2)} = \begin{pmatrix} 0 & 1 & 0 \\ 0 & 0 & 0 \\ 0 & 0 & 0 \end{pmatrix}.$$

Using the diad products of the basis vectors, the matrix presentation can be rewritten as a subscript format by way of expanding the matrices with respect to the basis of diads $e_i^{(k)}e_j^{(l)}$. For instance, for the most general type of anisotropy such a presentation will have the following format:

$$w_i = -\frac{1}{\mu}[k_{11}e_i^{(1)}e_j^{(1)} + k_{12}(e_i^{(1)}e_j^{(2)} + e_i^{(2)}e_j^{(1)}) + k_{22}e_i^{(2)}e_j^{(2)} + k_{33}e_i^{(3)}e_j^{(3)} + \\ + k_{13}(e_i^{(1)}e_j^{(3)} + e_i^{(3)}e_j^{(1)}) + k_{23}e_i^{(2)}e_j^{(2)} + k_{33}(e_i^{(2)}e_j^{(3)} + e_i^{(3)}e_j^{(2)})]\frac{\partial p^*}{\partial x_j}. \quad (18.52)$$

By decreasing the number of k_{ij} coefficients not equal to zero, it is possible to come up with the filtration law for any kind of anisotropic or isotropic media. For instance, for the orthotropic media:

$$w_i = -\frac{1}{\mu}[k_1e_i^{(1)}e_j^{(1)} + k_2e_i^{(2)}e_j^{(2)} + k_3e_i^{(3)}e_j^{(3)}]\frac{\partial p^*}{\partial x_j}, \quad (18.53)$$

for the transverse-isotropic:

$$w_i = -\frac{1}{\mu}[k_1e_i^{(1)}e_j^{(1)} + k_1e_i^{(2)}e_j^{(2)} + k_3e_i^{(3)}e_j^{(3)}]\frac{\partial p^*}{\partial x_j}, \quad (18.54)$$

and for isotropic:

$$w_i = -\frac{1}{\mu}[e_i^{(1)}e_j^{(1)} + e_i^{(2)}e_j^{(2)} + e_i^{(3)}e_j^{(3)}]\frac{\partial p^*}{\partial x_j}. \quad (18.55)$$

The latter equation can be transformed as the brackets include three matrices which in the summation form a unit matrix:

$$\begin{pmatrix} 1 & 0 & 0 \\ 0 & 1 & 0 \\ 0 & 0 & 1 \end{pmatrix}.$$

A special symbol, δ_{ij}, is use to denote the unit matrix. It is called the Kronecker delta. So, the last equality can be rewritten as:

$$w_i = -\frac{1}{\mu}\delta_{ij}\frac{\partial p^*}{\partial x_j}$$

or, after summing-up:

$$w_i = -\frac{1}{\mu}\frac{\partial p^*}{\partial x_i}.$$

Using the rule of calculating the directions of permeability Eq. (18.48), it is a simple operation to calculate permeability for the most general case Eq. (18.50):

$$k_{ij}n_in_j = [k_{11}e_i^{(1)}e_j^{(1)} + k_{12}(e_i^{(1)}e_j^{(2)} + e_i^{(2)}e_j^{(1)}) + k_{22}e_i^{(2)}e_j^{(2)} + k_{33}e_i^{(3)}e_j^{(3)} + k_{13}(e_i^{(1)}e_j^{(3)} + e_i^{(3)}e_j^{(1)}) +$$
$$+ k_{23}(e_i^{(2)}e_j^{(3)} + e_i^{(3)}e_j^{(2)})]n_in_j = k_{11}\cos^2\alpha + 2k_{12}\cos\alpha\cos\beta + k_{22}\cos^2\beta + k_{33}\cos^2\gamma +$$
$$+2k_{13}\cos\alpha\cos\gamma + 2k_{23}\cos\beta\cos\gamma,$$

where α, β and γ are the angles between the unit vector **n** and the coordinate lines.

By decreasing the number of k_{ij} coefficients not equal to zero, it is possible to provide with the directions of permeability for any kind of anisotropic or isotropic media.

Mechanics of Fluid Flow
by Kaplan S. Basniev, Nikolay M. Dmitriev and George V. Chilingar

CHAPTER XIX

MATHEMATICAL MODELS OF UNIPHASE FILTRATION

1. Introductory notes. The concept of the mathematical model of a physical process

Various equations and methods of their solution, depending on a specific problem, are used for the description of real physical processes. As mentioned earlier, the most common and well developed such technique in the subsurface hydrodynamics is the macroscopic technique. It is based on the continuity hypothesis, laws and methods of the mechanics of continuous medium. Therefore, oil and gas subsurface hydromechanics should be treated as a special branch of the mechanics of continuous medium.

Now the major concepts utilized by the mechanics of continuous medium in construction of mathematical models will be repeated applied to the oil and gas subsurface hydromechanics.

Different fields in their physical nature are defined in the continuous medium. They form under influence of the internal and external factors and may change in space and time. Various fields of major physical values occur under the conservation laws, which are the fundamental laws of nature. The main conservation laws in the subsurface hydromechanics (as in the other branches of the continuous medium mechanics) are the laws of conservation of mass, momentum (impulse) and kinetic momentum (momentum of impulse), conservation of energy and entropy balance.

The conservation laws are valid for all continuous media whose properties can be quite different. Thus using only the conservation laws are insufficient for the generation of closed systems of equations needed for the description of physical processes and solution of the specific problems. In order to assign properties of the specific continuous media, the defining equations and laws are added to the conservation laws. These defining equations and laws assign the specific properties of a given medium.

A result of combining the conservation laws with defining equations and laws is a closed system of equations where the number of equations is equal to the number of the unknown functions. Such close system defines a mathematical model of the continuous medium describing the specific physical processes.

From this point on only the isothermal fluid flow in porous media, wherein the temperature of the fluid flowing in a porous medium is equal to the medium's

temperature and remains constant, is considered. Indeed, as filtration is a very slow process, fluid's temperature changes due to the resistance on the walls of pore channels and fractures, and due to the fluid's expansion as pressure changes, have sufficient time to compensate through heat exchange with the surrounding rocks. It is possible not to include the energy equation for such isothermal processes.

In the oil and gas field development, however, non-isothermal filtration effects exist locally at the bottomhole locations due to the significant pressure gradients. Study of non-isothermal processes is important in connection with enhanced oil recovery by injecting hot fluid in the reservoirs (water, steam), with the development of gas-hydrate fields, and in some other cases. The energy conservation law equation must be always added to the model in these cases.

In order to describe physical processes and solve corresponding problems, the problem should be set accurately, i. e., the conditions at the initial moment in time should be given as well as the conditions at the reservoir boundaries. The result is a differential equation with the initial and boundary conditions. By integrating this differential equation, it is possible to determine the distribution of the pressures and filtration velocities in the reservoir at any moment in time, i. e., to construct the functions:

$$P = p(x,y,z,t),\ w_x = w_x(x,y,z,t),\ w_y = w_y(x,y,z,t),\ w_z = w_z(x,y,z,t).$$

If the fluid inside the reservoir is a incompressible fluid (ρ = const) in the non-deformable reservoir ($\varnothing$ = const, k = const), then the number of the functions to be determined is limited to these four. For a description of a compressible fluid in the compressible porous medium, it is also necessary to determine the fluid density ρ. For more complex processes, the unknown functions to be determined are viscosity μ, porosity $\varnothing$ and permeability k. In such a case, eight equations, both differential and finite, are required to determine the eight parameters of the filtration flow, fluid and porous medium.

The analytical solution of a system of differential equations is feasible only in a few simplest cases, for instance, in the problem of an elastic fluid flow into a well in a reservoir of infinite expanse at a constant rate.

In more complex cases, the system can be solved by the application of the numerical techniques on computers. There are well-developed numerical techniques for the solution of diverse and very complex subsurface hydromechanics problems. The mentioned analytical solutions are very important for testing the numerical techniques.

The system of differential equations can be used also for the qualitative study of a process. If the obtained equations are reduced to the dimensionless format, the dimensionless conformity parameters will serve as their coefficients. By analyzing their structure and numerical values, it is possible to judge which forces are most important in the process, which terms in the equations can be disregarded, etc.

Now the major conservation laws are formulated by considering the specifics of the subsurface hydromechanics.

2. Mass conservation laws in a porous medium

For the integral format of the mass conservation law, the mass of fluid within the control volume of the porous medium is computed.

The mass of the fluid within an infinitely-small (physical) volume of a porous medium is equal to $m\rho dV$. Indeed, the pore volume within an elementary volume of the porous medium is equal to $dV_{\text{pore}} = \varnothing dV$. The fluid mass within the elementary porous volume is:

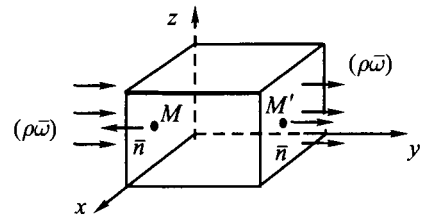

Fig. 19.1

$$dM = \rho dV_{\text{pore}} = m\rho dV.$$

By integrating this relationship over the entire control volume, the fluid mass within the control volume is obtained:

$$M = \int_V \varnothing \rho dV .$$

The fluid can flow in and out through the control surface (Fig. 19.1). Thus, the fluid mass changes in time. The changes are calculated as follows:

$$\frac{\partial}{\partial t} M = \frac{\partial}{\partial t} \int_V \varnothing \rho dV .$$

The change in the mass is equal to the mass inflow through the control surface:

$$\oint_{S_{\text{pore}}} \rho v_i n_i \, dS_{\text{pore}} = \oint_S \rho w_i n_i \, dS ,$$

where n is the external normal to the control surface.

Indeed, the mass flow through an elementary area dS, by definition, is equal to:

$$\rho \overline{w} \overline{n} \, dS \quad \text{or} \quad \rho w_i n_i \, dS ,$$

i. e., to the scalar product of the mass velocity vector and the vector of the normal to the elementary area multiplied by the area. In order to calculate the mass flow through the entire surface, the elementary flows with respect to the entire surface should be integrated.

Therefore, the balance equation becomes:

$$\frac{\partial}{\partial t} \int_V \varnothing \rho dV = -\oint_S \rho w_i n_i \, dS , \qquad (19.1)$$

which means that the mass changes in the control volume are equal to the fluid flow through the control surface. The minus sign is a results of the vector's normal orientation with respect to the control surface. As the normal is external with respect to the control surface, the fluid "inflow" into the control volume should be

accompanied by the increase in mass, a positive derivative with respect to time in the left part of Eq. (19.1) and a negative value of the scalar product $w_i n_i$ under the integral on the right. In order to equalize the signs, minus is needed. A similar train of thought is valid for the fluid "outflow".

Eq. (19.1) is the integral format of the fluid mass conservation law in a porous medium. In comparison to the integral format of the mass conservation law derived in Chapter II, the integral equation for a porous medium includes the $\varnothing\rho$ value instead of ρ; $m\rho$ is a fictitious fluid density, the density spread over the entire volume. In a transient-free flow, the time derivative is equal to zero, and following Eq. (19.1):

$$\oint_S \rho w_i n_i \, dS = 0 .$$

So, if a flow tube for the filtration velocity is considered as the control volume:

$$\int_{S_1} \rho_1 w_{1n} ds = \int_{S_2} \rho_2 w_{2n} ds , \tag{19.2}$$

where $S(\alpha)$ ($\alpha = 1, 2$) are areas of the flow tube's two cross-sections (at the "input" and "output"). The following properties were used in the derivation of Eq. (19.2):

– the scalar product of the filtration velocity vector and the normal's vector is equal to $w_i n_i = w_n$, where w_n is the projection of the velocity vector upon the normal,

and

– in one case it is positive (for instance, in the cross-section 2) and in the other case it is negative.

For an incompressible fluid, $\rho_1 = \rho_2 = \rho$, so:

$$\int_{S_1} w_{1n} ds = \int_{S_2} w_{2n} ds .$$

If the velocities in both cross-sections are constant over the entire cross-section:

$$w_{1n} S_1 = w_{2n} S_2 .$$

These relationships in their physical meaning and format are similar to the formulas derived in Part I of this book.

It is possible to switch from the integral format of the mass conservation law to the differential one. For this purpose, as the control volume is fixed in the space, the $\partial / \partial t$ operator is placed under the sign of the integral and then, using Gauss–Ostrogradsky theorem, transform the surface integral into a volume one. The result is:

$$\int_V \left(\frac{\partial \varnothing \rho}{\partial t} + \operatorname{div} \rho \bar{w} \right) dV = 0 . \tag{19.3}$$

Following the condition that Eq. (19.3) is valid for any volume V, that the expression under the sign of the integral is equal to zero, i. e.:

$$\frac{\partial \varnothing \rho}{\partial t} + \operatorname{div} \rho \bar{w} = 0. \qquad (19.4)$$

Eq. (19.4) is the differential format of the mass conservation law in a porous medium or ***the continuity equation for the fluid filtration in a porous medium.***

If porosity m is constant, it can be carried out from the sign of the derivative, and the continuity equation can be rewritten as follows:

$$\varnothing \frac{\partial \rho}{\partial t} + \operatorname{div} \rho \bar{w} = 0.$$

For an incompressible fluid ρ = const; so, the continuity equation is even simpler:

$$\operatorname{div} \rho \bar{w} = 0.$$

In the derivation of both differential and integral mass conservation law it was assumed that the porous medium volume does not have either fluid source or sink, that neither chemical reactions nor phase transformations, etc., occur there. If this is not so, a function q must be added to the right side of Eq. (19.4). The function q is the fluid mass entering (exiting) the unit volume during unit time, i. e.:

$$\frac{\partial \varnothing \rho}{\partial t} + \operatorname{div} \rho \bar{w} = q.$$

The q value is positive if the fluid enters the volume and negative if it exits the volume.

3. Differential equation of fluid flow

Another universal conservation law in mechanics is the law of the kinetic momentum. In the mechanics of continuous medium the differential form of this law has a format of continuous medium equation expressed in stresses. Its further transformation is determined by rheologic (or definitive) equations of the medium. In our case, Newton's law of viscous friction (leading to Navier–Stokes equations) serves as definitive equations.

As subsurface hydromechanics deals with the flow averaged over the entire volume of the porous medium, these equations must be averaged. The averaging results in the earlier discussed Darcy's law. The mathematical techniques applied for such derivation of Darcy's law are outside the scope of the subsurface hydromechanics. In Chapter I derivations based on hydraulic relationships were reviewed. It is now desired to demonstrate another derivation proposed by Zhukovsky.

Zhukovsky's train of thought was based on Euler's ideal fluid flow equation. To simplify the reasoning, the unidimensional flow described by the following equation is considered:

$$\rho \frac{\partial v}{\partial t} + \rho v \frac{\partial v}{\partial x} = -\frac{\partial p}{\partial x} + \rho f,$$

where f is the projection of the volume (mass) forces' projection density onto the flow direction, and v is true average flow velocity.

When a fluid is flowing within a porous medium, the friction force occurs on the separation boundary "medium-fluid". The surface of the pore channels is sufficiently great, and in transition from the true average filtration velocity to the filtration velocity, the friction force is spread all over the volume. Thus the friction force can be considered a volume force. Therefore, the volume forces' density can be represented as:

$$f = f_1 + f_2,$$

where f_1 is the projection of the volume gravitational force, $f_1 = g\sin\alpha = (z_1 - z_2)g/l$ in a case where the flow axis is inclined at the angle α to a horizontal plane (see 18.6), f_2 is the projection of the viscous friction volume force caused by the flow in a porous medium.

Further, assuming that the medium is isotropic and clearance is constant, the true average velocity is switched to the filtration velocity:

$$\frac{\rho}{s}\frac{\partial w}{\partial t} + \rho\frac{w}{s^2}\frac{\partial w}{\partial x} = -\frac{\partial p}{\partial x} + \rho(f_1 + f_2).$$

Assuming the velocity changes in time are small, we can disregard the $\partial v/\partial t$ term. The second component in the left part (the inertia term) is also negligibly small at low filtration velocities. Then:

$$\frac{\partial p}{\partial x} = \rho(f_1 + f_2). \tag{19.5}$$

Assuming the viscous friction force is linearly proportional to filtration velocity w (i. e., assuming $f_2 = \rho\lambda w$), Eq. (19.5) can be transformed into:

$$\frac{\partial p}{\partial x} = \rho\lambda w + \rho\frac{z_1 + z_2}{l}g.$$

If it is assumed that $\lambda = -\mu/\rho k$, this assumption leads to Darcy's law.

4. Closing equations. Mathematical models of isothermal filtration

As derived earlier, the conservation laws for any given porous medium are:
for the isotropic porous medium:

$$\begin{aligned} &\frac{\partial \varnothing\rho}{\partial t} + \operatorname{div}\rho\bar{w} = 0, \\ &\bar{w} = -\frac{k}{\mu}(\operatorname{grad}p + \rho\bar{f}); \end{aligned} \tag{19.6}$$

for the anisotropic porous medium:

$$\begin{aligned} &\frac{\partial \varnothing\rho}{\partial t} + \operatorname{div}\rho\bar{w} = 0, \\ &\bar{w} = -\frac{k_{ij}}{\mu}\left(\frac{\partial p}{\partial x_j} + \rho f_j\right). \end{aligned} \tag{19.7}$$

Of these four scalar equations, three are given by Darcy's law, and one is the mass conservation law. These equations include six unknown scalar functions: three

components of the velocity vector, density, pressure and porosity. In the general case, permeability and viscosity can be added to the list of the unknown functions. This makes it clear that the systems Eqs. (19.6) and (19.7) are not closed. Moreover, it is clear why just the conservation laws in themselves are insufficient for the production of a closed equation system. The conservation laws are valid at viscous fluid filtration within all porous media. The porous media and viscous fluids can have various properties. For instance, the fluid can be compressible and non-compressible, the porous medium can be deformable and non-deformable, etc. Thus, to assign the properties of a specific porous medium and fluid equations determining these additional properties are required (thus equations are called definitive).

With the isothermal filtration flows under consideration the definitive equations usually have the format of correlation between density, porosity (permeability, viscosity) and pressure, for instance, $\rho = \rho(p)$, etc. In this case, the most general representation of a closed system of equations (i. e., the mathematical model) is:

$$\begin{aligned} &\frac{\partial \varnothing \rho}{\partial t} + \operatorname{div} \rho \bar{w} = 0, \\ &\bar{w} = -\frac{k}{\mu}(\operatorname{grad} p + \rho \bar{f}), \\ &\rho = \rho(p),\ \varnothing = \varnothing(p),\ k = k(p),\ \mu = \mu(p). \end{aligned} \tag{19.8}$$

Here, the format of the pressure functions is assumed to be given. In the next section various types of these function and the corresponding mathematical models will be reviewed.

5. Filtration model of incompressible viscous fluid under Darcy's law in a non-deformable reservoir

The simplest model of isothermal filtration is when the fluid is assumed to be incompressible, viscosity is constant and the reservoir is non-deformable. In this case the definitive equations are assigned by the following equalities:

$$\rho = \text{const},\ \varnothing = \text{const},\ k = \text{const},\ \mu = \text{const}, \tag{19.9}$$

and the closed equation system of filtration in isotropic reservoir has the following format:

$$\begin{aligned} &\operatorname{div} \rho \bar{w} = 0, \\ &\bar{w} = -\frac{k}{\mu}(\operatorname{grad} p + \rho \bar{f}). \end{aligned} \tag{19.10}$$

The system Eq. (19.10) includes four equations and four unknown functions (three components of velocity vector and pressure). Density is no longer the unknown function as it does not change. If necessary, it is assigned at the problem setting (as well as the mass forces vector).

The system Eq. (19.10) can be transformed. To simplify the arguments, the mass forces are disregarded and the Darcy's law is substituted into the continuity equation. The result is:

$$\operatorname{div}\left(-\frac{k}{\mu}\operatorname{grad}p\right)=-\frac{k}{\mu}\operatorname{div}\operatorname{grad}p=-\frac{k}{\mu}\Delta p=0,\ \text{or}\ \Delta p=0,$$

where Δ is Laplace's operator.

Therefore, the system Eq. (19.10) can be rewritten as follows:

$$\begin{aligned}&\Delta p=0,\\ &\bar{w}=-\frac{k}{\mu}\operatorname{grad}p.\end{aligned}\tag{19.11}$$

The closed equation systems Eqs. (19.10) and (19.11) are a mathematical model of the theory of a incompressible viscous fluid filtration in the isotropic porous medium.

The equation systems of the theory of a incompressible viscous fluid filtration in the anisotropic porous medium look similarly and are derived by substituting in Eqs. (19.10) and (19.11) the Darcy's law for anisotropic porous media [Eq. (18.46)] for the Darcy's law for isotropic porous media.

Equations in the systems Eqs. (19.10) and (19.11) are written in the universal no-subscript format valid for any coordinate system. By projecting these equations, for example, onto the Cartesian coordinate system, respectively, for Eq. (19.10):

$$\begin{aligned}&\frac{\partial w_1}{\partial x_1}+\frac{\partial w_2}{\partial x_2}+\frac{\partial w_3}{\partial x_3}=0,\\ &w_1=-\frac{k}{\mu}\left(\frac{\partial p}{\partial x_1}+\rho f_1\right),\\ &w_2=-\frac{k}{\mu}\left(\frac{\partial p}{\partial x_2}+\rho f_2\right),\\ &w_3=-\frac{k}{\mu}\left(\frac{\partial p}{\partial x_3}+\rho f_3\right),\end{aligned}\tag{19.12}$$

and for Eq. (19.11):

$$\begin{aligned}&\frac{\partial^2 p}{\partial x_1^2}+\frac{\partial^2 p}{\partial x_2^2}+\frac{\partial^2 p}{\partial x_3^2}=0,\\ &w_1=-\frac{k}{\mu}\frac{\partial p}{\partial x_1},\\ &w_2=-\frac{k}{\mu}\frac{\partial p}{\partial x_2},\\ &w_3=-\frac{k}{\mu}\frac{\partial p}{\partial x_3}.\end{aligned}\tag{19.13}$$

The mathematical model for a compressible fluid also includes the equation of state. Let's review the consequences of this circumstance.

6. Gas filtration model under Darcy's law. Leibensohn's function

As mentioned, when considering fluid's (gas's) compressibility in filtration through a non-deformable reservoir, it is necessary to assign in a decisive format the equation of state (definitive equation) connecting density with pressure. The equations of state can be different, but the model generation and all needed mathematical transformations can be performed in a general form.

The general form of a mathematical model for the compressible fluid (gas) filtration through a non-deformable isotropic porous medium with no consideration of the gravitational force is defined by the following system of equations:

$$\begin{aligned} &\frac{\partial \varnothing \rho}{\partial t} + \operatorname{div} \rho \bar{w} = 0, \\ &\bar{w} = -\frac{k}{\mu} \operatorname{grad} p, \\ &\rho = \rho(p). \end{aligned} \tag{19.14}$$

This system can be converted into the format more convenient for practical applications. It is done by reducing it to a single equation relative to one unknown function. To derive such equation, Darcy's law is substituted into the continuity equation:

$$\varnothing \frac{\partial \rho}{\partial t} + \operatorname{div}\left(-\rho \frac{k}{\mu} \operatorname{grad} p \right) = \varnothing \frac{\partial \rho}{\partial t} - \frac{k}{\mu} \operatorname{div}(\rho \operatorname{grad} p) = 0.$$

The further transformation is the introduction of the function P, which enables the linearization of the expression under the divergence operator:

$$\operatorname{grad} P = \rho \operatorname{grad} p. \tag{19.15}$$

The function P is called Leibenson's function. Integrating Eq. (19.15) and considering that $\rho = \rho(p)$, results in:

$$P = \int \rho(p)\, dp. \tag{19.16}$$

Eq. (19.16) provides the Leibenson's function format when equation of state $\rho = \rho(p)$ is given, and by substituting the equation of state into the earlier derived equation:

$$\varnothing \frac{\partial \rho}{\partial t} - \frac{k}{\mu} \operatorname{div}(\operatorname{grad} P) = 0,$$

producing equation relative to only one function, pressure p. In a more general form these transformations will be analyzed when discussing the elastic regime theory.

After Leibenson's function was introduced, the system Eq. (19.14) can be rewritten as follows:

$$\begin{aligned} &\varnothing\frac{\partial\rho}{\partial t}-\frac{k}{\mu}\Delta P=0,\\ &\rho\bar{w}=-\frac{k}{\mu}\text{grad}P,\\ &\rho=\rho(p),\\ &P=\int\rho dp. \end{aligned} \tag{19.17}$$

The closed equation systems Eqs. (19.14) and (19.17) define a mathematical model of the viscous compressible fluid (gas) filtration theory within a non-deformable porous isotropic medium.

The Mathematical models Eqs. (19.14) and (19.17) are equivalent and describe non-stationary filtration flow. The systems become simpler for a non-transient process, respectively:

$$\begin{aligned} &\text{div}\,\rho\bar{w}=0,\\ &\bar{w}=-\frac{k}{\mu}\text{grad}\,p,\\ &\rho=\rho(p), \end{aligned} \tag{19.18}$$

and:

$$\begin{aligned} &\Delta P=0,\\ &\rho\bar{w}=-\frac{k}{\mu}\text{grad}P,\\ &\rho=\rho(p),\\ &P=\int\rho dp. \end{aligned} \tag{19.19}$$

Thus, under the transient-free filtration, the first equation in the Eq. (19.19) system is Laplace's equation for Leibenson's function. By integrating it, this function can be determined and after that, the pressure and velocity distribution in the reservoir can be found. The first equation includes two unknown functions (density and Leibenson's function). If, however, the equation of state (equation before the last in the system) is given, it also can be represented as a differential equation only for Leibenson's function.

For the mathematical model Eq. (19.18) the reservoir is taken to be deformable as porosity and permeability are assumed to be functions of pressure. Therefore, the pressure changes in the reservoir are so significant that viscosity is also assumed to be a function of pressure. Thus, substitution of Darcy's law into the continuity equation results in the generalized Leibenson's function:

$$\frac{\partial\varnothing(p)\rho}{\partial t}-\text{div}\left(\frac{k(p)}{\mu(p)}\rho(p)\text{grad}P\right)=0.$$

For this reason, Leibenson's function defined by Eq. (18.16) can be generalized assuming:

$$\text{grad}P = \frac{k(p)}{\mu(p)}\rho(p)\text{grad}P.$$

Solving this equation relative to the generalized Leibenson's function, the equation to calculate P is obtained as:

$$P = \int \frac{k(p)}{\mu(p)}\rho(p)dp. \tag{19.20}$$

After all these transformation, equation system Eq. (19.8) takes the following format:

$$\begin{aligned} &\frac{\partial \varnothing \rho}{\partial t} - \Delta P = 0, \\ &\bar{w} = -\frac{k}{\mu}\text{grad}\, p, \\ &\rho = \rho(p),\ \varnothing = \varnothing(p),\ k = k(p),\ \mu = \mu(p), \\ &P = \int \frac{k(p)}{\mu(p)}\rho(p)dp. \end{aligned} \tag{19.21}$$

A specific implementation of the model Eq. (19.21) will be analyzed in Chapter XXI when deriving the main equation of the elastic drive.

7. Uniphase filtration models in non-deformable reservoir under nonlinear filtration laws

As mentioned earlier, Darcy's law has the upper and lower applicability limits. The mathematical models generated in the previous sections are valid only for the filtration flows under Darcy's law. If the linear filtration law is broken, these models are invalid and must be expanded to cover the nonlinear filtration laws. As was shown, a filtration law is derived from the law on variation of kinetic momentum. The general concept in generating the mathematical model is: the mathematical model is a closed equation system with equations representing the conservation laws with the addition of the definitive equations. And under a nonlinear case, Darcy's law must be replaced with the nonlinear filtration law.

With the nonlinear filtration of incompressible fluid (disregarding the gravitational force) under Forchheimer law equation system Eq. (19.10) is replaced by:

$$\begin{aligned} &\text{div}\ \bar{w} = 0, \\ &\text{grad}\ p = -\frac{k}{\mu}\bar{w} - \beta\frac{\rho}{\sqrt{k}}|w|\bar{w} \end{aligned}$$

and in filtration under the exponential law, by:

$$\operatorname{div} \overline{w} = 0,$$

$$\overline{w} = c|\operatorname{grad} p|^{\frac{1-n}{n}} \operatorname{grad} p.$$

Similarly, the mathematical model under non-transient gas filtration is:

$$\operatorname{div} \rho \overline{w} = 0,$$

$$\operatorname{grad} p = -\frac{k}{\mu} \overline{w} - \beta \frac{\rho}{\sqrt{k}} |w| \overline{w},$$

$$\rho = \rho(p),$$

and:

$$\operatorname{div} \rho \overline{w} = 0,$$

$$\overline{w} = c|\operatorname{grad} p|^{\frac{1-n}{n}} \operatorname{grad} p,$$

$$\rho = \rho(p).$$

The analysis and integration of these systems will be dealt with in the next Chapter.

8. Correlation between fluid parameters and porous medium parameters with pressure

For a practical application of the generated models of uniphase filtration, the functions $\rho = \rho(p)$, $\varnothing = \varnothing(p)$, $k = k(p)$ and $\mu = \mu(p)$ must be given in the decisive format. Let's write down main relationships between the fluid parameters of the porous medium and pressure.

Under non-stationary processes, a substantial amount of oil can be extracted due to the increase in its volume as pressure declines. In these processes, the fluid compressibility must be taken into account. In gas, it is necessary to consider the gas density correlation with pressure. Thus, the equations *of elastic liquid, ideal and real gases* are treated as main equations of state.

In the future, pressure is assumed as a function of density only. As mentioned previously, the processes where $p = f(\rho)$ are called barotropic processes. An example of such processes is isothermal filtration.

By definition, liquid's volume compression factor β_{liq} is equal to the ratio of relative change in the liquid's volume dV_{liq}/V_{liq} to pressure change dp:

$$\beta_{liq} = -\frac{1}{V_{liq}} \frac{dV_{liq}}{dp}. \tag{19.22}$$

The minus sign is introduced in order to make the liquid's volume compression factor a positive value. Indeed, when pressure grows ($dp > 0$), the liquid's volume decreases ($dV_{liq} < 0$), and vice versa. I. e., the differentials in the numerator

and denominator of Eq. (19.22) have opposite signs. It is usually believed that the liquid's volume compression factor is a universal constant, i. e., it does not depend either on temperature or on pressure, but it is different for different liquids.

In Russian oilfields, β_{liq} for oil ranges between $7*10^{-10}$ Pa^{-1} and $30*10^{-10}$ Pa^{-1}, and for the formation water, between $2.7*10^{-10}$ Pa^{-1} and $5*10^{-10}$ Pa^{-1}.

Eq. (19.22) is a subtended form of the correlation between pressure and density in an elastic liquid; i. e., it is equation of state. In order to derive the decisive format from Eq. (19.22), liquid volumes are switched to densities. For a uniform liquid, mass and volume are related as $M = \rho V_{liq}$, so at M = const:

$$dV_{liq} = d\frac{M}{\rho} = -\frac{M}{\rho^2}d\rho.$$

Substituting this expression into Eq. (19.22), results in:

$$\beta_{liq} = \frac{\rho}{M}\frac{M}{\rho^2}\frac{d\rho}{dp} = \frac{d\rho}{\rho dp},$$

wherefrom:

$$\frac{d\rho}{\rho} = \beta_{liq}dp.$$

Integrating the latter relationship as follows:

$$\int_{\rho_0}^{\rho}\frac{d\rho}{\rho} = \beta_{liq}\int_{p_0}^{p}dp,$$

the result is:

$$\log\frac{\rho}{\rho_0} = \beta_{liq}(p - p_0).$$

From this equation:

$$\rho = \rho_0 e^{\beta_{liq}(p-p_0)}. \qquad (19.23)$$

The exponent $\beta_{liq}(p - p_0)$ is usually small, and the exponential function can be expanded into a series. Limiting this expression to only linear terms, results in:

$$e^{\beta_{liq}(p-p_0)} \approx 1 + \beta_{liq}(p - p_0).$$

From all these transformations, we come up with equation of state for an elastic slightly-compressible fluid at low pressure gradients:

$$\rho = \rho_0[1 + \beta_{liq}(p - p_0)]. \qquad (19.24)$$

Equation of state [Eq. (19.23)] must be used for large $\beta_{liq}(p - p_0)$ values. Instead of the volume compression factor, the inverse value is often used; $K_{liq} = 1/\beta_{liq}$. This value is called liquid's elasticity modulus.

Equation of state for ideal gas is often used as the equation of state for natural gases (Clapeyron's equation of state):

$$P = \rho RT, \tag{19.25}$$

where R is gas constant, T is absolute temperature. For isothermal processes, this equation assumes the following format:

$$\frac{p}{\rho} = RT = \text{const}.$$

Usually, the constant in equation of state is determined by assigning the gas density and pressure under the atmospheric conditions assuming that temperature is equal to the formation temperature T_{res}:

$$\frac{p_{atm}}{\rho_{atm}} = \text{const},$$

where ρ_{atm} is gas density at atmospheric pressure p_{atm} .Therefore, the ideal gas equation of state is:

$$\rho = \frac{\rho_{atm}}{p_{atm}} p. \tag{19.26}$$

A different version of the equation of state (called the real gas equation of state) is applied in the high-pressure gas fields (on the order of 40 to 60 MPa):

$$p = z\rho RT, \tag{19.27}$$

Where z is the gas super-compressibility factor equal to the ratio of ideal gas density to the real gas density at given P and T. The factor accounts for the deviations of the real gas state from the state prescribed by the equation of ideal gas. The z factor depends on normalized temperature and pressure values T_r and p_r:

$$p_r = \frac{p}{p_{avg.crit}}, \; T_r = \frac{T}{T_{avg.crit}} \tag{19.28}$$

and can be determined either analytically or graphically using the cross-plot of Fig. 19.2. $p_{avg.crit}$ and $T_{avg.crit}$ are average critical pressure and temperature. Natural gas includes numerous components (methane, ethane, propane, etc.); so, average critical pressure and temperature are determined as follows:

$$p_{avg.crit} = \frac{\sum n_j p_{crit\,j}}{\sum n_j}, \; p_{avg.crit} = \frac{\sum n_j T_{crit\,j}}{\sum n_j},$$

where n_j is the content in gas of the j^{th} component, $p_{crit,j}$ and $T_{crit,j}$ are critical pressure and temperature of the j^{th} component, respectively.

The RT value for isothermal filtration is constant and can be determined for the real gas equation of state under atmospheric conditions:

$$\frac{p_{atm}}{\rho_{atm}} = z\, p_{atm} RT\,.$$

In this case, equation of state for the real gas assumes the following format:

$$\rho = \frac{\rho_{atm}\, z(p_{atm})\, p}{p_{atm} z(p)}\,. \tag{19.29}$$

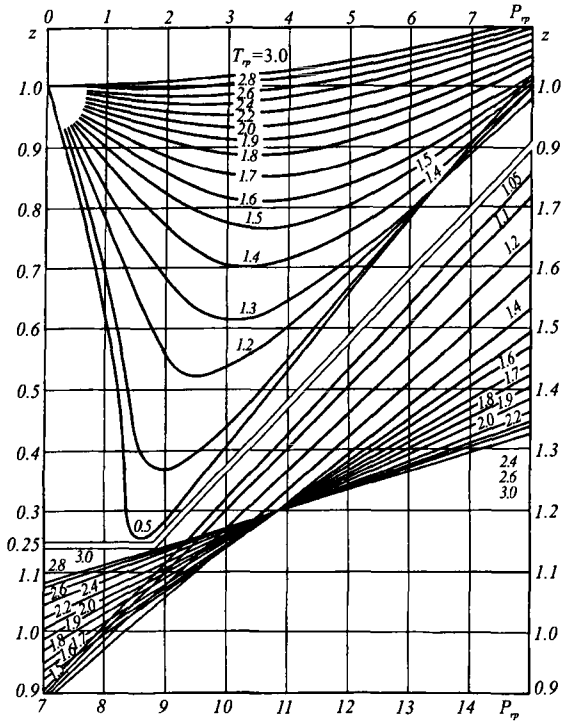

Fig. 19.2

Using Eqs. (19.23), (19.24), (19.26) and (19.29), Leibenson's function can be calculated for each particular case.

For the elastic liquid with equation of state Eq. (19.23), Leibenson's function is:

$$P = \int \rho_0 e^{\beta_{liq}(p-p_0)} dp = \frac{\rho_0}{\beta_{liq}} \int e^{\beta_{liq}(p-p_0)} d\beta_{liq}(p-p_0) =$$
$$= \frac{\rho_0}{\beta_{liq}} e^{\beta_{liq}(p-p_0)} + C = \frac{\rho_0}{\beta_{liq}} + C. \tag{19.30}$$

When the $\beta_{liq}(p-p_0)$ value is small, Eq. (19.30) can be transformed by expanding the exponent into a series, so that:

$$P=\frac{\rho_0}{\beta_{liq}}[1+\beta_{liq}(p-p_0)]+C=\frac{\rho_0}{\beta_{liq}}+\rho_0 p-\rho_0 p_0+C=\rho_0 p+C^*, \quad (19.31)$$

where $C^*=C+\frac{\rho_0}{\beta_{liq}}-\rho_0 p_0$.

For the elastic liquid with equation of state Eq. (19.24):

$$P=\int\rho_0[1+\beta_{liq}(p-p_0)]dp=\rho_0 p+\rho_0\beta_{liq}\left(\frac{p^2}{2}-\rho_0 p\right)+C$$

or, as the fluid is only slightly compressible and the β_{liq} factor is small:

$$P=\rho_0 p+C.$$

Thus, Leibenson's function for equations of state [Eqs. (19.23) and (19.24)] at small pressure changes in a slightly compressible fluid, as it was expected, is the same and is identical to Leibenson's function for incompressible fluid. Indeed, for a incompressible fluid $\rho=\rho_0=\text{const}$, and Leibenson's function is:

$$P=\int\rho dp=\rho p+C.$$

For an ideal gas with equation of state (19.25), Leibenson's function is:

$$P=\int\frac{\rho_{atm}p}{p_{atm}}dp=\rho p+C=\frac{\rho_{atm}p^2}{2p_{atm}}+C. \quad (19.32)$$

For a real gas in the case of the isothermal filtration, Leibenson's function is:

$$P=\frac{\rho_{atm}z(p_{atm})}{p_{atm}}\int\frac{p}{z(p)}dp.$$

The $z(p)$ correlation at constant temperature and small pressure changes can be considered linear:

$$z=z_0[1+a_z(p_0-p)], \quad (19.33)$$

where z_0 is super-compressibility factor at $p=p_0$; at large pressure changes it is exponential:

$$z=z_0e^{-a_z(p_0-p)}, \quad (19.34)$$

and the constant a_z should be selected in such a way that the Eqs. (19.33) or (19.34) curve was as close as possible to the empirical curve in Brown's graphs for $z=z(p)$.

The procedure illustrated here was the simplest way to account for the changes in properties of the real gas depending on changes in pressure and temperature. More complex equations of state must be used under complex thermobaric conditions, at filtration of multicomponent gases.

Experiments showed that the oil viscosity factor (at pressures above the saturation pressure) and gas viscosity factor increase with the rising pressure. If pressure

ranges significantly (up to 100 MPa), viscosity of the formation oil and natural gases correlation with pressure can be considered exponential:

$$\mu = \mu_0 e^{-a_\mu(p_0 - p)}. \tag{19.35}$$

When the pressure change is small, the correlation is close to be linear:

$$\mu = \mu_0[1 - a_\mu(p_0 - p)], \tag{19.36}$$

where μ_0 is viscosity at foxed pressure p_0, and a_μ is experimentally found factor determined by the oil and gas composition.

To find the correlation between porosity and pressure, the stresses acting in the fluid-filled porous medium will be reviewed.

Overburden covering the productive reservoir creates the so-called mining pressure p_{min}, which can be considered constant in the process of the reservoir development. Mining pressure is determined as $p_{min} = \rho_{min} gH$, where ρ_{min} is average density of overburden's rocks, and H is the reservoir depth. If it is assumed that the reservoir's top and base are completely impermeable and totally assume the load from overburden, the mining pressure is compensated by the stress σ in the reservoir's matrix and pressure p of the fluid, i. e.,

$$\rho_{min} = (1 - \varnothing)\,\sigma + \varnothing p. \tag{19.37}$$

Here, σ is true stress in the matrix of the porous medium per unit of the horizontal area mentally identified at any point in the reservoir. It acts on the part of the area $(1 - \varnothing)$. It is more convenient to introduce the so called effective stress σ_{eff} which is defined as the stress difference between the matrix and fluid phase. It can be found as:

$$\sigma_{eff} = (1 - \varnothing)(\sigma - p). \tag{19.38}$$

Then, following Eq. (19.37):

$$\rho_{min} = \sigma_{eff} + p. \tag{19.39}$$

Effective stress is physically interpreted as that portion of true stress σ in the solid phase, which is transmitted through the contacts of the matrix grains, is independent of the presence of fluids and will exist also in the dry medium. The concept of the effective stress is convenient also because it can be determined experimentally: it is possible to measure load Γ, which models mining pressure ρ_{min}, and pore pressure p, and find $\sigma_{eff} = \Gamma - p$.

Formation pressure p declines in the process of the accumulation's development, and the stress σ_{eff} in the matrix increases.

Porosity depends on pore pressure p as well as on the effective stress σ_{eff}: $\varnothing = \varnothing(p, \sigma_{eff})$. As pressure declines, the forces compressing each grain of rock decreases; thus, the grain volume increases and the pore volume decreases. Increase in σ_{eff} results in additional deformations of the grains: the grain contact surface increases, the grain packing become denser (see Fig. 19.3). Some grain regrouping, the destruction of the cement and of the grains, etc., can occur.

It is usually assumed in cases where $p_{min} = \text{const}$, that porosity depends only on pressure: $\varnothing = \varnothing(p)$.

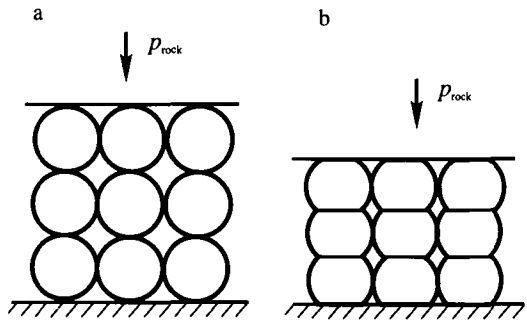

Fig. 19.3 Simlplified scheme of grain deformation in porous medium: a. before deformation; b. after deformation. $p_z = p_0$ (overburden pressure).

The solid phase's deformation is small, so it is usually assumed that porosity correlation with pressure is linear. The rock's compressibility law is presented, with the introduction of the elasticity factor β_c, as follows:

$$\beta_c = \frac{dV_p}{Vdp}, \tag{19.40}$$

where dV_p is the change in pore volume within the reservoir element of volume V as pressure changes by dp. If the volume of the reservoir element is considered constant, then $\frac{dV_p}{Vdp} = d\frac{V_p}{V} = d\varnothing$, and the rock compressibility law assumes the following format:

$$d\varnothing = \beta_c dp. \tag{19.41}$$

After integrating this equation:

$$\varnothing = \varnothing_0 + \beta_c(p - p_0), \tag{19.42}$$

where $\varnothing_0$ is porosity at $p = p_0$.

Laboratory and field studies of various granular media showed that the reservoir's volume elasticity factor is on the order of β_c = (0.3 to 2)10^{-10} Pa^{-1}. If pressure changes are significant, porosity changes are described by this equation:

$$\varnothing = \varnothing_0 e^{-\beta_c(p_0 - p)/\varnothing_0}. \tag{19.43}$$

Experiments also showed that not only porosity but permeability as well significantly changes with the change in pressure, and sometimes even larger than porosity. Under small pressure changes the correlation can be assumed to be linear:

$$k = k_0[1 - a_k(p - p_0)],\ a_k(p - p_0) << 1. \tag{19.44}$$

Under large pressure changes the correlation is exponential:

$$k = k_0 e^{-a_k(p_0 - p)}. \tag{19.45}$$

The above arguments are appropriate for porous rocks only. Permeability of fractured reservoirs more significantly changes with the change of pressure.

Mechanics of Fluid Flow
by Kaplan S. Basniev, Nikolay M. Dmitriev and George V. Chilingar

CHAPTER XX

UNIDIMENSIONAL TRANSIENT-FREE FILTRATION OF INCOMPRESSIBLE FLUID AND GAS IN AN UNIFORM POROUS MEDIUM.

1. Schematics of unidimensional filtration

Real hydrocarbon reservoirs have complex geometry, structure, etc., so simplified setting of edge problems is often used for modeling of the filtration flows. These settings are called model settings. The simplest models deal with unidimensional transient-free filtration within a uniform non-deformable isotropic reservoir.

In the simplest unidimensional problems, the coordinate system is selected so that filtration parameters (velocity, pressure) will be functions of a single coordinate. Unidimensional filtration flows possess different symmetries. Depending on the symmetry, there are rectilinear-parallel, radial-plane and radial-spherical flows. In a rectilinear-parallel flow the particle trajectories (flow-lines) are straight parallel lines.

Examples of a rectilinear-parallel flow are: the fluid flow in the Darcy's experimental device, the fluid or gas flow in laboratory equipment for the determination of permeability (Fig. 18.6), etc.

In a radial-plane flow, the flow-lines are rays on the plane radiating from a common center (pole). An example is the fluid flow to the central well in a circular reservoir (Fig. 20.1).

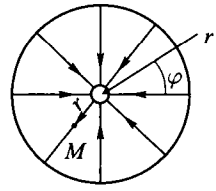

Fig. 20.1 Flow lines at radial-plane flow

At the radial-spherical flow, the particle trajectories are directed toward the center (or from the center) of a hemisphere. Such a filtration flow may occur when the reservoir top is penetrated and the fluid flow is directed toward the hemisphere (Fig. 20.2).

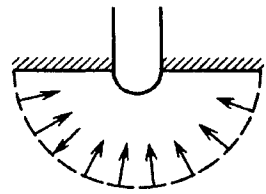

Fig. 20.2 Radial-spherical flow

In deriving the schematics for the unidimensional flows, the concepts of trajectory and flow-lines are used. In definitions, kinematic parameters of the filtration flow were used, and they reflect not the try, but averaged flow representation, i. e., the true particles' trajectories and flow-lines may not coincide with average, modeled parameters of the filtration flow.

2. Rectiliner-parallel filtration of incompressible fluid

In this section the unidimensional filtration flow parameters of a incompressible uniform Newtonian fluid within an isotropic noncompressible reservoir are determined. In such a case, the mathematical model is assigned by the following equation system:

$$\Delta p = 0, \quad w = -\frac{k}{\mu}\operatorname{grad} p\,. \tag{20.1}$$

Projecting this equation onto the Cartesian coordinate system, results in:

$$\begin{gathered}\frac{\partial^2 p}{\partial x^2}+\frac{\partial^2 p}{\partial y^2}+\frac{\partial^2 p}{\partial z^2}=0,\\ w_x=-\frac{k}{\mu}\frac{\partial p}{\partial x},\ w_y=-\frac{k}{\mu}\frac{\partial p}{\partial y},\ w_z=-\frac{k}{\mu}\frac{\partial p}{\partial z}.\end{gathered} \tag{20.2}$$

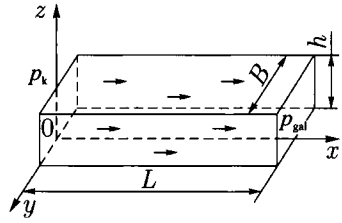

Fig. 20.3 Rectilinear-parallel filtration

Suppose the reservoir is a rectangular 3D-box of a width B and thickness h, limited at the top and base by impermeable planes, and by a charge contour (exter-

nal reservoir boundary) on the left and a gallery on the right. Let's select the coordinate system as shown in Fig. 20.3, i. e., place the origin on the charge contour plane. The name "charge contour" indicates that, under the problem setting, through the plane $x = 0$ a fluid inflow into the reservoir occurs, and the fluid further flows to the gallery $x = L$. The axis $0x$ is directed parallel to the filtration velocity. In this case, it is possible to assume that the unknown functions (pressure and filtration velocity) depend only on x coordinate. So, Eq. (20.2) may be rewritten as:

$$\frac{d^2p}{dx^2} = 0, \quad w_x = -\frac{k}{\mu}\frac{dp}{dx}, \quad w_y = w_z = 0. \tag{20.3}$$

By integrating the first equation:

$$\frac{dp}{dx} = C_1, \text{ and from there } dp = C_1 dx, \text{ and further, } p = C_1 x + C_2.$$

To find the integration constants C_1 and C_2, it is necessary to assign the boundary conditions, i. e., the pressure values at two points on the flow-line. Usually, pressures p_k at the source contour and at the gallery ($p_k > p_{gal}$) are known. So, to find C_1 and C_2, from the boundary conditions:

$$p = p_k \text{ at } x = 0 \text{ and } p = p_{gal} \text{ at } x = L.$$

By substituting the boundary conditions in the pressure equation:

$$p_k = C_2 \text{ and } p_{gal} = C_1 L + C_2,$$

wherefrom:

$$C_1 = \frac{p_k - p_{gal}}{L} \text{ and } C_2 = p_k.$$

After substituting the values for the integration constants into equations for pressure and the velocity, the problem of the rectilinear-parallel filtration is solved.

$$\begin{aligned} p(x) &= p_k - \frac{p_k - p_{gal}}{L}x, \\ w_x &= -\frac{k}{\mu}\frac{\partial p}{\partial x} = -\frac{k}{\mu}C_1 = \frac{k}{\mu}\frac{p_k - p_{gal}}{L}. \end{aligned} \tag{20.4}$$

Let's reformat this result. Multiplying the filtration velocity by the gallery area $S = Bh$ (Fig. 20.3), the value for the throughflow Q is obtained:

$$w_x S = Q = \frac{k}{\mu}\frac{p_k - p_{gal}}{L}S. \tag{20.5}$$

As the pressure gradient is:

$$\frac{p_k - p_{gal}}{L} = \frac{Q\mu}{kS},$$

And after substituting it into equation for the pressure distribution in the reservoir:

$$p(x) = p_k - \frac{Q\mu}{kS}x. \tag{20.6}$$

As Eq. (20.4) indicates, pressure in the reservior at rectilinear-parallel filtration is linearly distributed along the x cordinate with the filtration velocity constant in the entire reservoir. It is also important that Eq. (20.5), derived as a result of solving the problem for mathematical model of incompressible fluid filtration, exactly matches the experimental results by Darcy.

A different interpretation of the Eq. (20.4) is often used for applied studies (like the determination of reservoir parameters in the field). When determining the reservoir filtration parameters by the transient-free withdrawal technique, an indicator curve is plotted. The curve is the graph of throughflow *vs.* pressure differences at the charge contour and the gallery (this difference is called pressure drawdown). Thus, the indicator curve is a graph:

$$Q = C\Delta p,$$

where the proportionality factor C is called the productivity index. Apparently:

$$C = \frac{kS}{\mu L}.$$

Therefore, when Darcy's law is observed, the indicator curve is a straight line.

Another problem deals with the determination of time required for "marked particles" to move within the reservoir. In order to determine reservoir parameters of a petroleum interval, some isotopes or other particles identifiable with special techniques may be injected into the reservoir. The motion time of the "marked particles" is found from the motion law using the determination of the average true velocity.

First the formula is derived in the standard way under which porosity is equal to the clearance. Then, the corrections associated with the use of clearance instead of porosity is introduced to the equation when determining the relationship between the filtration velocity and true average velocity, see Eq. (18.12).

Suppose equation for the true average velocity is formatted as follows:

$$v = \frac{dx}{dt} = \frac{w}{\text{Ø}}. \tag{20.7A}$$

and after the separation of the variable:

$$dt = \frac{\text{Ø}}{w}dx.$$

Let's now substitute the filtration vector modulus [Eq. (20.4)] into the latter expression:

$$dt = \frac{\emptyset\mu}{k}\frac{L}{p_k - p_{gal}}dx.$$

By integrating this equation, the time taken by the "marked particle" to move from the charge contour ($x = 0$ at $t = 0$) to an arbitrary point within the reservoir can be found ($x = x_1$, $t = t_1$):

$$t_1 = \frac{\emptyset\mu}{k}\frac{Lx_1}{p_k - p_{gal}}. \tag{20.8A}$$

For the particle to move along the entire reservoir from the charge contour to the gallery (i. e., $x_1 = L$):

$$T = \frac{\emptyset\mu}{k}\frac{L^2}{p_k - p_{gal}}. \tag{20.9A}$$

However, in the initial equation clearance must have been used rather that porosity. As a result, a different equation instead of the initial one should be used:

$$v = \frac{dx}{dt} = \frac{w}{s_\alpha}. \tag{20.7B}$$

Now, to switch from porosity to clearance, the structural factor introduced in Chapter I is used to determine the capillary diameter in ideal porous medium

$$s_\alpha = \frac{\emptyset}{\varphi_\alpha},$$

transform Eq. (20.7B) into the following format:

$$v = \frac{dx}{dt} = \frac{\varphi_\alpha w}{\emptyset}.$$

As φ_α is a constant in an uniform porous medium, all further calculations remain the same as above, and the final result accounting for the fact that porosity rosity is not equal to clearance, gives the following equations:

$$t_1 = \frac{\emptyset\mu}{\varphi_\alpha k}\frac{Lx_1}{p_k - p_{gal}} \tag{20.8B}$$

and

$$T = \frac{\emptyset\mu}{\varphi_\alpha k}\frac{L^2}{p_k - p_{gal}}. \tag{20.9B}$$

Eqs. (20.8B) and (20.9B) differ from usually applied Eqs. (20.8A) and (20.9A) by the structural factor φ_α, whose value satisfies the inequality $\varphi_\alpha \geq 1$. Therefore, the inclusion of the structural factor results in a decreased travel time of the "marked particles".

Another important parameter utilized in the solution of applied problem is average formation pressure $\overline{p}$ weighted over the pore space volume. It usually is found as:

$$\overline{p} = \frac{1}{V_{\text{por}}} \int_{V_{\text{por}}} p dV_{\text{por}}, \tag{20.10}$$

where V_{por} is total pore volume of the reservoir. This definition, however, is not exactly accurate. Indeed, under porosity definition ($\text{Ø} = dV_{\text{por}} / dV$), the pore volume is represented by a function similar to the following:

$$V_{\text{por}} = \int_V \text{Ø} dV,$$

which is defined over the same multitude of "physical points" as the reservior volume V in which the voids are "spread". Thus, the correct definition Eq. [(20.10)] should be:

$$\overline{p} = \frac{1}{V_{\text{por}}} \int_V \text{Ø} p dV, \tag{20.11}$$

i. e., the volume over which integration is performed must be changed. It is clear that another parameter may also be introduced. It is the reservoir's average pressure:

$$\overline{p}_{\text{res}} = \frac{1}{V} \int_V p dV. \tag{20.12}$$

Now, the introduced parameters are compared. For a uniform reservoir ($dV_{\text{por}} = \text{Ø} dV$ and $\text{Ø} = \text{const}$):

$$\overline{p} = \frac{1}{\text{Ø}V} \int_V p \text{Ø} dV = \overline{p}_{\text{res}} = \frac{1}{V} \int_V p dV.$$

Thus, the average formation pressure for a uniform reservoir is equal to average value weighted over the pore volume. If the reservoir is non-uniform, the average formation pressure may not be equal to average value weighted over the pore volume:

$$\overline{p} = \frac{\int_V p \text{Ø} dV}{\int_V \text{Ø} dV} \neq p_{\text{res}} = \frac{\int_V p dV}{\int_V \text{Ø} dV}.$$

Substitute Eq. (20.4) for pressure distribution in the reservoir into the Eq. (20.11) and compute average pressure weighted over volume (which in this case is equal to case is equal to the average reservoir pressure).

$$\bar{p} = \frac{1}{BhL}\int_0^L Bh\left(p_k - \frac{p_k - p_{gal}}{L}x\right)dx = \frac{p_k + p_{gal}}{2}. \qquad (20.13)$$

Therefore, major filtration parameters at rectiliner-parallel filtration for an incompressible fluid are determined from Eqs. (20.4), (20.8A), (20.8B) and (20.13).

3. Radial-plane filtration of incompressible fluid

Let's now determine the pressure and filtration velocity distribution in the reservoir under the radial-plane environment. Suppose there is a central well with the diameter r_c intersecting a round reservoir with the thickness h and radius R_K (Fig. 20.4). A constant pressure p_k ($p_k > p_c$) is maintained at the bottomhole. A constant pressure is also maintained on the side surface $r = R_K$. Fluid inflow equal to the well's flow rate occurs through the side surface.

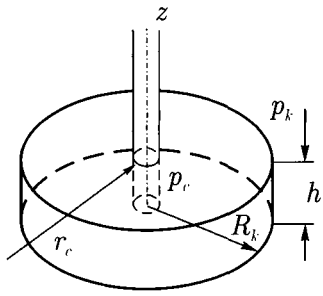

Fig. 20.4. Radial-plane flow in a circular reservoir

Filtration is transient-free. The side surface through which the inflow occurs is called charge contour. The equation system remains the same and in a no-subscript format is represented by Eq. (20.1). Projecting these equations onto a cylindrical coordinate system, results in:

$$\frac{1}{r}\frac{\partial}{\partial r}\left(r\frac{\partial p}{\partial r}\right) + \frac{1}{r^2}\frac{\partial^2 p}{\partial \varphi^2} + \frac{\partial^2 p}{\partial z^2} = 0,$$
$$w_r = -\frac{k}{\mu}\frac{\partial p}{\partial r},\quad w_\varphi = -\frac{k}{\mu}\frac{\partial p}{\partial \varphi},\quad w_z = -\frac{k}{\mu}\frac{\partial p}{\partial z}. \qquad (20.14)$$

According to the accepted flow scheme, the sought-for functions depend neither on φ (the flow is axisymmetric) nor on z (the flow is flat); so, in our problem

$\frac{\partial p}{\partial \varphi} = \frac{\partial p}{\partial z} = 0$, $p = p(r)$, and $w_\varphi = w_z = 0$, $w_r = w(r)$. Under these conditions, the system Eq. (20.14) takes the following format:

$$\frac{d}{dr}\left(r\frac{dp}{dr}\right) = 0, \quad w = \frac{k}{\mu}\frac{dp}{dr}. \tag{20.15}$$

It is important to note the fact that in the projection of Darcy's law, or the second Eq. (20.15), onto the coordinate axis r, the signs in the left and right parts are the same. The reason is that the flow is occurring toward the well, and filtration velocity is projected with the minus sign.

Now, the first equation $r\frac{dp}{dr} = C$ is integrated and, after separating the variables and integrating the last expression, results in:

$$p_K - p = C\log\frac{R_K}{r}. \tag{20.16}$$

When integrating, a following boundary condition is used:

$$p = p_K \text{ at } r = R_K.$$

It is possible to use a different boundary condition such as:

$$p = p_c \text{ at } r = R_c,$$

Thus:

$$p - p_c = C\log\frac{r}{r_c}. \tag{20.17}$$

Both Eqs. (20.16) and (20.17) are equivalent.

The constant C can be found by the following procedure: multiply filtration velocity Eq. (20.15) by the area of a side cylinder of arbitrary radius r ($r_c \le r \le r_K$):

$$2\pi rhw = 2\pi rh\frac{k}{\mu}\frac{dp}{dr},$$

or:

$$Q = 2\pi h\frac{k}{\mu}C,$$

and C is found from this equation:

$$C = \frac{Q\mu}{2\pi kh}.$$

Another approach is also possible: supposing in Eq. (20.17) $r = R_k$; then:

$$p_k - p_c = C\log\frac{R_k}{r_c}$$

Solving this equation for C, results in:

$$C = \frac{p_k - p_c}{\log \frac{R_k}{r_c}}.$$

After substituting the determined value of the integration constant C into Eqs. (20.16) and (20.17), gives equations for the pressure distribution in the reservoir:

$$p = p_k - \frac{Q\mu}{2\pi kh} \log \frac{R_k}{r} \quad \text{and} \quad p = p_c + \frac{Q\mu}{2\pi kh} \log \frac{r}{r_c}. \tag{20.18}$$

At $r = r_c$ for the first Eq. (20.18) and $r = R_k$ for the second one, the well flow rate (volume throughflow) may be found as:

$$Q = \frac{2\pi kh}{\mu} \frac{p_k - p_c}{\log \frac{R_k}{r_c}}. \tag{20.19}$$

Eq. (20.19) is called Dupois formula.

Using this formula, the pressure distribution in the reservoir can be transformed into the following format:

$$p = p_k - \frac{p_k - p_c}{\log \frac{R_k}{r_c}} \log \frac{R_k}{r} \quad \text{and} \quad p = p_c + \frac{p_k - p_c}{\log \frac{R_k}{r_c}} \log \frac{r}{r_c}. \tag{20.20}$$

Eqs. (20.18) and (20.20) are equivalent and indicate that the pressure in the reservoir is logarithmically distributed. Thus, at the radius values close to the source contour radius, pressure changes insignificant, but on approaching the well they change drastically (Fig. 20.5). Eqs. (20.18) and (20.20) in space define the surfaces generated by the generatrix rotation about the well's axis. This surface of pressure distribution is called the depression cone.

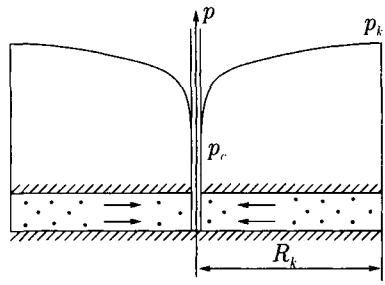

Fig. 20.5. Pressure distribution in a radial-plane flow

The pressure gradient and, hence, the filtration velocity behave in a similar way. The difference is that on approaching the well pressure drastically declines, whereas velocity drastically increases. This velocity behavior may be shown by analyzing equation relating velocity and the throughflow:

$$w = \frac{Q\mu}{2\pi h}\frac{1}{r}. \tag{20.21}$$

Such behavior of reservoir pressure and filtration velocity is physically understandable. Indeed, the same volume of the incompressible fluid flows through any cylindrical surface concentric relative to the well (Q = const). The side surface area near the charge contour is very high, so velocity there is small. Apporoaching the well, the area gradually declines, and velocity increase (Fig. 20.6). In order for this to occur, the pressure gradient must increase.

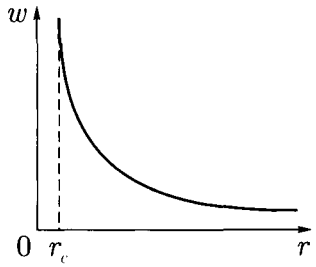

Fig. 20.6. Fluid's filtration velocity in a radial-plane flow vs. radius

As follows from Dupois formula, the indicator curve equation under the radial-plane flow, same as in the case of filtration in a gallery, is the equation of a straight line (Fig. 20.7):

$$Q = C\Delta p = \frac{2\pi kh}{\mu \log \frac{R_k}{r_c}}(p_k - p_c) \tag{20.22}$$

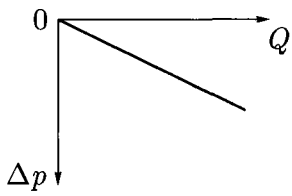

Fig. 20.7 Indicator curve of incompressible fluid flow under the Darcy law

With the productivity index $C = \dfrac{2\pi kh}{\mu \log \dfrac{R_k}{r_c}}$.

Let's now derive equations regarding the time the "marked particle" takes to move in a radial-plane flow. As in the case of rectilinear-parallel filtration, two options are reviewed. The first option is a one with porosity being equal to clearance, whereas the second one is using correction factor for clearance. From Eqs. (20.7A) and (20.21), time required for a "marked particle" to move from the charge contour to an arbitrary point in the reservoir is:

$$\frac{dr}{dr} = v = \frac{w}{\varnothing} = \frac{Q}{2\pi rh\varnothing}.$$

After separating the variables in this differential equation and integrating it with the integration limits from 0 to an arbitrary moment in time t_1 and from the charge contour radius to r_1, results in:

$$t_1 = \frac{\pi h \varnothing (R_k^2 - r_1^2)}{Q}.$$

After the application of Dupois' formula Eq. (20.19):

$$t_1 = \frac{\mu \varnothing \log \dfrac{R_k}{r_c} (R_k^2 - r_1^2)}{2k(p_k - p_c)}. \tag{20.23}$$

Following Eq. (20.23) that a "marked particle" will traverse the distance from the charge contour to the well over a time interval T:

$$T = \frac{\mu \varnothing \log \dfrac{R_k}{r_c} (R_k^2 - r_c^2)}{2k(p_k - p_c)}. \tag{20.24}$$

The replacement of porosity by clearance, as in case of rectilinear-parallel filtration, results in the appearance of the structural factor $s_\alpha = \dfrac{\varnothing}{\varphi_\alpha}$ in Eqs. (20.23) and (20.24):

$$t_1 = \frac{\mu \varnothing \log \left(R_k / r_c \right) (R_k^2 - r_1^2)}{2k\varphi_\alpha (p_k - p_c)} \text{ and } T = \frac{\mu \varnothing \log \left(R_k / r_c \right) (R_k^2 - r_c^2)}{2k\varphi_\alpha (p_k - p_c)}.$$

Next, the average pressure at parallel-plane filtration weighted over the pore space is determined. For this purpose the pressure, distribution Eq. (20.20) is substituted into Eq. (20.10):

$$\bar{p} = \frac{1}{\pi h \varnothing (R_k^2 - r_c^2)} \int_0^h dz \int_0^{2\pi} d\varphi \int_{r_c}^{R_k} \left[p_k - \frac{p_k - p_c}{\log \frac{R_k}{r_c}} \log \frac{R_k}{r} \right] \varnothing r \, dr,$$

and after integrating with respect to z and φ:

$$\bar{p} = \frac{2}{(R_k^2 - r_c^2)} \left[\int_{r_c}^{R_k} \left(p_k - \frac{p_k - p_c}{\log \frac{R_k}{r_c}} \log R_k \right) r \, dr + \int_{r_c}^{R_k} \frac{p_k - p_c}{\log \frac{R_k}{r_c}} r \log r \, dr \right].$$

The first integral in brackets is easy to calculate, and the second one is integrated part-by-part. The result is:

$$\bar{p} = p_k - \frac{p_k - p_c}{\log \frac{R_k}{r_c}} \log R_k + \frac{2}{(R_k^2 - r_c^2)} \frac{p_k - p_c}{\log \frac{R_k}{r_c}} \left[\frac{R_k^2}{2} \log R_k - \frac{r_c^2}{2} \log r_c - \frac{1}{4}(R_k^2 - r_c^2) \right].$$

Now, this equation is transformed by adding and subtracting the expression $R_k^2 \log r_c / 2$ within the brackets. After some transformations, the result is:

$$\bar{p} = p_k - \frac{r_c^2 (p_k - p_c)}{R_k^2 - r_c^2} - \frac{p_k - p_c}{2 \log \frac{R_k}{r_c}}.$$

As $\frac{R_k}{r_c} >> 1$, the second component may be disregarded; so, the final average pressure over the pore space is:

$$\bar{p} = p_k - \frac{p_k - p_c}{2 \log \frac{R_k}{r_c}}. \qquad (20.25)$$

4. Radial-spherical filtration of incompressible fluid

Let's analyze the incompressible fluid's radial-spherical filtration within an isotropic nondeformable reservoir. Suppose there is a well with the radius r_c which penetrated the top of a reservoir. Constant pressure p_c is maintained at the bottom-hole. Assuming the reservoir thickness is sufficiently large, it is possible to identify

a hemisphere with the radius R_k (Fig. 20.8) at the surface of which constant pressure p_k is maintained and through which fluid filtrates at a rate equal to well's flow rate. The flow is non-transient, and the surface of the hemisphere is the charge contour. It is possible to assume that the penetrated reservoir top in the well has the shape of a hemisphere, the filtration velocity vector at any point in the reservoir between the charge contour and the bottomhole is directed toward the center of the sphere. In this case the problem has spherical symmetry, and it is convenient to solve it in the spherical coordinate system.

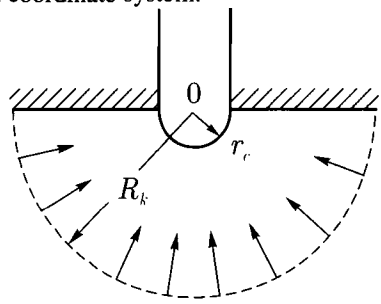

Fig. 20.8. Radial-spherical filtration

The equation system remains the same and is represented in the no-subscript format by Eq. (20.1). In the spherical coordinate system, Eq. (20.1) has the following format:

$$\frac{1}{r^2}\left[\frac{\partial}{\partial r}\left(r^2\frac{\partial p}{\partial r}\right)+\frac{1}{\sin\varphi}\frac{\partial}{\partial\varphi}\left(r^2\frac{\partial p}{\partial r}\right)+\frac{1}{\sin^2\varphi}\frac{\partial^2 p}{\partial\theta^2}\right]=0,$$
$$w_x=-\frac{k}{\mu}\frac{\partial p}{\partial x},\quad w_\varphi=-\frac{1}{r}\frac{k}{\mu}\frac{\partial p}{\partial\varphi},\quad w_\theta=-\frac{k}{\mu}\frac{1}{r\sin\varphi}\frac{\partial p}{\partial\theta}. \tag{20.26}$$

Under the condition of the process' spherical symmetry, all unknown functions depend only on r, so the system Eq. (20.26) becomes simpler:

$$\frac{d}{dr}\left(r^2\frac{dp}{dr}\right)=0,\qquad w_r=\frac{k}{\mu}\frac{\partial p}{\partial r} \tag{20.27}$$

The integration of the first equation of the Eq. (20.27) system results in:

$$r^2\frac{dp}{dr}=C,$$

where C is the integration constant. After separating the variables and integrating, the result is:

$$\int_p^{p_k}dp=C\int_r^{R_k}\frac{dr}{r^2},\ \text{and from here,}\ p_k-p=C\left(\frac{1}{r}-\frac{1}{R_k}\right).$$

To determine C, it is also possible to assume in the latter equation $r = r_c$. As a result:

$$C = (p_k - p_c)/(1/r_c - 1/R_k),$$

but as $R_k >> r_c$:

$$C = r_c (p_k - p_c),$$

and the pressure distribution equation will transform into the following format:

$$p = p_k - r_c(p_k - p_c)\left(\frac{1}{r} - \frac{1}{R_k}\right). \tag{20.28}$$

Using the second Eq. (20.27) and Eq. (20.28), the flow rate is obtained:

$$Q = \pi r^2 w_r = -2\pi r^2 \frac{k}{\mu}\frac{dp}{dr} = \frac{2\pi k}{\mu} r_c(p_k - p_c).$$

The remaining parameters of the radial-spherical flow may be derived similarly as the first two cases of the unidimensional flow.

As it is evident, the Laplace operator for all three reviewed cases of the unidimensional flow may be written as

$$\frac{d}{d\xi}\left(\xi^\alpha \frac{dp}{d\xi}\right) = 0, \tag{20.29}$$

where the exponent $\alpha = 0$, 1, 2 and may be called the shape factor. At $\alpha = 0$, the flow is rectilinear-parallel flow ($\xi = x$); at $\alpha = 1$, the flow is the parallel-plane flow ($\xi = r$); and at $\alpha = 2$, it is the radial-spherical flow ($\xi = r$). However, using the format common for all three cases in is not possible to obtain the universal solution format, as the integral assigning pressure distribution is not computed uniquely:

$$\int \frac{d\xi}{\xi^\alpha} = \frac{\xi^{1-\alpha}}{1-\alpha} + C \quad \text{at } \alpha \neq 1 \text{ and } \int \frac{d\xi}{\xi^\alpha} = \log \xi + C \quad \text{at } \alpha = 1.$$

However, the Eq. (20.29) may be used as a common rule for memorizing the Laplace's operator format for different types of unidimensional flows.

5. Filtration similarity between incompressible liquid and gas

The previous solutions for the unidimensional flow are valid for the filtration of an incompressible fluid. Now, these solutions will be expanded for gases. For this purpose, the mathematical models of the transient-free filtration are reviewed for an incompressible liquid and gas and establish their similarity. As it is shown in

Chapter XIX, equation systems for an incompressible liquid and gas (equation systems Eqs. (19.10) and (19.18) disregarding mass forces) are, respectively:

$$\begin{aligned} &\operatorname{div}\rho\bar{w}=0, && \operatorname{div}\rho\bar{w}=0,\\ &\bar{w}=-\frac{k}{\mu}\operatorname{grad}p, && \bar{w}=-\frac{k}{\mu}\operatorname{grad}p,\\ &\rho=\text{const} && \rho=\rho(p). \end{aligned}$$

Now, it is required to switch to Leibensohn's function. For this purpose, Darcy's law is multiplied in the gas model by density; grad P is used instead of ρ grad p; and in the continuity equation Darcy's law is substituted. The results are the system Eqs. (19.11) and (19.19):

$$\begin{aligned} &\Delta p=0, && \Delta P=0,\\ &\bar{w}=-\frac{k}{\mu}\operatorname{grad}p, && \rho\bar{w}=-\frac{k}{\mu}\operatorname{grad}P,\\ &\rho=\text{const}; && P=\int\rho dp\\ & && \rho=\rho(p), \end{aligned} \tag{20.30}$$

It is important to note that the gas equation of state is considered to be known. A comparison of the first two equations of Eq. (20.30) shows that they are equivalent but for the unknown functions (pressure p as opposed to Leibensohn's function P and filtration velocity w as opposed to filtration's mass velocity ρw). So, if the reservoir geometry and boundary conditions in the problems are similar, the solutions will have the similar format. Therefore, if the earlier obtained solutions is considered for the unidimensional filtration flow of an incompressible fluid and replace the functions, the solutions valid for the gas filtration are obtained. For instance, the solutions for pressure distribution and filtration velocity in the reservoir for the rectilinear-parallel flow [Eq. (20.4)] of a incompressible fluid will transform as follows for the gas filtration:

for incompressible liquid	*for gas*
$p(x)=p_k-\dfrac{p_k-p_{\text{gal}}}{L}x,$	$P(x)=P_k-\dfrac{P_k-P_{\text{gal}}}{L}x,$
$w=-\dfrac{k}{\mu}\dfrac{p_k-p_{\text{gal}}}{L}.$	$\rho w=-\dfrac{k}{\mu}\dfrac{P_k-P_{\text{gal}}}{L}.$

(20.31)

In order to obtain pressure and mass velocity distribution at gas filtration in the decisive format, the equation of state should be assigned. It is clear that after the substitution of Leibensohn's function, different pressure and mass velocity distributions are obtained, as well as equations for average pressure in the reservoir for each of equations of state reviewed in Chapter III.

Let's analyze each case individually.

6. Unidimensional filtration flow of ideal gas

After establishing the similarity in the transient-free filtration of a incompressible liquid and a gas, and assigning equations of state, the solutions for each of the unidimensional filtration case should be considered. Suppose the ideal gas is followings.

Rectilinear-parallel filtration flow of the ideal gas. For the ideal gas, the substitution of Leibensohn's function Eq. (19.32) into Eq. (20.31) results in the following pressure and velocity distribution, respectively:

$$\frac{\rho_{atm} p^2}{2p_{atm}} + C = \frac{\rho_{atm} p_k^2}{2p_{atm}} + C - \frac{\frac{\rho_{atm} p_k^2}{2p_{atm}} - \frac{\rho_{atm} p_{gal}^2}{2p_{atm}}}{L} x,,$$

$$\rho w = \frac{k}{\mu} \frac{\frac{\rho_{atm} p_k^2}{2p_{atm}} - \frac{\rho_{atm} p_{gal}^2}{2p_{atm}}}{L}.$$

After the transformations and multiplication of filtration velocity at the gallery area results in:

$$p(x) = \sqrt{p_k^2 - \frac{p_k^2 - p_{gal}^2}{L} x}, \tag{20.32}$$

$$\rho w = \frac{k}{\mu} \frac{\rho_{atm} (p_k^2 - p_{gal}^2)}{2p_{atm} L}, \tag{20.33}$$

$$\rho w Bh = Q_m = \frac{k}{\mu} \frac{\rho_{atm} (p_k^2 - p_{gal}^2)}{2p_{atm} L} Bh. \tag{20.34}$$

Eqs. (20.32)–(20.34) enable the calculation of major filtration parameters in rectilinear-parallel filtration of the ideal gas. Analyzing the mass throughflow Eq. (20.34) it is easy to see that it may be derived from equation for the rate of an incompressible fluid by substituting Leibensohn's function for pressure and the mass throughflow for the volume throughflow. Therefore, a complete similarity

between the incompressible liquid and gas filtration is established by the following ing substitutions of variables:

for incompressible liquids	*for gas*
$p(x)$	$p(x)$
w	ρw
Q	Q_m

At the gas filtration studies, beside the mass flow rate, a concept of the volume throughflow Q_{atm} normalized for the atmospheric conditions is commonly used. It is defined by the following equation:

$$Q_{atm} = \frac{Q_m}{\rho_{atm}}.$$

Equation for the gas volume throughflow, normalized for the atmospheric conditions, is:

$$Q_{atm} = \frac{k}{\mu}\frac{p_k^2 - p_{gal}^2}{2p_{atm}L}Bh. \tag{20.35}$$

Using the obtained solution for the mass filtration velocity, it is possible to derive equation for the "marked particles" flow time in a gas reservoir. For this purpose, the filtration velocity Eq (20.33) is substituted into Eq. (20.7):

$$t = \emptyset\int_0^x \frac{dx}{w} = \frac{2\mu\emptyset L}{k(p_k^2 - p_{gal}^2)}\int_0^x p(x)\,dx = \frac{2\mu\emptyset L p_k}{k(p_k^2 - p_{gal}^2)}\int_0^x \sqrt{1 - \frac{p_k^2 - p_{gal}^2}{p_k^2 L}x}\,dx, \tag{20.36}$$

where Eq. (20.32) was used for $p(x)$.

Upon integrating of Eq. (20.36):

$$t = \frac{4\mu\emptyset L^2 p_k^3}{3k(p_k^2 - p_{gal}^2)^2}\left[1 - \sqrt{\left(1 - \frac{p_k^2 - p_{gal}^2}{p_k^2 L}x\right)^3}\right].$$

This expression may be transformed by way of transferring p_k^3 into the brackets. The result is:

$$t = \frac{4\mu\emptyset L^2(p_k^3 - p^3(x))}{3k(p_k^2 - p_{gal}^2)^2}. \tag{20.37}$$

Eq. (20.37) enables determining time necessary for a "marked particle" to flow to any point in the reservoir. In particular, at $x = L$:

$$T = \frac{4\mu\emptyset L^2(p_k^3 - p_{gal}^3)}{3k(p_k^2 - p_{gal}^2)^2}. \tag{20.38}$$

Eq. (20.38) can be made simpler with the use of a formula for weighted average formation pressure. Average formation pressure weighted over the pore space in the ideal gas filtration is determined from the following equation:

$$\bar{p} = \frac{1}{V_{\Pi}} \int_V p \varnothing dV = \frac{1}{BhL} \int_0^L \int_0^h \int_0^B p(x)\, dx\, dy\, dz =$$

$$= \frac{1}{L} \int_0^L p(x) dx = \frac{p_k}{L} \int_0^L \sqrt{1 - \frac{p_k^2 - p_{gal}^2}{L p_k^2} x}\, dx,$$

where the same integral as in Eq. (20.36) needs to be calculated. Using the result obtained earlier:

$$\bar{p} = \frac{2}{3} \frac{p_k^3 - p_{gal}^3}{p_k^2 - p_{gal}^2}. \tag{20.39}$$

After that, Eq. (20.38) may be rewritten as:

$$T = \frac{2 \varnothing \mu L^2 \bar{p}}{k (p_k^2 - p_{gal}^2)}. \tag{20.40}$$

As mentioned earlier, Leibensohn's function for elastic fluid at small pressure changes coincides with Leibensohn's function for incompressible fluid. So, the solutions for elastic liquid at small pressure changes look exactly as for incompressible liquid.

Comparing the solutions for rectilinear-parallel filtration of incompressible liquid and ideal gas, Eq. (20.32) indicates that pressure in a gas reservoir changes not linearly (as it is for the flow of incompressible fluid), but in proportion with square root of the coordinate (Fig. 20.9). Pressure gradient (the angle between curve 2 in Fig. 20.9 and the x axis) increases as the gas is flowing in the reservoir, and reaches its maximum at the gallery. Pressure nonlinearity in the reservoir causes changes in pressure gradient, and under Darcy's law, in filtration velocity. A comparison of rectilinear-parallel filtration velocities for the flow of a incompressible liquid and ideal gas is illustrated in Fig. 20.10. Ideal gas filtration velocity increases on approaching the gallery. That causes equation of the "marked particle" motion to become nonlinear. A comparison of "marked particle" motion time for the flow of a incompressible liquid and ideal gas is illustrated in Fig. 20.11.

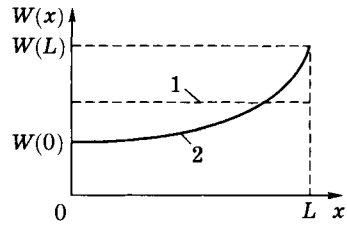

Fig. 20.9. Pressure distribution at rectilinear-parallel flow: 1. incompressible liquid, 2. gas

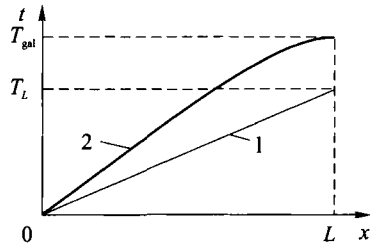

Fig. 20.10. Velocity vs. coordinate correlation for rectilinear-parallel filtration: 1 — incompressible liquid, 2 — gas

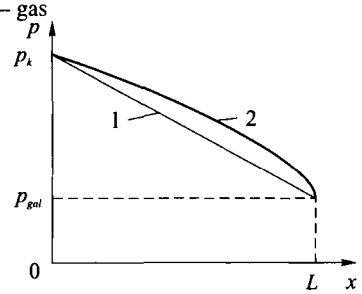

Fig. 20.11. Time vs. coordinate correlation of a marked particle under rectilinear-parallel filtration: 1 — incompressible liquid, 2 — gas

Radial-plane filtration flow of the ideal gas. Using the similarity between the incompressible liquid and gas filtration, the above solutions [Eqs. (20.19), (20.20) and (20.21)] are transformed by replacing Leibensohn's function for pressure, mass velocity for filtration velocity, and mass flow rate for the volume flow rate. The result is:

$$P = P_k - \frac{P_k - P_c}{\log(R_k / r_c)} \log \frac{R_k}{r},$$

$$\rho w = \frac{Q_m}{2\pi kh} \frac{1}{r}, \qquad (20.41)$$

$$Q_m = \frac{2\pi kh}{\mu} \frac{P_k - P_c}{\log(R_k / r_c)}.$$

We will now replace Leibensohn's function in Eq. (20.41) by its representation for an ideal gas [Eq. (1 9.32)]. As follows from this representation, $P = \rho_{atm} p^2 / 2p_{atm} + C$, $P_k = \rho_{atm} p_k^2 / 2p_{atm} + C$, and $P_c = \rho_{atm} p_c^2 / 2 p_{atm} + C$. Thus:

$$p^2 = p_k^2 - \frac{p_k^2 - p_c^2}{\log(R_k / r_c)} \log \frac{R_k}{r},$$

$$\rho w = \frac{Q_m}{2\pi h} \frac{1}{r},$$

$$Q_m = \frac{\pi kh \rho_{atm}}{\mu p_{atm}} \frac{p_k^2 - p_c^2}{\log(R_k / r_c)}.$$

Therefore, pressure distribution under radial-plane filtration of ideal gas is found from:

$$p = \sqrt{p_k^2 - \frac{p_k^2 - p_c^2}{\log(R_k / r_c)} \log \frac{R_k}{r}}. \tag{20.42}$$

Fig. 20.12 illustrates a comparison between pressure distribution curves in the reservoir under transient-free filtration of an incompressible liquid [Eq. (20.20)] and that of ideal gas [Eq. (20.42)] with the same boundary conditions and the same reservoir size. The curves show that pressure in a gas reservoir changes more slowly near the accumulation limit and more rapidly, near the well than it does in an oil reservoir (usually, the model of incompressible liquid is utilized for the calculations). The rate of pressure change determined pressure gradient, which, in turn, determined filtration velocity. Thus, the indicated pressure behavior of the gas reservoir results in the violation of the Darcy's law in the near-hole zone of the fields. Thus, the solutions derived from nonlinear filtration laws are better suited for the applied calculations of ideal gas flows. Later the solution of the corresponding ponding problems will be reviewed and analyzed.

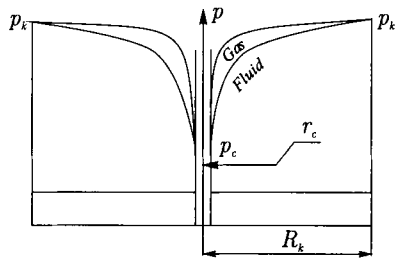

Fig. 20.12. Comparison of pressure distribution in the reservoir under transient-free filtration of incompressible liquid and perfect gas

The gas mass flow-rate equation in a gas reservoir is usually converted for the volume flow-rate equation under atmospheric conditions. This is done by dividing by the gas density under atmospheric conditions:

$$Q_{\text{atm}} = \frac{Q_m}{\rho_{\text{atm}}} = \frac{\pi k h}{\mu p_{\text{atm}}} \frac{p_k^2 - p_c^2}{\log(R_k / r_c)}. \tag{20.43}$$

The indicator curve for gas wells is usually a correlation graph of volume flow-rate *vs.* $(p_k^2 - p_c^2)$. Therefore, following Eq. (20.43), the indicator curve is a straight line (Fig. 2.13), and the productivity index is:

$$\frac{\pi k h}{\mu p_{\text{atm}}} \frac{1}{\log(R_k / r_c)}. \tag{20.44}$$

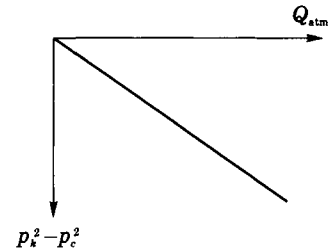

Fig. 20.13. Indicator diagram for gas wells

Mass velocity equation under the ideal gas radial-plane filtration, after the expression for the mass flow-rate is substituted, may be converted into:

$$\rho w = \frac{k}{\mu}\frac{\rho_{atm}}{2p_{atm}}\frac{p_k^2 - p_c^2}{\log(R_k / r_c)}\frac{1}{r}. \tag{20.44}$$

Volume throughflow and filtration velocity equations under the ideal gas radial-plane filtration are:

$$Q(r) = \frac{Q_m}{\rho} = \frac{Q_m p_{atm}}{\rho_{atm}\rho} = \frac{\pi kh}{\mu p_{atm}}\frac{p_k^2 - p_c^2}{\log(R_k / r_c)p(r)}, \tag{20.45}$$

$$w = \frac{Q(r)}{2\pi rh} = \frac{k}{\mu}\frac{p_k^2 - p_c^2}{2\log R_k / r_c}\frac{1}{p(r)r}. \tag{20.46}$$

Now, let's determine average pressure weighted over the pore volume under the ideal gas radial-plane filtration:

$$p = \frac{1}{V_\Pi}\int_V p\varnothing dV = \frac{1}{\pi h(R_k^2 - r_c^2)}\int_0^h dz\int_0^{2\pi} d\varphi\int_{r_c}^{R_k}\sqrt{p_k^2 - \frac{p_k^2 - p_c^2}{\log(R_k / r_c)}\log\frac{R_k}{r_c}}\,r\,dr.$$

After integrating this equation with respect to z and φ, and the subsequent removal of p_k^2 from under the integral, the result is:

$$p = \frac{2p_k}{R_k^2 - r_c^2}\int_{r_c}^{R_k}\sqrt{1 - \frac{1 - p_c^2 / p_k^2}{\log(R_k / r_c)}\log\frac{R_k}{r_c}}\,r\,dr. \tag{20.47}$$

The integral Eq. (20.47) cannot be taken in a finite form and is calculated approximately. To demonstrate the approximate calculation and simplifications, the following expression is introduced:

$$y = \frac{1 - p_c^2 / p_k^2}{\log(R_k / r_c)}\log\frac{R_k}{r_c}.$$

At $r_c < r < R_k$, the inequality $0 < y < 1$ is valid for the new variable (indeed, at $r = R_k$, we have $\log R_k/r = \log 1 = 0$, and $y = 0$; at $r_c < r < R_k$, $0 < \log R_k/r / \log R_k / r_c < 1$, and $0 < 1 - p_c^2 / p_k^2 < 1$, so $0 < y < 1$). Let's expand the radical into series:

$$\sqrt{1-y} = 1 - \frac{y}{2} - \frac{y^2}{8} - \ldots$$

Taking only y-linear term:

$$\sqrt{1-y} = 1 - \frac{1 - p_c^2 / p_k^2}{2\log(R_k / r_c)} \log \frac{R_k}{r}.$$

After the simplification, Eq. (20.47) takes the following format:

$$p = \frac{2p_k}{R_k^2 - r_c^2} \int_{r_c}^{R_k} \left[1 - \frac{1 - p_c^2 / p_k^2}{\log(R_k / r_c)} \log \frac{R_k}{r_c} \right] r\, dr.$$

This integral is integrated part-by-part (see the calculation of average pressure weighted over the pore volume under radial filtration of incompressible liquid in Section 2 of this Chapter). Disregarding the component containing r_c^2 / R_k^2, the result is:

$$p \approx p_k \left[\frac{1 - p_c^2 / p_k^2}{4\log(R_k / r_c)} \right]. \tag{20.48}$$

Now, let's determine the "marked particles" motion time in the gas reservoir under the radial filtration. This time is:

$$t = \varnothing \int_{r_c}^{r} \frac{dr}{w(r)}.$$

Substituting this term into the filtration velocity Eq. (20.46), results in:

$$t = \varnothing \int_{r_c}^{r} \frac{2\mu \log R_k / r_c}{k(p_k^2 - p_c^2)} p(r)\, dr.$$

The time required for the "marked particle" to move from the charge contour to the well is determined. For this purpose, the above equation is transformed by substituting, under the sign of integral, pressure distribution Eq. (20.42) at radial filtration of ideal gas:

$$T = \frac{2\varnothing\mu \log R_k / r_c}{k(p_k^2 - p_c^2)} p_k \int_{r_c}^{R_k} \sqrt{\left[1 - \frac{1 - p_c^2 / p_k^2}{2\log(R_k / r_c)} \log \frac{R_k}{r} \right]} r\, dr.$$

This integral was already derived for average pressure weighted over the pore volume Eq. (20.47). So, as in the previous case, it can be computed approximately by expanding the expression under integral into a series:

$$T = \frac{\varnothing \mu \log(R_k / r_c)(R_k^2 - r_c^2)}{k(p_k^2 - p_c^2)} p. \tag{20.49}$$

The assumption, while deriving Eq. (20.49), was that porosity is equal to clearance. If this assumption is neglected and the porosity/clearance correlation is accpted as $\varnothing = \varphi_\alpha S_\alpha$, the Eq. (20.49) becomes:

$$T = \frac{\varnothing \mu \log(R_k / r_c)(R_k^2 - r_c^2)}{\varphi_\alpha k(p_k^2 - p_c^2)} p.$$

The introduction of the structural factor shortens the motion time of the "marked particles".

Note about the radial-spherical filtration flow of ideal gas. Using Eqs. (20.27) and (20.28) and the similarity in filtration of incompressible liquid and the gas, it is possible to derive major filtration parameters also for the radial-spherical filtration flow of ideal gas.

7. Parallel-plane filtration of real gas under Darcy's law

In Chapter XIX, the generalized Leibensohn's function Eq. (19.20) is introduced. Let's now assume that permeability is constant, and the density is associated with pressure as in equation of state for the real gas [Eq. (19.27)]. In such a case, Leibensohn's function takes the following format:

$$P = \frac{k\rho_{atm} z(p_{atm})}{p_{atm}} \int \frac{p}{\mu(p) z(p)} dp. \tag{20.50}$$

After assigning the Eqs. (20.33), (20.34), (20.35) and (20.36), Leibensohn's for function [Eq. (20.50)] may be used for solving unidimensional filtration problems for compressible fluids accounting for the super-compressibility factor and the correlation pressure *vs.* viscosity. Let's review as an example the problem of a well flow-rate under the parallel-plane filtration.

To compute the flow-rate, the analogy between filtration of an incompressible liquid and compressible fluid is used, as well as the equation for the mass flow-rate utilizing Leibensohn's formula:

$$Q_m = \frac{2\pi kh}{\mu} \frac{P_k - P_c}{\log(R_k / r_c)},$$

Let's now substitute the Leibensohn's function [Eq. (20.49)]:

$$Q_m = \frac{2\pi kh}{\mu} \frac{\rho_{atm} z(p_{atm})}{\log(R_k / r_c)} \int_{p_c}^{p_k} \frac{p}{\mu(p) z(p)} dp.$$

There are different ways to calculate the integral in the above equation. The simplest way is to use the graphs in Fig. 19.2 to determine the values $z(p_k) = z_k$, $z(p_c) = z_c$, and $\mu(p_k) = \mu_k$, $\mu(p_c) = \mu_c$; and to replace the variables $z(p)$ and $\mu(p)$ under the integral by constant values equal to arithmetic averages:

$$\tilde{z} = \frac{z_k + z_c}{2} \text{ and } \tilde{\mu} = \frac{\mu_k + \mu_c}{2}. \qquad (20.51)$$

After that, equation of the mass flow-rate is formatted as follows:

$$Q_m = \frac{2\pi kh}{\mu} \frac{\rho_{atm} z(p_{atm})}{\tilde{\mu}\tilde{z} \log(R_k / r_c)} \int_{p_c}^{p_k} p dp.$$

Now, the integral is computable, and equation for the real gas's mass flow rate considering the pressure and viscosity is:

$$Q_m = \frac{\pi kh}{\mu} \frac{\rho_{atm} z(p_{atm})(p_k^2 - p_c^2)}{\tilde{\mu}\tilde{z}\, p_{atm} \log(R_k / r_c)}.$$

Inclusion of the real gas properties' deviations from those determined from equation of state for ideal gas, as well as of correlation of viscosity *vs.* pressure results in the flow-rate accuracy of up to 30 %.

Filtration parameters for unidimensional flow of elastic liquids. As mentioned in the derivation of Eq. (19.31), under small pressure changes, Leibensohn's function for the elastic liquid coincides with Leibensohn's function for incompressible liquid. So, the elastic liquid under the transient-free filtration may be considered as incompressible, and the solutions derived for the incompressible fluid may be used for for the calculations. However, when the pressure changes are large (such as in high-pressure reservoir with a large pressure drawdown), the use of equation of state for the incompressible fluid may cause significant errors. In such a case, equation of state [Eq. (19.23)] and the corresponding responding Leibensohn's function [Eq. (19.30)] should be used. But in such a case the soultions will be exponential, and usually they are not utilized in this form. Thus, models of ideal and real gas are considered. The elastic liquid's model is used in the filtration theory for solving problems under non-stationary flows.

8. Radial-plane filtration of incompressible liquid and gas under binomial filtration law

Let's now review the ways to determine major parameters of the radial-plane liquids and gas filtration at high velocity, when deviations from Darcy's law are caused by significant inertial components of the total filtration resistance.

The incompressible liquid and gas filtration models in this case are as following:

$$\operatorname{div}\bar{w}=0, \qquad \operatorname{div}\rho\bar{w}=0,$$

$$\operatorname{grad}p=-\frac{k}{\mu}\bar{w}-\beta\frac{\rho}{\sqrt{k}}|\bar{w}|\bar{w}, \qquad \operatorname{grad}p=-\frac{k}{\mu}\bar{w}-\beta\frac{\rho}{\sqrt{k}}|\bar{w}|\bar{w},$$

$$\rho=\text{const} \qquad \rho=\rho(p).$$

If the Leibensohn's function is introduced, both models allow for the analogy between the liquid and gas filtration also under the nonlinear filtration law. Let's multiply by density the filtration law in the gas model, and introduce Leibensohn's function. As e result, for the first two equations:

$$\operatorname{div}\bar{w}=0, \qquad \operatorname{div}\rho\bar{w}=0,$$

$$\operatorname{grad}p=-\frac{k}{\mu}\bar{w}-\beta\frac{\rho}{\sqrt{k}}|\bar{w}|\bar{w}; \qquad \operatorname{grad}p=-\frac{k}{\mu}\rho\bar{w}-\frac{\beta}{\sqrt{k}}|\rho\bar{w}|\rho\bar{w}.$$

Therefore, both models allow for the same analogy as under the linear filtration law.

To make the results more general, let's obtain the solution of the transient-free parallel filtration problem under the binomial law for the gas, and write down the solution for incompressible liquid as a particular case of Leibensohn's function for equation of state, $\rho = \text{const}$.

Let's project the binomial filtration law onto the flowline (onto the r axis of the cylindrical coordinate system):

$$\frac{dP}{dr}=\frac{\mu}{k}\rho w_r+\frac{\beta}{\sqrt{k}}(\rho w_r)^2. \tag{20.52}$$

In order to reduce differential equation [Eq. (20.72)] to a format for integration, the continuity equation is reviewed and the connection between the throughflow and filtration velocity is found by integrating the continuity equation. The transient-free flow continuity equation in the cylindrical coordinate system is:

$$\frac{\partial\rho w_r r}{\partial r}+\frac{\partial\rho w_\varphi}{\partial\varphi}+r\frac{\partial\rho w_z}{\partial z}=0.$$

As the flow is unidimensional and parallel-plane, all sought-for functions depend only on r, and the continuity equation becomes simpler:

$$\frac{d\rho w_r r}{dr}=0,$$

and after integrating:

$$\rho w_r r = C = \text{const.}$$

By multiplying this result by $2\pi h$ (where h is the reservoir thickness):

$$2\pi\rho w_r rh = Q_m = \text{const},$$

and from here, the mass filtration velocity is:

$$\rho w_r = \frac{Q_m}{2\pi h}\frac{1}{r}.$$

Substituting this expression into Eq. (20.52), results in:

$$\frac{dP}{dr} = \frac{\mu}{k}\frac{Q_m}{2\pi h}\frac{1}{r} + \frac{\beta}{\sqrt{k}}\left(\frac{Q_m}{2\pi h}\right)^2\frac{1}{r^2}.$$

By integrating this equation from the contour radius to an arbitrary point within the reservoir:

$$P = P_k - \frac{\mu}{k}\frac{Q_m}{2\pi h}\log\frac{R_k}{r} - \frac{\beta}{\sqrt{k}}\left(\frac{1}{r} - \frac{1}{R_k}\right). \tag{20.53}$$

As $r << R_k$, we may disregard the expression in parentheses. Assuming $r = r_c$, Eq. (20.53) may be rewritten as:

$$P = P_k - \frac{\mu}{k}\frac{Q_m}{2\pi h}\log\frac{R_k}{r} + \frac{\beta}{\sqrt{k}}\left(\frac{Q_m}{2\pi h}\right)^2\frac{1}{r_c}. \tag{20.54}$$

Eqs. (20.53) and (20.54) represent, respectively, the Leibensohn'd function distribution in the reservoir and the correlation of pressure drawdown *vs.* flow-rate. Now, the following equations will be used:

$$P = \frac{\rho_{\text{atm}} p^2}{2p_{\text{atm}}} + C \text{ for ideal gas, and}$$

$$P = \rho_0 p + C \text{ for a incompressible liquid}$$

to transit from Leibensohn's function to pressure. This results in the derivation from Eqs. (20.53) and (20.54) equations for pressure distribution and the throughflow *vs.* pressure drawdown correlation with radial-plane filtration under the binomial law. For the incompressible liquid, the distribution of pressure in the reservoir is found from:

$$p = p_k - \frac{\mu}{k}\frac{Q}{2\pi h}\log\frac{R_k}{r} - \frac{\beta\rho_0}{\sqrt{k}}\left(\frac{Q}{2\pi h}\right)^2\left(\frac{1}{r} - \frac{1}{R_k}\right), \tag{20.55}$$

and the pressure drawdown *vs.* throughflow correlation, from:

$$p_k - p_c = \frac{\mu}{k}\frac{Q}{2\pi h}\log\frac{R_k}{r_c} + \frac{\beta\rho_0}{\sqrt{k}}\left(\frac{Q}{2\pi h}\right)^2\frac{1}{r_c}. \tag{20.56}$$

For ideal gas, pressure distribution in the reservoir is found from:

$$p = \sqrt{p_k - \frac{\mu}{k}\frac{Q_{atm}p_{atm}}{\pi h}\log\frac{R_k}{r} - \frac{\beta\rho_{atm}p_{atm}}{2\sqrt{k}}\left(\frac{Q}{\pi h}\right)^2\left(\frac{1}{r}-\frac{1}{R_k}\right)}, \tag{20.57}$$

and the pressure drawdown *vs.* throughflow correlation, from:

$$p_k^2 - p_c^2 = \frac{\mu}{k}\frac{Q_{atm}p_{atm}}{\pi h}\log\frac{R_k}{r_c} + \frac{\beta\rho_{atm}p_{atm}}{2\sqrt{k}}\left(\frac{Q_{atm}}{2\pi h}\right)^2\frac{1}{r_c}. \tag{20.58}$$

Eqs. (20.56) and (20.58) show that the indicator curves plotted,in the, Q, Δp coordinates for the liquids and Q_{atm}, $(p_k^2 - p_c^2)$ for the gases, are parables (Figs. 20.14 and 20.15).

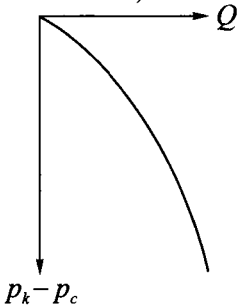

Fig. 20.14. Indicator diagram at liquid's filtration under the binomial law

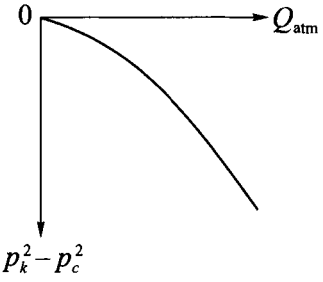

Fig. 20.15 Indicator diagram at gas flow under the binomial law

Let's now write down equation for the inflow into a well in a different form: for a noncompressible liquid:

$$p_k - p_c = AQ + BQ^2, \tag{20.59}$$

and for gas:

$$p_k^2 - p_c^2 = A_1 Q_{atm} + B_1 Q_{atm}^2. \tag{20.60}$$

In these equations:

$$A = \frac{\mu}{2\pi kh}\log\frac{R_k}{r_c},\quad B = \frac{\beta\rho_0}{\sqrt{k(2\pi h)^2}}\frac{1}{r_c}$$

$$A_1 = \frac{\mu p_{atm}}{\pi kh}\log\frac{R_k}{r},\quad B_1 = \frac{\beta\rho_{atm}p_{atm}}{2\sqrt{k(\pi h)^2}}\frac{1}{r_c}.$$

are filtration resistivity factors constant for a given well. They are found experimentally from well test results under a stabilized regime. The wells are studied under five or six regimes with the flow-rate and bottomhole pressure measured for each regime. After that the well is shut-in, and the stabilized bottomhole pressure in the shut-in well is assumed to be the contour pressure p_k. For interpretation of the well test results, Eqs. (20.59) and (20.60) are divided by Q and Q_{atm}, respectively, which turns them into straight line equations:

$$\frac{p_k - p_c}{Q} = A + BQ, \tag{20.61}$$

$$\frac{p_k^2 - p_c^2}{Q} = A_1 + B_1 Q_{atm}. \tag{20.62}$$

The graphs in coordinates Q, $(p_k - p_c)/Q$ and Q_{atm}, $(p_k^2 - p_c^2)/Q_{atm}$ are straight lines for which $A(A_1)$ is the interval cut on the y axis, and $B(B_1)$ is tangent of the angle between the straight line and the x axis (Fig. 2.16).

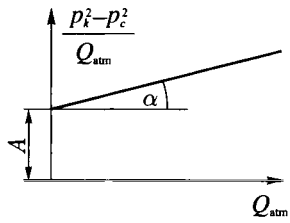

Fig. 20.16 Correlation at filtration under the binomial law

The flow-rate Eqs. (20.59) and (20.60) with experimentally determined factors are widely used in the designs of field development. Besides, $A(A_1)$ value found from well test results provides an opportunity for the determination of reservoir properties, such as hydroconductivity factor:

$$(p_k^2 - p_c^2)/Q_{atm} \text{ vs. } Q_{atm}$$

for an oil well:

$$\frac{kh}{\mu} = \frac{1}{2\pi A}\log\frac{R_k}{r_c};$$

and for a gas well:

$$\frac{kh}{\mu} = \frac{p_{atm}}{\pi A_1}\log\frac{R_k}{r_c}.$$

Equation of the real gas inflow to the well under the binomial filtration law is:

$$p_k^2 - p_c^2 = \frac{\tilde{\mu}\tilde{z}}{k}\frac{Q_{atm}p_{atm}}{\pi h}\log\frac{R_k}{r} + \frac{\beta\tilde{z}\rho_{atm}p_{atm}}{2\sqrt{k}}\left(\frac{Q_{atm}}{\pi h}\right)^2\frac{1}{r_c}, \qquad (20.63)$$

where $\tilde{\mu}$ and $\tilde{z}$ are determined from Eq. (20.51).

One should keep in mind that in real life it is incorrect to assume that a single nonlinear filtration law is valid within the entire reservoir, from the well-bore to the charge contour. At significant flow-rates, Darcy's law is broken in a near the bottom-hole, whereas within the rest of the reservoir the linear law is observed. As the flow-rate increases, the volume where Darcy's law is broken, grows.

9. Radial-plane filtration of incompressible liquid and gas under the exponential filtration law

Let's now project the exponential filtration law [Eq. (18.45)] onto a cylindrical coordinate system. For a radial-plane filtration flow:

$$w_r = c\left(\frac{dp}{dr}\right)^{1/n}, \quad w_\varphi = w_z = 0.$$

The mathematical model includes, besides the filtration law, the continuity equation. Integration of the continuity equation is similar to that performed in Section 8 and gives the same result:

$$2\pi\rho w_r rh = Q_m = \text{const}.$$

Because of this, the mass throughflow equation has the following format:

$$Q_m = 2\pi\rho w_r rh = 2\pi rhc\rho\left(\frac{dp}{dr}\right)^{\frac{1}{n}} = \text{const}.$$

To integrate this differential equation, let's raise to the power of n:

$$Q_m^n = (2\pi hc)^n r^n \rho^n \left(\frac{dp}{dr}\right)$$

and transform it to the following format:

$$A = r^n\rho^n\frac{dp}{dr},$$

where $A = (Q_m / 2\pi hc)^n = \text{const}$.

Separating the variables:

$$A = \frac{dr}{r^n}\rho^n dp \qquad (20.64)$$

and introducing the pressure function P^*:

$$P^* = \int \rho^n dp, \tag{20.65}$$

so that:

$$P^* = d\int \rho^n dp = \rho^n p.$$

After that, Eq. (20.64) may be rewritten as follows:

$$A\frac{dr}{r^n} = P^*. \tag{20.66}$$

After integrating from the bottomhole to the charge contour (i. e., using for integrating Eq. (20.66), the boundary conditions; $r = r_c, P^* = P_c^*$ and $r = R_k$, $P^* = P_k^*$), the result is:

$$\int_{P_c^*}^{P_k^*} dP^* = P_k^* - P_c^* = \int_{r_c}^{R_k} A\frac{dr}{r^n} = \frac{A}{n-1}\left(\frac{1}{r_c^{n-1}} - \frac{1}{R_k^{n-1}}\right) \approx \frac{A}{(n-1)r_c^{n-1}}. \tag{20.67}$$

Substituting A, represented through reservoir parameters and filtration parameters, in Eq. (20.67):

$$P_k^* - P_c^* = \frac{Q_m^n}{(2\pi hc)^n (n-1) r_c^{n-1}},$$

and from this, the flow-rate equation is obtained:

$$Q_m = 2\pi hc r_c^{\frac{n-1}{n}} \left[(n-1)(P_k^* - P_c^*)\right]^{\frac{1}{n}}. \tag{20.68}$$

On assuming an arbitrary point (r,P^*) as the lower integration limit in Eq. (20.67), the result is equation for the pressure function distribution in the reservoir:

$$P_k^* - P_c^* = \frac{A}{n-1}\left(\frac{1}{r^{n-1}} - \frac{1}{R_k^{n-1}}\right) \tag{20.69}$$

Or, eliminating A through Eq. (20.67),

$$P^*(r) = P_k^* - (P_k^* - P_c^*) r_c^{n-1}\left(\frac{1}{r^{n-1}} - \frac{1}{R_k^{n-1}}\right), \quad r_c \le r \le R_k. \tag{20.70}$$

The pressure function derived from Eq. (20.65) is:
for an incompressible liquid:

$$P^* = \rho_0^n p + C, \tag{20.71}$$

for an ideal gas (under the isothermal filtration):

$$P^* = \int \left(\frac{\rho_{atm} p}{p_{atm}}\right)^n dp = \left(\frac{\rho_{atm}}{p_{atm}}\right)^n \frac{p^{n-1}}{n-1} + C. \tag{20.72}$$

By substituting Eqs. (20.71) and (20.72) into Eqs. (20.68) and (20.70) equations for the flow-rate and pressure distribution is obtained for the liquid and ideal gas, respectively. Filtration velocity equation is then derived from the flow-rate equation.

Now, let's list all equations for the radial-plane filtration under the exponential law for an incompressible liquid.

The mass flow-rate:

$$Q_m = 2\pi h \rho_0 c r_c^{\frac{n-1}{n}} \left[(n-1)(p_k - p_c)\right]^{\frac{1}{n}}; \tag{20.73}$$

the volume flow-rate:

$$Q_m = 2\pi h c r_c^{\frac{n-1}{n}} \left[(n-1)(p_k - p_c)\right]^{\frac{1}{n}}; \tag{20.74}$$

pressure distribution in the reservoir:

$$p(r) = p_k - (p_k - p_c) r_c^{n-1} \left(\frac{1}{r^{n-1}} - \frac{1}{R_k^{n-1}} \right), \quad r_c \le r \le R_k; \tag{20.75}$$

filtration velocity:

$$w = \frac{Q}{2\pi r h} = \frac{c r_c^{\frac{n-1}{n}}}{r} \left[(n-1)(p_k - p_c)\right]^{\frac{1}{n}}. \tag{20.76}$$

If $n = 2$ is chosen in Eqs. (20.73)–(20.76), the result is Krasnopolsky filtration law formulae:

The mass flow-rate:

$$Q_m = 2\pi h \rho_0 c \sqrt{r_c (p_k - p_c)}; \tag{20.77}$$

pressure distribution in the reservoir:

$$p(r) = p_k - (p_k - p_c) r_c \left(\frac{1}{r} - \frac{1}{R_k} \right), \quad r_c \le r \le R_k; \tag{20.78}$$

filtration velocity:

$$w = \frac{Q}{2\pi r h} = \frac{c r_c^{\frac{1}{2}}}{r} \left[(p_k - p_c)\right]^{\frac{1}{2}}. \tag{20.79}$$

The formulae for radial-plane filtration of ideal gas under the exponential law are:

for the mass flow-rate:

$$Q_m = 2\pi h \rho_0 c r_c^{\frac{n-1}{n}} \frac{\rho_{atm}}{p_{atm}} \left[\frac{(n-1)}{(n+1)} (p_k^{n+1} - p_c^{n+1}) \right]^{\frac{1}{n}}; \tag{20.80}$$

for the volume tric flow-rate normalized for the atmospheric conditions:

$$Q_{am} = \frac{2\pi h \rho_0 c r_c^{\frac{n-1}{n}}}{p_{\text{atm}}} \left[\frac{(n-1)}{(n+1)} (p_k^{n+1} - p_c^{n+1}) \right]^{\frac{1}{n}}; \qquad (20.81)$$

for pressure distribution in the reservoir:

$$p(r) = p_k^{n+1} - (p_k^{n+1} - p_c^{n+1}) r_c^{n-1} \left(\frac{1}{r^{n-1}} - \frac{1}{R_k^{n-1}} \right), \quad r_c \le r \le R_k; \qquad (20.82)$$

and for filtration velocity:

$$w = \frac{Q}{2\pi r h} = \frac{c r_c^{\frac{n-1}{n}}}{r p(r)} \left[\frac{(n-1)}{(n+1)} (p_k^{n+1} - p_c^{n+1}) \right]^{\frac{1}{n}}. \qquad (20.83)$$

If $n = 2$is chosen in Eqs. (20.80)–(20.83), the result is the formulae of the Krasnopolsky filtration law.

Following Eq. (20.75), the pressure distribution curve for incompressible liquid has the shape of a hyperbola to a power on n–1, i. e., the drawdown funnel is a rotational hyperboloid. The funnel's steepness near the borehole is higher than that of a logarithmic curve. The $p(r)$ curve for the gas, Eq. (20.82), is positioned higher than for the liquid (at the same p_k and p_c values). Calculations show that for any p_k, p_c, R_k and r_c values over 80 % of the total drawdown ($p_k - p_c$) is lost at a distance of 1 meter from the borehole. The mass throughflow for fluids, Eq. (20.73), is proportional to the pressure drawdown to the power of $1/n$. Thus, the indicator curve $Q = f(\Delta p)$ at $1 < n < 2$ has the appearance of an exponential curve convex towards the flow-rate axis, and the curve's exponent is a fraction, less than 2. At filtration under Krasnoselsky law, as Eq. (20.76) shows, the indicator curve is a parabola. Fig. 20.17 displays the incompressible liquid flow indicator curves under the linear filtration law (n = 1), under nonlinear filtration laws ($1 < n < 2$) and n = 2. All the above is valid also for the gas indicator curves if they are plotted in the coordinates Q_m (or Q_{atm}) and $p_k^{n+1} - p_c^{n+1}$. Both for liquids and gases, the throughflow value is in proportion with the well radius to the $(n-1)/n$ power ($\sqrt{r_c}$ for Krasnoselsky's law), i. e., this correlation is much stronger than under Darcy's law.

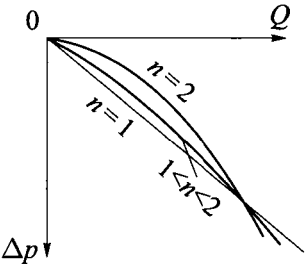

Fig. 20.17

Filtration velocity along the flow line changes same way under the nonlinear filtration as it does under the linear filtration; for the liquid, w is in inverse proportion with the radius, and for the gas, in inverse proportion with $rp(r)$.

Mechanics of Fluid Flow
by Kaplan S. Basniev, Nikolay M. Dmitriev and George V. Chilingar

CHAPTER XXI

UNIDIMENSIONAL FILTRATION OF INCOMPRESSIBLE LIQUID AND GAS IN A NONUNIFORM RESERVOIRS UNDER DARCY'S LAW

1. Major types of reservoir nonuniformities

In nature, productive hydrocarbon reservoirs are rarely uniform, i. e., such that the reservoir properties are identical for the entire reservoir. If permeability, porosity clearance, specific surface area, etc. change in a reservoir, such reservoir is called nonuniform.

However, permeability changes in the reservoir are sometimes so chaotic that significant reservoir volume may be considered as uniformly permeable on the average. Filtration flow parameters in such reservoirs with great accuracy repeat parameters of the filtration flows reviewed in the preceding paragraphs for uniform reservoirs.

Often, however, substantial reservoir volumes significantly differ from one another in their reservoir properties. These are so-called macro-nonuniform reservoirs whose parameter differences strongly affect the nature of the filtration flow. It may be acceptable for the calculations of elementary filtration flows within the macro-nonuniform reservoirs to resort to simplified flow geometry and to derive equivalent values of the filtration resistance factors. These values may be used with the equations derived in the preceding paragraph for a uniform reservoir.

The following types of the macro-nonuniformities are identified in the hydrocarbon reservoirs:

(1) Lamination nonuniformity. In such a case, the reservoir's thickness is subdivided into several laminae. Reservoir properties within each lamina are considered to be uniform and different from those in the adjacent laminae. Such reservoirs are also called thickness-nonuniform. The separation boundaries between the laminae of different permeabilities are considered plane. Thus, it is assumed in a lamination nonuniformity reservoir model that permeability, porosity, etc. change only from one lamina to the next and

are a piecewise-constant functions of the vertical coordinate. It may be assumed either that individual laminae – interbeds are separated by impermeable boundaries (the case of hydraulically isolated laminae) or cross-flows between the laminae must be taken into consideration (the case of hydraulically communicating laminae). In the first case, it is possible to determine the filtration parameters using unidimensional flow schematics. In the second case, an accurate determination, generally speaking, requires the solution of two-dimensional filtration problems.

(2) Zonal nonuniformity. In such a case, filtration properties change in the lamination plane, i. e., the reservoir includes several zones (areas of the reservoir). Reservoir properties within each zone are assumed to be identical and are assumed to change abruptly at the zones' boundaries.

(3) Continuous or random nonuniformity. In real life, some reservoirs have reservoir properties which change continuously or randomly from one point in the reservoir to the next. In solving forward problems of the subsurface hydromechanics, reservoir properties are assumed given. So, for the reservoirs with a continuous or random nonuniformity these properties are assumed to be given by the known continuous or random functions of the coordinates of filtration volume points.

For instance, in the process of drilling, the drilling mud filters into the hydrocarbon reservoir and degrade its reservoir properties. The reservoir invasion into the reservoir while drilling occurs uniformly, and reservoir properties degrade continuously from the well into the reservoir. However, such nonuniformity may be modeled as zonal as well as continuous.

Thus, the following may be identified as a result of simplifying filtration flows:

(1) Rectilinear-parallel, radial-plane and radial-spherical flows within nonuniformly laminated reservoir.

(2) Rectilinear-parallel, radial-plane and radial-spherical flows within zonally nonuniform reservoir.

(3) Rectilinear-parallel, radial-plane and radial-spherical flows within reservoirs where permeability is a continuous or random function of the filtration volume points.

For completeness, filtration within nonuniform reservoir should be analyzed for various fluids (incompressible and compressible fluids; and also for non-Newtonian liquids under the linear and nonlinear filtration laws). However, the volume of this monograph does not allow for such a detailed consideration, so the review is limited to the analysis of most typical cases and will note that the methodological approch remains he same.

Now the unidimensional liquid and gas flows are analyzed within the nonuniform reservoirs under Darcy's law.

2. Rectilinear-parallel flow within nonuniformly-stratified reservoir

Suppose a horizontal layer with thickness h and width B includes n laminae with permeability k_i and porosity $\varnothing_i$, $i = 1, 2, \ldots, n$ (Fig. 21.1). The reservoir is saturated with a liquid or gas. Constant pressure p_k is maintained at the charge contour. Constant pressure p_{gal} ($p_k > p_{gal}$) is maintained at the other boundary (gallery) positioned at a distance L from the charge contour. In the case where no crossflows exist between the lamina, the flow is rectilinear-parallel flow within each lamina using Eqs. (20.4) and (20.5) for determining pressure, filtration velocity and flow-rate for the incompressible liquid filtration derived in the preceding Chapter:

$$p(x) = p_k - \frac{p_k - p_{gal}}{L} x,$$

$$w_x = -\frac{k}{\mu}\frac{\partial p}{\partial x} = -\frac{k}{\mu} C_1 = \frac{k}{\mu}\frac{p_k - p_{gal}}{L},$$

$$w_x S = Q = \frac{k}{\mu}\frac{p_k - p_{gal}}{L} S.$$

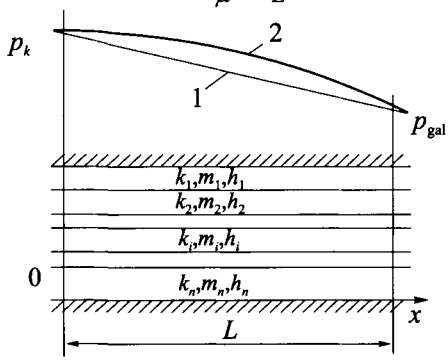

Fig. 21.1. Rectilinear-nonuniform flow in a nonuniformly-stratified reservoir: 1 — $p(x)$ for the liquid, 2 — $p(x)$ for the gas

The difference, however, is that the pressure distribution equation is the same for all beds, but the filtration velocity and flow-rate will be distinct for each of them:

$$p(x) = p_k - \frac{p_k - p_{gal}}{L} x, \tag{21.1}$$

$$w^i = \frac{k_i}{\mu}\frac{p_k - p_{gal}}{L}, \tag{21.2}$$

$$Q^i = \frac{k_i}{\mu}\frac{p_k - p_{gal}}{L} h_i B. \tag{21.3}$$

Eqs (21.1), (21.2) and (21.3) include the subscript i, which indicates the number of the lamina ranging between 1 and n.

The differences in Eqs. (21.1), (21.2) and (21.3) are, clearly, due to the fact that although the pressure drawdown in all laminae is the same, the laminae reservoir properties and size differ. Apparently, the filtration velocity will be higher wherever permeability is greater, and the flow-rate will be greater wherever the lamina cross-section is larger and permeability is higher.

Using the similarity between the filtration of incompressible liquid and gas, from Eqs. (21.1)–(21.3), expressed through Leibensohn' function, formulas are derived, which are also valid for the gas filtration:

$$P(x) = P_k - \frac{P_k - P_{\text{gal}}}{L} x, \tag{21.4}$$

$$\rho w^i = \frac{k_i}{\mu} \frac{P_k - P_{\text{gal}}}{L}, \tag{21.5}$$

$$Q_m^i = \frac{k_i}{\mu} \frac{P_k - P_{\text{gal}}}{L} h_i B. \tag{21.6}$$

Therefore, if we assume an ideal gas, and substitute the Leibensohn' s function [Eq. (19.32)] into Eqs. (21.4)–(21.6), the equations are derived for ideal gas filtration in the nonuniformly-laminated reservoir:

$$p(x) = \sqrt{p_k^2 - \frac{p_k^2 - p_{\text{gal}}^2}{L} x}, \tag{21.7}$$

$$\rho w^i = \frac{k_i \rho_{\text{atm}}}{\mu p_{\text{atm}}} \frac{p_k^2 - p_{\text{gal}}^2}{L} = \frac{k_i \rho(x)}{\mu p(x)} \frac{p_k^2 - p_{\text{gal}}^2}{L}, \tag{21.8}$$

$$Q_m^i = \frac{k_i \rho_{\text{atm}}}{\mu p_{\text{atm}}} \frac{p_k^2 - p_{\text{gal}}^2}{L} h_i B. \tag{21.9}$$

Now, let's again use the filtration similarity of incompressible liquid and gas and make calculations in a general format for both liquid and gas.

The mass throughflow for the entire reservoir is the sum of the throughflows in individual laminae:

$$Q_m = \sum_{i=1}^{n} Q_m^i = \sum_{i=1}^{n} \frac{k_i}{\mu} \frac{P_k - P_{\text{gal}}}{L} h_i B = \frac{B(P_k - P_{\text{gal}})}{\mu L} \sum_{i=1}^{n} k_i h_i. \tag{21.10}$$

It is convenient in hydrodynamic calculations to replace equations of the fluid flow within a nonuniform bed with the equation for the uniform bed of the same size with the average permeability k_{avg}. The value of this average permeability may be determined from the condition of the flow-rates equality, i. e., from:

$$Q_m = \frac{k_{\text{avg}}(P_k - P_{\text{gal}})}{\mu L} Bh = \frac{B(P_k - P_{\text{gal}})}{\mu L} \sum_{i=1}^{n} k_i h_i, \tag{21.11}$$

one obtains:

$$k_{\text{avg}} = \sum_{i=1}^{n} k_i h_i / h, \quad h = \sum_{i=1}^{n} h_i. \tag{21.12}$$

Therefore, average permeability of a nionuniformly-laminated reservoir does not depend on a fluid and is the same for both incompressible liquid and gas.

By substituting the Leibensohn's function values for the incompressible liquid and ideal gas into Eq. (21.11), the flow-rate equations for the entire nionuniformly-laminated reservoir are obtained:
For the incompressible liquid:

$$Q_m = \frac{B\rho_0(p_k - p_{gal})}{\mu L}\sum_{i=1}^{n} k_i h_i, \tag{21.13}$$

for the gas:

$$Q_m = \frac{B\rho_{atm}(p_k^2 - p_{gal}^2)}{2\mu p_{atm} L}\sum_{i=1}^{n} k_i h_i. \tag{21.14}$$

Fluid particles movement time for the incompressible liquid (not taking the difference between porosity and clearance into account) may be determined from Eqs. (20.8A) and (20.9A). However, individual values of porosity and permeability will pertain to each lamina:

$$t_i = \frac{\emptyset_i \mu}{k_i}\frac{Lx}{p_k - p_{gal}} \text{ and } T_i = \frac{\emptyset_i \mu}{k_i}\frac{L^2}{p_k - p_{gal}}.$$

Similarly for the gas, Eqs. (20.37) and (20.38) transform considering reservoir properties for each lamina:

$$t_i = \frac{4\emptyset_i \mu L^2(p_k^3 - p^3(x))}{3k_i(p_k^2 - p_{gal}^2)^2} \text{ and } T_i = \frac{4\emptyset_i \mu L^2(p_k^3 - p_{gal}^3)}{3k_i(p_k^2 - p_{gal}^2)^2}.$$

3. Rectilinear-parallel flow in zonally-nonuniform bed

Suppose a horizontal bed of a constant thickness h and constant width B includes n zones of different permeabilities k_i, porosities $\emptyset_i$, and lengths l_i ($i = 1, 2, 3, \ldots, n$). Constant pressures p_k and p_{gal} are maintained at the bed's boundaries ($p_k > p_{gal}$), [Fig. 21.2]. Boundaries of each filtration zone are perpendicular to the flow direction along the x axis.

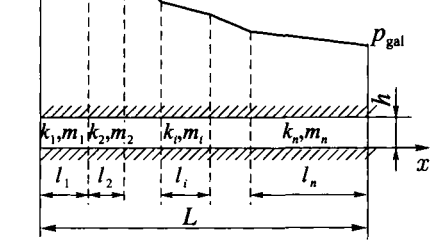

Fig. 21. 2. Rectilinear-parallel flow in zonally-nonuniform reservoir. $p(x)$ curve for a liquid.

A transient-free filtration of a uniform fluid occurs within the bed. So, in each zone of the zonally-nonuniform bed we have a rectilinear-parallel flow described by the same equations for pressure, filtration velocity and flowrate. For instance, at the filtration of incompressible liquid:

$$p(x) = p_k - \frac{p_k - p_{gal}}{L} x,$$

$$w_x = -\frac{k}{\mu}\frac{\partial p}{\partial x} = -\frac{k}{\mu}C_1 = \frac{k}{\mu}\frac{p_k - p_{gal}}{L},$$

$$w_x S = Q = \frac{k}{\mu}\frac{p_k - p_{gal}}{L} S,$$

where pressures in the beginning and at the end of each zone are assumed to be, respectively, the pressures at the charge source and the gallery, and the length is equal to the zone length. Remember that in a nonuniformly-laminated reservoir, pressure equation was the same for all laminae with different filtration velocities and flow-rates. In this case, the filtration velocities and flow-rates are equal in all zones, but the pressure distribution equations are different for each zone.

The amount entering the reservoir at the charge contour is exiting it at the gallery. This is a consequence of the mass conservation law at the transient-free flow for the flow-tube. Therefore, the volume throughflow is the same in all zones, and at the reservoir's cross-section having constant area the filtration velocity is also the same in all zones.

So, the pressure distribution, filtration velocity and flow-rate equations for rectilinear-parallel flow in zonally-nonuniform reservoir have the following format for each zone of the reservoir ($1 \le i \le n$):

$$p_i(x) = p_i - \frac{p_i - p_{i+1}}{l_i} x, \quad x_i < x < x_{i+1}, \tag{21.15}$$

$$w = \frac{k_i}{\mu}\frac{p_i - p_{i+1}}{l_i}, \tag{21.16}$$

$$Q = \frac{k_i}{\mu}\frac{p_i - p_{i+1}}{l_i} hB. \tag{21.17}$$

From Eq. (21.15), we can obtain the pressure gradient value for each zone:

$$\frac{dp_i(x)}{dx} = -\frac{p_i - p_{i+1}}{l_i}, \quad x_i < x < x_{i+1}.$$

Thus, the pressure gradient is constant within each zone but different from one zone to the next. So the pressure distribution graph is a broken line with straight-line segments inclined at different angles (Fig. 21.2).

To set the problem, it is sufficient to assign pressures only at the charge source and at the gallery. That is why the only known values are $p_1 = p_k$ at $x_1 = 0$ and $p_{n+1} = p_{gal}$ at $x_{n+1} = L = \sum_{i=1}^{n} l_i$. Therefore, in order to use Eqs. (21.15)–(21.17) for the computations, pressures at the boundaries of all zones must be calculated. To determine these pressures, we will find a flow-rate equation expressed through the parameters given in the problem. Let's solve Eq. (21.17) for all zones relative to the pressure drawdown:

$$\begin{aligned} p_k - p_2 &= Q\mu l_1 / k_1 Bh, \\ p_2 - p_3 &= Q\mu l_2 / k_2 Bh, \\ &\cdots\cdots\cdots\cdots \\ p_n - p_{gal} &= Q\mu l_n / k_n Bh. \end{aligned} \tag{21.18}$$

After addition of Eqs. (21.18), the result is:

$$p_k - p_{gal} = \frac{Q\mu}{Bh} \sum_{i=1}^{n} l_i / k_i.$$

Solving this equation relative to Q, we will obtain equation for the flow-rate in zonally-nonuniform bed at rectilinear-parallel filtration of incompressible liquid:

$$Q = \frac{Bh}{\mu} \frac{p_k - p_{gal}}{\sum_{i=1}^{n} l_i / k_i}. \tag{21.19}$$

Using Eqs. (21.17) and (21.19), it is possible to determine pressures at the zone boundaries. To find p_2, Eq. (21.17) is used for the first zone as well as Eq. (21.19):

$$k_1 \frac{p_k - p_2}{l_1} = \frac{p_k - p_{gal}}{\sum_{i=1}^{n} l_i / k_i},$$

where the only unknown variable is pressure at the boundary between zones 1 and 2 (all other values are given at the problem setting). Solving it relative to p_2, results in:

$$p_2 = p_k - \frac{l_1}{k_1} = \frac{p_k - p_{gal}}{\sum_{i=1}^{n} l_i / k_i}.$$

In a case the reservoir includes two zones of nonuniformity, from the above expression, the equation for pressure at the zones' boundary is derived:

$$p_2 = \frac{p_k \frac{l_2}{k_2} - p_{gal} \frac{l_1}{k_1}}{\sum_{i=1}^{n} l_i / k_i}.$$

Pressures at the other nonuniformity zone boundaries are found similarly. Now, the nonuniform reservoir's average permeability will be determined using Eq. (21.19):

$$Q = \frac{Bh}{\mu} \frac{p_k - p_{\text{gal}}}{\sum_{i=1}^{n} l_i / k_i} = \frac{k_{\text{avg}}}{\mu} \frac{p_k - p_{\text{gal}}}{L} Bh,$$

and:

$$k_{\text{avg}} = L \Big/ \sum_{i=1}^{n} l_i / k_i . \tag{21.20}$$

Thus, average permeability in a zonally-nonuniform reservoir is determined differently from the Eq. (21.12) law for average permeability in a zonally-uniform reservoir.

Using the similarity in the filtration of incompressible liquid and gas, from Eqs. (21.15)–(21.17) and (21.19) (expressed through Leibensohn's function) the transient-free rectilinear-parallel gas filtration through a zonally-nonuniform reservoir is derived:

$$P_i(x) = P_i - \frac{P_i - P_{i+1}}{l_i} x, \; x_i < x < x_{i+1}, \tag{21.21}$$

$$\rho w = \frac{k_i}{\mu} \frac{P_i - P_{i+1}}{l_i}, \tag{21.22}$$

$$Q_m = \frac{k_i}{\mu} \frac{P_i - P_{i+1}}{l_i} hB, \tag{21.23}$$

$$Q_m = \frac{Bh}{\mu} \frac{P_k - P_{\text{gal}}}{\sum_{i=1}^{n} l_i / k_i}. \tag{21.24}$$

Let's now insert Leibensohn's function for ideal gas into these Eqs. (21.21)–(21.24). The result is equations for pressure distribution, mass velocity, mass throughflow and volume throughflow under atmospheric conditions at transient-free rectilinear-parallel filtration of ideal gas through the zonally-nonuniform reservoir:

$$p_i(x) = \sqrt{p_i^2 - \frac{p_i^2 - p_{i+1}^2}{l_i} x}, \; x_i < x < x_{i+1}, \tag{21.25}$$

$$\rho w = \frac{k_i \rho_{\text{atm}}}{2\mu p_{\text{atm}}} \frac{p_i^2 - p_{i+1}^2}{l_i}, \tag{21.26}$$

$$Q_m = \frac{k_i \rho_{\text{atm}}}{2\mu p_{\text{atm}}} \frac{p_i^2 - p_{i+1}^2}{l_i} hB, \tag{21.27}$$

$$Q_m = \frac{Bh}{\mu} \frac{p_k^2 - p_{gal}^2}{\sum_{i=1}^{n} l_i / k_i}. \tag{21.28}$$

Using Eq. (21.28), it is possible to determine average permeability value of a zonally nonuniform reservoir at gas filtration. It is easy to see that the result will be the same Eq. (21.20) as for incompressible liquid. The result is clear remembering the permeability is a parameter of the medium and does not depend on the fluid properties.

Using Eqs. (21.27) and (21.28) the pressures at the zonal boundaries for gas filtration can be found. To find p_2, we will equate the expressions from Eqs. (21.28) and (21.27) for the flow-rate in the zone 1 and will obtain the following equation:

$$k_1 \frac{p_k^2 - p_2^2}{l_i} = \frac{p_k^2 - p_{gal}^2}{\sum_{i=1}^{n} l_i / k_i},$$

where the only variable is pressure at the boundary of the zones 1 and 2 (all other values are given at the problem setting). Pressures at the other nonuniformity zone boundaries are found similarly.

The time of a fluid particle run in the zone i of an incompressible liquid model will be found from equations:

$$t_1 = \frac{\emptyset_i \mu}{k_i} \frac{x l_i}{p_i - p_{i+1}} \text{ and } T_i = \frac{\emptyset_i \mu}{k_i} \frac{l_i^2}{p_i - p_{i+1}}. \tag{21.29}$$

Similarly, for the gas model:

$$t_i = \frac{4\emptyset_i \mu l_i^2 (p_i^3 - p^3(x))}{3k_i (p_i^2 - p_{i+1}^2)^2} \text{ and } T_i = \frac{4\emptyset_i \mu l_i^2 (p_i^3 - p_{i+1}^3)}{3k_i (p_i^2 - p_{i+1}^2)^2}. \tag{21.30}$$

In all equations for t_i determination, the x value ranges as $x_i \le x \le x_{i+1}$. The total run-time of the particles within a zonally-nonuniform reservoir is clearly $T = \sum_{i=1}^{n} T_i$.

4. Calculation of continuously-nonuniform reservoirs

If non-transient rectilinear flow of incompressible fluid occurs in a reservoir with continuously changing permeability (i. e., $k = k(x)$), the liquid and gas flow-rates are calculated from the following equations:

$$Q_m = -\frac{k(x)}{\mu} \frac{dp}{dx} Bh \text{ and } Q_m = -\frac{k(x)}{\mu} \frac{dP}{dx} Bh;$$

Upon separating variables in these differential equations:

$$dp = -\frac{Q\mu}{Bh}\frac{dx}{k(x)} \quad \text{and} \quad dP = -\frac{Q_m\mu}{Bh}\frac{dx}{k(x)},$$

and integrating them:

$$\int_{p_k}^{p_{gal}} dp = -\frac{Q\mu}{Bh}\int_0^L \frac{dx}{k(x)} \quad \text{and} \quad \int_{P_k}^{P_{gal}} dP = -\frac{Q_m\mu}{Bh}\int_0^L \frac{dx}{k(x)},$$

gives the distribution in the reservoir of pressure and Leibensohn's function, respectively:

$$p_k - p_{gal} = \frac{Q\mu}{Bh}\int_0^L \frac{dx}{k(x)} \quad \text{and} \quad P_k - P_{gal} = -\frac{Q_m\mu}{Bh}\int_0^L \frac{dx}{k(x)}. \tag{21.31}$$

Therefore, in this case it is possible to determine all parameters of the fluid flow if the function $k(x)$ is given.

5. Radial-plane flow in a nonuniformly stratified reservoir

Suppose a round horizontal reservoir of thickness h comprises n interbeds of thickness h_i, permeability k_i, and porosity $\emptyset_i$ each, where $i = 1, 2, \ldots, n$ (Fig. 21.3). The reservoir is saturated by a liquid or gas, and there is a radial-plane flow to the central well. The charge source is removed from the well by the distance R_k, and constant pressure p_k is maintained there, and constant pressure p_c is maintained in well of radius r_c ($p_k > p_c$). In such a case (provided there are no cross-flows between the interbeds), there is a radial-plane flow in each of them, and the Eqs. (20.22)–(20.22) are applicable:

$$p(r) = p_k - \frac{p_k - p_c}{\log\frac{R_k}{r_c}}\log\frac{R_k}{r}$$

$$w_r = -\frac{k}{\mu}\frac{dp}{dr} = \frac{k(p_k - p_c)}{\mu \log\frac{R_k}{r_c}}\frac{1}{r}$$

$$w_r S = Q = \frac{2\pi kh(p_k - p_c)}{\mu \log\frac{R_k}{r_c}}.$$

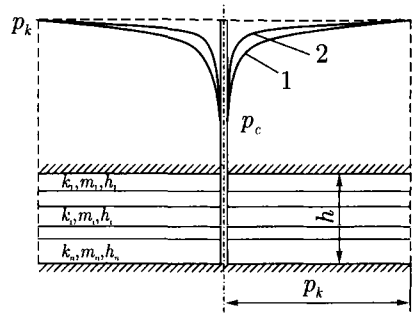

Fig. 21.3. Pressure distribution curves for a liquid (1) and gas (2) at radial-plane flow in a nonuniformly-laminated reservoir.

These are equations for pressure, filtration velocity and flow-rate for an incompressible liquid with the difference that the pressure distribution equation is the same for all interbeds, whereas the filtration velocity and flow-rate will be individual for each of them:

$$p(r) = p_k - \frac{p_k - p_c}{\log\frac{R_k}{r_c}} \log\frac{R_k}{r}$$

$$w_r^i = -\frac{k}{\mu}\frac{dp}{dr} = \frac{k(p_k - p_c)}{\mu \log\frac{R_k}{r_c}} \frac{1}{r} \tag{21.32}$$

$$w_r^i S_i = Q^i = \frac{2\pi k_i h_i (p_k - p_c)}{\mu \log\frac{R_k}{r_c}}.$$

The flow-rate for the entire reservoir is determined as the total of flow-rates from all interbeds:

$$Q = \sum_{i=1}^{n} w_r^i S_i = \sum_{i=1}^{n} Q^i = \frac{2\pi(p_k - p_c)}{\mu \log\frac{R_k}{r_c}} \sum_{i=1}^{n} k_i h_i . \tag{21.33}$$

Average reservoir permeability value k_{avg} is determined from the condition of the flow-rate equality in a nonunifomly-laminated and uniformly-laminated reservoirs:

$$\frac{2\pi k_{avg} h (p_k - p_c)}{\mu \log\frac{R_k}{r_c}} = \frac{2\pi(p_k - p_c)}{\mu \log\frac{R_k}{r_c}} \sum_{i=1}^{n} k_i h_i$$

and is given by equation $k_{avg} = \sum_{i=1}^{n} k_i h_i \Big/ h$, where $h = \sum_{i=1}^{n} h_i$ is total reservoir thickness. Equations for average reservoir permeability in a nonunifomly-laminated reservoir turn out to be the same for radial and rectilinear-parallel filtration.

Using similarity between the incompressible liquid and gas filtration, we derive from Eq. (21.32) equations for ideal gas filtration in a nonunifomly-laminated reservoir:

$$p(r) = \sqrt{p_k^2 - \frac{p_k^2 - p_c^2}{\log\frac{R_k}{r_c}} \log\frac{R_k}{r}},$$

$$w_r^i \rho = -\frac{k_i}{\mu}\frac{dP}{dr} = \frac{k_i \rho_{atm}(p_k^2 - p_c^2)}{2\mu p_{atm} \log\frac{R_k}{r_c}} \frac{1}{r} \qquad (21.34)$$

$$w_r^i \rho S_i = Q_m^i = \frac{2\pi k_i h_i (p_k^2 - p_c^2)}{\mu p_{atm} \log\frac{R_k}{r_c}}.$$

6. Rectilineal-parallel flow in a nonuniformly stratified reservoir

Suppose a round horizontal reservoir of thickness h comprises n ring-like zones with different permeabilities k_i, and porosity $\emptyset_i$ each, where $i = 1, 2, \ldots, n$. The boundary of each zone has the shape of the side surface of the cylinder coaxial with the well. At the external boundary on the zone n, which is the charge source $r = R_k$ ($r_{n+1} = R_k$), constant pressure p_k ($p_n = p_k$) is maintained, and constant pressure p_c ($p_c = p_1$) is maintained at the reservoir's internal boundary, i. e., at the bottomhole, $r = r_c$ ($r_1 = r_c$) (Fig.21.4).

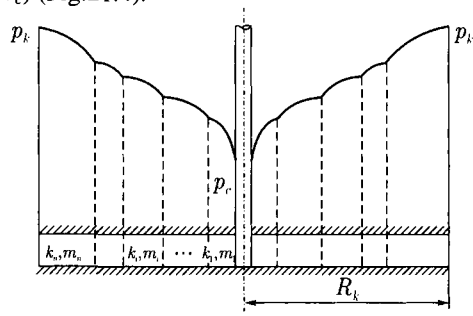

Fig. 21.4. Pressure distribution at radial-plane flow of incompressible liquid in a zonally-nonuniform reservoir.

The problem setting is such that there is the unidimensional transient-free flow of a uniform fluid. So, in each zone of this zonally-nonuniform reservoir there there is a radial-plane filtration with the same calculation equations as for the uniform reservoir:

$$p_i(r) = p_{i+1} - \frac{p_{i+1} - p_i}{\log\frac{R_{i+1}}{r_i}} \log\frac{r_{i+1}}{r},$$

$$w_r^i = -\frac{k_i}{\mu}\frac{dp}{dr} = \frac{k_i(p_{i+1}-p_i)}{\mu \log\frac{r_{i+1}}{r_i}}\frac{1}{r}, \qquad (21.35)$$

$$w_r^i S = Q = \frac{2\pi k_i h(p_{i+1}-p_i)}{\mu \log\frac{r_{i+1}}{r_i}}.$$

Here, pressures in the beginning and at the end of the zone, respectively, are taken for pressures at the charge contour and at the well, and the radii of the zone's beginning and end are taken for the charge contour and well radii.

Compared with the nonuniformly-laminated reservoir where the pressure distribution equation was the same for all interbeds, whereas the filtration velocity and flow-rate were individual for each of them, in this case the flow-rate equations for all zones will be the same, whereas the pressure and filtration velocity distribution equation will be individual for each zone. Indeed, the same fluid amount entering the reservoir at the charge contour is exiting it through the well. This conclusion is based on the mass conservation law at the transient-free flow. Therefore, the volume flow-rate is the same in each zone, but the reservoir cross-sections have different areas. Thus, the filtration velocity will be changing not only from one zone to the next but also within individual zones. And pressure, filtration velocity and flow-rate distribution equations at the zonally-nonuniform parallel-plane filtration within each zone of the reservoir nonuniformity ($0 \le i \le n$) have the format of Eq. (21.35).

As in the case of the rectilinear-parallel filtration, Eqs. (21.35) cannot be used for calculations as pressures in the problem setting are given only at the charge contour and in the well. So, with the first step is finding equation for the flow-rate expressed through pressures assigned in the problem setting. For this purpose the flow-rate equations are solved for each zone relative to the pressure difference:

$$p_k - p_n = \frac{Q\mu}{2\pi k_i h}\log\frac{R_k}{r_n},$$

$$p_n - p_{n-1} = \frac{Q\mu}{2\pi k_i h}\log\frac{r_n}{r_{n-1}},$$

$$\cdots\cdots\cdots\cdots\cdots\cdots\cdots\cdots$$

$$p_1 - p_c = \frac{Q\mu}{2\pi k_i h}\log\frac{r_1}{r_c}.$$

Adding these together gives:

$$p_k - p_c = \frac{Q\mu}{2\pi h}\sum_{i=1}^{n}\log\frac{r_{i+1}/r_i}{k_i}.$$

thus:

$$Q = \frac{2\pi h}{\mu}\frac{p_k - p_c}{\sum\limits_{i=1}^{n}\log\frac{r_{i+1}/r_i}{k_i}}. \qquad (21.36)$$

Using Eq. (21.36), one can derive the average permeability equation:

$$Q = \frac{2\pi h}{\mu} \frac{p_k - p_c}{\sum_{i=1}^{n} \log \frac{r_{i+1}/r_i}{k_i}} = \frac{2\pi k_{avg} h (p_k - p_c)}{\mu \log \frac{R_k}{r_c}},$$

and:

$$k_{avg} = \log \frac{R_k}{r_c} \Big/ \sum_{i=1}^{n} \log \frac{r_{i+1}/r_i}{k_i}. \tag{21.37}$$

Using Eqs. (21.35) and (21.36), it is possible to determine pressures at the zonal boundaries. To find $p_{(2)}$ equating Eq. (21.35) (written for the flow-rate in zone 1) to Eq. (21.36):

$$k_2 \frac{p_2 - p_c}{\log r_2 / r_c} = \frac{p_k - p_c}{\sum_{i=1}^{n} \log \frac{r_{i+1}/r_i}{k_i}}, \tag{21.38}$$

where the only unknown variable is pressure at the boundary between zones 1 and 2 (all other values are given at the problem setting). The other pressure values at the zone nonuniformity boundaries may be determined similarly.

Using analogy between filtration of the incompressible liquid and gas, Eq. (21.35) is used to obtain equations for ideal gas filtration in a zonally-nonuniform reservoir:

$$p_i(r) = \sqrt{p_{i+1}^2 - \frac{p_{i+1}^2 - p_{i+1}^2}{\log \frac{r_{i+1}}{r_i}} \log \frac{r_{i+1}}{r_i}},$$

$$w_r^i \rho = -\frac{k_i}{\mu} \frac{dP}{dr} = \frac{k_i \rho_{atm} (p_{i+1}^2 - p_i^2)}{2\mu p_{atm} \log \frac{r_{r+1}}{r_i}} \frac{1}{r} \tag{21.39}$$

$$w_r^i \rho S_i = Q_m = \frac{\pi k_i h \rho_{atm} (p_{i+1}^2 - p_i^2)}{\mu p_{atm} \log \frac{r_{i+1}}{r_i}}.$$

To find pressures at the zone boundaries, as we did for incompressible liquid: first, derive the flow-rate equation expressed through pressures p_k and p_c, and and after that derive equation similar to Eq. (21.38).

The particle movement-time in each zone may be found from Eqs. (20.23) and (20.24) for incompressible liquid and Eq. (20.49) for the gas with the only difference that the nonuniformity zone boundaries will play the role of the charge contour and the well.

CHAPTER XXII

FLAT TRANSIENT-FREE FILTRATION

1. Major definitions and concepts

Previously, the flow models to a gallery or to a single central well in a round reservoir have been studied. Real-life oil and gas fields are developed by numerous wells. Hydrodynamic problems arising in field development include bottomhole pressure determination at given flow-rates or, conversely, flow-rate determination at given pressures.

In solving these problems, one has to remember the existence of several operating wells interfering with one another. The result is that when new wells are started-up in the field, the total production increases slower than the increase in the number of wells (Fig. 22.1).

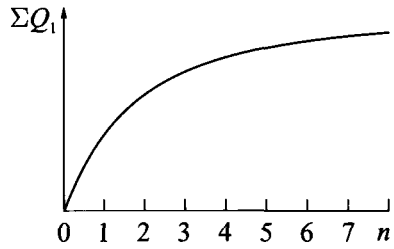

Fig. 22.1. Production vs. number of wells

Therefore, making the problems more complex in order to provide more adequate description of the processes occurring in a hydrocarbon field, it is necessary to review the setting and solution of the problems involving the simultaneous operation of several wells. The simplest problems occur when the reservoir is assumed to be flat, and the wells are assumed to be point sources or sinks. The solution of such problems acquires a supposition of the potential nature of flow and the potential.

The flow is called potential if there is a scalar function Φ such that its gradient is equal to velocity v, i. e., the following equality is valid:

$$\bar{v} = -\text{grad}\,\Phi,$$

where the scalar function Φ is called the potential. This equation is similar to the Darcy's law:

$$\bar{w} = -(k/\mu)\text{grad}\, p.$$

If k and μ are constants, then:

$$\bar{w} = -\text{grad}(kp/\mu) \tag{22.1}$$

and:

$$\Phi = kp/\mu\,. \tag{22.2}$$

Thus, filtration of a liquid with a constant viscosity in an undeformable reservoir (k = const) is a potential flow.

2. Potential of a point source and sink on an isotropic plane. Superposition method

Let's call a point sink the point on a plane which takes in the liquid. A production well may be considered as a sink on an assumption that its diameter is infinitely small. The flowlines on a plane around the point sink are straight lines directed towards the well, and the equal potential lines are circles (Fig. 22*a*). An injection well from which the fluid enters the reservoir is a source (Fig. 22.2*b*).

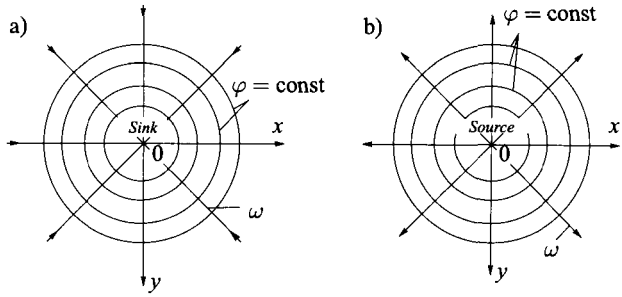

Fig. 22.2. Source and sink on the plane

Let's determine the potential of a production well (sink). For this purpose, Eq. (22.1) is projected onto a cylindrical coordinate system. The result is:

$$w = \frac{d\Phi}{dr}\,. \tag{22.3}$$

Because the well is a producer, velocity directed toward the pole of a polar coordinate system is projected onto the 0r-axis with the minus sign, and as a result Eq. (22.3) does not include the minus sign. Now, let's introduce the specific flow-rate q per unit of the reservoir thickness, $q = Q/h$, and express it through filtration velocity:

$$q = \frac{Q}{h} = \frac{2\pi rhw}{h} = 2\pi rw\,.$$

Therefore, Eq. (22.3) may be rewritten as:

$$\frac{q}{2\pi r} = \frac{d\Phi}{dr}\,.$$

Let's separate the variables in this equation:

$$\frac{qdr}{2\pi r} = d\Phi$$

and integrate it:

$$\Phi = (q/2\pi)\log r + C, \tag{22.4}$$

where C is the integration constant. Obviously, the same calculations are valid for a case of the source on the plane:

$$\Phi = -(q/2\pi)\log r + C. \tag{22.5}$$

Not only the pressure, but also the potentials introduced by Eqs. (22.4) and (22.5) satisfy Laplace's equation:

$$\frac{\partial^2\Phi}{\partial x^2} + \frac{\partial^2\Phi}{\partial y^2} = 0. \tag{22.6}$$

Laplace's equation is linear and uniform, and for this reason its solutions have a very important property: the sum of equation's particular solutions and the product of a partial solution and of the constant is also a solution. This property allows for the application in problem solving of a technique called superposition. The mathematical definition of this technique is as follows. If there are N flows with potentials:

$$\Phi_i = (q_i/2\pi)\log r + C_i, \text{ where } i = 1, 2, \ldots, N,$$

each of which satisfies Laplace's equation, then the linear combination of these potentials $\Phi = \sum_{i=1}^{N} c_i\Phi_i$ where c_i are arbitrary constants, also satisfies Laplace's Eq. (22.6).

Hydrodynamically, this means that if the potential of i^{th} well is found for a case when the only operating well in the reservoir is this i^{th} well, then in a joint operation of all N wells the solution is found by algebraic addition. Therefore, velocity in the reservoir is determined as total summation of the filtration velocity vectors produced by the operation of each well. Thus, when N wells jointly operate in the reservoir, the resulting potential in an arbitrary point M is the sum of potentials of all wells (Fig. 22.2*a*):

$$\Phi_M = \sum_{i=1}^{N}(q_i/2\pi)\log r_i + C \text{ at } C = \sum_{i=1}^{N} C_i, \tag{22.7}$$

where r_i is the distance between the point M and the i^{th} well ($i = 1, 2, \ldots, N$), and C_i are constants.

The filtration velocity vector $\bar{w}$ at the point M is equal to the sum of the filtration velocities in each well (Fig. 22.2*b*):

$$\bar{w} = \bar{w}_1 + \bar{w}_2 + \ldots + \bar{w}_N, \tag{22.8}$$

where the velocity vector modulus $|w_i|$ is equal to:

$$|w_i| = q_i/2\pi r_i.$$

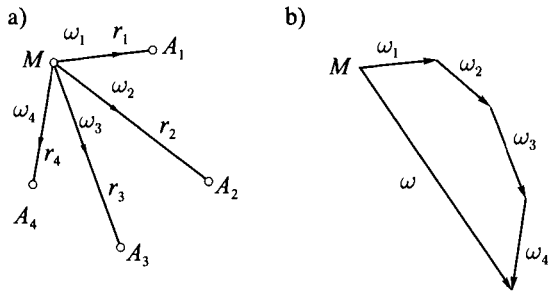

Fig. 22.3. Schematics of the filtration velocities at point M when four sinks (wells) are operating (a) and the calculation of a resulting velocity at point M (b)

The superposition method can be used both in the case of an infinite reservoir and in the cases when there is a charge contour of an impermeable boundary. In the latter cases, imaginary wells are introduced for the problem solving. They help satisfying the necessary boundary conditions. Then, the performance of the aggregation of real and imaginary wells in an infinite reservoir is reviewed. This method is called the reflection of sources and sinks technique.

3. Liquid flow to a group of wells with the remote charge contour

Using the superposition technique, it is possible to calculate the flow-rates, bottomhole potentials (pressures), filtration velocities, etc., for a group of wells operating in the reservoir with the remote charge contour.

Suppose there are n wells (Fig. 22.4) of radiuses r_i, at which the potentials Φ_i are given; also, the charge contour radius R_k and the potential Φ_k (contour pressure p_k) are given, as well as the distances between wells r_{ij} (the distance between i^{th} and j^{th} wells; obviously, $r_{ij} = r_{ji}$). It is required to determine the well (sink) flow-rates q_i.

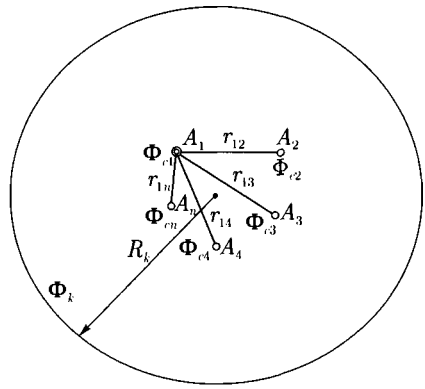

Fig. 22.4. Schematics of a group of wells with the remote charge contour.

The potential at an arbitrary point M is given by Eq. (22.7). First, the point M is placed at the bottomhole of each well to obtain n equations:

$$\begin{aligned}
\Phi_{c1} &= \frac{1}{2\pi}(q_1 \log r_{c1} + q_2 \log r_{12} + ... + q_n \log r_{1n}) + C, \\
\Phi_{c2} &= \frac{1}{2\pi}(q_1 \log r_{12} + q_2 \log r_{c2} + ... + q_n \log r_{2n}) + C, \\
&\cdots\cdots\cdots\cdots\cdots\cdots\cdots\cdots\cdots\cdots\cdots\cdots\cdots\cdots\cdots\cdots\cdots\cdots \\
\Phi_{cn} &= \frac{1}{2\pi}(q_1 \log r_{1n} + q_2 \log r_{2n} + ... + q_n \log r_{cn}) + C,
\end{aligned} \tag{22.9}$$

which contain $n + 1$ of variables q_i (i = 1, 2, ..., n) and C. To be able to solve this system of equations, one more equation is added which occurs when the point M is placed at the charge contour:

$$\Phi_k = \frac{1}{2\pi}(q_1 \log R_k + q_2 \log R_k + ... + q_N \log R_k) + C\,. \tag{22.10}$$

It is clear that Eq. (22.10) assumes the distance between all wells and the charge contour equal to R_k.

The obtain system of equations [Eqs. (22.9) and (22.10)] include $n + 1$ variables and can be solved appropriately. To find q_i, parameter C is excluded from the system. For this purpose each equation of the Eq. (22.9) is subtracted sequentially from Eq. (22.10). The result is n equations:

$$\begin{aligned}
\Phi_k - \Phi_{c1} &= \frac{1}{2\pi}\left(q_1 \log\frac{R_k}{r_{c1}} + ... + q_i \log\frac{R_k}{r_{1i}} + ... + q_N \log\frac{R_k}{r_{1n}}\right), \\
&\cdots\cdots\cdots\cdots\cdots\cdots\cdots\cdots\cdots\cdots\cdots\cdots\cdots\cdots\cdots\cdots\cdots\cdots \\
\Phi_k - \Phi_{cn} &= \frac{1}{2\pi}\left(q_1 \log\frac{R_k}{r_{1n}} + ... + q_i \log\frac{R_k}{r_{in}} + ... + q_N \log\frac{R_k}{r_{cn}}\right).
\end{aligned} \tag{22.11}$$

After the numerical values are substituted, the system Eq. (22.11) is a linear system of equations with respect to q_i. It can be solved using any technique for solving systems of linear equations (Kramer, Gauss, etc.).

Let's now review some application examples of reflection of sources and sinks technique.

4. Liquid inflow to a well in the reservoir with a rectilinear charge contour

Suppose the production well is in the reservoir with a rectilinear charge contour, i. e., the reservoir is a semiplane through whose boundary the flow to the well occurs. The distance between the well and the charge contour is equal to a, the potentials at the charge contour (Φ_k) and in the well (Φ_c) are given (Fig. 22.5). It is required to determine the well flow-rate and the potential at any point in the reser-

voir. In this case, the actual well is mirrored relatively to the rectilinear charge contour. But the flow-rate of the reflected well is given the sign opposite to that of the actual well's flow-rate.

Let's write down the potential for an arbitrary point M:

$$\Phi_M = \frac{1}{2\pi}(q\log r_1 - q\log r_2) + C,$$

and then place the point M first at the well's wall, and then, on the charge contour. The result is the system of equations:

$$\Phi_c = \frac{1}{2\pi}(q\log r_c - q\log 2a) + C,$$

$$\Phi_k = \frac{1}{2\pi}(q\log r_k - q\log r_k) + C.$$

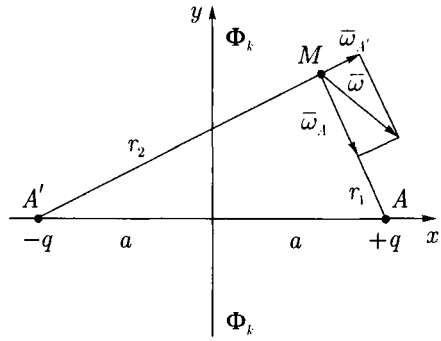

Fig. 22.5. Schematics of liquid inflow to a well operating next to the rectilinear charge contour.

Let's solve this system relative to q:

$$q = \frac{2\pi(\Phi_k - \Phi_c)}{\log 2a/r_c}. \tag{22.12}$$

Using the potential expression Eq. (22.4), it is possible to rewrite Eq. (22.12) as follows:

$$Q = \frac{2\pi kh(p_k - p_c)}{\mu\log 2a/r_c}. \tag{22.13}$$

After the flow-rate is found, we will determine the potential at any point in the reservoir:

$$\Phi_M = \frac{1}{2\pi}q\log r_1/r_2 + \Phi_k, \tag{22.14}$$

where q is determined from Eq. (22.12).

If the charge contour were a circle of radius a, the flow-rate would have been determined from Dupois' equation:

$$Q = \frac{2\pi kh(p_k - p_c)}{\mu \log a / r_c}.$$

In real life, the charge contour form is often unknown. It is evident, however, that the charge contour MN (Fig. 22.6) is somewhere between a circle and a straight line. Therefore, the well flow-rate under these conditions will be:

$$\frac{2\pi kh(p_k - p_c)}{\mu \log a / r_c} \geq Q \geq \frac{2\pi kh(p_k - p_c)}{\mu \log 2a / r_c}.$$

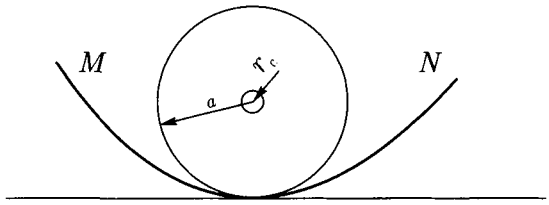

Fig. 22.6. Schematics of a reservoir with different charge contours

Filtration velocity at the point M is determined as a geometrical sum of filtration velocities caused by the performance of the actual and imaginary source wells (Fig. 22.5), i. e.:

$$\bar{w} = \bar{w}_A + \bar{w}_{A'},$$

where $|\bar{w}_A| = q/2\pi r_1$ and is directed to well A; $|\bar{w}_{A'}| = q/2\pi r_2$ and is directed away from well A. At the charge contour where $r_1 = r_2$, the filtration velocity vector is clearly perpendicular to the charge contour line.

Following Eq. (22.14), the equation of the equipotential lines has the following format:

$$r_1/r_2 = \text{const or } r_1^2 + r_2^2 = c$$

Expressing r_1^2 and r_2^2 through the coordinates of the point $M(x,y)$ and coordinates of the well centers A(0,a) and A'(0,–a), gives $r_1^2 = (x-a)^2 + y^2$ and $r_1^2 = (x+a)^2 + y^2$. After substituting these expressions into the equation for the equipotentials and performing the necessary transformations:

$$\left(x - a\frac{1+c}{1-c}\right)^2 + y^2 = \frac{4a^2c}{(1-c)^2},$$

which is the equation of a circle with the center at the point $x_0 = a\frac{1+c}{1-c}$, $y = 0$ and the radius $R = 2a\sqrt{c}/(1-c)$.

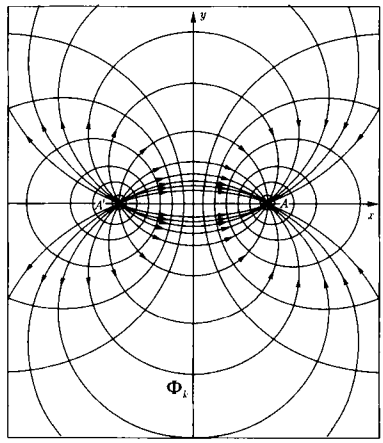

Fig. 22.7. Flow-line and equipotential line families at the liquid flow to a well sink in a reservoir with the straight-line charge contour (or in an indefinite reservoir to the source and to the sink).

Changing the value of the constant c, results in generating a family of the equipotential curves. They represent circles of different radius and the centers located at different points of the x axis. The flow-line family is circles running through the centers of both wells, and whose centers are located on the rectilinear segment of the charge contour. And the equipotentials (isobars) are always orthogonal to the flow-lines (Fig. 22.7).

5. Liquid inflow to a well in the reservoir near the impermeable boundary

Suppose the production well is in the reservoir with the impenetrable boundary, i. e., the reservoir is a semiplane. The distance between the well and impenetrable boundary is a, the potentials at the charge contour Φ_k and in the well Φ_c are given; the charge contour radius is R_k (Fig. 22.8). It is required to determine well's flow-rate. In real life, such a problem may occur when a production well is located near a fault on reservoir pinch-out line. In such a case, the actual well is mirrored relative to the impermeable boundary, and the same sign is assigned to the flow-rate of the reflected well as of the actual well.

Then the potential at an arbitrary point M is:

$$\Phi_M = \frac{1}{2\pi}(q\log r_1 + q\log r_2) + C\,.$$

Let's place the point M first on the well's wall, and then on the charge contour. The result is:

$$\Phi_c = \frac{1}{2\pi}(q\log r_c + q\log 2a) + C \text{ and } \Phi_k = \frac{1}{2\pi}(q\log R_k + q\log R_k) + C.$$

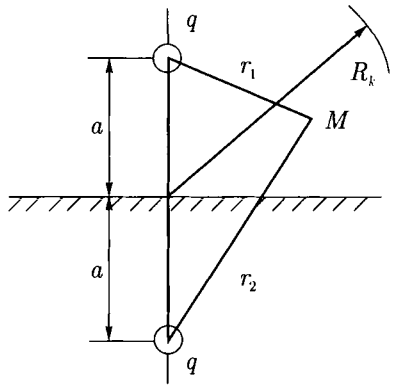

Fig. 22.8. Liquid inflow to a well operating close to a straight-line boundary.

Solving this system relative to q, results in:

$$q = \frac{2\pi(\Phi_k - \Phi_c)}{\log R_k^2 / 2ar_c}. \tag{22.15}$$

Using the potential expression Eq. (22.4), it is appropriate to rewrite Eq. (22.15) as follows:

$$Q = \frac{2\pi kh(p_k - p_c)}{\mu \log R_k^2 / 2ar_c}. \tag{22.16}$$

6. Liquid inflow to a well positioned eccentrically in a round reservoir

Suppose the well is in a reservoir with the circular charge contour but it is located at a distance δ from the center of the circle (Fig. 22.9). The distance between the reservoir center and the charge contour is R_k; the potentials at the charge contour Φ_k and in the well Φ_c are given. It is required to determine the well flow-rate and the potential at any point in the reservoir. In this case, as previously, the actual well – sink A is mirrored into the imaginary well – source A' located at a distance a from the well A on the extension of the line OA. The distance a is determined from a condition of a constant potential at the contour; therefore, at points M_1 and M_2 located at the charge contour.

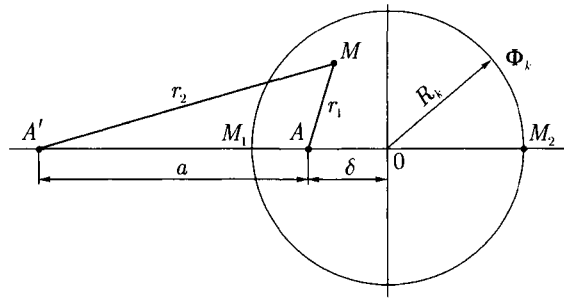

Fig.22.9. Liquid flow to a well eccentrically positioned in a circular reservoir.

Under the superposition technique, the potential at the points M_1 and M_2 are:

$$\Phi_k = \Phi_{M_1} = \frac{q}{2\pi}\log\frac{R_k - \delta}{a-(R_k-\delta)} + C, \tag{22.17}$$

$$\Phi_k = \Phi_{M_2} = \frac{q}{2\pi}\log\frac{R_k + \delta}{a+(R_k+\delta)} + C. \tag{22.18}$$

From the condition of the potential equality at the points M_1 and M_2, equation for a is:

$$\frac{R_k - \delta}{a-(R_k-\delta)} = \frac{R_k+\delta}{a+(R_k+\delta)},$$

wherefrom:

$$a = (R_k^2 - \delta^2)/\delta. \tag{22.19}$$

In order to determine the flow-rate of well A, it is necessary to determine its its bottomhole potential:

$$\Phi_c = \Phi_A = \frac{q}{2\pi}(\log r_c - \log r_c) + C. \tag{22.20}$$

Subtracting Eq. (22.20) from Eq. (22.17):

$$\Phi_k - \Phi_c = \frac{q}{2\pi}\log\frac{a(R_k-\delta)}{r_c[a-(R_k-\delta)]}$$

or, substituting the a expression [Eq. (22.19)] instead of a:

$$\Phi_k - \Phi_c = \frac{q}{2\pi}\log\frac{(R_k^2-\delta^2)/\delta(R_k-\delta)}{r_c\delta[(R_k^2-\delta^2)/\delta-(R_k-\delta)]}.$$

Transforming in this equation the expression under the logarithm sign and solving it relative to q gives the flow rate of a well eccentrically positioned in a round reservoir:

$$q = \frac{2\pi(\Phi_k - \Phi_c)}{\log \frac{R_k}{r_c}\left(1 - \frac{\delta^2}{R_k^2}\right)}. \tag{22.21}$$

When the eccentricity is equal to 0, this equation converts to Dupois equation.

To find potential at all points of the reservoir, the superposition technique is used by writing the potential at an arbitrary point M:

$$\Phi_M = \frac{q}{2\pi}(\log r_1 - \log r_2) + C = \frac{q}{2\pi}\log\frac{r_1}{r_2} + C. \tag{22.22}$$

Subtracting Eq. (22.22) from Eq. (22.20) and using Eq. (22.19), results in:

$$\Phi_M = \Phi_c + \frac{q}{2\pi}\left(\log\frac{r_1}{r_2}\frac{R_k^2 - \delta^2}{r_c\delta}\right). \tag{22.23}$$

Potential at an arbitrary point in the reservoir may also be derived by subtracting Eq. (22.22) from Eq. (22.17). In this case:

$$\Phi_M = \Phi_k - \frac{q}{2\pi}\left(\log\frac{r_1}{r_2}\frac{\delta}{R_k}\right). \tag{22.24}$$

Clearly, Eqs. (22.23) and (22.24) are equivalent.

7. On the use of the superposition technique at the gas filtration

The problems solved earlier dealt with transient-free filtration of incompressible liquids. Now, in this section these solutions will be expanded for transient-free filtration of the gas.

As the reader may recall, the superposition technique is based on Laplace's equation linearity and uniformity. As it was shown in the previous Chapter, at transient-free filtration Laplace equation in the case of incompressible liquid is satisfied by the pressure distribution, and in the case of compressible liquid and gas, Leibensohn's function. Therefore, the superposition technique may be used also at gas filtration, but only for the potentials defined through Leibensohn's function.

As the reader may recall, the system of equations for the incompressible fluid and compressible fluid have, respectively, the following format:

$$\Delta p = 0, \qquad \Delta P = 0,$$

$$\bar{w} = -\frac{k}{\mu}\operatorname{grad} p, \qquad \rho\bar{w} = -\frac{k}{\mu}\operatorname{grad} P,$$

$$\rho = \text{const}, \qquad \rho = \rho(p).$$

Thus, it is necessary to introduce the potential not for the filtration velocity vector **w** but for the filtration mass velocity vector $\rho\mathbf{w}$, i. e., the following equation must be realized:

$$\rho\bar{w} = -\text{grad}\,\Phi^*. \tag{22.25}$$

Because of gas filtration:

$$\rho\bar{w} = -\text{grad}\,\Phi^* = -\frac{k}{\mu}\text{grad}\,P,$$

and from there:

$$\Phi^* = \frac{k}{\mu}P. \tag{22.26}$$

Therefore, under transient-free gas filtration the potential linearly correlates with Leibensohn's function.

To determine the potential of a producing gas well (sink), Eq. (22.25) is projected onto a cylindrical coordinate system:

$$\rho w = \frac{d\Phi^*}{dr}. \tag{22.27}$$

Let's introduce the mass flow-rate q_m per-unit thickness of the reservoir ($q_m = Q_m/h$) and express it through mass filtration velocity:

$$q_m = \frac{Q_m}{h} = \frac{2\pi r h \rho w}{h} = 2\pi r \rho w.$$

Then Eq. (22.27) can be rewritten as:

$$\frac{q_m}{2\pi r} = \frac{d\Phi^*}{dr}.$$

After separating the variables:

$$\frac{q_m dr}{2\pi r} = d\Phi^*$$

and integrating this equation:

$$\Phi^* = \frac{q_m}{2\pi}\log r + C \tag{22.28}$$

where C is the integration constant.

The same train of thought is applicable for a case when there is a source on the plane. Then:

$$\Phi^* = -\frac{q_m}{2\pi}\log r + C.$$

The potential thus introduced, just as the potential introduced through Eq. (22.20), satisfies Laplace equation:

$$\frac{\partial^2\Phi^*}{\partial x^2} + \frac{\partial^2\Phi^*}{\partial y^2} = 0. \tag{22.29}$$

So, to find solutions through the superposition technique at the transient-free gas filtration, it is possible to use the earlier solutions for transient-free filtration of incompressible liquids. The analogy between filtration of an incompressible liquid and gas is established through the following substitution of variables:

For the incompressible liquid	*For the gas*
$p(x)$	$P(x)$
w	ρw
q	q_m
$\Phi = \frac{k}{\mu} p,$	$\Phi^* = \frac{k}{\mu} P$

(22.30)

Therefore, substituting the variables in the solutions for the transient-free filtration of incompressible liquid gives equations for the transient-free gas filtration.

The system of equations Eq. (22.11) for the flow-rate of a group of wells producing from the reservoir with a remote charge contour (gas wells), under the analogy defined by Eq. (22.30), will transform as follows:

$$\Phi^*_k - \Phi^*_{c1} = \frac{1}{2\pi}\left(q_{m1} \log\frac{R_k}{r_{c1}} + ... + q_{mi} \log\frac{R_k}{r_{1i}} + ... + q_{mN} \log\frac{R_k}{r_{1n}} \right),$$

$$\text{.....} \qquad (22.31)$$

$$\Phi^*_k - \Phi^*_{cn} = \frac{1}{2\pi}\left(q_{m1} \log\frac{R_k}{r_{1n}} + ... + q_{mi} \log\frac{R_k}{r_{in}} + ... + q_{mN} \log\frac{R_k}{r_{cn}} \right).$$

For a gas well case, the equation for the per-unit thickness of a well operating in the reservoir with impermeable boundary Eq. (22.12) transforms to the following format:

$$q_m = \frac{2\pi\left(\Phi^*_k - \Phi^*_c\right)}{\ln R_k^2 / 2ar_c}. \qquad (22.32)$$

Eqs. (22.15) and (22.16) for the unit thickness flow-rate and the flow-rate of an oil well from a reservoir with the rectilinear charge contour will transform for a gas well as follows:

$$q_m = \frac{2\pi(\Phi^*_k - \Phi^*_c)}{\log 2a / r_c} \qquad (22.33)$$

$$Q_m = \frac{2\pi kh(P_k - P_c)}{\mu \log 2a / r_c}. \qquad (22.34)$$

Equation for the potential at any point in the gas reservoir with a rectilinear charge contour is:

$$\Phi^*_{\text{M}} = \frac{1}{2\pi} q_m \log r_1 / r_2 + \Phi^*_k,$$

where q is determined from Eq. (22.33).

Similar changes will occur in equations for the flow-rate of a well eccentrically positioned in a round reservoir [Eq. (22.21)]. and for the potential at any point in the reservoir [Eqs. (22.23) and (22.24)]. The result is:

$$q_m = \frac{2\pi(\Phi^*_k - \Phi^*_c)}{\log \frac{R_k}{r_c}\left(1 - \frac{\delta^2}{R_k^2}\right)}, \tag{22.35}$$

$$\Phi^*_{\text{M}} = \Phi^*_c + \frac{q_m}{2\pi}\left(\log \frac{r_1}{r_2}\frac{R_k^2 - \delta^2}{r_c \delta}\right),$$

$$\Phi^*_{\text{M}} = \Phi^*_k - \frac{q_m}{2\pi}\left(\log \frac{r_1}{r_2}\frac{\delta}{R_k}\right). \tag{22.36}$$

Eqs. (22.35) and (22.36), and Eqs. (22.21)–(22.24), at $\delta \to 0$, have the passage to the limit and become the equations for the potential of an arbitrary point under the central well case. Indeed:

$$a = \frac{R_k^2}{\delta} - \delta,$$

therefore, at $\delta \to 0$:

$$r_2 \approx a \to \frac{R_k^2}{\delta} \text{ and } r_1 \to r$$

where r is the distance between the central well and an arbitrary point M. Therefore:

$$\Phi_{\text{M}} \to \Phi_c + \frac{q}{2\pi}\left(\log \frac{r}{r_2}\left(\frac{r_2}{r_c}\right)\right) = \Phi_c + \frac{q}{2\pi}\log \frac{r}{r_c} = \Phi_k - \frac{q}{2\pi}\log \frac{R_k}{r}.$$

8. Fluids inflow to infinite well lines and ring well rows

Let's now review the equivalent filtration resistance technique commonly used in the oil field development designing (Borisov). The technique uses the analogy between the fluid flow in a porous medium and the electric current in wires.

Let's go, without a derivation, over a solution of the problem of a fluid flow to a single infinite well line. The well spacing is 2σ, and they are located at a distance L from a rectilinear charge contour. Let's assume that the potential at the

charge contour is $\Phi_к$, and on the well walls, Φ_c (Fig. 22.10). It is required to determine the flow-rate of each well and the total rate N of the well in the line.

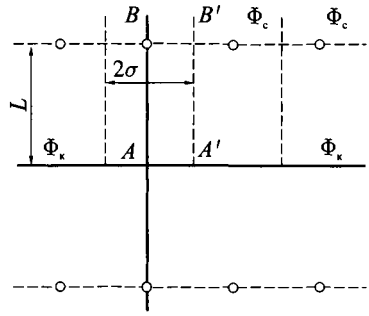

Fig. 22.10. A rectilinear well line

The problem is solved using the superposition technique. The line of the sink wells is mirrored relative to the charge contour into the source wells. Then, the interference of both well lines in an infinite reservoir is analyzed. The particles will move at the highest velocity along the line AB running through the sink well and the source well. The particles will move at the slowest velocity along the line $A'B'$ dividing in-half the distance between the wells, as due to the flow symmetry the lines are impermeable boundaries.

The flow-rate of each well is determined from the following equation:

$$q = \frac{2\pi(\Phi_к - \Phi_c)}{\ln 2sh\dfrac{\pi L}{\sigma} + \ln\dfrac{\sigma}{\pi r_c}}$$

where $sh\dfrac{\pi L}{\sigma} = \dfrac{1}{2}\left(e^{\pi L/\sigma} - e^{-\pi L/\sigma}\right)$ is hyperbolic sine. In a case $L > \sigma$, the value $e^{-\pi L/\sigma}$ is small, and $\ln 2sh(\pi L/\sigma) \approx \ln e^{\pi L/\sigma} = \pi L/\sigma$.

Thus, when $L > \sigma$, the well flow-rate may be found as:

$$q = \frac{2\pi(\Phi_к - \Phi_c)}{\dfrac{\pi L}{\sigma} + \ln\dfrac{\sigma}{\pi r_c}} = \frac{\Phi_к - \Phi_c}{\dfrac{L}{2\sigma} + \dfrac{1}{2\pi}\ln\dfrac{\sigma}{\pi r_c}}, \qquad (22.37)$$

or, designating:

$$\frac{L}{2\sigma} = \rho, \quad \frac{1}{2\pi}\ln\frac{\sigma}{\pi r_c} = \rho',$$

Eq. (22.37) may be formatted as follows:

$$q = \frac{(\Phi_к - \Phi_c)}{\rho + \rho'} \qquad (22.38)$$

Eq. (22.38) is analogous to the Ohm's law. For this reason, Borisov called the ρ value the ring well row external filtration resistance, and the ρ value, the internal resistance.

Thus, the fluids flow to the well line may be represented by the wiring of equivalent filtration resistances as shown in Fig. 22.11.

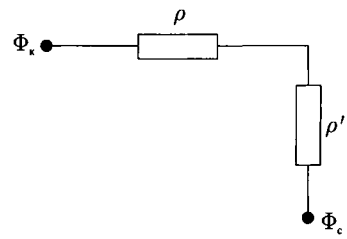

Fig. 22.11. Wiring of filtration resistances at the flow to an infinite well line.

The amperage here is an analog of the flow-rate q, and the electric potential difference is an analog of the filtration potential difference. The composite rate N of the well in the rectilinear line is:

$$Q_N = QN = qhN = \frac{(\Phi_к - \Phi_c)}{\frac{\pi L}{2\sigma Nh} + \frac{1}{2\pi Nh}\ln\frac{\sigma}{\pi r_c}} = \frac{p_к - p_c}{\frac{\mu L}{kh2\sigma N} + \frac{\mu}{2\pi khN}\ln\frac{\sigma}{\pi r_c}} \qquad (22.39)$$

Comparing Eqs. (22.38) and (22.39) gives the external filtration resistance of $\rho = L/2\sigma hN$, and the internal resistance, $\rho' = \ln(\sigma/\pi r_c)/2\pi hN$.

Suppose a semi-infinite reservoir with the rectilinear charge contour is developed by three parallel well lines of m_1, m_2 and m_3 wells. Suppose all wells have equal radiuses r_{c1}, r_{c2}, r_{c3} and bottomhole pressures p_{c1}, p_{c2}, p_{c3}. The composite rates of the lines are Q_1', Q_2', Q_3'.

Te wiring of the corresponding filtration resistances is shown in Fig. 22.12.

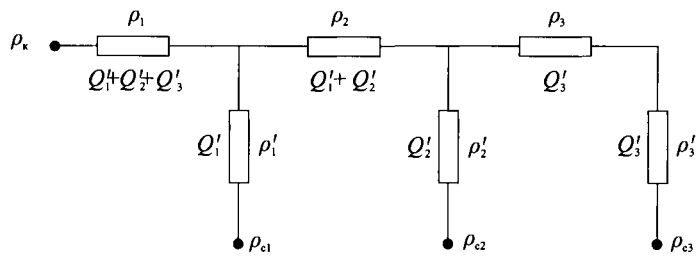

Fig. 22.12. Wiring of filtration resistances at the flow to three well lines.

The wiring is designed similar to the electric wiring using the Ohm's and Kirchhoff's laws. Depending on what is given and what is required, linear algebraic equations are written either for the rates Q_1', Q_2', Q_3' or for the bottomhole pressures p_{c1}, p_{c2}, p_{c3}. The external resistances are determined as:

$$\rho_1 = L_1/2\sigma_1 hm_1\,,\ \rho_2 = L_2/2\sigma_2 hm_2\,,\ \rho_3 = L_3/2\sigma_3 hm_3\,, \qquad (22.40)$$

where L_1, L_2, L_3 are distances, correspondingly, between the charge contour and the first line, between the first and second lines, and between the second and third lines (if the problem is being solved using potentials in Eqs. (22.39)), and:

$$\rho_1 = \mu L_1/khB_1\,,\ \rho_2 = \mu L_2/khB_2\,,\ \rho_3 = \mu L_3/khB_3\,, \qquad (22.41)$$

where $B_i = 2\sigma_i m_i$ (do not sum over i !), problem is being solved using pressures in Eqs. (22.39).

Internal resistances are determined from the following equations:

$$\rho_1' = \frac{\mu}{2\pi khm_1}\ln\frac{\sigma_1}{\pi r_{c1}},\ \rho_2' = \frac{\mu}{2\pi khm_2}\ln\frac{\sigma_2}{\pi r_{c2}},\ \rho_3' = \frac{\mu}{2\pi khm_3}\ln\frac{\sigma_3}{\pi r_{c3}} \qquad (22.42)$$

The rate of a single well in a ring well row which is composed of m wells (Fig. 22.13)

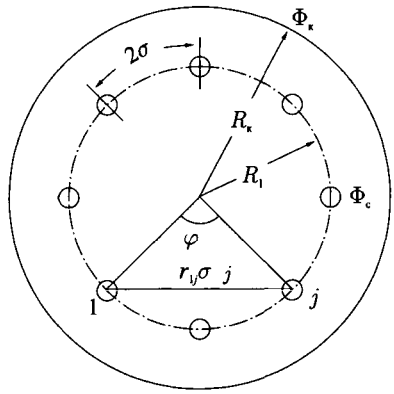

Fig. 22.13. Design of a ring well row

In a circular reservoir of the radius R_k:

$$Q' = \frac{2\pi h(\Phi_к - \Phi_c)}{\ln\left[\dfrac{R_k^m}{mr_c R_1^{m-1}}\left(1-\dfrac{R_1^{2m}}{R_k^{2m}}\right)\right]} = \frac{2\pi kh(p_к - p_c)}{\mu\ln\left[\dfrac{R_k^m}{mr_c R_1^{m-1}}\left(1-\dfrac{R_1^{2m}}{R_k^{2m}}\right)\right]} \qquad (22.43)$$

where R_1 is the ring well row radius; r_c is the well radius.

If the number of wells in he ring row is greater than five, $(R_1/R_k)^{2m} << 1$, Eq. (22.43) may be simplified. Besides, if $R_1/mr_c = \sigma/\pi r_c$ is subtracted, the approximate equation is:

$$Q' = \frac{2\pi kh(p_к - p_c)}{\mu(m \ln R_k/R_1 + \ln \sigma/\pi r_c)}. \quad (22.44)$$

The external and internal filtration resistances are defined as:

$$\rho = \frac{\mu}{2\pi kh} \ln \frac{R_k}{R_1} \quad \text{and} \quad \rho' = \frac{\mu}{2\pi khm} \ln \frac{\sigma}{\pi r_c} \quad (22.45)$$

For a case of two ring well rows coaxial with the circular charge contour, the flow to the wells is calculated using the equivalent filtration resistance wiring as shown in Fig. 22.14.

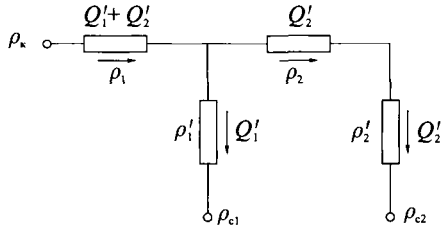

Fig. 22.14. Wiring of filtration resistances in the case of a flow to two ring well rows

The external and internal filtration resistances are found from the following equations:

$$\rho_1 = \frac{\mu}{2\pi kh} \ln \frac{R_k}{R_1} \quad \text{и} \quad \rho_2 = \frac{\mu}{2\pi kh} \ln \frac{R_1}{R_2}$$

$$\rho_1' = \frac{\mu}{2\pi khm_1} \ln \frac{\sigma_1}{\pi r_c} \quad \text{и} \quad \rho_2' = \frac{\mu}{2\pi khm_2} \ln \frac{\sigma_2}{\pi r_c} \quad (22.46)$$

where R_1, R_2 are ring well rows radiuses, and m_1, m_2 are a number of wells in a row.

For a case of three ring well rows coaxial with the circular charge contour, the flow to the wells is calculated using the equivalent filtration resistance wiring as shown in Fig. 22.12. The external and internal filtration resistances are found from equations:

$$\rho_1 = \frac{\mu}{2\pi kh} ln \frac{R_k}{R_1}, \quad \rho_2 = \frac{\mu}{2\pi kh} ln \frac{R_1}{R_2}, \quad \rho_3 = \frac{\mu}{2\pi kh} ln \frac{R_2}{R_3}$$

$$\rho_1' = \frac{\mu}{2\pi khm_1} \ln \frac{\sigma_1}{\pi r_c}, \quad \rho_2' = \frac{\mu}{2\pi khm_2} \ln \frac{\sigma_2}{\pi r_c}, \quad \rho_3' = \frac{\mu}{2\pi khm_3} \ln \frac{\sigma_3}{\pi r_c} \quad (22.47)$$

where R_1, R_2, R_3 are ring well rows radiuses, m_1, m_2, m_3 are a number of wells in a ring row.

Mechanics of Fluid Flow
by Kaplan S. Basniev, Nikolay M. Dmitriev and George V. Chilingar

CHAPTER XXIII

NON-STATIONARY FLOW OF AN ELASTIC FLUID IN AN ELASTIC RESERVOIR

1. Elastic reservoir drive

In the process of hydrocarbon field development, non-stationary processes often arise in the reservoirs. They may be associated with well infill or shut-ins, changes in the rate of fluid withdrawal from wells, etc. Typically, for the non-stationary processes the formation pressure redistribution changes in the filtration velocity with time subsequent to the change in well flow-rates. The quantitative parameters of the non-stationary processes (the values of pressure, velocity, flow-rate changes) depend on the elastic properties of the reservoirs and their saturating fluids This means that the major form of the reservoir energy providing for the fluid flow to the wells in the non-stationary process environment is the energy of fluids' (oil and water) and rock matrix's elastic deformation.

A mathematical model introduced below considers the elastic forces in a single-phase filtration flow. Thus, it is assumed that pressure at any point in the flow is is above the liquid-by-gas saturation pressure.

When a well is put on-production in the elastic drive environment, the fluids' motion begins at the expense of using the potential energy of the reservoir's elastic deformation. It begins near the bottomhole first, and then spreads to the more distant reservoir areas. Indeed, when formation pressure declines, the elastic counteraction of the reservoir against the overlying rock mass decreases. This results in a decrease in the pore volume, which, in turn, increases fluids' compression. These entire phenomenons facilitate the displacement of the fluid from the reservoir to wells. The volume elastic deformation factors for both fluids and the solid rock matrix are very small. But due to significant reservoir volume and volume of its saturating fluids, the fluid amounts recovered from the reservoir due to the reservoir and fluids elasticity may be quite significant.

In some cases, the fluid flow to the wells is supported by pressure of the water entering the reservoir from the charge area. In such cases, the reservoir drive is called elastic water drive. There is also another variety of the elastic drive. It is the enclosed elastic drive. There are oil accumulations within traps closed from all sides: the productive reservoir pinches-out at a small distance from the oil accumu-

lation or sliced by a fault or faults. At the initial stages of the development of such accumulations, until the formation pressure declines to the saturation pressure limit, the fluid flows under the closed elastic drive.

A typical feature of the elastic drive in the process of oilfield development is the long time it takes for the formation pressure to redistribute or the fluid withdrawal rate to change after the well began producing. The reason is that very significant resistance arises as the viscous fluid flows in the reservoir. The nonstationary processes are in direct proportion with the reservoir permeability k and in inverse proportion with fluid's viscosity μ, fluid's volume compressibility β_{liq} and solid rock's matrix compressibility β_c.

The initial studies of the elastic drive by Muskat, Schilthuis, Hearst, Tseis and Jacob did not take the volume elasticity of the reservoir into consideration. The elastic drive theory which did consider the matrix's elastic properties was developed by Shchelkachev (1999).

2. Calculation of elastic fluid reserves of a reservoir

The elastic fluid reserves are the amounts of the fluids that may be extracted from the reservoir under declining pressure as a result of the reservoir solid matrix's and its saturating fluid's volume elasticity. Although the elastic volume deformation factors are very low for both fluids and reservoir's solid matrix (see Chapter XIX), the reservoir volume is very big so that the fluid's elastic reserves in the reservoir may be very significant. As the formation pressure declines, the fluid's elastic reserves of a reservoir naturally decrease. If the formation pressure increases, the fluid's elastic reserves increase subsequently.

The fluid's elastic reserves in a reservoir may be calculated as follows. Let's conceptually identify a reservoir volume's element V_0. Suppose $V_{0\,liq}$ is the fluid's volume saturating this reservoir volume's element V_0 at formation pressure p_0. Let's determine the fluid's elastic reserves from its volume as measured under the initial formation pressure. Let's designate ΔV_{res} as a change in the fluid's elastic reserves within V_0 volume when pressure at all points of the reservoir changes by Δp. According to Eqs. (19.22) and (19.40), replacing the differentials of the fluid's pressure and volume and pore volume by finite differences, results in:

$$-\beta_{liq} V_{0\,liq} \Delta p = \Delta V_{liq} \text{ and } \beta_c V_0 \Delta p = \Delta V_{rock}.$$

It was assumed, when deriving the formula for the fluid's volume compressibility factor β_{liq}, that only the hydrostatic pressure acted on the fluid. For this reason, when pressure increases (the compression environment), fluid's volume decreases, and vice versa. Thus β_{liq} factor has the minus sign. Under the elastic drive, when pressure in the reservoir declines, fluid's volume decreases. Such fluid's behavior is caused by the fact that the fluid in question is positioned within pores, and following the equation for β_c, under decreased pressure the pore volume also decreases, and the fluid experiences the compressing action from the solid matrix.

Thus, the minus sign in front of β_{liq} is omitted. Assuming that the change in the elastic reserves includes ΔV_{liq} and ΔV_{rock}:

$$\Delta V_{res} = \beta_{liq} V_{0\,liq} \Delta p + \beta_c V_0 \Delta p. \tag{23.1}$$

The initial volume of fluid saturating the reservoir volume element V_0 is equal to the total pore volume within the element:

$$V_{0\,liq} = \varnothing V_0, \tag{23.2}$$

where $\varnothing$ is reservoir porosity.

Now it is possible tp rewrite Eq. (23.1) as follows:

$$\Delta V_{res} = (\varnothing \beta_{liq} + \beta c) V_0 \Delta p, \tag{23.3}$$

or:

$$\Delta V_{res} = \beta^* V_0 \Delta p, \tag{23.4}$$

where:

$$\beta^* = \varnothing\, \beta_{liq} + \beta_c. \tag{23.5}$$

β^* factor is called reservoir storativity or elastic capacity. Following Eq. (23.4), the storativity β^* is equal to the change in fluid's elastic reserves per reservoir unit volume at the formation pressure change by one unit:

$$\beta^* = \frac{\Delta V_{res}}{V_0 \Delta p}.$$

If Eqs. (23.3) and (23.4) are related to an oilfield under development in the environment of the closed elastic drive, the V_0 should be treated as the reservoir volume where pressure by a given moment in time changed by Δp. At that, by definition, it is assumed that:

$$\Delta p = p_k - p_{w.avg} \tag{23.6}$$

where p_k is initial formation pressure and $p_{w.avg}$ is average pressure weighted over the disturbed volume V_0. $p_{w.avg}$ may be calculated if the geometry of the disturbed reservoir volume and pressure distribution within this volume are known.

By differentiating Eq. (23.4):

$$d(\Delta V_{res}) = \beta^* d[V_0(t) \Delta p].$$

On the other hand, the change in the elastic fluid volume within the reservoir over the time interval dt may be found from:

$$d(\Delta V_{res}) = Q(t) dt,$$

where $Q(t)$ is the flow-rate of all wells producing from a given oil accumulation.

By equating the right portions of these two equations, the differential equation of the oil accumulation depletion under the closed elastic drive is obtained:

$$\beta^* d[V_0(t)\Delta p] = Q(t)dt. \tag{23.7}$$

This equation for finding approximate solutions under the elastic drive theory will be used.

3. Mathematical model of the elastic fluid non-stationary filtration in an elastic porous medium

Hydrodynamics of the elastic filtration drive is extremely important not only theoretically, but also in practice of oil gas field development. The knowledge of these basics enables the most complete utilization of the formation fluids' elastic reserves for providing the flow into the wells, the correct understanding of the elastic water-head system's potential capability to displace the fluids, and the solution of the so-called inverse problems of reservoir property determination based on the flow-rate or pressure changes. As a rule, only a small portion of the hydrocarbon reserves (2 to 5 %) is recovered under the natural elastic drive. However, there are cases where the elastic forces are so great that a much greater fraction of the reserves may be produced. For instance, the oil recovery factor from a major Tengiz Field in Kazakhstan under the elastic drive is expected to reach 20 %.

To derive major differential equations of the elastic fluid's filtration in an elastic porous medium, the flow continuity equation, the motion equations (Darcy's law) and equations of state of the porous medium and its saturating fluid will be used. Also the mathematical model described in Chapter XIX with system of equations of Eq. (19.8) is used:

$$\begin{aligned}
&\frac{\partial \varnothing \rho}{\partial t} + \operatorname{div} \rho \bar{w} = 0, \\
&\bar{w} = -\frac{k}{\mu}(\operatorname{grad} p + \rho \bar{f}), \\
&\rho = \rho(p),\ \varnothing = \varnothing(p),\ k = k(p),\ \mu = \mu(p).
\end{aligned} \tag{23.8}$$

After discarding the mass forces and introduction of Leibensohn's generalized function, the system converts to the following format [Eq. (19.21)]:

$$\begin{aligned}
&\frac{\partial \varnothing \rho}{\partial t} - \Delta P = 0, \\
&\rho \bar{w} = -\operatorname{grad} P, \\
&\rho = \rho(p),\ \varnothing = \varnothing(p),\ k = k(p),\ \mu = \mu(p), \\
&P = \int \frac{k(p)}{\mu(p)} \rho(p) dp.
\end{aligned} \tag{23.9}$$

The equations of state for an elastic fluid and an elastic porous medium as derived earlier Eqs. (19.24) and (19.42) are used as equations of state for the medium and fluid:

$$\rho = \rho_0[1 + \beta_{liq}(p - p_0)] \tag{23.10}$$

and:

$$\varnothing = \varnothing_0 + \beta_c(p - p_0). \tag{23.11}$$

It is assumed that permeability k and viscosity μ are constant. Laboratory studies and the field development practice indicate, however, that on a number of occasions as a result of arising deformations reservoir permeability also changes. It is especially typical for the deep hydrocarbon accumulations. This case, however, is not considered in the model under consideration. Therefore, the introduction of another equation of state, $k = k(\varnothing(p))$, will make the model much more complex. Thus, despite numerous developments in the elastic drive theory accounting for $k = k(\varnothing)p)$ correlation, the introduction of this more general treatment would make this Section too complicated, so the authors recommend all interested readers to refer to the specialized monographs.

4. Derivation of the differential equation of the elastic fluid filtration in an elastic porous medium under Darcy's law

Let's now review a mathematical model of non-stationary flow of the elastic fluid. It is assumed that the fluid complies with the Darcy's law and flows within a deformable porous medium [Eq. (23.9)] with equations of state [Eqs. (23.10) and (23.11)] at $k =$ const and $\mu =$const. The complete system of equations has the following format:

$$\frac{\partial \varnothing \rho}{\partial t} - \Delta P = 0,$$

$$\rho \bar{w} = -\text{grad}\, P,$$

$$\rho = \rho_0[1 + \beta_{liq}(p - p_0)],$$

$$\varnothing = \varnothing_0 + \beta_c(p - p_0),$$

$$k = \text{const}, \quad \mu = \text{const},$$

$$P = \frac{k}{\mu}\int \rho dp.$$

It is demonstrated that all equations in the system define the mathematical model. However, for the problem setting and solution within the model's framework, it is desirable to transform equations to a single equation for the function to be determined.

After substituting Leibensohn's function into first equation:

$$\frac{\partial(\varnothing\rho)}{\partial t} = \frac{k}{\mu}\Delta\int\rho dp. \tag{23.12}$$

Let's now transform the left part by using equation of state for an elastic fluid and elastic porous medium [Eqs. (23.10) and (23.11)]:

$$\rho = \rho_0[1+\beta_{liq}(p-p_0)],\ \varnothing = \varnothing_0 + \beta_c(p-p_0)$$

and calculate the product $\varnothing\rho$:

$$\varnothing\rho = \varnothing_0\rho_0 + (\varnothing_0\rho_0\beta_{liq} + \rho_0\beta_c)(p-p_0) + \rho_0\beta_c\beta_{liq}(p-p_0)^2.$$

The last member of this equation is small compared to two others and may be disregarded (as a reminder: for the oils, β_{liq} is $7*10^{-10}$ to $30*10^{-10}$ Pa^{-1}; for the formation water it is $2.7*10^{-10}$ to $5*10^{-10}$ Pa^{-1}; the volume compressibility factor of the reservoir $\beta_c = 0.3$ to $2*10^{-10}$ Pa^{-1}). Then, considering Eq. (23.5), results in:

$$\varnothing\rho = \varnothing_0\rho_0[1+\beta^*(p-p_0)/\varnothing_0],$$

and from there, after differentiating with respect to time t:

$$\frac{\partial(\varnothing\rho)}{\partial t} = \rho_0\beta^*\frac{\partial p}{\partial t}. \tag{23.13}$$

Next, let's transform the right part of Eq. (23.12):

$$\frac{k}{\mu}\Delta\left(\int\rho dp\right).$$

Substituting the equation of state for the elastic fluid Eq. (23.10) under integral, results in:

$$\frac{k}{\mu}\Delta\left(\int\rho dp\right) = \frac{k}{\mu}\Delta\left(\rho_0 p + \rho_0\beta_{liq}\left(\frac{p^2}{2} - p_0 p\right) + C\right). \tag{23.14}$$

Again, as the fluid is slightly-compressible and the β_{liq} factor is small, the second component can be disregarded:

$$\frac{k}{\mu}\Delta\left(\int\rho dp\right) = \frac{k}{\mu}\rho_0\Delta p. \tag{23.15}$$

Substituting Eqs. (23.13) and (23.15) into the source differential Eq. (23.12) and obtaining the differential equation with respect to pressure:

$$\beta^*\frac{\partial p}{\partial t} = \frac{k}{\mu}\Delta p, \tag{23.16}$$

or in Cartesian coordinates:

$$\frac{\partial p}{\partial t} = \kappa\left(\frac{\partial^2 p}{\partial x^2} + \frac{\partial^2 p}{\partial y^2}\frac{\partial^2 p}{\partial z^2}\right). \tag{23.17}$$

The notation κ is:

$$\kappa = \frac{k}{\mu\beta^*}. \tag{23.18}$$

Eq. (23.16) is the main differential equation of the elastic filtration drive theory. It is so called the piezo-conductivity equation. This equation is similar to the heat-transfer type differential equations (Fourier equations), which is one of the basic equations of mathematical physics.

The κ factor describes velocity at which formation pressure redistributes at non-stationary filtration of an elastic fluid in the elastic porous medium. It is usually called the piezo-conductivity factor by analogy with the thermal conductivity factor in heat transfer equation.

The dimensionality of the κ factor may be found from Eq. (23.18):

$$[\kappa] = \frac{k}{[\mu][\beta^*]} = \frac{\mathrm{L}^2}{\mathrm{L}^{-1}\mathrm{M}\mathrm{T}^{-1}\mathrm{L}\mathrm{M}^{-1}\mathrm{T}^2} = \frac{\mathrm{L}^2}{\mathrm{T}},$$

where L, M and T are, respectively, the dimensions of length, mass and time. The most common values of the piezo-conductivity factor encountered in the oil industry are between 0.1 and 5 m^2/s.

The piezo-conductivity equation is only applicable for a slightly-compressible elastic fluid with $\beta_{liq}(p - p_0) << 1$. If this condition is not observed, then in transforming from Eqs. (23.14) to (23.15) the component with β_{liq} cannot be disregarded. It would result in a significant increase of equation's complexity and its becoming nonlinear.

5. Unidimensional filtration of an elastic fluid. Point-solutions of the piezo-conductivity equation. Main equation of the elastic drive theory

In this section the simplest point-solutions of the piezo-conductivity Eq. (23.16) for the unidimensional flows will be reviewed.

5.1. Rectilinear-parallel filtration of an elastic fluid

Case 1. Inflow to the gallery at which constant pressure is maintained. Suppose constant initial formation pressure p_k is maintained in the semi-infinite hori-

zontal reservoir of a constant thickness h and width B. At the gallery (at $x = 0$) pressure is instantaneously dropped to p_{gal} and is subsequently maintained at the same level (i. e., $p_{gal} = \text{const}$). At any remote point ($x \to \infty$) pressure is equal p_k at any moment in time.

Under these conditions, non-stationary rectilinear-parallel flow of an elastic fluid emerges in the elastic deformable reservoir. Pressure an any point x of the flow and at any time may be determined by integrating the piezo-conductivity Eq. (23.17), which for the unidimensional flow in the Cartesian coordinates is:

$$\frac{\partial p}{\partial t} = \kappa \frac{\partial^2 p}{\partial x^2}, \quad 0 < x < \infty . \tag{23.19}$$

The initial and boundary conditions formulated earlier are as follows:

$$\begin{aligned} &p(x,t) = p_k \text{ at } t = 0; \\ &p(x,t) = p_{gal} \text{ at } x = 0, \ t > 0; \\ &p(x,t) = p_k \text{ at } x = \infty, \ t \geq 0. \end{aligned} \tag{23.20}$$

The problem requires the gallery flow-rate $Q(t)$ and pressure at any point in the flow and at any point in time, i. e., the function $p(x,t)$.

Let's use the dimensionality analysis to show that., arguments on which pressure is dependent may be combined into a single dimensionless complex on which the function $p(x,t)$ will depend.

Let's denote $P = (p - p_{gal})/(p_k - p_{gal})$ as the dimensionless pressure which, as Eqs. (23.19) and (23.20) show, depends on the time t, coordinate x and piezo-conductivity factor κ, i. e.:

$$P = f(x,t,\kappa).$$

Dimensionalities of these variables are as follows: $[x] = \text{L}$, $[t] = \text{T}$, and $[\kappa] = \text{L}^2\text{T}^{-1}$. They may be used to construct a dimensionless complex $x/\sqrt{\kappa t}$. By assuming the value $u = x/(2\sqrt{\kappa t})$ as a new variable, the problem is then limited to finding the dimensionless pressure P which depends only on u: $P = f(u)$. As a result of such transition, the boundary conditions [Eq. (23.20)] can be rewritten:

$$\begin{aligned} &P = 0 \ \text{ at } u = 0; \\ &P = 1 \ \text{ at } u = \infty. \end{aligned} \tag{23.21}$$

Because the differential Eq. (23.19) is linear, similar equation exists for the dimensionless pressure P as for the dimensional pressure p:

$$\frac{\partial P}{\partial t} = \kappa \frac{\partial^2 P}{\partial x^2}. \tag{23.22}$$

Using the complex function differentiation rule, partial derivative with respect to the coordinate and time may be expressed through a derivative with respect to dimensionless variable. As a result of differentiation:

$$\frac{\partial P}{\partial x}=\frac{dP}{du}\frac{\partial u}{\partial x}=\frac{dP}{du}\frac{1}{2\sqrt{\kappa t}},$$

$$\frac{\partial P}{\partial t}=\frac{dP}{du}\frac{\partial u}{\partial t}=\frac{dP}{du}\left(-\frac{1}{2\sqrt{t^3}}\right)=\frac{dp}{du}\frac{d^2P}{du^2},$$

$$\frac{\partial P}{\partial x^2}=\frac{\partial}{\partial x}\left(\frac{\partial P}{\partial x}\right)=\frac{\partial}{\partial x}\left(\frac{dP}{du}\frac{1}{2\sqrt{\kappa t}}\right)=\frac{1}{2\sqrt{\kappa t}}\frac{d^2P}{du^2}\frac{\partial u}{\partial x}=\frac{1}{4\kappa t}\frac{d^2P}{du^2}.$$

Substituting the values of the derivatives into Eq. (23.22), results in an ordinary differential equation:

$$\frac{d^2P}{du^2}+2u\frac{dP}{du}=0, \tag{23.23}$$

which must be solved under conditions listed in Eq. (23.21). For this purpose, the parameter $dP/du = \xi$ is introduced; then, Eq. (23.23) changes to:

$$\frac{d\xi}{du^2}+2u\xi=0. \tag{23.24}$$

And, after separating the variables:

$$\frac{d\xi}{\xi}=-2udu,$$

and, performing integration:

$$\log\xi=-u^2+\log C_1,$$

finally results in:

$$\xi=\frac{dP}{du}=C_1e^{-u^2}, \tag{23.25}$$

where C_1 is integration constant.

After integrating Eq. (23.25) and applying the first condition in Eq. (23.21):

$$P=C_1\int_0^u e^{-u^2}du.$$

Now, the second condition in Eq. (23.20) is used to find the integration constant C_1. Taking the upper limit in the integral to infinity, results in:

$$1 = C_1 \int_0^{\infty} e^{-u^2} du .$$

It is known form integral calculus that $\int_0^{\infty} e^{-u^2} du = \sqrt{\pi}/2$, so the preceding equation gives $C_1 = 2/\sqrt{\pi}$, and finally:

$$P = \frac{2}{\sqrt{\pi}} \int_0^{\frac{x}{2\sqrt{\kappa t}}} e^{-u^2} du . \qquad (23.26)$$

Integral Eq. (23.26) is called the probability integral. It is a tabulated function ranging in value between 0 and 1 and has a special notation

$$\frac{2}{\sqrt{\pi}} \int_0^{\frac{x}{2\sqrt{\kappa t}}} e^{-u^2} du = \operatorname{erf}\left(\frac{x}{2\sqrt{\kappa t}}\right).$$

Thus, $P = \operatorname{erf}\left(\frac{x}{2\sqrt{\kappa t}}\right)$ and the pressure distribution law in non-stationary rectilinear-parallel filtration flow of an elastic fluid has the following format:

$$p = p_{gal} + (p_k - p_{gal})\operatorname{erf}\left(\frac{x}{2\sqrt{\kappa t}}\right). \qquad (23.27)$$

Typical pressure distribution curves at different moments in time in the non-stationary rectilinear-parallel flow of an elastic fluid in a gallery produced at constant bottomhole pressure $p_{gal} = \text{const}$ are displayed in Fig. 23.1.

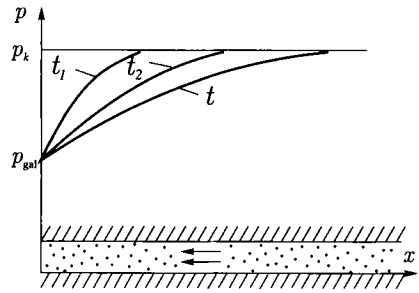

Fig. 23.1. Pressure distribution at different moments in time within a non-stationary rectilinear-parallel flow of an elastic fluid with p_{gal} = const.

Let's find the gallery flow-rate Q. The plus sign is associated to the flow-rate from gallery ($x = 0$) when the flow is moving against the x axis, and $\partial p/\partial x > 0$. Under Darcy's law:

$$w = \frac{k}{\mu}\left(\frac{\partial p}{\partial x}\right)_{x=0}, \quad Q = \frac{k}{\mu}Bh\left(\frac{\partial p}{\partial x}\right)_{x=0}, \tag{23.28}$$

where B and h are, respectively, reservoir's width and thickness. After taking derivative of Eq. (23.27):

$$\left(\frac{\partial p}{\partial x}\right)_{x=0} = (p_k - p_{gal})\left(\frac{2}{\sqrt{\pi}}e^{-\left(\frac{x}{2\sqrt{\kappa t}}\right)^2}\frac{1}{2\sqrt{\kappa t}}\right)_{x=0} = \frac{p_k - p_{gal}}{\sqrt{\pi\kappa t}}. \tag{23.29}$$

Gallery's flow-rate at any moment in time may be determined by substituting pressure gradient $\partial p/\partial x$ from Eq. (23.29) into Eq. (23.28):

$$Q = \frac{k}{\mu}\frac{p_k - p_{gal}}{\sqrt{\pi\kappa t}}Bh. \tag{23.30}$$

The latter equation indicates that gallery's rate declines with time in proportion with $1/\sqrt{t}$ and tends to zero at $t \to \infty$. At $t = 0$, Eq. (23.30) gives in the infinite value of the flow-rate, which is a consequence of pressure jump at the gallery from p_k to p_{gal} at the initial moment in time.

Cumulative oil production V_{cum} by the time t is determined by:

$$V_{cum} = \int_0^t Q(t)dt = \frac{k}{\mu}\frac{p_k - p_{gal}}{\sqrt{\pi\kappa t}}Bh\int_0^t \frac{dt}{\sqrt{t}} = \frac{2k(p_k - p_{gal})Bh}{\mu\sqrt{\pi\kappa}}\sqrt{t},$$

i. e., immediately upon the beginning of the production it rapidly increases, but subsequently grows very slowly (Fig. 23.2).

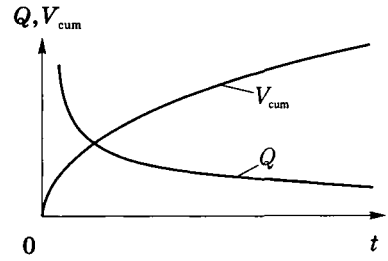

Fig. 23.2. Fluid's flow rate and production level vs. time after the gallery startup with p_{gal} = const.

Case 2. Flow into the gallery where a constant flow-rate is maintained. Suppose from the same kind of semi-infinite reservoir as in Case 1 at the moment in time $t = 0$ a gallery begins producing at a constant volume flow-rate Q. It is required to determine formation pressure at any point in the reservoir at any moment in time.

Mathematically, the problem reduces to the integration of the same equation Eq. (23.22) with different initial and boundary conditions:

$$\begin{aligned} &p(x,t) = p_k \text{ at } t = 0; \\ &w(x,t) = \frac{k}{\mu}\frac{\partial p}{\partial x} = w_1 = \text{const at } x = 0,\ t > 0; \\ &p(x,t) = p_k \text{ at } t > 0,\ x \to \infty. \end{aligned} \tag{23.31}$$

The first condition, as in previous Case, gives the pressure distribution in the reservoir prior to the gallery start-up. Thus, at the initial moment in time pressure at any points in the reservoir is constant and is equal to the contour pressure. The second condition sets permanency of gallery's flow-rate after its start-up. Following condition 3, the disturbed zone boundary with time moves to infinity.

For integrating the piezo-conductivity equation, both portions of the Eq. (23.22) are multiplied by κ/μ and then take derivative with respect to x. The result is:

$$\frac{\kappa}{\mu}\frac{\partial^2 x}{\partial x}\frac{p}{\partial t} = \frac{\kappa}{\mu}\kappa\frac{\partial^3 p}{\partial x^3},$$

then, changing the order of calculating the derivatives:

$$\frac{\partial}{\partial t}\left(\frac{\kappa}{\mu}\frac{\partial p}{\partial x}\right) = \kappa\frac{\partial^2 p}{\partial x^2}\left(\frac{\kappa}{\mu}\frac{\partial p}{\partial x}\right). \tag{23.32}$$

Considering:

$$\frac{\kappa}{\mu}\frac{\partial p}{\partial x} = w(x,t),$$

Eq. (23.32) can be rewritten as follows:

$$\frac{\partial w(x,t)}{\partial t} = \kappa\frac{\partial^2 w(x,t)}{\partial x^2}. \tag{23.33}$$

This latter equation in its format also coincides with the heat-transfer Eq. (23.22). Therefore, the solution of Eq. (23.33) will be similar to Eq. (23.26), with pressure p being replaced by the filtration velocity w:

$$w = C_1 \operatorname{erf}\left(\frac{x}{2\sqrt{\kappa t}}\right) + C_2. \tag{23.34}$$

And one has to keep in mind that the initial and boundary conditions for w are:

$$w(x,0) = 0, \quad w(0,t) = w_1.$$

Using these conditions we will find the integration constants. At $t = 0$ following Eq. (23.34):

$$0 = C_1 \frac{2}{\sqrt{\pi}} \int_0^{\infty} e^{-u^2} du + C_2$$

and as $\int_0^{\infty} e^{-u^2} du = \sqrt{\pi}/2$, then:

$$0 = C_1 + C_2.$$

The second condition at $x = 0$ provides:

$$w_1 = C_1 \frac{2}{\sqrt{\pi}} \int_0^{0} e^{-u^2} du + C_2.$$

From these two equations $C_2 = w_1$ and $C_2 = -w_1$; therefore:

$$w(x,t) = w_1 \left[1 - \operatorname{erf}\left(\frac{x}{2\sqrt{\kappa t}} \right) \right] = \frac{\kappa}{\mu} \frac{\partial p}{\partial x}. \tag{23.35}$$

In order to find pressure distribution in the flow, it is necessary to integrate Eq. (23.35) with respect to x with constant time t.

$$\frac{\kappa}{\mu} \int_0^x \frac{\partial p}{\partial x} = w_1 \int_0^x \left(1 - \frac{2}{\sqrt{\pi}} \int_0^{\frac{1}{2\sqrt{\kappa t}}} e^{-u^2} du \right) dx.$$

After integrating:

$$p(x,t) - p(0,t) = \frac{k}{\mu} w_1 x - \frac{k}{\mu} \frac{2}{\sqrt{\pi}} w_1 \int_0^x \left(\int_0^{\frac{1}{2\sqrt{\kappa t}}} e^{-u^2} du \right) dx. \tag{23.36}$$

The last component is then integrated part-by-part as:

$$\frac{k}{\mu} \frac{2}{\sqrt{\pi}} w_1 \int_0^x \left(\int_0^{\frac{1}{2\sqrt{\kappa t}}} e^{-u^2} du \right) dx =$$

$$= \frac{k}{\mu}\frac{2}{\sqrt{\pi}} w_1 \left[x * \int_0^{\frac{2}{2\sqrt{\kappa t}}} e^{-u^2} du \Big|_0^x - \int_0^x x e^{-x^2/4\kappa t} \frac{dx}{2\sqrt{\kappa t}} \right] =$$

$$= \frac{2\mu w_1}{k\sqrt{\pi}} \left[x * \int_0^{\frac{2}{2\sqrt{\kappa t}}} e^{-u^2} du \Big|_0^x - \sqrt{\kappa t}\left(1 - e^{-x^2/4\kappa t}\right) \right].$$

So, Eq. (23.36) can be rewritten as:

$$p(x,t) - p(0,t) = \frac{\mu w_1}{k} x \left[1 - \operatorname{erf}\left(\frac{x}{2\sqrt{\kappa t}} \right) + \frac{1 - e^{-x^2/4\kappa t}}{\sqrt{\pi} x / 2\sqrt{\kappa t}} \right]. \tag{23.37}$$

Considering that $p(0,t)$ is pressure at the gallery, i. e., $p(0,t) = p_{gal}(t)$, from Eq. (23.37) it is possible to determine the pressure at any point in the flow:

$$p(x,t) = p_{gal} \frac{\mu w_1}{k} \left[x\left(1 - \operatorname{erf}\left(\frac{x}{2\sqrt{\kappa t}} \right) \right) + \frac{2\sqrt{\kappa t}}{\sqrt{\pi}} \left(1 - e^{-x^2/4\kappa t} \right) \right]. \tag{23.38}$$

In order to determine the pressure change at the gallery $p_{gal}(t)$, the boundary condition $p(x,t) = p_k$ at $x \to \infty$ is substituted into Eq. (23.38). As at $x \to \infty$, $\operatorname{erf}\left(\frac{x}{2\sqrt{\kappa t}} \right) \to 1$, the product $x\left(1 - \operatorname{erf}\left(\frac{x}{2\sqrt{\kappa t}} \right) \right)$ gives invalid solution of a $\infty * 0$ kind. Expanding this equation under Lopitale's rule, it is possible to show that this product tends to zero. Also, considering that $e^{-x^2/4\kappa t} \to 0$ when $x \to \infty$:

$$p_{gal}(t) = p_k - \frac{2\mu w_1}{k\sqrt{\pi}} \sqrt{\kappa t}$$

or:

$$p_{gal}(t) = p_k - \frac{Q\mu}{Bh} \frac{2\sqrt{\kappa t}}{k\sqrt{\pi}}. \tag{23.39}$$

At long time the solution of Eq. (23.39) loses its physical meaning. Indeed, as the process is not time-limited, it is possible to indicate such t values at which $p_{gal}(t) < 0$. This result means that the accepted boundary condition $w(0,t) = \text{const} = w_1$ is excessively "rigid", and its implementation would require large negative pressure over a long t. In real life, such pressure will not occur but, rather, cavitations near the gallery will arise.

5.2. Rectilinear-parallel filtration flow of an elastic fluid. The main equation of the elastic filtration regime theory

Suppose there is a production well of the "zero" radius (point sink) in an unlimited horizontal reservoir of thickness h. Initial formation pressure within the entire reservoir is the same and is equal to p_k. The well is started-up at the moment in time $t = 0$ at a flow-rate Q_0. As a result, a non-stationary radial-plane flow of an elastic fluid occurs.

Pressure distribution in the reservoir $p(r,t)$ at any point and any place in time is determined by integrating Eq (23.16), which for the radial flow in the cylindrical coordinate system is:

$$\frac{\partial p}{\partial t} = \kappa\left(\frac{\partial^2 p}{\partial r^2} + \frac{1}{r}\frac{\partial p}{\partial r}\right). \tag{23.40}$$

The problem has the following initial and boundary conditions:

$$\begin{aligned} &p(r,t) = p_k \text{ at } t = 0; \\ &p(r,t) = p_{gai} \text{ at } t > 0 \text{ and } r \to \infty; \\ &Q = \frac{2\pi kh}{\mu}\left(r\frac{\partial p}{\partial r}\right)_{r=0} = Q_0 = \text{const at } t > 0. \end{aligned} \tag{23.41}$$

The first condition implies that at initial time $t = 0$ pressure within the entire reservoir was constant and equal to the contour pressure. The second condition indicates that the boundary of the disturbed zone (i. e., the radius at which pressure is equal o the contour pressure) is moving with time and for long time tends to infinity. Following the third condition, the well's flow-rate is maintained constant.

Let's write the latter condition as:

$$\left(r\frac{\partial p}{\partial r}\right)_{r=0} = \frac{Q_0\mu}{2\pi kh}. \tag{23.42}$$

As previously shown, the dimensionalities of the equations should be examined. The pressure distribution in the reservoir depends on the five definitive variables: r, t, κ, p_k and $Q_0\mu/(2\pi kh)$. Dimensionalities of these variables are as follows:

$$[r] = \mathrm{L},\ [t] = \mathrm{T}, \text{ and } [\kappa] = \mathrm{L}^2\mathrm{T}^{-1},\ [p_k] = [p],\ [Q_0\mu/(2\pi kh)] = [p],$$

where $[p]$ is the dimensionality of pressure. Thus the pressure dimensionality reduces to a dimensionless format, $P = p/p_k$, depending only on two dimensionless parameters (because out of five parameters, three have independent dimensionalities (r, t, p_k)). Therefore:

$$P = f\left(\xi, \frac{Q_0\mu}{2\pi khp_k}\right), \quad \xi = \frac{r}{2\sqrt{\kappa t}}. \tag{23.43}$$

Thus, Eq. (23.40) can be converted to a regular differential equation. Let's take derivative of Eq. (23.43) and find the representation of the partial derivatives with respect to independent variables t and r through the variables with respect to the variable:

$$\frac{\partial P}{\partial t} = -\frac{\partial P}{\partial \xi}\frac{\xi}{2t}, \quad \frac{\partial P}{\partial r} = \frac{\partial P}{\partial \xi}\frac{\xi}{2\sqrt{\kappa t}}, \quad \frac{\partial^2 P}{\partial r^2} = \frac{1}{4\kappa t}\frac{\partial^2 P}{\partial \xi^2}.$$

Substituting these expressions into Eq. (23.40), results in an ordinary differential equation:

$$\frac{\partial^2 P}{\partial \xi^2} + \left(\frac{1}{\xi} + 2\xi\right)\frac{dP}{d\xi} = 0, \tag{23.44}$$

which should be integrated with the conditions obtained from Eq. (23.41) through the transformation to dimensionless format:

$$P(\xi) = 1 \text{ at } \xi \to \infty,$$
$$\left(\xi \frac{dP}{d\xi}\right)_{\xi=0} = \frac{Q_0 \mu}{2\pi k h p_\kappa}. \tag{23.45}$$

Let's now use a substitution:

$$\frac{dP}{d\xi} = v$$

and obtain from Eq. (21.44):

$$\frac{dv}{d\xi} + \left(\frac{1}{\xi} + 2\xi\right)v = 0$$

or:

$$\frac{d\xi}{\xi} + \frac{dv}{v} = -2\xi d\xi. \tag{23.46}$$

After integrating Eq. (23.46):

$$\log \xi + \log v = -\xi^2 + \log C_1, \tag{23.47}$$

where C_1 is the integration constant.

Rearranging Eq. (23.47), gives:

$$v = \frac{dP}{d\xi} = C_1 \frac{e^{-\xi^2}}{\xi}. \tag{23.48}$$

After integrating Eq. (23.48) from ξ to infinity, and accounting for the first condition from Eq. (23.41):

$$P(\xi) = -C_1 \int_{\xi}^{\infty} \frac{e^{-\xi^2}}{\xi} d\xi. \tag{23.49}$$

C_1 can be found by multiplying Eq. (23.49) by ξ, directing ξ to infinity and using the second condition of Eq. (23.45):

$$C_1 = \frac{Q_0 \mu}{2\pi k h p_\kappa}.$$

Then, Eq. (23.49) can be transformed to appear as:

$$P(\xi) = 1 - \frac{Q_0 \mu}{2\pi k h p_\kappa} \int_{\xi}^{\infty} \frac{e^{-\xi^2}}{\xi} d\xi. \tag{23.50}$$

This integral is easily reduced to the tabular format by a substitution:

$$u = \xi^2 = \frac{r^2}{4\kappa t}, \qquad \frac{d\xi}{\xi} = \frac{du}{2u}.$$

Back substitution from the dimensionless pressure P to dimensional $p = Pp_\kappa$, results in:

$$p(r,t) = p_\kappa - \frac{Q_0 \mu}{2\pi k h} \int_{r^2/(4\kappa t)}^{\infty} \frac{e^{-u}}{u} du. \tag{23.51}$$

The integral in Eq. (23.51) is called the integral exponential function. It is a tabular integral and is denoted:

$$-\mathrm{Ei}\left(-\frac{r^2}{4\kappa t}\right) = \int_{r^2/(4\kappa t)}^{\infty} \frac{e^{-u}}{u} du.$$

Thus, pressure at any point in the rectilinear-parallel flow under the elastic filtration regime is determined from the following equation:

$$p(r,t) = p_\kappa - \frac{Q_0 \mu}{2\pi k h} \left[-\mathrm{Ei}\left(-\frac{r^2}{4\kappa t}\right) \right]. \tag{23.52}$$

This equation is called the major equation of the elastic regime theory. It is widely used in practical applications for the interpretation of well testing results, for calculations of pressure distribution at the elastic fluids' filtration, etc.

The integral exponential function may be represented as a series:

$$-\mathrm{Ei}(-x) = \log\frac{1}{x} - \gamma + \sum_{n=1}^{\infty}\frac{(-1)^{n+1}}{n*n!}x^n,$$

which converges at any x values ($0 < x < \infty$), γ is Euler's constant (an irrational value whose approximate value for hydrodynamic calculation is accepted as 0.5772).

When the variable x changes from 0 to ∞, the function $-\mathrm{Ei}(-x)$ rapidly declines from ∞ to 0. The graph of this function is displayed in Fig. 23.3. At small x values, the series total may be disregarded; then:

$$-\mathrm{Ei}(-x) = \log\frac{1}{x} - 0.5772.$$

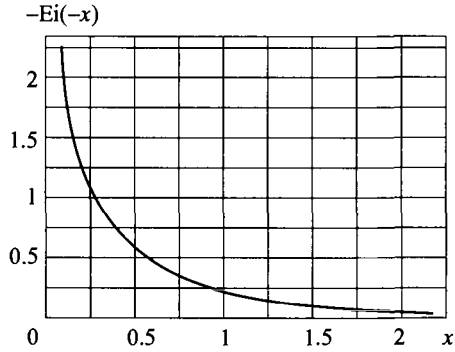

Fig. 23.3. An integral exponential function.

The estimated error is:

$$0.25\ \%\ \text{when}\ x = \frac{r^2}{4\kappa t} \le 0.01;$$

$$5.7\ \%\ \text{when}\ x = \le 0.1;$$

$$9.7\ \%\ \text{when}\ x = \le 0.14.$$

Therefore, for the values $x = \dfrac{r^2}{4\kappa t} \le 1$, pressure may be determined from equation:

$$p(r,t) = p_\kappa - \frac{Q_0\mu}{2\pi kh}\left[\log\frac{4\kappa t}{r^2} - 0.5772\right]. \tag{23.53}$$

From Eq. (23.52), the fluid throughflow through any cylindrical surface of radius r and filtration velocity can be determined, respectively, from equations:

$$Q(r,t) = \frac{k}{\mu}\frac{\partial p}{\partial r}2\pi rh = Q_0 e^{-r^2/4\kappa t}, \tag{23.54}$$

$$w = \frac{Q_0}{2\pi rh} e^{-r^2/4\kappa t}. \tag{23.55}$$

The latter equation tells us that the stationary velocity $w_{stat} = Q_0/2\pi rh$ is reached very rapidly at a short distance from the well as the value of the piezoconductivity factor is usually very high.

In theoretical studies of non-stationary formation pressure redistribution processes, it is convenient to use dimensionless Fourier parameter fo and Fo, serving as dimensionless time and determined from the following equations:

$$\text{fo} = \frac{\kappa t}{r_c^2}, \quad \text{Fo} = \frac{\kappa t}{R_k^2}. \tag{23.56}$$

Depending on the problem, one or the other Fourier parameter may be used.

Strictly speaking, the major equation of the elastic drive [Eq. (23.52)] is valid only for a point sink (at $r_c = 0$) in a limitless reservoir ($R_k = \infty$).

Shchelkachev (1990) compared the results obtained from Eq. (23.52) with the results computed with the precise equation (Van Everdingen, Hurst), which considers the finite radius of the well r_c. He found that the pressure error as determined from Eq. (23.52) is

0.6 % at fo = 100

2.3 % at fo = 25

5 % at fo = 10

and 9.4% at fo = 5

of the charge contour radius (or the radius of the circular impermeable reservoir boundary).

Let's now estimate the practical meaning of this error. Suppose $\kappa = 1$ m^2/s, $r_c = 0.1$ m. Then, assuming fo = 100:

$$t = \text{fo}\frac{r_c^2}{\kappa} = 100\frac{0.1^2}{1} = 1s.$$

Therefore, already 1 second after the well startup the bottomhole pressure calculations from Eq. (23.52) will have an error of no greater that 0.6 %. Therefore, for the wells of a regular size, Eq. (23.52) provides for a high accuracy at the very early stage (and even more so, at the later stages) of the pressure redistribution process.

Direct calculation showed that in most practical cases, when a well was producing from a finite open reservoir, a simple Eq. (23.52) for an infinite reservoir may be used for a long period of time. The error of the bottomhole pressure does not exceed 0.08 % at $\text{Fo} \le 0.2$, 1 % at $\text{Fo} \le 0.35$ and 1.9 % at $\text{Fo} \le 0.5$.

To calculate formation pressure at any point in the open circular reservoir at $r \le 0.1R_k$, it is also possible to use Eq. (23.52) with accuracy of up to 0.2 % for the infinite reservoir (provided $R_k \ge 10^5 r_c$, $0.1R_k$, $\mathrm{Fo} \le 0.2$).

In addition to these estimations, it is important to note that the bottomhole pressure difference in the finite (open and closed) and infinite reservoirs does not exceed 1 % if $\mathrm{Fo} \le 0.33$, $R_k \ge 50r_c$ or if $\mathrm{Fo} \le 0.35$, $R_k \ge 1{,}000r_c$.

Solutions of Fourier's differential Eq. (23.40) for different cases of the elastic fluid filtration within limited open and closed reservoirs are represented by infinite series of the special Bessel's functions.

In conclusion, let's see how the piezometric curves look near a well producing at a constant flow-rate Q_0 (Fig. 23.4). For the point close to the bottomhole Eq. (23.53) can be used. By taking derivative of this equation with respect to the coordinate r, the pressure gradient can be found as follows:

$$\partial p / \partial r = Q_0 \mu / (2\pi k r).$$

This equation shows that pressure gradient for r values satisfying the inequality $r^2 \le 0.03 * 4\kappa t$ for any practical purpose does not depend on t and is determined from the same equation as for non-transient parallel-plane filtration of an incompressible fluid. For these r values, the piezometric curves are logarithmic curves (Fig. 23.4). Bottomhole pressure declines with time; the θ angles of the tangents at the bottomhole are equal for all curves.

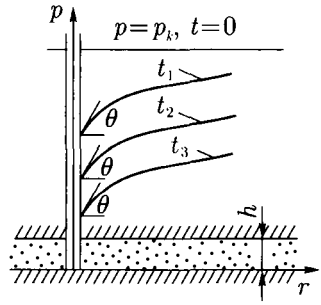

Fig. 23.4. Piezometric curves at startup of a well with a constant flow-rate Q_0; r_c — well radius; R_k — radius of the circular charge contour or radius of the circular impermeable reservoir boundary.

6. Approximate solution techniques of the elastic drive problems

It was shown in the preceding paragraphs that the solutions of boundary problems for the non-stationary filtration of an elastic fluid in an elastic porous medium within infinite and finite reservoirs may be obtained using the well-known integra-

tion methods of the piezo-conductivity (heat-transfer) differential Eq. (23.16). However, in many cases such solutions are represented by the complicated equations in form of infinitely-slowly converging series or an improper integral containing special functions. For this reason, attempts were undertaken to find effective approximate solutions of the non-stationary filtration of an elastic fluid in an elastic porous medium. In the next section some of these methods, which gained wide acceptance in the solution of the elastic drive problems, will be reviewed.

6.1. Method of sequential change of stationary states

One of the simplest approximate techniques for the solution of the elastic drive problems is the sequential change of stationary states (SCSS) method developed by I.A. Charny (1963) and commonly used in practice.

At each movement, the reservoir is subdivided into two areas, one disturbed and the other, undisturbed. It is assumed that in the disturbed area, which begins from the well's wall, pressure is distributed so that the fluid flow within the area is non-transient, and the external boundary of the area is serving at a given moment in time as the charge contour. Pressure within the undisturbed reservoir area is constant anywhere and is equal to the initial contour pressure. The motion pattern of the movable boundary between the disturbed and undisturbed areas is determined from the material balance equation and boundary conditions.

The separation of the flow into two areas (disturbed and undisturbed) calls for the consideration of the formation pressure redistribution process as if occurring into two phases. During phase one, the disturbed area boundary continuously expands. As soon as it reaches the reservoir boundary, phase two begins. In a theoretical study of the process in conditions of an infinite reservoir, we are dealing only with phase one whose duration is not restricted.

Let's now conduct the calculation of non-stationary unidimensional flows of an elastic fluid using the SCSS technique.

A rectilinear non-stationary filtration of an elastic fluid.

Case 1. Inflow to the gallery where a constant flow-rate Q is maintained. Suppose at the time $t = 0$, a rectilinear gallery is started-up from a horizontal reservoir of the thickness h and width B. A constant flow-rate Q is maintained in the gallery. Prior to the start-up, pressure in the entire reservoir was constant and equal to p_k.

By the moment in time t after the gallery start-up the disturbed area boundary will spread to length $l(t)$ (Fig. 23.5). Pressure distribution within this area is considered to be steady-state (see Chapter XX, sec. 2), i. e., it is described by the linear equation:

$$p(x,t) = p_k - \frac{Q\mu}{kBh}(l(t) - x),\ 0 \le x \le l(t). \tag{23.57}$$

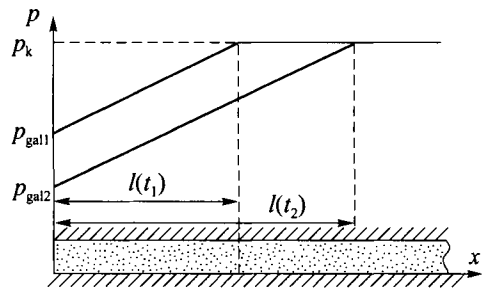

Fig. 23.5. Pressure distribution in the rectilinear –parallel flow after the PSSS technique.

It is required to find the rule of motion in time of the disturbed area's external boundary $l(t)$.

Eq. (23.7) is used, which is the condition of the production over a period dt being equal to the change in the fluid's elastic reserve within the disturbed reservoir area over the same period of time:

$$Qdt = \beta^* d[V(t)\Delta p], \tag{23.58}$$

where $V(t)$ is the volume of the disturbed reservoir area:

$$V(t) = Bhl(t); \tag{23.59}$$

$$\Delta p = p_k - p_{w.avg} = p_k - \frac{p_k + p_{gal}}{2} = \frac{p_k - p_{gal}}{2}. \tag{23.60}$$

Inasmuch as at $x = 0$, $p_x(t) = p_{gal}(t)$, from Eq. (23.57):

$$Q = \frac{k}{\mu}\frac{p_k - p_{gal}}{\mu}Bh,$$

and from there

$$\frac{Q\mu l(t)}{2kBh} = \frac{p_k - p_{gal}}{2}. \tag{23.61}$$

After substituting Eqs. (23.59)–(23.61) into Eq. (23.58):

$$Q = \beta^* \frac{d}{dt}\left(Bhl\frac{Q\mu l}{2kBh}\right),$$

and, as Q = const:

$$2Q = \frac{\beta^*\mu}{k}Q\frac{d}{dt}(l^2),$$

and from there:

$$2\kappa dt = dl^2 \quad \left(\kappa = k/(\mu\beta^*)\right).$$

After performing integration:

$$l(t) = \sqrt{2\kappa t}\,. \tag{23.62}$$

Therefore, Eq (23.57) for pressure distribution in the reservoir will have the following format:

$$\begin{aligned} p(x,t) &= p_k - \frac{Q\mu}{kBh}(\sqrt{2\kappa t} - x), \quad 0 \le x \le \sqrt{2\kappa t}, \\ p(x,t) &= p_k, \quad x > \sqrt{2\kappa t}. \end{aligned} \tag{23.63}$$

The $p_k - p_{gal}$ pressure drawdown found using the approximate Eq. (23.63) differs by 25 % from the value determined from the exact Eq. (23.39).

Case 2. Inflow to the gallery where constant bottomhole pressure is maintained (p_{gal} = const). In the same reservoir as in Case 1 the production gallery started-up at the moment in time $t = 0$ with a constant bottomhole pressure p_{gal} = = const. Before the production startup pressure in the entire reservoir was constant and equal to p_k It is required to find pressure distribution, the rule of motion in time of the disturbed area's external boundary $l(t)$, and change in time of gallery's flow-rate $Q(t)$.

Gallery's flow-rate under the transient-free conditions is:

$$Q(t) = \frac{k(p_k - p_{gal})}{\mu l(t)} Bh = \frac{k}{\mu} Bh \frac{\partial p}{\partial x}\Big|_{x=0}.$$

The problem is solved similarly to Case 1 with the only difference that the following expressions should be substituted into Eq. (23.58) for fluid's elastic reserve:

$$V(t) = Bhl(t),$$

$$\Delta p = p_k - p_{w.avg} = p_k - \frac{p_k + p_{gal}}{2} = \frac{p_k - p_{gal}}{2}$$

$$Q(t) = \frac{k(p_k - p_{gal})}{\mu l(t)} Bh,$$

and as a result:

$$\frac{k(p_k - p_{gal})}{\mu l(t)} Bh\,dt = \beta^* s\left[Bhl\frac{p_k - p_{gal}}{2}\right].$$

After performing the arithmetic transformation and integration:

$$l(t) = 2\sqrt{\kappa t}\,.$$

Therefore, pressure distribution within the disturbed reservoir area is determined by the expression:

$$p(x,t) = p_k - (p_k - p_{gal})\left(1 - \frac{1}{2\sqrt{\kappa t}}\right), \quad 0 < x \le 2\sqrt{\kappa t},$$
$$p(x,t) = p_k, \quad x > 2\sqrt{\kappa t}, \tag{23.64}$$

and the gallery flow-rate:

$$Q(t) = \frac{k(p_k - p_{gal})}{2\mu\sqrt{\kappa t}} Bh. \tag{23.65}$$

The gallery flow-rate error as determined from Eq. (23.65) compared to the precise Eq. (23.27) is 11 %. Therefore, it is better to use the sequential change of stationary states method in the case of non-stationary rectilinear-parallel flows when a constant pressure drawdown is given.

Radial-plane non-stationary flow of an elastic fluid.

Case 1. Flow to the well whose flow-rate Q is maintained constant. Suppose in an infinite horizontal reservoir of a constant thickness h at the moment in time $t = 0$, a production well of a radius r_c begins producing at a constant flow-rate Q. Prior to the well start-up, pressure in the entire reservoir was constant and equal to p_k.

Under the SCSS technique, it is assumed in the time t since the well start-up a disturbed area of a radius $R(t)$ forms around the well. Pressure within this area will be distributed under the stationary law:

$$p(r,t) = p_k - \frac{Q\mu}{2\pi kh} \log \frac{R(t)}{r}. \tag{23.66}$$

Pressure within the rest of the reservoir is constant and equal to initial formation pressure p_k.

It is required to find the rule of motion in time of the disturbed area's external boundary $R(t)$.

Pressure distribution curves at different moments in time in such a flow are displayed in Fig. 23.6. The well flow-rate can be found from equation similar to Dupois formula:

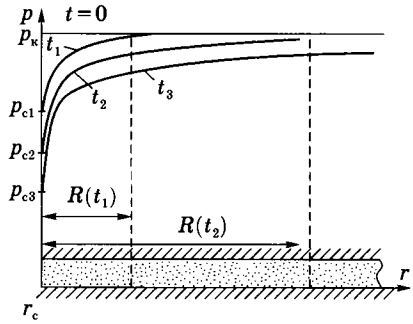

Fig. 23.6. Pressure distribution in the radial-plane flow at different moments in time under the PSSS technique (withdrawal is conducted at Q = const).

$$Q = \frac{2\pi kh(p_k - p_c(t))}{\mu \log\left(R(t)/r_c\right)}. \tag{23.67}$$

The size of the disturbed area may be found from material balance Eq. (23.58) at:

$$V(t) = \pi\left(R^2(t) - r_c^2\right)h, \quad \Delta p = p_k - p_{w.avg}. \tag{23.68}$$

Weighted average formation pressure $p_{w.avg}$ in the transient-free radial-plane flow (see Chapter XX, sec. 3) is determined from Eq. (20.25):

$$p_{w.avg} = p_k - \frac{p_k - p_c}{2\log\dfrac{R(t)}{r_c}},$$

and from there, in considering of Eq. (23.66):

$$\Delta p = p_k - p_{w.avg} = \frac{p_k + p_{gal}}{2\log\dfrac{R(t)}{r_c}} = \frac{Q\mu}{2\pi kh}. \tag{23.69}$$

The rule of motion in time of the disturbed area $R(t)$'s external boundary may be found by substituting Eqs. (23.68) and (23.69) into the material balance Eq. (23.58):

$$4\kappa\, dt = d\left(R^2(t) - r_c^2\right),$$

and after integrating from 0 to t and from r_c to $R(t)$:

$$R(t) = \sqrt{r_c^2 + 4\kappa t}. \tag{23.70}$$

Then, Eq. (23.66) is used to determine pressure at any point in the reservoir at any point in time t:

$$p(x,t) = p_k - \frac{Q\mu}{2\pi kh}\log\frac{\sqrt{r_c^2 + 4\kappa t}}{r}, \quad r_c \le r \le \sqrt{r_c^2 + 4\kappa t},$$
$$p(x,t) = p_k, \quad r > \sqrt{r_c^2 + 4\kappa t}. \tag{23.71}$$

The pressure drawdown at the moment t:

$$\Delta p_c \equiv p_k - p_c(t) = \frac{Q\mu}{2\pi kh}\log\frac{\sqrt{r_c^2 + 4\kappa t}}{r_c}. \tag{23.72}$$

Comparison of Eq. (23.71) results with the pressure drawdown determined from the exact Eq. (23.52), shows that the relative error decreases with time and is 10.6% when $fo = \kappa t / r_c = 100$, 7.5 % when $fo = 10^3$, and 5.7 % when $fo = 10^4$.

Case 2. Flow to the well where constant pressure p_c = const is maintained. In case of the radial-plane fluid flow into the well started-up at a constant bottomhole pressure p_c = const, the rule of motion in time of the disturbed area's boundary is expressed by an integral in the form of a slowly converging series, so the solution is not quoted here. The calculation of motion in time of the disturbed area's boundary in this case may be determined from the graph (Fig. 23.7).

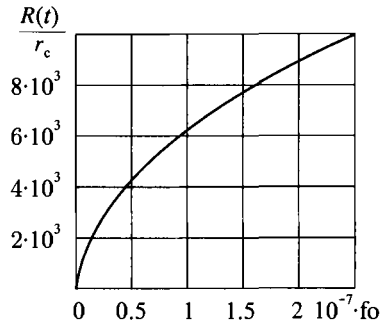

Fig. 23.7. Dimensionless radius of the disturbed area $R(t)/r_c$ vs. dimensionless time f_o at fluid withdrawal with a constant bottomhole pressure p_c = const.

Well's flow-rate is determined from Dupois' Eq. (23.67) at p_c = const.

A comparison with the exact calculations shows that the error in rate's determination using the SCSS technique is about 5 %.

It is important to note that in case of both linear and radial filtration, the pressure gradient in the transition point from the disturbed to undisturbed area experiences a disruption, which is one of the reasons of discrepancies between the SCSS calculations and the exact calculations. The SCSS, however, is an effective calculation technique, and thus it is commonly used not only in the problems associated with filtration of single-phase fluids but even in the problems of gas and liquid flow and problems of fluid/gas separation boundary motion.

Pressure distribution in the filtration area as determined by SCSS technique is a rather rough approximation. The technique works much better for the flow-rate *vs.* pressure drawdown correlation, especially at radial filtration.

6.2. Pirverdian's technique

This method is similar to the SCSS, but is more accurate. According to the SCSS, the non-stationary flow at each moment in time is mentally subdivided into two areas, disturbed and undisturbed. Their boundary is also determined based on material balance equation. As opposed to the SCSS technique, however, pressure distribution in the disturbed area is assigned in the form of a squared parabola, so that the piezometric curve at the boundary of the areas were tangential to a horizontal

line representing pressure in the undisturbed area. Pressure distribution will no longer be stationary, and the pressure gradient at the boundary of the areas becomes equal to zero. This provides for a smooth connection of the pressure profile in the disturbed and undisturbed areas.

Let's review the rectilinear-parallel non-stationary flow of an elastic fluid.

Case 1. Inflow into a gallery where a constant flow-rate Q is maintained. Suppose a gallery started-up producing at a constant flow-rate Q from a horizontal reservoir of a constant thickness h and width B. Prior to the production start-up, pressure p_k in the entire reservoir was equal.

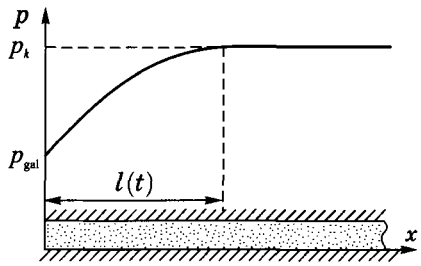

Fig. 23.8. Pressure distribution in a rectilinear-parallel flow under the Pirverdyan's technique.

By the moment in time t after the start-up, the disturbed area boundary will advance by the length $l(t)$, and the pressure distribution curve within this area will be a parabola. The pressure distribution graph in the reservoir by the time t after the gallery start-up is displayed in Fig. 23.8. The parabolas equation describing the pressure distribution in the disturbed area is as follows:

$$p(x,t) = p_k - (p_k - p_{gal})\left(1 - \frac{x}{l(t)}\right)^2, \quad 0 < x \le l(t). \tag{23.73}$$

The gallery's flow-rate is determined from Darcy's law:

$$Q = \frac{k}{\mu} Bh \frac{\partial p}{\partial x}\Big|_{x=0}. \tag{23.74}$$

The pressure gradient at the gallery $\frac{\partial p}{\partial x}\Big|_{x=0}$ can be found by differentiating Eq. (23.73) and substituting $x = 0$ in the obtained expression:

$$\frac{\partial p}{\partial x}\Big|_{x=0} = \frac{2(p_k - p_{gal})}{l(t)}. \tag{23.75}$$

Substituting Eq. (23.75) into Eq. (23.74), the equation for the gallery flow-rate can be obtained:

$$Q = 2\frac{k}{\mu}\frac{(p_k - p_{gal})}{l(t)}Bh. \tag{23.76}$$

The rule of the disturbed area boundary motion is determined from the material balance Eq. (23.58) and considering Eq. (23.59) at $\Delta p = p_k - p_{w\,avg}$. Now, it is possible to determine the weighted average formation pressure within the disturbed area by the moment t in time using the distribution Eq. (23.73):

$$p_{w.avg} = \frac{1}{V(t)}\int_{V(t)} p(x,t)dv = \frac{1}{l(t)}\int_0^{l(t)}\left[p_k - (p_k - p_{gal})\left(1 - \frac{x}{l(t)}\right)^2\right]dx = p_k - \frac{(p_k - p_{gal})}{3}.$$

Therefore, the pressure change is:

$$\Delta p = p_k - p_{w.avg} = \frac{(p_k - p_{gal})}{3}.$$

Using Eq. (23.76), the above equation can be transformed to:

$$\Delta p = \frac{(p_k - p_{gal})}{3} = \frac{Q\mu l(t)}{6kBh} \tag{23.77}$$

and further, by substituting Eqs. (23.59) and (23.77) into the material balance Eq. (23.58):

$$Qdt = \beta^* d\left[Bhl^2(t)\frac{Q\mu}{6kBh}\right],$$

wherefrom:

$$6\kappa dt = dl^2(t),$$

and, after integrating from 0 to t and from 0 to l:

$$l(t) = \sqrt{6\kappa t}. \tag{23.78}$$

Thus, the pressure distribution equation in the disturbed area assumes the following format:

$$p(x,t) = p_k - \frac{Q\mu}{2kBh}\sqrt{6\kappa t}\left(1 - \frac{x}{\sqrt{6\kappa t}}\right)^2,\ 0 < x \le \sqrt{6\kappa t}), \tag{23.79}$$

$$p(x,t) = p_k,\ x > \sqrt{6\kappa t}.$$

The calculation of pressure drawdown $(p_k - p_{gal})$ from Eq. (23.79) results in an error of about 9 % compared with the exact solution, i. e., 2.5 times smaller than using the SCSS technique.

Case 2. Inflow into a gallery where a constant pressure p_{gal} is maintained. Suppose there is the rectilinear-parallel flow of an elastic fluid to the gallery, which is started-up producing at a constant bottomhole pressure p_{gal} = const. Prior to the production start-up, pressure p_k in the entire reservoir was equal.

To obtain an approximate solution using the Pirverdian's technique the same approach as in Case 1 is used. Let's substitute the expressions for the throughflow, volume and pressure drawdown into the material balance Eq. (23.58):

$$Q = 2\frac{k}{\mu}\frac{(p_k - p_{gal})}{l(t)}Bh,\ V(t) = Bhl(t),\ \Delta p = p_k - p_{w.avg} = \frac{(p_k - p_{gal})}{3}.$$

The result is differential equation:

$$6\kappa dt = l(t)dl(t),$$

after integrating, the rule for the flow in the disturbed area boundary is obtained:

$$l(t) = \sqrt{12\kappa dt}.$$

Substituting the found rule into equations for pressure distribution Eq. (23.73) and flow-rate Eq. (23.76), gives the pressure equation within the reservoir's disturbed area:

$$p(x,t) = p_k - (p_k - p_{gal})\left(1 - \frac{x}{\sqrt{12\kappa dt}}\right)^2,$$

and from the gallery's flow-rate:

$$Q = 2\frac{k}{\mu}\frac{(p_k - p_{gal})}{l(t)}Bh = 2\frac{k}{\mu}\frac{(p_k - p_{gal})}{\sqrt{12\kappa dt}}Bh. \qquad (23.80)$$

The calculation of the gallery flow-rate from the approximate Eq. (23.80) results in an error of about 2.5 % compared with the exact solution, i. e., better than 2 times more precise than using the SCSS technique.

6.3. Integral relationships technique

The integral ratios technique proposed by Barenblatt, similar to the boundary layer techniques for the viscous fluid flow, provides approximate solution of some problems of non-stationary filtration for an elastic fluid with the needed accuracy.

The technique is base on the following assumptions:

1. At any moment in time the reservoir is subdivided into the finite disturbed area and non-disturbed area where there is no motion.
2. The pressure distribution in the disturbed area is represented by a binomial in the powers of the coordinate x or r (in a case of the radial flow, a logarithmic term is added) with the time-dependent coefficients so that for a rectilinear-parallel flow:

$$p(x,t) = a_0(t) + a_1(t)\frac{x}{l(t)} + ... + a_n(t)\frac{x^n}{l^n(t)},\ 0 \le x \le l(t), \tag{23.81}$$

for a radial-plane filtration:

$$p(r,t) = a_0(t)\log\frac{r}{R(t)} + a_1(t) + a_2(t)\frac{r}{R(t)} + ... + a_{n+1}(t)\frac{r^n}{R^n(t)},\ r_c \le r \le R(t), \tag{23.82}$$

where the number of terms n is selected depending on the desired solution accuracy.

3. The binomial coefficients $a_0, a_1, a_2, ..., a_n$, and the size of the disturbed area $l(t)$ – or $R(t)$ are derived from (a) the conditions at the gallery (or the bottom-hole), (b) the conditions of pressure continuity and smoothness of the pressure curve at the boundary of the disturbed area, and (c) special integral ratios which are found as follows:

In the case of inflow to the gallery, both the right and left portions of piesoconductivity Eq. (23.19) are multiplied by x^k ($k = 1, 2, ...,$) and integrated over the the entire disturbed area:

$$\int_0^{l(t)} x^k \frac{\partial p}{\partial t} dx = \kappa \int_0^{l(t)} x^k \frac{\partial^2 p}{\partial x^2} dx. \tag{23.83}$$

In the case of inflow to the well, the right and left portions of differential equation is multiplied by r^k ($k = 1, 2, ...$) and integration is performed over the entire disturbed area:

$$\int_{r_c}^{R(t)} r^k \frac{\partial p}{\partial t} dr = \kappa \int_{r_c}^{R(t)} \frac{1}{r}\frac{\partial}{\partial r}\left(r\frac{\partial p}{\partial r}\right) r^k dr. \tag{23.84}$$

If the Eqs. (23.81) and (23.82) are substituted into Eqs. (23.83) and (23.84), respectively, and the necessary integrations is performed, the missing relationships for the determination of the factors $a_0(t)$, $a_1(t)$, ... and $l(t)$ — or $R(t)$ will be obtained.

The first of these integral relationships (at $k = 0$ in the case of inflow to the gallery, $k = 1$ in the case of inflow to the well) is material balance equation from which the coordinate of the disturbed area boundary $l(t)$ or $R(t)$ is found.

If it is assumed $n = 1$ in Eq. (23.81) and $n = 0$ in Eq. (23.82), the solution corresponding to the SCSS technique Eqs. (23.63), (23.64), (23.71), depending on conditions at the gallery or the bottomhole, will be obtained. If $n = 2$ in Eq. (23.81), then a specific case of the integral relationships technique is the Pirverdian's method.

Now, the integral relationships technique will be used to solve, for example, a problem of the parallel-plane non-stationary filtration of an elastic fluid to the well of radius r_c put on production at the moment in time $t = 0$ with a constant flow-rate Q. The formation pressure at the initial moment is constant within the entire reservoir and is equal to p_k.

The pressure distribution is assigned within the disturbed area $[r_c \le r \le R(t)]$ as:

$$p(r,t) = a_0 \log \frac{r}{R(t)} + a_1 + a_2 \frac{r}{R(t)}, \tag{23.85}$$

i. e., a linear binomial.

Factors a_0, a_1 and a_2 are determined from the conditions at the bottomhole and at the disturbed area boundary.

The condition at the bottomhole, according to Eq. (23.41), is:

$$Q = \frac{2\pi kh}{\mu} r \frac{\partial p}{\partial r} \text{ at } r = r_c. \tag{23.86}$$

At the boundary of the disturbed area:

$$p = p_k \text{ at } r = R(t),$$

$$\frac{\partial p}{\partial r} = 0 \text{ at } r = R(t), \tag{23.87}$$

where the second condition is the pressure curve smoothness condition.
The factors determined from these conditions are:

$$a_0 = \frac{Q\mu}{2\pi kh}, \; a_1 = p_k + \frac{Q\mu}{2\pi kh}, \; a_3 = -\frac{Q\mu}{2\pi kh} \tag{23.88}$$

(the components proportional to r_c and a_c^2 are discarded in view of their smallness).

Substituting Eq. (23.88) into the right portion of Eq. (23.85), results in:

$$p(r,t) = p_k + \frac{Q\mu}{2\pi kh}\left[\log \frac{r}{R(t)} + 1 - \frac{r}{R(t)}\right]. \tag{23.89}$$

The movement rule for the disturbed area boundary $R(t)$ is found from the material balance Eq. (23.58) and considering Eq. (23.68) (this equation may be obtained from the integral relationship Eq. (23.84) at $k = 1$).

Weighted average formation pressure $p_{w.avg}$ in the disturbed area may be determined using the pressure distribution Eq. (23.85):

$$p_{w.avg} = \frac{1}{V(t)} \int_{V(t)} p(r,t)dV =$$

$$= \frac{1}{\pi\left(R^2(t) - r_c^2\right)} \int_{r_c}^{R(t)} \left[p_k - \frac{Q\mu}{2\pi kh} \log \frac{r}{R(t)} + \frac{Q\mu}{2\pi kh} \left(1 - \frac{r}{R(t)}\right) \right] 2\pi hr\, dr$$

After integrating and discarding the resulting expression of the terms with r_c^2: $p_{w.avg} = p_k - \frac{Q\mu}{12\pi kh}$, and then, from Eq. (23.68),

$$\Delta p = p_k - p_{w.avg} = \frac{Q\mu}{12\pi kh}. \tag{23.90}$$

Substituting Eq. (23.68) for $V(t)$ and Eq. (23.90) into the material balance Eq. (23.58), after simple transformations:

$$12\kappa dt = d\left(R^2(t) - r_c^2\right),$$

and after integrating:

$$R(t) = \sqrt{r_c^2 + 12\kappa t}\ .$$

Therefore, the pressure distribution within the disturbed area will be:

$$p(r,t) = p_k - \frac{Q\mu}{2\pi kh} \left[\log \frac{\sqrt{r_c^2 + 12\kappa t}}{r} - 1 - \frac{r}{\sqrt{r_c^2 + 12\kappa t}} \right], \tag{23.91}$$

$$r_c \le r \le \sqrt{r_c^2 + 12\kappa t},\ p(r,t) = p_k,\ r > \sqrt{r_c^2 + 12\kappa t}.$$

Relative error δ in the pressure drawdown calculations $[p_k - p_c(t)]$ using Eq. (23.91) for different values of the Fourier's parameter fo $(= \kappa t / r_c^2)$ is: $\delta = -4.9$ % at $\text{fo} = 100$, $\delta = -4$ % at $\text{fo} = 10^3$, $\delta = -3.2$ % at $\text{fo} = 10^4$.

Thus, the approximate values of the average pressure drawdown Δp_c found by the integral relationships technique are underestimated compared with the precise values.

6.4 "Averaging" technique

The essence of the "averaging" technique (Sokolov, Guseynov, ...) is in that the time derivative $\partial p / \partial t$ in the elastic drive Eq. (23.40) is averaged over the entire disturbed area and is replaced by some time function:

$$F(t) = \frac{2}{R^2(t) - r_c^2} \int_{r_c}^{R(t)} \frac{\partial p}{\partial t} r\, dr \tag{23.92}$$

whose value is determined from the initial and boundary conditions. Eq. (23.40) will then assume the following format:

$$F(t) = \kappa \frac{1}{r}\frac{\partial}{\partial r}\left(r\frac{\partial p}{\partial r}\right). \tag{23.93}$$

This substitution makes the equation simpler and its integration easier.

Let's determine the pressure distribution at the non-stationary flow of an elastic fluid to the well with a constant flow-rate Q. The conditions at the bottomhole and at the disturbed area boundary are represented by Eqs. (23.86) and (23.87). Integrating Eq. (23.93) with respect to r under those conditions:

$$p = p_k + \frac{Q\mu}{2\pi kh}\log\frac{r}{R(t)} + \frac{F(t)}{2\kappa}\left[\frac{1}{2}\left(r^2 - R^2(t)\right) - r^2\log\frac{r}{R(t)}\right]. \tag{23.94}$$

The function $F(t)$ is determined from the second condition: Eq. (23.87):

$$F(t) = -\frac{Q\mu\kappa}{\pi kh\left(R^2(t) - r_c^2\right)}. \tag{23.95}$$

Substituting Eq. (23.95) into Eq. (23.94) and disregarding the terms with r_c^2:

$$p = p_k + \frac{Q\mu}{2\pi kh}\log\frac{r}{R(t)} + \frac{Q\mu}{2\pi kh}\left(1 - \frac{r^2}{R^2(t)}\right), \quad r_c \le r \le R(t). \tag{23.96}$$

In order to determine the disturbed area coordinate $R(t)$, it is necessary to take derivative of Eq. (23.96) with respect to t, substitute the result into Eq. (23.92) and considering Eq. (23.53) for $F(t)$:

$$R(t) = \sqrt{r_c^2 + 8\kappa t}. \tag{23.97}$$

Comparing Eq. (23.96), and considering Eq. (23.97), with the exact solution Eq. (23.53) shows that the relative error in the determination of pressure drawdown $p_k - p_c$ does not exceed 5 %.

In conclusion, we would like to mention an approximate result by Chekalyuk (1965). He proposed to determine the rate for a well started-up at a constant bottomhole pressure using Dupois' Eq. (23.67), where the disturbed area radius is found as:

$$R(t) = r_c + \sqrt{\pi\kappa t}.$$

This equation is very important for practical applications as there is no simple exact solution of the elastic fluid production on condition p_c = const. Calculations indicate that Chekalyuk's equation is precise, with the flow-rate determination error no greater than 1 %.

7. Elastic fluid flow to an aggregate well

Many oil and gas fields are associated with water-bearing reservoirs are developed under the water-drive. In the course of the development, pressure in the accumulation declines, and the bottom or edge water encroaches into the accumulation. The areal extent of the oil (or gas) accumulation decreases. It is important in designing the development of such a field to know the amount of the encroached water as well as formation pressure at any moment in time (it is usually assumed that pressure in the entire accumulation at a given moment in time is constant, i. e., the calculations deal with weighted average pressure). Such a problem taking into account the fluid contact advance is highly complex. However, at the initial development stages, with small amount of information about the reservoir and its specifics, the estimation may be made without consideration of the water encroachment into the accumulation. The oil or gas accumulation is modeled as a round one and is considered as an aggregate well of a constant radius R_z. The aquifer around the well is considered to be either infinite or finite.

Let's set the problem as follows. A hydrocarbon accumulation of the areal extent S is considered as an aggregate well with the radius $R_z = \sqrt{S/\pi}$. The aquifer extends to infinity. Prior to the production start-up, pressure within the entire aquifer is R_k. At the moment in time assumed to be the initial time t = 0, bottomhole pressure declines to p_c and is maintained so during the entire production period. It is required to determine the amount of water entering the aggregate well during the time interval t.

Assuming the aquifer's thickness is constant and equal to h, with permeability k, water viscosity μ_w and elastic capacity β^*, we may use the elastic drive equation for the radial-plane water flow to the aggregate well Eq. (23.40):

$$\frac{\partial p}{\partial t} = \kappa\left(\frac{\partial^2 p}{\partial r^2} + \frac{1}{r}\frac{\partial p}{\partial r}\right), \tag{23.98}$$

which should be solved under the following conditions:

$$p = p_k \text{ at } t = 0,\ R_z \le r < \infty; \tag{23.99}$$

$$p = p_c \text{ at } r = R_z,\ t > 0; \tag{23.100}$$

$$p = p_k \text{ at } r = \infty. \tag{23.101}$$

By integrating Eq. (23.98) under the conditions of Eqs. (23.99)–(23.101) the pressure distribution within the aquifer $p(r,t)$ is determined. Water flow-rate is determined from the following equation:

$$Q_w = \frac{k}{\mu_w}\left(\frac{\partial p}{\partial r}\right)_{r=R_z} 2\pi R_z h, \tag{23.102}$$

and the produced water volume, from this equation:

$$\int_0^t Q_w(t)dtQ = \frac{2\pi khR_z}{\mu_w}\int_0^t \left(\frac{\partial p}{\partial r}\right)_{r=R_z} dt. \qquad (23.103)$$

This problem was solved by Van Everdingen and Hurst (1949) using the Laplace transform. First of all, equation for the produced water volume was reduced to dimensionless format:

$$\overline{Q}(\text{fo}) = \frac{\mu_w \eta}{2\pi khR_z^2(p_k - p_c)}\int_0^t Q_w(t)dt, \qquad (23.104)$$

where $\text{fo} = \dfrac{\eta t}{R_z^2}$ is Fourier's parameter, i. e., dimensionless time.

Equation obtained for $\overline{Q}$ is:

$$\overline{Q}(\text{fo}) = \frac{4}{\pi^2}\int_0^\infty \frac{\left(1 - e^{-u^2 \text{fo}}\right)du}{u^3\left[J_0^2(u) + Y_0^2(u)\right]}. \qquad (23.105)$$

Here, $J_0(u)$and $Y_0(u)$ are zero order Bessel's functions, respectively, of the first and second kind. Tables were prepared and the graph plotted for $\overline{Q}(\text{fo})$ function (Fig. 23.9).

The problems become more complex if the assigned bottomhole pressure in the aggregate well is variable, i. e. $p_c = p_c(t)$. In such a case, the superposition principle under elastic drive conditions may be used.

Suppose, pressure declines with time as shown in Fig. 23.10. Let's designate the moment in time under consideration as t_n, and subdivide the entire interval $0 \le t \le t_n$ into n segments at a stem equal to Δt. Then $t_n = \Delta t * n$. We will replace the $p_c(t)$ curve by a step-correlation and will assume that pressure within one step is constant. Under the superposition principle and from Eq. (23.104):

$$\int_0^t Q_w(t)dtQ = \frac{2\pi khR_z^2}{\mu_w \kappa}[\Delta p_0 \overline{Q}(\text{fo}) + \Delta p_1 \overline{Q}(\text{fo} - \text{fo}_1) + \\ + \Delta p_2 \overline{Q}(\text{fo} - \text{fo}_2) + \ldots + \Delta p_{n-1}\overline{Q}(\text{fo} - \text{fo}_{n-1}), \qquad (23.106)$$

where $\text{fo} - \text{fo}_i = \dfrac{\kappa t}{R_z^2} - \dfrac{\kappa t_i}{R_z^2} = \dfrac{\kappa(t - t_i)}{R_z^2}$,

i. e., pressure decline at bottomhole of the operating aggregate well has the same effect as if at the moment in time $t_1 = \Delta t$, in addition to the well operating with pressure drawdown Δp_0; a second well with pressure drawdown Δp_1 began operating in the same location. By the moment t_n, this second well would have been operating during the time interval $t_n - t_1$, so its variable is $\text{fo} - \text{fo}_1 = \eta(t_n - t_1)/R_z^2$, etc.

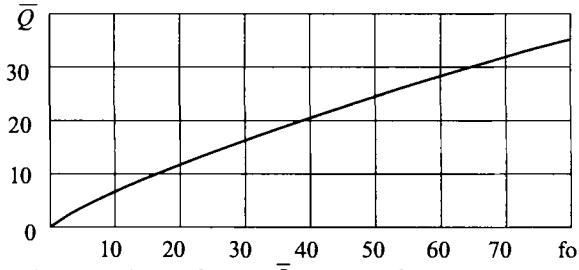

Fig. 23.9. Dimensionless volume of water $\bar{Q}$ extracted from the aggregate well vs. Fourier's parameter f_o for an indefinite reservoir (p_c = const).

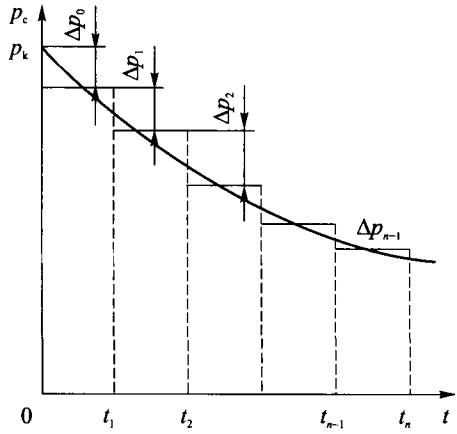

Fig. 23.10. Pressure dynamics at the bottomhole of an aggregate well.

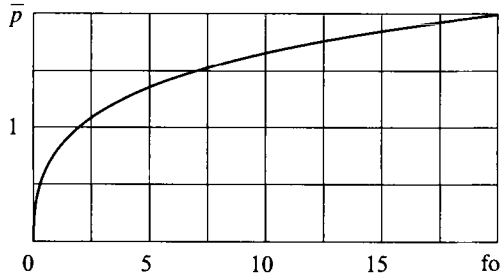

Fig. 23.11. Dimensionless pressure drawdown p vs. Fourier's parameter f_o for an aggregate well in an indefinite reservoir at Q_a = const.

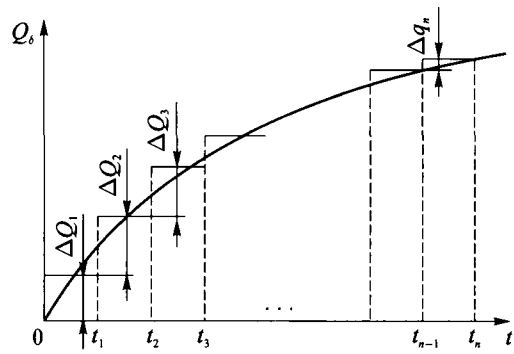

Fig. 23.12. Aggregate well flow-rate dynamics.

Eq. (23.106) is the solution of the set problem if bottomhole pressure is time-variable.

Significant for field development may be the problem of determining bottomhole pressure $p_c(t)$ in the aggregate well if the flow-rate Q_w is given. This problem may be solved by integrating Eq. (23.98) with the conditions of Eqs. (23.99) and (23.100), and the Eq. (23.101) must be replaced by the following:

$$r\frac{\partial p}{\partial r} = \frac{Q_w \mu_w}{2\pi kh} \text{ at } r = R_z. \tag{23.107}$$

Let's denote the dimensionless pressure drawdown as:

$$\overline{p}(\text{fo}) = \frac{2\pi kh}{Q_w \mu_w R_z^2}[p_k - p_c(\text{fo})]. \tag{23.108}$$

The Van Everdingen and Hurst (1949) solution is:

$$\overline{p}(\text{fo}) = \frac{4}{\pi^2}\int_0^\infty \frac{\left(1 - e^{-u^2 \text{fo}}\right)du}{u^3\left[J_1^2(u) + Y_1^2(u)\right]}, \tag{23.109}$$

where $J_1(u)$ and $Y_1(u)$ are first-order Bessel's functions, respectively, of the first and second kind. The graph of the $\overline{p}(\text{fo})$ function is presented in Fig. 23.11.

If the flow-rate Q_w is variable, we will replace the continuous $Q_w(t)$ curve by a step-correlation (Fig. 23.12) and will subdivide the time interval $t = t_n$ into n steps $t_n = n\Delta t$, where $t_n = \Delta t$, $t_1 = 2\Delta t$, etc. then the superposition principle is applied as-

suming that at the moments in time t_1, t_2, etc., new wells located in the same place will start operating at the flow-rates ΔQ_1, ΔQ_2, etc.

$$p_k - p_c(R_z, t) = \frac{\mu_w}{2\pi kh}[\Delta\overline{Q}_1\,\overline{p}(\text{fo}) + \Delta\overline{Q}_1\,\overline{p}(\text{fo} - \text{fo}_1) + \ldots + \Delta\overline{Q}_n\,\overline{p}(\text{fo} - \text{fo}_{n-1})]. \quad (23.110)$$

If a finite closed aquifer of radius R_k is assumed, the following condition is realized at the boundary:

$$\partial p / \partial r = 0 \text{ at } r = R_k. \quad (23.111)$$

The solution at p_c = const in the dimensionless format as a function of fo and $R = R_k/R_z$ is an infinite series:

$$\overline{Q}(\text{fo}) = \frac{R^2 - 1}{2} - 2\sum_{a_1, a_2, \ldots}^{\infty} \frac{e^{-a_n^2 \text{fo}} J_1^2(a_n R)}{a_n^2\left(J_0^2(a_n) - J_1^2(a_n R)\right)}, \quad (23.112)$$

Where a_1, a_2, ... are the equation roots:

$$J_1(a_n R)Y_0(a_n) - Y_1(a_n R)J_0(a_n) = 0. \quad (23.113)$$

The $\overline{Q}(\text{fo})$ curves for various values of the reservoir's dimensionless radius R are listed in Fig. 23.13 and Att.1. The smaller the reservoir's radius, the smaller is the elastic reserves, and the shorter time is needed for the extraction of the entire fluid's volume, which may be recovered from the reservoir on the account of fluid's elasticity at a given pressure drawdown $p_k - p_c$. For instance, for R = 1.5 beginning from fo = 0.8, $\overline{Q}$ = 0.625 and remains constant, which means no extraction; for R = 2 the extraction stops at fo = 3, etc.

If a finite aquifer at a constant given flow-rate Q_k is assumed, the dimensionless pressure drawdown will be:

$$\overline{p}(\text{fo}) = \frac{2}{R^2 - 1}\left(\frac{1}{4} + \text{fo}\right) - \frac{\left(3R^4 - 4R^4 \log R - 2R^2 - 1\right)}{4(R^2 - 1)} + 2\sum_{\beta_1, \beta_2, \ldots}^{\infty} \frac{e^{-\beta_n^2 \text{fo}} J_1^2(\beta_n R)}{\beta_n^2\left(J_0^2(\beta_n R) - J_1^2(\beta_n)\right)}, \quad (23.114)$$

Where β_1, β_2 are the roots of equation

$$J_1(\beta_n R)Y_1(\beta_n) - J_1(\beta_n)Y_1(\beta_n R) = 0. \quad (23.115)$$

Fig. 23.14 and Att. 1 show that the smaller the reservoir size, the more drastic pressure drawdown increases at the water production at a constant flow-rate. When the time value is low, the boundary effect is not noticeable (for instance, with R = 6 to the fo value equal to 6, $\overline{p}$ values are the same as for the infinite reservoir).

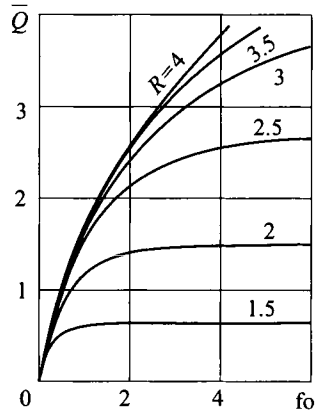

Fig. 23.13. Dimensionless volume $\bar{Q}$ withdrawn from aggregate well vs.Fourier parameter f_o for a closed reservoir of the finite size (p_c = const, $R = R_к/R_з$).

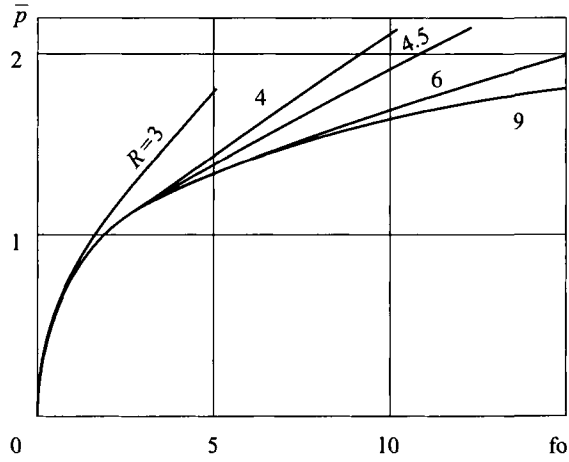

Fig. 23.14 Dimensionless pressure drawdown $\bar{p}$ vs. Furier's parameter f_o for the aggregate well operating in a finite-size closed reservoir (Q_e = const, R $R_к/R_з$).

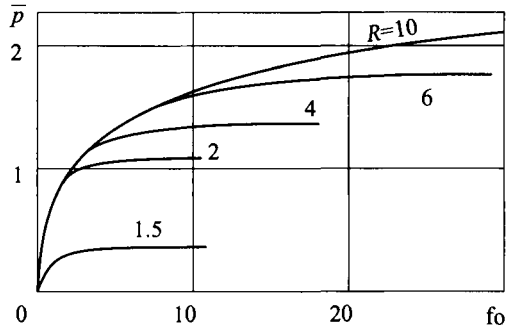

Fig. 23.15. Dimensionless pressure drawdown $\bar{p}$ vs. Furier's parameter f_0 for the aggregate well in a finite-size open reservoir (Q_s = const, $R = R_к/R_э$).

In this section the graphs for the dimensionless pressure drawdown $\bar{p}$ (fo) for a finite open reservoir with a constant pressure at the boundary ($p = p_k$ at $r = R_k$) from a constant withdrawal (Q_w = const) will be displayed (Fig. 23.15), The smaller the reservoir size, the sooner the constant depression sets up, i.e., the sooner the first phase of the elastic drive ends and the second phase, the stationary filtration, begins.

The problem of an elastic fluid flow to the aggregate well in an infinite reservoir at the flow-rate $Q_w(t)$ may also be solved approximately using the integral relationships technique. The problem setting is described by Eqs. (23.98), (23.99), (23.101) and (23.107). Let's find the pressure distribution in the reservoir and bottomhole pressure in the aggregate well.

Under the integral relationship technique (see Section 6), the solution is sought for as a binomial with powers of r with the addition of a logarithmic term for a parallel-plane flow (see Eq. (23.82)) where $R(t)$ is the disturbed area radius, and a_0, a_1, a_2, ... are time functions. The pressure distribution Eq. (23.82) is valid for the disturbed area, i. e., for the values $R_z \le r \le R(t)$; for the values $R(t) \le r \le \infty$, pressure equals to initial pressure p_k. The first power binomial will be considered:

$$p(r,t) = a_1 \log\frac{r}{R(t)} + a_0 + a_2\frac{r}{R(t)}. \qquad (23.116)$$

For the determination of parameters a_1, a_0, a_2, we will use the conditions at bottomhole of the aggregate well [Eq. (23.107)] and at the disturbed area boundary:

$$p = p_k \text{ at } r = R(t); \qquad (23.117)$$

$$\partial p / \partial r = 0 \text{ at } r = R(t). \tag{23.118}$$

The latter equation is the condition of the $p(r,t)$ curve smoothness. From this condition:

$$\begin{aligned} a_1 = a_2 &= \frac{Q_w(t)\mu_w}{2\pi kh} \frac{R(t)}{R(t) - R_z}; \\ a_0 = p_k &= \frac{Q_w(t)\mu_w}{2\pi kh} \frac{R(t)}{R(t) - R_z}. \end{aligned} \tag{23.119}$$

Substituting this Eq. (23.119) into Eq. (23.116) gives the pressure distribution:

$$p(r,t) = p_k - \frac{Q_w(t)\mu_w}{2\pi kh[R(t) - R_z]} \left[R(t) \log \frac{R(t)}{r} - R(t) + r \right]. \tag{23.120}$$

Note, that in Eq. (23.120) and all subsequent equations it is not possible to disregard the well radius R_z compared to the disturbed area radius $R(t)$, as it was done previously when we were analyzing the flow to a regular well with $r_c \approx 0.1$ m.

The disturbed area radius is determined from the material balance Eq. (23.58) which is reduced to the following format:

$$\frac{\int_0^t Q_w(t)}{Q_w(t)} = \frac{R_z}{\kappa[R(t) - R_z]} \left[\frac{R^3(t)}{12R_z^2} + \frac{R(t)}{4} - \frac{R_z}{3} - \frac{R(t)}{2} \log \frac{R(t)}{R_z} \right]. \tag{23.121}$$

If $Q_w = \text{const}$, $\int_0^t Q_w(t)dt = Q_w(t)$, and Eq. (23.121) becomes:

$$\frac{\kappa t}{R_z^2} = \text{fo} = \frac{1}{R(t) - R_z} \left[\frac{R^3(t)}{12R_z^2} + \frac{R(t)}{4} - \frac{R_z}{3} - \frac{R(t)}{2} \log \frac{R(t)}{R_z} \right]. \tag{23.122}$$

Eqs. (23.121) and (23.122) are transcendent equations relative to $R(t)$. By solving them graphically or on the computer for different moments in time and substituting the found $R(t)$ values into Eq. (23.120), the pressure distribution in the reservoir at any time will be found. In particular, at $r = R_z$ bottomhole pressure in the aggregate well from Eq. (23.120) is:

$$p(R_z,t) = p_c(t) = p_k - \frac{Q(t)\mu_w}{2\pi kh[R(t) - R_z]} \left[R(t) \log \frac{R(t)}{R_z} - R(t) + R_z \right]. \tag{23.123}$$

The calculation procedure using the approximate Eqs. (23.120), (23.123), (23.121) or (23.122) is as follows: (1) find the production amount $\int_0^t Q_w(t)dt$ from the given water flow-rate *vs.* time correlation $Q_w(t)$ by the moment in time under consideration; (2) calculate $\int_0^t Q_w(t)dt / Q_w(t)$; (3) find $R(t)$ for the same moment in time using Eqs. (23.121) and (23.122); (4) substitute found $R(t)$ value into Eqs. (23.120) and (23.123), thereby finding pressure distribution $p(r,t)$ and bottom-hole pressure $p_c(t)$. one can evaluate the error by using Eq. (23.123) by reducing it to a dimensionless format and comparing its values with the values listed in tables. It is important to note that for large time values, when $R(t) >> R_z$, it is possible to leave in the right part of Eqs. (23.121) and (23.122) only the first term and in the denominator to disregard R_z value compared to the $R(t)$ value. In such a case:

$$\int_0^t Q_w(t)dt / Q_w(t) = R^2(t)/12\kappa t . \tag{23.124}$$

Denoting:

$$\frac{\eta}{R_z^2}\int_0^t Q_w(t)dt / Q_w(t) = \text{fo}', \tag{23.125}$$

where fo' is a known dimensionless time function:

$$R(t) = \sqrt{12\,\text{fo}'}\, R_z . \tag{23.126}$$

If, however, Q_w = const:

$$R(t) = \sqrt{12\,\kappa t} . \tag{23.127}$$

The use of Eqs. (23.126) and (23.127) substantially simplifies pressure calculations.

CHAPTER XXIV

NON-STATIONARY FLOW OF GAS IN A POROUS MEDIUM

1. Mathematical model of non-stationary gas filtration

Basics of the gas flow in a porous medium have been developed by L. S. Leibensohn. He was the first to derive differential equations for non-stationary ideal gas filtration in a porous medium under Darcy's law. This non-linear parabolic differential equation was later called Leibensohn's equation.

It was assumed in the derivation of this equation that porosity and permeability do not depend on pressure (i. e., the reservoir is non-deformable), and gas viscosity also does not depend on pressure, i. e., the gas is ideal. It is also assumed that filtration is isothermal, i. e., the gas and reservoir temperature remains constant. It was shown later that the non-stationary gas filtration may indeed be approximated as isothermal because the gas temperature change occurring under changed pressure is to a significant extent compensated through heat-exchange with the porous reservoir matrix, ant the gas contact surface with matrix is huge.

However, at gas filtration in the bottomhole zone of the reservoir non-isothermal behavior of gas filtration is substantial due to the localization of the major pressure drawdown near the borehole wall. (This effect is utilized in interpretation of thermograms in operating wells for fine-tuning the inflow profile across the reservoir thickness, so-called depth flow-rate metering). In analyzing filtration process in the reservoir as a whole these local effects may be disregarded.

Mathematical model of non-stationary isothermal gas filtration includes flow continuity equation, motion equation (Darcy's law) and equations of state of the gas and porous medium:

$$\frac{\partial \varnothing \rho}{\partial} + \operatorname{div} \rho \bar{w} = 0,$$

$$\bar{w} = -\frac{k}{\mu} \operatorname{grad} p,$$

$$p / \rho = p_{atm} / \rho_{atm},\ \varnothing = \text{const},\ \text{k} = \text{const},\ \mu = \text{const}.$$

After the substitution of Darcy's law into continuity equation and introduction of Leibensohn's function, the equation system is transformed as follows:

$$\begin{aligned} &\frac{\partial \varnothing \rho}{\partial} - \frac{k}{\mu}\Delta P = 0, \\ &\rho \bar{w} = -\frac{k}{\mu}\operatorname{grad} p, \\ &P = \frac{\rho_{\text{atm}} P^2}{2p_{\text{atm}}} + \text{const.} \end{aligned} \tag{24.1}$$

First equation of Eq. (24.1) after substituting the Leibensohn's function, may be rewritten as:

$$\frac{\partial \varnothing \rho}{\partial t} - \frac{\rho_{\text{atm}} k}{2p_{\text{atm}}\mu}\Delta p^2. \tag{24.2}$$

Let's now transform the left part of the above equation. Considering the porosity is constant and the ideal gas equation of state in the isothermal process is:

$$\rho = \frac{\rho_{\text{atm}} p}{p_{\text{atm}}}$$

or:

$$\frac{\partial \varnothing \rho}{\partial t} - \frac{\rho_{\text{atm}} \varnothing}{p_{\text{atm}}}\frac{\partial p}{\partial t},$$

after the transformation the following equation with only one unknown variable, pressure:

$$\frac{\partial \rho}{\partial t} = \frac{k}{2\mu\varnothing}\Delta p^2. \tag{24.3}$$

The derived differential equation for non-stationary isothermal filtration of ideal gas Eq. (24.3) is Leibensohn's equation. It is a parabolic type nonlinear differential equation in partial derivatives. It is valid in a case where Darcy's law is realized. Porosity variability is disregarded because the porosity factor enters the equation as a product $\rho\varnothing$, where gas density is much more variable than porosity.

Eq. (24.3) is represented in a no-subscript format valid for any coordinate system. In the Cartesian coordinate system the equation is:

$$\frac{\partial \rho}{\partial t} = \frac{k}{2\mu\varnothing}\left(\frac{\partial^2 p^2}{\partial x^2} + \frac{\partial^2 p^2}{\partial y^2} + \frac{\partial^2 p^2}{\partial z^2}\right)\Delta p^2.$$

It also may be written differently by multiplying it by pressure p and keeping in mind that:

$$p\frac{\partial p}{\partial t}=\frac{1}{2}\frac{\partial p^2}{\partial t}:$$

$$\frac{\partial p^2}{\partial t}=\frac{kp}{\mu\emptyset}\Delta p^2$$

or in Cartesian coordinate system:

$$\frac{\partial p^2}{\partial t}=\frac{kp}{\mu\emptyset}\left(\frac{\partial^2 p^2}{\partial x^2}+\frac{\partial^2 p^2}{\partial y^2}+\frac{\partial^2 p^2}{\partial z^2}\right). \tag{24.2}$$

In this format, under both coordinate and time derivatives is one and the same function p^2 but the factor in front of Laplace's operator is variable and contains the sought-for function $p(x,y,z,t)$.

It is easy to show that non-stationary filtration of a real gas with equation of state:

$$\rho=\frac{\rho_{\text{atm}}p}{p_{\text{atm}}z(p)}$$

and in consideration of viscosity being a function of pressure $\mu(p)$ and porous medium being non-deformable ($\emptyset=\text{const}$, $k=\text{const}$), is described by the following parabolic type nonlinear differential equation:

$$\frac{\partial}{\partial t}\frac{p}{z(p)}=\frac{k}{2\emptyset}\left(\frac{\partial}{\partial x}\left(\frac{1}{\mu(p)z(p)}\frac{\partial p^2}{\partial x}\right)+\frac{\partial}{\partial y}\left(\frac{1}{\mu(p)z(p)}\frac{\partial p^2}{\partial y}\right)+\frac{\partial}{\partial z}\left(\frac{1}{\mu(p)z(p)}\frac{\partial p^2}{\partial z}\right)\right).$$

To solve the specific problems in non-stationary gas filtration, differential equation in the Eq. (24.3) or Eq. (24.4) format should be integrated over the entire gas accumulation with the initial and boundary conditions.

Eq. (24.3) or (24.4) is a complex nonlinear equation in partial derivatives. In most cases it does not have exact analytical solution. It may be integrated using the computer or solve it approximately. The approximate solutions techniques are well developed. Some of them have already been reviewed earlier in this book as applied to the elastic drive problems (for instance, the technique of sequential change of the stationary state, etc.).

Numerical techniques in solving various non-stationary gas filtration problems based on Leibensohn's equation are also well substantiated in applied problems of gas field development. The most common are the techniques of finite difference and finite elements. The practice of the gas field development changed over time (increase in depth, pressure and temperature, multi-component nature of many gases). All these needed to be taken into account in the main Leibensohn's equa-

tion. It is possible to use Leibensohn's function for ideal gas under low pressures in deformable reservoirs. For real gases under high pressure and in deformable reservoirs, Leibensohn's function should be calculated as Eq. (19.20):

$$P = \int \frac{k(p)}{\mu(p)} \rho(p)\, dp. + \text{const.}$$

At non-isothermal filtration, changes in gas properties with temperature should be considered.

Eq. (24.3) was derived using Darcy's law as the motion equation. Subsequent studies (Charny, Minsky, etc.) showed, however, that for the natural gas filtration the nonlinear (binomial) filtration law should be used. The mathematical difficulties in solving the so produced differential equation become even greater.

One of the efficient directions in solving Leibensohn's equation is its linearization, i. e., reducing it to linear Fourier's equation.

2. Linearization of Leibensohn's equation and the main solution of linearized equation

If nonlinear differential equation [Eq. (24.3) or Eq. (24.4)] is replaced by a linear equation (i. e., if it is linearized), the differential equation simplifies to a linear equation with exact analytical solutions. Clearly, such exact solutions would be approximations for the nonlinear equation. The error of such replacement may be estimated by the comparison with a computer-found solution of exact equation.

Different ways for linearization of Eq. (24.3) or Eq. (24.4) have been proposed. In the case of the radial-plane flow to a well, the non-transient gas filtration theory (see Chapter IV) predicts a very steep pressure drawdown funnel, and pressure over most of the reservoir is only slightly different from contour pressure. Based on this, Leibensohn proposed to replace variable pressure p in the coefficient in front of Laplace's operator in Eq. (24.4) by constant pressure p_k equal to initial reservoir pressure. Then, denoting $\tilde{\eta} = kp_k / \mu \varnothing$, another equation will be obtained instead of Eq. (24.4):

$$\frac{\partial p^2}{\partial t} = \tilde{\eta}\left(\frac{\partial^2 p^2}{\partial x^2} + \frac{\partial^2 p^2}{\partial y^2} + \frac{\partial^2 p^2}{\partial z^2}\right). \tag{24.5}$$

This is linear piezo-conductivity equation relative to p^2 (compare with Eq. (23.17), where $\tilde{\eta}$ is a constant similar to the piezo-conductivity factor). This way of linearization, when the variable factor in Eq. (7.109) is taken for a constant, is called Leibensohn's linearization. For instance, Charny (1961) proposed to reduce Eq. (24.4) to the linear format by replacing variable pressure in the coefficient in front of Laplace's operator by:

$$p_{avg} = p_{min} + 0.7(p_{max} - p_{min}),$$

where p_{max} and p_{min} are maximum and minimum gas accumulation's formation pressures during the estimation period.

Now, the linearized Eq. (24.5) is used to solve a problem of gas flow into a well of infinitely small diameter (a point drain) located in an infinite size reservoir of thickness h. At the initial moment the reservoir is undisturbed, i. e., formation pressure in the entire reservoir is constant an equal to p_k. From this point forward, the gas production begins at a constant flow-rate Q_{atm}. The goal is to find the formation pressure in the reservoir with respect to time $p(r,t)$.

For the radial-plane filtration, Fourier's Eq. (23.40), and for gas filtration:

$$\frac{\partial p^2}{\partial t} = \tilde{\eta}\left(\frac{\partial^2 p^2}{\partial r^2} + \frac{1}{r}\frac{\partial p^2}{\partial r}\right). \tag{24.6}$$

This equation needs to be integrated under the initial condition:

$$p^2(r,t) = p_k{}^2 \text{ at } t = 0; \tag{24.7}$$

with the boundary condition for remote points of the reservoir being:

$$p^2(r,t) = p_k^2 \text{ at } t > 0 \text{ and } r \to \infty. \tag{24.8}$$

Let's write the condition for bottomhole pressure. For this purpose, let's introduce the expression for the mass flow-rate based on Darcy's law for radial-plane filtration in the differential format:

$$Q_m = \rho w S = \frac{\rho_{atm}}{p_{atm}} p \frac{k}{\mu}\frac{\partial p}{\partial r} 2\pi r h.$$

Using equations:

$$2p\frac{\partial p}{\partial r} = \frac{\partial p^2}{\partial r}$$

and:

$$Q_m = \rho_{atm} Q_{atm},$$

one obtains:

$$Q_{atm} = \rho w S = \frac{\pi h k}{p_{atm}\mu} r \frac{\partial p^2}{\partial r}.$$

From this equation the condition at the wall of an infinitely small radius gas well is obtained:

$$r\frac{\partial p^2}{\partial r} = \frac{Q_{atm} p_{atm} \mu}{\pi k h} \text{ at } r = 0. \tag{24.9}$$

Thus, to solve the assigned problem, Eq. (24.6) should be integrated under the conditions of Eqs. (24.7)–(24.9).

In this Chapter, a similar problem is solved with the elastic liquid production from an infinite and initially undisturbed elastic reservoir through a well at a constant flow-rate Q. The mathematical setting of the problem is represented by Eq. (23.40) under the condition of Eq. (23.41). Then these relationships for the elastic liquid are quoted and compared with the relationships of Eq. (24.6) and Eqs. (24.7)–(24.9) for the gas.

$$\frac{\partial p}{\partial t} = \kappa\left(\frac{\partial^2 p}{\partial r^2} + \frac{1}{r}\frac{\partial p}{\partial r}\right). \qquad \frac{\partial p^2}{\partial t} = \tilde{\eta}\left(\frac{\partial^2 p^2}{\partial r^2} + \frac{1}{r}\frac{\partial p^2}{\partial r}\right).$$

$$p(r,t) = p_k \text{ at } t = 0; \qquad p^2(r,t) = p_k{}^2 \text{ at } t = 0;$$

$$p(r,t) = p_{gal} \text{ at } t > 0 \text{ and } r \to \infty; \qquad p^2(r,t) = p_k^2 \text{ at } t > 0 \text{ and } r \to \infty;$$

$$r\frac{\partial p}{\partial r} = \frac{Q\mu}{2\pi kh} \quad r = 0. \qquad r\frac{\partial p^2}{\partial r} = \frac{Q_{atm}\, p_{atm}\mu}{\pi kh} \text{ at } r = 0.$$

As it can be seen, pressure in all ideal gas equations is squared, whereas it is to power one for the elastic liquid. The piezoconductivity factor for liquid is replaced by $\tilde{\eta} = kp_k$ for the gas, and $Q\mu/2\pi kh$ is replaced by $Q_{atm}\, p_{atm}\mu/\pi kh$. The rest remains the same.

As it was shown, the solution of the problem for an elastic liquid is the major equation of the elastic drive-Eq. (23.52):

$$p(r,t) = p_k - \frac{Q_0\mu}{2\pi kh}\left[-\mathrm{Ei}\left(-\frac{r^2}{4\kappa t}\right)\right].$$

The similarity between filtration of an elastic liquid and gas indicates that if in Eq. (23.52) pressure is substituted by p^2, κ by $\tilde{\eta}$, $Q\mu/2\pi kh$ by $Q_{atm}p_{atm}\mu/\pi kh$, this gives the solution of the set problem for the gas:

$$p^2(r,t) = p_k^2 - \frac{Q_{atm}\, p_{atm}\mu}{2\eta kh}\left[-\mathrm{Ei}\left(-\frac{r^2}{4\tilde{\eta}t}\right)\right]. \tag{24.10}$$

or:

$$p(r,t) = \sqrt{p_k^2 - \frac{Q_{atm}\, p_{atm}\mu}{2\eta kh}\left[-\mathrm{Ei}\left(-\frac{r^2}{4\tilde{\eta}t}\right)\right]}. \tag{24.11}$$

This is the main solution of Leibensohn's linearized equation.

For small values of the variable $\frac{r^2}{4\eta t}$, as in the main equation of the elastic drive theory Eq. (23.53), the integral exponential function can be replaced by a logarithmic one:

$$p^2(r,t) = p_k^2 - \frac{Q_{atm} p_{atm} \mu}{2\eta kh}\left(\ln\frac{4\eta t}{r^2} - 0.5772\right) \tag{24.12}$$

or:

$$p(r,t) = \sqrt{p_k^2 - \frac{Q_{atm} p_{atm} \mu}{2\eta kh}\left(\ln\frac{4\eta t}{r^2} - 0.5772\right)}. \tag{24.13}$$

Once again, the solution Eqs. (24.10)–(24.13) are approximate ones as they are obtained from integration of Leibensohn's linearized equation.

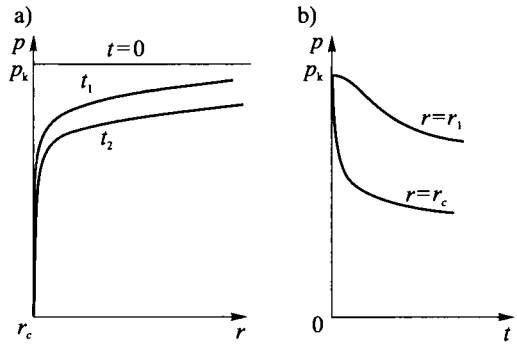

Fig. 24.1. Pressure distribution in the reservoir under non-stationary gas flow to a well at different moments in time (a) and pressure dynamics at certain points in the reservoir (b).

Eqs. (24.12) and (24,13) determine pressure distribution around the gas well operating at a constant flow-rate from the moment in time t_0. These depression curves have the same shape as for non-transient filtration: they are very steep next to the well (Fig. 24.1a). If the value of r is assigned, it is possible to find pressure change at a given point with time. In particular, it is posible to determine pressure change at the bottomhole ($r = r_c$) after the well began operating (Fig. 24.1b):

$$p_c(r,t) = \sqrt{p_k^2 - \frac{Q_{atm} p_{atm} \mu}{2\eta kh}\left(\ln\frac{4\eta t}{r^2} - 0.5772\right)}. \tag{24.14}$$

3. Point solution of an automodel problem on axisymmetric gas flow to a well with a constant flow-rate

The previous section includes a solution of the problem of non-stationary ideal gas flow at a constant flow-rate to a well of infinitely small diameter. The solution was obtained by integrating the linearized differential equation.

Barenblatt (1982) used analysis of dimensions to show that at certain initial and boundary conditions the non-linear Leibensohn's equation has exact solution. This is important as the derived exact solution may serve as the standard for comparison with approximate solutions.

As in Sec. 2, the problem of non-stationary radial-plane gas flow at a constant flow-rate to a well in an infinite reservoir will be analyzed. In this case it is necessary to integrate the non-linear Leibensohn's equation:

$$\frac{\partial p}{\partial t} = \frac{k}{2\mu\varnothing}\left(\frac{\partial^2 p^2}{\partial r^2} + \frac{1}{r}\frac{\partial p^2}{\partial r}\right). \tag{24.15}$$

under the same initial and boundary conditions [Eqs. (24.7)–(24.9)].

Barenblatt showed that as set here, the problem is an automodel one, i. e., pressure depends on some complex, which includes both variables r and t, and partial derivatives differential Eq. (24.15) is reduced to a regular differential equation which is integrable.

In order to establish the variables on which pressure is dependent, a dimensionality analysis should be performed. As follows from the problem setting, pressure distribution in the reservoir depends on five definitive parameters ($n = 5$): r, t, p_k, $k/2\mu\varnothing$; $Q_{atm}p_{atm}\mu/\pi kh$.

Let's denote length dimensionality as $[L]$, time dimensionality as $[T]$, pressure dimensionality as $[p]$. Then dimensionalities of these parameters will be:
$[r] = L$, $[t] = T$, $[p_k] = [p]$, $[k/2\mu\varnothing] = L^2[p]^{-1}T^{-1}$, $[Q_{atm}p_{atm}\mu/\pi kh] = [p]^2$.

Three of these parameters have independent dimensionalities: r, t, p_k ($i = 3$). As follows from Π-theorem (Chapter V, p. 4), the sought-for function, i. e., pressure reduced to dimensionless format $F = p/p_k$, will depend on two dimensionless complexes ($n - k = 5 - 3 = 2$). It is easy to check that these complexes are:

$$\xi = \frac{r}{\sqrt{\frac{k}{2\mu\varnothing}p_k t}} = \frac{r}{\sqrt{\frac{\eta t}{2}}} \text{ and } \lambda = \frac{Q_{atm}p_{atm}\mu}{2khp_k^2},$$

i. e.,

$$F = p/p_k = F(\xi,\lambda).$$

Taking derivative of the F function with respect to r and t and substituting derivatives into Eq. (24.15), gives the function F satisfying the regular differential equation:

$$\frac{d^2F^2}{d\xi^2}+\frac{1}{\xi}\frac{dF^2}{d\xi}+\frac{\xi}{2}\frac{dF}{d\xi}=0. \tag{24.16}$$

The initial and boundary conditions [Eqs. (24.7)–(24.9)] are as follows:

$$\xi\frac{dF^2}{d\xi}=\lambda \text{ at } \xi=0;\ F(\xi,\lambda)=1 \text{ at } \xi=\infty. \tag{24.17}$$

Eq. (24.16) was numerically integrated under the conditions of Eq. (24.7). The results are presented (Table 24.1) for the values $\lambda = 0.01$ and $\lambda = 0.04994$. ξ^* in the table is such value of the variable ξ that for $\xi < \xi^*$, the values of $\xi dF^2/d\xi$ differ from λ by less than 0.01 %. This means that for $\xi < \xi^*$, it may be stated that $\xi dF^2/d\xi = \lambda$. Upon integrating this equation:

$$F^2 = F^2(\xi^*,\lambda)+\lambda\log(\xi/\xi^*)$$

or:

$$F=\sqrt{F^2(\xi^*,\lambda)+\lambda\log(\xi/\xi^*)} \text{ for } \xi<\xi^*. \tag{24.18}$$

For this reason the values of $F(\xi,\lambda)$ for $\xi < \xi^*$ are not included into the table.

By comparing the dimensionless pressure values $p/p_k = F(\xi,\lambda)$ in Table 24.1 with those calculated from Eq. (24.12), it is possible to find the error introduced by linearization of Leibensohn's equation.

Table 24.1

Numerical values of automodel solution

$\lambda = 0.01$		$\lambda = 0.004994$	
ξ	$F(\xi,\lambda)$	ξ	$F(\xi,\lambda)$
$\xi^* = 0.005787$	0.9701	$\xi^* = 0.003886$	0.9842
0.01157	0.9737	0.01555	0.9877
0.01923	0.9763	0.03109	0.9894
0.03472	0.9793	0.06218	0.9912
0.06553	0.9825	0.2487	0.9947
0.09645	0.9845	0.4974	0.9964
0.1582	0.9870	0.9949	0.9980
0.2816	0.9899	1.492	0.9988
0.5285	0.9930	2.487	0.9996
0.7754	0.9948	3.482	0.9999
1.269	0.9970		
1.763	0.9982		
2.751	0.9994		
3.738	0.9999		

4. Solution of the problem of gas flow to a well using sequential change of stationary states technique

As indicated in Chapter XXIII, Section 6, this technique is based on the following assumptions: at each time the reservoir is subdivided into two areas, one disturbed and the other, undisturbed. It is assumed that in the disturbed area, which begins from the well's wall, pressure is distributed so that the liquid flow within the area is non-transient, and the external boundary of the area is serving at a given moment in time as the charge contour. Pressure within the undisturbed reservoir area is constant and is equal to the initial contour pressure. The motion pattern of the movable boundary between the disturbed and undisturbed areas is determined from the material balance equation and boundary conditions.

Let's apply this technique to the solution of the problem reviewed in Sections 1 and 2, i. e., the problem of non-stationary flow of gas to the well at a constant rate Q_{atm}. However, as opposed to the problem in Section 1, the finite well radius equal to r_c is considered.

At any time, the disturbed area is a round area of radius $R(t)$, pressure within which is distributed under the stationary condition [Eq. (20.42)]:

$$p = \sqrt{p_k^2 - \frac{p_k^2 - p_c^2}{\log(R_k / r_c)} \log \frac{R(t)}{r}}. \quad r_c \le r \le R(t). \tag{24.19}$$

Outside of the disturbed area, pressure is equal to the initial pressure (the undisturbed state):

$$p = p_k, \; r > R(t).$$

It is also possible to write the expression Eq. (20.43) for the flow-rate of the disturbed area:

$$Q_{atm} = \frac{\pi k h}{\mu p_{atm}} \frac{p_k^2 - p_c^2}{\ln(R(t)/r_c)}. \tag{24.20}$$

In the problem under review, bottomhole pressure is a function of time. For the convenience of further discussion, Eq. (24.20) is rearranged to:

$$\frac{p_k^2 - p_c^2}{\ln \dfrac{R(t)}{r_c}} = \frac{Q_{atm} p_{atm} \mu}{\pi k h}$$

Substituting this equation into the pressure Eq. (24.19), gives:

$$p = \sqrt{p_k^2 - \frac{Q_{atm} p_{atm} \mu}{\pi k h} \ln \frac{R(t)}{r}}. \quad r_c \le r \le R(t), \tag{24.21}$$

i. e., pressure distribution expressed through the given flow-rate and reservoir parameters.

In order to find $R(t)$, material balance equation is used. The initial gas reserves (at $p = p_k$) within the reservoir area of radius $R(t)$ are:

$$M_0 = \pi\left(R^2(t) - r_c^2\right)h\varnothing\rho_k = \pi\left(R^2(t) - r_c^2\right)h\varnothing\frac{\rho_{atm}}{p_{atm}}p_k . \qquad (24.22)$$

The current gas reserves may be expressed through weighted average pressure $\hat{p}$:

$$M_{cur} = \pi\left(R^2(t) - r_c^2\right)h\varnothing\hat{p} = \pi\left(R^2(t) - r_c^2\right)h\varnothing\frac{\rho_{atm}}{p_{atm}}\hat{p}, \qquad (24.23)$$

where $\hat{p}$ is determined from Eq. (20.48) for transient-free filtration:

$$\hat{p} \approx p_k\left[\frac{1 - p_c^2/p_k^2}{4\ln(R_k/r_c)}\right]. \qquad (24.24)$$

The gas is produced at a constant flow-rate Q_{atm}, so that the gas mass produced by the moment in time t is equal to $\rho_{atm}Q_{atm}t$. Therefore:

$$M_0 - M_t = \rho_{atm}Q_{atm}t$$

or, by using Eqs. (24.22) and (24.23):

$$\pi\left(R^2(t) - r_c^2\right)h\varnothing\frac{\rho_{atm}}{p_{atm}}(p_k - \hat{p}) = \rho_{atm}Q_{atm}t. \qquad (24.25)$$

Substituting Eqs. (24.23) and (24.24) into Eq. (24.25), results in:

$$\pi\left(R^2(t) - r_c^2\right)h\varnothing\frac{\rho_{atm}}{p_{atm}}\frac{(p_k^2 - p_c^2)}{4p_k\ln(R(t)/r_c)} = \rho_{atm}\frac{\pi kh(p_k^2 - p_c^2)t}{\mu p_{atm}\ln(R(t)/r_c)},$$

and thus:

$$R^2(t) - r_c^2 = \frac{4kp_k}{\mu\varnothing}t = 4\tilde{\eta}t$$

or:

$$R(t) = \sqrt{r_c^2 + 4\tilde{\eta}t}\,. \qquad (24.26)$$

For the time values for which $4\tilde{\eta}t >> r_c^2$:

$$R(t) = 2\sqrt{\tilde{\eta}t}\,. \qquad (24.27)$$

Now that the motion rule of the disturbed area boundary is known according to Eq. (24.16) or Eq. (24.27), it is possible to determine pressure at any point of the reservoir at any time using Eq. (24.21), as well as bottomhole pressure change at any point in time:

$$p = \sqrt{p_k^2 - \frac{Q_{atm} p_{atm} \mu}{\pi k h} \ln \frac{\sqrt{4\tilde{\eta} t + r_c^2}}{r}} \qquad (24.28)$$

$$r_c \le r \le \sqrt{r_c^2 + 4\tilde{\eta} t}, \; p = p_k, \; r > \sqrt{r_c^2 + 4\tilde{\eta} t},$$

$$p_c = \sqrt{p_k^2 - \frac{Q_{atm} p_{atm} \mu}{\pi k h} \ln \frac{\sqrt{4\tilde{\eta} t + r_c^2}}{r_c}} \; . \qquad (24.29)$$

Eqs. (24.28) and (24.29) are valid for the infinite reservoir and for finite open and closed reservoir of radius R_k. In the latter case, they are only valid for the first phase of the motion until the pressure drawdown funnel reaches the reservoir boundary, i. e. for:

$$R(t) = 2\sqrt{\tilde{\eta} t} \le R_k \; .$$

Pressure changes in the second phase depend on the reservoir's boundary conditions. If the reservoir is closed, pressure will continue declining over the entire reservoir, including the boundary. If the reservoir is open ($p = p_k$ or $r = R_k$), i. e., under the water drive, then a stationary regime will form in the second phase with the constant pressure drawdown $p_k - p_c$, where:

$$p_c = \sqrt{p_k^2 - \frac{Q_{atm} p_{atm} \mu}{\pi k h} \ln \frac{\sqrt{R_k}}{r_c}} \; .$$

5. Solution of the gas flow to well problem using averaging technique

Let's review another technique applicable to the problems of non-stationary gas filtration – the technique of averaging time derivative over the space domain.

Consider an example of rectilinear parallel filtration of a real gas. The exact differential equation for this case is:

$$\frac{\partial}{\partial t} \frac{p}{z(p)} = \frac{k}{\mu \varnothing} \left(\frac{\partial}{\partial x} \left(\frac{p}{z(p)} \frac{\partial p}{\partial x} \right) \right).$$

Suppose, it is possible to substitute $\tilde{z} = z(p_{avg})$ instead of supercompressibility $z(p)$, where p_{avg} is some average pressure in the moving gas. Let's now introduce the denotation $p_1 = p/z(p)$. Then the latter equation becomes:

$$\frac{\partial}{\partial t} p_1 = \frac{k\tilde{z}}{\mu \varnothing} \left(\frac{\partial}{\partial x} \left(p_1 \frac{\partial p_1}{\partial x} \right) \right). \qquad (24.30)$$

Suppose, there is an initially undisturbed gas-saturated reservoir of the width B, thickness h and length L. From one side ($x = 0$) the reservoir is penetrated in a gallery, and from all other sides it is bounded by impermeable planes. At the moment in time $t = 0$ the gas begins to produce trough the gallery at a constant mass flow-rate, which may be expressed, under Darcy's law, as follows:

$$Q_m = \rho w B h = \frac{\rho_{atm} p k}{p_{atm} \tilde{z} \mu} \frac{\partial p}{\partial x} B h = B h \tilde{z} \frac{Q_{atm} \rho_{atm} k}{2 p_{atm} \mu} \frac{\partial p_1^2}{\partial x}.$$

It is required to determine pressure in the reservoir at any moment in time $t > 0$. For this purpose, Eq. (24.30) should be solved within the domain $0 \le x \le L, t \ge 0$, which satisfies the initial condition [Eq. (24.31)] and boundary conditions [Eqs. (24.32) and (24.33)]:

$$p_1 = p_{10} \text{ at } t = 0; \tag{24.31}$$

$$\frac{\partial p_1^2}{\partial x} \frac{Q\mu}{k} \text{ at } x = 0 \text{ where } Q = \frac{2 Q_m p_{atm}}{B h \tilde{z} \rho_{atm}}, \tag{24.32}$$

$$\frac{\partial p_1^2}{\partial x} = 0 \text{ at } x = L. \tag{24.33}$$

As under the change of stationary states technique, it is assumed that at each moment in time there is a finite disturbed area, $l(t)$, at the boundaries of which the following conditions are realized:

$$p_1^2 = p_{10.}^2 \quad \frac{\partial p_1^2}{\partial x} = 0 \text{ at } x = l(t). \tag{24.34}$$

The pivot in this technique is the acceptance of the condition:

$$\frac{\partial p_1}{\partial t} = F(t) \tag{24.35}$$

which is equivalent to a supposition that pressure in the entire disturbed portion of the reservoir changes at an equal rate; then, Eq. (24.30) changes to the following format:

$$\tilde{z} \frac{\partial^2 p_1^2}{\partial x^2} = \frac{2 \varnothing \mu}{k} F(t). \tag{24.36}$$

Integrating this equation twice with respect to x, gives:

$$p_1^2 = \frac{\varnothing \mu}{k} \frac{F(t)}{2} x^2 + bx + c = F(t). \tag{24.37}$$

Using the boundary conditions at the gallery [Eq. (24.32)] and at the disturbed zone boundary [Eq. (24.34)], let's find the integration constants b and c as well as the function $F(t)$:

$$b = \frac{Q\mu}{k},\ c = p_{10}^2 = \frac{Q\mu l(t)}{2k},\ F(t) = \frac{Q\tilde{z}}{2\varnothing l(t)}.$$

The result is:

$$p_1^2 = p_{10}^2 - \frac{Q\mu l(t)}{2k}\left(1 - \frac{x}{l(t)}\right)^2,\ 0 \le x \le l(t). \tag{24.38}$$

Determine the $l(t)$ function. For this purpose, the initial Eq. (22.30) is integrated twice with respect to the coordinate and time:

$$\frac{2\varnothing\mu}{k}\int_0^{l(t)}\int_0^t \frac{\partial p_1}{\partial t}dtdx = \tilde{z}\int_0^t\int_0^{l(t)} \frac{\partial^2 p_1^2}{\partial x^2}dtdx.$$

Then, using the boundary conditions [Eqs. (24.32) and (24.34)], the equation for weighted average pressure is obtained:

$$\hat{p} = p_{10} - \frac{\tilde{z}Qt}{2\varnothing l(t)}. \tag{24.39}$$

Let's accept a hypothesis that weighted average pressure is:

$$\hat{p} = \frac{1}{l}\int_0^l p_1(x,t)dx$$

for this particular case, then it is determined from this equation:

$$\hat{p} = \sqrt{\frac{1}{l}\int_0^l p_1(x,t)dx} = \sqrt{\frac{1}{l}\int_0^l\left[p_{10}^2 - \frac{Q\mu l}{2k}\left(1 - \frac{x}{l}\right)^2\right]dx} = \sqrt{p_{10}^2 - \frac{Q\mu l}{6k}}. \tag{24.40}$$

Reduce equations for $\hat{p}_1$ [Eqs. (24.39) and (24.40)] to a dimensionless format format and equate them:

$$1 - \frac{\tilde{z}Qt}{2\varnothing l(t)p_{10}} = \sqrt{1 - \frac{Q\mu l(t)}{6kp_{10}^2}}. \tag{24.41}$$

This equation is used for the determination of $l(t)$. However, a very simple approximate equation may be derived. Denoting $Q\mu l \Big/ 6kp_{10}^2 = u$ and expanding the right part of Eq. (24.41) into a series:

$$\sqrt{1-u} = 1 - \frac{u}{2} - \frac{u^2}{8} - \ldots$$

Keeping two first terms of the series:

$$\sqrt{1-\frac{Q\mu l(t)}{6kp_{10}^2}} \approx 1-\frac{Q\mu l(t)}{12kp_{10}^2}.$$

In this case, Eq. (24.41) takes the following format:

$$1-\frac{\tilde{z}Qt}{2\varnothing l(t)p_{10}} \approx 1-\frac{Q\mu l(t)}{12kp_{10}^2},$$

and from there:

$$l(t)=\sqrt{6\frac{k}{\mu}\frac{\tilde{z}p_{10}}{\varnothing}t}. \qquad (24.42)$$

Substituting this expression into Eq. (24.38), gives the pressure as a decisive function of the coordinate and time.

At the time T when the disturbed zone reaches the impermeable reservoir boundary ($l(t) = L$), the first phase has ended. To determine its duration, let's assign in Eq. (24.41), $l(t) = L$ and find the time T:

$$T=\frac{2\varnothing p_{10}L}{\tilde{z}Q}\left(1-\sqrt{1-\frac{Q\mu L}{6kp_{10}}}\right). \qquad (24.43)$$

One can find the approximate T value from Eq. (24.42) and see that the error does not exceed 3 to 4 %.

During phase two, pressure at the boundary $x = L$ declines, and the condition of Eq. (24.33) is realized. Equations for the phase two of the gas reservoir depletion are constructed in a similar way. After similar calculations, we establish pressure distribution law in the reservoir:

$$p_1^2 = p_{1g}^2 - \frac{Q\mu x}{2k}\left(1-\frac{x}{2L}\right),\ 0 \le x \le L, \qquad (24.44)$$

and pressure distribution law at the gallery:

$$p_{1g}^2 = \left(p_{10}-\frac{Q\tilde{z}}{2\varnothing L}t\right)^2 - \frac{Q\mu l}{3k}. \qquad (24.45)$$

6. Application of superposition principle to problems of non-stationary gas filtration

The superposition technique (flow superposition method) is used to solve linearized equation of non-stationary filtration [Eq. (24.5)]. This equation is linear and uniform relative to p^2. Therefore, if $p_i^2(x,y,z,t)$, where $i = 1, 2, \ldots, n$, defines pres-

sure distribution as a result of the performance of i^{th} well and is a solution of Eq. (24.5), their linear combination $p^2 = \sum_i^n c_i p_i^2$ is also a solution of Eq. (24.5).

The superposition technique enables the solution of numerous problems occurring in the design of gas field development.

Using the superposition technique, we will derive equation of bottomhole pressure buildup after gas well shut-in and will show how the gas interval reservoir properties may be determined from the pressure buildup curve.

Suppose a gas well in an infinite reservoir was producing over a long period of time T at a constant flow-rate Q_{atm} and was suddenly shut-in at the moment T in time (i. e., flow of gas to the well suddenly stopped).

Using the superposition technique, it is assumed that at the moment in time $t = T$ an injection well began operating at the same injection rate simultaneously with the production well. Then:

$$p_k^2 - p_c^2 = \frac{Q_{atm} p_{atm} \mu}{2\pi kh}\left(\log\frac{2.25\tilde{\eta}t}{r_c^2} - \ln\frac{2.25(t-T)}{r_c^2}\right). \tag{24.46}$$

Besides, at the moment of the well shut-in the following equation is realized:

$$p_k^2 - p_c^2(T) = \frac{Q_{atm} p_{atm} \mu}{2\pi kh}\left(\ln\frac{2.25\tilde{\eta}t}{r_c^2}\right). \tag{24.47}$$

Let's subtract Eq. (24.46) from Eq. (24.47):

$$\begin{aligned} p_k^2(t) - p_c^2(T) &= \frac{Q_{atm} p_{atm} \mu}{2\pi kh}\left(\ln\frac{2.25\tilde{\eta}T}{r_c^2} - \ln\frac{2.25\tilde{\eta}t}{r_c^2} + \ln\frac{2.25(t-T)}{r_c^2}\right) = \\ &= \frac{Qp\mu}{2\pi kh}\left(\ln\frac{2.25\tilde{\eta}(t-T)}{r_c^2} - \ln\frac{t}{T}\right). \end{aligned} \tag{24.48}$$

If prior to shut-in the well operated for a long time T, and $t - T << T$, then:

$$\ln\frac{t}{T} << \ln\frac{2.25\tilde{\eta}(t-T)}{r_c^2}$$

and the term log t/T in Eq. (24.48) may be disregarded. Then:

$$p_c^2(t) - p_c^2(T) = \frac{Q_{atm} p_{atm} \mu}{2\pi kh}\left(\ln\frac{2.25\tilde{\eta}T}{r_c^2}\right). \tag{24.49}$$

Suppose the moment of the well shut-in T is a new beginning of the time count: $t' = t - T$. Then Eq. (24.49) may be written as:

$$p_c^2(t') - p_c^2(0) = \frac{Q_{atm} p_{atm} \mu}{2\pi kh}\left(\ln\frac{2.25\tilde{\eta}t'}{r_c^2}\right). \tag{24.50}$$

The bottomhole pressure buildup curve is shown in Fig. 24.2. One can see from Eq. (24.50) that the correlation $p_c^2(t') - p_c^2(0)$ vs. log t' is linear (Fig. 24.3).

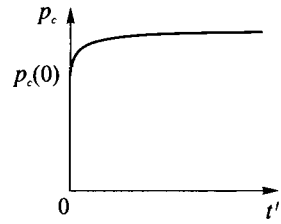

Fig. 24.2. Bottomhole pressure distribution after the well is shut-in.

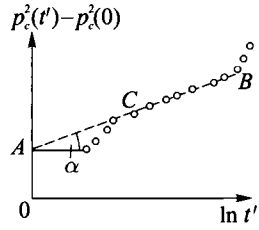

Fig. 24.3. $p_c^2(t') - p_c^2(0)$ vs. $\ln t'$.

Let's identify in the right portion of Eq. (24.50), a term containing log t'.

$$p_c^2(t') - p_c^2(0) = \frac{Q_{atm} p_{atm} \mu}{2\pi kh} \ln t' + \frac{Q_{atm} p_{atm} \mu}{2\pi kh} \ln \frac{2.25\tilde{\eta}}{r_c^2}. \qquad (24.51)$$

$i = \dfrac{Qp\mu}{2\pi kh}$ is the tangent of the angle between the straight line AB and x-axis, and OA is the segment cut by the AB line on the y-axis, which is equal to:

$$OA = \frac{Q_{atm} p_{atm} \mu}{2\pi kh} \ln \frac{2.25\tilde{\eta}}{r_c^2} = i \ln \frac{2.25\tilde{\eta}}{r_c^2}. \qquad (24.52)$$

During the well testing under non-stationary regime (conducted in order to derive reservoir properties), p_c values are obtained at different times t' after the well is shut-in. These data are processed in coordinates $p_c^2(t') - p_c^2(0)$ and ln t' (or log t').

The experimental points are shown in Fig. 24.3. Usually a straight-line segment may be identified on the experimental line. From this segment, the values of $i = \mathrm{tg}\alpha$ and OA are determined. Knowing these values and the well flow-rite prior to the shut-in, it is possible to determine the reservoir hydroconductivity factor:

$$\frac{kh}{\mu} = \frac{Q_{atm} p_{atm}}{2\pi i} \qquad (24.53)$$

and the complex parameter:

$$\frac{\tilde{\eta}}{r_c^2} = \frac{1}{2.25} e^{OA/i}. \tag{24.54}$$

On the AC segment, the experimental points deflect from the straight line due to the gas inflow into the well after the shut-in, which was not taken into account in Eqs. (24.46)–(24.48), and due to some other factors.

Eq. (24.46) may be rewritten as follows:

$$p_k^2 - p_c^2 = \frac{Q_{atm} p_{atm} \mu}{2\pi kh} \ln \frac{t}{t-T}$$

or:

$$p_c^2(t') = p_k^2 - i \ln \frac{T+t'}{t'}. \tag{24.55}$$

Pressure buildup curves after the well was shut-in are also processed using Horner's technique in coordinates $p_c^2(t')$ and $\ln \frac{T+t'}{t'}$. Eq. (24.55) in this coordinates represent a straight line. From the inclination angle of this line one may determine hydroconductivity factor [Eq. (24.53)]. By extrapolating the line to the y-axis ($\ln \frac{T+t'}{t'} = 0$), formation pressure p_k (which is usually unknown) is found.

7. Approximate solution of gas production from closed reservoir problems using the material balance equation

Let's review several problems associated with the gas production from a closed round accumulation of radius r_c. Prior to well penetration of the reservoir, pressure in the entire accumulation is constant and equal to p_k.

Two simple cases are considered: (a) the gas extraction occurs at a constant flow-rate Q_{atm}; (b) bottomhole pressure p_c remains constant.

In the case (a), we are interested in the pressure decline at the reservoir boundary $p_k(t)$, and in case (b), the pressure decline at the reservoir boundary $p_k(t)$ and the decline of the flow-rate $Q_{atm}(t)$.

Both problems are solved using the technique of the sequential change of stationary states, i. e., using the laws of non-transient gas filtration and equation of gas accumulation depletion. The substance of this latter equation (the material balance equation) is in that the amount of gas extracted from the reservoir over some time interval is equal to the decrease of the gas reserves in the reservoir. Because the reservoir is closed, the reserves are limited and not replenished from the outside.

If $\tilde{\rho}$ is gas density corresponding to weighted average formation pressure $\hat{p}$, and $V_П$ is the pore volume which is assumed to be constant, the gas reserves decline over an infinitely small time interval dt will be:

$$-V_П d\tilde{\rho} = -V_П d \frac{\rho_{atm} p}{p_{atm}} = -\frac{\rho_{atm}}{p_{atm}} V_П d\tilde{p}. \tag{24.56}$$

The mass of the gas extracted over the same time interval is:

$$Q_m(t)dt = \rho_{atm} Q_{atm} dt . \tag{24.57}$$

By equating Eq. (24.56) and Eq. (24.57), differential equation of the gas accumulation depletion is obtained:

$$-V_{\Pi} d\hat{p} = \rho_{atm} Q_{atm} dt . \tag{24.58}$$

It was shown in Eq. (20.58) of Chapter IV on transient-free radial-plane gas filtration that the difference between weighted average pressure $\hat{p}$ and contour pressure p_k is small (in our case p_k is pressure at the closed reservoir boundary). It was found by Lapuk (1948) that under the same boundary conditions the formation pressure distribution curve in the case of non-stationary filtration is positioned somewhat above the corresponding curve for transient-free filtration. So, the condition $\hat{p} = p_k$ is assumed and p_k is substituted for $\hat{p}$ in Eq. (24.58):

$$-V_{\Pi} dp_k = \rho_{atm} Q_{atm} dt . \tag{24.59}$$

Let's review case (a) where Q_{atm} = const. In this case:

$$dp_k = -\frac{\rho_{atm} p_{atm}}{V_{\Pi}} dt . \tag{24.60}$$

Upon integrating this equation under the initial condition $p = p_n$ at $t = 0$:

$$p_k = p_n - \frac{\rho_{atm} Q_{atm}}{V_{\Pi}} t , \tag{24.61}$$

i. e., pressure at the reservoir boundary linearly declines with time (Fig. 24.4).
In order to find how bottomhole pressure changes with time, Eq. (20.43) is used to find the well flow-rate:

$$Q_{atm} = \frac{\pi kh}{\mu p_{atm}} \frac{p_k^2 - p_c^2}{\ln(R_k / r_c)} \tag{24.62}$$

and find bottomhole pressure from it:

$$p_c = \sqrt{p_k^2 - \frac{p_{atm} Q_{atm}}{\pi kh} \ln(R_k / r_c)} .$$

Substituting Eq. (24.61) into this equation results in:

$$p_c = \sqrt{\left(p_n - \frac{p_{atm} Q_{atm}}{V_{\Pi}} t \right)^2 \frac{Q_{atm} p_{atm}}{\pi kh} \ln(R_k / r_c)} . \tag{24.63}$$

The p_c vs. t graph is displayed in Fig. 24.4.

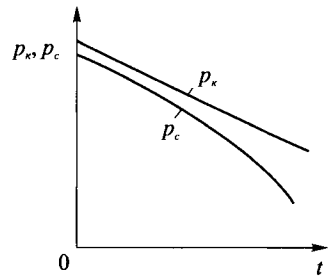

Fig. 24.4. Pressure $p_к(t)$ and bottomhole pressure $p_c(t)$ dynamics at the boundary of a closed gas reservoir at gas withdrawal with constant flow-rate.

To determine p_k vs. t correlation in the case (b) with p_c = const, let's substitute the flow-rate Eq. (24.62) into Eq. (24.60) and divide the variable:

$$-V_П \frac{dp_k Q_{atm}}{p_k^2 - p_c^2} p_c = \frac{\pi kh}{\mu} \frac{dt}{\ln(R_k / r_c)}. \tag{24.64}$$

Introducing the notation $A = \dfrac{\pi kh}{\mu \ln(R_k / r_c)}$ and integrating Eq. (24.64) from 0 to t and from $p_п$ to p_k:

$$\int_0^t dt = -\frac{V_П}{A} \int_{p_п}^{p_k} \frac{dp_k}{p_k^2 - p_c^2},$$

and from there:

$$t = -\frac{V_П}{2Ap_c} \frac{(p_п - p_c)(p_k + p_c) dp_k}{(p_п + p_c)(p_k - p_c)}. \tag{24.65}$$

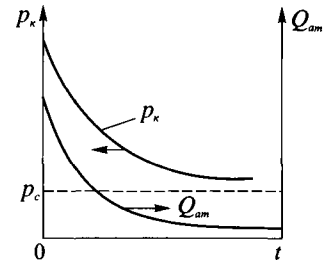

Fig. 24.5. Pressure $p_к(t)$ and flow-rate $Q_{am}(t)$ dynamics at gas withdrawal with constant bottomhole pressure.

Assigning different p_k values at the accumulation's boundary, starting with $p_п$ and smaller, it is possible to find the corresponding t values in the accumulation's development life. Substituting the same p_k values into Eq. (24.62), the flow-rates at the same moments in time will be found. The graph of $p_k(t)$ vs. $Q_{atm}(t)$ is presented in Fig. 24.5.

CHAPTER XXV

FILTRATION OF NON-NEWTONIAN LIQUID

There are cases of unusual hydrocarbon behavior in some oil and gas fields, which can be explained by the manifestation of non-Newtonian properties by the fluids in the process of filtration. These properties are usually called anomalous. Filtration specifics of the non-Newtonian oils are mostly due to elevated contents of high-molecular-weight components (resins, asphaltenes, paraffin).

With the evolution of enhanced oil and gas recovery techniques ever more numerous substances are being injected into the productive reservoirs. Many of such substances (high-molecular-weight compounds, polymers) also display non-Newtonian properties. Same goes with the drilling mud. A classification of non-Newtonian liquids was provided in Chapter XVI. Here and thereafter it is quoted just as non-Newtonian viscoplastic liquid (NVL).

1. Viscoplastic liquid: filtration law and mathematical model

In Chapter XVIII, the NVL filtration law Eq. (18.26) was quoted without derivation, just as an experimental fact. Now the hydrodynamic law for the simplest case of the NVL filtration flow in the ideal tube formed by a single capillary system will be derived. The velocity profile under the stationary flow is displayed in Fig. 16.10, and the equation for the liquid throughflow in a tube is Eq. (16.48), which indicates that the average velocity V of a viscoplastic fluid in a tube of the diameter d is found as:

$$V = \frac{d^2 \Delta p}{32 \mu l}\left[1 - \frac{4}{3}\left(\frac{4\tau_0 L}{d\Delta p}\right) + \frac{1}{3}\left(\frac{4\tau_0 L}{d\Delta p}\right)^4\right], \tag{25.1}$$

where Δp is pressure gradient in the capillary over a segment of length L, τ_0 is initial (cutoff) shear stress, and μ is plastic viscosity factor.

Let us consider an ideal single capillary system (Fig. 18.14). In such a case, the the flow in each capillary is described by Buckingham's equation [Eq. (25.1)]. A modified format of this equation is usually applied for the description of NVL in ideal

porous media, with the last bracketed term discarded. So, the NVL "filtration" flow in a capillary is found as:

$$V = \frac{d^2 \Delta p}{32 \mu l}\left[1 - \frac{4}{3}\left(\frac{4\tau_0 L}{d\Delta p}\right)\right]. \tag{25.2}$$

Note, that both Eqs. (25.1) and (25.2) determine the true average filtration velocity under the pressure gradient only along the capillary axis of the symmetry.

In order to transfer from true average velocity to filtration velocity, it is necessary to determine the throughflow through an elementary cell and then "spread" it over the entire cell facet, i. e., by multiplying Eq. (25.2) by $\pi d^2/4$ and dividing the result by a^2 (see Fig. 18.14 for the size of elementary cell). As a result of such transformation:

$$w = \frac{\pi d^4}{128 \mu a^2}\left[1 - \frac{4}{3}\left(\frac{4\tau_0 L}{d\Delta p}\right)\right]\frac{\Delta p}{L}, \tag{25.3}$$

where w is the modulus of filtration velocity.

As mentioned, Eq. (25.3) determines filtration velocity in a single capillary system for a case when the pressure gradient direction coincides with the direction of the capillary axis of symmetry. Generally speaking, the mutual orientation of the direction of the capillary axis of symmetry and of the pressure gradient can be arbitrary. For this reason it is necessary to review a problem of the NVL filtration in a single capillary system. The results of such a transformation, without the derivation, is:

$$w_i = -\frac{k}{\mu_0}\left(1 - \frac{4}{3}\frac{\gamma}{|l_j \nabla_j p|}\right) l_i l_j \nabla_j p. \tag{25.4}$$

Here, l_i is the basis vector assigning the direction of the capillary system's axis of symmetry (its direction coincides with the direction of the filtration velocity vector); $|l_j \nabla_j p|$ is modulus of the scalar product of the basis vector and pressure gradient; $\gamma = 4\tau_0 / d$ is the value of the initial (cutoff) gradient for the capillary system; $k = \pi d^4 / 128 \mu a^2$ is permeability. The Latin subscripts i and j indicate vector and tensor components; the summation is assumed with respect to them. Eq. (25.4) is not yet the NVL's filtration law as it is valid only if the flow initiation conditions are met (for an isotropic case, $|\nabla p| > \gamma$). In order to evaluate the NVL filtration law in the ideal tube formed by a single capillary system, it is necessary to formulate the condition for the flow initiation. For such formulation, one can be use the inequality that follows from the condition of negative work of the friction forces during the liquid flow in a porous medium:

$$w_i \nabla_i p < 0. \tag{25.5}$$

After substituting filtration Eq. (25.4) into inequality (25.5), the condition of the flow initiation in the direction l_i is:

$$\frac{k}{\mu}\left(1-\frac{4}{3}\frac{\gamma}{|l_j\nabla_j p|}\right)l_i l_j \nabla_i p \nabla_j p > 0.$$

It follows from there that:

$$|l_j\nabla_j p| > 4/3\gamma. \tag{25.6}$$

Thus, in the model of ideal tube formed by a single capillary system, the NVL flow initiates on condition that the vector gradient projection length onto the capillary axes of the symmetry direction is greater than the cutoff gradient, which is $4\gamma/3$. After the condition of the flow initiation is determined, the filtration law of the NVL in the ideal tube is:

$$w_i = -\frac{k}{\mu}\left(1-\frac{4}{3}\frac{\gamma}{|l_j\nabla_j p|}\right)l_i l_j \nabla_i p, \text{ at } |l_i\nabla_i p| > \frac{4}{3}\gamma \tag{25.7}$$

$$w_i = 0 \qquad \text{at } |l_i\nabla_i p| \le \frac{4}{3}\gamma.$$

Similar transformations can be performed on Buckingham's Eq. (25.1) (i. e., without discarding the nonlinear term). Then the filtration law can be obtained as follows:

$$w_i = -\frac{k}{\mu}\left(1-\frac{4}{3}\frac{\gamma}{|l_j\nabla_j p|}+\frac{1}{3}\left(\frac{\gamma}{|l_j\nabla_j p|}\right)^4\right)l_i l_j \nabla_j p, \text{ at } |l_i\nabla_i p| > \frac{4}{3}\gamma. \tag{25.8}$$

Note, that the flow initiation condition in Eq. (25.8) includes the value of γ, whereas the filtration law Eq. (25.7) includes the value of the cutoff gradient with the numerical factor. This is due to linearization of the exact solution when switching to the NVL law used in the filtration theory. The numerical factor, by analogy with the Kozeny-Karman theory, can be considered as the shape factor. The filtration laws [Eqs. (25.7) and (25.8)] can be expanded for the case of isotropic porous media. In the case of isotropic porous media, the linear and nonlinear NVL filtration laws assume, respectively, the following formats:

$$w_i = -\frac{k}{\mu}\left(1-\frac{4}{3}\frac{\gamma}{|\nabla_j p|}\right)\nabla_i p, \text{ at } |\nabla_i p| > \frac{4}{3}\gamma \tag{25.9}$$

$$w_i = 0 \qquad \text{at } |\nabla_i p| \le \frac{4}{3}\gamma,$$

$$w_i = -\frac{k}{\mu}\left(1 - \frac{4}{3}\frac{\gamma}{|\nabla_j p|} + \frac{1}{3}\left(\frac{\gamma}{|\nabla_j p|}\right)^4\right)\nabla_i p, \text{ at } |\nabla_i p| > \gamma \qquad (25.10)$$

$$w_i = 0 \qquad \text{at } |\nabla_i p| \le \gamma,$$

where $|\nabla_j p|$ is modulus of the pressure gradient.

The filtration laws [Eqs. (25.7)–(25.10)] are written in the subscript format. In the vector format, the Eq. (9.15) filtration law takes the format similar to Eq. (18.26), and the nonlinear filtration law Eq. (25.10) is:

$$\vec{w} = -\frac{k}{\mu}\left(1 - \frac{4}{3}\frac{\gamma}{|\text{grad } p|} + \frac{1}{3}\left(\frac{\gamma}{|\text{grad } p|}\right)^4\right)\text{grad } p \text{ at } |\text{grad } p| \ge \gamma,$$

$$\vec{w} = 0 \qquad \text{at } |\text{grad } p| \le \gamma.$$

The NVL filtration mathematical model includes the continuity equation and the filtration law. The viscoplastic liquid is assumed incompressible; so, the equation system in the mathematical model is:

$$div\,\vec{w} = 0$$

$$\vec{w} = -\frac{k}{\mu}\left(1 - \frac{4}{3}\frac{\gamma}{|\text{grad } p|}\right)\text{grad } p \text{ at } |\text{grad } p| \ge \frac{4}{3}\gamma. \qquad (25.11)$$

$$\vec{w} = 0 \qquad \text{at } |\text{grad } p| \le \frac{4}{3}\gamma$$

The NVL filtration law can also be expressed differently. As the pressure gradient vector can be formatted as follows:

$$\text{grad } p = |\text{grad } p|\vec{n},$$

where $\vec{n}$ is a basis vector assigning the direction of the pressure gradient vector. Then, multiplying the expression in the right part of this equation by the gradient gives:

$$\vec{w} = -\frac{k}{\mu}\text{grad } p + \frac{4}{3}\frac{k}{\mu}\gamma\vec{n}.$$

So, if the first equation (assigning the NVL filtration law) is substituted into the continuity equation, it results in:

$$\Delta p + \frac{4}{3}\gamma\nabla\vec{n} = 0$$

$$\vec{w} = -\frac{k}{\mu}\text{grad } p\frac{4}{3}\frac{k}{\mu}\gamma\vec{n} \text{ at } |\text{grad } p| > \frac{4}{3}\gamma. \qquad (25.12)$$

$$\vec{w} = 0 \qquad \text{at } |\text{grad } p| \le \frac{4}{3}\gamma$$

For parallel-rectilinear filtration in the Cartesian coordinate system, $\vec{n} = \text{const}$ and $\nabla\vec{n} = 0$. So, the mathematical model of NVL filtration is different from the Newtonian liquid filtration mathematical model [Eq. (5.1)] only in the filtration law. But for unidimensional flows in the generalized curvilinear coordinate systems (the cylindrical and spherical), $\vec{n} \neq \text{const}$ and $\nabla\vec{n} \neq 0$. Therefore, in a general case, the mathematical model of NVL filtration is different from the Newtonian liquid filtration model not only in the filtration law.

2. Rectilinear-parallel filtration flow for the viscoplastic liquid

The solution of the flow-to-gallery problem is important for the processing of laboratory core study results, where the rectilinear-parallel flow is realized.

Suppose a reservoir comprising of a rectilinear block of width B and thickness h. The reservoir is bounded on the top and base by impermeable planes, on the left by the charge contour, and on the right, by the gallery. The coordinate system (as indicated in Fig. 25.1) is selected, i. e., the origin is placed at the charge contour plane. $0x$ axis is directed parallel to the filtration velocity vector.

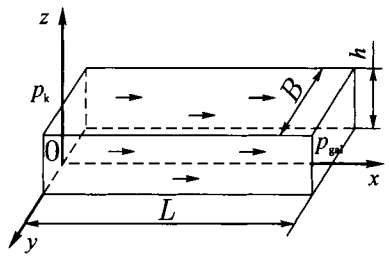

Fig. 25.1. Rectilinear-parallel filtration flow of viscoplastic liquid (VPL).

It is possible to assume that the sought-for functions (pressure p and filtration velocity $\vec{w}$) are dependent only on the x coordinate, and equation of the system Eq. (25.12) becomes:

$$\frac{d^2p}{dx^2} = 0,\ w_x = \frac{k}{\mu}\left|\frac{dp}{dx}\right| - \frac{4k\gamma}{3\mu},\ w_y = w_z = 0. \qquad (25.13)$$

The first Eq. (25.13) is easily integrable:

$$\frac{dp}{dx} = C_1, \text{ therefore, } dp = C_1dx, \text{ and further } p = C_2,$$

i. e., the same result as for a Newtonian liquid (see Chapter XX).

To find the integration constants C_1 and C_2, we need the boundary conditions (pressure values at some points along the flow line). Let's assume that pressure values are known at the charge contour and at the gallery:

$$p = p_k \text{ at } x = 0 \text{ and } p = p_{gal} \text{ at } x = L.$$

Let's now insert these values into the expression for pressure:

$$p_k = C_2 \text{ and } p_{gal} = C_1 L + C_2,$$

and from there:

$$C_1 = -\frac{p_k - p_{gal}}{L} \text{ and } C_2 = p_k ,$$

so the pressure distribution equation is:

$$p(x) = p_k - \frac{p_k - p_{gal}}{L} x . \tag{25.14}$$

Therefore, pressure distribution in the reservoir at NVL filtration is distributed under the same law as for filtration of a Newtonian liquid [see Chapter XX, Eq. (20.4)]. The difference with the Newtonian liquid is that the above pressure distribution in the reservoir is valid not for all pressure gradients, but only when the following condition is realized:

$$|\text{grad } p| > \frac{4}{3}\gamma .$$

So, using Eq. (25.14), it is possible to find the pressure gradient modulus:

$$|\text{grad } p| = \left|\frac{dp}{dx}\right| = \frac{p_k - p_{gal}}{L} \tag{25.15}$$

and by adding the flow initiation condition to equation that gives pressure distribution during NVL filtration:

$$p(x) = p_k - \frac{p_k - p_{gal}}{L} x \text{ at } \frac{p_k - p_{gal}}{L} > \frac{4}{3}\gamma . \tag{25.16}$$

This is the correct format of the pressure distribution equation at NVL filtration. This equation, however, can be formulated differently when NVL's rheological properties are included into it. Before presenting this equation, let's find the solution of filtration velocity and flow-rate problem.

Let's substitute the expression for pressure gradient [Eq. (25.15)] into Eq. (25.13):

$$w_x = \frac{k}{\mu}\frac{p_k - p_{gal}}{L} - \frac{4k\gamma}{3\mu} . \tag{25.17}$$

Moreover, the obtained result can be used to determine the flow-rate. For this purpose, the filtration velocity should be multiplied by the gallery area $S = Bh$. The result is:

$$w_x S = Q = \frac{k}{\mu}\frac{p_k - p_{gal}}{L} S - \frac{4k\gamma}{3\mu} S$$

or

$$Q = \frac{k}{\mu}\left(\frac{p_k - p_{gal}}{L} - \frac{4}{3}\gamma\right) S . \tag{25.18}$$

This is equation for the flow-rate determination at viscoplastic liquid filtration to the gallery. As it can be seen, if it is assumed $\gamma = 0$, then it results in the expression for the Newtonian liquid flow-rate Eq. (20.5).

From Eq. (25.18), the pressure gradient can be derived:

$$\frac{p_k - p_{gal}}{L} = \frac{Q\mu}{kS} + \frac{4}{3}\gamma$$

and substituting into the equation for pressure distribution in the reservoir Eq. (25.16), results in:

$$p_x = p_k - \frac{Q\mu}{kS} x - \gamma x . \tag{25.19}$$

The same equation can be derived in a shorter way. Let's use the second equation of Eq. (25.13):

$$w_x = \frac{k}{\mu}\left|\frac{dp}{dx}\right| - \frac{4k\gamma}{3\mu} .$$

Let's open the modulus sign, and as $|dp/dx < 0|$:

$$w_x = -\frac{k}{\mu}\frac{dp}{dx} - \frac{4k\gamma}{3\mu} .$$

After solving this equality relative to the differential and separating the variables:

$$-dp = \frac{\mu}{k} w_x dx + \frac{4}{3}\gamma dx .$$

As $w_x = Q/Bh$, it is possible to exclude velocity out of this equation:

$$-dp = \frac{\mu}{k}\frac{Q}{Bh} dx + \frac{4}{3}\gamma dx \tag{25.20}$$

and integrate it from the charge contour to arbitrary x value ($0 < x \le L$):

$$\int_{p}^{p_k} dp = \int_{0}^{x} \left(\frac{\mu}{k} \frac{Q}{Bh} + \frac{4}{3}\gamma \right) dx .$$

The result is Eq. (25.19):

$$p(x) = p_k - \frac{Q\mu}{kS} x - \gamma x .$$

It is possible to integrate Eq. (25.20) from the gallery to arbitrary x value:

$$\int_{p_{gal}}^{p} dp = \int_{x}^{L} \left(\frac{\mu}{k} \frac{Q}{Bh} + \frac{4}{3}\gamma \right) dx$$

and obtain:

$$p_x = p_{gal} + \left(\frac{\mu}{k} \frac{Q}{Bh} + \frac{4}{3}\gamma \right)(L - x) . \qquad (25.21)$$

Similar calculations can be performed also for the nonlinear filtration law Eq. (25.10). However, due to nonlinearity of differential equation associating velocity and pressure gradient, a simple analytical solution is difficult to arrive at. Indeed, after projecting the filtration equation onto the coordinate axis:

$$w_x = \frac{k}{\mu} \left[\frac{dp}{dx} - \frac{4}{3}\gamma + \frac{1}{3} \frac{\gamma^4}{\left(\frac{dp}{dx} \right)^3} \right] .$$

After multiplying this equation by the gallery cross-sectional area and transforming gives this format:

$$Q = \frac{kBh}{\mu} \left[\frac{dp}{dx} - \frac{4}{3}\gamma + \frac{1}{3} \frac{\gamma^4}{\left(\frac{dp}{dx} \right)^3} \right] , \qquad (25.22)$$

The indicator curves can be plotted for Eqs. (25.18) and (25.22). The plotted lines are displayed in Fig. 25.2.

A particular feature of the indicator curves at filtration of the viscoplastic liquid is that all lines do not run through the origin, but cut some segment on the "pressure drawdown" axis. The segment cut by curves 2 and 3 corresponds to the initial gradient value, and the segment cut by curve 1 corresponds to the value $4\gamma/3$.

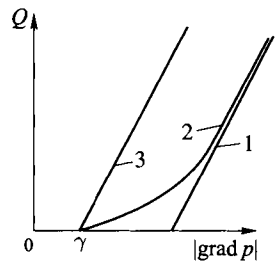

Fig. 25.2. Indicator curves using Eqs. (25.18) — 1, Eq. (25.22) — 2 and Eq. (25.18), without the numeric parameter 4/3 at γ — 3.

Thus, the filtration law Eq. (25.9) approximates well the nonlinear filtration law [Eq. (25.10)] at pressure gradients greater that $4\gamma/3$. If the numerical factor 4/3 at the initial gradient γ is not included into the filtration law Eq. (25.9), the indicator curve will be the straight line 3. This figure shows that the approximation without this numerical factor results in greater errors than the filtration law Eq. (25.9).

Moreover, the real porous medium comprises numerous micro-capillaries of diverse diameters. So, as pressure declines, the capillaries are being "plugged" starting with the smallest ones and then the largest. Thus, the indicator curves in Fig. 25.2 correspond to some averaged parameters, and the "increase" of the cutoff gradient value in the filtration law Eq. (25.9) enables the consideration of the smallest "plugged" capillaries.

The initial (cutoff) gradient value in the porous medium can be determined using Eq. (25.5) obtained for the NVL flow in a capillary, i. e., the value based on the ideal tube model, but accounting for linearization of Buckingham's equation:

$$\gamma^* = \frac{4}{3}\gamma = \frac{16\tau_0}{3d}, \tag{25.23}$$

where γ^* is "new" cutoff gradient taking the 4/3 factor into account, which by analogy with the Kozeny-Karman theory can be dubbed the shape factor.

3. Rectilinear-parallel filtration flow of viscoplastic liquid in a nonuniformly-stratified reservoir

In this section, the rectilinear-parallel filtration in a nonuniformly laminated reservoir will be reviewed. Usually, permeability and porosity differ from one bed to the next. Therefore, as follows from Eq. (25.23), the cutoff gradient will also differ. The same equation indicates that the higher permeability (k is proportional to d), the lower the cutoff gradient, and vice versa.

Let's assume that the filtration law with the cutoff gradient is valid for each interbed/lamina:

$$\begin{aligned} w_i^\alpha &= -\frac{k_\alpha}{\mu}\left(1 - \frac{\gamma_\alpha^*}{|\nabla_j p|}\right)\nabla_j p, \text{ at } = |\nabla_j p| > \gamma_\alpha^* \\ w_i &= 0 \qquad\qquad\qquad\qquad \text{at } = |\nabla_j p| \le \gamma_\alpha^*, \end{aligned} \tag{25.24}$$

where α is the lamina/interbed number.

Let's review the bed composed of three interbeds of different permeability $k_1 > k_2 > k_3$, then $\gamma_1 < \gamma_2 < \gamma_3$. It is assumed that the pressures at the charge contour and at the gallery in all interbeds are the same.

In this case, as pressure grows, the interbeds will sequentially begin to transmit liquid. Indeed, if $|\text{grad}| < \gamma_1^*$, there is no motion in the entire reservoir. At $\gamma_1^* < |\text{grad}| < \gamma_2^*$

filtration will occur only within the first interbed, and so on. In order to introduce parameters average for the reservoir, it is possible to use Eqs. (25.24) and "spread" the result over the entire reservoir:

$$w = \frac{1}{H}\sum_{\alpha=1}^{3} w^{\alpha} = -\frac{1}{H}\sum_{\alpha=1}^{3} \frac{k_\alpha h_\alpha}{\mu}\left(1 - \frac{\gamma_\alpha^*}{|\nabla_j p|}\right)\frac{dp}{dx}, \qquad (23.25)$$

where h_α is the interbed's thickness. Eq. (25.25) describes filtration through a piecewise-linear broken line (line 1 in Fig 25.3).

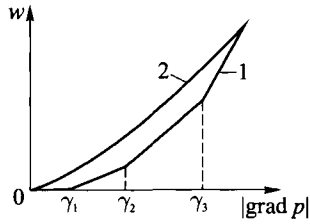

Fig. 25.3. Filtration velocity vs. pressure gradient modulus. 1 — piecewise-linear (in a laminated reservoir); 2 —nonlinear, under the exponential filtration law.

Along with the reviewed NVL filtration laws, the exponential filtration law is also used:

$$\vec{w} = -C|\text{grad}\, p|^{n}\,\text{grad}\, p\,, \qquad (25.26)$$

where C is the experimental constant, $n > 0$.

The exponential law Eq. (25.26) corresponds with the pseudoplastic fluid behavior and adequately describes the polymer solution flow in a porous medium. It is used in designing polymer flooding of reservoirs as an EOR technique. The indicator curve corresponding to Eq. (25.26) filtration law is displayed in Fig. 25.3 (line 2).

4. Radial-plane filtration of viscoplastic liquid

In this section, the pressure distribution and filtration velocity in the reservoir under the parallel-plane symmetry will be reviewed. Suppose there is a round central well of radius r_c with constant bottomhole pressure p_c located in a circular reservoir of thickness h and charge contour radius R_k. A constant pressure p_k is maintained in the reservoir (see Fig. 20.4).

To solve the problem of a viscoplastic liquid flow to the central well in a circular reservoir, let's rearrange the flow equation in the viscoplastic liquid filtration law Eq. (25.11) by solving it relative to the pressure gradient. For this purpose, let's represent the pressure gradient as the product of a unitary vector **n** and the pressure gradient modulus $|\text{grad}\, p|$:

$$\text{grad}\, p = |\text{grad}\, p|\vec{n}$$

and open the parentheses in the right part of the first filtration equation:

$$\vec{w} = -\frac{k}{\mu}\text{grad}\, p + \frac{4}{3}\frac{k}{\mu}\gamma^*\vec{n} = -\frac{k}{\mu}\text{grad}\, p + \frac{k}{\mu}\gamma^*\vec{n}\,.$$

This equation is easy to solve relative the pressure gradient:

$$\text{grad}\, p = -\frac{\mu}{k}\vec{w} + \gamma^*\vec{n}. \tag{25.27}$$

Therefore, the NVL filtration law solved relative to the pressure gradient can be formatted as follows:

$$\text{grad}\, p = -\frac{\mu}{k}\vec{w} + \gamma^*\vec{n} \text{ at } |\text{grad}\, p| > \gamma^* \text{ and } |\vec{w}| > 0$$

$$|\text{grad}\, p| < \gamma^* \text{ and } |\vec{w}| = 0.$$

Furthermore, let's return to Eq. (25.27) and, assume that the flow is axisymmetric and only dp/dr and $w_r = w(r)$ are different from zero. So, after projecting Eq. (25.27) onto a polar coordinate system:

$$\frac{dp}{dr} = \frac{\mu}{k}w + \gamma^*. \tag{25.28}$$

To find pressure distribution in the reservoir, we will separate the variables in Eq. (25.28):

$$dp = \frac{\mu}{k}w dr + \gamma^* dr$$

and, use the ratio:

$$w = \frac{Q}{2\pi h r}, \tag{25.29}$$

Canceling the velocity from the equation:

$$dp = \frac{\mu}{k}\frac{Q}{2\pi h}\frac{dr}{r} + \gamma^* dr. \tag{25.30}$$

After having integrated this equation from the charge contour R_k to an arbitrary r value ($r_c \le r \le R_k$):

$$p(r) = p_k - \frac{\mu}{k}\frac{Q}{2\pi h}\ln\frac{R_k}{r} - \gamma^*(R_k - r). \tag{25.31}$$

By assuming $r = r_c$ in Eq. (25.31) and solving this equation relative to the flow-rate Q, the equation for the well flow-rate under the viscoplastic liquid filtration will be derived:

$$Q = \frac{2\pi p_k h}{\mu}\left(\frac{p_k - p_c}{\ln R_k / r_c} - \frac{\gamma^*(R_k - r_c)}{\ln R_k / r_c}\right). \tag{25.32}$$

Eqs. (25.30)–(25.32) are valid only if the conditions of the flow initiation are met, i. e., when the inequality:

$$|\text{grad } p| > \gamma^* \tag{25.33}$$

is realized. Let's see, then, to what inequality leads the condition of Eq. (25.33) in solving this problem. The pressure gradient modulus is equal to:

$$|\text{grad } p| = \frac{dp}{dr} = \gamma^* + \frac{\mu Q}{2\pi kh}\frac{1}{r}.$$

Therefore, it is possible to rewrite the inequality Eq. (25.33) as:

$$\frac{\mu Q}{2\pi kh}\frac{1}{r} > 0$$

or, using Eq. (25.32):

$$\frac{p_k - p_c}{R_k - r_c} > \gamma^*$$

or, as $R_k >> r_c$:

$$\frac{p_k - p_c}{R_k} > \gamma^* \text{ , and from there } \Delta p > \gamma^* R_k \text{ .}$$

The indicator curve under the viscoplastic liquid filtration is shown in Fig. 25.4.

As it can be seen, the line does not run through the origin and cuts some segment $0A$ on the "pressure drawdown" axis. The size of the segment determines the value of the initial gradient. Indeed, the following equality is realized at the point A:

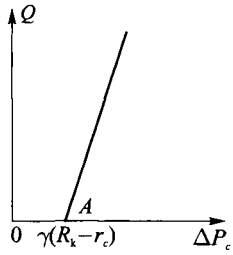

Fig. 25.4. Indicator curve corresponding to the VPL filtration law.

$$\frac{p_k - p_c}{R_k - r_c} > \gamma^* \text{ or } \frac{p_k - p_c}{R_k} \approx \gamma^*$$

In the field, however, the value of the initial gradient is determined differently.

It is assumed that after the well is shut-in ($Q = 0$), pressure distribution is still determined from Eq. (25.31). Then after the well shut-in, its bottomhole pressure will be:

$$p_{c'} = p_k - \gamma(R_k - r_c)\,, \tag{25.34}$$

where $p_{c'}$ pressure in the well after the shut-in (Fig. 25.5). Because the oil by default is incompressible, theoretically pressure distribution Eq. (25.34) sets up instantaneously after the well is shut-in. However, as opposed to the model oil, the real oil is slightly compressible; the pressure distribution Eq. (25.34) will be reached after a while. Also, due to the non-Newtonian oil properties, the "restored" pressure in the well turns out lower than charge contour pressure and not equal to it as it would be under the Darcy's law filtration for a Newtonian liquid ($\gamma = 0$).

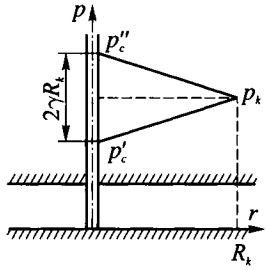

Fig. 25.5. Definition of cut-off gradient in a reservoir

After $p_{c'}$ pressure is measured, some amount of the same oil is injected back into the well. As a result, the oil begins to flow into the reservoir. After the injection is finished and the flow stops, a new pressure distribution will set up, and the well pressure will be:

$$p_{c''} = p_k + \gamma(R_k - r_c) . \tag{25.35}$$

Subtraction of Eq. (25.34) from Eq. (25.32), results in:

$$\gamma = \frac{p_{c''} - p_{c'}}{2R_k} . \tag{25.36}$$

The described procedure takes a few hours in the field. Initial pressure gradient measured in the Gryazevaya Sopka in Azerbaijan was: $\gamma = 0.007$ MPa.

5. Non-stationary filtration of viscoplastic liquid

In this section, the non-stationary filtration of elastic NVL within an elastic reservoir will be reviewed. The mathematical model of such process includes:

$$\frac{\partial \varnothing \rho}{\partial t} - \Delta P = 0,$$

$$\rho w = -\rho\left(1 - \frac{\gamma}{|\text{grad } p|}\right)\text{grad } p,$$

$$\rho = \rho_0[1\beta_{\text{Liq}}(p - p_0)],\ \varnothing = \varnothing_0 + \beta_C(p - p_0),$$

$$k = \text{const},\ \ \mu = \text{const},\ \ P = \frac{k}{\mu}\int \rho dp.$$

So, repeating the same procedure with a different motion equation results in the piezoconductivity equation for a compressible NVL:

$$\frac{\partial p}{\partial t} = \kappa \mathrm{div}\left[\left(1 - \frac{\gamma}{|\nabla p|}\right)\nabla p\right], \quad |\nabla \mathrm{p}| > \gamma \tag{25.37}$$

where κ is piezoconductivity factor.

Eq. (25.37) is the base on which to construct the nonlinear theory of the elastic filtration drive. In solving specific filtration problems, initial and boundary conditions are formed for Eq. (25.37), similar to those reviewed in the elastic drive theory. At the same time, what is important is that under filtration at a cutoff gradient, a variable area forms in the reservoir. At the boundary of this area (until such time when it reaches the reservoir boundary), the pressure gradient modulus must be equal to the cutoff gradient, and pressure must be equal to the initial formation pressure.

Let's review some unidimensional problems of this kind.

Rectilinear-parallel filtration of an elastic NVL. Let's review non-stationary filtration of an elastic NVL within the uniform semi-indefinite reservoir. Suppose at the initial moment in time $t = 0$ a production gallery begins operating at the reservoir boundary $x = 0$. Constant pressure p_{gal} is maintained at the gallery. Two areas form in the reservoir: the filtration zone and the no-flow zone. Their boundary is moving with time under the $l = l(t)$ rule, and $l(0) = 0$.

Suppose pressure in the no-flow zone is equal to the initial formation pressure, and the cutoff gradient is constant.

Piezoconductivity equation projected onto the coordinate axis x is:

$$\frac{\partial p}{\partial t} = \kappa \frac{\partial}{\partial x}\left[\left(\frac{\partial p}{\partial x} - \gamma\right)\right], \quad |\nabla \mathrm{p}| > \gamma \quad 0 < x < l \tag{25.38}$$

Outside the filtration zone, pressure is equal to the initial formation pressure:

$$p(x,t) = p_0 \quad \text{at} \quad x > l(t)$$

The following conditions are realized at the zone boundary $x = l(t)$:

$$p(l,t) = p_0 \tag{25.39}$$

$$\left(\partial p / \partial x\right)_{x=l} = \gamma \tag{25.40}$$

It is required to find in the $0 < x < l$ area the solution of Eq. (25.38) equation, to determine the flow-rate $Q = Q(t)$ and the $l = l(t)$ law under the conditions of Eqs. (25.39) and (25.40) at the zone boundary; and with the initial and boundary conditions:

$$p(x,0) = p_0 \quad \text{and} \quad p(0,t) = p_{\mathrm{gal}} \tag{25.41}$$

Let's solve this problem approximately using the integral relationships technique (Chapter XXIV, Sec. 3). Restricting to only one integral, relationship gives only the solution in the following format:

$$p(x,t)=\gamma x+a_0(t)+a_1(t)\frac{x}{l}+a_2(t)\left(\frac{x}{l}\right)^2 \tag{25.42}$$

where a_0, a_1, a_2 are unknown variables determined from the boundary conditions of Eqs. (25.39), (25.40) and the second condition of Eq. (25.41).

From the condition of Eq. (25.40):

$$\left(\frac{\partial p(x,t)}{\partial x}\right)_{x=l}=\gamma+a_1(t)\frac{1}{l}+2a_2(t)\left(\frac{1}{l}\right)=\gamma.$$

It follows from there that:

$$a_1(t)=-2a_2(t)$$

From the second condition of Eq. (25.41):

$$p(0,t)=p_{gal}=a_0(t)=\text{const}, \tag{25.43}$$

and it follows from the condition of Eq. (25.39) that:

$$p_0(l,t)=\gamma l+a_0(t)+a_1(t)+a_2(t)$$

The obtained values of the factors are constant [see Eq. (25.43)] and by subtracting from Eq. (25.42) results in the following equation for pressure distribution in the reservoir:

$$p(x,t)=p_0-\gamma(l-x)-(\Delta p_0-\gamma l)\left(1-\frac{x}{l}\right)^2 \tag{25.44}$$

where $\Delta p_0 = p_0 - p_{gal} = \text{const}$.

Equation for the gallery flow-rate is derived from filtration equation by multiplying it by the gallery area Bh, where B and h are, respectively, gallery's width and thickness:

$$Q(0,t)=\frac{k}{\mu}\left(\frac{\partial p}{\partial x}-\gamma\right)Bh \tag{25.45}$$

After substituting Eq. (25.44) into Eq. (25.45):

$$Q(0,t)=\frac{k}{\mu}\left(\frac{2\Delta p_0}{l}-\gamma\right)Bh \tag{25.46}$$

To determine $l(t)$, the integral relationship characterizing the condition of the material balance is used:

$$\int_0^{l(t)}\frac{\partial p}{\partial t}dx=\kappa\left(\frac{\partial p(x,t)}{\partial x}-\gamma^*\right)_0^{l(t)}$$

From there, and considering Eq. (25.44):

$$6\kappa\frac{\partial t}{\partial l}=l+\frac{2\gamma^{*}l^{2}}{\Delta p_0-\gamma^{*}l}$$

Integrating this equation under $l(0)=0$ condition, gives a subtended algebraic equation for the zone boundary $l(t)$ motion law:

$$3\kappa t=\left(\frac{\Delta p_0}{\gamma^{*}}\right)^{2} ln\frac{\Delta p_0}{\Delta p_0-\gamma^{*}l}-\left(\frac{\Delta p_0}{\gamma^{*}}+\frac{l}{4}\right)l \tag{25.47}$$

Analysis of Eq. (25.47) shows that $l(t)$ has the asymptote:

$$l=l^{*}=\Delta p_0/\gamma^{*}$$

Cutoff $(t\to\infty)$ pressure distribution and flow-rate, respectively, will be: $p=p(x)=p_{gal}+\gamma^{*}$ at $0\le x\le l^{*}$

$$p=p(x)=p_0 \quad \text{at} \quad x>l^{*} \tag{25.48}$$

$$Q(\infty)=0$$

For better understanding of derivations and formulas, it is important to analyze Eqs. (25.44)–(25.48). This would help better understanding the major features of non-stationary filtration with the cutoff gradient.

Problem of the well startup at a constant flow-rate under filtration of an elastic viscoplastic fluid in an elastic reservoir. In this case Eq. (25.37) is:

$$\frac{\partial p}{\partial t}=\kappa\frac{1}{r}\frac{\partial}{\partial r}\left[r\left(\frac{\partial p}{\partial r}-\gamma\right)\right], \quad |\nabla p|>\gamma \quad 0<r<l \tag{25.49}$$

At the initial point in time, the reservoir is undisturbed:

$$p=p_k \quad \text{at} \quad t=0 \tag{25.50}$$

The condition at the well is derived from the filtration equation:

$$Q=\frac{k}{\mu}\left(\frac{\partial p}{\partial r}-\gamma\right)2\pi rh,$$

and from there:

$$\frac{\partial p}{\partial r}=\frac{Q\mu}{2\pi khr_c}+\gamma \quad \text{at} \quad r=r_c \tag{25.51}$$

Let's search for an approximate solution of the assigned problem using the integral relationships technique. Suppose, pressure distribution in the disturbed zone of radius $R(t)$ is:

$$p(r,t) = a_0 ln\frac{r}{R(t)} + a_1 + a_2\frac{r}{R(t)} \quad \text{at} \quad r \le R(t) \tag{25.52}$$

$$p(r,t) = p_k \text{ at } r > R(t),$$

where a_0, a_1, a_2 are unknown factors to be determined, $R(t)$ is the disturbed zone (where filtration is occurring) radius; there is no filtration outside of this zone. With time, the disturbed zone boundary advances under the rule $R = R(t)$, and at $R(0) = r_c$.

The following conditions are realized at the disturbed zone boundary:

$$p(R,t) = p_k, \quad \partial p/\partial r = \gamma \text{ at } r = R(t) \tag{25.53}$$

Factors a_0, a_1, a_2 can be found from the conditions of Eqs. (25.51) and (25.53). Then, Eq. (25.52) is transformed to the following format:

$$p(r,t) = p_k + \frac{Q\mu}{2\pi kh}\left(ln\frac{r}{R(t)} - \frac{r}{R(t)} + 1\right) - \gamma\left[R(t) - r\right] \tag{25.54}$$

The disturbed zone radius is found from the material balance Eq. (23.7), which in the case $Q = \text{const}$ can be written as:

$$Q = \beta^* \pi R^2(t) h(p_k - \tilde{p}), \tag{25.55}$$

where $\tilde{p}$ is weighted average pressure within the reservoir disturbed zone. It is determined from Eq. (20.11). After substituting into Eq. (25.54) and integrating it, the result is:

$$\tilde{p} = p_k + \frac{Q\mu}{12\pi kh} - \frac{\gamma}{3}R(t) \tag{25.56}$$

From Eq. (25.55) and considering Eq. (25.56), the disturbed zone boundary advance rule is found:

$$R^2(t)\left[1 + \frac{4\pi kh\gamma}{Q\mu}R(t)\right] = 12\kappa t \tag{25.57}$$

Finding from Eq. (25.27) the $R(t)$ values at different times and substituting into Eq. (25.54), $p(r,t)$ values can be found.

Of a special interest are bottomhole pressure changes (at $r = r_c$):

$$p(r_c,t) = p_k + \frac{Q\mu}{2\pi kh}\left(\ln\frac{r_c}{R(t)} - \frac{r_c}{R(t)} + 1\right) - \gamma\left[R(t) - r_c\right]$$

or, a almost immediately after the well startup $R(t) >> r_c$:

$$p(r,t) \approx p_k + \frac{Q\mu}{2\pi kh}\left(\ln\frac{r}{R(t)} + 1\right) - \gamma R(t) \qquad (25.58)$$

In order to analyze bottomhole pressure change under non-stationary filtration with the cutoff gradient, Eq. (25.57) will be studied.

For the values $R(t) << Q\mu/4\pi kh\gamma$, the second component in parentheses is less than 1 and can be disregarded. Then:

$$R^2(t) = 12\kappa\tau \qquad (25.59)$$

Which is typical of the elastic drive (Chapter XXIII). This relationship is realized for the small time values:

$$t << \frac{1}{12\kappa}\left(\frac{Q\mu}{4\pi kh\gamma}\right)^2.$$

At that, $\gamma R(t) << Q\mu/4\pi kh$, and the major role in the Eq. (25.58) belongs to the logarithmic term:

$$p(r,t) \approx p_k - \frac{Q\mu}{2\pi kh}\ln\frac{12\kappa\tau}{r_c^2}$$

At long times, when the one in parentheses of Eq. (25.58) can be discarded compared with the other components, i. e., $R(t) >> Q\mu/4\pi kh\gamma$, the disturbed zone boundary advance rule looks as follows:

$$R(t) = \left(\frac{3Q\mu\kappa\tau}{\pi kh\gamma}\right)^{1/3},$$

and bottomhole pressure vs. time correlation is:

$$p(r_c,t) \approx p_k - \frac{Q\mu}{6\pi kh}\ln\frac{3Q\mu\kappa\tau}{\pi kh\gamma r_c^3} - \gamma\left(\frac{3Q\mu\kappa\tau}{\pi kh\gamma}\right)^{1/3} + \frac{Q\mu}{2\pi kh} \qquad (25.60)$$

With some parameter values, the exponential term acquires the main significance; so, the bottomhole pressure decline rule changes from a logarithmic to the ex-

ponential one. Therefore, at long times the shape of the bottomhole pressure change curves, under filtration with the cutoff gradient, significantly changes compared with the elastic liquid filtration. In principle, it enables to identify the manifestation of the cutoff pressure gradient.

7. Formation of bypass zones in the process of oil-by-water displacement

An important effect of filtration with the cutoff pressure gradient is the possibility of formation in the reservoir of bypass zones, where oil or gas remain immobile. These zones form in the reservoir areas where pressure gradient is below the cutoff value. Occurrence of the bypass zones results in a decrease of the oil recovery. Such bypass zone located between two production wells operating at equal flow-rates is shaded (3) in Fig. 25.6a.

Let's review the oil-by-water displacement from a reservoir under the 5-spot waterflooding system (Fig. 25.6b). Well 1 is the injection well, wells 2 are oil producers.

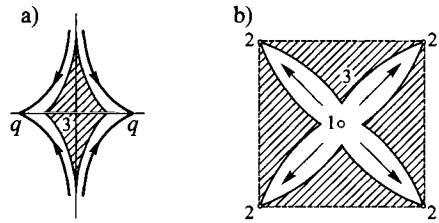

Fig. 25.6. Schematics of formation of bypass zone.

Analysis of the two-dimensional flow demonstrates, that the flow velocity in zones 3 is small compared to velocities in the areas next to the straight lines connecting the injector with the producers. The result is that these zones are bypassed. The ratio of the shaded areas in Fig. 25.6b to the entire area of the 5-spot cell can be viewed as the water-flooding sweep factor. It was shown that the size of the bypass zone and the reservoir sweep factor are functions of the parameter:

$$\lambda = Q\mu / k\gamma L,$$

where Q is the production well flow-rate and L is the characteristic linear dimension (such as half-distance between two wells).

It turns out that the reservoir sweep factor increases as the λ parameter increases.

At the same time, in order to derive a sweep factor change due to the cutoff pressure gradient as applied to a real oil field, it is necessary to eliminate the

effect from the other wells, reservoir non-uniformity, physicochemical phenomena, etc.

8. Specifics of viscoplastic liquid filtration in anisotropic porous media

For a description of NVL filtration flow in anisotropic porous media, the results of Sec. 3 in this chapter will be used. Equations derived for the ideal tube formed by one system of capillaries for the ideal tube formed by three mutually perpendicular systems of cylindrical capillaries will be expanded. Each capillary system will have its own diameter d_α and laying step $a_\alpha, \alpha = 1,2,3$.

It is usually assumed, in generating definitive equations for idealized models, that it is acceptable to disregard the flows interaction in the channels. In such a case it is possible to derive formulas for the vector components for the true filtration velocity for each channel system. To do so, the true filtration velocity in the case of NVL Bukingham's equation Eq. (25.2) can be used. The last component in brackets can be ignored. In this case, such a transformation should be made for each capillary system. So, as a result of the transformation of the approximate equation:

$$w^\alpha = \frac{\pi d_\alpha^4}{128\mu_0 a_\beta a_\gamma}\left[1-\frac{4}{3}\left(\frac{4\tau_0 L}{d_\alpha \Delta p}\right)\right]\frac{\Delta p}{L}\ , \qquad (25.61)$$

where w^α is filtration velocity for the flow along the axis α of the Cartesian coordinate system, a_β and a_γ are the capillary laying steps along the corresponding axes of the coordinate system. Subscripts α, β, γ here and thereafter form a cyclical permutation of numbers 1, 2, 3. As indicated earlier, Eq. (25.61) determines filtration velocity in the capillary system α for a case when the pressure gradient direction coincides with the capillary axis of symmetry. As a general case, we need to solve the problem of the NVL filtration within one capillary system, with the mutual relationship between the capillary axis of symmetry and the pressure gradient being arbitrary. In such a case, Eq. (25.61) takes the format of Eq. (25.4).

Let's expand the parentheses in Eq. (25.4) for each capillary system:

$$w_i^\alpha = -\frac{k_\alpha}{\mu_0} l_i^\alpha l_j^\alpha \nabla_j p + \frac{k_\alpha \gamma_\alpha}{\mu_0} l_i^\alpha l_j^\alpha \frac{\nabla_j p}{\left| l_j^\alpha \nabla_j p \right|} \qquad (25.62)$$

Here and thereafter the Greek subscripts usually indicate the channel system number, and the Latin ones, the vector and tensor components. The summation is assumed with respect to the repetitive Latin subscripts. The summation with re-

spect to the repetitive Greek subscripts, if necessary, is indicated the usual way, using the summation symbol.

Using the assumption of the independent flows in the capillaries, Eqs. (25.62) can be summed up over all the capillary systems and transit to a 3D NVL filtration equation:

$$w_i = -\frac{1}{\mu_0}\left[k_1 l_i^1 l_j^1 + k_2 l_i^2 l_j^2 + k_3 l_i^3 l_j^3\right]\nabla_j p + \frac{1}{\mu_0}\sum_{\alpha=1}^{3} k_\alpha \gamma_\alpha l_i^\alpha l_j^\alpha \frac{\nabla_j p}{\left|l_n^\alpha \nabla_n p\right|} \quad (25.63)$$

Let's analyze the obtained Eq. (25.63). The grid formed by the three mutually perpendicular capillary systems, depending on geometrical parameters d_α, a_α, can have either isotropic or anisotropic filtration properties. At $d_1 = d_2 = d_3$ and $a_1 = a_2 = a_3$ we have the grid with isotropic filtration properties, and on almost all other occasions the grid will have anisotropic properties. For the isotropic properties, Eq. (25.63) will be:

$$w_i = -\frac{k}{\mu_0}\delta_{ij}\nabla_j p + \frac{k}{\mu_0}\gamma\sum_{\alpha=1}^{3} l_i^\alpha l_j^\alpha \frac{\nabla_j p}{\left|l_n^\alpha \nabla_n p\right|}, \quad (25.64)$$

where δ_{ij} is Kroneker's delta.

Let's compare the derived Eq. (25.64) with equation for the NVL filtration in the isotropic porous medium Eq. (25.9). Usually the rule of NVL filtration in the isotropic porous medium is written as:

$$w_i = -\frac{k}{\mu_0}\left(1 - \frac{\gamma}{|\nabla p|}\right)\nabla_i p, \quad (25.65)$$

where $|\nabla p|$ is modulus of filtration pressure gradient. The ratio $\nabla_i p/|\nabla p|$ is equal to a unitary vector directed along the applied action. So, Eq. (25.65) can be rearranged differently as:

$$w_i = -\frac{k}{\mu_0}\delta_{ij}\nabla_j p + \frac{k}{\mu_0}\gamma\delta_{ij} n_i, \quad (25.66)$$

where n_i is the unitary vector which assigns the direction of the action: $\nabla_i p = |\nabla p| n_i$.

Despite their mathematical equivalency, Eqs. (25.65) and (25.66) allow for different physical interpretations. Eq. (25.65) is usually considered to be a nonlinear filtration equation, where the expression $k(1-\gamma/|\nabla p|)$ sets up nonlinear

permeability. Eq. (25.66) can be considered to be the sum containing two tensors: the permeability tensor ($k_{ij} = k\delta_{ij}$) and the cutoff (initial) gradient tensor ($t_{ij} = k\gamma\delta_{ij}$).

Eq. (25.66) is more general as it allows possible symmetry independence of the properties given by the tensors k_{ij} and t_{ij}. As it follows for the model permeability equation ($k^{\alpha} = \pi d_{\alpha}^{4}/128 a_{\beta} a_{\gamma}$), a situation is possible when at $d_1 \neq d_2 \neq d_3$ the medium manifests isotropic properties during filtration of a Newtonian fluid, but in the filtration equation of NVL, with the isotropic tensor k_{ij}, we will have the anisotropic tensor t_{ij}.

Indeed, permeability tensor k_{ij} is represented as a composition of two parameters (the shape factor $d_{\alpha}^{2}/32$ and clearance $\pi d_{\alpha}^{2}/4 a_{\beta} a_{\gamma}$), and the cutoff gradients tensor is represented as a combination of three parameters (the shape factor, clearance and $4\tau_0/d_{\alpha}$ factor, which is the cutoff pressure gradient for the α^{th} capillary). With the isotropic permeability tensor, anisotropic tensor of the cutoff gradients can be found. So, it is important to assume that for NVL filtration within porous media, filtration equation has the following format:

$$w_i = -\frac{1}{\mu_0} k_{ij} \nabla_j p + \frac{1}{\mu_0} t_{ij} n_j . \tag{25.67}$$

Let's now come back to Eq. (25.63). Remembering, that $\nabla_i p = |\nabla p| n_i$:

$$w_i = -\frac{k}{\mu_0} \delta_{ij} \nabla_j p + \frac{k}{\mu_0} \gamma \sum_{\alpha=1}^{3} l_i^{\alpha} \operatorname{sgn} \ (n_j l_j^{\alpha}) . \tag{25.68}$$

where $\operatorname{sgn}(n_j l_j^{\alpha})$ is the signum function, which is equal to one if $n_j l_j^{\alpha} > 0$, and –1 if $n_j l_j^{\alpha} < 0$.

Let's further review Eqs. (25.67) and (25.68). Comparing them shows that the cutoff gradient value in Eq. (25.67) is assigned any direction using the second rank tensor. At the same time, in Eq. (25.68) the cutoff gradient is determined as the sum of the cutoff gradients along the major directions of the permeability tensor. In either case, the cutoff gradient value does not depend on the filtration pressure gradient. Thus, the cutoff gradient in Eq. (25.67) can be variable and is determined and assigned continuously for any direction. In Eq. (25.68), the cutoff gradient is represented by a constant vector in each quadrant of the Cartesian coordinate system. For a continuum model, the Eq. (25.67) appears to be more natural.

However, Eq. (25.67), as in the case of a single capillary system, does not completely define the NVL filtration rule as they only give filtration equations if the conditions of the flow beginning are met (for the isotropic case, $|\nabla p| > \gamma$). Thus, in order to derive the rule of the NVL filtration in anisotropic media, it is necessary to formulate the condition for the beginning of the flow and write down all possible options of filtration flows, which arise due to the fact that the cutoff gradient values in anisotropic media vary depending on the direction.

A condition for the flow beginning, as in the case of a single capillary system, can be the inequality based on the condition of negative friction at the fluid flow in a porous medium:

$$w_i \nabla_i p < 0. \tag{25.69}$$

After substituting filtration Eq. (25.67) into this inequality, the condition for the flow beginning in the direction n_i is:

$$|\nabla p| > \frac{t_{ij} n_i n_j}{k_{ij} n_i n_j}. \tag{25.70}$$

It follows from there that for the isotropic case the flow is possible at $|\nabla p| > \gamma$. For anisotropic media, however, this representation has low information value. By analogy with the definition of the directional permeability, the factor of "the directional movability" is introduced:

$$P(|\nabla p|, n_i) = -\mu_0 w_i n_i / |\nabla p| = k_{ij} n_i n_j - t_{ij} n_i n_j / |\nabla p|. \tag{25.71}$$

In this case the flow beginning condition boils down to the requirement of positivity of the movability factor: $P(|\nabla p|, n_i) > 0$. Therefore, filtration Eq. (25.67) is valid if the movability factor on application of action in the direction n_i is greater than zero.

For an isotropic medium, the addition of the no-flow condition ($w_i = 0$) to this system in the case of a negative movability factor, would be a complete definition of the filtration rule. In the anisotropic porous media, however, motion Eq. (25.67) results in numerous possible outcomes in the formulation of the NVL filtration rule.

Indeed, in the anisotropic media, the realization of the flow beginning condition $P(|\nabla p|, n_i) > 0$ is a guarantee of 3D NVL motion under Eq. (25.67). However, the second rank tensors in the main directions assume extremal values of the directional

properties. For this reason, the fact that $P(|\nabla p|, n_i) < 0$ does not mean that NVL filtration is impossible.

Indeed, let's assume with certainty that $\gamma_1 > \gamma_2 > \gamma_3$. Then, when the condition $P(|\nabla p|, n_i) < 0$ is realized, inequality $|\nabla_i pb_i| > \gamma_3$ can also be realized (see Fig. 25.7). And this means that the pressure gradient attached in the direction n_i can be sufficient to realize the flow beginning condition for only one system of channels. In this case the filtration flow will be unidimensional and will be described by motion Eq. (25.60) at $\alpha = 3$. The two-dimensional flow is possible if $P(|\nabla p|, n_i) < 0$, but $(k_2 n_2^2 + k_3 n_3^2)|\nabla p||n_0| - (k_2\gamma_2 n_2^2 + k_3\gamma_3 n_3^2) > 0$, where $|n_0|$ is the length of vector n_i projection onto the Ox_2x_3 plane.

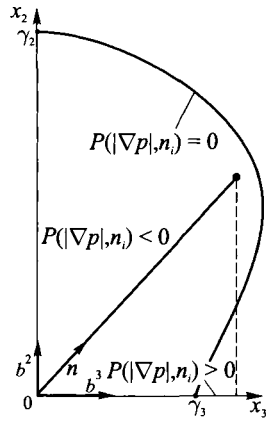

Fig. 25.7. Cross-section of the surface of zero directional movability (initial gradients) at $k_3 = k_2$ and $d_3/d_2 = 3$.

Thus, the NVL filtration rule in anisotropic media allows for the single-, two- and three-dimensional formulations.

Mechanics of Fluid Flow
by Kaplan S. Basniev, Nikolay M. Dmitriev and George V. Chilingar

CHAPTER XXVI

LIQUID AND GAS FLOW IN FRACTURED AND FRACTURED-POROUS MEDIA

As the demand for oil and gas increases, petroleum exploration goes deeper, enters new areas, encounters more complex geology. Significant number of large fields discovered in the Middle East, North America, Europe and other regions are associated with carbonate reservoirs which are fractured.

Certain anomalous behavior was observed in some fields. Intense circulation loss occurred in the wells against low-permeability section; high flow-rates were obtained in wells with the stationary regime from the low-permeability intervals. These and similar occurrences indicated the presence of systems of communicating fractures, which served as avenues for the fluid inflow or circulation loss.

Field data and laboratory studies of cores and thin-sections showed that the fractures have complicated structure, and liquids and gas flow in them has certain specifics compared to the porous medium. Fractured rocks have micro- and macro-fractures, small and large caverns and cavities. At the same time, the rock matrix may be totally impermeable or just a regular porous rock. The macro-fracture width may be 1 mm, sometimes greater. The width of micro-fractures is usually 1 to 100 μm. The resistance to the fluid flow in the fractured rock is substantial. Based on this, it is believed that the macro-fractures are not very long and in most cases connect with one another through micro-fractures, and the micro-features create higher resistance to the flow.

Liquid and gas filtration models created for the clastic granular reservoirs do not fully describe filtration specifics in the carbonate reservoirs whose main distinction was the variable nature of the fracturing.

Generation of the new filtration models for the fractured rocks involved more detailed studies of the geology and physical properties of these rocks.

This chapter deals with the most common model and concepts associated with filtration in fractured rocks.

1. Specifics of filtration in fractured and fractured-porous media

The subsurface hydromechanics describes the filtration processes in fractured reservoirs using two models, purely fractured (Fig. 26.1a) and fractured-porous (Fig. 26.1b). In the former case, the rock between the fractures is impermeable, and

the fluid flow occurs only through the fractures. Such rocks include shales, crystalline rocks, marls and some limestones and dolomites.

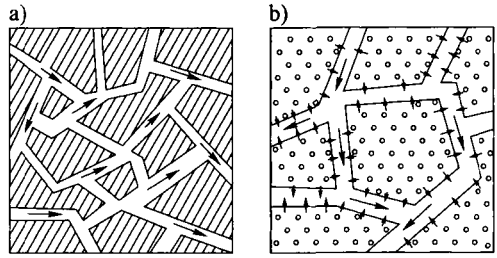

Fig. 26.1. Schematic representation of a purely-fractured (a) and fractured-porous (b) media.

Suppose a fluid-saturated fractured rock is considered as a continuous medium. Then a representative volume for which averaged filtration parameters are introduced must be much larger than in the case of the filtration parameter determination for a porous medium. For instance, if the fractured reservoir is represented as a system of fractures, then the number of fractures in the representative volume should be at least ten.

Fractured-porous medium is a combination of porous blocks separated by the fractures (Fig. 26.1b). The fluid saturates both the porous blocks and fractures. The sizes of the fractures significantly exceed characteristic sizes of the pores, so the fracture permeability is much greater than that of the porous blocks. At the same time, the fractures occupy substantially smaller void volume than the pores. For this reason, the fracturing factor $\varnothing_1$, i. e., the ratio of the fracture volume to the entire rock volume, is much smaller that the block porosity $\varnothing_2$. Fractured porous reservoirs are mostly limestones and dolomites, sometimes sandstones and siltstones.

Let's review a purely fractured rock. The fracture is viewed as a narrow slit with two dimensions (breadth and length) much larger than the third one (the distance between the walls called the fracture width). The fracturing factor $\varnothing_1$, as well as permeability k_1, is determined by the fracture density and width. To determine the introduced parameters, a simplified fractured reservoir model is usually considered. The simplest fractured reservoir is viewed as slits formed by two parallel planes with the constant opening width δ and laying period b (Fig. 26.2). Such a model is called the fractured medium with ordinary fracture system or just fracture system. Fracture density Γ is the number of fractures per unit length of the axis perpendicular to the fractures. By definition, the fracture system density is:

$$\Gamma = \frac{n}{h}$$

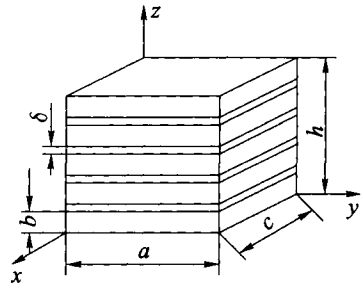

Fig. 26.2. Model of the fractured medium with the orderly fracture system.

For an orderly fracture system, this equation may be written as follows:

$$\Gamma = \frac{n}{h} = \frac{n}{n(b+\delta)} = \frac{1}{b+\delta} \tag{26.1}$$

The fracturing factor for an orderly fracture system is $\varnothing_1 = \Gamma\delta$. If there are two fracture system in the reservoir, with the equal density and width, then $\varnothing_1 = 2\Gamma\delta$, etc.

In a general case, it is believed that for the fractured reservoirs:

$$\varnothing_1 = \theta\Gamma\delta \tag{26.2}$$

where θ is a dimensionless factor depending on the fracture system geometry in the reservoir.

2. Filtration laws in fractured media

The liquid or gas flow through an orderly fracture system may be described similarly to the way it was done for a single capillary system in a porous medium (Chapter XXVIII), but using Boussinesq's (rather than Poiseuille's) equation:

$$v = \frac{\delta^2}{12\mu}\frac{\Delta p}{l} \tag{26.3}$$

which associates the average velocity v in one plane of the slit and the pressure drawdown Δp at the distance l. For the case of an orderly fracture system and the pressure gradient directed parallel to the fracture planes, Eq. (26.3) determines true

filtration velocity. To transfer to filtration velocity w, let's calculate the through-flow through the fracture

$$v\delta a = \frac{\delta^2}{12\mu}\frac{\Delta p}{l}\delta a$$

and "spread" it over the entire area of the elementary cell. The result is the motion equation of the filtering liquid:

$$w = \frac{v\delta a}{(b+\delta)a} = \frac{\delta^2}{12}\cdot\frac{\delta a}{(b+\delta)a}\cdot\frac{1}{\mu}\frac{\Delta p}{l} \tag{26.4}$$

This equation coincides in its format with Darcy's law Eq. (18.11) and with the motion equation in an ideal tube Eq. (18.37), although with a different representation of the factor in front of $\Delta p/\mu l$:

$$w = \frac{\delta^2}{12}\cdot\frac{\delta a}{(b+\delta)a}\cdot\frac{1}{\mu}\frac{\Delta p}{l} \tag{26.5}$$

Darcy's law Eq. (1.11) indicates that the resulting factor:

$$\frac{\delta^2}{12}\cdot\frac{\delta}{(\delta+b)} = \frac{\delta^3}{12(\delta+b)} = k \tag{26.6}$$

is permeability of the orderly fractures. The format of numerical factors in the right part of Eq. (26.6) is preserved (as in the ideal tube model) in order to emphasize the physical meaning of its components. The first component $\delta^2/12$ assigns fracture system's "conductivity"; its format is determined by the form of the channels cross-section (for a cylindrical tubule $d^2/32$). The second component $\delta/(b+\delta)$ assigns clearance, which plays the role of averaging scale. The sinuosity factor is often included in equations for permeability determination. In fractured media, the earlier introduced dimensionless factor θ plays the role of sinuosity.

Eq. (26.5) can be presented both in the vector and matrix format. With a single orderly system of fractures, filtration is only possible in the $0xy$ plane (Fig. 26.2). The medium is impermeable in the direction of the axis z ($k_3 = 0$). Thus, the matrix presentation has the following format:

$$\begin{pmatrix} w_1 \\ w_2 \\ w_3 \end{pmatrix} = -\frac{1}{\mu}\begin{pmatrix} k & 0 & 0 \\ 0 & k & 0 \\ 0 & 0 & 0 \end{pmatrix}\begin{pmatrix} \partial p/\partial x_1 \\ \partial p/\partial x_2 \\ \partial p/\partial x_3 \end{pmatrix}, \tag{26.7}$$

where $k = \delta^3/12(\delta+b)$.

Using the dyadic representation Eq. (18.55), the matrix format Eq. (26.7) can be reduced to the vector format:

$$w_i = -\frac{1}{\mu}\left(k_1 e_i^{(1)} e_j^{(1)} + k_2 e_i^{(2)} e_j^{(2)}\right) \frac{\partial p}{\partial x_j} \tag{26.8}$$

Eq. (26.5) was derived for a single orderly fracture system. The same train of thought will be valid for a 3D model of three mutually perpendicular systems of fractures (Fig. 26.3). The only difference would be that the subscripts will be needed to the parameters δ and b. The purpose is to indicate to which fracture the written equation corresponds and to take into account the fact that the flows in the fractures will sum up. Eq. (26.5) in the matrix format Eq. (26.7) can be written for each orderly fracture system:

$$\begin{pmatrix} w_1^1 \\ w_2^1 \\ w_3^1 \end{pmatrix} = -\frac{1}{\mu}\begin{pmatrix} 0 & 0 & 0 \\ 0 & k_1 & 0 \\ 0 & 0 & k_1 \end{pmatrix}\begin{pmatrix} \partial p/\partial x_1 \\ \partial p/\partial x_2 \\ \partial p/\partial x_3 \end{pmatrix}$$

$$\begin{pmatrix} w_1^2 \\ w_2^2 \\ w_3^2 \end{pmatrix} = -\frac{1}{\mu}\begin{pmatrix} k_2 & 0 & 0 \\ 0 & 0 & 0 \\ 0 & 0 & k_2 \end{pmatrix}\begin{pmatrix} \partial p/\partial x_1 \\ \partial p/\partial x_2 \\ \partial p/\partial x_3 \end{pmatrix}$$

$$\begin{pmatrix} w_1^3 \\ w_2^3 \\ w_3^{31} \end{pmatrix} = -\frac{1}{\mu}\begin{pmatrix} k_3 & 0 & 0 \\ 0 & k_3 & 0 \\ 0 & 0 & 0 \end{pmatrix}\begin{pmatrix} \partial p/\partial x_1 \\ \partial p/\partial x_2 \\ \partial p/\partial x_3 \end{pmatrix},$$

where the fracture number is determined by the number of a coordinate axis, to which the perpendicular to the fractures is parallel. Then, the total result can be by summing up $\vec{w} = \sum_{\alpha} \vec{w}^{\alpha}$:

$$\begin{pmatrix} w_1 \\ w_2 \\ w_3 \end{pmatrix} = -\frac{1}{\mu}\begin{pmatrix} k_2 + k_3 & 0 & 0 \\ 0 & k_1 + k_3 & 0 \\ 0 & 0 & k_1 + k_2 \end{pmatrix}\begin{pmatrix} \partial p/\partial x_1 \\ \partial p/\partial x_2 \\ \partial p/\partial x_3 \end{pmatrix} \tag{26.9}$$

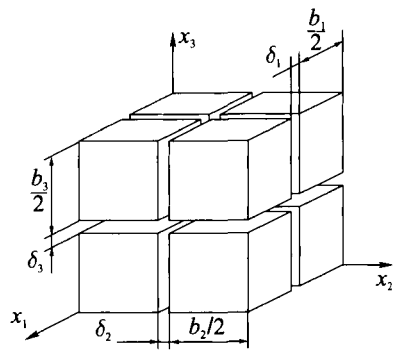

Fig. 26.3. 3D model of a fractured rock.

It follows from Eq. (26.9), that, for instance, by applying the pressure gradient parallel to the α^{th} axis the following equation is obtained:

$$\vec{w} = -\frac{1}{12}\cdot\left(\frac{\delta_\beta^3}{\delta_\beta + b_\beta} + \frac{\delta_\gamma^3}{\delta_\gamma + b_\gamma}\right)\cdot\frac{1}{\mu}\cdot \text{grad}p = -\frac{k_\beta + k_\gamma}{\mu}\text{grad}p\,. \quad (26.10)$$

There, the subscripts α, β, γ correspond to the number of the coordinate axis, onto which the lengths of the fracture parameters are projected, and form a cyclical permutation of the numbers 1, 2 and 3. k_β and k_γ are permeabilities of the orderly orderly fracture systems with subscripts β and γ determined, respectively, from Eqs. (26.6).

From Eq. (26.10), we will derive permeability K_α, in the direction of the coordinate axis α, for the 3D fractured medium model:

$$K_\alpha = \frac{1}{12}\left(\frac{\delta_\beta^3}{\delta_\beta + b_\beta} + \frac{\delta_\gamma^3}{\delta_\gamma + b_\gamma}\right) = k_\beta + k_\gamma \quad (26.11)$$

The technique of obtaining the filtration rule for purely fractured reservoir by summing-up of the filtration rules for orderly fracture systems is called the matrix technique.

The other reservoir parameters of a 3D fractured system model are also easy to calculate:

$$\varnothing = \sum_{\alpha=1}^{3}\frac{\delta_\alpha}{\delta_\alpha + b_\alpha},\ \Sigma = 2\sum_{\alpha=1}^{3}\frac{1}{\delta_\alpha + b_\alpha},\ s_\alpha = \frac{\delta_\beta}{\delta_\beta + b_\beta} + \frac{\delta_\gamma}{\delta_\gamma + b_\gamma} \quad (26.12)$$

It follows from Eq. (26.12) that $2\varnothing = (s_1 + s_2 + s_3)$, and the equality of clearance and porosity is only realized when $\delta_2 = \delta_3 = 0$, i. e., as was the case for an

ideal rock model, only for a single orderly fracture system. One can observe from Eqs. (26.9) and (26.11) that fractured reservoirs are as a rule anisotropic, although to simplify we will treat them as isotropic.

3. Permeability vs. pressure in fractured and fractured-porous media

Laboratory experiments and field practice showed that there is a much stronger dependence of permeability on pressure in fractured and fractured-porous reservoirs than in the porous ones. Let's review several ways to model this correlation $k(p)$.

First, Eq. (26.6) is rearranged using Eqs. (26.1) and (26.2):

$$k = \frac{\delta^3}{12(\delta + b)} = \frac{\varnothing_1 \delta^2}{12} = \frac{\theta \Gamma \delta^3}{12} \tag{26.13}$$

Then, similar to the case of porosity vs. pressure Eq. (19.40), the correlation of openness/width vs. pressure using the elasticity factor β of a fractured reservoir is introduced:

$$\beta = \frac{d\delta}{\delta dp}, \tag{26.14}$$

where $d\delta$ is the change in the fracture openness/width as pressure changes by dp. Now the fracture compressibility rule can be integrated to find correlation between the opening/width and pressure $\delta = \delta(p)$. Upon separating the variables:

$$\beta dp = d \ln \delta$$

and integrating:

$$\beta \int_{p_0}^{p} dp = \int_{\delta_0}^{\delta} d \ln \delta$$

results in:

$$\beta (p - p_0) = \ln \frac{\delta}{\delta_0}$$

or:

$$\delta = \delta_0 e^{\beta (p - p_0)} \tag{26.15}$$

Assuming the exponent $\beta(p-p_0)$ is usually small, it is possible to expand it into a series and, limiting ourselves only to the linear term of the expansion:

$$\delta=\delta_0\left[1+\beta(p-p_0)\right] \tag{26.16}$$

At large values of $\beta(p-p_0)$, it is necessary to use Eq. (26.15) for the equation of state of the elastic liquid.

Let's now return to Eq. (26.13). By definition, θ is a dimensionless factor determined by the fracture system geometry in the reservoir. Therefore, it does not depend on pressure, and Γ, as Eq. (26.1) shows, at $\delta/b<<1$:

$$\Gamma=\frac{n}{h}=\frac{n}{n(b+\delta)}=\frac{1}{b+\delta}\approx\frac{1}{b},$$

then permeability as a function of pressure can be presented as follows:

$$k=\frac{\theta\Gamma\delta^3}{12}=\frac{\theta\Gamma}{12}\delta_0^3\left[1+\beta(p-p_0)\right]^3$$

or, as at $p=p_0$:

$$k_0=\frac{\theta\Gamma\delta_0^3}{12},$$

then:

$$k=k_0\left[1+\beta(p-p_0)\right]^3. \tag{26.17}$$

When the $\beta(p-p_0)$ value is high, similar calculations will result in an exponential correlation between permeability and pressure like Eq. (19.45):

$$k=k_0e^{\alpha(p-p_0)} \quad \text{where } \alpha=3\beta \tag{26.18}$$

In granular reservoirs, at small pressure changes the Eq. (26.17) correlation usually can be assumed linear:

$$k=k_0\left[1+a(p-p_0)\right] \tag{26.19}$$

It is usually believed that under the stationary filtration in a fractured-porous reservoir, permeability k_1 strongly depends on pressure and is defined by one of Eqs. (26.17)–(26.19), whereas permeability k_2 of the porous blocks does not depend on pressure and is assumed to be constant.

In fractured rocks, where the true flow cross-section is relatively small, the flow-rates are usually high; a deviation from Darcy's law due to inertia forces is highly probable. Usually, the binomial filtration law Eq. (18.22) is used.

4. Fluid crossflow in fractured-porous media

These filtration specifics are especially clear in the fractured-porous rocks under non-stationary processes. The fracture system and the pore system are two media with different linear scales. The average pore size is 10 μm, and the average fracture opening/width is 10^2 μm (and their length is between a few centimeters and hundreds of meters). At the same time, the block/matrix porosity $\varnothing_2$ is one to two orders of magnitude higher than porosity of fractures $\varnothing_1$. Permeability is proportional to the squared characteristic linear size. For this reason fracture permeability is much higher than the block/matrix permeability, so most of the fluid is contained in pores but filtration occurs in fractures. In the process, the fluid moves in pores and fractures with cross-flows from the matrix blocks into fractures.

Let's review the cross-flow process in more detail. Suppose bottomhole pressure drastically changes (for instance, during the well startup). If the matrix blocks are considered impermeable, the regular elastic drive theory can be used. Piezoconductivity $\kappa = k_1 / \left[\left(\beta_{liq} \varnothing_1 + \beta \right) \mu \right]$ as determined through the fracture system parameters can turn out to be very large compared with the porous reservoir (because permeability k_1 of the fractured rock is high, and the fracturing factor $\varnothing_1$ is low). It means that the pressure distribution process will occur at a higher velocity in the fractures than in the matrix blocks. Indeed, pressure change under the elastic drive is found as:

$$p(x,t) = p_к - \frac{Q\mu}{kBh}\left(\sqrt{2\kappa t} - x\right), \quad 0 \le x \le \sqrt{2\kappa t}\,.$$

It follows from there that at the x value set, the greater η, the faster pressure changes. So, a new pressure distribution sets up in the fractures over a relatively short period of time. Pressure within the matrix blocks changes more slowly, so pressure difference emerges between the matrix blocks and the fractures. As a result of the liquids partial cross-flow from the matrix blocks to the fractures, pressure in the entire reservoir will level. The lower the matrix blocks permeability k_2, the higher their porosity $\varnothing_2$ larger their size, and larger liquid and matrix compressibilities β_l and β, the longer is the process.

Thus, the flow parameters in the matrix blocks and fractures are different: the matrix blocks pressure p_2 is greater that pressure in the fractures p_1, the filtration velocity in the matrix blocks w_2 is much lower that filtration velocity in fractures w_1. For this reason, a fractured-porous medium under the non-stationary processes can be considered as a combination of two porous media with pores at different scale. Medium 1 is an amalgamated medium where the porous matrix

blocks play the role of grains and considered to be impermeable. The fractures play the role of pore channels. Pressure in this medium is p_1, and filtration velocity, w_1. Medium 2 is porous matrix blocks composed of grains separated by small pores. Pressure in this medium is p_2, and filtration velocity, w_2.

Thus, an important feature of the non-stationary processes in fractured-porous reservoirs is intensive fluid exchange between both media, i. e., between the porous matrix blocks and the fractures. The exchange is caused by the pressure difference between the media.

Clearly, during the motion of a slightly-compressible liquid out of the matrix blocks into the fractures per unit time per unit volume, the intensity q of the cross-flow is in direct proportion to the pressure difference $p_2 - p_1$, density ρ_0 (provided density changes little in the pressure interval of p_1 to p_2), and in inverse proportion to viscosity μ, i. e.:

$$q = \alpha_0 \frac{\rho_0}{\mu}(p_2 - p_1), \tag{26.20}$$

where α_0 is dimensionless factor determined by the matrix block permeability k_2, characteristic linear size l, and dimensionless values describing the matrix block shape; $\alpha_0 = \tilde{\alpha} k_2 / l^2$.

Eq. (26.20) should be considered in cases where density strongly depends on pressure. For instance, in the ideal gas filtration the cross-flow intensity from the matrix blocks into the fractures is:

$$q = \alpha_0 \frac{\rho_0}{\mu^2 p_0}\left(p_2^2 - p_1^2\right), \tag{26.21}$$

where p_0 is pressure corresponding to density ρ_0.

5. Derivation of differential equations for liquids and gas flow within the fractured and fractured-porous media

Now, the differential equations are derived for the liquids and gas flow within a deformable fractured-porous medium on the assumption that there are two pressures at each point of the medium (p_1 in the fracture system, p_2 in the porous matrix blocks), and two respective filtration velocities w_1 and w_2. The cross-flows between the media are determined from Eqs. (26.20) and (26.21).

Therefore, under the initial assumption the fractured-porous medium is a multi-velocity continuum where there is the mass transfer from the component 2 into the component 1 or the other way around.

In this case, the balance of mass equation written for the control volume, as opposed to Eq. (19.4), derived earlier in Chapter XIX, has an additional integral over the volume with the cross-flow function q_{ji}. This function represents the liquid (or gas) mass flowing per unit time within the control volume from the j^{th} component to the i^{th} component and has the following format:

$$\frac{\partial}{\partial t}\int_V \varnothing_i \rho_i dV = -\oint_S \rho w_i^n ds + \int_V q_{ji} dV, \tag{26.22}$$

where the subscript i assumes the values 1 and 2 and corresponds to the number of the medium (1, fractures; 2, matrix blocks). At that, q_{12} corresponds to the cross-flow from 1 to 2, q_{21}, tj the cross-flow from 2 to 1, $q_{11} = q_{22} = 0$.

It is possible to transfer the integral formulation of the mass conservation law Eq. (26.22) to a differential formulation. For this purpose let's do the following: first, the control volume is set in space, its position does not depend on time, so it is possible to move the operator $\partial/\partial t$ under the integral; second, the surface integral is changed into a volume integral using Gauss–Ostrogradsky theorem:

$$\int_V \left(\frac{\partial \varnothing_i \rho_i}{\partial t} + div \rho_i \vec{w}_i - q_{ji} \right) dV = 0. \tag{26.23}$$

The condition of Eq. (26.23) is realized for any "physical" volume, the expression under the integral is equal to zero:

$$\frac{\partial \varnothing_i \rho_i}{\partial t} + div \rho_i \vec{w}_i - q_{ji} = 0. \tag{26.24}$$

Eq. (26.24) is the differential format of the mass conservation law both for the fractures ($i = 1$) and the matrix blocks ($i = 2$). In the equation for fractures, the matrix blocks-to-fractures cross-flow function is $q_{21} = q$, and in the equation for the matrix blocks, the matrix blocks-to-fractures cross-flow function is $q_{12} = -q$, i. e., $q_{21} = -q_{12}$. Density values ρ_i in Eqs. (26.24) correspond to the pressure values p_i.

Clearly, for a purely fractured reservoir $q_{21} = -q_{12} = 0$, and a single Eq. (26.24) remains at $i = 1$.

Let's now introduce Leibensohn's functions for the fracture system P_1 and for the pore matrix blocks P_2 according to Eq. (19.20):

$$P_1 = \int \frac{k_1(p_1)}{\mu(p_1)} \rho(p_1) dp_1 + \text{const}. \tag{26.25}$$

$$P_2 = \int \frac{k_2(p_2)}{\mu(p_2)} \rho(p_2) dp_2 + \text{const}. \tag{26.26}$$

Assuming that the linear Darcy's law is realized, it is possible to write differential equations as follows:

$$\rho \vec{w}_i = -\text{grad}\, P_i$$

or in Cartesian coordinates:

$$\rho w_{1x} = -\frac{\partial P_1}{\partial x}, \quad \rho w_{1y} = -\frac{\partial P_1}{\partial y}, \quad \rho w_{1z} = -\frac{\partial P_1}{\partial z_1} \tag{26.27}$$

$$\rho w_{2x} = -\frac{\partial P_2}{\partial x}, \quad \rho w_{2y} = -\frac{\partial P_2}{\partial y}, \quad \rho w_{2z} = -\frac{\partial P_2}{\partial z_1} \tag{26.28}$$

Substituting Eqs. (26.27), (26.28) and (26.20) for an elastic liquid or Eq. (26.21) for the gas, into the continuity Eqs. (26.24), gives the system of equations for the non-stationary filtration of any uniform fluid in a fractured-porous medium. In the Cartesian coordinate system:

$$\frac{\partial^2 P_1}{\partial x_1^2} + \frac{\partial^2 P_1}{\partial x_2^2} + \frac{\partial^2 P_1}{\partial x_3^2} = \frac{\partial}{\partial t}[\rho(p_1)\varnothing_1(p_1)] - \frac{\alpha_0}{\mu}[f(p_2) - f(p_1)] \tag{26.29}$$

$$\frac{\partial^2 P_2}{\partial x_1^2} + \frac{\partial^2 P_2}{\partial x_2^2} + \frac{\partial^2 P_2}{\partial x_3^2} = \frac{\partial}{\partial t}[\rho(p_2)\varnothing_1(p_2)] + \frac{\alpha_0}{\mu}[f(p_2) - f(p_1)], \tag{26.30}$$

where $f(p) = \rho_0 p$ for an elastic liquid, $f(p) = \rho_0 p^2 / 2p_0$ for the ideal gas.

In order to solve the above system relative to p_1 and p_2, the initial and boundary conditions must be added.

6. Stationary unidimensional liquids and gas filtration in a fractured and fractured-porous reservoir

In this section the stationary liquid and gas filtration is considered in a deformable purely fractured reservoir where permeability depends on pressure under one of the rules of Eqs. (26.17)–(26.19). In this case, Eq. (26.29) is reduced to Laplace's equation for Leibensohn's function as defined by Eq. (11.25):

$$\frac{\partial^2 P_1}{\partial x_1^2} + \frac{\partial^2 P_1}{\partial x_2^2} + \frac{\partial^2 P_1}{\partial x_3^2} = 0 \tag{26.31}$$

Let's find the solution for filtration of an uncompressible liquid ($\rho_0 = \text{const}$) with constant viscosity ($\mu = \text{const}$) in a reservoir, whose permeability is an exponential function of pressure Eq. (26.18). First, let's calculate Leibensohn's function:

$$P_l = \int \frac{\rho_0}{\mu} k_1^0 e^{\alpha(p-p_0)} dp + \text{const} = \frac{\rho_0 k_1^0 e^{\alpha(p-p_0)}}{\alpha\mu} + \text{const}$$

The solution for a radial-plane filtration flow expressed through Leibensohn's function was derived in Chapter XX (see Eq. (20.41)). The P and Q_m distributions have the following format:

$$P = P_k - \frac{P_k - P_c}{\ln\frac{R_k}{r_c}} \ln\frac{R_k}{r},$$
$$Q_m = \frac{2\pi kh}{\mu} \frac{P_k - P_c}{\ln\frac{R_k}{r_c}} \tag{26.32}$$

Now the Leibensohn's function is derived at the charge contour and in the well:

$$P_к = \frac{\rho_0 k_1^0 e^{\alpha(p_к - p_0)}}{\alpha\mu} + \text{const}, \quad P_c = \frac{\rho_0 k_1^0 e^{\alpha(p_c - p_0)}}{\alpha\mu} + \text{const} \tag{26.33}$$

substituting into Eq. (26.32):

$$e^{\alpha(p-p_0)} = e^{\alpha(p_к - p_0)} - \frac{e^{\alpha(p_к - p_0)} - e^{\alpha(p_c - p_0)}}{\ln\frac{R_k}{r_c}} \ln\frac{R_k}{r},$$
$$Q_m = \frac{2\pi k_1^0 h\rho_0}{\alpha\mu} \frac{e^{\alpha(p_к - p_0)} - e^{\alpha(p_c - p_0)}}{\ln\frac{R_k}{r_c}} \tag{26.34}$$

If it is assumed that $p_0 = p_к$, Eqs. (26.34) become:

$$e^{\alpha(p-p_к)} = 1 - \frac{1 - e^{-\alpha(p_к - p_c)}}{\ln\frac{R_k}{r_c}} \ln\frac{R_k}{r},$$
$$Q_m = \frac{2\pi k_1^0 h\rho_0}{\alpha\mu} \frac{1 - e^{-\alpha(p_к - p_c)}}{\ln\frac{R_k}{r_c}} \tag{26.35}$$

Equation for the volume flow-rate is:

$$Q = \frac{2\pi k_1^0 h}{\alpha\mu} \frac{1 - e^{-\alpha(p_к - p_c)}}{\ln \frac{R_k}{r_c}} \tag{26.36}$$

The indicator diagram defined by Eq. (26.36) is a curve convex toward the flow-rate axis for the production wells (Fig. 26.4, curve 1), and toward the pressure drawdown axis for the injection wells ($p_c > p_к$; curve 2).

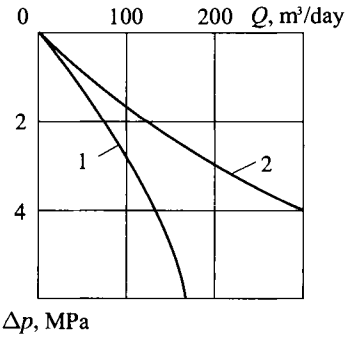

Fig. 26.4. Indicator curves for a production well (1) and injection well (2) in a deformable fractured reservoir.

Rearranging the first Eq. (26.35), gives the rule for the pressure distribution in the reservoir:

$$p = p_c + \frac{1}{\alpha} \ln \left[1 - \frac{1 - e^{-\alpha(p_к - p_c)}}{\ln \frac{R_k}{r_c}} \ln \frac{R_k}{r} \right] \tag{26.37}$$

Fig. 26.5 represents the pressure distribution curves constructed based on Eqs. (26.37) and for undeformable reservoir. Comparison of the curves shows that in the deformable fractured reservoir (due to a decrease in the fracture opening/width as pressure decreases) the resistance increases and pressure declines more drastically that in an undeformable reservoir.

The qualitative features of Eqs. (26.36) and (26.37) are also valid in the case of the permeability vs. pressure correlation as expressed by Eqs. (26.17)–(26.19).

The determination of fractured reservoir parameters (permeability k_1 and factor α) is of a great practical importance.

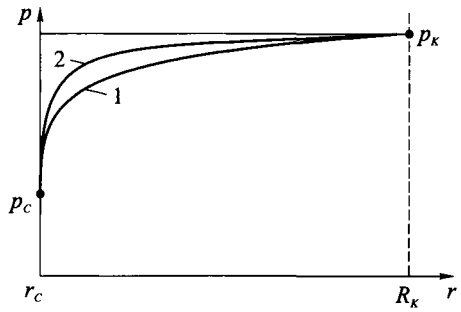

Fig. 26.5. Pressure distribution curves: 1. undeformable reservoir ($k = \text{const}$), 2. fractured reservoir ($k = k^0 e^{\alpha(p-p_0)}$).

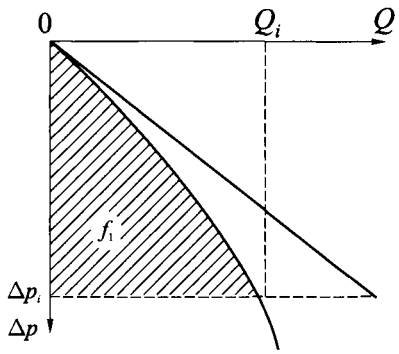

Fig. 26.6. Indicator curve for a fractured reservoir (for parameter determination of fractured tured reservoirs).

Nikolayevsky and Gorlunov (1970) proposed a technique for the processing of indicator curves convex toward the flow-rate axis for the production wells in fractured reservoirs. This technique is now reviewed as it applies to the first equation of Eq. (26.35).

Two areas are recognized in the indicator diagram (Fig. 26.4):

$$f_1 = \int_0^{\Delta p_i} Q d\Delta p$$

the area between the curve $Q(\Delta p)$ and Y-axis (shaded in Fig. 26.6) and:

$$f_2 = Q_i \Delta p_i ,$$

i. e., the quadrangle area for the corresponding point of the indicator curve.

The ratio of these areas $z_m = f_1/f_2$ is calculated analytically through Eq. (26.35). The z depends only on one dimensionless values $\alpha\Delta p$:

$$z = \frac{f_1}{f_2} = \frac{1}{1 - e^{-\alpha\Delta p}} = \frac{1}{\alpha\Delta p} \text{ where } \Delta p = p_0 - p . \qquad (26.38)$$

Various values of $\alpha\Delta p$ are assigned, and the z values calculated from Eq. (26.38) and tabulated. Besides, the $z = f_1/f_2$ ratios are determined for different points of the indicator curve from the actual curve (the area is calculated by hand for instance, with the trapezoid formula). Then from the table $\alpha\Delta p$ is determined for the found z value. As the actual pressure differences Δp_i are known, it is possible to determine α. The α values are found for several Δp_i values, and the average is calculated. Knowing α, it is possible to calculate from flow-rate Eq. (26.36) the hydroconductivity factor $k_1^0 h/\mu$, and then permeability k_1^0 (if the reservoir thickness h and viscosity μ are known).

Field practice showed that α is within the following range: $\alpha = (0.1 - 20) \cdot 10^{-17}\ \text{Pa}^{-1}$.

The indicator curve curvature with the increase of pressure drawdown can be caused not only by the permeability dependence on pressure, but also by some other factors (deviation from Darcy's law, the presence in the reservoir of the initial pressure gradient, etc.) So, possible effect of the other factors must be taken into account in the indicator curve interpretation.

The well flow-rate from a fractured-porous reservoir is a sum total of the liquid's rate from fractures and that from the porous matrix blocks. For instance, if Eq. (26.18) is observed, the total flow-rate of a production well is:

$$Q = \frac{2\pi k_2 h (p_к - p_c)}{\mu \ln \frac{R_к}{r_c}} + \frac{2\pi k_1^0 h}{\alpha\mu} \frac{1 - e^{-\alpha(p_к - p_c)}}{\ln \frac{R_к}{r_c}} , \qquad (26.39)$$

where it is assumed that $k_2 = \text{const}$. Usually, porous matrix block permeability k_2 is much lower than fracture permeability k_1^0, and the major contribution is from the flow in fractures. Thus, discarding the first component in Eq. (26.39) does not result result in a significant flow-rate determination error.

Now, let's find the solution for filtration of the compressible fluid (ideal gas) with constant viscosity ($\mu = \text{const}$) in the reservoir whose permeability is a linear function of pressure Eq. (26.19). The Leibensohn's function can be presented as (assuming $p_0 = p_к$):

$$P_1 = \int \frac{\rho(p)}{\mu} k_1^0(p)\,dp + \text{const} = \int \frac{\rho_{atm} p k_1^0 \left[1 - \alpha(p_к - p)\right]}{p_{atm}\mu} dp + \text{const} =$$

$$= \frac{\rho_{atm} k_1^0}{p_{atm}\mu}\left[(1 - \alpha p_к)\int p\,dp + \alpha \int p^2 dp\right] + \tag{26.40}$$

$$+ \text{const} = \frac{\rho_{atm} k_1^0}{p_{atm}\mu}\left[(1 - \alpha p_к)\frac{p^2}{2} + \alpha \frac{p^3}{3}\right] + \text{const}$$

Gas mass flow-rate at radial-plane filtration in a circular reservoir can be derived by the substitution of Eq. (26.40) into Dupois equation at $p = p_к$ and $p = p_c$ Eq. (20.41):

$$Q = \frac{2\pi k_1^0 h \rho_{atm}}{\mu p_{atm}} \frac{\left[(1 - \alpha p_к)\frac{p_к^2}{2} + \alpha \frac{p_к^3}{3}\right] - \left[(1 - \alpha p_c)\frac{p_c^2}{2} + \alpha \frac{p_c^3}{3}\right]}{\ln \frac{R_k}{r_c}} \tag{26.41}$$

The normalized volume flow-rate can be used by differently representing the expression in the numerator of the second component:

$$Q_{atm} = \frac{\pi k_1^0 h\left(p_к^2 - p_c^2\right)}{\mu p_{atm} \ln R_к / r_c}\left(1 - \frac{\alpha}{3} p_к + \frac{2}{3}\alpha \frac{p_c^2}{p_к + p_c}\right) \tag{26.42}$$

Here, the component in front of the parentheses is the gas flow-rate from the undeformable reservoir. Thus, it is possible to estimate the parameter α effect on the gas flow in the circular reservoir.

If the gas flow-rate from the undeformable reservoir is denoted as Q^* ($\alpha = 0$), then from equation:

$$\frac{Q_{atm}}{Q^*} = \left(1 - \frac{\alpha}{3} p_к + \frac{2}{3}\alpha \frac{p_c^2}{p_к + p_c}\right) \tag{26.43}$$

it is possible to determine the deviation of the gas flow-rate from the deformable reservoir from the gas flow-rate from the undeformable reservoir (for a reservoir with constant permeability).

If, for instance, $\alpha = 2 \cdot 10^{-17}$ Pa^{-1}, $p_к = 10$ MPa and $p_c = 7$ MPa, then $Q^*/Q_{am} = 0.78$, i. e., the flow-rate declines by 28 %.

Using the similar technique, it is possible to derive equations for the flow-rate and pressure distribution of the liquid and gas (at rectilinear-parallel filtration to the gallery) in a fractured deformable reservoir.

7. Non-stationary liquid and gas flow in fractured and fractured-porous reservoirs

To determine the parameters of a non-stationary filtration in fractured and fractured-porous reservoirs, we need to integrate the system of differential Eqs. (26.29) and (26.30) at the assigned initial and boundary conditions.

Let's make the following assumptions: (1) the liquid is weakly-compressible, i. e., the equation of state is Eq. (19.23) — $\rho = \rho_0 e^{\beta_{liq}(p-p_0)}$; (2) viscosity is constant ($\mu = \text{const}$); (3) both media (fractures and porous blocks) are elastic, i. e., porosity is a function of pressure under Eq. (19.42) individually for each reservoir component medium $m_i = m_{0i} + \beta_{ci}(p - p_0)$, $i = 1,2$; (4) permeabilities of both media are constant: $k_1 = \text{const}$, $k_2 = \text{const}$; (5) there is mass exchange between the fractures and blocks, and (6) the mass flowing from the blocks to the fractures is governed by Eq. (26.20).

Under these assumptions, the Leibensohn's functions, as defined by Eqs. (26.25) and (26.26), accurate to small values, are as follows:

$$P_1 = \frac{\rho k_1}{\mu} \int \left[1 + \beta_{liq}(p_1 - p_0)\right] dp_1 + \text{const} \approx \frac{\rho_0 k_1}{\mu} p_1 + \text{const} \qquad (26.44)$$

$$P_2 = \frac{\rho_0 k_2}{\mu} \int \left[1 + \beta_{liq}(p_2 - p_0)\right] dp_2 + \text{const} \approx \frac{\rho_0 k_2}{\mu} p_2 + \text{const} \qquad (26.45)$$

Let's transform the right portions of Eqs. (26.29) and (26.30):

$$\rho(p_i) m_i(p_i) = \rho_0 \left[m_{0i} + \beta_i^*(p_i - p_0) + \beta_{ж}\beta_c (p_i + p_0)^2 \right] \approx$$
$$\approx \rho_0 \left[m_{0i} + \beta_i^*(p_i - p_0) \right] \quad , i = 1,2$$

where the last component is discarded due to its smallness; β_i^* are elastic capacity factors of both media:

$$\beta_i^* = \beta_{ci} + m_{0i}\beta_{ж}$$

Then:

$$\frac{\partial}{\partial t}\left[\rho(p_i)m_i(p_i)\right]=\rho_0\beta_i^*\frac{\partial p_i}{\partial t} \tag{26.46}$$

Substituting Eqs. (26.44), (26.45), (26.46), and (26.20) into the system Eq. (26.29) and (26.30), results in:

$$\frac{k_1}{\mu}\left(\frac{\partial^2 p_1}{\partial x_1^2}+\frac{\partial^2 p_1}{\partial x_2^2}+\frac{\partial^2 p_1}{\partial x_3^2}\right)=\beta_1^*\frac{\partial p_1}{\partial t}-\frac{\alpha_0}{\mu}(p_2-p_1) \tag{26.47}$$

$$\frac{k_2}{\mu}\left(\frac{\partial^2 p_2}{\partial x_1^2}+\frac{\partial^2 p_2}{\partial x_2^2}+\frac{\partial^2 p_2}{\partial x_3^2}\right)=\beta_2^*\frac{\partial p_2}{\partial t}-\frac{\alpha_0}{\mu}(p_2-p_1) \tag{26.48}$$

where p_1 and p_2 are pressures, correspondingly, in the fractures and porous blocks.

Let's introduce the following notations:

$$\eta=\frac{k_1}{\mu\beta_2^*},\quad \varepsilon_1=\frac{\beta_1^*}{\beta_2^*},\quad \varepsilon_2=\frac{k_2}{k_1},\quad \tau=\frac{\mu\beta_2^*}{\alpha_0}$$

Using the $\eta,\varepsilon_1,\varepsilon_2,\tau$ parameters, Eqs. (26.47) and (26.48) look as follows:

$$\eta\nabla^2 p_1=\varepsilon_1\frac{\partial p_1}{\partial t}-\frac{(p_2-p_1)}{\tau} \tag{26.49}$$

$$\eta\varepsilon_2\nabla^2 p_2=\frac{\partial p_2}{\partial t}+\frac{(p_2-p_1)}{\tau} \tag{26.50}$$

where $\nabla^2 p_i=\Delta p_i$ is the Laplace's operator.

It is important to note that piezoconductivity factor η is defined through the fracture system permeability k_1 and blocks' elastic capacity β_2^*; the factor τ has the dimension of time and is called the delay time. It is a very important factor in the theory of liquid's non-stationary flow within a fractured-porous medium. It describes the time lag between pressure redistribution in the fractured-porous medium compared to a porous reservoir with piezoconductivity η. The lag is caused by the liquid exchange between the system of porous blocks and the fracture system. The time lag τ can also be formatted differently:

$$\tau=\frac{\mu\beta_2^*}{\alpha_0}=\frac{\mu\beta_2^* l^2}{\tilde{\alpha}k_2}=\frac{l^2}{\tilde{\alpha}\eta_2}$$

It follows from this equation that large τ values correspond to small piezoconductivity η_2 values and to large block size l (either factor makes the overflow from the blocks into the fractures more difficult).

The following conclusions can be made analyzing the Eq. system (26.49) and (26.50). At $\tau = 0$, $p_1 = p_2$, i. e., the pressures in the fractures and blocks are equal, and the medium behaves as if it is uniform. At $\tau = \infty$, the system falls apart into two filtration equations in the fractures and blocks, i. e., the blocks are now isolated, impermeable, and the medium behaves as if it were purely fractured. The intermediate τ values correspond to the fractured-porous medium. Then, regardless of a specific solution format for a problem, as the time t increases, the solution is tending to the solution of the elastic regime problem coming asymptotically close to it after the time duration of several t's.

The system of equations Eqs. (26.49) and (26.50) can be simplified as the fracture porosity $\varnothing_1$ and block permeability k_2 are small, i. e., $\varnothing_1/\varnothing_2 << 1$ and $k_1/k_2 >> 1$; therefore, $\varepsilon_1 << 1$ and $\varepsilon_2 << 1$, and the components $\varepsilon_1 \partial p_1/\partial t$ and $\eta\varepsilon_2\nabla^2 p_2$ can be discarded. The result is:

$$\eta\nabla^2 p_1 + \frac{(p_2 - p_1)}{\tau} = 0 \text{ and } \frac{\partial p_2}{\partial t} + \frac{(p_2 - p_1)}{\tau} = 0 \qquad (26.51)$$

The above assumption ($\varnothing_1 = 0$ and $k_2 = 0$) means that the liquid is "stored" in the blocks and flows only in the fractures (as the mass change in the fracture system and the liquid flow in the blocks are disregarded).

There are numerous solutions of the system Eqs. (26.49) and (26.50) and of the truncated system Eq. (26.51) derived by way of integrating differential equations and using approximation techniques (integral ratios, averaging, etc.) All these solutions are complex and unwieldy.

Here, the graphs resulting from the solution of the radial-plane problem are included for the elastic liquid withdrawal at a constant flow-rate Q from a well with the radius r_c in an indefinite fractured-porous reservoir.

The problem setting is as follows:

Eqs. (26.49) and (26.50) for radial-plane flow are:

$$\eta\frac{1}{r}\frac{\partial}{\partial r}\left(r\frac{\partial p_1}{\partial r}\right) = \varepsilon_1\frac{\partial p_1}{\partial t} - \frac{(p_2 - p_1)}{\tau} \qquad (26.52)$$

$$\eta\varepsilon_2\frac{1}{r}\frac{\partial}{\partial r}\left(r\frac{\partial p_2}{\partial r}\right) = \frac{\partial p_2}{\partial t} + \frac{(p_2 - p_1)}{\tau} \qquad (26.53)$$

At the initial time, the pressures in the fractures and blocks are equal (p_0):

$$p_1(r,0) = p_2(r,0) = p_0 \tag{26.54}$$

This pressure is maintained at all times in distant locations:

$$p_1(r,t) = p_2(r,t) = p_0 \quad \text{at } r \to \infty, t > 0 \tag{26.55}$$

The condition at the bore hole is as follows:

$$r\frac{\partial p_1}{\partial r} + \varepsilon_2 \frac{\partial p_2}{\partial r} = \frac{\mu Q}{2\pi k_1 h} \quad \text{at } r = r_c \tag{26.56}$$

Fig. 26.7 displays the graphs corresponding to a solution of the above problem. On the Y-axis are values of the dimensionless pressure gradients $u_1 = 2\pi k_1 h(p_0 - p_1)/\mu Q$ and $u_2 = 2\pi k_1 h(p_0 - p_2)/\mu Q$, and on the X-axis, the dimensionless radial coordinate $r\sqrt{\eta\tau}$. The curves are plotted for different t/τ values. The figure shows that the pressure distributes in the blocks much slower than in the fractures. For the ratio $t/\tau = 3$, the curve $u_1\left(r\sqrt{\eta\tau}\right)$ is almost coincident with the curve $u = -\frac{1}{2}Ei\left(-r^2/4\eta t\right)$, which describes a usual porous medium with the piezoconductivity η. Therefore, for the times much greater than the delay time τ, the pressures in the fractures and pores are the same, and the filtration equation for a regular porous medium can be used.

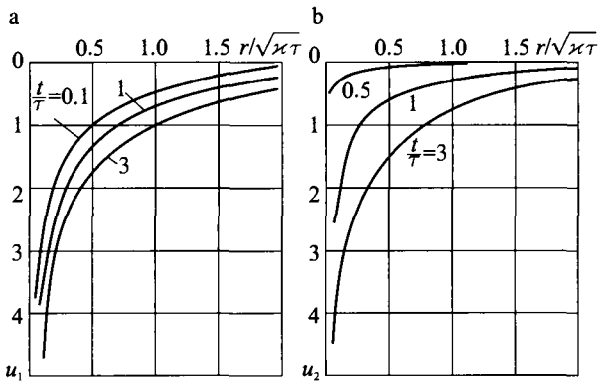

Fig. 26.7. Dimensionless pressure distribution in the fractures (a) and blocks (b) at different times.

Analyzing the elastic liquid's flow to the well in a fractured-porous reservoir, Warren and Root (1963) disregarded the liquid's flow within the blocks (i. e., $\varepsilon_2 << 1$); thus, they discarded the right part of Eq. (26.50). Using the Laplace's transform they came up with an approximate and relatively simple solution for the pressure fractures at the bottomhole:

$$u_{1c} = \frac{1}{2}\left[0.80908 + \ln \bar{t} + Ei\left(-\frac{\lambda \bar{t}}{\omega(1-\omega)}\right) - Ei\left(-\frac{\lambda \bar{t}}{1-\omega}\right)\right] \quad (26.57)$$

where $u_{1c} = 2\pi k_1 h(p_0 - p_{1c})/\mu Q$; $\bar{t} = k_1 t/(\beta_1^* + \beta_2^*)\mu r_c^2$;

$$\omega = \frac{\beta_1^*}{\beta_1^* + \beta_2^*} = \frac{\varepsilon_1}{\varepsilon_1 + \varepsilon_2}; \quad \lambda = \tilde{\alpha}\frac{k_2}{k_1}\frac{r_c^2}{l^2} = \tilde{\alpha}\varepsilon_2\frac{r_c^2}{l^2} \quad (26.58)$$

As Eq. (26.57) shows, the pressure decline at the bottomhole depends on two dimensionless parameters ω and λ determined from Eq. (26.28) describing a fractured-porous reservoir: ω is the ratio of the elastic reserves of the fractures to the total reserves, and λ is the intensity of blocks-to-fractures overflow.

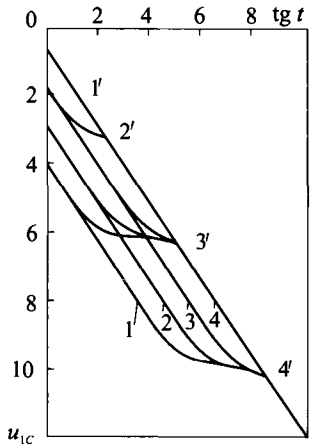

Fig. 26.8. Pressure dynamics in fractures at bottomhole for different ω and λ values, ω: 1 — 0.001; 2 — 0.01; 3 — 0.1; 4 — 1. λ: 1' — 0; 2' — $5 \cdot 10^3$; 3' — $5 \cdot 10^6$; 4' — $5 \cdot 10^9$.

Graphs plotted using Eq. (26.57) for different ω and λ values are presented in Fig. 26.8. Each curve can be subdivided into three segments. At small values of the dimensionless time $\bar{t}$ (when the liquid enters the well mostly from the fractures),

parameter ω plays a major role. For such time values, the asymptotic expression of the integral exponential function can be used:

$$-\mathrm{Ei}(-x) = \ln\frac{1}{x} - 0.5772 \quad \text{at } x << 1;$$

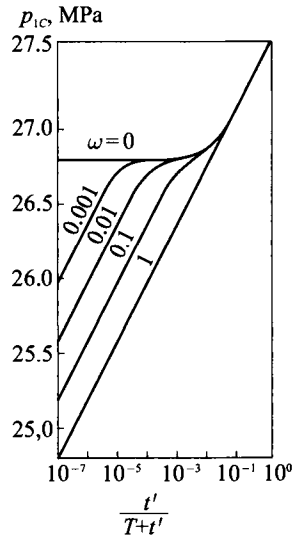

Fig. 26.9. Pressure buildup curves for different ω values ($\lambda = 5\cdot10^{-6}$, $Q = 18.3$ m^3/day).

then

$$\mathrm{Ei}\left(-\frac{\lambda\bar{t}}{\omega(1-\omega)}\right) \approx \ln\frac{\omega(1-\omega)}{\lambda\bar{t}} + 0.5772$$

$$-\mathrm{Ei}\left(-\frac{\lambda\bar{t}}{(1-\omega)}\right) \approx \ln\frac{(1-\omega)}{\lambda\bar{t}} - 0.5772$$

Inserting these expression into Eq. (26.57), results in:

$$u_{1c} = \frac{1}{2}\left[0.80908 + \ln\bar{t} + \ln\frac{1}{\omega}\right], \tag{26.59}$$

i. e., the first segment in coordinates u_{1c} — $\ln \bar{t}$ is a straight line with the slope 1.15. This line cuts on the axis a segment equal to $[0.80908 - \ln \omega]/2$.

For the second segment, the pressure in fractures u_{1c} remains almost constant. The liquid enters the well both from the fractures and matrix blocks.

The third segment occurs at large time values when the values of the integral exponential functions Eq. (26.57) can be disregarded. Then:

$$u_{1c} = [0.80908 + \ln \bar{t}]/2 . \tag{26.60}$$

This is a straight line parallel to the first straight line and describing the flow in a uniform reservoir. The distance between these straight lines depends on parameters ω and $\bar{t}$ (see Fig. 26.8).

The pressure buildup curves of Fig. 26.9 in coordinates p_{1c} — $\ln t/T + t$, (T is the production well operating time prior to shut-in, t is the time after shut-in) have a similar format. The curves are plotted for the value $\lambda = 5 \cdot 10^{-6}$ and different ω values.

The ω and λ parameters can be determined in the process of pressure buildup or drawdown.

For additional information on behavior of fractured reservoirs, see Chilingarian et al. (1992, 1996).

Mechanics of Fluid Flow
by Kaplan S. Basniev, Nikolay M. Dmitriev and George V. Chilingar

APPENDIX A

Inasmuch as the authors believe that petroleum engineers and geologists must be familiar with both the SI and FPS systems of weights and measures and be able to easily make necessary conversions, some concepts and problems using FPS system are presented here.

Some fundamental fluid mechanics concepts and sample problems

Fundamental equation of fluid statics

The fundamental equation of fluid statics states that pressure increases with depth, the increment per unit length being equal to the weight per unit volume (Binder, 1962, p. 13):

$$dp = -\rho g\, dz \tag{A-1}$$

where dp is increment in pressure; dz is increment in depth (z is a vertical distance measured positively in the direction of decreasing pressure); ρ is density (mass per unit volume); and g is gravitational acceleration. The minus sign indicates that pressure decreases with increasing z. The above relationship can be clearly understood on examining Fig. A-1, which shows vertical forces on the infinitesimal element in the body of a static fluid. In this figure, dA represents an infinitesimal cross-sectional area, p is the pressure on the top surface of the element and $(p + dp)$ is the pressure on the bottom surface.

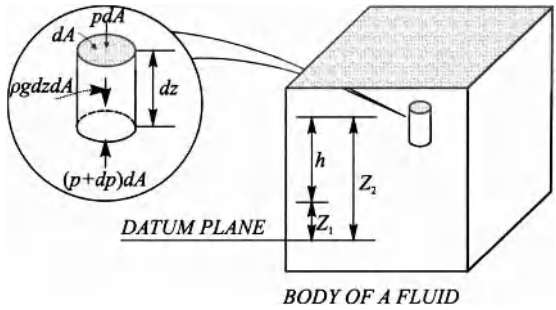

Fig. A-1. Schematic diagram of vertical forces on an infinitesimal element in body of any fluid. (Modified after Binder, 1962, fig. 2-2, p. 13)

Inasmuch as the pressure is due to the fluid weight, the weight of the element ($\rho\, g\, dz\, dA$) is balanced by the force due to pressure difference ($dp\, dA$):

$$dp\, dA = -\rho\, g\, dz\, dA \tag{A-2}$$

or:

$$dp = -\rho\, g\, dz$$

In integral form, the above equation can be expressed as follows (see Fig. A-2):

$$\int_1^2 \frac{dp}{\rho g} = -\int_1^2 dz = -(z_2 - z_1) \tag{A-3}$$

If ρ is assumed to be constant, eq. A-3 becomes:

$$p_2 - p_1 = -\rho\, g\, (z_2 - z_1) \tag{A-4}$$

or:

$$\Delta p = \gamma h \tag{A-5}$$

where h is the difference in depth between two points, which is commonly referred to as the "pressure head"; and $\gamma\,(=\rho\, g)$ is the specific weight. On expressing γ in *lb/cu ft* and h in *ft*, pressure difference Δp is found in *lb/sq ft*.

Buoyancy

When a body is completely or partly immersed in a static fluid, there is an upward vertical buoyant force on this body equal in magnitude to the weight of displaced fluid. This force is a resultant of all forces acting on the body by the fluid. The pressure is greater on the parts of the body more deeply immersed. The pressures at different points on the immersed body are independent of the body material. For example, if the same fluid is substituted for the immersed body, this fluid will remain at rest. This means that the buoyant, upward force on the substituted fluid is equal to its weight.

If the immersed body is in static equilibrium, the buoyant force and the weight of the body are equal in magnitude and opposite in direction, passing through the center of gravity of the body. For a comprehensive treatment of fluid statics, the reader is referred to an excellent book on fluid mechanics by Binder (1962).

General energy equation

[The heat added to unit weight of the flowing fluid between entrance and exit.] + [The work transferred to (done upon) unit weight of the flowing fluid between entrance (1)and exit (2).] = [The total gain in energy by unit weight of the fluid between entrance and exit.]

$$q+\frac{p_1v_1}{778}-\frac{p_2v_2}{778}+\frac{W}{778}=u_2-u_1+\frac{V_2^2-V_1^2}{2g(778)}+\frac{Z_2-Z_1}{778} \tag{A-6}$$

where p = pressure in *psia*; v = specific volume in ft^3/lb; V = velocity in *ft/sec*; Z = = potential head in *ft*; q = heat transferred to fluid; $p_1v_1/778$ = external work in pushing 1 *lb* of fluid across the entrance; W = work in *ft-lb* per *lb* fluid flowing; u_2-u_1 = gain in internal energy; $\left[\left(V_2^2-V_1^2\right)/2g(778)\right]$ = gain in kinetic energy; and $\left(Z_2-Z_1\right)/778$ = gain in potential energy. Point 1 = entrance; point 2 = exit; 1 Btu = = 778 *ft-lb*; $u_2-u_1=c_v\left(T_2-T_1\right)$; c_v = specific heat at constant volume.

Inasmuch as enthalpy $=h=u+(pv)/778$, eq. 1.1-6 becomes:

$$q+\frac{W}{778}=h_2-h_1+\frac{V_2^2-V_1^2}{2g(778)}+\frac{Z_2-Z_1}{778} \tag{A-7}$$

where $h_2-h_1=c_p\left(T_2-T_1\right)$; c_p = specific heat at constant pressure.

For a number of cases, the process is adiabatic and change in internal energy is negligible. Thus:

$$\frac{p_1v_1}{778}-\frac{p_2v_2}{778}+\frac{W}{778}=\frac{V_2^2-V_1^2}{2g(778)}+\frac{Z_2-Z_1}{778} \tag{A-8}$$

and each term in the latter equation is in Btu/lb fluid flowing. On multiplying through by 778:

$$W=\left[\frac{p_2}{\gamma_2}+\frac{V_2^2}{2g}+Z_2\right]-\left[\frac{p_1}{\gamma_1}+\frac{V_1^2}{2g}+Z_1\right] \tag{A-9}$$

where γ = specific weight in lb/ft^3 $(1/v)$; p/γ = pressure head in *ft*; $V^2/2g$ = velocity head in *ft*; and Z = potential head in *ft*.

For frictionless incompressible fluid with no work done:

$$\frac{p_2}{\gamma_2}+\frac{V_2^2}{2g}+Z_2=\frac{p_1}{\gamma_1}+\frac{V_1^2}{2g}+Z_1=\text{const.} \tag{A-10}$$

which is the well-known Bernoulli's equation.

Derivation of formula for flow through orifice meter

A schematic diagram of incompressible fluid flow through an orifice meter is presented in Fig. A-2. For an ideal flow with no friction losses the following relation will hold true:

$$V_1^2/2g+p_1/\gamma+Z_1=V_2^2/2g+p_2/\gamma+Z_2 \tag{A-11}$$

where V = velocity in ft/sec; p = pressure in *psia*; γ= specific weight in *lb/cu ft*; and Z = potential head above any datum plane in ft.

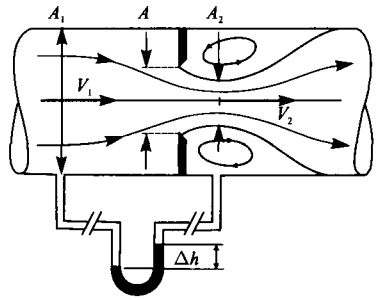

Fig. A-2. Schematic diagram of an orifice meter

Inasmuch as volumetric rate of flow (in cu ft/sec) $Q = V_1A_1 = V_2A_2$:

$$V_1 = V_2A_2/A_1 \tag{A-12}$$

Substituting eq. A-12 in eq. A-11 and solving for V_2:

$$V_2 = \left[\frac{2g\left(p_1/\gamma - p_2/\gamma + Z_1 - Z_2\right)}{1-\left(A_2/A_1\right)^2}\right]^{1/2} \tag{A-13}$$

For an actual flow one has to introduce correction factor for velocity (C_v) and correction factor for area (C_c). The latter is termed coefficient of contraction and is equal to A_2/A. Thus:

$$Q = C_VC_cV_2A \tag{A-14}$$

The term discharge coefficient (C or C_d) often is substituted for C_VC_C. Another term flow coefficient (K) is defined as:

$$K = C/\left[1-\left(A_2/A_1\right)^2\right]^{1/2} \tag{A-15}$$

Thus:

$$\text{actual } Q = KA\left[2g\left(p_1/\gamma - p_2/\gamma + Z_1 - Z_2\right)\right]^{1/2} \tag{A-16}$$

If Δh is manometer deflection in inches. of Hg, then:

$$p_1/\gamma + Z_1 - p_2/\gamma - Z_2 = \frac{\Delta h}{12}\left(sp\,gr_{Hg} - sp\,gr_f\right)/sp\,gr_f \tag{A-17}$$

where $sp\,gr_f$ = specific gravity of fluid flowing.

Flow equation for the Venturi meter (Fig. A-3) can be derived similarly; however, $C_c = 1$ in this case.

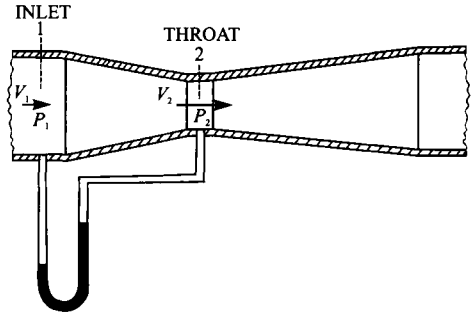

Fig. A-3. Schematic diagram of a venturi meter

Compressible flow formula

For a compressible flow, one can derive the following equation starting with the general energy equation (also see Binder, 1962):

$$G = CA_2\gamma_2\left[\frac{[(2gk)(k-1)][(p_1/\gamma_1)][(1-p_2/p_1)^{(k-1)/k}]}{1-(A_2/A_1)^2(p_2/p_1)^{2/k}}\right]^{1/2} \qquad \text{(A-18)}$$

where G = weight rate of flow in lb/sec, and k = (specific heat at constant pressure)/(specific heat at constant volume) = c_p/c_v. As shown in Nelson (1958, p. 211), constant k can be obtained for various hydrocarbons.

Example problem A-1. Maximum reliable flow

Two reservoirs shown below are connected by a 4-in. 10,000-ft long pipe having friction factor of 0.02. Determine: (1) pump horsepower required to maintain a flow rate of 0.33 cu ft/sec of water (γ= 62.4 lb/cu ft); and (2) the maximum distance x for dependable (reliable) flow.

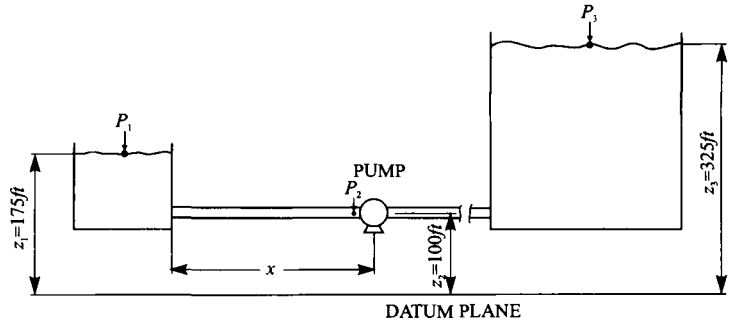

Fig. A-4. Diagram for example problem A-1

Solution:

(1) One can use Bernoulli's equation between points 1 and 3:

$$p_1/\gamma + V_1^2/2g + z_1 + E_p = p_3/\gamma + V_3^2/2g + z_3 + h_{lf} + h_{le} + h_{lx}$$

where E_p = energy output of the pump, ft-lb/lb of fluid flowing; h_{lf} = head loss due to friction = $f(l/d)(V_p^2/2g)$, ft-lb/lb; h_{le} = head loss due to entrance = = $0.5V_p^2/2g$ in the case of sharp entrance, ft-lb/lb; h_{lx} = head loss due to the exit = = dissipated kinetic energy ($=V_p^2/2g$); V_p = velocity in the pipe, ft/sec; d = inside diameter of the pipe, ft; l = length of the pipe, ft; γ = specific weight of the flowing fluid, lb/ft^3; g = gravitational acceleration, ft/sec^2; and z = elevation above some datum plane, ft.

Inasmuch as velocities at the surface of two reservoirs (V_1 and V_3) can be considered negligible and pressures p_1 and p_3 are atmospheric (0 gage), the above equation reduces to:

$$E_p = (z_3 - z_1) + h_{lf} + h_{le} + h_{lx} = (z_3 - z_1) + V_p^2/2g\,(f\,l/d + 0.5 + 1)$$

Inasmuch as:

$$V_p = Q/A = 0.33\,\text{cuft/sec}/(\pi(4/12)^2/4) = 3.78\ \text{ft/sec},$$

$$E_p = (325 - 175) + 3.78^2/64.4[(0.02)(10000)/(4/12) + 0.5 + 1.0)] = 285\ \text{ft-lb/lb}.$$

Thus, horsepower of the pump is equal to:

$$HP = Q\gamma E_p/550 = (0.33)(62.4)(285)/550 = 10.6,$$ where 550 ft-lb/sec = 1 HP.

(2) For maximum and yet reliable flow of water (i. e., no cavitation), the pressure at the inlet side of the pump (p_2) should be 2/3 of the barometric head of water. With safety factor incorporated, it is equal to –21 ft of water (= p_2/γ). Thus, using Bernoulli's equation between points 1 and 2:

$$p_1/\gamma + V_1^2/2g + z_1 = p_2/\gamma + V_2^2/2g + z_2 + h'_{lf} + h_{le},$$

one can solve for unknown distance x, inasmuch as terms p_1/γ and $V_1^2/2g$ can be neglected. Thus: $175 = -21 + (3.78)^2/64.4 + 100 + 0.02[(x)/(4/12)]\ (3.78^2/64.4) + + 0.5(3.78)^2/64.4$ and solving for x: $x = 7180$ ft.

Example problem A-2. Compressible flow (nozzle)

A convergent-divergent nozzle is connected to a tank with air, having pressure of 100 psia and temperature of 100 °F. The tip diameter (point 3) is equal to two inches, and air discharges to atmosphere ($p'_3 = 14.7$ psi and $T'_3 = 60$°F). Determine throat diameter (point 2) necessary to maintain maximum flow rate through this nozzle. Adiabatic constant k for air is equal to 1.4. (See Fig. A-5.)

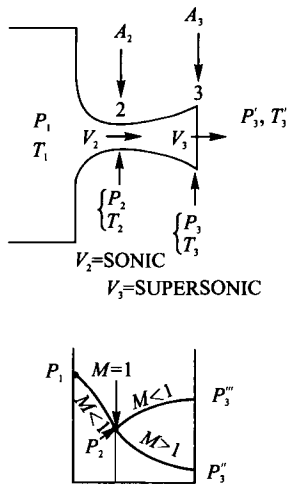

Fig. A-5. Diagram for example problem A-2

Solution:

For maximum flow rate, the velocity in the throat must be sonic, because maximum velocity attainable in a convergent nozzle is sonic. Inasmuch as p_3'/p_1 (=14.7/100 = 0.147) is less than $(p_2/p_1)_{critical} = \{2/(k+1)\}^{k/k-1} =$ $= \{2/(1.4+1)\}^{1.4/1.4-1} = 0.528$), velocity V_3 in the divergent passage will be supersonic.

To attain sonic velocity in the throat (point 2), pressure p_2 must be critical:

$$p_2 = p_1(2/(k+1))^{k/k-1} = 100 \times 0.528 = 52.8 \text{ psia.}$$

The specific weight of air in the tank, γ_1 is equal to: $\gamma_1 = p_1/RT_1 = 100 \times$ $\times$ 144/53.3$\times$560 = 0.483 lb/ft^3, where gas constant for air, R, is equal to 53.3 and T_1 is the absolute temperature in °R (= °F + 460).

Inasmuch as $\gamma_2/\gamma_1 = (p_2/p_1)^{1/k}$, $\gamma_2 = (0.528)^{1/14} \times 0.483 = 0.3$ lb/cu ft. In order to attain sonic velocity in the throat, temperature in the throat must be critical:

$$T_2 = T_1(2/k + 1) = 560(2/2.4) = 466 \text{ °R.}$$

Thus, velocity V_2 is equal to V_c: $V_2 = V_c = c_2 = (kgRT_2)^{1/2} = (1.4 \times 32.2 \times$ $\times 53.3 \times 466)^{1/2} = 1060$ ft/sec.

Temperature at point 3 can be determined from the following equation*: $T_3 = T_1(p_3/p_1)^{k-1/k} = 560(0.147)^{0.4/1.4} = 320°R$, and γ_3 is equal to: $\gamma_3 = p_3/RT_3 =$ $= 14.7\times144/53.3\times320 = 0.12$ lb/ft^3.

Velocity at point 3 can be determined on using the following equation:

$$V_3^2/2g = (p_1/\gamma_1)(k/k-1)\{1-(p_3/p_1)^{(k-1)/k}\}$$

$$V_3^2 = 64.4\times(100\times144/0.483)(1.4/0.4)\{1-(0.147)^{0.4/1.4}\}$$

Solving for V_3:

$V_3 = 1700$ ft/sec, i. e., supersonic speed.

Inasmuch as for adiabatic flow the weight rate of flow in the throat (W_2) is equal to the weight rate of flow at the exit (W_3):

$$W_2 = A_2V_2\gamma_2 = W_3 = A_3V_3\gamma_3$$

$(\pi d_2^2/4\times144)(1060)(0.3) = (\pi2^2/4\times144)(1700)(0.12)$, one can solve for throat diameter d_2: $d_2 = 1.161$ inches.

Example problem A-3: Compressor problem

Air at standard conditions is handled at a rate of 1000 lb/hr by a compressor. Cross-sectional area of inlet is 0.6 ft^2 and that of outlet is 0.11 ft^2. Air is compressed to 100 psia and 180 °F, and the heat taken from air is 50,000 Btu/hr; c_p = = 0.239. If the change in elevation is negligible, what is the work done on the air? Solution:

$$q = \frac{-50{,}000\,Btu/hr}{1000\,lb/hr} = -50\,Btu/lb$$

Weight rate of flow:

$$G = AV\gamma\,lb/\sec$$

where A = cross-sectional area in ft^2; V = velocity in ft/sec; γ= specific weight in lb/ft^3.

$$G = A_1V_1\gamma_1 = A_2V_2\gamma_2$$

---

* $p_1v_1 = RT_1$; $p_3v_3 = RT_3$; $v_1 = 1/\gamma_1$; $v_3 = 1/\gamma_3$. Thus: $T_1 = p_1/\gamma_1R$ and $T_3 = p_3/\gamma_3R$. Dividing T_3 by T_1: $T_3/T_1 = (p_3/p_1)(\gamma_1/\gamma_3)$, and inasmuch as $\gamma_3/\gamma_1 = (p_3/p_1)^{1/k}$; $T_3/T_1 = (p_3/p_1)(p_3/p_1)^{-1/k} =$ $= (p_3/p_1)^{k-1/k}$.

$$V_1 = \frac{G}{A_1\gamma_1} = \frac{1000/3600}{(0.60)\times(0.07651)} = 6.06\, ft/s$$

where 0.07651 is the specific weight of standard sea-level air (59 °F and 14.7 psia).

$$\gamma_2 = \frac{p_2}{RT_2} = \frac{100(144)}{(53.3)(640)} = 0.421\, lb/ft^3$$

$$V_2 = \frac{G}{A_2\gamma_2} = \frac{1000/3600}{(0.11)\times(0.421)} = 5.97\, ft/s$$

$$q + \frac{W}{778} = h_2 - h_1 + \frac{V_2^2 - V_1^2}{2gJ}$$

$$h_2 - h_1 = 0.239(180-59) = 29\ Btu/lb$$

$$\frac{W}{778} = 50 + 29 + \frac{(5.97)^2 - (6.06)^2}{(64.4)\times(778)}$$

$$W = 61{,}600 \text{ ft-lb/lb}$$

If the answer is desired in *HP* then one has to use the following equation:

$$HP = \frac{(W\ ft-lb/lb)\times(G\, lb/\sec)}{(550\, ft-lb/\sec)/HP}$$

Example problem A-4. Friction Losses in Circular Pipes

Calculate the pressure drop in benzene-flowing 200 feet commercial steel pipe 6 inches in diameter. Given; temperature = 50 °F; sp. gr. = 0.90; velocity =11.0 ft/sec; absolute roughness of pipe = 0.00015 ft; dynamic viscosity of benzene = 1.6×10^{-5} slugs/ ft-sec; and g = gravitational acceleration = 32.2 ft/sec/sec.

Solution:

The Reynolds Number is equal to:

$$\text{Re} = \frac{Vd\rho}{\mu} = 11.0\times(\frac{6}{12})\times(\frac{0.90\times62.4}{32.2})/1.6\times10^{-5} = 6\times10^5.$$

Using Fig. A-6,

$$\frac{e}{D} = 0.0003 - 0.0004.$$

Thus, from Fig. A-7, the friction factor, $f = 0.016$.

The head loss, h, is equal to:

$$h = f\frac{l}{d}\frac{V^2}{2g} = 0.016(\frac{200}{0.5})(\frac{11.0^2}{2x\,32.2}) = 12.02 \text{ ft or ft-lb/lb.}$$

Pressure drop $\Delta p = \gamma h = 0.90(62.4)\dfrac{12.02}{144} = 4.69$ psi.

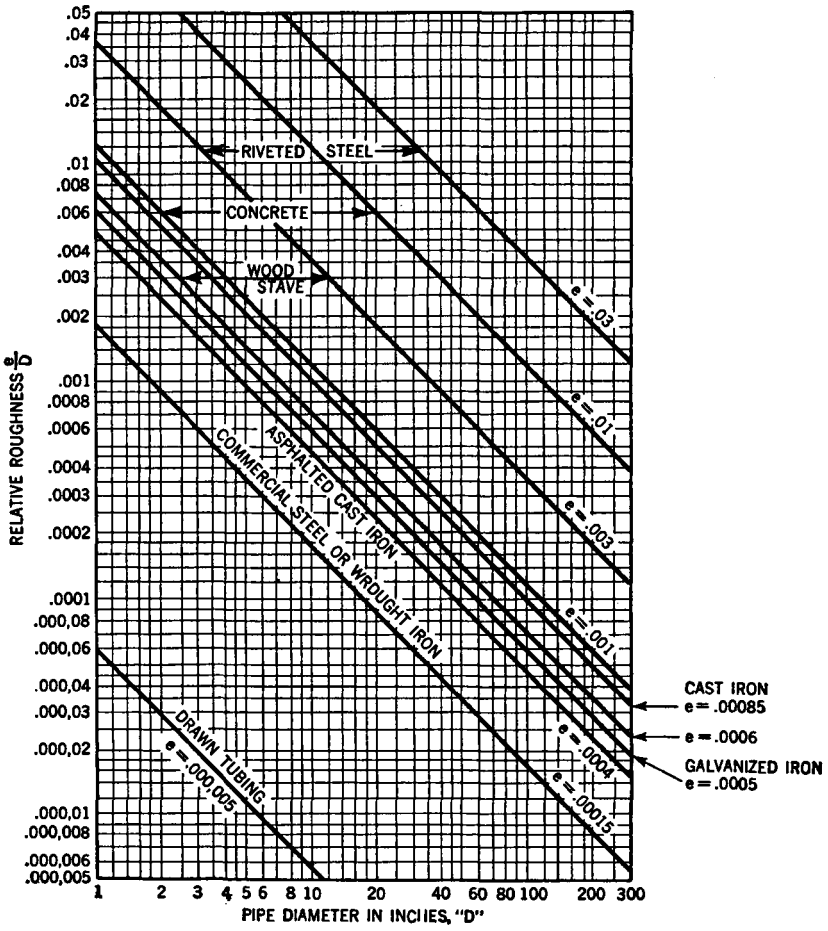

Fig. A-6. Chart for determining relative roughness of pipes (After Moody, 1944.)

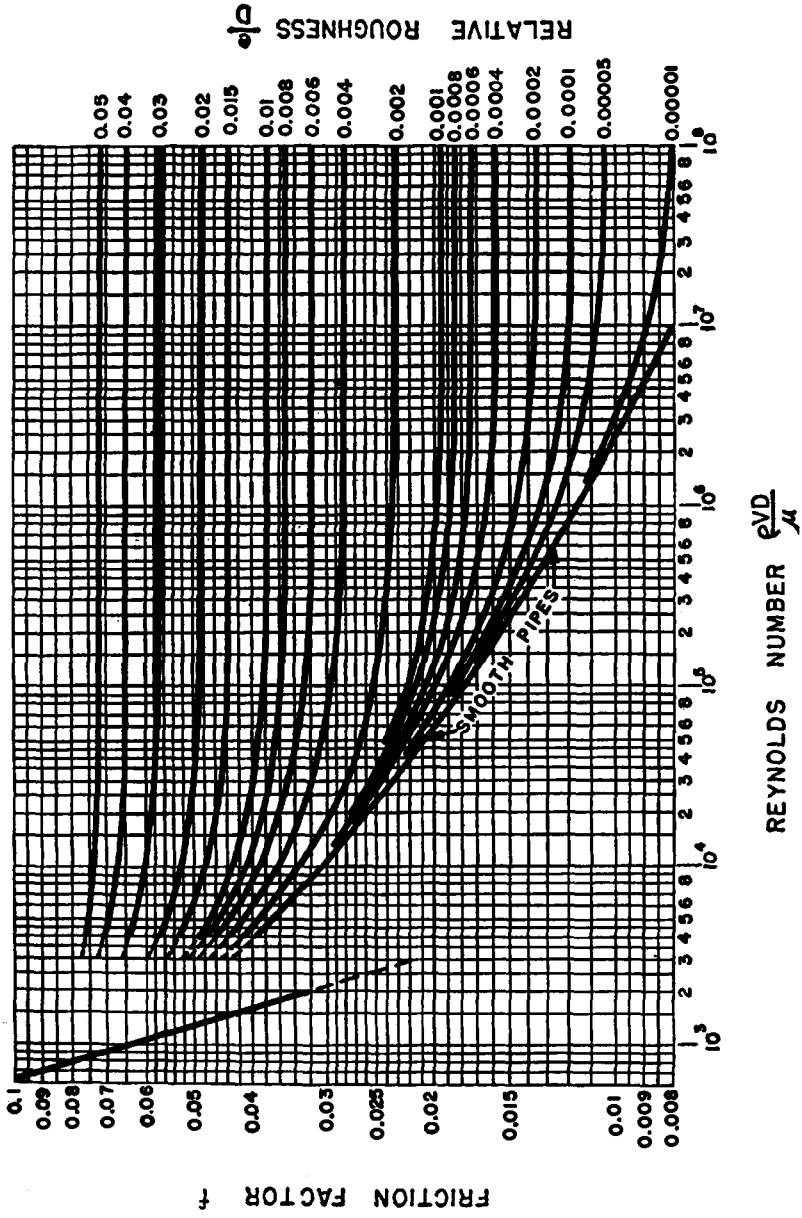

Fig. A-7. Friction factors for flow in circular pipes (After Moody, 1944.)

Farshad's surface roughness values and relative-roughness equations

Surface roughness for various recently-developed pipes is presented in Table A-1. The surface roughness of internally plastic-coated pipes is the lowest compared to the other pipes in this group. The bare Cr13 pipe exhibits the highest average surface-roughness value.

A relative-roughness chart (Fig. A-8) was developed for (1) internally plastic-coated, (2) honed-bare carbon steel, (3) electro-polished bare Cr13, (4) cement-lining, (5) bare carbon steel, (6) fiberglass lining, and (7) bare Cr13 pipes. The relative roughness *e/d* (dimensionless) is related to the absolute *e* (in inches) and pipe diameter *d* (in inches).

A set of nonlinear mathematical models is offered to describe the log/log relationship between the average relative roughness and pipe diameter for various modern pipes (Table A-2).

Table A-1.

Farshad's surface roughness values for modern pipes

Material	Average measured absolute roughness (inches x 10^{-3})	Average measured absolute roughness (micrometers)
Internally plastic coated	0.2	5
Honed bare carbon steel	0.492	12.5
Electro-polished bare Cr 13	1.18	30
Cement lining	1.3	33
Bare carbon steel	1.38	36
Fiber glass lining	1.5	38
Bare Cr 13	2.1	55

Table A-2.

Farshad's relative roughness (*e/d*) equations for modern pipes

Material	Equation (diameter, *d* in inches)
Internally plastic coated	$e/d = 0.0002\,d^{-1.0098}$
Honed bare carbon steel	$e/d = 0.0005\,d^{-1.0101}$
Elcetro-polished bare Cr13	$e/d = 0.0012\,d^{-1.0086}$
Cement lining	$e/d = 0.0014\,d^{-1.0105}$
Bare carbon steel tubing	$e/d = 0.0014\,d^{-1.0112}$
Fiber glass lining	$e/d = 0.0016\,d^{-1.0086}$
Bare Cr13	$e/d = 0.0021\,d^{-1.055}$

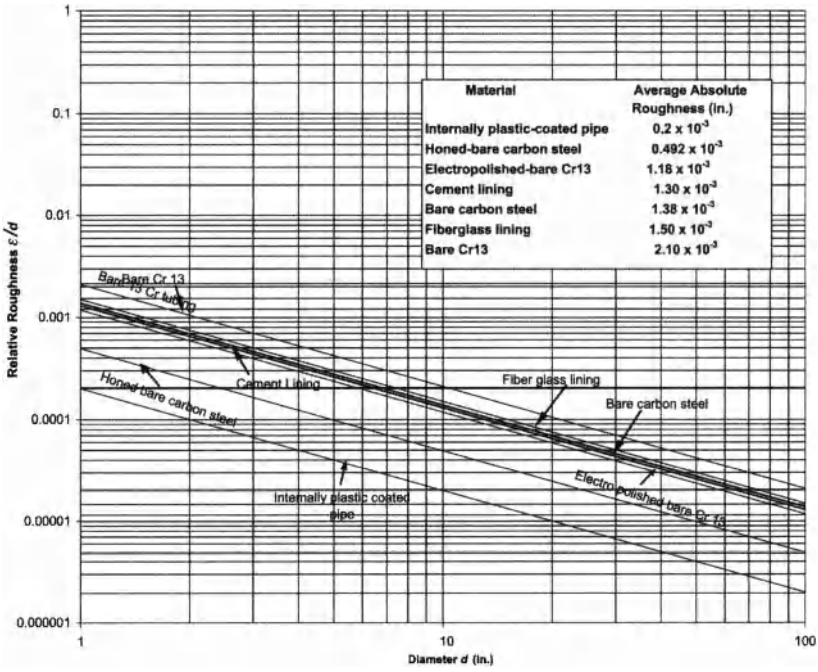

Fig. A-8. Farshad's surface roughness chart for modern pipes

Flow though fractures

The writers have placed strong emphasis on the importance of fractures in carbonate reservoirs. It has been shown in the geological and engineering literature that fractures can constitute the most important heterogeneity affecting production. Craze (1950) cited carbonate reservoirs in Texas, U.S.A., which have low matrix permeabilities, that produce moveable oil from fractures and vugs. Also, Daniel (1954) discussed the influence of fractures on oil production from carbonate reservoirs of low matrix permeability in the Middle East. Reservoirs are not mechanically continuous owing to the presence of fractures. In this sense, the reservoir rock is a discontinum rather than a continuum. The nature and spatial relationship of discontinuities, such as fractures, dissolution channels, and conductive stylolites that affect fluid flow in carbonate rocks are best evaluated using large-core analysis.

Geological conditions which create fractures and control fracture spacing in rocks include: (1) variations in lithology; (2) physical and mechanical properties of the rocks and fluids in the pores; (3) thickness of beds; (4) depth of burial; (5) orientation of the earth's stress field; (6) amount of differential stress (tectonic forces); (7) temperature at depth; (8) existing mechanical discontinuities; (9) rate of

overburden loading or unloading; (10) gravitational compaction (rock or sediment volume reduction as a result of water loss during compaction); (11) anisotropy; and (12) continuum state at depth (competent versus incompetent character of the rocks).

Permeability of a fracture-matrix system

One is interested in the total permeability of the fracture-matrix system rather than the permeability contributions of its various parts. The studies of Huitt (1956) and Parsons (1966) provided the following two equations for determining permeability values in a horizontal direction (k_H) through an idealized fracture-matrix system (using English units):

$$k_H = k_m + 5.446\times10^{10} w^3 \cos^2(\alpha / L), \tag{A-19}$$

where k_m is the matrix permeability (mD); w is the fracture width (in.); L is the length of the fracture; and α is the angle of deviation of the fracture from the horizontal plane in degrees. If w and L are expressed in mm, then Eq. A-19 becomes:

$$k_H = k_m + 8.44\times10^{7} w^3 \cos^2(\alpha / L).$$

Various mathematical models have been proposed to describe the velocity of a fluid in a fracture, to estimate tank oil-in-place in fractured reservoirs, to determine the fracture porosity, and to calculate average "height" of fractures (Chilingarian et al., 1992).

Fluid flow in deformable rock fractures

Witherspoon et al. (1980) proposed a model analyzing fluid flow in deformable rock fractures. This study has ramifications with respect to the migration and production of subsurface fluids. The withdrawal of fluids from carbonate rocks can cause a fracture to close due to induced compaction of the reservoir.

The above proposed model consists of a single-phase fluid flowing between smooth parallel plates. The pressure drop is proportional to the cube of the distance between plates (w = width or aperture of a fracture). For laminar flow (Witherspoon et al., 1980):

$$q = 5.11\times10^{6}\left[w^3 \Delta p a / L\mu\right], \tag{A-20}$$

where q is the volumetric rate of flow (bbl/D); w is the width (or aperture) of a fracture (in.); Δp is the pressure drop (psi); α is the width of the fracture face (ft); L is the length of the fracture (ft); and μ is the viscosity of the fluid (cP).

But natural fractures are rarely smooth and, therefore, head loss owing to friction, h_{Lf}, is equal to:

$$h_{Lf} = f\left[\frac{LV^2}{d_e 2g}\right] \tag{A-21}$$

where f is the friction factor, which is a function of the Reynolds Number, N_{Re}, and relative roughness that is equal to the absolute roughness, e, divided by the width (height or aperture) of the fracture, w (or b) (Fig. A-9). The Reynolds Number is equal to $Vd_e\rho/\mu$, where V is the velocity of flowing fluid (ft/sec); d_e is the equivalent diameter (ft); ρ is the mass per unit volume, i. e., specific weight, γ, in lb/ft^3 divided by the gravitational acceleration, g, in ft/sec/sec (= 32.2). Effective diameter, d_e, is equal to hydraulic radius, R_h, times four (R_h = area of flow/wetted perimeter).

Lomize (1951) and Louis (1969) studied the effect of absolute and relative roughness on flow through induced fractures, sawed surfaces and fabricated surfaces (e. g., by gluing quartz sand onto smooth plates). They found that results deviate from the classical cubic law at small fracture widths. Jones et al. (1988) studied single-phase flow through open-rough natural fractures. They found that N_{Rec} (critical Reynolds Number where laminar flow ends) decreases with decreasing fracture width (b or w) for such fractures.

Jones et al. (1988) suggested the following equations for open, rough fractures with single-phase flow:

$$q = 5.06\times10^4 a\left[\Delta p w^3 / f L\rho\right]^{0.5} \tag{A-22}$$

and

$$k = 5.39\times10^5 \mu\left[wL / f\Delta p\rho\right]^{0.5}, \tag{A-23}$$

where k is the permeability in darcys; ρ is the density of the fluid (lb/ft^3); and f is the friction factor, which is dimensionless.

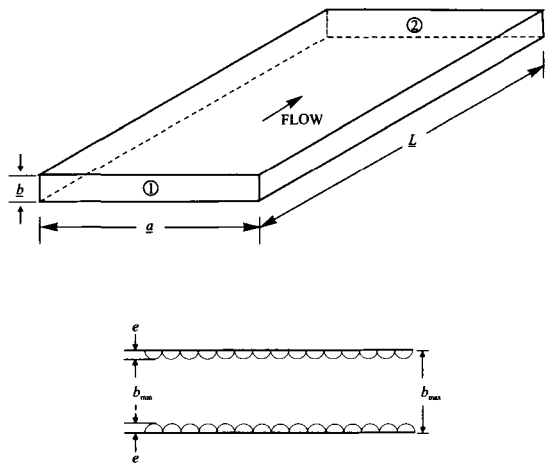

Fig. A-9. Simple fracture-fluid-flow model showing the length of the fracture, L; width, a; thickness, b; and the absolute roughness, e

Based on experimental data, Lomize (1951) developed many equations relating friction factor (f) and Reynolds Number (N_{Re}) for both laminar and turbulent flows. He also prepared elaborate graphs relating friction factor, Reynolds Number, and relative roughness of fractures (e/b or e/w) (Fig. A-10).

Lomize (1951) found that at the relative roughness (e/b) of less than 0.065, fractures behave as smooth ones ($e/b = 0$) and friction factor (f) is equal to:

$$f = 6/N_{Re} \tag{A-24}$$

In the turbulent zone, with e/b varying from 0.04 to 0.24 and $N_{Re} < 4000\text{-}5000$, friction factor is equal to:

$$f = B/(N_{Re})^n \tag{A-25}$$

Coefficient B is equal to 0.056 and n can be found from Fig. A-11 or by using the following equation:

$$n = 0.163 - [0.684(e/b)] + [2.71/e^{76.5(e/b)}] \tag{A-26}$$

The following example illustrates how to use the discussed equations and graphs, and the significance of the results.

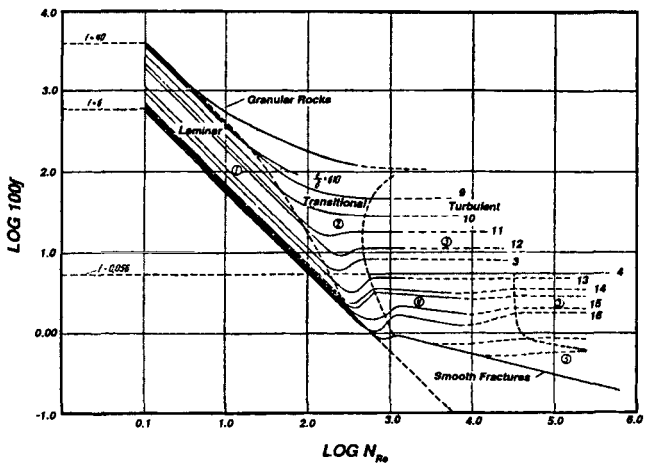

No.	e, см	e/b
3	0.055	0.327
4	0.055	0.205
9	0.175	0.854
10	0.175	0.687
11	0.175	0.574
12	0.175	0.432
13	0.055	0.150
14	0.055	0.120
15	0.055	0.069
16	0.055	0.054

Fig. A-10. Chart showing the relation between friction factor, f, and Reynolds number, N_{Re}, for laminar, transitional and turbulent fluid flow in granular rocks and smooth fractures. (Modified after Lomize, 1951)

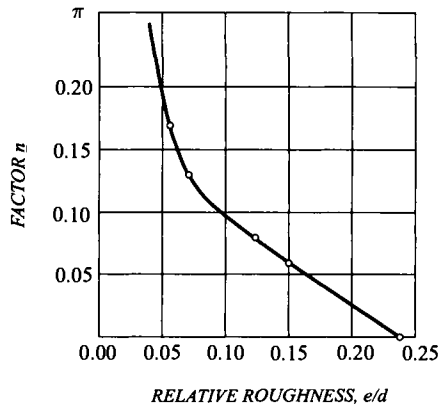

Fig. A-11. Chart showing the relation between coefficient, n, and the relative roughness, e/b ($b = d$), where the coefficient $B = 0.056$. (Modified after Lomize, 1951)

Example problem A-5: Effect of fractures on total permeability

If $w = 0.005$ in., $L = 1$ in., $\alpha = 0°$, and $k_m = 1$ mD, then using Eq. A-19. $k_H =$ $= 6{,}800$ mD.

This example shows the overwhelming contribution which relatively small fracture can exert on total permeability.

Example problem A-6: Pressure drop in a vertical fracture

Determine the pressure drop in psi in a vertical fracture (flow is in upward direction) given the following information: absolute roughness, $e = 0.065$ mm; fracture width (w) or height (b) = 0.68 mm; width of fracture face, $a = 5$ mm ($a > b$); length of fracture, $L = 5$ cm; volumetric rate of flow, $q = 1$ cm^3/sec; specific gravity of flowing oil (sp. gr.) = 0.8; and Reynolds Number ($N_{Re} = 4000$) (see Fig. A-9).

Using Bernouli's Equation for flow from point 1 to point 2:

$$p_1/\gamma + V_1^2/2g + z_1 = p_2/\gamma + V_2^2/2g + z_2 + h_{lf}$$

and

$$p_1/\gamma - p_2/\gamma = \Delta p/\gamma = (z_2 - z_1) + h_{lf} = L + h_{lf}$$

where p_1 and p_2 are pressures at points 1 and 2, respectively, in lb/ft^2 absolute; V = = velocity of flowing fluid in ft/sec; z_1, and z_2 = potential heads at points 1 and 2 in ft; g = gravitational acceleration, ft/sec/sec (=32.2); h_{lf} = head loss due to friction in ft. All terms in the above equation are in *ft-lb* per lb of fluid flowing or in ft.

$$q = 1 \text{ cm}^3/\text{sec} = 1 \text{ (cm}^3/\text{sec)} \times 3.531 \times 10^{-5}(\text{ft}^3/\text{cm}^3) = 3.531 \times 10^{-5}\text{ft}^3/\text{sec}$$

A (cross-sectional area of flow) = $a \times b = 5 \times 0.68$ mm $\times (1.07639 \times 10^{-5}$ ft^2/mm^2) = = 3.6597 x 10^{-5} ft^2;

$$V = q/A = 3.531 \times 10^{-5}/3.6597 \times 10^{-5} = 0.965 \text{ ft/sec}$$

Hydraulic radius R = (flow area)/(wetted perimeter) = $(a \times b)/(2a + 2b)$ = = 9.814×10^{-4} ft

Equivalent diameter = $d_e = 4R = 2ab/(a + b) = 3.9277 \times 10^{-3}$ ft

Inasmuch as N_{Re} is 4000 and relative roughness, $e/b = 0.065/0.68 = 0.095$, one can use Eq. A-26 (and Fig. A-11 to determine n):

$$f = B/(N_{Re})^n = 0.056/(4000)^{0.12} = 0.0207$$

Thus:

$$h_{lf} = f\,(l/d_e)(V^2/2g) =$$

$$= 0.0207(0.164/3.93 \times 10^{-3})\,[(0.965)^2/(2 \text{ x } 32.2)] = 0.0197 \text{ ft}$$

$$\text{Pressure drop } \Delta p = r\,(L + h_{ef}) = [(0.8 \times 62.4)(0.164 + 0.0197)]{:}144$$

$$= 0.062 \text{ psi}$$

REFERENCES

1. Abramovich, G. N., 1960. *Theory of Turbulent Streams.* Fizmatgiz. Moscow, 715 pp.
2. Abramovich, G. N., 1976. *Applied Gas Dynamics.* Nauka, Moscow, 888 pp.
3. Alishayev, M. G., Rozenberg, M. D., Teslyuk, E. V., 1985. *Non-Isothermal Flow in Oilfield Development.* Nedra, Moscow. 271 pp.
4. Altshul, A. D., Kiselev, P. G., 1965. *Hydraulics and Aerodynamics.* Construction Literature Publishing House, Moscow, 274 pp.
5. Aravin, V. N., Numerov, S. N., 1953. *Therory of Liquids and Gas Flow in Undeformable Porous Medium.* Gostekhteorizdat, Moscow, 616 pp.
6. Astarita, J. Marucci, J., 1978. *Basics of Non-Newtonian Liquids Hydrodynamics.* Mir, Moscow, 309 pp.
7. Aziz, H., Settari E., 1982. *Mathematical Modeling of Reservoir Systems.* Nedra, Moscow, 407 pp.
8. Batchelor, G. K., 1973. *Introduction to Dynamics of the Liquid.* Mir. Moscow, 758 pp.
9. Barenblatt, G. I., 1982. *Similarity, Automodelity, Intermediate Asymptotics.* Hydrometeoizdat, Leningrad, 255 pp.
10. Barenblatt, G. I., Entov, V. M., Ryzhik, V. M., 1984. *Liquid and Gas Flow in Natural Reservoirs.* Nedra, Moscow, 416 pp.
11. Barenblatt, G. I., Entov, V. M., Ryzhik, V. M., 1990. *Theory of Fluid Flow Through Natural Rocks.* Kluwer Academic Publishers, Dordrecht, Boston, London, 395 pp.
12. Barenblatt, G. I., Zheltou, Y. P. and Kochina, I. N., 1960. Basic concepts in the theory of seepage of homogeneous liquids in fissured rocks. *J. Appl. Math. Mech.*, 24(5): 852–864.
13. Basniev, K. S., Kochina, I. N., Maksimov, V. M., 1993. *Underground Hydrodynamics.* Nedra, Moscow, 416 pp.
14. Bear, J., 1967. *Dynamics of Fluids in Porous Media.* Amer. Elsevier, N.Y., 764 pp.

15. Ber, Ya, Zaslavsky, D., Ermey, S., 1971. *Physico-Mathematical Basics of Flow.* Mir. Moscow, 452 pp.

16. Bernadiner, M. G., Entov, V. M. 1975. *Hydrodynamic Theory of Anomalous Liquids Flow.* Nauka, Moscow, 199 pp.

17. Binder, R. C., 1962. *Fluid Mechanics*, 4th Ed. Prentice – Hall, Englewood Cliffs, N.D., 453 pp.

18. Birgof, G., 1963. *Hydrodynamics.* IL, Moscow, 199 pp.

19. Butterworth, D., Hewitt, G. (Editors), 1980. *Heat Transfer in Dual-Phase Flow.* Energy, Moscow, 328 pp.

20. Carman, P. C., 1937. Fluid flow through granular beds. Trans. list. *Chem. Eng. Lond*, 30: 150–156.

21. Chang, J. and Yortsos, Y. C., 1990. Pressure transient analysis of fractal reservoirs. *Soc. Petrol. Eng. Form. Evaluation*, 5(1): 31–38.

22. Charny, I. A., 1961. *Fundamentals of Gas Dynamics.* Gostoptekhizdat, Moscow, 200 pp.

23. Charny, I. A., 1963. *Reservoir Hydrogasdynamics.* Gostoptekhizdat. Moscow, 396 pp.

24. Charny, I. A., 1975. *Stationary Flow of Real Fluid in Tubes.* Nedra, Moscow, 296 pp.

25. Cheeseholm, D., 1986. *Two-Phase Flow in Pipelines and Heat Exchangers.* Nedra, Moscow, 204 pp.

26. Chekalyuk, E. B., 1965. *Thermodynamics of Oil Reservoirs.* Nedra, Moscow, 238 pp.

27. Cherny, G. G., 1988. *Gas Dynamics.* Nauka, Moscow, 424 pp.

28. Chilingarian, G. V., Mazzullo, S. J., and Rieke, H. H., 1992. *Carbonate Reservoir Characterization: A Geological Engineering Analysis, Part I.* Elsevier, Amsterdam, The Netherlands, 639 pp.

29. Chilingarian, G. V., Mazzullo, S. J., and Rieke, H. H., 1996. *Carbonate Reservoir Characterization: A Geological Engineering Analysis, Part II.* Elsevier, Amsterdam, The Netherlands, 994 pp.

30. Christianovich, S. A., 1938. *Non-Stationary Flow in Canals and Rivers.* In: Some New Issues in Mechanics of Continua (Kochin, N. E., Editor). AN USSR Publishers, Moscow-Leningrad, 15–154.

31. Cinco-ley, H. and Samaniego, V. F., 1981. Transient pressure analysis for fractured wells. *J. Petrol. Techn.*, 33(9): 1749–1766.

32. Collinse, R., 1964. *Flow of Fluids Through Porous Materials.* Mir, Moscow, 350 pp.

33. Danilov, V. L., Kats, R. M., 1980. *Hydrodynamic Calculations of Mutual Liquid's Displacement in Porous Medium.* Nedra, Moscow, 264 pp.

34. Dancy, H. J., 1856. Determination of the law of flow of water through sand. In: *Les Fontaines Publigues de la Ville de Dijon.* Libraire de Corps Impériaux des Pont et Chaussées et des Mines, Paris, pp. 590–594.

35. Darcy, H., 1856. *Les Fontaines Publiques de la Ville de Dijon.* Paris.

36. Deich, M. E., Filippov, G. A., 1981. *Gas-Dynamics of the Double-Phase Media.* Energoizdat, Moscow, 472 pp.

37. Dupuit, J., 1863. *Etudes Theoriques et Pratiques sur le Mouvement des Eaux dans le Canaux de et a Travers les Terrains Permeables.* 2-eme ed. Paris.

38. Dvukhsherstov, G. I., 1948. *Hydraulic Shock in Non-Round Cross-section Pipes Mechanics.* vol II, 17–76 pp.

39. Earlougher, Jr., R. C., 1977. *Advances in Well Test Analysis.* SPE Monograph Vol. 5, Dallas, TX, 264 pp.

40. Efros, D. A., 1963. *Studies in the Nonuniform Systems Flow.* Gostoptekhizdat, Leningrad, 351 pp.

41. Eglit, M. E. (Editor), 1996. *Mechanics of Continua (Problems).* Moscow Lyceum, Moscow, vol. 1 — p. 394; vol. 2 — p. 395.

42. Eirich, (Editor), 1962. *Rheology. Theory and Applications.* Moscow, 824 pp.

43. Emtsev, B. T., 1987. *Technical Hydrodynamics.* Mashinostroyeniye, Moscow, 440 pp.

44. Entov, V. M., Zazovsky, A. F., 1989. *Hydrodynamics of the Improved Oil Recovery Processes.* Nedra, Moscow, 232 pp.

45. Evdokimova, V. A., Kochina, I. M., 1979. *Problems in Underground Hydraulics.* Nedra, Moscow, 169 pp.

46. Farshad, F. F., Garber, J. D., Polaki, V., 2000. *Comprehensive Model for Predicting Corrosion Rates in Gas Wells Containing* CO_2. SPE PF 15(3): 183–190.

47. Farshad, F. F., Pesacreta, T. S., 2003. *Coated Pipe Interior Surface Roughness as Measured by Three Scanning Probe Instruments.* Anti-Crrosion Methods and Materials, 50 (1): 6–16.

48. Farshad, F. F., Rieke, H. H., 2006. *Surface-Roughness Design Values for Modern Pipes. J.SPE* Drilling and Completion.

49. Farshad, F. F., Rieke, H. H., Gandy, J., 2002. *Flow Test Validation of Direct Measurment Methods Used to Determine Surface Roughness in Pipes (OCTG).* SPE 76768 Presented at the SPE Western Regional/ AAPG Pacific Section Joint Meeting, Anchorage, 20–22 May.

50. Farshad, F. F., Rieke, H. H., Garber, J. D., 2001. *New Development in Surface Roughness Measurements, Characterization, and Modeling Fluid Flow in Pipe. J. Petroleum Science and Engineering*, 29 (2): 139–150.

51. Forchheimer, P., 1914. *Hydraulik.* Teubner, Leipzig and Berlin, pp. 211–216.

52. Germain, P. P., 1965. *Mechanics of Continua.* Mir, Moscow, 479 pp.

53. Gimatudinov, Sh. K., Shirkovsky, A. I., 1982. *Physics of Oil and Gas Reservoirs.* Nedra, Moscow, 308 pp.

54. Ginsburg, I. P., 1958. *Applied Hydrogasodynamics.* LGU Publishers, 338 pp.

55. Ginsburg, I. P., 1966. *Aerogasodynamics.* Vysshaya Shkola, Moscow, 404 pp.

56. Ginsburg, I. P., 1970. *Theory of Resistance and Heat Transfer.* LGU Publishers, 375 pp.

57. Goldshitk, M. A., Shtern, V. N., Javorsky, N. I., 1989. *Viscous Flow with Paradoxical Properties.* Nauka, Novosibirsk, 336 pp.

58. Golf-Racht, T. D., van, 1982. *Fundamentals of Fractured Reservoir Engineering.* Elsevier, Amsterdam, 710 pp.

59. Golf-Racht, T. D. van, 1986. *Basics of Oilfield Geology and Development of Fractured Reservoirs (translated from English).* Nedra, Moscow, 608 pp.

60. Golubeva, O. V., 1972. *Course of the Mechanics of Continua.* Vysshaya Shkola, Moscow, 368 pp.

61. Godunov, S. K., 1978. *Elements of the Mechanics of Continua.* Nauka, Moscow, 304 pp.

62. Greenkorn, R. A., 1983. *Flow Phenomena in Porous Media.* M. Dekker, Inc., N.Y. Basel, 550 pp.

63. Gritsenko, A. I., Klapchuk, O. V., Kharchenko, Yu. A., 1994. *Hydrodynamics of Gas-Liquid Mixtures in Wells and Pipelines.* Nedra, Moscow, 238 pp.

64. Gussein-Zadeh, M. A., Kolosovskaya, A. K., 1972. *Elastic Regime in Single-bed and Multi-bed Systems.* Nedra, Moscow, 454 pp.

65. Haifets, L. I., Neimark, A. V., 1982. *Multiphase Processes in Porous Media.* Chemistry, Moscow, 319 pp.

66. Hazebrock, P., Rainbow, H. and Matthews, C. S., 1958. Pressure fall-off in water injection wells. *Trans. AIME*, 213: 250–260.

67. Hintze, I. O., 1963. *Turbulence.* Fizmatizdat, Moscow, 680 pp.

68. Hinze, J. O., 1959. *Turbulence (An Introduction to its Machanism and Theory.* McGraw-Hill Book Co., New York.

69. Houpeurt, A., 1958. *Elements de Mechanique des Fluides dans les Milieux Poeux.* Editions Technic, Paris, 231 pp.

70. Huitt, J. L., 1956. *Fluid flow in simulated fractures.* AIChE J., 2(2): 259–264.

71. Idelchik, I. E., 1975. *Reference Book on Hydraulic Resistances.* Mashinostroyeniye, Moscow.

72. Ikoku, C. V., Ramey, H. J., 1979. *Transient Flow of Non-Newtonian Fluids in Porous Media.* Stanford University, 220 pp.

73. Jones, T. A., Wooten, S. O. and Kaluza, T. J., 1988. *Single-Phase Flow Through Natural Fractures.* Soc. Petrol. Engrs. 63d Ann. Tech. Conf. and Exhibit., Houston, TX, 7 pp.

74. Kochin, N. B., Kibel, I. A., Roze, N. V., 1963.*Theoretical Hydrodynamics, Pt.I.* Fizmatgiz, Moscow, 583 pp.

75. Kochin, N. B., Kibel, I. A., Roze, N. V., 1963.*Theoretical Hydrodynamics, Pt.II.* Fizmatgiz, Moscow, 727 pp.

76. Konovalov, A. N., 1988. *Problems in Filtration of Multiphase Incompressible Liquids.* Nauka, Novosibirsk, 165 pp.

77. Kotyakhov, F. I., 1997. *Physics of Oil and Gas Reservoirs.* Nedra, Moscow, 287 pp.

78. Kozeny, J., 1927. Uber kapillare Leitung des Wassers im Boden. Sitzunger, *Akad Wiss. Wien, Math. Naturw.* Kl. Alt., 136(IIa): 271–306.

79. Kuteladze, S. S., Starikovich, M. A., 1976. *Hydrodynamics of Double-Phase Systems.* Energy, Moscow, 296 pp.

80. Lamb, G., 1947. *Hydrodynamics.* GITTL, Moscow, 928 pp.

81. Landau, L. D., Livshitz, E. M., 1986. *Hydrodynamics.* Nauka, Moscow, 736 pp.

82. Langnes, G. L., Robertson, J. O., Jr. and Chilingar, G. V., 1972. *Secondary Recovery and Carbonate Reservoirs*, Am. Elsevier Publ. Co., New York, N.Y., 304 pp.

83. Lapuk, B. B., 1948. *Theoretical Grounds for the Development of Natural Gas Fields.* Nauka, Moscow, 295 pp.

84. Lavrentyev, M. A., Shabat, B. V., 1973. *Problems of Hydrodynamics and their Mathematical Models.* Nauka, Moscow. 416 pp.

85. Leibenzon, L. S., 1947. *Flow of Natural Liquids and Gases in Porous Medium.* Gostekhizdat, Moscow, 244 pp.

86. Lodge, A., 1969. *Elastic Liquids.* Nauka, Moscow, 463 pp.

87. Lomize, G. M., 1951. *Flow in Fractured Rocks.* Gos. Energ. Lzd., Moscow – Leningrad, 127 pp. (In Russian).

88. Loytsyanskiy, L. G., 1987. *Mechanics of Liquids and Gases.* Nauka, Moscow, 840 pp.

89. Luis, C., 1969. *A study of groundwater in jointed rocks and its influence on the stability of rock masses.* Rock Mech. Res., Imp. Coll., London, Rept. No. 10, 90 pp.

90. Mase, G., 1974. *Theory and Problems in of Continuum Mechanics.* Mir, Moscow, 518 pp.

91. Matthews, C. S. and Russell, D. G., 1967. Pressure Buildup and Flow Tests in Wells. *Soc. Petrol. Engrs. Trans. AIME*, Monograph 1, Dallas TX, 167 pp.

92. Millheim, K.K. and Chichowiez, L., 1968. Testing and analyzing low-permeability fractured gas wells. *Trans. AIME*, 243: 193–198.

93. Monin, A. S., Yaglom, A. M., 1965. *Statistical Hydrodynamics, Pt.1.* Mir, Moscow, 655 pp.

94. Monin, A. S., Yaglom, A. M., 1967. *Statistical Hydrodynamics, Pt.2.* Mir, Moscow, 720 pp.

95. Muscat, M., 1949. *Flow of Uniform Liquids in Porous Media.* Gostoptekh-izdat, Moscow, 628 pp.

96. Muscat, M., 1949. *Physical Principles of Oil Production.* McGraw-Hill, New York, 922 pp.

97. Nakaznaya, L. G., 1972. *Liquid and Gas Flow in Fractured Reservoirs.* Nedra, Moscow, 184 pp.

98. Nelson, W. I., 1958. *Petroleum Refinery Engineering.* Mc Graw-Hill, New York, N.Y., 4th ed., 960 pp.

99. Nigmatulin, R. I., 1987. *Dynamics of Multiphase Media.* vol. I. Nauka, Moscow, 464 pp.

100. Nigmatulin, R. I., 1987. *Dynamics of Multiphase Media.* vol. II. Nauka, Moscow, 359 pp.

101. Nikolaevskiy, V. N., Basniev, K. S., Gorbunov, A. T., Zotov, G. A., 1970. *Mechanics of Saturated Porous Media.* Nedra, Moscow, 335 pp.

102. Nikolaevsky, V. N., 1990. *Mechanics of Porous and Fractured Media.* World Scientific, Singapore, 472 pp.

103. Nikolaevsky, V. N., 1996. *Geomechanics and Fluid Dynamics.* Nedra, Moscow, 447 pp.

104. Novozhilov, V. V., 1977. *Theory of Turbulent Boundary Layer in Incompressible Liquid.* Shipbuilding Publishers, Leningrad, 165 pp.

105. Parsons, R. W., 1966. Permeability of idealized fractured rock. *Trans. AIME*, 237: 126–136.

106. Perez-Rozales, C. 1978. Use of Pressure Buildup Tests for Describing Hetrogeneous Reservoirs. SPE 7451. *Soc. Petrol. Engrs.* 53rd Ann. Techn. Conf. and Exhibition, Houston, TX, 8 pp.

107. Polubarinova-Kochina, P. Ya. (Editor), 1969. *Evolution of Flow Theory in the USSR.* Nauka, Moscow, 545 pp.

108. Polubarinova-Kochina, P. Ya. (Editor), 1977. *Theory of Groundwater Flow.* Nauka, Moscow, 664 pp.

109. Prager, W., 1968. *Introduction to the Mechanics of Continua.* IL, Moscow, 311 pp.

110. Prandtl, L., 1949. *Hydroaeromechanics.* IL, Moscow, 520 pp.

111. Prandtl, L., 1952. *Essentials of Fluid Dynamics.* Hafner Publ. Co., New York.

112. Periverdian, A. M., 1982. *Physics and Hydraulics of Oil Reservoir.* Nedra, Moscow, 192 pp.

113. Pykhachev, G. B., Isayev, R. G., 1973. *Reservoir Hydraulics.* Nedra, Moscow, 360 pp.

114. Raghavan, R., Scorer, J. D. T. and Miller, F. G., 1972. An investigation of

numerical methods of the effect of pressure-dependent rock and fluid properties on well flow tests. *Soc. Pet. Eng. J.*

115. Rakhmatulin, Kh. A., Sagomonian, A. Ya., Bunimovich, A. I., Zverev, I. N., 1965. *Gas Dynamics.* Vysshaya Shkola, Moscow, 722 pp.
116. Reiner, M., 1965. *Rheology.* Nauka, Moscow, 223 pp.
117. Romm, E. S., 1985. *Structural Models of Rock's Porous Media.* Nedra, Leningrad, 240 pp.
118. Rosenberg, M. D., Kundin, S. A., 1976. *Multiphase Multicomponent Flow in Oil and Gas Production.* Nedra, Moscow, 335 pp.
119. Rouse, H., 1959. *Advanced Mechanics of Fluids.* John Wiley and Sons, New York.
120. Scheideggar, A. E., 1960. *Physics of Liquid Flow Through Porous Media.* Gostoptekhizdat, Moscow, 249 pp.
121. Scheidegger, A. E., 1974. *The Physics of Flow Through Porous Media.* Toronto University Press, Toronto, 353 pp.
122. Schlichting, G., 1974. *Theory of Boundary Layer.* Nauka, Moscow, 711 pp.
123. Schwidler, M. I., 1985. *Statistical Hydrodynamics of Porous Media.* Nedra, Moscow, 288 pp.
124. Sedov, L. I., 1987. *Similarity and Dimensionality Methods in Mechanics.* Nauka, Moscow, 430 pp.
125. Sedov, L. I., 1994. *Mechanics of Continua.* vol.I. Nauka, Moscow, 528 pp.
126. Sedov, L. I., 1994. *Mechanics of Continua.* vol.II. Nauka, Moscow, 560 pp.
127. Shchelkachev, V. N., 1990. *Selecta.* vol. I-II. Nedra, Moscow.
128. Shchelkachev, V. N., 1995. *Fundamentals and Applications of Non-Stationary Flow Theory.* Oil and Gas. Pt. I. 586 pp., Pt. II. 493 pp. Moscow.
129. Shchelkachev, V. N., Lapuk, B. B., 1949. *Reservoir Hydraulics.* Gostoptekhizdat, Moscow, 358 pp.
130. Slezkin, N. A., 1955. *Dynamics of Viscous Incompressible Liquids.* GITTL, Moscow, 519 pp.
131. Sou, S., 1971. *Hydrodynamics of Multiphase Systems.* Mir, Moscow, 536 pp.
132. Sternlicht, D. V., *Hydraulics.* Energoatomizdat, Moscow, 639 pp.
133. Targ, S. M., 1951. *Basic Problems of the Laminar Flow Theory.* GITTL, Moscow, 420 pp.

134. Tatashev, K. K., 1968. Effect of the change in layer pressure on the oil displacement from blocks of fissured-porous oil reservoirs by water injection. *Geol. Nefti i Gaza*, 1: 55–59.

135. Truesdail, K., 1975. *Initial Course of Rational Mechanics of Continua.* Mir, Moscow, 592 pp.

136. Vakhitov, G. G., Kuznetsov, O. L., Simkin, E. M., 1978. Thermodynamics of *Oil Reservoirs Near-bottom Zone.* Nedra, Moscow, 212 pp.

137. Van Everdingen, A.F. and Hurst, W., 1949. The application of the Laplace transformation to flow problems in reservoirs. *Trans. AIME*, 186: 305–324.

138. Van Everdingen, A. F. and Kriss, H. S., 1980. New approach to improved recovery efficiency. *J. Petrol. Techn.*, 32(6): 1164–1168.

139. von Karman, T., 1954. *Aerodynamics.* Cornell Univ. Press, Ithaca, New York.

140. Vulis, L. A., Kashkarov, V. P., 1965. *Theory of Viscous Liquid Streams.* Nauka, Moscow, 431 pp.

141. Wallis, G., 1972. *One-dimensional Two Phase Flow.* Mir, Moscow, 440 pp.

142. Warren, J. E. and Root, P. J., 1963. The behavior of naturally fractured reservoirs. *Trans. AIME*, 228: 245–255.

143. Wilkinson, W. L., 1964. *Non-Newtonian Liquids.* Mir, Moscow, 440 pp.

144. Witherspoon, P. A., Wang, J. S. Y., Iwai, K. and Gale, J. E., 1980. Validity of the cubic law for fluid in a deformable rockW fracture. *Water Resources Res.*, 16(6): 1016–1024.

145. Zeldovich, A. B., 1946. Theory of Shock Wave and an Introduction to Gas *Dynamics.* Moscow, AN USSR Publishers. Leningrad. 185 pp.

146. Zheltov, Yu. P. 1975. *Mechanics of an Oil Reservoir.* Nedra, Moscow, 216 pp.

147. Zhukovsky, N. E., 1949. *Collected Works.* vol. 3. Goslitizdat, Moscow, Leningrad, 700 pp.

148. Zommerfeld, A., 1954. *Mechanics of Deformable Media.* IL, Moscow, 486 pp.

Mechanics of Fluid Flow
by Kaplan S. Basniev, Nikolay M. Dmitriev and George V. Chilingar

SUBJECT INDEX

Also of Interest

Check out these other related titles from Scrivener Publishing

Fundamentals of the Petrophysics of Oil and Gas Reservoirs, by Buryakovsky, Chilingar, Rieke, and Shin. Coming in July 2012, ISBN 9781118344477. The most comprehensive book ever written on the basics of petrophysics for oil and gas reservoirs.

Petroleum Accumulation Zones on Continental Margins, by Grigorenko, Chilingar, Sobolev, Andiyeva, and Zhukova. Coming in August 2012, ISBN 9781118385074. Some of the best-known petroleum engineers in the world have come together to produce one of the first comprehensive publications on the detailed (zonal) forecast of offshore petroleum potential, a must-have for any petroleum engineer or engineering student.

Zero-Waste Engineering, by Rafiqul Islam, ISBN 9780470626047. In this controversial new volume, the author explores the question of zero-waste engineering and how it can be done, efficiently and profitably. *NOW AVAILABLE!*

Sustainable Energy Pricing, by Gary Zatzman, ISBN 9780470901632. In this controversial new volume, the author explores a new science of energy pricing and how it can be done in a way that is sustainable for the world's economy and environment. *NOW AVAILABLE!*

Flow Assurance, by Boyun Guo and Rafiqul Islam, January 2013, ISBN 9780470626085. Comprehensive and state-of-the-art guide to flow assurance in the petroleum industry.

An Introduction to Petroleum Technology, Economics, and Politics, by James Speight, ISBN 9781118012994. The perfect primer for anyone wishing to learn about the petroleum industry, for the layperson or the engineer. *NOW AVAILABLE!*

Ethics in Engineering, by James Speight and Russell Foote, ISBN 9780470626023. Covers the most thought-provoking ethical questions in engineering. *NOW AVAILABLE!*

Formulas and Calculations for Drilling Engineers, by Robello Samuel, ISBN 9780470625996. The most comprehensive coverage of solutions for daily drilling problems ever published. *NOW AVAILABLE!*

Emergency Response Management for Offshore Oil Spills, by Nicholas P. Cheremisinoff, PhD, and Anton Davletshin, ISBN 9780470927120. The first book to examine the Deepwater Horizon disaster and offer processes for safety and environmental protection. *NOW AVAILABLE!*

Advanced Petroleum Reservoir Simulation, by M.R. Islam, S.H. Mousavizadegan, Shabbir Mustafiz, and Jamal H. Abou-Kassem, ISBN 9780470625811. The state of the art in petroleum reservoir simulation. *NOW AVAILABLE!*

Energy Storage: A New Approach, by Ralph Zito, ISBN 9780470625910. Exploring the potential of reversible concentrations cells, the author of this groundbreaking volume reveals new technologies to solve the global crisis of energy storage. *NOW AVAILABLE!*